ORGANOMETALLICS

Volume 1, Number 2, February 1982

Addition of Isocyanides to $[CpMo(CO)_2]_2$. The Crystal and Molecular Structure of $Cp_2Mo_2(CO)_4(\mu\text{-}\eta^2\text{-CNPh})$ Which Contains a Bridging η^2-Isocyanide Ligand

Richard D. Adams,* Dean A. Katahira, and Li-Wu Yang

Department of Chemistry, Yale University, New Haven, Connecticut 06511

Received June 26, 1981

The isocyanides, CNR, R = Me, Ph, *t*-Bu, react with $[CpMo(CO)_2]_2$ to form the 1:1 adducts $Cp_2Mo_2(CO)_4(\mu\text{-}\eta^2\text{-CNR})$, R = Me, Ph, *t*-Bu. The products have been investigated by IR, ^1H NMR, and ^{13}C NMR spectroscopy. The phenyl isocyanide adduct has also been characterized by X-ray crystallographic methods: space group $P2_1/n$, at 23 °C, a = 9.144 (1) Å, b = 19.574 (3) Å, c = 11.409 (2) Å, β = 96.10 (1)°, V = 2030.5 (9) Å^3, Z = 4, ρ_{calcd} = 1.757 g/cm^3. For 2951 reflections ($F_o \geq 3.0\sigma(F_o^2)$) R_1 = 0.023 and R_2 = 0.025. The molecule contains two molybdenum atoms joined by a Mo–Mo single bond, Mo–Mo = 3.212 (1) Å. The two metal atoms are bridged by an isocyanide ligand which is σ bonded to one metal atom and π bonded to the other. The C–N multiple bond at 1.244 (3) Å is significantly longer than that normally found for terminally coordinated isocyanide ligands. ^{13}C NMR shifts of the isocyano carbons of the $\sigma + \pi$-bonded isocyanide ligands occur at approximately 215-ppm downfield from Me_4Si.

Introduction

Organometallic molecules containing metal–metal multiple bonds have been shown to exhibit a wealth of new and unusual reaction chemistry.[1,2] Probably the most thoroughly studied of these is $[CpMo(CO)_2]_2$ (**I**).[3-11] Formally this molecule contains a Mo≡Mo triple bond.[3] It readily adds donors, either two two-electron donors or one four-electron donor,[4,6] to yield molecules containing a Mo—Mo single bond (eq 1–3). The third reaction X≡Y = N≡C—R[5] or CN^-[7] has resulted in a few of the rare examples of the $\sigma + \pi$ coordination of the heteronuclear triple bond. It has been proposed that such coordination may play an important role in the activation of these ligands toward catalytic reduction about polynuclear metal centers.[12] We have now found that isocyanides also react with **I** according to eq 3 to produce 1:1 adducts where the isocyanide ligand engages in the $\sigma + \pi$-bonding mode.

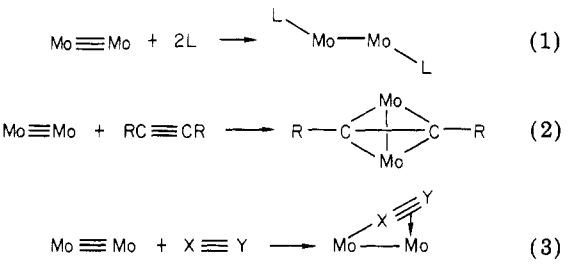

Experimental Section

General Information. Since the compounds, particularly when in solution, were air sensitive, all reactions and purifications were routinely performed under a prepurified nitrogen atmosphere. Hexane and toluene solvents were purified by distillation from sodium–benzophenone; other solvents were stored over 4-Å molecular sieves and degassed with a dispersed stream of nitrogen. $[CpMo(CO)_2]_2$ was prepared according to the method of Curtis.[13] MeNC and PhNC were prepared by reported methods.[14,15]

(1) Chisholm, M. H.; Cotton, F. A. *Acc. Chem. Res.* **1978**, *11*, 356.
(2) (a) Clauss, A. D.; Dimas, P. A.; Shapley, J. R. *J. Organomet. Chem.* **1980**, *201*, C31. (b) Boag, N. M.; Green, M.; Mills, R. M.; Pain, G. N.; Stone, F. G. A.; Woodward, P. *J. Chem. Soc., Chem. Commun.* **1980**, 1171.
(3) Klinger, R. J.; Butler, W. M.; Curtis, M. D. *J. Am. Chem. Soc.* **1978**, *100*, 5034.
(4) Bailey, W. I.; Chisholm, M. H.; Cotton, F. A.; Rankel, L. A. *J. Am. Chem. Soc.* **1978**, *100*, 5764.
(5) Chisholm, M. H.; Cotton, F. A.; Extine, M. W.; Rankel, L. A. *J. Am. Chem. Soc.* **1978**, *100*, 807.
(6) Curtis, M. D.; Klingler, R. J. *J. Organomet. Chem.* **1978**, *161*, 23.
(7) Curtis, M. D.; Han, K. R.; Butler, W. M. *Inorg. Chem.* **1980**, *19*, 2096.
(8) Curtis, M. D.; Butler, W. M. *J. Chem. Soc., Chem. Commun.* **1980**, 988.
(9) Curtis, M. D.; Messerle, L. *J. Am. Chem. Soc.* **1980**, *102*, 7791.
(10) Wachter, J.; Mitschler, A.; Riess, J. G. *J. Am. Chem. Soc.* **1981**, *103*, 2121.
(11) Brunner, H.; Meier, W.; Wachter, J. *J. Organomet. Chem.* **1981**, *210*, C23.
(12) (a) Muetterties, E. L. *Bull. Soc. Chim. Belg.* **1976**, *85*, 451. (b) Muetterties, E. L.; Stein, J. *Chem. Rev.* **1979**, *79*, 479.
(13) Klingler, R. J.; Butler, W.; Curtis, M. D. *J. Am. Chem. Soc.* **1975**, *97*, 3535.

0276-7333/82/2301-0231$01.25/0

Table I. Spectral Properties[a]

compd	NMR, δ (J, Hz) ^{1}H	NMR, δ (J, Hz) ^{13}C	IR, cm^{-1}
$Cp_2Mo_2(CO)_4CNMe$ (II)	5.34 (C_5H_5), 5.33 (C_5H_5) 3.62 (CH_3)	245.99 (CO), 244.37 (CO) 233.84 (CO), 232.50 (CO) 210.53 (CN), 94.56 (C_5H_5) 92.26 (C_5H_5), 40.65 (CH_3)	ν_{CN} 1725 (m br) ν_{CO} 1825 (s), 1898 (s) 1930 (vs), 1971 (s)
$Cp_2Mo_2(CO)_4CNPh$ (III)	7.50 (d, ^3J = 8.1, C_6H_5) 7.40 (dd, ^3J = 8.1, ^3J = 7.0, C_6H_5) 7.21 (d, ^3J = 7.0, C_6H_5) 5.44 (C_5H_5), 5.42 (C_5H_5)	246.16 (CO), 244.47 (CO)[b] 232.96 (CO), 231.02 (CO) 213.90 (CN), 139.32 (C_6H_5) 129.29 (C_6H_5), 125.98 (C_6H_5) 122.74 (C_6H_5), 94.76 (C_5H_5) 92.89 (C_5H_5)	ν_{CN} 1666 (m br) ν_{CO} 1850 (s), 1898 (s) 1927 (vs), 1968 (s)
$Cp_2Mo_2(CO)_4CN$-*t*-Bu (IV)	5.33 (C_5H_5), 5.32 (C_5H_5) 1.39 (CH_3)	246.49 (CO), 244.48 (CO) 233.98 (CO), 232.90 (CO) 211.36 (CN), 94.41 (C_5H_5) 94.44 (C_5H_5), 59.49 (C_4H_9, tertiary) 31.09 (C_4H_9, primary)	ν_{CN} 1690 (m br) ν_{CO} 1849 (s), 1892 (s) 1920 (vs), 1963 (s)

[a] NMR spectra of compounds in $CDCl_3$ at 298 K; IR spectra of compounds in hexane solvent, ±5 cm^{-1}. [b] At −50 °C.

tert-Butyl isocyanide was obtained from Strem Chemicals Inc. Alumina for chromatography was Baker acid-washed aluminum oxide deactivated with 6% w/w water.

Melting points were determined in evacuated capillary tubes using a Thomas-Hoover apparatus are are uncorrected. Infrared spectra were recorded on a Perkin-Elmer 237B spectrophotometer. A Bruker HX270 NMR spectrometer was used to obtain ^{1}H and ^{13}C NMR spectra at 270 and 67.89 MHz, respectively.

Reaction of $[CpMo(CO)_2]_2$ with CNPh. At room temperature phenyl isocyanide (85.5 mg, 0.829 mmol) was added to a stirred solution of $[CpMo(CO)_2]_2$ (300.0 mg, 0.691 mmol) in methylene chloride (100 mL). As monitored by IR spectroscopy, the reaction was complete in 5 min. Volatile components of the reaction were removed under vacuum. The remaining red-browm residue was taken up in a minimal amount of methylene chloride and chromatographed on alumina. A single red-brown band was eluted with a methylene chloride/hexane solvent mixture (30%/70%, v/v) to yield 315.6 mg (85%) of crude $Cp_2Mo_2(CO)_4(CNPh)$ (III). Dark red-brown, rhombohedral crystals were obtained by slow crystallization of the crude product from hexane/methylene chloride (20%/80%, v/v) or from benzene at 6 °C; mp 156 °C.

The reactions of methyl and *tert*-butyl isocyanides with $Cp_2Mo_2(CO)_4$ were performed similarly. $Cp_2Mo_2(CO)_4$-(CNMe) (II): yield, 87%; mp 120 °C. Anal. Calcd: C, 40.44; H, 2.76; N, 2.95. Found: C, 40.18; H, 2.85; N, 3.03. $Cp_2Mo_2(CO)_4$(CN-*t*-Bu) (IV): yield 88%, mp 121 °C. Anal. Calcd: C, 44.12; H, 3.70; N, 2.71. Found: C, 44.13; H, 3.89; N, 2.44. See Table I for IR and NMR spectra.

Crystallographic Analyses. A crystal of Cp_2Mo_2-$(CO)_4(\mu$-η^2-CNPh) suitable for diffraction measurements was obtained from a benzene solution. It was mounted in a thin-walled glass capillary. Diffraction measurements were made on an Enraf-Nonius CAD-4 fully automated four-circle diffractometer using graphite-monochromatized Mo K$\bar{\alpha}$ radiation. Unit cells were determined and refined from 25 selected reflections ($2\theta > 45°$) by using the CAD-4 automatic center and least-squares routines. The space group $P2_1/n$ was identified by observation of the appropriate systematic absences during data collection. Crystal data and data collection parameters are listed in Table II. All data processing was performed on a Digital PDP 11/45 computer using the Enraf-Nonius SDP program library.

Table II. Crystallographic Data for X-ray Diffraction Study for $Cp_2Mo_2(CO)_4(\mu$-η^2-CNPh) (III)

(A) Crystal Data	
formula	$C_{21}H_{15}NO_4Mo_2$
temp, ±5 °C	23
space group	$P2_1/n$
a, Å	9.144 (1)
b, Å	19.574 (3)
c, Å	11.409 (2)
β, deg	96.10 (1)
V, Å^3	2030.5 (9)
mol wt	537.24
Z	4
ρ_{calcd}, g/cm^3	1.757
ρ_{obsd}, g/cm^3	1.78
(B) Measurement of Intensity Data	
radiation	Mo K$\bar{\alpha}$ (0.710 73 Å)
monochromator	graphite
detector aperture, mm	
horizontal ($A + B \tan\theta$)	
A	3.0
B	1.0
vertical	4.0
crystal faces	100, $\bar{1}$00, 010; 0$\bar{1}$0, 001, 00$\bar{1}$
crystal size, mm	0.23 × 0.33 × 0.30
crystal orientatn: direction; deg from ϕ axis	normal to 21$\bar{4}$; 14.0°
reflections measd	$+h, +k, \pm l$
max 2θ	52°
scan type	moving crystal-stationary counter
ω-scan width	
A + 0.347 tan θ	A = 0.90°
bkgd	one-fourth additional scan at each end of scan
ω-scan rate (variable)	
max, deg/min	10.0°
min, deg/min	1.3°
no. of reflections measd	5333
data used ($F^2 \geq 3.0\sigma(F)^2$)	2951
(C) Treatment of Data	
P factor	0.01
final residuals R	0.023
R_w	0.025
esd of unit weight	1.89
largest shift/error value on final cycle	0.01
largest peak in final diff Fourier, e/Å^3	0.35

The linear absorption coefficient is 12.4 cm^{-1}. No absorption correction was applied. Three standard reflections monitored every 4000 s showed only random ±2% fluctuation. Neutral atom scattering factors were calculated by the standard procedures.[16a] Anomalous dispersion

(14) Casanova, J.; Schuster, E. R.; Werner, N. D. *J. Chem. Soc.* **1963**, 4280.
(15) Ugi, I.; Meyer, R.; Lipinski, M.; Bodesheim, F.; Rosendahl, F. *Org. Synth.* **1961**, *41*, 13.

Table III. Fractional Atomic Coordinates, Thermal Parameters,[a] and Their Esds for $Cp_2Mo_2(CO)_4(\mu\text{-}\eta^2\text{-}CNPh)$ (III)

atom	x	y	z	B_{11}	B_{22}	B_{33}	B_{12}	B_{13}	B_{23}
Mo(1)	0.29947 (3)	0.10929 (1)	0.22387 (2)	2.806 (9)	2.61 (1)	2.677 (9)	−0.14 (1)	0.703 (8)	−0.35 (1)
Mo(2)	0.03298 (3)	0.21699 (1)	0.20517 (2)	3.35 (1)	3.42 (1)	2.79 (1)	0.67 (1)	0.394 (9)	0.22 (1)
O(1)	0.4329 (3)	0.2483 (1)	0.1562 (2)	6.8 (1)	4.2 (1)	7.4 (1)	−1.6 (1)	2.7 (1)	0.2 (1)
O(2)	0.5570 (3)	0.1397 (2)	0.4159 (2)	5.3 (1)	9.5 (2)	6.3 (1)	1.0 (1)	−1.8 (1)	−3.3 (1)
O(3)	0.0602 (4)	0.1869 (2)	−0.0613 (2)	9.6 (2)	8.8 (2)	3.1 (1)	1.8 (2)	0.2 (1)	−0.2 (1)
O(4)	−0.2616 (3)	0.1412 (2)	0.1369 (3)	4.7 (1)	11.8 (2)	11.0 (2)	−2.8 (2)	−1.6 (1)	3.3 (2)
N	0.1561 (3)	0.0932 (1)	0.365 (2)	3.3 (1)	3.4 (1)	3.0 (1)	0.39 (9)	1.03 (9)	0.42 (9)
Cp(11)	0.3056 (4)	0.0715 (2)	0.032 (3)	7.6 (2)	4.0 (2)	3.3 (1)	−1.2 (2)	1.5 (1)	−1.4 (1)
Cp(12)	0.4326 (4)	0.0477 (2)	0.100 (3)	4.1 (2)	4.7 (2)	6.1 (2)	−0.7 (1)	2.1 (1)	−2.7 (1)
Cp(13)	0.3907 (4)	0.0014 (2)	0.1821 (3)	5.0 (2)	3.4 (1)	5.8 (2)	0.6 (1)	0.6 (2)	−1.0 (1)
Cp(14)	0.2372 (4)	−0.0053 (2)	0.1639 (3)	6.0 (2)	2.9 (1)	6.0 (2)	−1.4 (1)	2.3 (1)	−1.1 (1)
Cp(15)	0.1839 (4)	0.0381 (2)	0.0716 (3)	4.8 (2)	4.3 (2)	5.2 (2)	−1.0 (1)	−0.2 (2)	−2.0 (1)
Cp(21)	0.1665 (5)	0.3073 (2)	0.3075 (3)	7.4 (2)	3.8 (2)	5.2 (2)	0.5 (2)	−0.8 (2)	−1.5 (1)
Cp(22)	0.0446 (6)	0.2926 (2)	0.3673 (3)	11.4 (3)	5.0 (2)	3.7 (2)	1.5 (2)	1.5 (2)	−1.1 (2)
Cp(23)	−0.0829 (5)	0.3072 (2)	0.2906 (4)	6.8 (2)	6.8 (2)	8.4 (2)	2.4 (2)	2.8 (2)	−1.7 (2)
Cp(24)	−0.0377 (5)	0.3311 (2)	0.1856 (4)	7.0 (2)	4.3 (2)	6.0 (2)	2.7 (2)	−0.0 (2)	0.1 (2)
Cp(25)	0.1149 (5)	0.3302 (2)	0.1944 (3)	7.9 (2)	3.1 (2)	5.2 (2)	0.1 (2)	0.5 (2)	0.1 (2)
C(1)	0.3760 (4)	0.1982 (2)	0.1823 (3)	4.2 (1)	3.7 (2)	3.9 (1)	−0.5 (1)	1.2 (1)	−0.2 (1)
C(2)	0.4587 (4)	0.1285 (2)	0.3465 (3)	3.9 (1)	5.1 (2)	3.9 (1)	0.5 (1)	0.4 (1)	−1.3 (1)
C(3)	0.0538 (4)	0.1968 (2)	0.0371 (3)	5.0 (2)	4.7 (2)	3.4 (1)	0.6 (1)	−0.1 (1)	0.2 (1)
C(4)	−0.1527 (4)	0.1696 (2)	0.1627 (3)	3.9 (2)	6.9 (2)	5.3 (2)	0.1 (2)	0.0 (1)	2.0 (2)
C(5)	0.0921 (3)	0.1379 (2)	0.3014 (3)	2.7 (1)	3.7 (1)	3.0 (1)	0.0 (1)	0.8 (1)	−0.0 (1)
C(31)	0.1528 (3)	0.0717 (2)	0.4845 (2)	3.0 (1)	3.1 (1)	2.7 (1)	−0.2 (1)	0.4 (1)	0.3 (1)
C(32)	0.0733 (4)	0.1087 (2)	0.5589 (3)	4.0 (1)	3.8 (1)	3.8 (1)	0.4 (1)	1.2 (1)	0.3 (1)
C(33)	0.0722 (4)	0.0874 (2)	0.6752 (3)	5.2 (2)	5.2 (2)	3.4 (1)	−0.6 (1)	1.7 (1)	−0.8 (1)
C(34)	0.1474 (4)	0.0302 (2)	0.7147 (3)	5.2 (2)	5.6 (2)	2.8 (1)	−0.9 (2)	0.4 (1)	0.5 (1)
C(35)	0.2252 (4)	−0.0066 (2)	0.6409 (3)	5.3 (2)	4.8 (2)	3.9 (2)	0.8 (2)	0.1 (1)	1.4 (1)
C(36)	0.2307 (4)	0.0147 (2)	0.5244 (3)	4.5 (2)	3.8 (2)	3.5 (1)	0.7 (1)	1.0 (1)	0.4 (1)

atom[b]	x	y	z	atom[b]	x	y	z
H(32)	0.0180	0.1487	0.5293	H(13)	0.4562	−0.0225	0.2427
H(33)	0.0183	0.1126	0.7296	H(14)	0.1783	−0.0352	0.2080
H(34)	0.1442	0.0152	0.7953	H(15)	0.0798	0.0436	0.0414
H(35)	0.2792	−0.0474	0.6702	H(21)	0.2717	0.3025	0.3394
H(36)	0.2872	−0.0108	0.4714	H(22)	0.0474	0.2749	0.4472
H(11)	0.3026	0.1058	−0.0310	H(23)	−0.1855	0.3021	0.3080
H(12)	0.5333	0.0603	0.0920	H(24)	−0.1011	0.3455	0.1153
				H(25)	0.1751	0.3428	0.1321

[a] The form of the anisotropic thermal parameter is exp $[-1/4\ (B_{11}h^2a^{*2} + B_{22}k^2b^{*2} + B_{33}l^2c^{*2} + B_{12}hka^*b^* + B_{13}hla^*c^* + B_{23}klb^*c^*)]$. [b] Hydrogen atom positions were not refined. $B = 5.00$ Å^2.

corrections were applied for all nonhydrogen atoms.[16b] The structure was solved by a combination of Patterson and difference Fourier techniques. Hydrogen atom positions were calculated on the basis of geometric considerations. Hydrogen atom contributions were included in structure factor calculations, but their positions were not refined. Full-matrix least-squares refinements minimized the function $\sum_{hkl} w(|F_o| - |F_c|)^2$, where $w = 1/\sigma(F)^2$, $\sigma(F) = \sigma(F_o^2)/2F_o$, and $\sigma(F_o^2) = [\sigma(I_{raw})^2 + (PF_o^2)^2]^{1/2}/Lp$. All nonhydrogen atoms were refined with anisotropic temperature factors. Final fractional atomic coordinates and interatomic distances and angles with errors obtained from the inverse matrix calculated on the final cycle of least-squares refinement are listed in Tables III–V. Structure factor amplitudes are available (see supplementary material).

Results and Discussion

When I is allowed to react with 1 equiv of isocyanide at room temperature, products with the formula $Cp_2Mo_2(CO)_4(CNR)$ (II, R = Me; III, R = Ph; IV, R = *t*-Bu) can be isolated in high yield. Their IR spectra show four absorptions in the terminal CO stretching region and a broad low-energy absorption (1725, 1666, and 1695 cm^{-1} for II, III, and IV, respectively) indicative of a bridging ligand. No absorptions are observed in the region 2000–2200 cm^{-1} which is characteristic of terminally coordinated isocyanide ligands.

Table IV. Interatomic Distances with Esds for $Cp_2Mo_2(CO)_4(\mu\text{-}\eta^2\text{-}CNPh)$ (III)

atoms	dist, Å	atoms	dist, Å
Mo(1)-Mo(2)	3.212 (1)	C(31)-C(32)	1.380 (3)
Mo(1)-C(1)	1.953 (3)	C(32)-C(33)	1.391 (3)
Mo(1)-C(2)	1.946 (3)	C(33)-C(34)	1.367 (4)
Mo(1)-C(5)	2.247 (2)	C(34)-C(35)	1.364 (4)
Mo(1)-N	2.207 (2)	C(35)-C(36)	1.398 (3)
Mo(1)-Cp(11)	2.317 (2)	C(36)-C(31)	1.376 (3)
Mo(1)-Cp(12)	2.301 (2)	Cp(11)-Cp(12)	1.406 (4)
Mo(1)-Cp(13)	2.339 (3)	Cp(12)-Cp(13)	1.387 (4)
Mo(1)-Cp(14)	2.397 (3)	Cp(13)-Cp(14)	1.403 (4)
Mo(1)-Cp(15)	2.384 (2)	Cp(14)-Cp(15)	1.399 (4)
Mo(2)-C(3)	1.986 (3)	Cp(15)-Cp(11)	1.406 (4)
Mo(2)-C(4)	1.950 (3)	Cp(21)-Cp(22)	1.397 (5)
Mo(2)-C(5)	1.942 (2)	Cp(22)-Cp(23)	1.410 (5)
Mo(2)-Cp(21)	2.382 (3)	Cp(23)-Cp(24)	1.388 (5)
Mo(2)-Cp(22)	2.363 (3)	Cp(24)-Cp(25)	1.389 (4)
Mo(2)-Cp(23)	2.326 (3)	Cp(25)-Cp(21)	1.400 (4)
Mo(2)-Cp(24)	2.330 (3)	C(1)-O(1)	1.163 (3)
Mo(2)-Cp(25)	2.347 (3)	C(2)-O(2)	1.154 (3)
C(5)-N	1.244 (3)	C(3)-O(3)	1.147 (3)
N-C(31)	1.426 (3)	C(4)-O(4)	1.151 (3)

The ^{1}H NMR spectra of II, III, and IV show resonances which can be assigned to inequivalent cyclopentadienyl rings and the R groups of the isocyanide ligands (see Table I). The ^{13}C NMR spectra show five low-field resonances in addition to those characteristic of the cyclopentadienyl ligands and R groups. These low-field resonances are arranged in two groups of two with the remaining reso-

(16) "International Tables for X-ray Crystallography"; Kynoch Press: Birmingham, England, 1975; Vol. IV: (a) Table 2.2B, pp 99–101; (b) Table 2.3.1, pp 149–50.

Table V. Interatomic Angles with Esds for $Cp_2Mo_2(CO)_4(\mu\text{-}\eta^2\text{-}CNPh)$ (III)

atoms	angles, deg	atoms	angles, deg	atoms	angles, deg
Mo(2)-Mo(1)-C(5)	36.55 (6)	C(2)-Mo(1)-Cp(13)	93.8 (1)	Mo(2)-C(5)-N	167.7 (2)
Mo(2)-Mo(1)-N	68.69 (5)	C(2)-Mo(1)-Cp(14)	121.6 (1)	Mo(1)-N-C(5)	75.5 (1)
Mo(2)-Mo(1)-C(1)	71.81 (8)	C(2)-Mo(1)-Cp(15)	151.3 (1)	Mo(1)-N-C(31)	144.4 (2)
Mo(2)-Mo(1)-C(2)	115.15 (8)	Mo(1)-Mo(2)-C(5)	43.56 (6)	C(5)-N-C(31)	135.2 (2)
C(5)-Mo(1)-N	32.41 (7)	Mo(1)-Mo(2)-C(3)	77.50 (8)	N-C(31)-C(32)	119.8 (2)
C(5)-Mo(1)-C(1)	102.3 (1)	Mo(1)-Mo(2)-C(4)	109.8 (1)	N-C(31)-C(36)	119.5 (2)
C(5)-Mo(1)-C(2)	105.48 (9)	C(5)-Mo(2)-C(3)	109.7 (1)	C(36)-C(31)-C(32)	120.6 (2)
C(5)-Mo(1)-Cp(11)	123.9 (1)	C(5)-Mo(2)-C(4)	86.8 (1)	C(31)-C(32)-C(33)	119.2 (2)
C(5)-Mo(1)-Cp(12)	153.62 (9)	C(5)-Mo(2)-Cp(21)	102.5 (1)	C(32)-C(33)-C(34)	120.4 (2)
C(5)-Mo(1)-Cp(13)	129.8 (1)	C(5)-Mo(2)-Cp(22)	94.0 (1)	C(33)-C(34)-C(35)	120.4 (2)
C(5)-Mo(1)-Cp(14)	99.25 (9)	C(5)-Mo(2)-Cp(23)	118.7 (1)	C(34)-C(35)-C(36)	120.4 (3)
C(5)-Mo(1)-Cp(15)	96.02 (9)	C(5)-Mo(2)-Cp(24)	151.2 (1)	C(35)-C(36)-C(31)	119.1 (2)
N-Mo(1)-C(1)	124.07 (9)	C(5)-Mo(2)-Cp(25)	135.4 (1)	Cp(15)-Cp(11)-Cp(12)	107.7 (3)
N-Mo(1)-C(2)	87.65 (9)	C(3)-Mo(2)-C(4)	80.6 (1)	Cp(11)-Cp(12)-Cp(13)	108.5 (3)
N-Mo(1)-Cp(11)	136.16 (9)	C(3)-Mo(2)-Cp(21)	121.6 (1)	Cp(12)-Cp(13)-Cp(14)	107.8 (3)
N-Mo(1)-Cp(12)	140.22 (9)	C(3)-Mo(2)-Cp(22)	151.6 (1)	Cp(13)-Cp(14)-Cp(15)	108.5 (2)
N-Mo(1)-Cp(13)	105.84 (9)	C(3)-Mo(2)-Cp(23)	130.5 (1)	Cp(14)-Cp(15)-Cp(11)	107.4 (3)
N-Mo(1)-Cp(14)	86.23 (8)	C(3)-Mo(2)-Cp(24)	98.8 (1)	Cp(25)-Cp(21)-Cp(22)	107.9 (3)
N-Mo(1)-Cp(15)	101.40 (9)	C(3)-Mo(2)-Cp(25)	94.2 (1)	Cp(21)-Cp(22)-Cp(23)	107.8 (3)
C(1)-Mo(1)-C(2)	75.0 (1)	C(4)-Mo(2)-Cp(21)	149.6 (1)	Cp(22)-Cp(23)-Cp(24)	107.5 (3)
C(1)-Mo(1)-Cp(11)	90.6 (1)	C(4)-Mo(2)-Cp(22)	117.3 (2)	Cp(23)-Cp(24)-Cp(25)	108.8 (3)
C(1)-Mo(1)-Cp(12)	95.2 (1)	C(4)-Mo(2)-Cp(23)	92.4 (1)	Cp(24)-Cp(25)-Cp(21)	108.0 (3)
C(1)-Mo(1)-Cp(13)	127.6 (1)	C(4)-Mo(2)-Cp(24)	102.0 (1)	Mo(1)-C(1)-O(1)	174.1 (2)
C(1)-Mo(1)-Cp(14)	147.7 (1)	C(4)-Mo(2)-Cp(25)	135.3 (1)	Mo(1)-C(2)-O(2)	177.3 (2)
C(1)-Mo(1)-Cp(15)	119.1 (1)	Mo(1)-C(5)-Mo(2)	99.89 (9)	Mo(2)-C(3)-O(3)	176.9 (3)
C(2)-Mo(1)-Cp(11)	130.5 (1)	Mo(1)-C(5)-N	72.0 (1)	Mo(2)-C(4)-O(4)	179.4 (3)
C(2)-Mo(1)-Cp(12)	98.0 (1)				

nance occurring at a somewhat higher field. In III these occur at at δ 246.16, 244.47, 232.96, 231.02, and 217.50 at −50 °C. We choose to assign the first four to the terminal carbonyl ligands since on the basis of the structural analysis (see below), these can be arranged into groups of two. The remaining resonance we assign to the isocyano (C≡N) carbon atom. This shift is considerably lower than that normally found for terminally coordinated isocyanide ligands which lie in the range δ 140–170[17-19] but is similar to those found for bridging isocyanide ligands.[15] The ^1H and ^{13}C NMR peaks remain sharp at room temperature; thus, unlike other molecules in this family,[4,7] these are stereochemically rigid.

Details of the molecular structure of III were established by an X-ray crystallographic analysis. An ORTEP diagram of the molecular structure is shown in Figure 1. The molecule contains two $(\eta^5\text{-Cp})Mo(CO)_2$ units joined by a metal–metal bond which on the basis of bond length (3.212 (1) Å) can be formulated as a single bond (e.g., $[CpMo(CO)_3]_2$, Mo—Mo = 3.235 (1) Å,[20] and $Cp_2Mo_2(CO)_5CNCH_3$, Mo—Mo = 2.320 (1) Å[21]). The metal–metal bond is bridged by an isocyanide ligand coordinated in a $\sigma + \pi$ fashion. The isocyano carbon is σ bonded to metal Mo(2), Mo(2)—C(5) = 1.942 (2) Å, while the C—N function is π bonded to Mo(1), Mo(1)—C(5) = 2.247 (2) Å and Mo(1)—N = 2.207 (1) Å. The C(5)≡N bond length at 1.244 (3) Å is significantly longer than those found for terminal isocyanide ligands.[19,21-26] For example, the C≡N

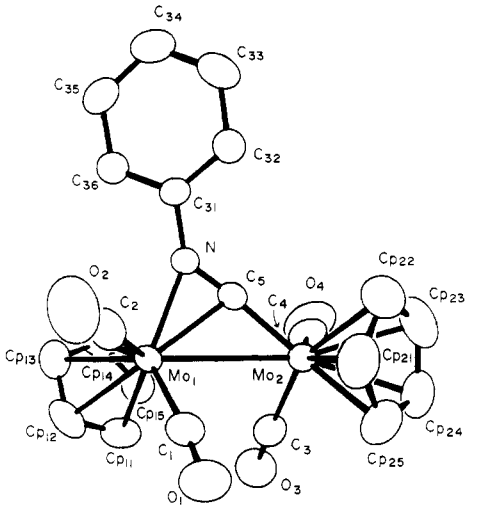

Figure 1. A perspective ORTEP diagram of $Cp_2Mo_2(CO)_4(\mu\text{-}\eta_2\text{-}CNPh)$ showing 50% electron density probability ellipsoids.

bond lengths of the terminal isocyanide ligands are 1.17 (1) Å in $Cp_2Mo_2(CO)_5CNMe$[21] and 1.153 (13) Å in $CpMo(CO)_2CNPhI$.[22] It is even longer than those found for the more common C-briding isocyanide ligands.[19,27,28] C≡N bond lengths for C-bridging isocyanide ligands generally lie in the range 1.19–1.23 Å.[15,23,24] The only other reported example of a $\sigma + \pi$-bonded isocyanide ligand was for the molecule $Mn_2(dpm)_2(CO)_4(\mu\text{-}\eta^2\text{-}CN\text{-}p\text{-}tol)$, and it had a C≡N bond length of 1.25 (1) Å.[29] The long bond length suggests a weakening of the C—N bond order, and this is supported by the low-energy position of the C—N absorption in the IR spectrum. Both observations support the notion advanced by Muetterties that polynuclear coordination will significantly reduce bond order in unsat-

(17) Novotny, M.; Lewis, D. F.; Lippard, S. J. *J. Am. Chem. Soc.* **1972**, *94*, 6961.
(18) Fanell, L. F.; Randall, E. W.; Rosenberg, E. *J. Chem. Soc. D* **1971**, 1078.
(19) Green, M.; Howard, J. A. K.; Murray, M.; Spencer, J. L.; Stone, F. G. A. *J. Chem. Soc., Dalton Trans.* **1977**, 1509.
(20) Adams, R. D.; Collins, D. M.; Cotton, F. A. *Inorg. Chem.* **1974**, *13*, 1086.
(21) Adams, R. D.; Brice, M.; Cotton, F. A. *J. Am. Chem. Soc.* **1973**, *95*, 6954.
(22) Sim, G. A.; Sime, J. G.; Woodhouse, D. I.; Knox, G. R. *Acta Crystallogr., Sect. B* **1979**, *B35*, 2406.
(23) Green, M.; Nyathi, J. Z.; Scott, C.; Stone, F. G. A.; Welch, A. J.; Woodward, P. *J. Chem. Soc., Dalton Trans.* **1978**, 1067.
(24) Davidson, J. L.; Green, M.; Nyathi, J. Z.; Stone, F. G. A.; Welch, A. J. *J. Chem. Soc., Dalton Trans.* **1977**, 2246.
(25) Lam, C. T.; Novotny, M.; Lewis, D. L.; Lippard, S. J. *Inorg. Chem.* **1978**, *17*, 2127.
(26) Lewis, D. L.; Lippard, S. J. *J. Am. Chem. Soc.* **1975**, *97*, 2697.
(27) Cotton, F. A.; Frenz, B. A. *Inorg. Chem.* **1974**, *13*, 253.
(28) Adams, R. D.; Cotton, F. A.; Rusholme, G. A. *J. Coord. Chem.* **1971**, *1*, 275.
(29) Benner, L. S.; Olmstead, M. M.; Balch, A. J. *J. Organomet. Chem.* **1978**, *159*, 289.

urated ligands.[12] Although the $\sigma + \pi$ unit is nearly linear, Mo(2)–C(5)–N = 167.7 (2)°, the C(5)–N–C(31) angle of 135.2 (2)° indicates a change in hybridization at the nitrogen atom away from the linear sp-type normally found for terminally coordinated isocyanide ligands.

Two other compounds in this series which have the $\sigma + \pi$ coordination are $Cp_2Mo_2(CO)_4(NCNMe_2)$[5] and $Et_4N[Cp_2Mo_2(CO)_4CN]$ (V).[7] The former has the nitrile function of the cyanimide ligand σ bonded via the nitrogen atom. In the latter the cyanide ligand is σ bonded via the carbon to one metal atom and π bonded to the other. This molecule was disordered in the crystal, and only crude structural parameters were obtained, but we feel a few useful comparisons can still be made. The π-bonding Mo–C and Mo–N distances in V lie in the range 2.3–2.6 Å and are significantly longer than the corresponding distances in III. One could reasonably infer that the cyanide ligand in V is not as strongly π bonded as the isocyanide in III. This notion is supported by the observation that V is a fluxional molecule which apparently rearranges to an equivalent form in which the σ- and π-bonding modes of the cyanide ligand have been interchanged between the two metal atoms. Intuitively, such a rearrangement would require some degree of metal-ligand bond breaking. Accordingly, we find that the molecules II–IV are not fluxional.

III also contains four terminal carbonyl ligands which could be grouped into pairs. C(1)–O(1) and C(3)–O(3) project toward the adjacent metal atom, Mo(2)–Mo(1)–C(1) = 71.81 (8)° and Mo(2)–Mo(1)–C(2) = 77.50 (8)°, while the other two, C(2)–O(2) and C(4)–O(4), point away from the second metal atom, Mo(2)–Mo(1)–C(2) = 115.15 (8)° and Mo(1)–Mo(2)–C(4) = 109.76 (10)°. We would hesitate to call the former semibridging CO's because the Mo···C distances at approximately 3.2 Å are clearly nonbonding, but the pairing of the environments of the CO ligands might explain the pairing of the resonance shifts of these ligands in the ^{13}C NMR spectra (see above).

Acknowledgment. This research has been supported by the Office of Basic Energy Sciences of the U.S. Department of Energy under Contract No. DE-AC02-78ER04900 and by the Alfred P. Sloan Foundation through a Fellowship to R.D.A. NMR studies were supported by Grant No. CHE-7916210 from the National Science Foundation.

Registry No. I, 56200-27-2; II, 79703-92-7; III, 79703-93-8; IV, 79703-94-9.

Supplementary Material Available: A listing of structure factor amplitudes (13 pages). Ordering information is given on any current masthead page.

Cleavage of Aryl Carbon–Sulfur Bonds by a Trinuclear Cluster. The Reaction of Alkyl Phenyl Sulfides with $Os_3(CO)_{12}$

Richard D. Adams,* Dean A. Katahira, and Li-Wu Yang

Department of Chemistry, Yale University, New Haven, Connecticut 06511

Received June 30, 1981

The reactions of the alkyl phenyl sulfides, RSPh (R = Me, *i*-Pr), with $Os_3(CO)_{12}$ have been shown to produce cleavage of the phenyl group from the sulfur atom and yield the molecules $HOs_3(\mu\text{-}SR)(\mu_3\text{-}\eta^2\text{-}C_6H_4)(CO)_9$ (I, R = Me; II, R = *i*-Pr). I has been analyzed by an X-ray crystallographic analysis: space group $P2_1/n$, at 23 °C, a = 8.697 (2) A, b = 13.442 (5) Å, c = 17.779 (7) Å, β = 99.29 (3)°, V = 2551 (2) Å^3, Z = 4, ρ_{calcd} = 3.07 g/cm^3. For 1999 reflections ($F_o \geq 3.0\sigma(F_o^2)$ R_1 = 0.052 and R_2 = 0.051. I contains an "open" cluster of three osmium atoms with a methanethiolato group bridging the open edge and a triply bridging benzyne, C_6H_4, ligand. In solution I exists as two rapidly equilibrating isomers at room temperature. ^1H DNMR studies have revealed two dynamical processes. A low-energy degenerate process (ΔG^* = 12.7 kcal/mol) which involves a migration of the hydride ligand between the two metal–metal bonds was established through a DNMR study of II. The higher energy isomerization process ($\Delta G^* \cong$ 14.7 kcal/mol) is believed to involve inversions of configuration of the trivalent sulfur atom of the bridging methanethiolato group.

Introduction

A number of workers have shown that triosmium cluster compounds can readily cleave aryl groups from phosphines and other ligands. Frequently, cluster compounds containing benzyne, C_6H_4, ligands are obtained.[1-6] Recently, the cleavage of carbon–sulfur bonds in CS_2 and related ligands by triosmium clusters has been demonstrated,[7] and it occurred to us that such cleavages in alkyl or aryl sulfide molecules might also be possible. Such processes are of fundamental importance to the desulfurization and purification of fossil fuels.[8] Herein we report results of our investigation of the cleavage of carbon–sulfur bonds of alkyl phenyl sulfide molecules by $Os_3(CO)_{12}$. Similar to the reactions with arylphosphines, these reactions also give a number of products. Not all of these have been characterized yet. In this report we will describe the structure and fluxional properties of the family of molecules which

(1) Bradford, C. W.; Gainsford, G. J.; Guss, J. M.; Ireland, P. R.; Mason, R. *J. Chem. Soc., Chem. Commun.* **1972**, 87.
(2) Gainsford, G. J.; Guss, J. M.; Ireland, P. R.; Mason, R.; Bradford, C. W.; Nyholm, R. S. *J. Organomet. Chem.* **1972**, *40*, C70.
(3) Deeming, A. J.; Kimber, R. E.; Underhill, M. *J. Chem. Soc., Dalton Trans.* **1973**, 2589.
(4) Brown, S. C.; Evan, J.; Smart, L. E. *J. Chem. Soc., Chem. Commun.* **1980**, 1021.
(5) Bradford, C. W.; Nyholm, R. S. *J. Chem. Soc., Dalton Trans.* **1973**, 529.
(6) Adams, R. D.; Golembeski, N. M. *J. Organomet. Chem.* **1979**, *172*, 239
(7) Adams, R. D.; Golembeski, N. M.; Selegue, J. P. *J. Am. Chem. Soc.* **1981**, *103*, 546.
(8) Schuman, S. C.; Shalit, H. *Catal. Rev.* **1970**, *4*, 245.

0276-7333/82/2301-0235$01.25/0

urated ligands.[12] Although the $\sigma + \pi$ unit is nearly linear, Mo(2)–C(5)–N = 167.7 (2)°, the C(5)–N–C(31) angle of 135.2 (2)° indicates a change in hybridization at the nitrogen atom away from the linear sp-type normally found for terminally coordinated isocyanide ligands.

Two other compounds in this series which have the $\sigma + \pi$ coordination are $Cp_2Mo_2(CO)_4(NCNMe_2)$[5] and $Et_4N[Cp_2Mo_2(CO)_4CN]$ (V).[7] The former has the nitrile function of the cyanimide ligand σ bonded via the nitrogen atom. In the latter the cyanide ligand is σ bonded via the carbon to one metal atom and π bonded to the other. This molecule was disordered in the crystal, and only crude structural parameters were obtained, but we feel a few useful comparisons can still be made. The π-bonding Mo–C and Mo–N distances in V lie in the range 2.3–2.6 Å and are significantly longer than the corresponding distances in III. One could reasonably infer that the cyanide ligand in V is not as strongly π bonded as the isocyanide in III. This notion is supported by the observation that V is a fluxional molecule which apparently rearranges to an equivalent form in which the σ- and π-bonding modes of the cyanide ligand have been interchanged between the two metal atoms. Intuitively, such a rearrangement would require some degree of metal-ligand bond breaking. Accordingly, we find that the molecules II–IV are not fluxional.

III also contains four terminal carbonyl ligands which could be grouped into pairs. C(1)–O(1) and C(3)–O(3) project toward the adjacent metal atom, Mo(2)–Mo(1)–C(1) = 71.81 (8)° and Mo(2)–Mo(1)–C(2) = 77.50 (8)°, while the other two, C(2)–O(2) and C(4)–O(4), point away from the second metal atom, Mo(2)–Mo(1)–C(2) = 115.15 (8)° and Mo(1)–Mo(2)–C(4) = 109.76 (10)°. We would hesitate to call the former semibridging CO's because the Mo···C distances at approximately 3.2 Å are clearly nonbonding, but the pairing of the environments of the CO ligands might explain the pairing of the resonance shifts of these ligands in the ^{13}C NMR spectra (see above).

Acknowledgment. This research has been supported by the Office of Basic Energy Sciences of the U.S. Department of Energy under Contract No. DE-AC02-78ER04900 and by the Alfred P. Sloan Foundation through a Fellowship to R.D.A. NMR studies were supported by Grant No. CHE-7916210 from the National Science Foundation.

Registry No. I, 56200-27-2; II, 79703-92-7; III, 79703-93-8; IV, 79703-94-9.

Supplementary Material Available: A listing of structure factor amplitudes (13 pages). Ordering information is given on any current masthead page.

Cleavage of Aryl Carbon–Sulfur Bonds by a Trinuclear Cluster. The Reaction of Alkyl Phenyl Sulfides with $Os_3(CO)_{12}$

Richard D. Adams,* Dean A. Katahira, and Li-Wu Yang

Department of Chemistry, Yale University, New Haven, Connecticut 06511

Received June 30, 1981

The reactions of the alkyl phenyl sulfides, RSPh (R = Me, *i*-Pr), with $Os_3(CO)_{12}$ have been shown to produce cleavage of the phenyl group from the sulfur atom and yield the molecules $HOs_3(\mu\text{-}SR)(\mu_3\text{-}\eta^2\text{-}C_6H_4)(CO)_9$ (I, R = Me; II, R = *i*-Pr). I has been analyzed by an X-ray crystallographic analysis: space group $P2_1/n$, at 23 °C, a = 8.697 (2) A, b = 13.442 (5) Å, c = 17.779 (7) Å, β = 99.29 (3)°, V = 2551 (2) Å^3, Z = 4, ρ_{calcd} = 3.07 g/cm^3. For 1999 reflections ($F_o \geq 3.0\sigma(F_o^2)$ R_1 = 0.052 and R_2 = 0.051. I contains an "open" cluster of three osmium atoms with a methanethiolato group bridging the open edge and a triply bridging benzyne, C_6H_4, ligand. In solution I exists as two rapidly equilibrating isomers at room temperature. ^1H DNMR studies have revealed two dynamical processes. A low-energy degenerate process (ΔG^* = 12.7 kcal/mol) which involves a migration of the hydride ligand between the two metal–metal bonds was established through a DNMR study of II. The higher energy isomerization process ($\Delta G^* \cong$ 14.7 kcal/mol) is believed to involve inversions of configuration of the trivalent sulfur atom of the bridging methanethiolato group.

Introduction

A number of workers have shown that triosmium cluster compounds can readily cleave aryl groups from phosphines and other ligands. Frequently, cluster compounds containing benzyne, C_6H_4, ligands are obtained.[1-6] Recently, the cleavage of carbon–sulfur bonds in CS_2 and related ligands by triosmium clusters has been demonstrated,[7] and it occurred to us that such cleavages in alkyl or aryl sulfide molecules might also be possible. Such processes are of fundamental importance to the desulfurization and purification of fossil fuels.[8] Herein we report results of our investigation of the cleavage of carbon–sulfur bonds of alkyl phenyl sulfide molecules by $Os_3(CO)_{12}$. Similar to the reactions with arylphosphines, these reactions also give a number of products. Not all of these have been characterized yet. In this report we will describe the structure and fluxional properties of the family of molecules which

(1) Bradford, C. W.; Gainsford, G. J.; Guss, J. M.; Ireland, P. R.; Mason, R. *J. Chem. Soc., Chem. Commun.* **1972**, 87.
(2) Gainsford, G. J.; Guss, J. M.; Ireland, P. R.; Mason, R.; Bradford, C. W.; Nyholm, R. S. *J. Organomet. Chem.* **1972**, *40*, C70.
(3) Deeming, A. J.; Kimber, R. E.; Underhill, M. *J. Chem. Soc., Dalton Trans.* **1973**, 2589.
(4) Brown, S. C.; Evan, J.; Smart, L. E. *J. Chem. Soc., Chem. Commun.* **1980**, 1021.
(5) Bradford, C. W.; Nyholm, R. S. *J. Chem. Soc., Dalton Trans.* **1973**, 529.
(6) Adams, R. D.; Golembeski, N. M. *J. Organomet. Chem.* **1979**, *172*, 239
(7) Adams, R. D.; Golembeski, N. M.; Selegue, J. P. *J. Am. Chem. Soc.* **1981**, *103*, 546.
(8) Schuman, S. C.; Shalit, H. *Catal. Rev.* **1970**, *4*, 245.

0276-7333/82/2301-0235$01.25/0

have the formula $HOs_3(\mu\text{-SR})(\mu_3\text{-}\eta^2\text{-}C_6H_4)(CO)_9$.

Experimental Section

General Comments. Although these compounds were air stable, the reactions were routinely performed under a prepurified nitrogen atomosphere. Nonane solvent was purified by stirring for 2 days over concentrated sulfuric acid and then allowing to stand overnight over anhydrous sodium carbonate. Hexane solvent was purified by distillation from sodium–benzophenone. Other solvents were stored over 4-Å molecular sieves and degassed with a dispersed stream of nitrogen gas. Osmium carbonyl was prepared from OsO_4.[9] Both phenyl methyl and phenyl isopropyl sulfides were obtained from commercial sources and were used without further purification.

Melting points were determined in evacuated capillary tubes using a Thomas-Hoover apparatus and are uncorrected. Infrared spectra were recorded on a Perkin-Elmer 237B spectrophotometer. Fourier transform ^1H NMR spectra were obtained at 270 MHz on a Bruker HX 270.

Preparation of $HOs_3(\mu\text{-SMe})(\mu_3\text{-}\eta^2\text{-}C_6H_4)(CO)_9$ (I). Phenyl methyl sulfide (0.15 mL, 1.28 mmol) was added to $Os_3(CO)_{12}$ (200 mg, 0.221 mmol) in nonane (70 mL). The reaction was maintained at reflux for 20 h. The solvent was removed in vacuo, and the remaining red-brown residue was taken up in a minimal amount of methylene chloride and applied to thin-layer silica plates. Elution with methylene chloride/hexane (10%/90%, v/v) yielded several bands. The product was the third of these. It is yellow in color and follows a red band. It crystallizes from hexane at −20 °C to yield 5.0 mg (2.4%) of yellow crystals, mp 172–174 °C; ^1H NMR (in $CDCl_3$): at 298 K, δ 8.70 (br, C_6H_4), 7.37 (br, C_6H_4), 2.88 (br, Me), −15.95 (OsH); at 213 K, major isomer, δ 8.93 (d, ^3J = 8.5 Hz C_6H_4), 8.48 (d, ^3J = 8.5 Hz C_6H_4), 7.11 (dd, ^3J = 8.5 Hz $^3J'$ = 6.1 Hz, C_6H_4), 6.86 (dd, ^3J = 8.5 Hz, $^3J'$ = 6.1 Hz, C_6H_4), 2.22 (CH_3), −15.97 (OsH); minor isomer, δ 8.89 (d, ^3J = 8.3 Hz, C_6H_4), 8.42 (d, ^3J = 8.3 Hz, C_6H_4), 7.34 (m, C_6H_4), 7.21 (m, C_6H_4), 2.90 (CH_3), −15.67 (OsH). IR (in hexane, $\nu_{CO} \pm 5$ cm^{-1}): 2100 (m), 2076 (vs), 2048 (vs), 2024 (s), 2008 (s), 2001 (s), 1982 (m), 1964 (m) cm^{-1}.

$HOs_3(\mu\text{-S-}i\text{-Pr})(\mu_3\text{-}\eta^2\text{-}C_6H_4)(CO)_9$ (II) was prepared and isolated similarly: yield, 5%; mp 142–143 °C. ^1H NMR (in $CDCl)_3$: at 298 K, δ 8.69 (m, C_6H_4), 6.96 (m, C_6H_4), 2.43 (sept, ^3J = 6.7 Hz, C_3H_7), 0.90 (d, ^3J = 6.7 Hz, C_3H_7), −16.05 (OsH). At 213 K, δ 8.90 (d, ^3J = 7.9 Hz, C_6H_4), 8.47 (d, ^3J = 7.9 Hz, C_6H_4), 7.08 (dd, ^3J = 7.9 Hz, ^3J = 5.9 Hz, C_6H_4), 6.83 (dd, ^3J = 7.9 Hz, J' = 5.9 Hz, C_6H_4), 2.33 (m, C_3H_7), 0.90 (d, ^3J = 6.3 Hz, C_3H_7), 0.70 (d, ^3J = 6.2 Hz, C_3H_7), −16.22 (OsH). IR (in hexane, ν_{CO}: 2105 (s), 2080 (vs), 2055 (vs), 2030 (vs), 2017 (vs), 2010 (vs), 1990 (s), 1985 (m), 1970 (s) cm^{-1}.

Crystallographic Analysis. Crystals of $HOs_3(\mu\text{-SMe})(\mu_3\text{-}\eta^2\text{-}C_6H_4)(CO)_9$ suitable for diffraction measurements were obtained as described above and were mounted in thin-walled glass capillaries. Diffraction measurements were made on an Enraf-Nonius CAD-4 fully automated four-circle diffractometer using graphite-monochromatized Mo K$\bar{\alpha}$ radiation. The unit cell was refined from 25 selected reflections ($2\theta > 31°$) by using the CAD-4 automatic center and least-squares routines. The space group $P2_1/n$ was determined from the systematic absences observed during data collection. Crystal data and data collection parameters are listed in Table I. All data processing was performed on a Digital PDP 11/45 computer using the Enraf-Nonius SDP program library. An absorption correction of a Gaussian integration type was applied to all the data. Neutral atom scattering factors were calculated by the standard procedures.[10a] Anomalous dispersion corrections were applied for all nonhydrogen atoms.[10b] The structure was solved by a combination of Patterson and difference Fourier techniques. Hydrogen atom positions for the benzyne ligand were calculated by assuming idealized sixfold symmetry and C–H distances of 0.95 Å. These hydrogen atom contributions were included in structure factor calculations, but their positions were not refined. Hydrogen atom positions for the methyl group were not observed and were ignored. Full-matrix least-squares refinements minimized the function $\sum_{hkl} w(|F_o| - |F_c|)^2$, where $w = 1/\sigma(F)^2$, $\sigma(F) = \sigma(F_o^2)/2F_o$ and $\sigma(F_o^2) = [\sigma(I_{raw})^2 + (PF_o^2)^2]^{1/2}/Lp$. All atoms heavier than oxygen were refined with anisotropic temperature factors. All other atoms were refined with isotropic temperature factors only. Final fractional atomic coordinates, thermal parameters, and interatomic distances and angles with errors obtained from the inverse matrix calculated on the final cycle of least-squares refinement are listed in Tables II–IV. Structure factor amplitudes are available (see supplementary material).

Table I. Crystallographic Data for X-ray Diffraction Study of $HOs_3(\mu\text{-SMe})(\mu_3\text{-}\eta^2\text{-}C_6H_4)(CO)_9$

(A) Crystal Data	
formula	$Os_3SO_9C_{16}H_8$
temp, ±5 °C	23
space group	$P2_1/n$
a, Å	8.697 (2)
b, Å	13.442 (5)
c, Å	17.779 (7)
β, deg	99.29 (3)
V, Å^3	2551 (2)
mol wt	946.9
ρ_{calcd}, g/cm^3	3.07
(B) Measurement of Intensity Data	
radiation	Mo K$\bar{\alpha}$ (0.710 73 Å)
monochromator	graphite
detector aperture, mm	
horizontal ($A + B \tan \theta$)	
A	3.0
B	1.0
vertical	4.0
cryst faces	$0\bar{2}1$, $02\bar{1}$, 001; $00\bar{1}$, $11\bar{1}$, $\bar{1}11$
cryst size, nm	0.16 × 0.15 × 0.09
cryst orientation:	
direction; deg from ϕ axis	normal to 120; 10.8
reflctns measd	$h, k, \pm l$
max 2θ	50°
scan type	moving crystal–stationary counter
ω-scan width, deg	
A + 0.347 tan θ	A = 0.85°
bakgd	one-fourth additional scan at each end of scan
ω-scan rate (variable)	
max, deg/min	6.7°
min, deg/min	1.2°
no of reflctns measd	3934
data used ($F^2 \geq 3.0\sigma(F)^2$)	1999
(C) Treatment of Data	
abs correctn coeff, cm^{-1}	198.6
grid	12 × 10 × 8
transmissn coeff	
max	0.26
min	0.07
P factor	0.01
final residuals R	0.052
R_w	0.051
esd of unit wt	2.57
largest shift/error value on final cycle	0.02

Results

The reactions of alkyl phenyl sulfides, RSPh (R = Me, i-Pr) with $Os_3(CO)_{12}$ in refluxing nonane solvent give low yields (<5%) of the molecules $HOs_3(\mu\text{-SR})(\mu_3\text{-}\eta^2\text{-}C_6H_4)(CO)_9$ (I, R = Me; II, R = i-Pr) which have been characterized by IR and ^1H DNMR spectroscopies and an X-ray crystallographic analysis of I.

Description of the Structure. The molecular structure of I is shown in Figure 1. The molecule contains an "open" cluster of three osmium atoms with a bridging

(9) Johnson, B. F. G.; Lewis, J.; Kilty, P. A. *J. Chem. Soc. A* **1968**, 2859.

(10) "International Tables for X-ray Crystallography"; Kynoch Press: Birmingham, England, 1975; Vol. IV, (a) Table 2.2B, pp 99–101; (b) Table 2.3.1, pp 149–50.

Table II. Final Fractional Atomic Coordinates, Thermal Parameters, and Their Estimated Standard Deviations for $HOs_3(\mu\text{-SMe})(\mu_3\text{-}\eta^2\text{-}C_6H_4)(CO)_9$

atom	x	y	z	B_{11} [b]	B_{22}	B_{33}	B_{12}	B_{13}	B_{23}
Os(1)	0.3215 (1)	0.19720 (8)	0.05626 (5)	2.80 (4)	2.72 (5)	2.13 (3)	0.00 (5)	0.32 (3)	−0.17 (4)
Os(2)	0.5894 (1)	0.20806 (8)	0.17004 (5)	2.47 (4)	2.42 (4)	2.37 (4)	0.42 (5)	0.47 (3)	0.19 (4)
Os(3)	0.3969 (1)	0.35375 (8)	0.23576 (6)	2.68 (4)	2.57 (4)	2.36 (4)	0.13 (5)	0.59 (3)	−0.29 (4)
S(1)	0.1870 (8)	0.2746 (6)	0.1510 (4)	3.2 (3)	4.1 (4)	3.0 (3)	0.1 (3)	0.0 (3)	−0.6 (3)

atom	x	y	z	B, Å²	atom	x	y	z	B, Å²
O(1)	0.506 (2)	0.091 (2)	−0.053 (1)	5.1 (5)	C(7)	0.313 (3)	0.482 (2)	0.222 (1)	3.4 (6)
O(2)	0.141 (2)	0.006 (2)	0.082 (1)	5.6 (5)	C(8)	0.562 (3)	0.406 (2)	0.306 (1)	3.3 (6)
O(3)	0.094 (2)	0.283 (1)	−0.076 (1)	4.8 (4)	C(9)	0.282 (3)	0.316 (2)	0.317 (1)	3.5 (6)
O(4)	0.815 (2)	0.148 (2)	0.062 (1)	5.4 (5)	C(10)	0.065 (4)	0.380 (2)	0.101 (2)	4.9 (7)
O(5)	0.518 (2)	−0.008 (1)	0.210 (1)	5.0 (5)	C(11)	0.478 (3)	0.317 (2)	0.071 (1)	2.9 (5)
O(6)	0.867 (3)	0.241 (2)	0.296 (1)	6.6 (6)	C(12)	0.521 (3)	0.374 (2)	0.139 (1)	2.5 (5)
O(7)	0.266 (2)	0.564 (2)	0.210 (1)	6.0 (5)	C(13)	0.632 (3)	0.453 (2)	0.145 (1)	3.0 (5)
O(8)	0.669 (2)	0.437 (1)	0.347 (1)	4.9 (4)	C(14)	0.700 (3)	0.481 (2)	0.083 (1)	3.8 (6)
O(9)	0.224 (2)	0.286 (2)	0.366 (1)	5.5 (5)	C(15)	0.672 (3)	0.424 (2)	0.015 (2)	4.6 (7)
C(1)	0.435 (3)	0.128 (2)	−0.012 (1)	3.4 (6)	C(16)	0.567 (3)	0.349 (2)	0.009 (1)	3.2 (5)
C(2)	0.202 (3)	0.075 (2)	0.073 (1)	3.7 (6)	H(13)[a]	0.6617	0.4878	0.1928	5.0
C(3)	0.183 (3)	0.247 (2)	−0.027 (1)	2.8 (5)	H(14)[a]	0.7684	0.5389	0.0853	5.0
C(4)	0.723 (3)	0.167 (2)	0.104 (1)	3.7 (6)	H(15)[a]	0.7269	0.4400	−0.0274	5.0
C(5)	0.543 (3)	0.074 (2)	0.194 (1)	3.2 (6)	H(16)[a]	0.5473	0.3137	−0.0395	5.0
C(6)	0.761 (4)	0.232 (2)	0.249 (2)	4.3 (6)					

[a] Hydrogen atom positions were calculated and not refined. [b] The form of the general temperature factor expression is $\exp[-1/4(B_{11}h^2a^{*2} + B_{22}k^2b^{*2} + B_{33}l^2c^{*2} + B_{12}hka^*b^* + B_{13}hla^*c^* + B_{23}klb^*c^*)]$.

Table III. Interatomic Distances with Esds for $HOs_3(\mu\text{-SMe})(\mu_3\text{-}\eta^2\text{-}C_6H_4)(CO)_9$

atoms	dist, Å	atoms	dist, Å
Os(1)-Os(2)	2.833 (1)	S(1)-C(10)	1.90 (2)
Os(2)-Os(3)	2.939 (1)	C(11)-C(12)	1.42 (2)
Os(1)···Os(3)	3.791 (1)	C(12)-C(13)	1.43 (2)
Os(1)-S(1)	2.433 (5)	C(13)-C(14)	1.39 (2)
Os(1)-C(1)	1.92 (2)	C(14)-C(15)	1.42 (2)
Os(1)-C(2)	1.99 (2)	C(15)-C(16)	1.35 (2)
Os(1)-C(3)	1.87 (2)	C(16)-C(11)	1.52 (2)
Os(1)-C(11)	2.10 (2)	C(1)-O(1)	1.14 (2)
Os(2)-C(4)	1.86 (2)	C(2)-O(2)	1.09 (2)
Os(2)-C(5)	1.91 (2)	C(3)-O(3)	1.18 (2)
Os(2)-C(6)	1.90 (2)	C(4)-O(4)	1.21 (2)
Os(2)-C(11)	2.37 (2)	C(5)-O(5)	1.18 (2)
Os(2)-C(12)	2.35 (2)	C(6)-O(6)	1.15 (2)
Os(3)-S(1)	2.418 (4)	C(7)-O(7)	1.18 (2)
Os(3)-C(7)	1.87 (2)	C(8)-O(8)	1.14 (2)
Os(3)-C(8)	1.87 (2)	C(9)-O(9)	1.17 (2)
Os(3)-C(9)	1.95 (2)		
Os(3)-C(12)	2.19 (2)	av C-O	1.16 (3)

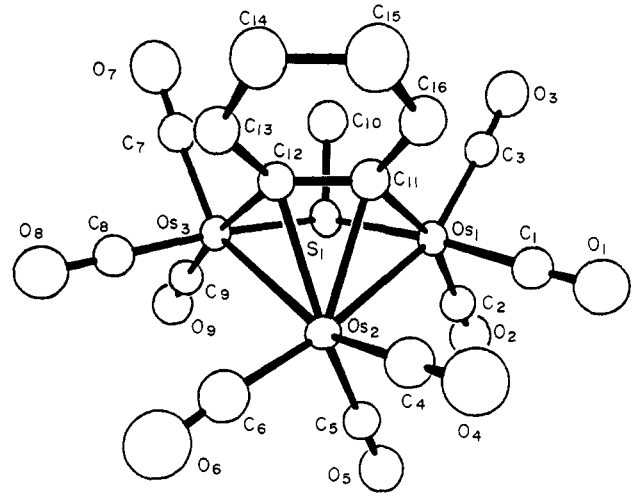

Figure 1. A perspective ORTEP drawing of $HOs_3(\mu\text{-SMe})(\mu_3\text{-}\eta^2\text{-}C_6H_4)(CO)_9$ showing 50% electron density probability ellipsoids.

methanethiolato group, a triply bridging benzyne ligand, C_6H_4, and a bridging hydride ligand. The Os(2)–Os(3) distance at 2.939 (1) Å is 0.106 Å longer than the Os(1)–Os(3) distance of 2.833 (1) Å. Although both distances are similar to those observed in $Os_3(CO)_{12}$ (i.e., 2.877 (3) Å),[11] the elongation of the one bond is significant and is a feature which is characteristic of the presence of bridging hydride ligands.[12] Spectroscopic measurements confirm the presence of a bridging hydride ligand in these molecules (vide infra) and accordingly, we conclude that the bridging hydride ligand straddles the Os(2)–Os(3) bond although this was not confirmed by "direct" observation in the crystallographic analysis. The Os(1)···Os(3) distance at 3.791 (1) Å is clearly too large to allow any significant direct metal–metal bonding.

The "open" edge of the cluster contains the bridging methanethiolato group which serves formally as a three-electron donor. Being tricoordinate and also containing a lone pair of electrons, the sulfur atom has a pyramidal structure, and as expected, the Os(1)–S–Os(3), Os(1)–S–C(10), and Os(3)–S–C(10) angles of 102.8 (2), 106.6 (6), and 105.9 (6)°, respectively, are approximately tetrahedral.

A triply bridging benzyne ligand, C_6H_4, is coordinated to one face of the cluster. Atom C(11) is asymmetrically bonded to Os(1) and Os(2), Os(1)–C(11) = 2.10 (2) Å and Os(2)–C(11) = 2.37 (2) Å, and atom C(12) is asymmetrically bonded to Os(3) and Os(2), Os(3)–C(12) = 2.19 (2) Å and Os(2)–C(12) = 2.35 (2) Å, although the asymmetry for C(12) is not as large as for C(11). The benzyne ligand serves formally as a four-electron donor, and the bonding can be viewed as σ bonds to Os(1) and Os(3) and a π-donor bond to Os(2). There does not appear to be any systematic pattern of long and short C–C bond alternations within the benzyne ring. The ring is planar and is inclined at an angle of 71.5° from the Os_3 plane. Similar incline angles have been found in other triosmium cluster compounds containing benzyne ligands.[1,2,4]

There are nine linear terminal carbonyl ligands. The average C–O bond distance is 1.16 (3) Å. The osmium–carbon distances which are trans to osmium–benzyne σ

(11) Churchill, M. R.; DeBoer, B. G. *Inorg. Chem.* **1977**, *16*, 878.
(12) (a) Churchill, M. R.; DeBoer, B. G.; Rotella, F. J. *Inorg. Chem.* **1976**, *15*, 1843. (b) Teller, R. G.; Bau, R. *Struct. Bonding (Berlin)* **1981**, *44*, 1.

Table IV. Interatomic Angles with Esds for $HOs_3(\mu\text{-SMe})(\mu_3\text{-}\eta^2\text{-}C_6H_4)(CO)_9$

atoms	angles, deg	atoms	angles, deg	atoms	angles, deg
Os(1)-Os(2)-Os(3)	82.09 (3)	C(4)-Os(2)-C(6)	90.8 (8)	Os(3)-S(1)-C(10)	105.9 (6)
Os(2)-Os(1)-S(1)	85.2 (1)	C(4)-Os(2)-C(11)	86.7 (6)	Os(1)-C(11)-Os(2)	78.4 (5)
Os(2)-Os(1)-C(1)	91.6 (5)	C(4)-Os(2)-C(12)	107.2 (7)	Os(1)-C(11)-C(12)	127 (1)
Os(2)-Os(1)-C(2)	109.0 (5)	C(5)-Os(2)-C(6)	99.5 (7)	Os(1)-C(11)-C(16)	121 (1)
Os(2)-Os(1)-C(3)	153.6 (5)	C(5)-Os(2)-C(11)	132.3 (6)	Os(2)-C(11)-C(12)	71.5 (8)
Os(2)-Os(1)-C(11)	55.1 (4)	C(5)-Os(2)-C(12)	153.3 (6)	Os(2)-C(11)-C(16)	121 (1)
S(1)-Os(1)-C(1)	175.2 (5)	C(6)-Os(2)-C(11)	128.1 (7)	Os(2)-C(12)-Os(3)	80.6 (5)
S(1)-Os(1)-C(2)	86.0 (5)	C(6)-Os(2)-C(12)	98.6 (7)	Os(2)-C(12)-C(11)	73.4 (9)
S(1)-Os(1)-C(3)	94.2 (5)	C(11)-Os(2)-C(12)	35.1 (5)	Os(2)-C(12)-C(13)	123 (1)
S(1)-Os(1)-C(11)	87.6 (5)	Os(2)-Os(3)-S(1)	83.1 (1)	Os(3)-C(12)-C(11)	120 (1)
C(1)-Os(1)-C(2)	91.7 (7)	Os(2)-Os(3)-C(7)	142.9 (5)	Os(3)-C(12)-C(13)	117 (1)
C(1)-Os(1)-C(3)	90.3 (7)	Os(2)-Os(3)-C(8)	95.1 (5)	C(11)-C(12)-C(13)	123 (1)
C(1)-Os(1)-C(11)	93.6 (7)	Os(2)-Os(3)-C(9)	120.9 (5)	C(12)-C(13)-C(14)	121 (1)
C(2)-Os(1)-C(3)	97.2 (7)	Os(2)-Os(3)-C(12)	52.0 (4)	C(13)-C(14)-C(15)	119 (2)
C(2)-Os(1)-C(11)	163.4 (6)	S(1)-Os(3)-C(7)	94.9 (5)	C(14)-C(15)-C(16)	119 (2)
C(3)-Os(1)-C(11)	98.6 (6)	S(1)-Os(3)-C(8)	175.6 (5)	C(15)-C(16)-C(11)	125 (2)
Os(1)-Os(2)-C(4)	93.6 (5)	S(1)-Os(3)-C(9)	85.5 (5)	C(16)-C(11)-C(12)	112 (1)
Os(1)-Os(2)-C(5)	86.2 (5)	S(1)-Os(3)-C(12)	89.0 (4)	Os(1)-C(1)-O(1)	177 (2)
Os(1)-Os(2)-C(11)	46.5 (4)	C(7)-Os(3)-C(8)	89.0 (7)	Os(1)-C(2)-O(2)	177 (2)
Os(1)-Os(2)-C(12)	74.5 (4)	C(7)-Os(3)-C(9)	95.7 (8)	Os(1)-C(3)-O(3)	176 (2)
Os(3)-Os(2)-C(4)	154.5 (6)	C(7)-Os(3)-C(12)	91.1 (7)	Os(2)-C(4)-O(4)	174 (2)
Os(3)-Os(2)-C(5)	112.6 (5)	C(8)-Os(3)-C(9)	92.0 (7)	Os(2)-C(5)-O(5)	178 (1)
Os(3)-Os(2)-C(6)	91.5 (6)	C(8)-Os(3)-C(12)	93.1 (7)	Os(2)-C(6)-O(6)	176 (2)
Os(3)-Os(2)-C(11)	72.0 (4)	C(9)-Os(3)-C(12)	171.6 (7)	Os(3)-C(7)-O(7)	176 (2)
Os(3)-Os(2)-C(12)	47.4 (4)	Os(1)-S(1)-Os(3)	102.8 (2)	Os(3)-C(8)-O(8)	173 (2)
C(4)-Os(2)-C(5)	92.1 (8)	Os(1)-S(1)-C(10)	106.6 (6)	Os(3)-C(9)-O(9)	177 (2)

bonds (i.e., C(2)–O(2) and C(9)–O(9)) are noticeably longer than others (see Table III). The shortest intermolecular contact was between the carbonyl oxygen atoms O(1) and O(5) at 3.00 (2) Å.

Dynamical Behavior and Solution Structures of I and II. At −60 °C of the ^1H NMR spectrum of I shows two resonances δ −15.67 and −15.97 of unequal intensity (ratio 1:5) which can be assigned to bridging hydride ligands. There are two methyl resonances with the same ratio of intensities for the bridging methanethiolato group. On this basis we conclude that I exists in solution as two inequivalent isomers one of which is probably the same isomer A as found in the solid state (see Scheme I).

We have not been able to establish unambiguously the structure of the second isomer in solution, but we consider structures B and C to be likely candidates, and on the basis of an analysis of the dynamical behavior we believe B is more probable than C. B differs from A only by an inversion of configuration at the pyramidal sulfur atom. C differs from A in the orientation of the benzyne ligand. In A, the benzyne ligand bridges the nonbonded osmium atoms via its osmium–carbon σ bonds. In C it bridges a pair of bonded osmium atoms. Interestingly, the molecule $Os_3(\mu_3\text{-PEt})(\mu_3\text{-}C_6H_4)(CO)_9$ was recently shown to have its benzyne ligand coordinated in a manner analogous to that in C.[4]

There are prominent doublets at 8.98 and 8.48 ppm of equal intensity and two apparent triplets (actually doublets of doublets) of equal intensity at 7.11 and 6.86 ppm. Low intensity doublets were observed near the prominent ones, but the expected low intensity triplets of the minor isomer were not clearly resolved. In A the protons of the benzyne ligand should appear in an ABCD pattern. The prominent doublets can be assigned to the A and D protons where the AC, AD, and BD couplings are approximately zero and the AB and CD couplings are equal (8.5 Hz), and the triplets can be assigned to the B and C protons where AC and BD couplings are zero, and the AB and CD couplings are 8.5 Hz, and the BC coupling is 6.1 Hz.

When the temperature is raised, the resonances of the benzyne ligand in both isomers broaden, coalesce, and average, doublets with doublets and triplets with triplets, $\Delta G_{228\,K}^* = 12.7$ kcal/mol[13] (coalescence temperature is approximately −10 °C)), but at −10 °C, the methyl and hydride resonances have not changed and remain sharp. As the temperature is raised still further, these resonances begin to broaden (hydrides and methyls to approximately the same extent), coalesce (30 °C, methyls; 20 °C, hydrides), and reform as singlets: $\Delta G_{263\,K}^* = 14.7$ kcal/mol (minor isomer to major isomer) and $\Delta G_{273\,K}^* = 15.3$ kcal/mol[13] (major isomer to minor isomer). Clearly two processes are operative. The lowest energy process, (1), produces a plane of symmetry in the benzyne ligand of both isomers. For the low-energy process the two most plausible mechanisms are as follows: (1a), a 180° rotation of benzyne ligand (this process has been observed in other triosmium clusters containing triply bridging benzyne ligands);[3,4] or (1b), an exchange of the hydride ligand between the metal–metal bonds (see Scheme I). Evidence which distinquishes between these mechanisms was obtained from a ^1H DNMR analysis of II. At −60 °C the ^1H NMR spectrum of II is consistent with the presence of only one isomer. The resonances of the benzyne ligand are similar to those in I. As expected for a structure of the type A, the isopropyl methyl groups are diastereotopic and appear as two doublets. As the temperature is raised, the resonances of the benzyne ligand are averaged in a manner analogous to those in I, but most importantly the isopropyl methyl doublets are also averaged at the same rate: $\Delta G_{223\,K}^* = 12.4$ kcal/mol.[13,15] This latter observation rules out mechanism (1a) and implies (1b).

Since the resonances of the benzyne ligand in the minor isomer of I are averaged similarly to those of the major isomer, we believe their structures must be similar too. As a result we prefer the structure B for the minor isomer since hydride shifts will produce a pairwise averaging of

(13) ΔG^* was estimated at the temperature where the limiting spectrum at slow exchange was just attained.[14]

(14) Faller, J. W., In "Transition Metal Olefin and Acetylene Complexes"; Bennett, M. A., Ed.; Wiley: New York, in press.

(15) We observed that the collapse of the two isopropyl methyl doublets is noticeably asymmetric near coalescence. We believe this could be caused by small amounts of a minor isomer (not significantly populated in the slow exchange region) which averages with the major isomer.

Scheme I

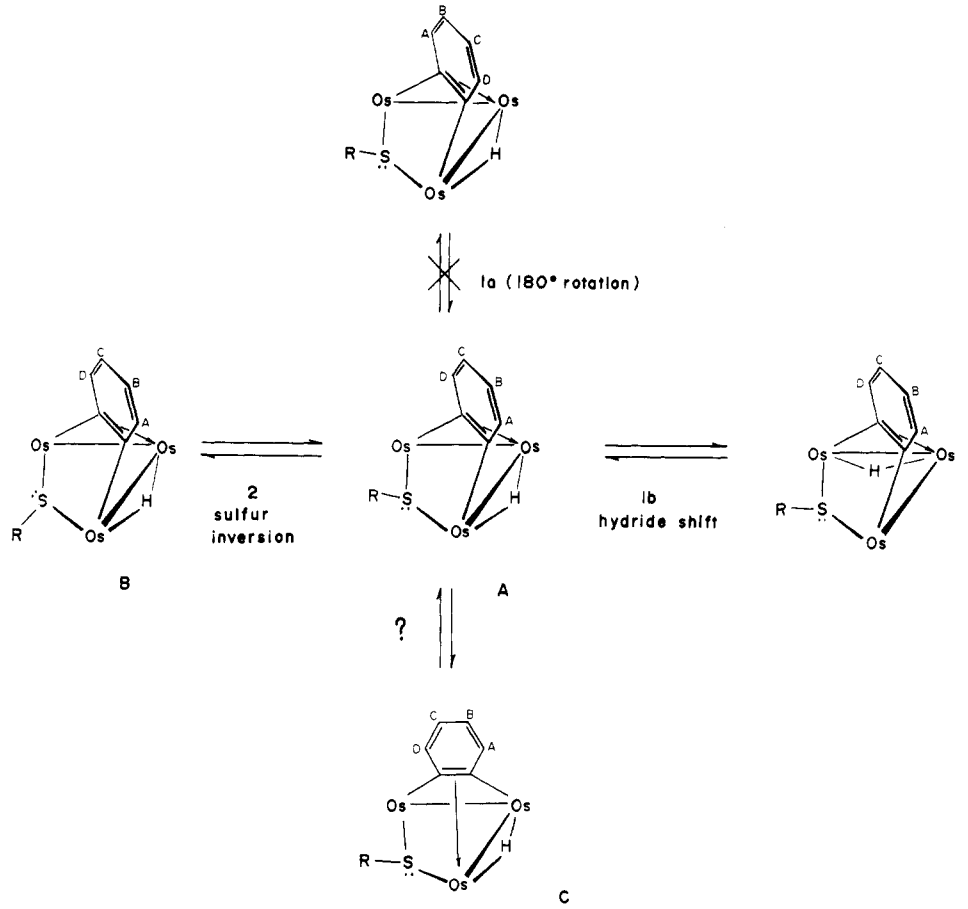

the resonances of the benzyne ligand. This would not occur in C. It is conceivable that the benzyne ligand resonances of an isomer like C could be averaged by 180° rotations,[3,4] but it is difficult to imagine a mechanism that would not involve A as an intermediate, and the spectra show that such isomerization does not occur in this temperature range.

The higher energy process interconverts the two isomers of I. If A and B are the correct structures, the isomerization involves only the inversion of configuration of the sulfur atom. While such inversions at trivalent sulfur are generally of fairly high energy when the three substituents are alkyl groups,[16] it has been shown that barrier can be reduced considerably when one of the substituents is a metal atom.[17]

In 1973 Deeming reported the preparation and dynamical behavior of the complexes $HOs_3(EMe_2)(C_6H_4)(CO)_9$ (E = P or As) and $HOs_3(PMe_2)(C_6H_4)(CO)_8PMe_2Ph$.[3] Structurally, he assumed that the triosmium clusters contained three metal–metal bonds. Thus, in order to maintain satisfactory electron configurations, he proposed that the benzyne ligand served as a two-electron donor. Although the benzyne ligand can serve as a two-electron donor in trosmium clusters,[6] in view of our present results, we propose to reformulate Deeming's complexes as "open" clusters containing benzyne ligands serving as four-electron donors.[18] The dynamical activity in his molecules showed a pairwise averaging of the benzyne ligand resonances which could also be explained by hydride shifts. The observation of phosphorus coupling to the hydride ligand in the fast exchange region[3] indicates that the hydride shift occurs by an intramolecular process in these molecules.

In summary, we found that triosmium clusters can readily cleave aryl groups from alkyl aryl sulfide molecules. We have characterized a new class of triosmium cluster which contains a triply bridging benzyne ligand serving as a four-electron donor. These molecules are dynamically active via two processes. A lower energy process involves rapid shifts of the hydride ligand between the metal–metal bonds, and a higher energy process appears to involve inversion of configuration of the sulfur atom of the bridging methanethiolato ligands.

Acknowledgment. This work was supported by the National Science Foundation through Grant No. CHE-8019041 and the Alfred P. Sloan Foundation through a fellowship to R.D.A. NMR studies were supported by Grant No. CHE-7916210 from the National Science Foundation. We wish to thank Engelhard Industries for a loan of osmium tetroxide, Dr. B. F. B. Johnson for converting it into $Os_3(CO)_{12}$ for us, and Dr. Zain Dawoodi for helpful discussions.

Registry No. I, 79435-97-5; II, 79435-98-6; $Os_3(CO)_{12}$, 15696-40-9; MeSPh, 100-68-5; *i*-PrSPh, 3019-20-3.

Supplementary Material Available: A listing of structure factor amplitudes for the X-ray structural analysis (9 pages). Ordering Information is given on any current masthead page.

(16) Darwish D.; Tomilson, R. C. *J. Am. Chem. Soc.* **1968**, *90*, 5938.
(17) (a) Abel, E. W.; Ahmed, A. K. S.; Farrow, G. W.; Orrell, K. G.; Sik, G. *J. Chem. Soc., Dalton Trans.* **1977**, 47. (b) Abel, E. W.; Farrow, G. W.; Orrell, K. G.; Sik, V. *J. Chem. Soc., Dalton Trans.* **1977**, 42. (c) Abel, E. W.; Farrow, G. W.; Orrell, K. G. *Ibid.* **1976**, 1160. (d) Abel, E. W.; Khan, A. R.; Kite, K.; Orrell, K. G.; Sik, V. *J. Organomet. Chem.* **1978**, *145*, C18.

(18) This has recently been confirmed. Deeming, A. J.; Rothwell, I. P.; Hursthouse, M. B.; Backer-Dirks, J. D. *J. Chem. Soc., Dalton Trans.* **1981**, 1879.

Cleavage of Metal–Metal Bonds in Heteronuclear Clusters. Reactions of $Os_3(\mu_3\text{-}S)(\mu_3\text{-}\eta^2\text{-}SCH_2)(CO)_8(PMe_2Ph)$ with HCl and $P(OMe)_3$

Richard D. Adams,* Nancy M. Golembeski, and John P. Selegue

Department of Chemistry, Yale University, New Haven, Connecticut 06511

Received July 20, 1981

The reactions of the cluster $Os_3(\mu_3\text{-}S)(\mu_3\text{-}\eta^2\text{-}SCH_2)(CO)_8(PMe_2Ph)$ (I), which contains a thioformaldehyde ligand, with HCl and $P(OMe)_3$ have been investigated. The reaction of I with HCl yields an addition product $HOs_3(\mu_3\text{-}S)(\mu_3\text{-}\eta^2\text{-}SCH_2)(CO)_8(PMe_2Ph)Cl$ (II), which has been characterized by X-ray crystallographic methods: space group $P2_1/c$, at 23 °C; a = 10.423 (2) Å, b = 11.014 (5) Å, c = 22.743 (9) Å, β = 101.98 (3); V = 2554 (3) Å^3; Z = 4; ρ_{calcd} = 2.72 g/cm^3. For 2689 reflections ($F_o \geq 3.0\sigma(F_o^2)$) R_1 = 0.044 and R_2 = 0.048. The molecule contains a group of three osmium atoms but only one osmium–osmium bond. The third osmium is linked to the others by a triply bridging sulfide and triply bridging thioformaldehyde ligand. The addition of HCl to I results in cleavage of one of its osmium–osmium bonds. The reaction of I with $P(OMe)_3$ yields the new molecule $Os_3(\mu_3\text{-}S)(\mu_3\text{-}\eta^2\text{-}SCH_2)(CO)_7(PMe_2Ph)[P(OMe)_3]$ (III). III was also analyzed by an X-ray crystallographic analysis: space group $P\bar{1}$, at 23 °C; a = 10.694 (2) Å, b = 11.630 (3) Å, c = 12.675 (2) Å, α = 111.16 (2)°, β = 99.63 (2)°, γ = 92.36 (2)°; V = 1441 (1) Å^3; Z = 2; ρ_{calcd} = 2.55 g/cm^3. For 4083 reflections ($F_o \geq 3.0\sigma(F_o^2)$) R_1 = 0.035 and R_2 = 0.038. III is formed from I by the substitution of one of the carbonyl ligands on the phosphine-substituted osmium atom with the $P(OMe)_3$ ligand. Thus, as in I, III contains a cluster with two osmium–osmium bonds a triply bridging sulfide ligand and a triply bridging thioformaldehyde ligand. The nature of the formations of II and III is compared in terms of probable mechanisms.

Introduction

In all examples of homogeneous catalysis involving transition-metal agents, at some point a metal complex is called upon to activate either a selected reagent, a target substrate, or both. Nucleophilic and oxidative additions[1,2] and electron-transfer[3] processes which are the principal activation steps have been well studied for mononuclear transition complexes.

Attention has recently been focused on transitional metal cluster compounds as a possible new source of homogeneous catalytic agents.[4] Once again, it can be expected that oxidative and nucleophilic additions and electron-transfer processes will play important roles in reagent and substrate activations. However, a feature that makes polynuclear metal complexes unique and chemically quite different from mononuclear ones is the existence of metal–metal bonds. Frequently, the metal–metal bonds are the weakest chemical bonds in the molecule, and as a result the basic activation processes may be altered by reaction with them. One obvious way this can happen is by cleavage of the metal–metal bond, and already much attention has been focused on nucleophilic, oxidative, and reductive cleavage of metal–metal bonds in polynuclear metal complexes.[2,5-8] Of course, if all the metal–metal bonds in the cluster are cleaved, the true catalytic agents may be only the mononuclear fragments. However, heteronuclear cluster compounds which contain a group of transition-metal atoms plus some bridging, supportive main-group element, where the bonds between the main-group element and the transition-metal atoms are stronger than the metal–metal bonds, may provide a means for circumventing cluster degradation and might even permit one to take advantage of the metal–metal bond cleavage processes in the activation of certain small molecules.[9,10]

At present, we are investigating the reactivity of such heteronuclear clusters with a variety of small molecules.[10] In this report we describe the nature of reactions of the cluster $Os_3(\mu_3\text{-}S)(\mu_3\text{-}\eta^2\text{-}SCH_2)(CO)_8(PMe_2Ph)$ (I) with HCl and $P(OMe)_3$. A preliminary report on some of this work has been published previously.[11]

Experimental Section

General Data. The compounds reported in this study showed no significant sensitivity to air. However, as a matter of routine all reactions were performed under an atmosphere of prepurified nitrogen. Hexane solvent was distilled from a sodium–benzophenone solution. $Os_3(\mu_3\text{-}S)(\mu_3\text{-}\eta^2\text{-}SCH_2)(CO)_8(PMe_2Ph)$ was prepared as previously reported.[12] All other reagents were used as purchased.

Melting points were determined by using a Thomas-Hoover apparatus and are uncorrected. Infrared spectra were recorded on a Perkin-Elmer 237B spectrophotometer and were calibrated with polystyrene. Fourier transform ^1H NMR spectra were obtained at 270 MHz on a Bruker HX270 spectrometer.

Preparation of $HOs_3(\mu_3\text{-}S)(\mu_3\text{-}\eta^2\text{-}SCH_2)(CO)_8(PMe_2Ph)Cl$ (II). A 37-mg (0.0365-mmol) sample of $Os_3(\mu_3\text{-}S)(\mu_3\text{-}\eta^2\text{-}SCH_2)(CO)_8(PMe_2Ph)$ was dissolved in 15 mL of methylene chloride.

(1) Cotton, F. A., Wilkinson, G. "Advanced Inorganic Chemistry", 4th ed.; Wiley: New York, 1980.
(2) Collman, J. P.; Hegedus, L. "Principles and Applications of Organotransition Metal Chemistry"; University Science Books: Mill Valley, CA, 1980.
(3) (a) Kochi, J. K. *Acc. Chem. Res.* **1974**, *7*, 351. (b) Lappert, M. F.; Lednor, P. W. *Adv. Organomet. Chem.* **1976**, *14*, 345.
(4) (a) Muetterties, E. L. *Science (Washington, D.C)* **1977**, *196*, 839. (b) Ugo, R. *Catal. Rev.* **1975**, *11*, 225.
(5) Meyer, T. J. *Prog. Inorg. Chem.* **1975**, *19*, 1.
(6) Kramer, G.; Patterson, J.; Poë, A.; Lily, N. *Inorg. Chem.* **1980**, *19*, 1161.
(7) Poë, A.; Malik, S. K. *Inorg. Chem.* **1979**, *18*, 1241.
(8) (a) Johnson, B. F. G.; Lewis, J.; Kilty, P. A. *J. Chem. Soc. A* **1968**, 2859. (b) Candlin, J. P.; Cooper, J. *J. Organomet. Chem.* **1968**, *15*, 230.
(9) (a) Huttner, G.; Schneider, J.; Muller, H. D.; Mohr, G.; von Seyerl, J.; Wohlfart, L. *Angew. Chem. Int. Ed. Engl.* **1979**, *18*, 76. (b) Langenback, H. J.; Vahrenkamp, H. *Chem. Ber.* **1979**, *112*, 3390. (c) Langenback, H. J.; Keller, E.; Vahrenkamp, H. *Angew. Chem., Int., Ed. Engl.* **1977**, *16*, 188. (d) Dawoodi, Z.; Mays, M. J.; Raithby, P. R. *J. Chem. Soc., Chem. Commun.* **1979**, 721.
(10) Adams, R. D.; Katahira, D. A. *Organometallics* **1981**, *1*, 0000.
(11) Adams, R. D.; Golembeski, N. M.; Selegue, J. P. *J. Organomet. Chem.* **1980**, *193*, C7.
(12) Adams, R. D.; Golembeski, N. M.; Selegue, J. P. *J. Am. Chem. Soc.* **1981**, *103*, 546.

0276-7333/82/2301-0240$01.25/0

Table I. Crystallographic Data for X-ray Diffraction Studies

	$Os_3ClS_2PO_8C_{17}H_{14}$	$Os_3S_2P_2O_{10}C_{19}H_{22}$
(A) Crystal Data		
temp (±5 °C)	23	23
space group	$P2_1/c$, No. 14	$P\bar{1}$, No. 2
a, Å	10.423 (2)	10.694 (2)
b, Å	11.014 (5)	11.630 (3)
c, Å	22.743 (9)	12.675 (2)
α, deg	90.00	111.16 (2)
β, deg	101.98 (3)	99.63 (2)
γ, deg	90.00	92.36 (2)
V (Å^3)	2554 (3)	1441 (1)
mol wt	1047.5	1107.1
Z	4	2
ρ_{calcd}, g/cm^3	2.72	2.55
(B) Measurement of Intensity Data		
radiation	Mo Kα (0.710 73 Å)	
monochromator	graphite	
detector aperture, mm		
horizontal ($A + B \tan \theta$)		
A	3.0	
B	1.0	
vertical	4.0	
cryst faces	$\bar{2}\bar{1}0$, $21\bar{2}$, $0\bar{1}2$, $01\bar{2}$, $2\bar{1}4$, $\bar{2}14$	$\bar{1}01$, $41\bar{4}$, $0\bar{1}2$, $01\bar{2}$, 011, $0\bar{1}\bar{1}$
crystal size, mm	0.12 × 0.17 × 0.17	0.12 × 0.12 × 0.21
crystal orientatn: direction, deg from ϕ axis	normal to $0\bar{1}2$, 22.0	b^*, 13.3
reflctns measd	$h,k,\pm l$	$h,\pm k,\pm l$
max 2θ, deg	50	52
scan type	moving crystal-stationary counter	
ω-scan width		
$(A + 0.347 \tan \theta)^0$	0.85	0.80
bkgd	one-fourth additional scan at each end of scan	
ω-scan rate (variable)		
max, deg/min	10.0	10.0
min, deg/min	1.3	1.3
no. of reflctns measd	4718	5310
data used ($F^2 \geq 3.0\sigma(F)^2$)	2689	4083
(C) Treatment of Data		
abs correction		
coeff, cm^{-1}	162	143
grid	10 × 10 × 8	10 × 10 × 8
transmission coeff		
max	0.22	0.33
min	0.09	0.04
P factor	0.02	0.01
final residuals		
R_1	0.044	0.035
R_2	0.048	0.038
esd of unit wt	2.44	3.40
largest shift/error value on final cycle	0.01	0.02
largest peaks in final doff fpiroer. e$^-$/Å^3	2.1	2.8

A solution of 12 M HCl–ethanol (1:1) was prepared, and 10 drops were added to the methylene chloride solution. The yellow solution was stirred 15 h at room temperature and became colorless. IR spectra showed the reaction to be complete, and the solution was then concentrated in vacuo to approximately 2-mL volume. A 5-mL sample of pentane was added, and when the mixture was cooled to −20 °C, a very pale yellow powder precipitated. Recrystallization of the pale yellow powder from CH_2Cl_2–octane solutions gave 20 mg of II as crystals: yield 52%; mp 151.0–151.5 °C; IR (ν CO), in methylene chloride) 2110 (m), 2095 (s), 2030 (s), 2022 (s), 1995 (m, br) cm^{-1}; ^{1}H NMR (δ, in $CDCl_3$) 7.41 (m, 5 H), 4.40 (d, 1 H), 3.98 (d, 1 H, $^2J_{H-H}$ = 11.0 Hz), 2.11 (d, 6 H, $^2H_{P-H}$ = 9.8 Hz), −15.12 (d, 1 H, $^2H_{P-H}$ = 8.55 Hz).

Preparation of $Os_3(\mu_3\text{-}S)(\mu_3\text{-}\eta^2\text{-}SCH_2)(CO)_7(PMe_2Ph)[P(OMe)_3]$ (III). A solution of I (68.0 mg, 0.067 mmol) and $P(OMe)_3$ (0.1 mL) in 50 mL of hexane was heated to reflux for 8 h. Infrared spectra indicated formation of a single product with no detectable intermediates. Chromatography on alumina (acid, 6% water) using benzene–hexane (3:7) gave a single yellow band. This was collected, reduced to a yellow oil, dissolved in a minimum of pentane, and precipitated at −78 °C. The product III was obtained as a yellow powder (19.2 mg, 26%): mp 155–156 °C; IR (ν (CO) in hexane) 2080 (s), 2045 (s), 2002 (s), 1995 (m), 1970 (mw) cm^{-1}; ^{1}H NMR (δ in $CDCl_3$) 7.54–7.38 (m, 5 H, C_6H_5), 3.72 (d, 9 H, $^3H_{PH}$ = 11.0 Hz OCH_3), 2.27 (dd, 1 H, $^2J_{HH'}$ = 11.4 Hz, J_{PH} = 11.1 Hz, SC*H*H′), 2.20 (d, 3 H, $^2H_{PH}$ = 11.0 Hz, PCH_3), 2.13 (d, 3 H, $^2H_{PH}$ = 10.6 Hz, PCH_3), 0.69 (dd, 1 H, $^2J_{HH'}$ = 11.4 Hz, $J_{H'P}$ = 4.9 Hz, SCH*H*′).

Crystallographic Analyses. Crystals of II and III suitable for diffraction measurements were obtained by slow crystallization from hexane solutions cooled to −20 °C. All crystals were mounted in thin-walled glass capillaries. Diffraction measurements were made on an Enraf-Nonius CAD-4 fully automated four-circle diffractometer using graphite-monochromatized Mo K$\bar{\alpha}$ radiation. Unit cells were determined and refined from 25 randomly selected reflections obtained by using the CAD-4 automatic search, center, index, and least-squares routines. For I the space group $P2_1/c$ was established from the systematic absences observed in the data. For II the space group $P\bar{1}$ was assumed and confirmed by the successful solution and refinement of the structure. Crystal data and data collections parameters are listed in Table I. All data processing was performed on a Digital PDP 11/45 computer using the Enraf-Nonius SDP program library (version 16). Absorption corrections of a Gaussian integration type were applied to the data

Table II. Final Fractional Atomic Coordinates, Thermal Parameters, and Their Esds for $HOs_3(\mu_3\text{-}S)(\mu_3\text{-}\eta^2\text{-}SCH_2)(CO)_8(PMe_2Ph)Cl$ (II)

atom	x	y	z	B,[a] Å²	atom	x	y	z	B,[a] Å²
Os(1)	0.39227 (7)	0.23765 (7)	0.11751 (3)		C(2)	0.337 (2)	0.109 (2)	0.0669 (7)	2.6 (3)
Os(2)	0.74224 (8)	0.07582 (7)	0.13494 (3)		C(3)	0.619 (2)	−0.031 (3)	0.0927 (8)	2.8 (4)
Os(3)	0.59225 (7)	0.39199 (7)	0.18016 (3)		C(4)	0.873 (2)	0.014 (2)	0.950 (8)	3.7 (4)
Cl	0.9159 (5)	0.2057 (5)	0.1880 (3)		C(5)	0.788 (2)	−0.041 (2)	0.2004 (9)	4.1 (5)
S(1)	0.5654 (5)	0.3312 (4)	0.0757 (2)		C(6)	0.580 (2)	0.408 (2)	0.2629 (8)	3.4 (4)
S(2)	0.5887 (5)	0.1710 (4)	0.1897 (2)		C(7)	0.776 (2)	0.433 (2)	0.1999 (9)	4.4 (5)
P	0.2260 (5)	0.3504 (5)	0.0554 (2)		C(8)	0.553 (2)	0.563 (2)	0.1629 (10)	5.0 (5)
O(1)	0.230 (1)	0.144 (1)	0.2034 (6)	4.9 (3)	C(10)	0.251 (2)	0.375 (2)	−0.0219 (9)	4.1 (5)
O(2)	0.295 (1)	0.027 (1)	0.0363 (6)	4.5 (3)	C(11)	0.196 (2)	0.502 (2)	0.0829 (8)	2.9 (4)
O(3)	0.545 (1)	−0.099 (1)	0.0658 (6)	5.0 (3)	C(12)	0.123 (2)	0.514 (2)	0.1261 (9)	4.8 (5)
O(4)	0.948 (2)	−0.023 (1)	0.0702 (7)	5.9 (4)	C(13)	0.101 (2)	0.631 (2)	0.1504 (11)	5.9 (6)
O(5)	0.806 (2)	−0.112 (1)	0.2374 (7)	6.3 (4)	C(14)	0.161 (2)	0.725 (2)	0.1298 (10)	4.9 (5)
O(6)	0.572 (1)	0.407 (1)	0.3118 (6)	4.7 (3)	C(15)	0.234 (2)	0.718 (2)	0.0895 (10)	5.1 (5)
O(7)	0.879 (2)	0.476 (2)	0.2102 (7)	7.1 (4)	C(16)	0.257 (2)	0.603 (2)	0.0645 (9)	4.6 (5)
O(8)	0.543 (2)	0.664 (2)	0.1549 (7)	6.8 (4)	C(17)	0.693 (2)	0.216 (2)	0.0684 (8)	2.9 (4)
C(1)	0.288 (2)	0.181 (2)	0.1693 (8)	3.1 (4)	C(9)	0.062 (2)	0.278 (2)	0.0427 (9)	4.5 (5)

atom	B(1,1) [b]	B(2,2)	B(3,3)	B(1,2)	B(1,3)	B(2,3)
Os(1)	2.24 (3)	2.03 (3)	2.79 (3)	0.01 (3)	0.70 (3)	0.16 (3)
Os(2)	2.68 (3)	2.56 (3)	3.63 (3)	0.49 (3)	0.96 (2)	0.11 (3)
Os(3)	2.69 (3)	2.15 (3)	3.44 (3)	−0.23 (3)	0.90 (2)	−0.29 (3)
P	3.0 (2)	2.6 (2)	3.1 (2)	0.4 (2)	0.6 (2)	0.2 (2)
S(1)	2.9 (2)	2.4 (2)	3.3 (2)	−0.3 (2)	0.9 (2)	0.1 (2)
S(2)	2.6 (2)	2.2 (2)	2.8 (2)	0.0 (2)	0.6 (2)	0.0 (2)
Cl	2.9 (2)	4.6 (3)	6.0 (3)	−0.3 (2)	0.4 (2)	−0.3 (3)

[a] Isotropic thermal parameters. [b] The form of the anisotropic thermal parameter is $\exp(-1/4[B(1,1)h^2a^{*2} + B(2,2)k^2b^{*2} + B(3,3)l^2c^{*2} + B(1,2)hka^*b^* + B(1,3)hla^*c^* + B(2,3)klb^*c^*])$.

for both structures. Neutral atom scattering factors were calculated by the standard procedures.[13a] Anomalous dispersion corrections were applied to all nonhydrogen atoms.[13b] Full-matrix least-squares refinements minimized the function $\sum_{hkl} w(|F_o| - |F_c|)^2$, where $w = 1/\sigma(F)^2$, $\sigma(F) = \sigma(F^2)/2F_o$, and $\sigma(F_o^2) = [\sigma(I_{raw})^2 + (PF_o^2)^2]^{1/2}/Lp$.

The structure of II was solved by the heavy-atom method. Hydrogen atom positions were calculated by assuming idealized geometry and staggered rotational conformations in the cases of the methyl groups. Hydrogen atom contributions were added to the structure factor calculations but their positions were not refined. Refinement converged with final values of the residuals being $R_1 = 0.044$ and $R_2 = 0.048$.

The structure of III was solved by the heavy-atom method. Hydrogen atom positions were calculated by assuming idealized geometry and by employing located positions whenever possible. The hydrogen atoms on the carbon atom of the thioformaldehyde ligand were located in a difference Fourier synthesis. Hydrogen atom contributions were added to the structure factor calculations, but their positions were not refined. Refinement converged with final values of the residuals being $R_1 = 0.035$ and $R_2 = 0.038$.

Final values of the fractional atomic coordinates, interatomic distances, and angles with errors obtained from the inverse matrix calculated on the final cycle of refinement for both structures are listed in Tables II–VII. Structure factor amplitudes are available for both structures (see supplementary material).

Results

The reaction of I with HCl yields a product which shows a resonance at δ −15.12 in its ^1H NMR spectrum. This can be attributed to a bridging metal hydride ligand that was apparently produced by protonation of one of the metal–metal bonds in I. Details of the molecular structure of II were established by a X-ray crystallographic analysis which revealed the presence also of a chloride ligand.

The molecular structure of II is shown in Figure 1. The molecule contains a group of three osmium atoms, but on the basis of their internuclear separations, Os(1)–Os(3) = 2.834 (1) Å, Os(1)···Os(2) = 4.005 (1) Å, and Os(2)···Os(3)

Table III. Bond Distances (Å) with Esds for $HOs_3(\mu_3\text{-}S)(\mu_3\text{-}\eta^2\text{-}SCH_2)(CO)_8(PMe_2Ph)Cl$ (II)

Os(1)-Os(3)	2.834 (1)	S(1)-C(17)	1.872 (12)
Os(3)-S(1)	2.427 (3)	C(1)-O(1)	1.158 (14)
Os(3)-S(2)	2.445 (3)	C(2)-O(2)	1.167 (13)
Os(3)-C(6)	1.919 (13)	C(3)-O(3)	1.162 (14)
Os(3)-C(7)	1.926 (16)	C(4)-O(4)	1.130 (14)
Os(3)-C(8)	1.952 (16)	C(5)-O(5)	1.134 (15)
Os(2)-S(2)	2.457 (3)	C(6)-O(6)	1.134 (13)
Os(2)-Cl	2.423 (4)	C(7)-O(7)	1.151 (17)
Os(2)-C(17)	2.147 (12)	C(8)-O(8)	1.125 (16)
Os(2)-C(3)	1.852 (13)	P-C(9)	1.853 (15)
Os(2)-C(4)	1.911 (14)	P-C(10)	1.851 (14)
Os(2)-C(5)	1.949 (15)	P-C(11)	1.835 (12)
Os(1)-P	2.350 (3)	C(11)-C(12)	1.371 (17)
Os(1)-S(1)	2.436 (3)	C(12)-C(13)	1.441 (20)
Os(1)-S(2)	2.455 (3)	C(13)-C(14)	1.348 (20)
Os(1)-C(1)	1.864 (13)	C(14)-C(15)	1.309 (19)
Os(1)-C(2)	1.841 (12)	C(15)-C(16)	1.422 (19)
		C(11)-C(16)	1.382 (18)

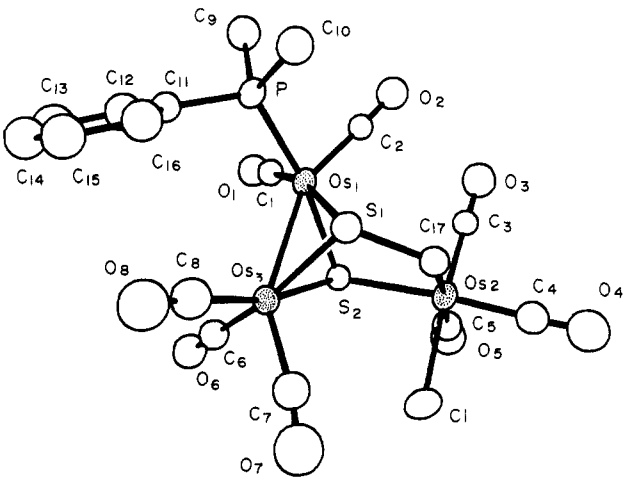

Figure 1. An ORTEP drawing of $HOs_3(\mu_3\text{-}S)(\mu_3\text{-}\eta^2\text{-}SCH_2)(CO)_8(PMe_2Ph)Cl$ (II) showing 50% electron density probability ellipsoids.

(13) "International Tables for X-ray Crystallography"; Kynoch Press: Birmingham, England, 1975; Vol. IV: (a) Table 2.2B, pp 99–101; (b) Table 2.3.1, pp 149–150.

Table IV. Intramolecular Angles (Deg) with Esds for $HOs_3(\mu_3\text{-}S)(\mu_3\text{-}\eta^2\text{-}SCH_2)(CO)_8(PMe_2Ph)Cl$ (II)

Os(3)-Os(1)-S(1)	54.21 (8)	S(1)-Os(3)-C(7)	101.5 (4)
Os(3)-Os(1)-S(2)	54.49 (7)	S(1)-Os(3)-C(8)	95.4 (5)
Os(3)-Os(1)-P	111.03 (9)	S(2)-Os(3)-C(6)	89.8 (4)
Os(3)-Os(1)-C(1)	110.2 (4)	S(2)-Os(3)-C(7)	104.3 (4)
Os(3)-Os(1)-C(2)	151.6 (3)	S(2)-Os(3)-C(8)	166.7 (5)
S(1)-Os(1)-S(2)	78.74 (10)	C(6)-Os(3)-C(7)	90.9 (6)
S(1)-Os(1)-P	93.19 (12)	C(6)-Os(3)-C(8)	93.2 (6)
S(1)-Os(1)-C(1)	164.2 (4)	C(7)-Os(3)-C(8)	88.6 (6)
S(1)-Os(1)-C(2)	104.2 (3)	Os(1)-S(1)-Os(3)	71.28 (9)
S(2)-Os(1)-P	165.50 (11)	Os(1)-S(1)-C(17)	110.2 (4)
S(2)-Os(1)-C(1)	89.5 (4)	Os(3)-S(1)-C(17)	109.6 (4)
S(2)-Os(1)-C(2)	107.4 (4)	Os(1)-S(2)-Os(2)	109.24 (12)
P-Os(1)-C(1)	95.9 (4)	Os(1)-S(2)-Os(3)	70.67 (9)
P-Os(1)-C(2)	86.6 (4)	Os(2)-S(2)-Os(3)	110.90 (12)
C(1)-Os(1)-C(2)	89.4 (5)	Os(2)-C(17)-S(1)	119.7 (6)
S(2)-Os(2)-Cl	89.65 (11)	Os(1)-P-C(9)	114.2 (5)
S(2)-Os(2)-C(3)	94.6 (4)	Os(1)-P-C(10)	114.7 (5)
S(2)-Os(2)-C(4)	174.5 (4)	Os(1)-P-C(11)	115.6 (4)
S(2)-Os(2)-C(5)	88.7 (4)	C(9)-P-C(10)	102.9 (6)
S(2)-Os(2)-C(17)	88.0 (3)	C(9)-P-C(11)	103.2 (6)
Cl-Os(2)-C(3)	175.7 (4)	C(10)-P-C(11)	104.8 (6)
Cl-Os(2)-C(4)	85.0 (4)	P-C(11)-C(12)	119 (1)
Cl-Os(2)-C(5)	88.2 (4)	P-C(11)-C(16)	121 (1)
Cl-Os(2)-C(17)	88.4 (3)	C(16)-C(11)-C(12)	120 (1)
C(3)-Os(2)-C(4)	90.8 (6)	C(11)-C(12)-C(13)	121 (1)
C(3)-Os(2)-C(5)	90.8 (6)	C(12)-C(13)-C(14)	116 (1)
C(3)-Os(2)-C(17)	92.9 (5)	C(13)-C(14)-C(15)	125 (2)
C(4)-Os(2)-C(5)	92.4 (6)	C(14)-C(15)-C(16)	120 (2)
C(4)-Os(2)-C(17)	90.5 (5)	C(15)-C(16)-C(11)	118 (1)
C(5)-Os(2)-C(17)	175.2 (5)	Os(1)-C(1)-O(1)	177 (1)
Os(1)-Os(3)-S(1)	54.51 (7)	Os(1)-C(2)-O(2)	176 (1)
Os(1)-Os(3)-S(2)	54.84 (8)	Os(2)-C(3)-O(3)	178 (1)
Os(1)-Os(3)-C(6)	110.8 (4)	Os(2)-C(4)-O(4)	178 (1)
Os(1)-Os(3)-C(7)	148.2 (4)	Os(2)-C(5)-O(5)	175 (1)
Os(1)-Os(3)-C(8)	112.1 (5)	Os(3)-C(6)-O(6)	175 (1)
S(1)-Os(3)-S(2)	79.12 (10)	Os(3)-C(7)-O(7)	170 (1)
S(1)-Os(3)-C(6)	165.1 (4)	Os(3)-C(8)-O(8)	173 (2)

= 4.037 (1) Å, there is only one metal–metal bond. The group of metal atoms is held together a triply bridging sulfide ligand and a triply bridging thioformaldehyde ligand. The osmium–sulfur distances (see Table III) are similar to those found in I.[12] The sulfur atom of the thioformaldehyde ligand bridges the Os(1)–Os(3) metal–metal bond while the carbon atom is coordinated solely to Os(2). The carbon–sulfur distance, C(17)–S, at 1.872 (12) Å is very similar to that observed in I (1.869 (6) Å) and is indicative of single bond.[12] Unexpectedly, a chloride ligand was found bonded to Os(2), Os(2)–Cl = 2.423 (4) Å. The hydride ligand was not observed crystallographically but is believed to bridge the Os(1)–Os(3) bond in the cavity circumscribed by the carbonyl ligands C(1)–O(1), C(6)–O(6), and C(8)–O(8) and the phosphine ligand. I also contains eight linear terminal carbonyl ligands and a phosphine distributed in the same way as those in I. The shortest intermolecular contacts were between oxygen atoms of the carbonyl ligands and lay in the range 3.06–3.09 Å.

The reaction of I with $P(OMe)_3$ in refluxing hexane gives III as the only isolable product. Its ^1H NMR spectrum indicates the presence of a $P(OMe)_3$ ligand, but its site of coordination could not be established. This was determined, however, by the use of a X-ray crystallographic analysis.

The molecular structure of III is shown in Figure 2. Overall III is simply a trimethyl phosphite substituted derivative of I. The cluster contains three osmium atoms with two metal–metal bonds, Os(1)–Os(2) = 2.894 (1) Å, Os(1)–Os(3) = 2.837 (1) Å, Os(2)···Os(3) = 4.079 (1) Å. There is a triply bridging sulfide ligand and a triply bridging thioformaldehyde ligand. As found in I, the osmium–sulfur distances to the central osmium atom, Os(1), are significantly longer than those to external osmium atoms, Os(1)–S(1) = 2.435 (2) Å and Os(1)–S(2) = 2.448 (1) Å vs. Os(2)–S(1) = 2.393 (2) Å, Os(2)–S(2) = 2.394 (2) Å, and Os(3)–S(2) = 2.406 (2) Å. The thioformaldehyde carbon–sulfur distance, C(17)–S(1), at 1.837 (7) Å is slightly shorter than those in I and II, but this is probably not significant. The two hydrogen atoms on C(17) were located in a difference Fourier synthesis and are shown in the figure at those sites. The trimethyl phosphite ligand is coordinated to osmium Os(2), the same osmium atom which contains the dimethylphenylphosphine ligand. There are seven linear terminal carbonyl groups arranged such that Os(1) and Os(3) have three each and Os(2) has only one. The shortest intermolecular contact was between the carbonyl oxygen atoms O(2) and O(3) at 3.003 (8) Å.

Discussion

Upon reaction, I adds 1 equiv of HCl to form III in which one metal–metal bond has been cleaved. Formally, the reaction is equivalent to an oxidative addition of HCl across a metal–metal bond in I. Mechanistically, we believe the reaction occurs in a sequence of two steps: (1) a protonation of one of the metal–metal bonds in I followed by (2) a nucleophilic addition of chloride ion which induced the cleavage of the metal–metal bond. It is well-known that protonic acids will protonate metal–metal bonds in transition-metal cluster compounds, and we have observed that I will react with protonic acids containing noncoordinating counterions to give hydride-containing clusters.[15]

(14) (a) Knight, K.; Mays, M. J. *J. Chem. Soc. A* **1970**, 711. (b) Deeming, A. J.; Johnson, B. F. G.; Lewis, J. *Ibid.* **1970**, 2967. (c) Bryan, E. G.; Jackson, W. G.; Johnson, B. F. G.; Kelland, J. W.; Lewis, J.; Schorpp, K. T. *J. Organomet. Chem.* **1976**, *108*, 385.

Table V. Final Fractional Atomic Coordinates, Thermal Parameters, and Their Esds for $Os_3(\mu_3\text{-}S)(\mu_3\text{-}\eta^2\text{-}SCH_2)(CO)_7(PMe_2Ph)[P(OMe)_3]$ (III)

atom	x	y	z	B, [a] Å²	atom	x	y	z	B, [a] Å²
Os(1)	0.42952 (4)	0.13164 (4)	0.25880 (4)		C(13)	−0.1139 (12)	0.3704 (12)	0.3521 (12)	5.3 (3)
Os(2)	0.29937 (4)	0.31390 (4)	0.18958 (4)		C(14)	−0.2146 (13)	0.4056 (14)	0.2996 (13)	6.3 (4)
Os(3)	0.27106 (4)	0.15052 (4)	0.42159 (4)		C(15)	−0.1996 (15)	0.4706 (15)	0.2304 (15)	7.5 (4)
S(1)	0.4400 (3)	0.3531 (2)	0.3697 (3)		C(16)	−0.0803 (14)	0.4964 (14)	0.2066 (13)	6.3 (4)
S(2)	0.2004 (2)	0.1510 (2)	0.2313 (2)		C(17)	0.3479 (10)	0.3421 (10)	0.4764 (10)	3.2 (2)
P(1)	0.1865 (3)	0.4829 (3)	0.2356 (3)		C(18)	0.2614 (11)	0.6097 (11)	0.3698 (11)	4.4 (3)
P(2)	0.1893 (3)	0.2302 (3)	0.0034 (3)		C(19)	0.1672 (12)	0.5597 (12)	0.1330 (12)	5.0 (3)
O(1)	0.6691 (8)	0.1193 (8)	0.4190 (8)	5.2 (2)	H(12) [b]	0.0796	0.3675	0.3688	5.0
O(2)	0.5710 (10)	0.1477 (9)	0.0738 (9)	7.3 (3)	H(13) [b]	−0.1252	0.3287	0.4045	5.0
O(3)	0.3611 (8)	−0.1507 (8)	0.1458 (7)	4.8 (2)	H(14) [b]	−0.3018	0.3863	0.3066	5.0
O(4)	0.4886 (9)	0.4704 (9)	0.1316 (9)	6.7 (3)	H(15) [b]	−0.2738	0.4999	0.1940	5.0
O(5)	0.0508 (10)	0.2277 (10)	0.5482 (10)	8.4 (3)	H(16) [b]	−0.0695	0.5397	0.1537	5.0
O(6)	0.1642 (9)	−0.1263 (9)	0.3250 (9)	6.5 (2)	H(171) [b]	0.2773	0.3828	0.4648	5.0
O(7)	0.4702 (9)	0.1480 (9)	0.6185 (9)	6.4 (2)	H(172) [b]	0.4180	0.3848	0.5586	5.0
O(8)	0.2264 (8)	0.2846 (8)	−0.0870 (8)	5.3 (2)	H(181) [b]	0.3320	0.6152	0.3477	5.0
O(9)	0.0416 (7)	0.2459 (7)	−0.0281 (7)	4.7 (2)	H(182) [b]	0.2720	0.5877	0.4359	5.0
O(10)	0.2028 (8)	0.0859 (8)	−0.0534 (7)	4.9 (2)	H(183) [b]	0.2214	0.6835	0.3848	5.0
C(1)	0.5757 (9)	0.1245 (9)	0.3572 (9)	2.9 (2)	H(91) [b]	−0.0547	0.1035	−0.0449	5.0
C(2)	0.5116 (12)	0.1462 (12)	0.1419 (12)	4.9 (3)	H(92) [b]	−0.1328	0.2186	0.0099	5.0
C(3)	0.3888 (10)	−0.0435 (10)	0.1842 (10)	3.6 (2)	H(93) [b]	−0.0232	0.1895	0.0901	5.0
C(4)	0.4139 (11)	0.4097 (11)	0.1527 (11)	4.1 (3)	H(81) [b]	0.3906	0.2324	−0.0918	5.0
C(5)	0.1364 (13)	0.1986 (13)	0.5030 (12)	5.6 (3)	H(82) [b]	0.3931	0.3441	−0.1170	5.0
C(6)	0.2074 (12)	−0.0229 (12)	0.3620 (11)	4.8 (3)	H(83) [b]	0.3324	0.2160	−0.2085	5.0
C(7)	0.3902 (11)	0.1468 (11)	0.5432 (10)	3.9 (3)	H(191) [b]	0.1280	0.5042	0.0581	5.0
C(8)	0.3413 (19)	0.2668 (19)	−0.1279 (18)	10.5 (6)	H(192) [b]	0.1156	0.6273	0.1567	5.0
C(9)	−0.0519 (12)	0.1858 (12)	0.0125 (12)	5.3 (3)	H(193) [b]	0.2488	0.5949	0.1293	5.0
C(10)	0.1461 (15)	0.0146 (14)	−0.1717 (14)	7.0 (4)	H(101) [b]	0.1623	−0.0726	−0.1939	5.0
C(11)	0.0260 (10)	0.4573 (10)	0.2606 (10)	3.7 (3)	H(102) [b]	0.0542	0.0133	−0.1868	5.0
C(12)	0.0076 (12)	0.3943 (12)	0.3307 (11)	4.6 (3)	H(103) [b]	0.1780	0.0440	−0.2246	5.0

atom	B(1,1) [c]	B(2,2)	B(3,3)	B(1,2)	B1,3)	B(2,3)
Os(1)	3.02 (2)	2.37 (2)	2.64 (2)	0.43 (1)	0.45 (1)	0.85 (1)
Os(2)	2.60 (2)	2.45 (1)	2.97 (2)	0.11 (1)	0.42 (1)	1.25 (1)
Os(3)	3.99 (2)	2.72 (2)	2.97 (2)	0.25 (1)	0.92 (2)	1.24 (1)
S(1)	3.0 (1)	2.2 (1)	3.5 (1)	−0.01 (9)	0.1 (1)	0.96 (9)
S(2)	3.0 (1)	2.3 (1)	3.1 (1)	−0.07 (9)	0.43 (9)	0.96 (8)
P(1)	3.4 (1)	2.5 (1)	3.7 (1)	0.3 (1)	0.2 (1)	1.21 (9)
P(2)	3.7 (1)	3.6 (1)	3.1 (1)	0.3 (1)	0.6 (1)	1.54 (9)

[a] Isotropic thermal parameters. [b] Hydrogen atom positions were not refined. [c] The form of the anisotropic thermal parameter is $\exp(-1/4[B(1,1)h^2a^{*2} + B(2,2)k^2b^{*2} + B(3,3)l^2c^{*2} + B(1,2)hka^*b^* + B(1,3)hla^*c^* + B(2,3)klb^*c^*])$.

Table VI. Interatomic Distances (Å) with Esds for $Os_3(\mu_3\text{-}S)(\mu_3\text{-}\eta^2\text{-}SCH_2)(CO)_7(PMe_2Ph)[P(OMe)_3]$ (III)

Os(1)-Os(2)	2.894 (1)	P(1)-C(19)	1.816 (8)
Os(1)-Os(3)	2.837 (1)	C(11)-C(12)	1.371 (9)
Os(2)···Os(3)	4.079 (1)	C(12)-C(13)	1.407 (10)
Os(1)-S(1)	2.435 (2)	C(13)-C(14)	1.328 (10)
Os(1)-S(2)	2.448 (1)	C(14)-C(15)	1.371 (12)
Os(1)-C(1)	1.855 (6)	C(15)-C(16)	1.404 (11)
Os(1)-C(2)	1.897 (9)	C(16)-C(11)	1.406 (10)
Os(1)-C(3)	1.906 (7)	P(2)-O(8)	1.590 (6)
Os(2)-S(1)	2.393 (2)	P(2)-O(9)	1.597 (5)
Os(2)-S(2)	2.394 (2)	P(2)-O(10)	1.593 (5)
Os(2)-P(1)	2.294 (2)	O(8)-C(8)	1.407 (12)
Os(2)-P(2)	2.284 (2)	O(9)-C(9)	1.460 (9)
Os(2)-C(4)	1.848 (7)	O(10)-C(10)	1.436 (10)
Os(3)-S(2)	2.406 (2)	C(1)-O(1)	1.180 (6)
Os(3)-C(5)	1.897 (9)	C(2)-O(2)	1.159 (9)
Os(3)-C(6)	1.928 (8)	C(3)-O(3)	1.167 (7)
Os(3)-C(7)	1.843 (7)	C(4)-O(4)	1.170 (8)
Os(3)-C(17)	2.160 (6)	C(5)-O(5)	1.159 (9)
S(1)-C(17)	1.837 (7)	C(6)-O(6)	1.164 (8)
P(1)-C(11)	1.828 (7)	C(7)-O(7)	1.166 (7)
P(1)-C(18)	1.828 (8)	S(1)···S(2)	3.192 (2)

An intermediate like A where the hydride ligand bridges the metal–metal bond to which the osmium atom containing the electron-rich phosphine ligand is attached seems to be very likely. The chloride ion then adds to the remaining osmium atom and yields II. As the electron pair from the chloride ion is added to the metal atom, the metal–metal bond is cleaved in order to maintain that metal atom's 18-electron configuration.

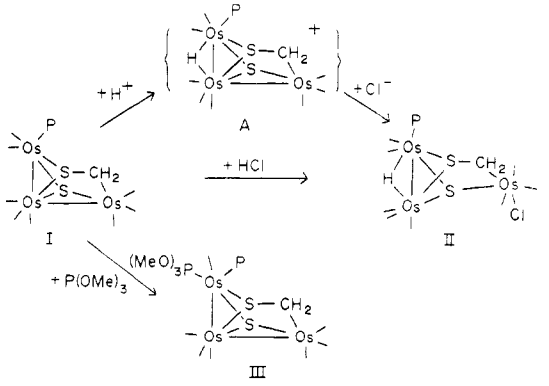

The addition of HCl to I differs significantly from the addition of HCl to the mononuclear thioformaldehyde complex $Os(\eta^2\text{-}SCH_2)(CO)_2(PPh_3)_2$.[16] In the latter reaction hydrogen is transferred to the carbon atom of the thioformaldehyde ligand and chlorine is added to the metal atom to give the methanethiolate complex $OsCl(SMe)(CO)_2(PPh_3)_2$. This reacts further with HCl to give methanethiol and $OsCl_2(CO)_2(PPh_3)_2$.

(15) Adams, R. D.; Selegue, J. P., unpublished results.

(16) Collins, T. J.; Roper, W. R. *J. Organomet. Chem.* **1978**, *159*, 73.

Table VII. Interatomic Angles (Deg) with Esds for $Os_3(\mu_3\text{-}S)(\mu_3\text{-}\eta^2\text{-}SCH_2)(CO)_7(PMe_2Ph)[P(OMe)_3]$ (III)

Os(2)-Os(1)-Os(3)	90.73 (1)	S(2)-Os(3)-C(17)	88.4 (2)
Os(2)-Os(1)-S(1)	52.49 (4)	C(5)-Os(3)-C(6)	93.0 (3)
Os(2)-Os(1)-S(2)	52.45 (4)	C(5)-Os(3)-C(7)	97.3 (3)
Os(2)-Os(1)-C(1)	139.0 (2)	C(5)-Os(3)-C(17)	90.7 (3)
Os(2)-Os(1)-C(2)	75.9 (2)	C(6)-Os(3)-C(7)	96.3 (3)
Os(2)-Os(1)-C(3)	125.0 (2)	C(6)-Os(3)-C(17)	175.6 (3)
Os(3)-Os(1)-S(1)	75.03 (4)	C(7)-Os(3)-C(17)	85.5 (3)
Os(3)-Os(1)-S(2)	53.55 (4)	Os(1)-S(1)-C(17)	97.5 (2)
Os(3)-Os(1)-C(1)	93.7 (2)	Os(2)-S(1)-C(17)	109.9 (2)
Os(3)-Os(1)-C(2)	166.6 (2)	Os(1)-S(1)-Os(2)	73.66 (5)
Os(3)-Os(1)-C(3)	93.4 (2)	Os(3)-C(17)-S(1)	107.4 (3)
S(1)-Os(1)-S(2)	81.62 (5)	Os(1)-S(2)-Os(2)	73.40 (4)
S(1)-Os(1)-C(1)	89.5 (2)	Os(1)-S(2)-Os(3)	71.52 (4)
S(1)-Os(1)-C(2)	96.6 (2)	Os(2)-S(2)-Os(3)	116.34 (6)
S(1)-Os(1)-C(3)	167.8 (2)	Os(2)-P(1)-C(18)	113.6 (2)
S(2)-Os(1)-C(1)	147.2 (2)	Os(2)-P(1)-C(19)	115.6 (3)
S(2)-Os(1)-C(2)	115.5 (2)	Os(2)-P(1)-C(11)	116.4 (2)
S(2)-Os(1)-C(3)	88.2 (2)	C(18)-P(1)-C(19)	102.2 (3)
C(1)-Os(1)-C(2)	96.8 (3)	C(18)-P(1)-C(11)	102.1 (3)
C(1)-Os(1)-C(3)	95.4 (3)	C(19)-P(1)-C(11)	105.2 (3)
C(2)-Os(1)-C(3)	94.0 (3)	P(1)-C(11)-C(12)	119.4 (5)
Os(1)-Os(2)-S(1)	53.85 (4)	P(1)-C(11)-C(16)	121.8 (6)
Os(1)-Os(2)-S(2)	54.16 (4)	C(16)-C(11)-C(12)	118.8 (7)
Os(1)-Os(2)-P(1)	148.91 (5)	C(11)-C(12)-C(13)	122.0 (7)
Os(1)-Os(2)-P(2)	111.92 (5)	C(12)-C(13)-C(14)	119.2 (8)
Os(1)-Os(2)-C(4)	109.7 (2)	C(13)-C(14)-C(15)	120.4 (9)
S(1)-Os(2)-S(2)	83.64 (5)	C(14)-C(15)-C(16)	122.2 (9)
S(1)-Os(2)-P(1)	101.42 (6)	C(15)-C(16)-C(11)	117.3 (9)
S(1)-Os(2)-P(2)	165.22 (6)	Os(2)-P(2)-O(8)	118.6 (2)
S(1)-Os(2)-C(4)	90.0 (2)	Os(2)-P(2)-O(9)	121.1 (2)
S(2)-Os(2)-P(1)	110.36 (6)	Os(2)-P(2)-O(10)	111.3 (2)
S(2)-Os(2)-P(2)	90.35 (6)	O(8)-P(2)-O(9)	92.8 (2)
S(2)-Os(2)-C(4)	163.1 (2)	O(8)-P(2)-O(10)	103.9 (3)
P(1)-Os(2)-P(2)	93.33 (6)	O(9)-P(2)-O(10)	92.0 (3)
P(1)-Os(2)-C(4)	86.2 (2)	P(2)-O(8)-C(8)	123.2 (6)
P(2)-Os(2)-C(4)	92.0 (2)	P(2)-O(9)-C(9)	119.3 (4)
Os(1)-Os(3)-S(2)	54.93 (4)	P(2)-O(10)-C(10)	121.2 (5)
Os(1)-Os(3)-C(5)	159.3 (3)	Os(1)-C(1)-O(1)	179.4 (6)
Os(1)-Os(3)-C(6)	96.3 (2)	Os(1)-C(2)-O(2)	172.9 (7)
Os(1)-Os(3)-C(7)	100.0 (2)	Os(1)-C(3)-O(3)	175.0 (6)
Os(1)-Os(3)-C(17)	79.4 (2)	Os(2)-C(4)-O(4)	178.4 (6)
S(2)-Os(3)-C(5)	107.1 (3)	Os(3)-C(5)-O(5)	177.0 (8)
S(2)-Os(3)-C(6)	88.3 (2)	Os(3)-C(6)-O(6)	174.4 (6)
S(2)-Os(3)-C(7)	154.9 (2)	Os(3)-C(7)-O(7)	176.4 (6)

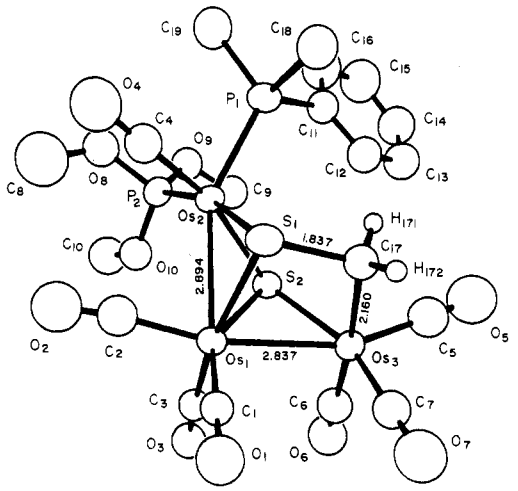

Figure 2. An ORTEP drawing of $Os(\mu_3\text{-}S)(\mu_3\text{-}\eta^2\text{-}SCH_2)(CO)_7(PMe_2Ph)[P(OMe)_3]$ (III) showing 50% electron density probability ellipsoids. Atoms H(171) and H(172) are shown with artificially reduced temperature factors.

Somewhat surprisingly the addition of trimethyl phosphite to I follows a different course. The phosphite ligand apparently attacks the cluster at the phosphine-substituted osmium atom and leads to CO substitution not metal–metal bond cleavage although the traversal of a transient intermediate with a cleaved metal–metal bond cannot be ruled out at this time.

In both cases the apparent nucleophilic additions have occurred at the external osmium atoms of the cluster. This seems to be reasonable since the internal osmium atom which is bonded to two other metal atoms would probably be more electron rich than the others and thus would be less likely to accept a nucleophile. All the factors which influence which of the external osmium atoms is actually attacked by a given nucleophile cannot be ascertained at this time, but the prior addition of a proton to one of the metal–metal bonds could be an important one in the case of the addition of HCl.

Acknowledgment. This work was supported by the National Science Foundation, Grant No. CHE-8019041, the Alfred P. Sloan Foundation through a fellowship to R.D.A. and in its initial stages[11] by the Division of Basic Energy Sciences of the U.S. Department of Energy, Contract No. ER-78-S-02-4900. NMR studies were supported by Grant No. CHE-7916210 from the National Science Foundation. We wish to thank Engelhard Industries for a loan of osmium tetraoxide.

Registry No. I, 71903-66-7; II, 75269-05-5; III, 79172-17-1.

Supplementary Material Available: Listings of structure factor amplitudes for both structures (49 pages). Ordering information is given on any current masthead.

The Organoaluminum Bond: Single vs. Multiple Bonding

Charles M. Cook and Leland C. Allen*

Department of Chemistry, Princeton University, Princeton, New Jersey 08544

Received July 28, 1981

Although Lewis dot structures would lead to the expectation of an AlC double bond in $AlCH_2$, Fox, Ray, Rubesin, and Schaefer III found strong evidence for a single bond from high accuracy ab initio calculations. These calculations have been extended by generating ab initio wave functions for $AlCH_2$, BCH_2, $HAlCH_2$, and $HBCH_2$ and making comparisons between them. The ground and first excited states of $AlCH_2$ are found to be single bonded: BCH_2 and $HBCH_2$ possess double bonds; $HAlCH_2$ is intermediate. The origin of these results has been investigated by analysis of orbital compositions, charge density difference maps, and energies. Considerable insight has been gained into the long-standing problem of multiple vs. single bonding in the second and third rows of the periodic table. Our results also suggest that control of Al substituent electronegativity can impose AlC bond order changes from 1 to 2.

Introduction

This paper is an extension of the recent important study by Fox, Ray, Rubesin, and Schaefer[1] on the organometallic model compounds $AlCH_3$, $AlCH_2$, and AlCH. The molecule $AlCH_2$ is of particular note because its dissociation energy, dipole moment, and bond length in the ground state is more representative of the Lewis dot structure, :Al—$\dot{C}H_2$, than the expected double bonded structure, ·Al=CH_2. Thus, Schaefer et al. found the optimized Al—C bond length in $AlCH_2$ (using a double-ζ basis set) to be 1.989 Å while a value of 2.013 Å was obtained for $AlCH_3$. Dissociation energies (using a double-ζ plus polarization basis and a two reference state CI) were 77.4 kcal/mol (Al—CH_2) and 67.8 kcal/mol (Al—CH_3).

One reason for special interest in these species is the long-standing question of multiple bonding between atoms of the second and third rows. In this respect we investigate some aspects of the Al—C bonding in $AlCH_2$ by comparative calculations on $AlCH_2$, $HAlCH_2$ and their boron analogues BCH_2 and $HBCH_2$.

Method

Energy-optimized geometries of $AlCH_2$, BCH_2, $HAlCH_2$, and $HBCH_2$ were determined ab initio by using the STO-3G basis set[2] in GAUSSIAN 70[3] (see Figure 1) with the force relaxation scheme of Pulay.[4] For reference, STO-3G optimized geometries of HAl, HB, and CH_2 are also reported (Figure 1). All open-shell SCF calculations were performed by using UHF wave functions, and closed-shells were calculated RHF.

In general, STO-3G level calculations have been found to give reliable geometries and our energy-optimized Al—C bond length in $^2B_1$ $AlCH_2$ (1.948 Å) compares well with the value calculated by Schaefer et al. (1.989 Å). We also find that our ground-state energy level ordering ($^2B_1$: $1a_1^2$, $1b_2^2$, $2a_1^2$, $1b_1$, $3a_1^2$) agrees with Schaefer's larger basis set. This substantial agreement supports the belief that the STO-3G basis set is adequate for explaining the qualitative nature of the bonding and characterizing the essential differences between the molecules in this study.

$AlCH_2$ and BCH_2. Energy Levels. Insight into why Al—C is a single bond in $AlCH_2$ can be gained from the one-electron energy levels of $AlCH_2$ (ground-state $^2B_1$) and its fragments ^2P Al and $^3B_1$ CH_2 (Figure 2a and Table I). Several features should be noted.

First, the orbital ordering shows a singly occupied $1b_1$ in $AlCH_2$ falling below the double occupied $3a_1$. This arises from the reduction in electron–electron repulsion upon removing one electron from the closed-shell species $AlCH_2^-$. Removal of an electron from the $1b_1$ results in a large stabilization of the remaining $1b_1$ electron and a smaller stabilization of the $3a_1$ electrons. This difference is accentuated by the large spatial separation of the $1b_1$ and $3a_1$ orbitals (the $1b_1$ is primarily a perpendicular p orbital on carbon while the $3a_1$ is a largely s lone pair on Al). A lesser effect is the differential stabilization of the α orbitals as a result of removing a $1b_1$ β electron. As shown, this splitting is greatest for those orbitals nearest the $1b_1$ β "hole" (i.e., $1a_1$). The reverse of this argument can be applied to the removal of a single electron from the $3a_1^\beta$ orbital. In this case, the remaining $3a_1^\alpha$ orbital would be expected to fall below the double-occupied $1b_1$ orbitals again because of the reduction in electron–electron repulsion. This in fact happens in BCH_2 (Figure 2b and Table I), leading to a $^2A_1$ ground state. The $1b_1$ itself mixes with the p_x of B where it did not in Al.

The second striking feature of the orbital level diagram for $AlCH_2$ (Figure 2a) is the destabilization of the "methylene" orbitals, namely, the $1a_1$, $1b_2$, $2a_1$, and $1b_1$ orbitals. This destabilization is countered by a large drop in the energy of the single Al p electron and the formation of the Al—C single bond (primarily the $2a_1$ orbital). Because of the sizeable electronegativity difference between Al and C, the methylene-like orbitals gain charge (destabilization) while Al loses charge (stabilization). That $AlCH_2$ should behave in this fashion can be seen in a third feature of the orbital level diagram—the single occupied orbitals of methylene ($2a_1$ and $1b_1$) fall below the doubly occupied Al 3s. Thus there is a mismatch of orbital energies. The 3s orbitals are not well suited for mixing with the methylene orbitals, but the 3p orbitals are much worse: in essence, the p's do not contribute greatly to the bonding. Instead, the lone p electron of Al will occupy the "s-like" $2a_1$ bonding orbital and the 3s electrons will become the $3a_1$ "s-like" lone pair. This can be formally likened to a charge-transfer process (to the $2a_1$ of methylene) followed by the formation of a coordinate-covalent bond to Al.[5]

(1) Fox, D. J.; Ray, D.; Rubesin, P. C.; Schaefer, H. F., III, *J. Chem. Phys.* **1980**, *73*, 3246.
(2) Hehre, W. J.; Stewart, R. F.; Pople, J. A. *J. Chem. Phys.* **1969**, *51*, 2657.
(3) Hehre, W. H.; Ditchfield, R.; Pople, J. A.; Latham, W.; Newton, M. D. GAUSSIAN 70, *QCPE* **1973**, *No. 236*.
(4) Pulay, P. *Mol. Phys.* **1969**, *17*, 197.
(5) Because of the formation of a coordinate covalent bond in the ground state the dipole moment is much smaller than might be expected on the basis of a simple charge-transfer process. A charge transfer to the $1b_1$ methylene orbital (leading to the $^2A_1$ excited state) does not permit the formation of the covalent coordinate bond and results in a higher dipole moment. (Schaefer reports a dipole moment of 3.15 D for the $^2A_1$ state and 0.74 D for the $^2B_1$ ground state.)

0276-7333/82/2301-0246$01.25/0

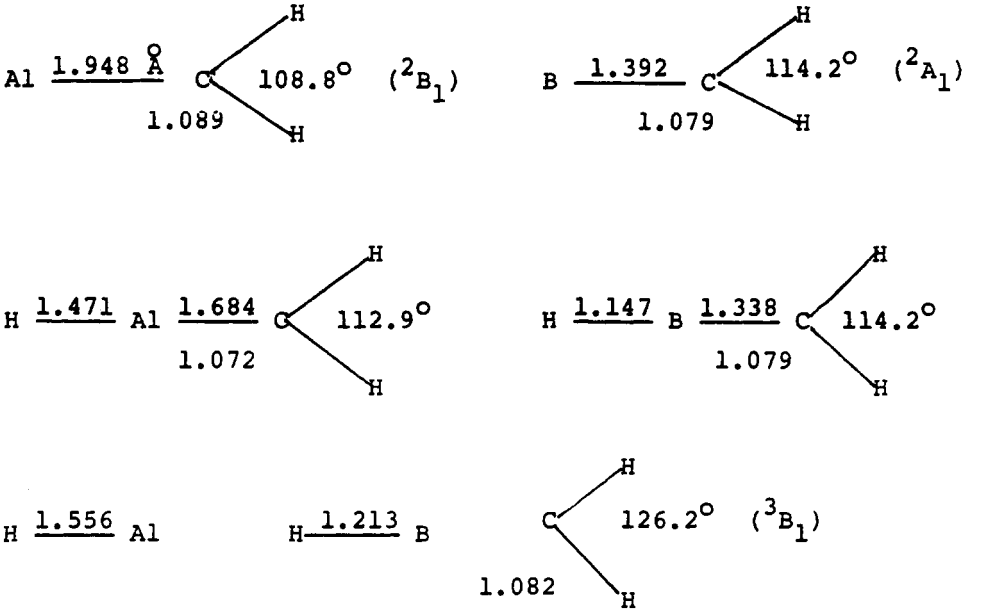

Figure 1. Optimized geometrical parameters (STO-3G) for $AlCH_2$, BCH_2, $HAlCH_2$, $HBCH_2$, HAl, HB, and CH_2.

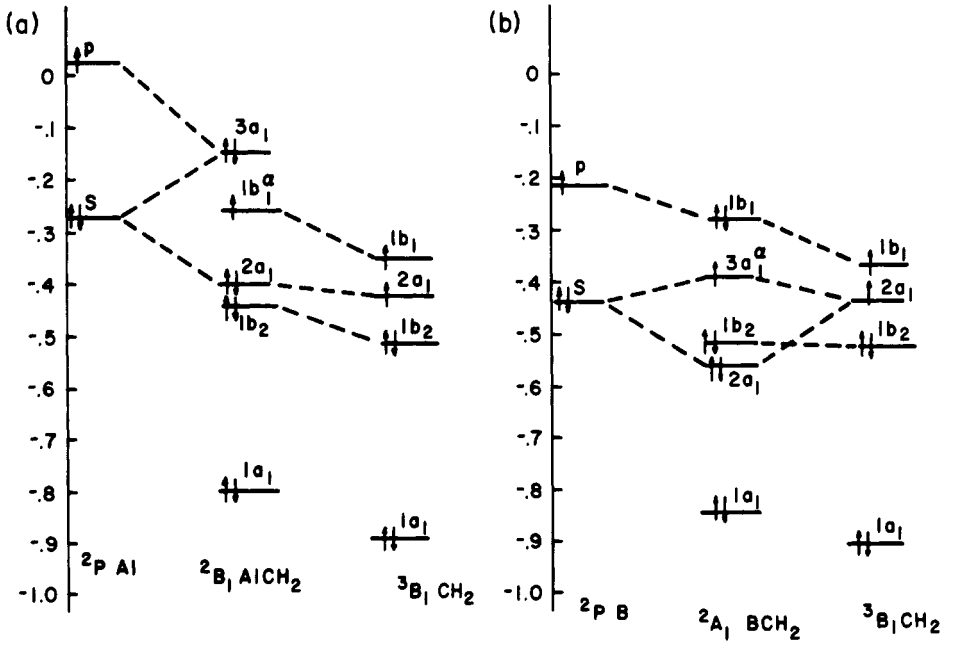

Figure 2. One-electron energy levels for α orbitals in (a) $AlCH_2$ and (b) BCH_2. All energies are in hartrees.

Table I. Molecular Orbital Energy Eigenvalues[a]

$AlCH_2$			BCH_2			$HAlCH_2$		$HBCH_2$	
	α	β		α	β				
$3a_1$	−0.1553	−0.1393	$1b_1$	−0.2635	−0.3012	$1b_1$	−0.1350	$1b_1$	−0.2739
$1b_1$	−0.2681		$3a_1$	−0.3744		$3a_1$	−0.3286	$3a_1$	−0.4950
$2a_1$	−0.4038	−0.3371	$1b_2$	−0.5041	−0.5129	$1b_2$	−0.4229	$1b_2$	−0.5148
$1b_2$	−0.4460	−0.4304	$2a_1$	−0.5506	−0.4960	$2a_1$	−0.4790	$2a_1$	−0.5928
$1a_1$	−0.8079	−0.7033	$1a_1$	−0.8259	−0.8672	$1a_1$	−0.7390	$1a_1$	−0.8623

[a] Energies are in hartrees.

For BCH_2 there is a strong stabilization of the $2a_1$ orbital upon formation of the B—C single bond consistent with the small difference in energy between the CH_2 $2a_1$ orbital and the B 2s orbital. The $3a_1$ orbital, made up from out-of-phase CH_2 and boron contributions, is stabilized by mixing with the unoccupied p_z orbital on B. This is possible for BCH_2 because the boron levels lie much closer to the CH_2 levels. The degree of charge transfer is much less in BCH_2 also. Thus there is only a slight destabilization of the $1a_1$ methylene-like orbital while the $1b_2$ orbital is essentially unchanged. In summary, the most important feature of Figure 2 is the stabilization of the 2s and 2p B orbitals relative to Al. The p orbitals are low enough to participate in the bonding leading to s,p mixing in the a_1 orbitals and π formation in the $1b_1$ orbitals of BCH_2.

Lewis Structures. In spite of modern advances in bonding theory, Lewis dot structures remain a remarkably powerful aid in guiding qualitative thinking.[6] It is

Table II. π orbital ($1b_1$) Mulliken Populations for M = Al and B

	M (%)	C (%)
$AlCH_2$	0.1142 (11)	0.9649 (89)
BCH_2	0.8877 (44)	1.1096 (56)
$HAlCH_2$	0.5673 (28)	1.4855 (72)
$HBCH_2$	0.8396 (42)	1.1603 (58)

therefore important to explore cases where a breakdown in the Lewis representation occurs, to make connection between Lewis structures and the quantum calculations, and to establish criteria that can help anticipate such cases. In contrast to the expected double bond in $AlCH_2$, the actual $^2B_1$ ground state is best pictured as :Al—$\dot{C}H_2$. This structure is entirely compatible with its Al—C bond length, Al—C dissociation energy, and small dipole moment (0.74 D). The $^2A_1$ state, now the first excited state instead of the expected ground state, contains an AlC double bond as one of the resonance contributors

$$\cdot Al{=}CH_2 \leftrightarrow \cdot Al^+{-}\ddot{C}H_2^-$$

We can estimate the dissociation energy of the $^2A_1$ state and compare it to that of the $^2B_1$ ground state in order to ascertain which of the above resonance contributors has the largest weight. The $^2A_1$ separates at infinity to ^2P Al + $^1A_1$ CH_2 which was been recently determined to be 10.9 kcal/mol higher[7] than the ^2P Al plus $^3B_1$ CH_2 separation of the $^2B_1$ ground state. Combining this value with the 22.9 kcal/mol $^2A_1 - {}^2B_1$ energy difference obtained from the double ζ with polarization plus CI calculation of Schaefer et al.[1] yields a $^2A_1$ dissociation energy of 65.4 kcal/mol, a smaller value than that of $^2B_1$ $AlCH_2$ or Al—CH_3. This line of reasoning points to the $\cdot Al^+$—$\ddot{C}H_2^-$ Lewis structure as a strong contributor (in spite of its six bonding electrons compared to eight in the double-bonding structure), and this assignment is supported by the 3.14 D dipole moment computed for the $^2A_1$. On the other hand, the internuclear separation is 1.802 Å, only 5% greater than the double bond length predicted form the average single-to-double bond length ratio generally observed.[6] As in the $^2B_1$ ground state, the origin of the reduced bond strength is mismatch in orbital energies between Al and methylene, in this case the Al p_x with $1b_1$ in CH_2. (Schaefer et al.[1] found a similarly weak bond with an extremely short (1.668 Å) AlC length in $^1\Sigma^+$ AlCH.) For BCH_2 the single structure, $\cdot B{=}CH_2$, is an adequate representation; the ionic structure can be eliminated by the usual arguments of formal charges (plus fewer bonding electrons).

As shown by the orbital energy levels discussed later, addition of hydrogen to BCH_2 leads to the expected Lewis dot structure H—B=CH_2. Addition of H to $AlCH_2$, on the other hand, shortens the AlC bond length by exactly that ratio expected in going from a single to a double bond. Nevertheless the AlC bond retains considerable ionic character and the two resonance contributors analogous to those for $^2A_1$ $AlCH_2$ are also those which must be considered here. As in that case, the bond strength is less, and the bond more polar, than that suggested by its length and associated Lewis structure, but there is considerably more double-bond character in $HAlCH_2$ than in $^2A_1$ $AlCH_2$.

The ability of a singly occupied orbital of intermediate electronegativity (like H) to significantly modify the aluminum carbon bond suggests the large range of organoaluminum compounds potentially available. It also suggests that a highly electronegative substituent should produce a full AlC double bond.

Orbital Composition. The molecular orbital shapes[8] (Figure 3a) further elucidate the bonding in $AlCH_2$. Because of the large differences in orbital energies between the aluminum and methylene, the lowest orbitals ($1a_1$ and $1b_2$) are essentially unchanged from their parent methylene orbitals. The $2a_1$ orbital consists largely of the methylene $2a_1$ with a small out-of-phase Al s contribution and can be interpreted as a coordinate covalent bond (recall that in the parent CH_2 orbitals, the $2a_1$ is only singly occupied). The singly occupied $1b_1$ is almost entirely localized on the carbon atom, thereby excluding the formation of even a partial π bond. Finally, the doubly occupied $3a_1$ shows a lone pair directed away from the Al—C bond and has a high degree of s character consistent with the poor energetics of the Al p orbitals. The directionality of the lone pair is obtained by an out-of-phase mixing with the methylene $2a_1$ orbital. The region of positive polarity enclosing the aluminum nuclei is primarily due to the radial node of the 3s orbital.

The bonding in BCH_2 stands in sharp contrast to that in $AlCH_2$. The B—C bond is unequivocally a double bond as shown by the shortening of the BC bond distance from 1.558 Å in BCH_3 to 1.392 Å in BCH_2 and by the shape of the $1b_1$ π orbital (Figure 3b). A comparison of the p_x Mulliken populations (Table I) displays a well-shared density between boron and carbon (44% on boron) while the singly occupied $1b_1$ in $AlCH_2$ is 89% on the carbon. The $1a_1$ orbitals in BCH_2 largely retain their CH_2 character, stabilized by a weak in-phase interaction with a B sp orbital. The $2a_1$ orbitals form the B—C σ bond from an in-phase combination of the CH_2 $2a_1$ and the boron s and p_z orbitals. The $2a_1^\alpha$ orbital is stabilized relative to the $2a_1^\beta$ orbital (because of the Fermi hole arising from the singly occupied $3a_1^\alpha$ orbital) and has more 2s character than the $2a_1^\beta$. The $1b_2$ orbitals are virtually unchanged from the CH_2 fragment. The singly occupied $3a_1$ consists of an sp hybrid on boron directed away from the CH_2 and a smaller contribution from the $2a_1$ CH_2 orbital in-phase with the tail of the B sp hybrid. Finally, the doubly occupied $1b_1$ is a pair of π spin orbitals with the α orbital polarized toward the boron (toward the Fermi hole) and the β orbital polarized toward carbon. The net polarization (as shown in Table I) is toward carbon.

Charge Density Difference Plots. The large differences in the bonding between $AlCH_2$ and BCH_2 is further illustrated in the charge density difference plots shown in Figure 4. These plots were generated from the total density minus the density of a spherically averaged Al (or B) atom (^2P ground state) and the density of the CH_2 biradical. This choice of reference fragments corresponds to that used in the MO splitting diagram, and the resultant plot shows the change in electron density upon formation of the bond. Both density plots are presented as two half planes through the C_{2v} axis. The xz plane contains the hydrogen atoms; the yz plane bisects the HCH angle.

The charge density difference plot for BCH_2 shows a large concentration of density in the yz plane at the expense of density in the xz plane. This shift is associated with the formation of the B—C π bond. (Since the reference density is based on spherically averaged boron

(6) DeKock, R. L.; Gray, H. B. "Chemical Structure and Bonding", Benjamin/Cummings: New York, 1980. Huheey, J. E. "Inorganic Chemistry"; Harper and Row: New York, 1978. Purcell, K. F.; Kotz, J. C. "Inorganic Chemistry"; W. B. Saunders: Philadelphia, Pa., 1977.

(7) Bauschlicher, C. W.; Shavitt, I. *J. Am. Chem. Soc.* **1978**, *100*, 739. As discussed in this article, there is one experimental measurement that suggests a $^3B_1 - {}^1A_1$ separation of 19.5 kcal/mol, but the resulting binding energy of $^2A_1$ $AlCH_2$ would still be less than that of its $^2B_1$ ground state.

(8) Jorgensen, W. L. *QCPE* **1977**, *No.* 340.

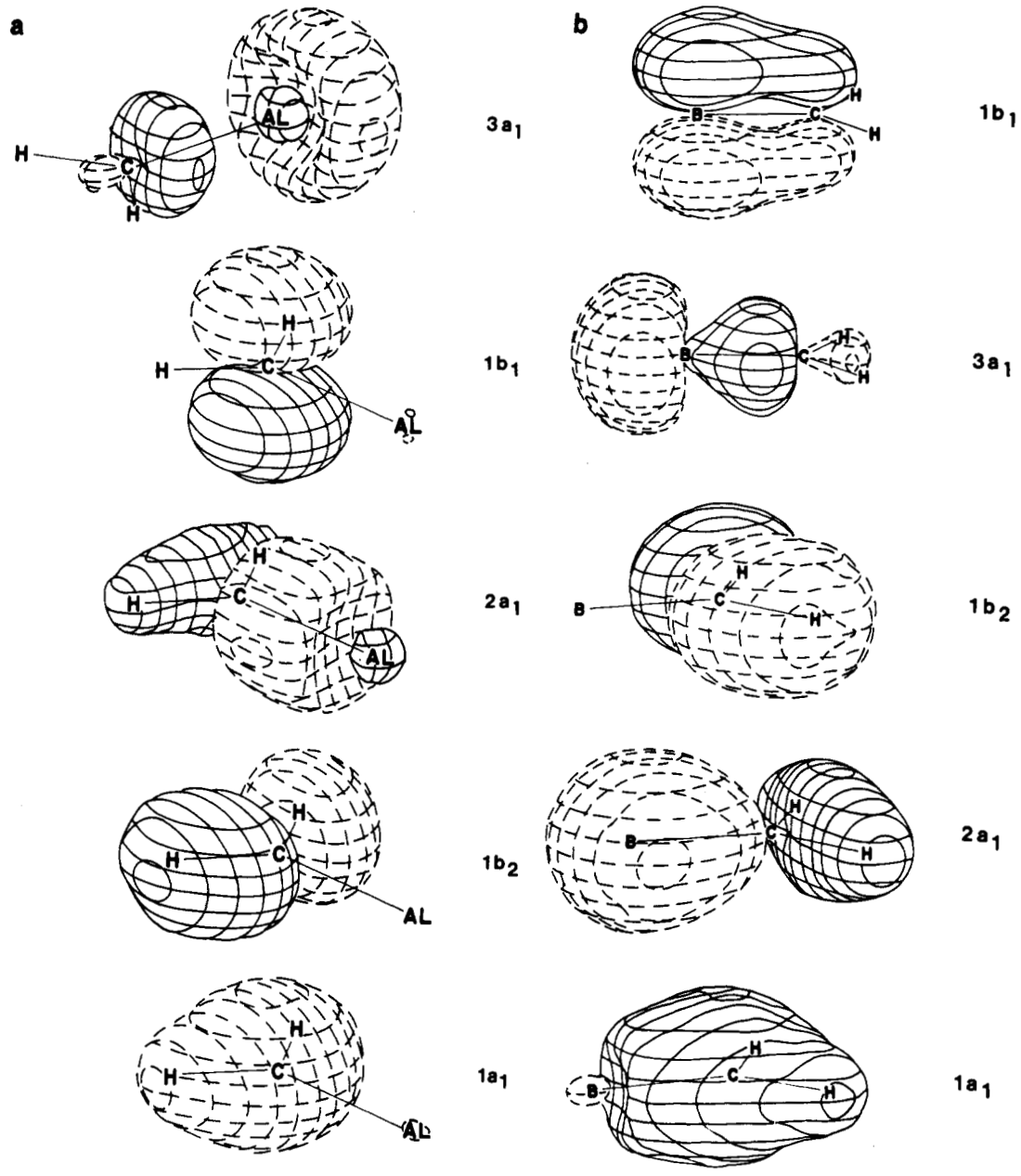

Figure 3. a. Valence orbitals for $AlCH_2$ (α spin). b. Valence orbitals for BCH_2 (α spin).

density, this shift reflects the orientation of the lone 2p electron of boron along the y axis.) There is also a large gain in charge along the B—C bond associated with the formation of the σ bond. The shape of this region, especially in the xz plane, is indicative of the covalent nature of the bond: both atoms contribute electrons to the region. Finally, there is a slight loss of density around the hydrogen atoms (relative to CH_2) and a gain in the region between them consistent with the increase in the HCH angle.

The corresponding plot for $AlCH_2$ shows a large loss in both the xz and yz planes in the region associated with the Al $3p_x$ and $3p_y$ orbitals and in the region along the Al—C bond nearest the aluminum. There is a large gain along the z axis both between the Al and C and in the Al lone pair region. The latter is due to the strong polarization of charge away from the Al as indicated in the $3a_1$ molecular orbital. The shape of the charge gain between the atoms is significantly different than in the boron case. Here the pattern is dominated by the gain of charge in the methylene $2a_1$ region and not by a sharing of charge. The pattern is essentially that of an ionic bond. (The smallness of the dipole moment is understandable: the dipole arising from the ionic bond is reduced by the polarization of the Al 3s electrons and by the small spatial separation of the component charges—which in turn is due to the hybridization of the carbon.) Also unlike the density in BCH_2 there is a region of large charge gain near the hydrogen atoms. This is another indication of the net gain on CH_2 by charge transfer from the aluminum. It is interesting that except for this region, the charge density difference plot has virtually pure σ symmetry.

$HAlCH_2$ and $HBCH_2$. To examine the effect of additional ligands on aluminum and boron, we have also carried out calculations for $HAlCH_2$ and $HBCH_2$[9] (geometries given in Figure 1). The AlC bond length in $HAlCH_2$ showed a considerable shortening relative to $AlCH_2$ (0.264 Å) while the BC bond length in $HBCH_2$ shortened only 0.054 Å compared to that of BCH_2. This is indicative of the formation of at least a partial aluminum carbon double bond.[10] Since the $3a_1$ orbital of $AlCH_2$ is doubly occupied,

(9) Previously reported: Dill, J. D.; Schleyer, P. v. R.; Pople, J. A. *J. Am. Chem. Soc.* **1975**, *97*, 3402.

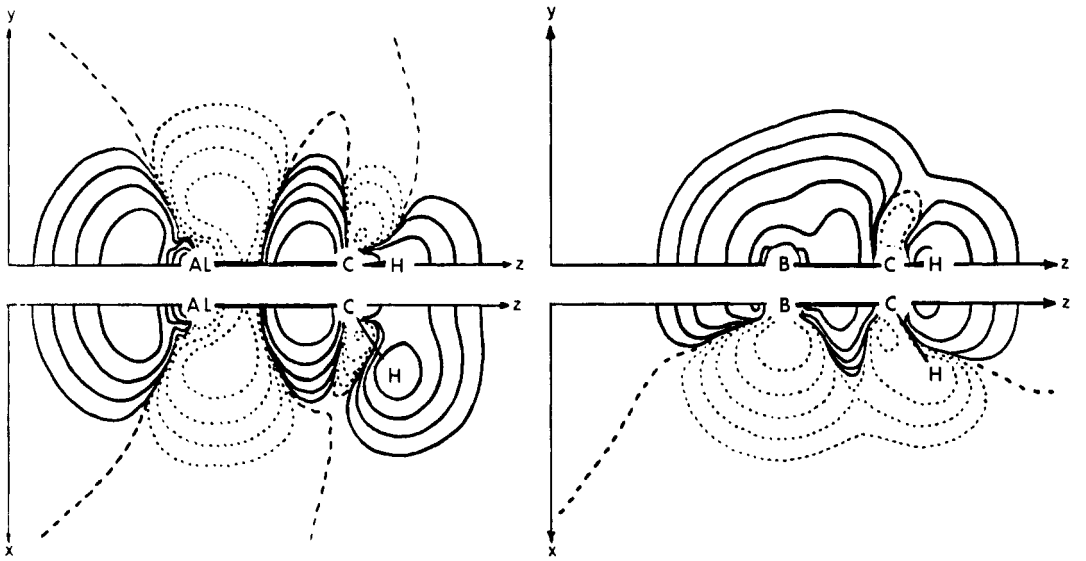

Figure 4. Charge density difference maps, $AlCH_2$ (left), BCH_2 (right). Total charge density minus spherical Al (B) minus CH_2 diradical in plane of molecule (xz) and the perpendicular plane (yz): solid lines, gain relative to separated fragments; dotted lines, loss; dashed lines, zero contour. Lowest gain (loss) contour is 0.000 316 e^-/a_0^3; successive contours increase by $10^{1/2}$.

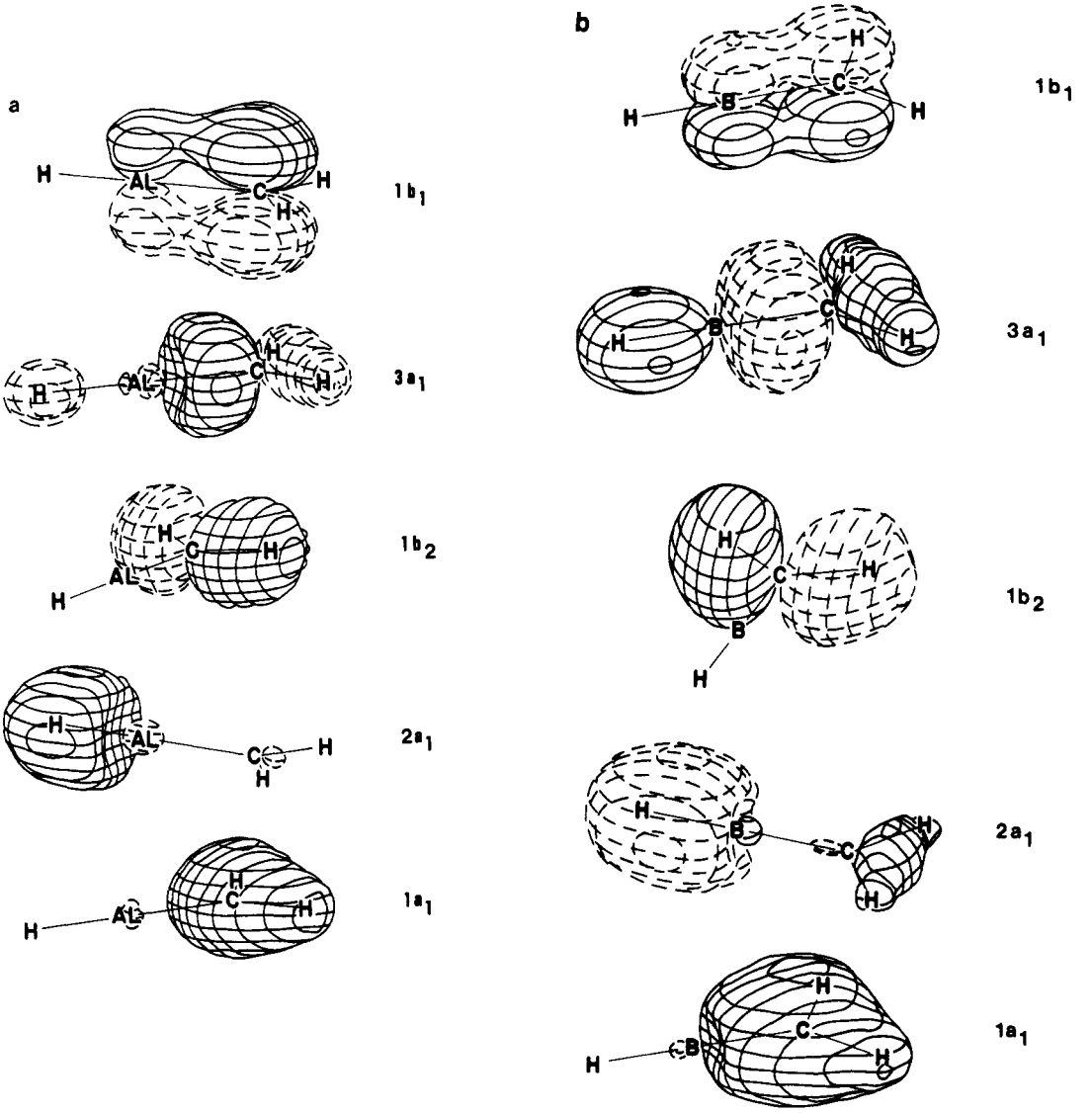

Figure 5. a. Valence orbitals for $HAlCH_2$. b. Valence orbitals for $HBCH_2$.

it is easiest to view the formation of $HAlCH_2$ as a protonation of the Al lone pair followed by the addition of an electron to the LUMO $1b_1^{\beta}$ orbital. The orbitals in $HAlCH_2$ and $HBCH_2$ are compared in parts a and b, re-

spectively, of Figure 5. The principal effect of the hydrogen is stabilization of the $3a_1$ orbital and withdrawal of charge from the aluminum. The charge withdrawal has two effects. First, it stabilizes the 3s Al orbitals by increasing the positive charge on Al, thus allowing them to participate more fully in bonding. Secondly, it greatly reduces the electron–electron repulsion between the $2a_1$ and the $3a_1$ orbitals. Both effects will tend to reduce the Al—C bond length. A shorter bond length also increases the Al $3p_x$—C $2p_x$ overlap leading to additional stabilization of the $1b_1$ orbital. We note, however, that the relative Mulliken population of the $1b_1$ orbital on the Al is only 28% (11% in $AlCH_2$) and thus remains highly polarized.

(10) As suggested by a reviewer, a thermodynamic measure of the degree of XC double bonding in these compounds as well as $AlCH_2$ and BCH_2 might be obtained by considering isodesmic reactions of the form

$$HXCH_2 + XH_n \rightarrow XCH_2 + XH_{n+1} \quad (1)$$

$$XH_2 + XH_n \rightarrow XH + XH_{n+1} \quad X = B, Al;\ n = 0, 1, 2 \quad (2)$$

In the table below we give heats of reaction for these two reactions with the same basis set employed throughout our study.

ΔE_m, kcal/mol	reaction 1		reaction 2	
n	X = Al	X = B	X = Al	X = B
0	−66.0	+29.7	−142.5	−48.1
1	+76.5	+77.8	0.0	0.0
2	−177.3	−87.3	−253.8	−165.1

It is clear from the energies for the second reaction that bonding to either Al or B is very sensitive to the value of n. This variability makes it difficult to evaluate changes in the XC bonding from reaction 1. Although the trends are interesting and worthy of future study, the differences in spin multiplicity and coordination number make a detailed analysis at the minimal basis set level impractical.

Note Added in Proof. We have implicitly assumed the BC double bonded species, $B{=}CH_2$ and $HB{=}CH_2$, to be the expected and normally occurring reference compounds. However, BC double bonds have not, in fact, been observed (Onak, Thomas "Organoborane Chemistry"; Academic Press: New York, 1975; p 4). This fact undoubtedly derives from the relative stability of isomers with BC single bonds and therefore does not invalidate the BC double bonds we have calculated. It may actually enhance the value of our computational results because they elucidate the nature of a bond which has proved difficult to isolate experimentally.

Acknowledgment. We wish to thank the NIH (Grant GM 26462) for financial support.

Registry No. $AlCH_2$, 76392-50-2; BCH_2, 79435-75-9; $HAlCH_2$, 79435-76-0; $HBCH_2$, 56125-75-8.

The Molybdenum–Molybdenum Triple Bond. 11.[1] 1,1- and 1,2-Disubstituted Dimolybdenum Compounds of Formula $Mo_2X_2(CH_2SiMe_3)_4$ (M≡M). Observation of Rotation about the Triple Bond

M. H. Chisholm,* K. Folting, J. C. Huffman, and I. P. Rothwell

Department of Chemistry and Molecular Structure Center, Indiana University, Bloomington, Indiana 47405

Received August 3, 1981

The preparation and characterization of a series of compounds of general formula $Mo_2X_2R_4$ (M≡M), where X = Br, Me, O-*i*-Pr, O-*t*-Bu, and NMe_2 and R = CH_2SiMe_3, are reported. The pattern of substitution may be 1,1-, $X_2RMo{\equiv}MoR_3$, or 1,2-, $XR_2Mo{\equiv}MoR_2X$, depending upon the nature of X and the preparative route. The 1,1- and 1,2-$Mo_2X_2R_4$ compounds do not isomerize, demonstrating the existence of a high kinetic barrier to R and X group transfer between molybdenum atoms. Alkyl group transfer may occur during the substitution reaction: 1,2-$Mo_2Br_2R_4$ and $LiNMe_2$ (2 equiv) yield 1,1-$Mo_2(NMe_2)_2R_4$, whereas 1,2-$Mo_2Br_2R_4$ and $HNMe_2$ yield 1,2-$Mo_2(NMe_2)_2R_4$. The formation of one isomer of $Mo_2(NMe_2)_2R_4$ must occur by kinetic control. Variable-temperature ^1H NMR spectra for 1,1- and 1,2-$Mo_2(NMe_2)_2R_4$ compounds provide the first observation of rotation about the Mo≡Mo bond. The energy barriers to rotation are reconcilable with steric restraints. By contrast, the barriers to rotations about Mo—N bonds in the 1,1- and 1,2-$Mo_2(NMe_2)_2R_4$ compounds are ΔG^* (kcal mol^{-1}) = 11.5 ± 0.5 and 15.0 ± 0.5, respectively, and the difference is correlated with electronic factors. The structure of 1,2-Mo_2(O-*t*-Bu)$_2R_4$, determined by a single-crystal X-ray diffraction study, revealed a staggered ethane-like (C_{2h}) *anti*-$Mo_2O_2C_4$ central skeleton with Mo—Mo = 2.209 (2) Å, Mo—O = 1.865 (8) Å, and Mo—C = 2.13 (1) and 2.14 (1) Å and internal angles Mo—Mo—O = 110.7 (3)° and Mo—Mo—C = 100.1 (5)° (averaged). Crystal data at −163 °C were a = 10.025 (3) Å, b = 18.473 (9) Å, c = 9.975 (5) Å, β = 102.03 (3)°, Z = 2, and d_{calcd} = 1.263 g cm^{-1} with space group $P2_1/n$. These new observations are discussed in the light of previous work.

Introduction

In the first paper of this series, the preparation and detailed characterization of $Mo_2(NMe_2)_6$ (M≡M) was reported.[2] This compound has since been the parent of an extensive family of others and affords an easy entry into the rich chemistry associated with the Mo≡Mo bond in Mo_2^{6+}-containing compounds.[3,4] Two views of the Mo_2-

(1) Chisholm, M. H.; Huffman, J. C.; Rothwell, I. P. *Inorg. Chem.* **1981**, *20*, 2215.

(2) Chisholm, M. H.; Cotton, F. A.; Frenz, B. A.; Reichert, W. W.; Shive, L. W.; Stults, B. R. *J. Am. Chem. Soc.* **1976**, *98*, 4469.

(3) Chisholm, M. H.; Cotton, F. A. *Acc. Chem. Res.* **1978**, *11*, 356.

(4) Chisholm, M. H. *Symp. Faraday Soc.* **1980**, *No. 14*, 194.

0276-7333/82/2301-0251$01.25/0

spectively, of Figure 5. The principal effect of the hydrogen is stabilization of the $3a_1$ orbital and withdrawal of charge from the aluminum. The charge withdrawal has two effects. First, it stabilizes the 3s Al orbitals by increasing the positive charge on Al, thus allowing them to participate more fully in bonding. Secondly, it greatly reduces the electron–electron repulsion between the $2a_1$ and the $3a_1$ orbitals. Both effects will tend to reduce the Al—C bond length. A shorter bond length also increases the Al $3p_x$—C $2p_x$ overlap leading to additional stabilization of the $1b_1$ orbital. We note, however, that the relative Mulliken population of the $1b_1$ orbital on the Al is only 28% (11% in $AlCH_2$) and thus remains highly polarized.

(10) As suggested by a reviewer, a thermodynamic measure of the degree of XC double bonding in these compounds as well as $AlCH_2$ and BCH_2 might be obtained by considering isodesmic reactions of the form

$$HXCH_2 + XH_n \rightarrow XCH_2 + XH_{n+1} \quad (1)$$

$$XH_2 + XH_n \rightarrow XH + XH_{n+1} \quad X = B, Al;\ n = 0, 1, 2 \quad (2)$$

In the table below we give heats of reaction for these two reactions with the same basis set employed throughout our study.

ΔE_m, kcal/mol	reaction 1		reaction 2	
n	X = Al	X = B	X = Al	X = B
0	−66.0	+29.7	−142.5	−48.1
1	+76.5	+77.8	0.0	0.0
2	−177.3	−87.3	−253.8	−165.1

It is clear from the energies for the second reaction that bonding to either Al or B is very sensitive to the value of n. This variability makes it difficult to evaluate changes in the XC bonding from reaction 1. Although the trends are interesting and worthy of future study, the differences in spin multiplicity and coordination number make a detailed analysis at the minimal basis set level impractical.

Note Added in Proof. We have implicitly assumed the BC double bonded species, $B{=}CH_2$ and $HB{=}CH_2$, to be the expected and normally occurring reference compounds. However, BC double bonds have not, in fact, been observed (Onak, Thomas "Organoborane Chemistry"; Academic Press: New York, 1975; p 4). This fact undoubtedly derives from the relative stability of isomers with BC single bonds and therefore does not invalidate the BC double bonds we have calculated. It may actually enhance the value of our computational results because they elucidate the nature of a bond which has proved difficult to isolate experimentally.

Acknowledgment. We wish to thank the NIH (Grant GM 26462) for financial support.

Registry No. $AlCH_2$, 76392-50-2; BCH_2, 79435-75-9; $HAlCH_2$, 79435-76-0; $HBCH_2$, 56125-75-8.

The Molybdenum–Molybdenum Triple Bond. 11.[1] 1,1- and 1,2-Disubstituted Dimolybdenum Compounds of Formula $Mo_2X_2(CH_2SiMe_3)_4$ (M≡M). Observation of Rotation about the Triple Bond

M. H. Chisholm,* K. Folting, J. C. Huffman, and I. P. Rothwell

Department of Chemistry and Molecular Structure Center, Indiana University, Bloomington, Indiana 47405

Received August 3, 1981

The preparation and characterization of a series of compounds of general formula $Mo_2X_2R_4$ (M≡M), where X = Br, Me, O-*i*-Pr, O-*t*-Bu, and NMe_2 and R = CH_2SiMe_3, are reported. The pattern of substitution may be 1,1-, $X_2RMo{\equiv}MoR_3$, or 1,2-, $XR_2Mo{\equiv}MoR_2X$, depending upon the nature of X and the preparative route. The 1,1- and 1,2-$Mo_2X_2R_4$ compounds do not isomerize, demonstrating the existence of a high kinetic barrier to R and X group transfer between molybdenum atoms. Alkyl group transfer may occur during the substitution reaction: 1,2-$Mo_2Br_2R_4$ and $LiNMe_2$ (2 equiv) yield 1,1-$Mo_2(NMe_2)_2R_4$, whereas 1,2-$Mo_2Br_2R_4$ and $HNMe_2$ yield 1,2-$Mo_2(NMe_2)_2R_4$. The formation of one isomer of $Mo_2(NMe_2)_2R_4$ must occur by kinetic control. Variable-temperature ^1H NMR spectra for 1,1- and 1,2-$Mo_2(NMe_2)_2R_4$ compounds provide the first observation of rotation about the Mo≡Mo bond. The energy barriers to rotation are reconcilable with steric restraints. By contrast, the barriers to rotations about Mo—N bonds in the 1,1- and 1,2-$Mo_2(NMe_2)_2R_4$ compounds are ΔG^* (kcal mol^{-1}) = 11.5 ± 0.5 and 15.0 ± 0.5, respectively, and the difference is correlated with electronic factors. The structure of 1,2-Mo_2(O-*t*-Bu)$_2R_4$, determined by a single-crystal X-ray diffraction study, revealed a staggered ethane-like (C_{2h}) *anti*-$Mo_2O_2C_4$ central skeleton with Mo—Mo = 2.209 (2) Å, Mo—O = 1.865 (8) Å, and Mo—C = 2.13 (1) and 2.14 (1) Å and internal angles Mo—Mo—O = 110.7 (3)° and Mo—Mo—C = 100.1 (5)° (averaged). Crystal data at −163 °C were a = 10.025 (3) Å, b = 18.473 (9) Å, c = 9.975 (5) Å, β = 102.03 (3)°, Z = 2, and d_{calcd} = 1.263 g cm^{-1} with space group $P2_1/n$. These new observations are discussed in the light of previous work.

Introduction

In the first paper of this series, the preparation and detailed characterization of $Mo_2(NMe_2)_6$ (M≡M) was reported.[2] This compound has since been the parent of an extensive family of others and affords an easy entry into the rich chemistry associated with the Mo≡Mo bond in Mo_2^{6+}-containing compounds.[3,4] Two views of the Mo_2-

(1) Chisholm, M. H.; Huffman, J. C.; Rothwell, I. P. *Inorg. Chem.* **1981**, *20*, 2215.

(2) Chisholm, M. H.; Cotton, F. A.; Frenz, B. A.; Reichert, W. W.; Shive, L. W.; Stults, B. R. *J. Am. Chem. Soc.* **1976**, *98*, 4469.

(3) Chisholm, M. H.; Cotton, F. A. *Acc. Chem. Res.* **1978**, *11*, 356.

(4) Chisholm, M. H. *Symp. Faraday Soc.* **1980**, *No. 14*, 194.

0276-7333/82/2301-0251$01.25/0

Scheme I

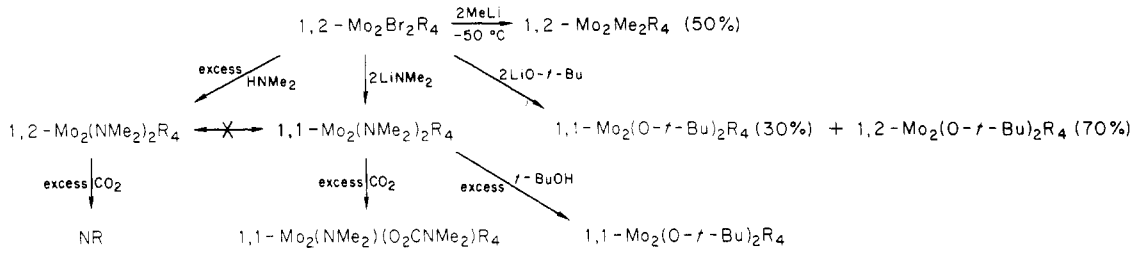

$1,1\text{-}Mo_2X_2R_4 = MoX_2R{\equiv}MoR_3$; $1,2\text{-}Mo_2X_2R_4 = MoXR_2{\equiv}MoXR_2$

$(NMe_2)_6$ molecule are shown from which it can be seen that there are six proximal and six distal methyl groups.

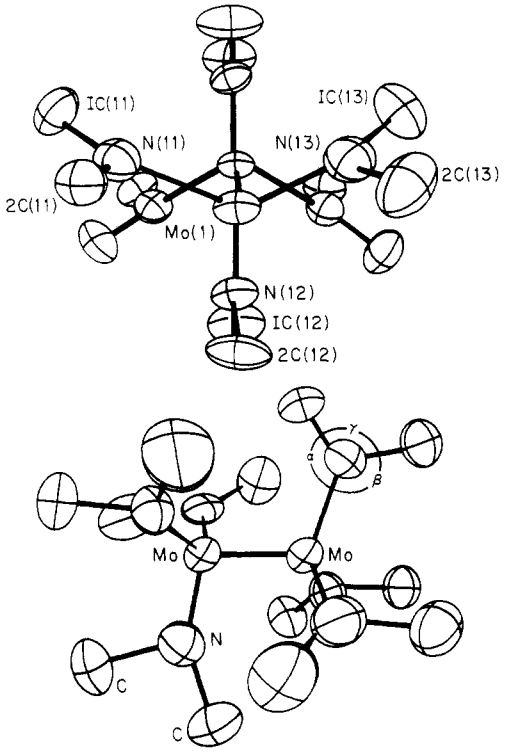

On the ^1H NMR time scale, these interconvert slowly at low temperature (<−60 °C) and rapidly at high temperature (>+60 °C), and the observation of this phenomenon is heightened by the large diamagnetic anisotropy exerted by the Mo≡Mo bond. We attributed[2] this proximal ⇌ distal methyl exchange to rotations about the Mo—N bonds. Subsequently, the characterization of the related compounds $1,2\text{-}W_2Cl_2(NEt_2)_4$[5] and $1,2\text{-}W_2(Me)_2(NEt_2)_4$[6] supported this mechanism over seemingly all reasonable alternate mechanisms. Two questions which were raised in the discovery of $Mo_2(NMe_2)_6$ have, however, remained unanswered. (1) Is there rotation about the Mo≡Mo bond and what factors influence the barrier to rotation?[7] (2) Do NMe_2 groups pass between the directly bonded molybdenum atoms? This type of scrambling, which is so common in dinuclear and polynuclear carbonyl chemistry,[8] might seem eminently reasonable for $Mo_2(NMe_2)_6$, since bridging dialkylamido ligands are known, e.g., as in $Cr_2(O_2CNEt_2)_4(\mu\text{-}NEt_2)_2$.[9]

Further work led to the isolation and characterization of $1,2\text{-}M_2R_2(NR'_2)_4$ compounds, where R = alkyl, R′ = Me or Et, and M = Mo and W.[10] These compounds exist in solution as mixtures of anti and gauche rotamers and show activation barriers to anti ⇌ gauche isomerization in the range 21–25 kcal mol^{-1}, depending on the nature of R and R′.[11] The mechanism of this isomerization either could involve a direct rotation about the M≡M bond or could be achieved by an indirect route in which NR_2 groups were scrambled across the Mo≡Mo bond.

Being afflicted with this uncertainty, we resolved to synthesize related molecules for which these two processes would be distinguishable. Since the cogging effect of the interlocking NC_2 units in $M_2R_2(NMe_2)_4$ compounds could be responsible for hindering rotation about the Mo≡Mo bond, we set out to prepare related $Mo_2X_2(CH_2SiMe_3)_4$ compounds which would be less sterically encumbered and would have methylene protons placed as stereochemical probes adjacent to the central Mo≡Mo bond. For an ethane-like molecule, these methylene protons would have to be diastereotopic, but a fluxional process involving passage through an intermediate or transition state of the type shown below would cause the methylene protons to be equivalent.

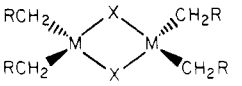

We report work which was prompted by these considerations. Preliminary reports of some of this work have appeared.[12,13]

Results and Discussion

Preparation of $Mo_2X_2R_4$ Compounds (R = CH_2SiMe_3). The careful addition of anhydrous HBr (2 equiv) to a saturated solution of $Mo_2(CH_2SiMe_3)_6$[14] in hexane at −78 °C leads to the precipitation of crude $1,2\text{-}Mo_2Br_2R_4$ and the formation of Me_4Si. The analytically pure compound $1,2\text{-}Mo_2Br_2R_4$ can be obtained by room-

(5) Chisholm, M. H.; Cotton, F. A.; Extine, M. W.; Millar, M.; Stults, B. R. *J. Am. Chem. Soc.* **1976**, *98*, 4486.
(6) Chisholm, M. H.; Cotton, F. A.; Extine, M. W.; Stults, B. R. *Inorg. Chem.* **1976**, *15*, 2244.
(7) For a nonlinear molecule having a triple bond consisting of a σ bond and two equivalent π bonds, which is therefore cylindrical; there should be no electrical barrier to rotation. For a detailed discussion of the Mo≡Mo bond in these molecules, see: Cotton, F. A. *Acc. Chem. Res.* **1978**, *11*, 225.
(8) Adams, R. D.; Cotton, F. A. In "Dynamic Nuclear Resonance Spectroscopy", Jackman, L. M., Cotton, F. A., Eds.; Academic Press: New York, 1975; p 489.
(9) Chisholm, M. H.; Cotton, F. A.; Extine, M. W.; Rideout, D. C. *Inorg. Chem.* **1978**, *17*, 3536.
(10) Chisholm, M. H.; Haitko, D. A. *J. Am. Chem. Soc.* **1979**, *101*, 6784. Chisholm, M. H.; Folting, K.; Haitko, D. A.; Huffman, J. C. *Ibid.* **1981**, *103*, 4046.
(11) Chisholm, M. H.; Extine, M. W. *J. Am. Chem. Soc.* **1976**, *98*, 6393.
(12) Chisholm, M. H.; Rothwell, I. P. *J. Am. Chem. Soc.* **1980**, *102*, 5950.
(13) Chisholm, M. H.; Rothwell, I. P. *J. Chem. Soc., Chem. Commun.* **1980**, 985.
(14) Huq, F.; Mowat, W.; Shortland, A.; Shapski, A. C.; Wilkinson, G. *J. Chem. Soc., Chem. Commun.* **1971**, 1071.

Table I. Analytical and Other Characterization Data for Compounds $Mo_2X_2(CH_2SiMe_3)_4$ [a]

compd	appearance	elemental analyses: C found	C calcd	H found	H calcd	X found	X calcd
1,2-$Mo_2Br_2R_4$	orange needles	27.8	27.7	6.42	6.36	23.14 [b]	23.3
1,2-$Mo_2Me_2R_4$	brown crystals	37.9	37.7	8.83	9.01		
1,1-$Mo_2(NMe_2)_2R_4$	yellow liquid	38.2	37.9	8.98	8.42	4.46 [c]	4.57
1,2-$Mo_2(NMe_2)_2R_4$	yellow liquid	38.2	36.2	8.98	8.43	4.46 [c]	4.71
1,1'-$Mo_2(NMe_2)(O_2CNMe_2)R_4$	brown liquid	37.5	36.9	8.39	8.76	4.76 [c]	4.91
1,2-$Mo_2(O\text{-}t\text{-}Bu)_2R_4$	red crystals	40.9	39.8	9.08	8.94		

[a] All compounds, including 1,1-$Mo_2(O\text{-}t\text{-}Bu)_2R_4$ and 1,2-$Mo_2(O\text{-}i\text{-}Pr)_2R_4$, for which elemental analyses were not obtained, gave molecular ions, $M_2X_2R_4^+$, in the mass spectrometer. [b] X = Br. [c] X = N.

temperature hexane extraction of this precipitate, followed by condensation of the solution and low-temperature crystallization. 1,2-$Mo_2Br_2R_4$ is only very sparingly soluble in hexane at low temperatures but is much more soluble in benzene and toluene. In the above procedure, any unreacted $Mo_2(CH_2SiMe_3)_6$ and the monobromo compound Mo_2BrR_5 (discussed later) remain in the mother liquid: only $Mo_2Br_2R_4$ and further bromo-substituted products are precipitated from the cold hexane solution and only 1,2-$Mo_2Br_2R_4$ dissolves in hexane at room temperature. We have not isolated any product of formula $Mo_2Br_xR_{6-x}$, where $x > 2$ as a hydrocarbon-soluble species. Related reactions involving anhydrous HCl (2 equiv) did not yield 1,2-$Mo_2Cl_2R_4$: only hexane-insoluble products and unreacted $Mo_2(CH_2SiMe_3)_6$ were recovered.

The bromide ligands in 1,2-$Mo_2Br_2R_4$ are labile to a number of metathetic reactions involving organolithium reagents, and some of these reactions and their products are summarized in Scheme I. Analytical data and other characteristics of the $Mo_2X_2R_4$ compounds are given in Table I. All the new compounds are air-sensitive and must be handled under dry and oxygen-free conditions. They are all soluble in hydrocarbon solvents and show molecular ions in the mass spectrometer. The calculated m/e distribution for the $Mo_2(NMe_2)_2R_4^+$ ion is shown in Figure 1. An identical m/e pattern was seen for both 1,1 and 1,2 isomers.

^{1}H NMR Studies. The substitution pattern 1,1- or 1,2- in $Mo_2X_2R_4$ compounds is readily deduced by ^{1}H NMR spectroscopy.[15] The compounds 1,2-$Mo_2X_2R_4$, where X = Me, O-*i*-Pr, O-*t*-Bu, and Br, show only one type of X group and one $SiMe_3$ resonance; the methylene protons which are diastereotopic appear as either an AB or AX spectrum. The chemical shift separation between the H_aH_b resonances increases in the order Me < O-*i*-Pr ~ O-*t*-Bu < Br, with the latter being ca. 4 ppm. The spectra are essentially temperature invariant in the range −50 to +90 °C at 220 MHz. These observations are interpretable in terms of either the existence of (i) only the anti rotamer, (ii) a rapidly (NMR time scale) interconverting mixture of anti and gauche rotamers, or (iii) a frozen out mixture of anti and gauche rotamers in which the methylene protons of the three R groups are accidentally magnetically degenerate. We are inclined to discount the last, since the shielding effects of the Mo≡Mo bond and the X group are so pronounced in all the other cases. By analogy with the $Mo_2X_2(NMe_2)_4$ compounds,[10] it is likely that in hydrocarbon solvents 1,2-$Mo_2X_2R_4$ compounds exist in the anti rotamer for X = Br ($\mu = 0$), while for X = Me, O-*i*-Pr, and O-*t*-Bu, a mixture of rapidly interconverting anti and gauche rotamers is present. By studies of the vibrational spectra and dipole moments, this point could have been established, but, as is shown below, it was not a necessary step in establishing the dynamic properties of the class as a whole.

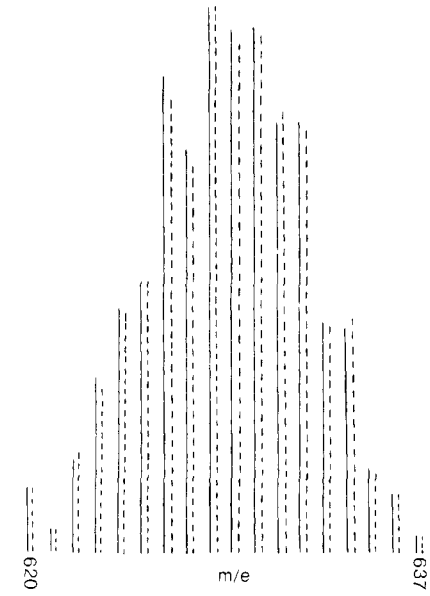

Figure 1. Observed (solid) vs. calculated (dotted) m/e distribution for the ion $Mo_2(NMe_2)_2(CH_2SiMe_3)_4^+$.

At −45 °C, 220 MHz in toluene-d_8, 1,2-$Mo_2(NMe_2)_4R_4$ shows two types of R groups in the integral ratio 1:1, each having diastereotopic methylene protons. There is only one type of NMe_2 group, though this gives rise to two singlets (1:1) assignable to proximal and distal methyl groups. Upon raising the temperature in toluene, the *N*-methyl resonances initially broaden, collapse into the base line, and sharpen to a singlet as rotations about the Mo—N bonds become fast on the NMR time scale. The resonances of the CH_2SiMe_3 groups show interesting changes with temperature, and at +95 °C, there is a single $SiMe_3$ resonance and an AB quartet for the methylene proton signals. The low-temperature spectrum is consistent with the presence of only the *gauche*-1,2-MoX_2R_2 isomer, while at high temperatures, rapid rotation about the Mo≡Mo bond leads to a time averaged spectrum akin to that expected for the *anti*-1,2-$Mo_2X_2R_4$ isomer. The threshold mechanism for rotation about the Mo≡Mo bond could be either gauche ⇌ gauche′ (enantiomerization) or gauche ⇌ anti ⇌ gauche. By analogy with R_2HSi—$SiHR_2$ molecules, the latter would seem more likely.[16] In any event, it is evident that a pairwise exchange of NMe_2 groups between the two molybdenum atoms of the type described in the Introduction is not occurring since this

(15) ^{1}H NMR spectra for 1,1- and 1,2-$Mo_2(NMe_2)_2R_4$, 1,2-$Mo_2Br_2R_4$, and 1,1′-$Mo_2(NMe_2)(O_2CNMe_2)R_4$ have been shown in ref 13 and 14.

(16) Baxter, S. G.; Dougherty, D. A.; Hummel, J. P.; Blount, J. F.; Mislow, K. *J. Am. Chem. Soc.* **1978**, *100*, 7795 and references cited therein.

would generate a plane of molecular symmetry and cause the methylene protons to collapse to a single resonance.

The low-temperature ^1H NMR spectrum for 1,1-$Mo_2(NMe_2)_2R_4$ in toluene-d_8 at 220 MHz shows three $SiMe_3$ signals in the integral ratio 1:1:2. The methylene proton resonances appear as an AB quartet, [4 H], and two singlets, [2 H] and [2 H]. There are also two signals in the integral ratio 1:1 assignable to proximal and distal *N*-methyl groups. This is entirely in accord with the predictions based on a consideration of the Newman projection shown below for a 1,1-disubstituted ethane-like diamer.

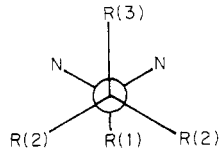

The methylene carbons associated with R(1) and R(3) are contained in the plane of symmetry of the molecule, and thus, with free rotation about Mo—C and C—Si bonds (fast on the NMR time scale), the methylene protons of each group are equivalent but, of course, different from each other (R(1) ≠ R(2)). The methylene protons associated with R(2), on the other hand, are diastereotopic: irrespective of rotations about Mo—C and C—Si bonds, they are never equivalent.

Upon raising the temperature, the proximal and distal *N*-methyl resonances initially broaden, then collapse into the base line, and finally (>60 °C), reform to a sharp singlet as proximal ⇌ distal exchange becomes rapid due to rotation about the Mo—N bonds. With increasing temperature, one of the singlets of the methylene groups and the AB quartet broaden, collapse, and reform as a singlet. The high-temperature limiting spectrum at 100 °C, 220 MHz, thus shows one *N*-methyl resonance, [12 H], two singlets, [2 H]:[6 H], for the methylene protons, and two singlets for the $SiMe_3$ protons, [9 H]:[27 H]. These observations are *only* interpretable in terms of a temperature-dependent rate of rotation about the Mo≡Mo bond. At +100 °C, R(2) and R(3) are rapidly interconverting, but not exchanging with R(1). Indeed, the fact that 1,1- and 1,2-$Mo_2(NMe_2)_2R_4$ compounds do not isomerize to an equilibrium mixture indicates that alkyl group transfer across the Mo≡Mo bond does not occur to any significant extent below 100 °C. Thus, formation of bridged intermediates or transition states for $Mo_2(NMe_2)_2R_4$ compounds must have a high energy of activation.

A similar conclusion can be made for 1,1- and 1,2-$Mo_2(O\text{-}t\text{-}Bu)_2R_4$ compounds. The 1,1 compound is obtained by addition of *t*-BuOH to 1,1-$Mo_2(NMe_2)_2R_4$, while the 1,2 isomer can be obtained by crystallization of the 1,1 (30%) and 1,2 (70%) mixture of isomers obtained from the reaction between 1,2-$Mo_2Br_2R_4$ and LiO-*t*-Bu (2 equiv) in hexane. The ^1H NMR spectra of both of these isomers are consistent with rapid rotation about Mo≡Mo bonds.

It is thus evident that $Mo_2X_2R_4$ compounds, once formed, are kinetically inert to alkyl group transfer but that the mechanism of substitution at the dimetal center may proceed with kinetic control and induce alkyl group transfer, though we do not know which of the isomers is the thermodynamically more stable one.

Partial Substitution Reactions. Addition of HBr (1 equiv) to $Mo_2(CH_2SiMe_3)_6$ leads to an essentially statistical mixture (1:2:1) of 1,2-$Mo_2Br_2R_4$, Mo_2BrR_5, and Mo_2R_6. The solubility of the monobromo product is so simlar to that of $Mo_2(CH_2SiMe_3)_6$ that we have been unable to separate the two. The ^1H NMR spectrum of the mixture leaves little doubt concerning the authenticity of Mo_2BrR_5 (see Experimental Section).

A ca. 1:2:1 mixture of 1,2-$Mo_2Br_2R_4$, $MoBrR_5$, and Mo_2R_6 was obtained from the reaction between 1,2-$Mo_2Br_2R_4$ and $LiCH_2SiMe_3$ (1 equiv) in hexane. However, 1,2-$Mo_2Br_2R_4$ and Mo_2R_6 do not react in toluene-d_8 (6 months at room temperature): no Mo_2BrR_5 was detected by ^1H NMR spectroscopy. Evidently, intermolecular alkyl-for-bromo group transfer does not occur, and in each of the reactions, (i) Mo_2R_6 + 2HBr and (ii) 1,2-$Mo_2Br_2R_4$ + 2LiR, the rates of the first and second substitutions are comparable.

Similar observations were made in studies of the reaction between 1,2-$Mo_2Br_2R_4$ and MeLi (1 equiv). The compound 1,2-$Mo_2(Br)(Me)R_4$ was not separated from 1,2-$Mo_2Me_2R_4$ because of their similar solubilities, but ^1H NMR data leave little doubt concerning the existence of this compound.

In the reaction between 1,2-$Mo_2Br_2R_4$ and $LiNMe_2$ (2 equiv), which yields 1,1- (95%) and 1,2-$Mo_2(NMe_2)_2R_4$ (5%), alkyl transfer could occur with the first or second substitution. Attempts to follow the course of the reaction when only 1 equiv of $LiNMe_2$ was used were not very informative. Many species were present and this reaction could be complicated by the presence of trace quantities of free $HNMe_2$ (arising from unavoidable hydrolysis) which would catalyze Mo—Br and Mo—NMe_2 group scrambling. Consequently, we followed in detail the course of the reaction between 1,2-$Mo_2Br_2R_4$ and LiO-*t*-Bu which leads ultimately to mixture of 1,1- (30%) and 1,2-$Mo_2(O\text{-}t\text{-}Bu)_2R_4$ (70%).

The reaction between 1,2-$Mo_2Br_2R_4$ and LiO-*t*-Bu (1 equiv) proceeds slowly at room temperature in hexane or toluene to give 1,2-$Mo_2Br(O\text{-}t\text{-}Bu)R_4$ which appears spectroscopically pure (see Figure 2). Evidently, an alkyl group transfer does not accompany the first O-*t*-Bu-for-Br substitution. Furthermore, the second substitution of Br by O-*t*-Bu must be significantly slower than the first: 1,2-$Mo_2Br_2R_4$ + LiO-*t*-Bu $\xrightarrow{k_1}$ 1,2-$Mo_2Br(O\text{-}t\text{-}Bu)R_4$; 1,2-$Mo_2Br(O\text{-}t\text{-}Bu)R_4$ + LiO-*t*-Bu $\xrightarrow{k_2}$ 1,1- + 1,2-$Mo_2(O\text{-}t\text{-}Bu)_2R_4$; where $k_1 \gg k_2$. It is tempting to suggest that the difference in rates reflects steric congestion [$Mo_2Br(O\text{-}t\text{-}Bu)R_4 > Mo_2Br_2R_4$] and that as crowding increases, the organolithium reagent (LiO-*t*-Bu or $LiNMe_2$) acts as a base and promotes a net alkyl transfer by a reversible deprotonation of the CH_2SiMe_3 ligand. This could occur at either the α- or γ-carbon with the formation of either a bridging carbene or dimetallacycle intermediate as shown below in eq 1 and 2.[17]

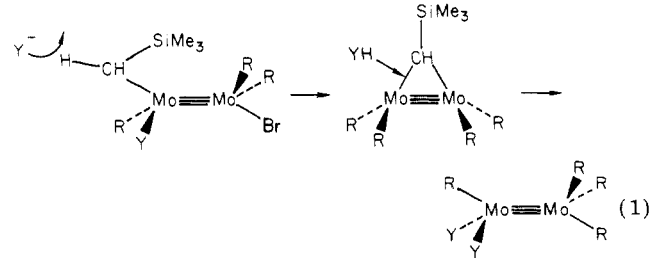

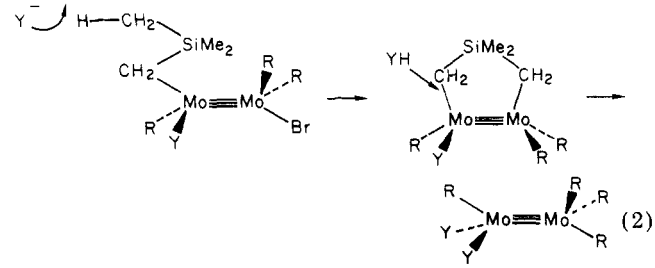

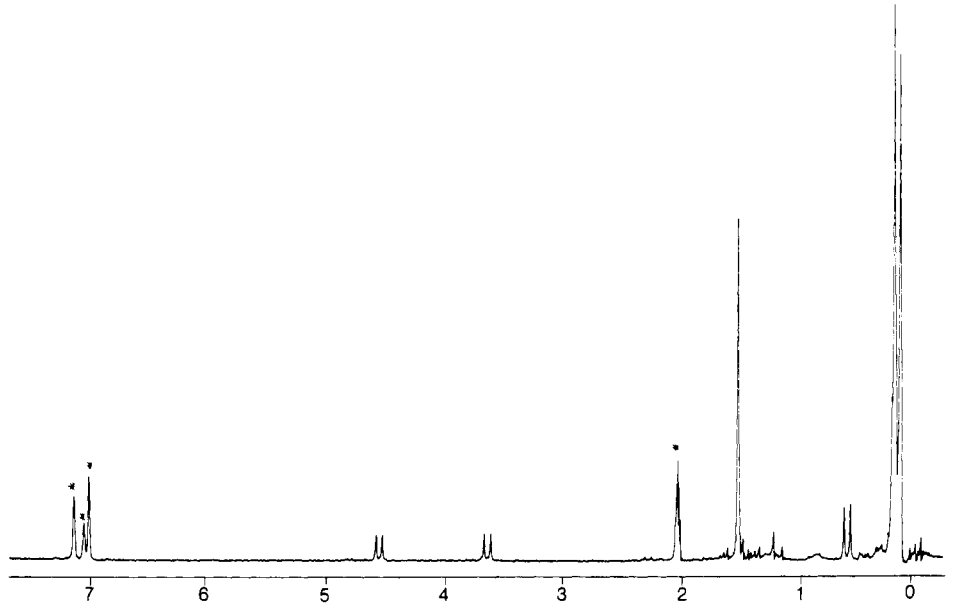

Figure 2. ^1H NMR spectrum of the crude hexane-soluble product from the reaction between 1,2-$Mo_2Br_2R_4$ and LiO-*t*-Bu (1 equiv) recorded at 220 MHz, 16 °C, in toluene-d_8 solvent. The methylene protons of the CH_2SiMe_3 groups appear as two AX spectra with the high-field doublets overlapping. The methyl signals of the O-*t*-Bu and CH_2SiMe_3 ligands appear as three singlets in the integral ratio 1:2:2 as expected for 1,2-$Mo_2Br(O\text{-}t\text{-}Bu)(CH_2SiMe_3)_4$. The signals arising from protio impurities in the solvent are denoted by asterisks.

Table II. Rotational Barriers about M≡M and M—N Bonds[a]

compd (R = CH_2SiMe_3)	$\Delta G^{\ddagger}$, kcal mol^{-1} M≡M	$\Delta G^{\ddagger}$, kcal mol^{-1} M–N	ref
$Mo_2(NMe_2)_6$	not measurable	11.5 ± 0.5	*b*
$W_2(NMe_2)_6$	not measurable	11.2 ± 0.5	*c*
$Mo_2(NEt_2)_6$	not measurable	13.6 ± 0.5	*b*
anti-1,2-$Mo_2Cl_2(NMe_2)_4$	not observed, >16 kcal mol	14.0 ± 0.5	*d*
1,2-$W_2Me_2(NEt_2)_4$	anti ⇌ gauche, 21 ± 1	(11-14)	*e*
1,2-$W_2R_2(NEt_2)_4$	anti ⇌ gauche, 24 ± 1	(11-14)	*f*
1,1-$Mo_2(NMe_2)_2R_4$	14.0 ± 1	10.3 ± 0.5	this work
1,2-$Mo_2(NMe_2)_2R_4$	15.6 ± 1	15.0 ± 0.5	this work
1,1-$Mo_2(O\text{-}t\text{-}Bu)_2R_4$	not observed, <8		this work

[a] Estimates from coalescence temperature by using the Gutowsky-Holm equation: Pople, J. A.; Schneider, W. G.; Burnstein, H. J. "High Resolution NMR Spectroscopy"; McGraw-Hill: New York, 1959; p 223. [b] Chisholm, M. H.; Cotton, F. A.; Frenz, B. A.; Reichert, W. W.; Shive, L. W.; Stults, B. R. *J. Am. Chem Soc.* **1976**, *96*, 4469. [c] Chisholm, M. H.; Cotton, F. A.; Extine, M. W.; Stults, B. R. *Ibid.* **1976**, *96*, 4477. [d] Akiyama, M.; Chisholm, M. H.; Cotton, F. A.; Extine, M. W.; Murillo, C. A. *Inorg. Chem.* **1977**, *16*, 2407. [e] Chisholm, M. H.; Cotton, F. A.; Extine, M. W.; Millar, M.; Stults, B. R. *Ibid.* **1976**, *15*, 2244. [f] Chisholm, M. H.; Extine, M. W. *J. Am. Chem. Soc.* **1976**, *98*, 6393.

However, neither of these mechanisms could account for the alkyl migration observed in the reaction between 1,1′-$Mo_2(NMe_2)(O_2CNMe_2)R_4$ and *t*-BuOH, which leads to a mixture 1,1- and 1,2-$Mo_2(O\text{-}t\text{-}Bu)_2R_4$.

Mo≡Mo and Mo—N Roational Barriers. Rotational barriers, calculated from the variable-temperature dependence of the ^1H NMR spectra, are given in Table II for the 1,1- and 1,2-$Mo_2(NMe_2)_2R_4$ compounds. For a nonlinear molecule having a cylindrical triple bond ($\sigma^2 + \pi^4$), there should be no electronic or quantum mechanical barrier to rotation. It is of significance, therefore, that of the $Mo_2X_2R_4$ compounds studied, only when X = NMe_2, have we observed a barrier to rotation in the range which is observable by NMR spectroscopy ($\Delta G^{\ddagger} > 8$ kcal mol^{-1}) and it is reasonable to assign the origin of the barrier to steric factors. The NC_2 units which are aligned along the axis introduce cogging between the two ends of the molecule. This is more pronounced for gauche 1,2-$Mo_2(NMe_2)_2R_4$ than for the 1,1 isomer, since the two NC_2 blades cannot allow a facile gauche–gauche′ (enantiomerization) rotation without a twisting or simultaneous rotation about Mo—N bonds. It is quite likely that this causes the slighlty higher activation to rotation about the Mo≡Mo bond in the 1,2 isomer.

Proximal ⇌ distal methyl exchange is quite significantly slower for the 1,2-$Mo_2(NMe_2)_2R_4$ isomer. One might initially be tempted to believe that this also correlates with the greater contact of the NC_2 units in the *gauche*-1,2-$Mo_2(NMe_2)_2R_4$ molecule. However, this idea falls into trouble when one recognizes that in $Mo_2(NMe_2)_6$, a molecule which has all six NC_2 blades meshed, the energy of activation is only 11 kcal mol^{-1}—as is found for the 1,1-$Mo_2(NMe_2)_2R_4$ isomer. Consequently, we believe that electronic factors must be responsible for the higher activation energy for the 1,2 isomer. As a result of forming three σ bonds and the Mo≡Mo bond, each molybdenum atom achieves only a 12 valence shell of electrons in $X_3Mo{\equiv}MoX_3$ compounds. This number falls short of satisfying the EAN rule and π donation from X is possible when X = NR_2 or OR, but not R. This ligand to metal π donation is favored when the NC_2 units are aligned along

(17) The compound $(Me_3SiCH_2)_2Mo(CH_2SiMe_2CH_2)Mo(PMe_3)_3$ (M≡M) has been isolated from the reaction between $Mo_2(OAc)_4$, Me_3SiCH_2MgCl, and PMe_3: Andersen, R. A.; Jones, R. A.; Wilkinson, G. *J. Chem. Soc., Dalton Trans.* **1978**, 446.

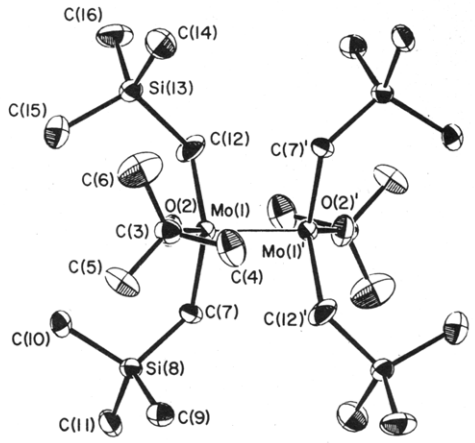

Figure 3. An ORTEP view of 1,2-$Mo_2(O\text{-}t\text{-}Bu)_2(CH_2SiMe_3)_4$ molecule showing the atom numbering scheme used in the tables.

the Mo—Mo axis (defined as the z axis): the d_{xz} and d_{yz} atomic orbitals are used in forming the Mo—Mo π bonds, while one set of in-plane atomic orbitals (p_x, p_y) or ($d_{x^2-y^2}$, d_{xy}) is avaiable for receiving ligand π electrons. In this way in 1,1-$Mo_2(NMe_2)_2R_4$, one molybdenum atom attains a 16 valence shell of electrons, but in the 1,2 isomer, a 14 valence shell is all that is possible. Thus, ligand to metal π bonding is expected to be more important in each Mo—N bond in the 1,2 isomer than in the 1,1 isomer. This in turn yields a higher Mo—N rotational barrier for the 1,2 isomer. Within this line of reasoning, it should be noted that the Mo—O bond distances in 1,2-$Mo_2(O\text{-}t\text{-}Bu)_2R_4$ (see below) are shorter than in the related compounds $Mo_2(OCH_2CMe_3)_6$,[18] $Mo_2(OSiMe_3)_6(HNMe_2)_2$[19] and $Mo(O\text{-}t\text{-}Bu)_2(py)_2(CO)_2$, which have decreasing degrees of oxygen-to-molybdenum π bonding.

Solid-State Structure of 1,2-$Mo_2(O\text{-}t\text{-}Bu)_2(CH_2SiMe_3)_4$. An ORTEP view of the molecule giving the atom numbering scheme is shown in Figure 3 and a view of the molecule looking down the Mo—Mo axis, which clearly emphasizes the disposition of alkyl ligands, is shown in Figure 4. Final atomic coordinates and thermal parameters are given in Table III and IV, respectively. Complete listings of bond distances and angles are given in Table V and VI, respectively.

In the solid state, 1,2-$Mo_2(O\text{-}t\text{-}Bu)_2R_2$ exists in the anti rotameric form and has a crystallographically imposed center of inversion. The Mo—Mo distance is 2.209 (2) Å, which is longer than in $Mo_2(CH_2SiMe_3)_6$ (2.169 (?) Å)[14] but shorter than that in $Mo_2(OCH_2CMe_3)_6$ (2.222 (2) Å).[18] The Mo—O distance, 1.865 (8) Å, is slighlty shorter than those in $Mo_2(OCH_2CMe_3)_6$[18] and $Mo_2(OSiMe_3)_6(HNMe_2)_2$[19] which, together with the obtuse Mo—O—C angle, 158.4 (7)°, is indicative of strong oxygen-to-molybdenum π bonding. The internal angles for the $Mo_2O_2C_4$ unit are similar to those in other ethane-like Mo_2^{6+}-containing compounds. The Mo—Mo—O angle (110.7 (3)°) and the Mo—Mo—C angles (100.0 (3)° and 100.2 (4)°) probably reflect the packing of the *tert*-butyl and trimethylsilyl groups which are proximal and distal to the Mo≡Mo bond, respectively.

Concluding Remarks. Rotation about the Mo≡Mo bond has been observed and rotational barriers appear very low (<8 kcal mol^{-1}) in the absence of dialkylamide ligands, consistent with the view that the origin of the barrier is steric and not electronic.

1,1- and 1,2-$Mo_2X_2R_4$ compounds do not isomerize readily which implies a high barrier to alkyl group migration across the Mo≡Mo bond. Bridged $Mo_2X_2R_4$ compounds must be relatively high-energy species, probably because the required rehybridization of metal atomic orbitals would involve a significant disruption of the Mo≡Mo bond. The threshold mechanism for anti ⇌ gauche isomerization in 1,2-$Mo_2X_2(NMe_2)_4$ compounds is, by inference, one of Mo≡Mo rotation.

The formation of 1,1-$Mo_2X_2R_4$ compounds from 1,2-$Mo_2X'_2R_4$ starting materials, and vice versa, which is seen

Table III. Fractional Coordinates for the 1,2-$Mo_2(C\text{-}t\text{-}Bu)_2(CH_2SiMe_3)_4$ Molecule[a]

atom	10^4x	10^4y	10^4z	$10B_{iso}$, Å^2
Mo(1)	5311 (1)	359.8 (5)	895 (1)	15
O(2)	6903 (9)	860 (5)	790 (8)	30
C(3)	8049 (12)	1098 (6)	228 (13)	25
C(4)	7875 (16)	871 (8)	−1257 (16)	43
C(5)	8110 (14)	1925 (7)	278 (16)	37
C(6)	9327 (15)	833 (11)	1204 (18)	53
C(7)	3525 (11)	1012 (6)	691 (11)	19
Si(8)	3730 (3)	1998 (2)	884 (3)	19
C(9)	4094 (12)	2394 (6)	−708 (12)	24
C(10)	5145 (12)	2196 (6)	2364 (11)	22
C(11)	2121 (13)	2418 (6)	1199 (13)	27
C(12)	5477 (13)	−409 (7)	2520 (14)	34
Si(13)	7070 (3)	−386 (2)	391 (3)	22
C(14)	8584 (14)	−791 (8)	3331 (15)	35
C(15)	7453 (14)	572 (8)	4540 (14)	35
C(16)	6768 (15)	−939 (8)	5355 (14)	39

atom	10^3x	10^3y	10^3z	$10B_{iso}$, Å^2
H(1)	706	108	−178	53
H(2)	863	103	−161	53
H(3)	782	36	−132	53
H(4)	823	208	120	47
H(5)	885	209	−10	47
H(6)	728	212	−24	47
H(7)	930	32	128	63
H(8)	1011	97	86	63
H(9)	938	104	208	63
H(10)	299	92	−20	29
H(11)	305	85	136	29
H(12)	490	218	−89	34
H(13)	335	230	−145	34
H(14)	421	290	−60	34
H(15)	494	200	317	32
H(16)	597	199	221	32
H(17)	525	271	247	32
H(18)	224	293	129	37
H(19)	139	231	45	37
H(20)	192	223	202	37
H(21)	472	−34	294	44
H(22)	542	−88	212	44
H(23)	840	−128	309	45
H(24)	874	−53	256	45
H(25)	937	−76	405	45
H(26)	825	58	524	45
H(27)	759	87	380	45
H(28)	671	76	489	45
H(29)	602	−75	569	50
H(30)	657	−142	505	50
H(31)	756	−93	607	50

[a] The isotropic thermal parameter listed for those atoms refined anisotropically are the isotropic equivalent. Numbers in parentheses in this and all following tables refer to the error in the least significant digits. Estimated standard deviations greater than 29 are not statistically significant but are left "unrounded", since the tables are all produced automatically by the X-TEL interactive programs.

(18) Chisholm, M. H.; Cotton, F. A.; Murillo, C. A.; Reichert, W. W. *J. Am. Chem. Soc.* **1977**, *99*, 1652; *Inorg. Chem.* **1977**, *16*, 1801.
(19) Chisholm, M. H.; Cotton, F. A.; Extine, M. W.; Reichert, W. W. *J. Am. Chem. Soc.* **1978**, *100*, 153.
(20) Chisholm, M. H.; Huffman, J. C.; Kelly, R. L. *J. Am. Chem. Soc.* **1979**, *101*, 7615.

Table IV. Anisotropic Thermal Parameters for the 1,2-$Mo_2(O\text{-}t\text{-}Bu)_2(CH_2SiMe_3)_4$ Molecule[a]

atom	U_{11}	U_{22}	U_{33}	U_{12}	U_{13}	U_{23}
Mo(1)	22 (1)	18 (1)	18 (1)	−0.1 (4)	6.5 (4)	0.5 (4)
O(2)	46 (5)	39 (5)	28 (5)	−14 (4)	3 (4)	−4 (4)
C(3)	31 (7)	26 (6)	38 (7)	−2 (5)	6 (5)	5 (5)
C(4)	64 (10)	50 (9)	55 (9)	−1 (8)	24 (8)	−14 (8)
C(5)	49 (8)	25 (7)	71 (10)	5 (6)	24 (8)	2 (7)
C(6)	38 (8)	100 (14)	66 (11)	10 (9)	16 (8)	20 (10)
C(7)	29 (6)	20 (6)	23 (6)	5 (5)	10 (5)	3 (5)
Si(8)	28 (2)	22 (2)	23 (2)	3 (1)	5 (1)	2 (1)
C(9)	31 (6)	26 (6)	36 (7)	−2 (5)	9 (5)	6 (5)
C(10)	36 (7)	29 (6)	21 (6)	−0 (5)	13 (5)	−4 (5)
C(11)	50 (8)	24 (6)	31 (7)	0 (6)	13 (6)	−3 (5)
C(12)	31 (7)	47 (8)	42 (8)	−7 (6)	−17 (6)	5 (7)
Si(13)	31 (2)	29 (2)	23 (2)	3 (1)	5 (1)	2 (1)
C(14)	43 (8)	43 (8)	52 (9)	4 (6)	17 (7)	−1 (7)
C(15)	41 (8)	49 (8)	39 (8)	−7 (6)	2 (6)	−9 (6)
C(16)	61 (8)	48 (9)	42 (8)	19 (7)	13 (7)	20 (7)

[a] The form of the exponent is $\exp[-2\pi^2(U_{11}h^2a^{*2} + U_{22}k^2b^{*2} + U_{33}lc^{*2} + 2U_{12}hka^*b^* + 2U_{13}hla^*c^* + 2U_{23}klb^*c^*)]$. All U's are $\times 10^3$.

Table V. Bond Distances for the 1,2-$Mo_2(O\text{-}t\text{-}Bu)_2(CH_2SiMe_3)_4$ Molecule

A	B	dist
Mo(1)	Mo(1)	2.209 (2)
Mo(1)	O(2)	1.865 (8)
Mo(1)	C(7)	2.133 (11)
Mo(1)	C(12)	2.135 (14)
Si(8)	C(7)	1.838 (11)
Si(8)	C(9)	1.852 (12)
Si(8)	C(10)	1.858 (12)
Si(8)	C(11)	1.875 (13)
Si(13)	C(12)	1.891 (13)
Si(13)	C(14)	1.893 (13)
Si(13)	C(15)	1.888 (14)
Si(13)	C(16)	1.833 (13)
O(2)	C(3)	1.449 (14)
C(3)	C(4)	1.514 (19)
C(3)	C(5)	1.528 (17)
C(3)	C(6)	1.520 (19)

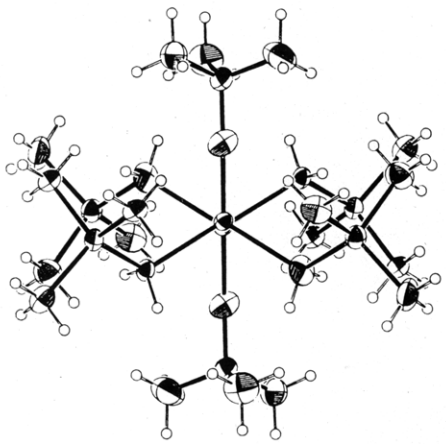

Figure 4. An ORTEP view of the 1,2-$Mo_2(O\text{-}t\text{-}Bu)_2(CH_2SiMe_3)_4$ molecule looking down the Mo≡Mo bond.

in certain reactions, shows that alkyl transfer can occur during the substitution reaction at the dimetal center. Further studies of the substitutional behavior of these $(Mo{\equiv}Mo)^{6+}$-containing compounds are warranted and will be undertaken.

Experimental Section

General procedures[1] and the preparation of $Mo_2(CH_2SiMe_3)_6$[14] have been described.

Preparation of 1,2-$Mo_2Br_2(CH_2SiMe_3)_4$. To a solution of $Mo_2(CH_2SiMe_3)_6$ (1.95 g) in hexane (25 mL), frozen at −198 °C (1. N_2), was added anhydrous HBr (5.5 mmol, 2 equiv) by use of a calibrated vacuum manifold. Upon being slowly warmed, the initially clear yellow solution darkened and, at temperatures between −50 and −20 °C, a pale brown precipitate formed. This was collected by filtration. The toluene-soluble solids were extracted (50 mL), and the filtrate was reduced in volume to ca. 20 mL and cooled to −15 °C in the refrigerator of the Dri-Lab, yielding orange crystals. These were collected by filtration and dried in vacuo: 1,2-$Mo_2Br_2(CH_2SiMe_3)_4$, 1.5 g (80% yield based on Mo).

Table VI. Bond Angles (Deg) for the 1,2-$Mo_2(O\text{-}t\text{-}Bu)_2(CH_2SiMe_3)_4$ Molecule

A	B	C	angle
Mo(1)′	Mo(1)	O(2)	110.7 (3)
Mo(1)′	Mo(1)	C(7)	100.0 (3)
Mo(1)′	Mo(1)	C(12)	100.2 (4)
O(2)	Mo(1)	C(7)	115.2 (4)
O(2)	Mo(1)	C(12)	116.1 (4)
C(7)	Mo(1)	C(12)	112.3 (5)
C(7)	Si(8)	C(9)	109.8 (5)
C(7)	Si(8)	C(10)	109.2 (5)
C(7)	Si(8)	C(11)	110.3 (5)
C(9)	Si(8)	C(10)	110.4 (5)
C(9)	Si(8)	C(11)	108.1 (5)
C(10)	Si(8)	C(11)	109.1 (5)
C(12)	Si(13)	C(14)	111.7 (7)
C(12)	Si(13)	C(15)	110.2 (6)
C(12)	Si(13)	C(16)	108.3 (7)
C(14)	Si(13)	C(15)	110.5 (6)
C(14)	Si(13)	C(16)	107.2 (6)
C(15)	Si(13)	C(16)	108.8 (7)
Mo(1)	O(2)	C(3)	158.4 (7)
O(2)	C(3)	C(4)	110.8 (10)
O(2)	C(3)	C(5)	108.7 (10)
O(2)	C(3)	C(6)	106.5 (10)
C(4)	C(3)	C(5)	107.7 (11)
C(4)	C(3)	C(6)	116.6 (12)
C(5)	C(3)	C(6)	106.2 (12)
Mo(1)	C(7)	Si(8)	118.5 (6)
Mo(1)	C(12)	Si(13)	117.8 (6)

Under similar conditions, addition of 1 equiv of HBr followed by stripping the solvent and toluene extraction gave an orange solution which, based on ^1H NMR spectroscopy, was a 1:2:1 mixture of 1,2-$Mo_2Br_2R_4$, Mo_2BrR_5, and Mo_2R_6. (NMR data is given later.) By careful crystallizations of this mixture in hexane at −15 °C, 1,2-$Mo_2Br_2R_4$ was removed, but the compounds Mo_2BrR_5 and Mo_2R_6 were inseparable by crystallization.

Addition of 1,2-$Mo_2Br_2R_4$ to a toluene solution of $LiCH_2SiMe_3$ (1 equiv) at −78 °C led to a hexane soluble extract which was indistinguishable by ^1H NMR spectroscopy from the 1:2:1 mixture of $Mo_2Br_2R_4$, Mo_2BrR_5, and Mo_2R_6 prepared in the above manner.

Reaction of 1,2-$Mo_2Br_2(CH_2SiMe_3)_4$ with $LiNMe_2$. Addition of $Mo_2Br_2R_4$ (0.56 g) to a suspension of $LiNMe_2$ (0.1 g, >2 equiv) in hexane (25 mL) at −50 °C led to a suspension of reagents which mostly went into solution upon warming to 0 °C over 2 h. The solution was filtered to remove finely divided LiCl and unreacted

$LiNMe_2$; the filtrate was collected and the solvent was stripped to yield a yellow liquid, which by ^1H NMR spectroscopy was identified as predominantly 1,1-$Mo_2(NMe_2)_2R_4$ (95%) with an NMR detectable impurity (5%) of the 1,2-$Mo_2(NMe_2)_2R_4$ isomer.

Preparation of 1,2-$Mo_2(NMe_2)_2(CH_2SiMe_3)_4$. To a suspension of 1,2-$Mo_2Br_2R_4$ (0.517 g), in pentane (20 mL), was added $HNMe_2$ (ca. 10 equiv) by use of a calibrated vacuum manifold. This led to the rapid precipitation of $H_2NMe_2^+Br^-$ and a clear solution. Filtration, followed by stripping the solvent, gave a yellow liquid which was identified as 1,2-$Mo_2(NMe_2)_2R_4$ by ^1H NMR spectroscopy. The elemental analyses obtained on the yellow liquid are slightly high in nitrogen and low in carbon, a fact which probably reflects some contamination by $H_2NMe_2^+Br^-$. The dimolybdenum compounds are volatile, and purification by vacuum distillation would presumably be possible. However, this was not undertaken since samples prepared in the above manner appeared spectroscopically pure (^1H NMR).

Preparation of 1,1′-$Mo_2(NMe_2)(O_2CNMe_2)(CH_2SiMe_3)_4$. Addition of bone-dry CO_2, by use of a vacuum manifold, to a hexane solution of 1,1-$Mo_2(NMe_2)_2R_4$ (plus its ca. 5% impurity of 1,2-$Mo_2(NMe_2)_2R_4$) led to an immediate reaction with the formation of 1,1′-$Mo_2(NMe_2)(O_2CNMe_2)R_4$ which was obtained as a yellow-brown liquid upon stripping the solvent. The ^1H NMR spectrum revealed the pattern of substitution, and furthermore, that the impurity of the 1,2-$Mo_2(NMe_2)_2R_4$ isomer remained unreacted.

These observations were confirmed in experiments carried out in NMR tubes: the 1,2-$Mo_2(NMe_2)_2R_4$ compound does not react with CO_2 (<5 atm) at temperatures below +80 °C.

Reaction of 1,2-$Mo_2Br_2(CH_2SiMe_3)_4$ with LiO-*t*-Bu. (a) A mixture of 1,2-$Mo_2Br_2R_4$ (0.417 g) and LiO-*t*-Bu (0.106 g, 2.2 equiv) was placed in a round-bottomed flask. Hexane (40 mL) was added, and the suspension was stirred for 5 h to give a red solution and gray solids. The solids were removed by filtration, and the filtrate was collected. Stripping the solvent yielded red microcrystalline solids which were identified by ^1H NMR spectroscopy as 70:30 mixture of 1,2- and 1,1-$Mo_2(O\text{-}t\text{-}Bu)_2R_4$. Crystallization of this mixture from cold pentane solutions (−15 °C) gave deep red crystals of the isomerically pure 1,2-$Mo_2(O\text{-}t\text{-}Bu)_2R_4$ compound. This compound sublimes at 80 °C (10^{-4} torr) with little decomposition and without detectable isomerization.

(b) To a suspension of 1,2-$Mo_2Br_2R_4$ (0.5 g) in hexane (40 mL) was added LiO-*t*-Bu (0.06 g, 1 equiv), and the reaction mixture was stirred for 1 h. The solvent was then stripped to give a red solid which was identified by ^1H NMR spectroscopy as 1,2-$Mo_2Br(O\text{-}t\text{-}Bu)R_4$. Addition of a further equivalent of LiO-*t*-Bu to this solid dissolved in hexane (20 mL) gave, after 4 h, a mixture of 1,2- and 1,1-$Mo_2(O\text{-}t\text{-}Bu)_2R_4$, indistinguishable from that in a above.

(c) Small scale reactions were carried out in sealed NMR tubes to monitor with time the reaction between LiO-*t*-Bu and 1,2-$Mo_2Br_2R_4$. These showed the initial, relatively fast, formation of 1,2-$Mo_2Br(O\text{-}t\text{-}Bu)R_4$, followed by formation of the 70:30 mixture of 1,2- and 1,1-$Mo_2(O\text{-}t\text{-}Bu)_2R_4$.

Reaction of 1,1-$Mo_2(NMe_2)_2(CH_2SiMe_3)_4$ with *t*-BuOH. A large excess of *t*-BuOH in benzene (azeotrope) was added to a solution of 1,1-$Mo_2(NMe_2)_2R_4$ (ca. 0.4 g) in hexane (10 mL). The solution was stirred for 12 h, and then the solvent was stripped to give a red solid which was identified by ^1H NMR spectroscopy as 1,1-$Mo_2(O\text{-}t\text{-}Bu)_2R_4$ contaminated with ca. 5% of 1,2-$Mo_2(O\text{-}t\text{-}Bu)_2R$, which presumably arose from the ca. 5% impurity of the 1,2-$Mo_2(NMe_2)_2R_4$ isomer in the sample of 1,1-$Mo_2(NMe_2)_2R_4$. The red solid sublimed at 80 °C (10^{-4} torr) with little decomposition and no apparent isomerization.

Neither the 1,1-, nor the 1,2-$Mo_2(O\text{-}t\text{-}Bu)_2R_4$ compounds reacted with CO_2 nor was isomerization observed in the presence of excess LiO-*t*-Bu or *t*-BuOH.

Reaction of 1,1′-$Mo_2(NMe_2)(O_2CNMe_2)(CH_2SiMe_3)_4$ with *t*-BuOH. Addition of an excess of *t*-BuOH in benzene (azeotrope) to a hexane solution of 1,1′-$Mo_2(NMe_2)(O_2CNMe_2)R_4$ yielded a red solution within 0.5 h. Stripping the solvent yielded red solids which, by ^1H NMR spectroscopy, were determined to be an ca. 4:1 mixture of 1,2- and 1,1-$Mo_2(O\text{-}t\text{-}Bu)_2R_4$, respectively.

^1H NMR Data. ^1H NMR data for the compounds 1,2-$Mo_2X_2(CH_2SiMe_3)_4$ recorded in toluene-d_8 at 220 MHz and 16 °C. (a) X = Br: 1.49 4.76 (d), 0.73 (d, J = 11.1 Hz); $\delta(SiMe_3)$ 0.22. (b) X = CH_3: δ(Mo–CH_3) 1.49 (s); δ(Mo–CH_2) 1.11 (d), 2.69 (d, J = 11.8 Hz); $\delta(SiMe_3)$ 0.20 (s). (c) X = O-*i*-Pr: δ(OCH) 5.36; $\delta(OCHMe_2)$ 1.45 (d, J = 6.5 Hz); δ(Mo–CH_2) 3.63 (d), 0.01 (d, J = 12.0 Hz); $\delta(SiMe_3)$ 0.21 (s). (d) X = O-*t*-Bu: $\delta(OCMe_3)$ 1.54 (s); δ(Mo–CH_2) 3.55 (d), 0.03 (d, J = 12.0 Hz); $\delta(SiMe_3)$ 0.20 (s). (e) X = NMe_2 at −35 °C: $\delta(NMe_2)$ 3.57 (s, proximal), 2.55 (s, distal); δ(Mo–CH_2) −0.25 (d), 3.45 (d, J = 11.0 Hz), 1.52 (d), 1.66 (d, J = 11.0 Hz); $\delta(SiMe_3)$ 0.17 (s), 0.23 (s).

^1H NMR data for $Mo_2Br(CH_2SiMe_3)_5$ obtained at 220 MHz, 16 °C in toluene-d_8: $(Me_3SiCH_2)_2BrMo$, $\delta(CH_2)$ 4.56 (d), 0.66 (d, J = 11.5 Hz); $\delta(SiMe_3)$ 0.34 (s); $Mo(CH_2SiMe_3)_3$, $\delta(CH_2)$ 2.00 (s); $\delta(SiMe_3)$ 0.26 (s).

^1H NMR data for 1,1-$Mo_2(NMe_2)_2(CH_2SiMe_3)_4$ obtained at 220 MHz, −42 °C in toluene-d_8: δ (NMe_2) 3.07 (br s); δ(Mo–CH_2) 1.37 (s), 1.52 (s), 1.67 (d), 2.24 (d, J = 11.2 Hz); $\delta(SiMe_3)$ 0.21 (s), 0.25 (s), 0.27 (s).

^1H NMR data for 1,1-$Mo_2(O\text{-}t\text{-}Bu)_2(CH_2SiMe_3)_4$ obtained at 220 MHz, 16 °C in toluene-d_8: δ(O-*t*-Bu) 1.39 (s); δ(Mo–Ch_2) 1.94 (s, intensity 6 H), 2.33 (s, intensity 2 H); $\delta(SiMe_3)$ 0.25 (s).

^1H NMR data for 1,1′-$Mo_2(NMe_2)(O_2CNMe_2)(CH_2SiMe_3)_4$ obtained at 220 MHz, 16 °C in toluene-d_8: $\delta(NMe_2)$ 3.80 (s, proximal), 2.81 (s, distal); $\delta(O_2CNMe_2)$ 2.58 (s); δ(Mo–CH_2) 2.18 (d), 1.65 (d, J = 11.0 Hz);, 1.61 (d), 1.42 (d, J = 12.1 Hz); $\delta(SiMe_3)$ 0.13 (s), 0.19 (s).

^1H NMR data for 1,2-$Mo_2Br(O\text{-}t\text{-}Bu)(CH_2SiMe_3)_4$ obtained at 220 MHz, 16 °C in toluene-d_8: δ(O-*t*-Bu) 1.62 (s); $(Me_3SiCH_2)_2BrMo$, $\delta(CH_2)$ 4.60 (d), 0.75 (d, J = 11.5 Hz); $\delta(SiMe_3)$ 0.22 (s); $(Me_3SiCH_2)_2(O\text{-}t\text{-}Bu)Mo$, $\delta(CH_2)$ 3.72 (d), 0.75 (d, J = 11.5 Hz); $\delta(SiMe_3)$ 0.19 (s).

^1H NMR data for 1,2-$Mo_2MeBr(CH_2SiMe_3)_4$ obtained at 220 MHz, 16 °C in toluene-d_8: δ(Mo–CH_3) 1.49 s; $(Me_3SiCH_2)_2BrMo$, $\delta(CH_2)$ 4.22 (d), 0.91 (d, J = 11.0 Hz); $\delta(SiMe_3)$ 0.21 (s); $(Me_3SiCH_2)_2MeMo$, $\delta(CH_2)$ 2.82 (d), 1.21 (d, J = 12.0 Hz); $\delta(SiMe_3)$ 0.20 (s).

X-ray Structural Determination for 1,2-$Mo_2(O\text{-}t\text{-}Bu)_2(CH_2SiMe_3)_4$. General procedures were described previously.[21]

An orange crystal of dimensions 0.21 × 0.21 × 0.19 mm was selected and transferred to the cold stream of the goniostat under an atmosphere of dry nitrogen. The cell dimensions obtained from 31 reflections at −163 °C with Mo Kα (λ = 0.71069 Å) were a = 10.025 (3) Å, b = 18.473 (9) Å, c = 9.975 (5) Å, β = 102.03 (3)°, Z = 2, and d_{calcd} = 1.263 g cm^{-3} with space group P_{21}/n.

A total number of 4057 reflections were collected by using standard moving-crystal moving-detector techniques with the following values: scan speed = 3.0 deg min^{-1}; scan width = 2.0 + dispersion; single background time at extremes of scan = 4 s; aperture size = 3.0 × 4.0 mm. The limits of data collection were $6° < 2\theta < 50°$. Of the 4057 reflections, 3189 were unique, and the number of $F > 2.33\sigma(F)$ was 2715.

The structure was solved by a combination of direct methods and Fourier techniques. All nonhydrogen atoms were located and refined by full-matrix least-squares using anisotropic thermal parameters. The final R was 0.083 for 2620 reflections having $F > 3\sigma(F)$. The hydrogen atoms were included as fixed atoms in calculated positions, each having an isotropic B equivalent to that of the parent C atom plus 1. An isotropic extinction parameter was included in the refinement: the final value was 1.878 × 10 exp(−6). No absorption correction was performed.

The maximum peak height in the final Difference map was 2.1 e/Å^3. The peaks could not be interpreted in terms of a solvent molecule or disorder. We are unable to account for the rather high value of R. Attempts at changing the weighting scheme by changing the uncertainty factor did not improve the refinement. We did note that R was fairly independent of sin θ and dependent of the magnitude of F: R increased with decreasing values of F. The overall R for 3190 reflections was 0.093.

Acknowledgment. We thank the donors of the Petroleum Research Fund, administered by the American Chemical Society, the National Science Foundation, and the Wrubel Computing Center at Indiana University for support of this work. M.H.C. is also grateful for a Camille

(21) Huffman, J. C.; Lewis, L. N.; Caulton, K. G. *Inorg. Chem.* **1980**, *19*, 2755.

and Henry Dreyfus Teacher-Scholar Grant.

Registry No. 1,2-$Mo_2Br_2(CH_2SiMe_3)_4$, 75059-90-4; 1,2-$Mo_2Me_2(CH_2SiMe_3)_4$, 75059-91-5; 1,1-$Mo_2(NMe_2)_2(CH_2SiMe_3)_4$, 75059-94-8; 1,2-$Mo_2(NMe_2)_2(CH_2SiMe_3)_4$, 76599-13-8; 1,1′-$Mo_2(NMe_2)(O_2CNMe_2)(CH_2SiMe_3)_4$, 76716-47-7; 1,2-$Mo_2(O\text{-}t\text{-}Bu)_2(CH_2SiMe_3)_4$, 75059-93-7; 1,2-$Mo_2(O\text{-}i\text{-}Pr)_2(CH_2SiMe_3)_4$, 75059-92-6; $Mo_2Br(CH_2SiMe_3)_5$, 79172-46-6; 1,1-$Mo_2(O\text{-}t\text{-}Bu)_2(CH_2SiMe_3)_4$, 75059-95-9; 1,2-$Mo_2Br(O\text{-}t\text{-}Bu)(CH_2SiMe_3)_4$, 79172-47-7; 1,2-$Mo_2MeBr(CH_2SiMe_3)_4$, 79172-75-1; $Mo_2(CH_2SiMe_3)_6$, 34439-17-3.

Supplementary Material Available: A listing of observed and calculated structure factors (20 pages). Ordering information is given on any current masthead page. The complete structural report, MSC Report 8024, is available in microfiche form only, from the Indiana University Library.

Unsaturated (π-Allyl)nickel Halide Complexes. Reactions To Produce Dienes

Louis S. Hegedus* and Sudarsanan Varaprath

Department of Chemistry, Colorado State University, Fort Collins, Colorado 80523

Received August 18, 1981

The (π-allyl)nickel halide complexes of 1-bromohexa-2,5-diene (**1**), 1-bromopenta-2,4-diene (**2**), 1-bromohexa-2,4-diene (**3**), and 2-(bromomethyl)-1,3-butadiene (**4**) were prepared from either nickel carbonyl or bis(cyclooctadiene)nickel and were characterized. The nonconjugated (π-1-(2-propenyl)allyl)nickel halide complex **1** reacted cleanly with iodobenzene, β-bromostyrene, cinnamyl bromide, iodocyclohexane, iodohexane, *o*-bromobenzamide, and *o*-bromoaniline to replace the halogen with the 1,4-hexadienyl group. The complexes from 1-bromopenta-2,4-diene (**2**) and 1-bromohexa-2,4-diene (**3**) were considerably less useful, reacting only with the very reactive substrates iodobenzene, cinnamyl bromide, and β-bromostyrene. The complex from 2-(bromomethyl)-1,3-butadiene (**4**) was used to synthesize myrcene, β-farnesene, and tagetol.

(π-Allyl)nickel halide complexes are easily prepared from the reaction of allylic halides with either nickel carbonyl or bis(cyclooctadiene)nickel in a nonpolar solvent such as benzene. The complexes are usually deep red crystalline, air-sensitive solids that can be stored in the absence of air for at least several years. In polar solvents such as DMF, they are generally reactive toward a wide range of organic halides, reacting to replace the halide in the substrate with the allyl group originally on nickel.[1] Under more severe conditions, some (π-allyl)nickel halide complexes react with ketones or aldehydes to produce homoallylic alcohols.[2] In relation to ongoing studies directed toward the synthesis of heterocycles by palladium-catalyzed cyclizations of amino olefins,[3-6] a number of diene-containing substrates were required. Although a number of new methods for the introduction of pentadienyl and hexadienyl groups into organic substrates have been recently reported,[7-9] none offered viable approaches to the desired substrates. Thus, we synthesized four new (π-allyl)nickel halide complexes containing an additional double bond and studied their reactions with organic halides and carbonyl compounds.

Results and Discussion

Preparation of (π-Allyl)nickel Halide Complexes

Complex **1** was prepared in 76% isolated yield on a 10-g scale by the reaction of a mixture of 1-bromo-2,5-hexadiene and 3-bromo-1,5-hexadiene with nickel carbonyl in benzene at 70 °C. This stable red crystalline solid was a typical (π-allyl)nickel halide complex in both its physical and chemical characteristics. In that regard, complex **1** is similar to other nonconjugated, unsaturated (π-allyl)nickel halide complexes such as those containing π-geranyl ligands.[10]

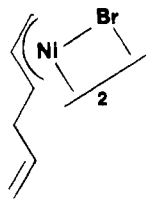

1

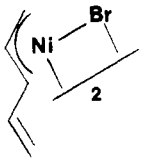

2

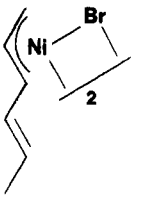

3

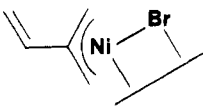

4

(1) For reviews concerning the preparation and reactions of (π-allyl)nickel halides see: (a) M. F. Semmelhack and P. Helquist, *Org. Synth.* **52**, 115 (1972); (b) M. F. Semmelhack, *Org. React.*, **19**, 115 (1972); (c) R. Baker, *Chem. Rev.*, **73**, 787 (1973); (d) L. S. Hegedus, *J. Organomet. Chem. Libr.*, 1, 329 (1976).

(2) (a) E. J. Corey and M. F. Semmelhack, *J. Am. Chem. Soc.*, **89**, 2755 (1967); (b) L. S. Hegedus, S. D. Wagner, E. L. Waterman, and K. Siirala-Hansen, *J. Org. Chem.*, **40**, 593 (1975).

(3) D. E. Korte, L. S. Hegedus, and R. K. Wirth, *J. Org. Chem.*, **42**, 1329 (1977).

(4) L. S. Hegedus, G. F. Allen, J. J. Bozell, and E. L. Waterman, *J. Am. Chem. Soc.*, **100**, 5800 (1978).

(5) L. S. Hegedus, G. F. Allen, and D. J. Olsen, *J. Am. Chem. Soc.*, **102**, 3583 (1980).

(6) L. S. Hegedus, P. M. Winton, and S. Varaprath, *J. Org. Chem.*, **46**, 2215 (1981).

(7) For the Lewis acid catalyzed reactions of dienylsilanes with electrophiles see: A. Hosomi, M. Saito, and H. Sakurai, *Tetrahedron Lett.*, **21**, 3783 (1980).

(8) For an approach to the isoprene synthon see: S. R. Wilson, L. R. Phillips, and K. J. Natalie, Jr., *J. Am. Chem. Soc.*, **101**, 3340 (1979).

(9) C. A. Henrick, *Tetrahedron*, **33**, 1845 (1977).

0276-7333/82/2301-0259$01.25/0

and Henry Dreyfus Teacher-Scholar Grant.

Registry No. 1,2-$Mo_2Br_2(CH_2SiMe_3)_4$, 75059-90-4; 1,2-$Mo_2Me_2(CH_2SiMe_3)_4$, 75059-91-5; 1,1-$Mo_2(NMe_2)_2(CH_2SiMe_3)_4$, 75059-94-8; 1,2-$Mo_2(NMe_2)_2(CH_2SiMe_3)_4$, 76599-13-8; 1,1′-$Mo_2(NMe_2)(O_2CNMe_2)(CH_2SiMe_3)_4$, 76716-47-7; 1,2-$Mo_2(O\text{-}t\text{-}Bu)_2(CH_2SiMe_3)_4$, 75059-93-7; 1,2-$Mo_2(O\text{-}i\text{-}Pr)_2(CH_2SiMe_3)_4$, 75059-92-6; $Mo_2Br(CH_2SiMe_3)_5$, 79172-46-6; 1,1-$Mo_2(O\text{-}t\text{-}Bu)_2(CH_2SiMe_3)_4$, 75059-95-9; 1,2-$Mo_2Br(O\text{-}t\text{-}Bu)(CH_2SiMe_3)_4$, 79172-47-7; 1,2-$Mo_2MeBr(CH_2SiMe_3)_4$, 79172-75-1; $Mo_2(CH_2SiMe_3)_6$, 34439-17-3.

Supplementary Material Available: A listing of observed and calculated structure factors (20 pages). Ordering information is given on any current masthead page. The complete structural report, MSC Report 8024, is available in microfiche form only, from the Indiana University Library.

Unsaturated (π-Allyl)nickel Halide Complexes. Reactions To Produce Dienes

Louis S. Hegedus* and Sudarsanan Varaprath

Department of Chemistry, Colorado State University, Fort Collins, Colorado 80523

Received August 18, 1981

The (π-allyl)nickel halide complexes of 1-bromohexa-2,5-diene (**1**), 1-bromopenta-2,4-diene (**2**), 1-bromohexa-2,4-diene (**3**), and 2-(bromomethyl)-1,3-butadiene (**4**) were prepared from either nickel carbonyl or bis(cyclooctadiene)nickel and were characterized. The nonconjugated (π-1-(2-propenyl)allyl)nickel halide complex **1** reacted cleanly with iodobenzene, β-bromostyrene, cinnamyl bromide, iodocyclohexane, iodohexane, *o*-bromobenzamide, and *o*-bromoaniline to replace the halogen with the 1,4-hexadienyl group. The complexes from 1-bromopenta-2,4-diene (**2**) and 1-bromohexa-2,4-diene (**3**) were considerably less useful, reacting only with the very reactive substrates iodobenzene, cinnamyl bromide, and β-bromostyrene. The complex from 2-(bromomethyl)-1,3-butadiene (**4**) was used to synthesize myrcene, β-farnesene, and tagetol.

(π-Allyl)nickel halide complexes are easily prepared from the reaction of allylic halides with either nickel carbonyl or bis(cyclooctadiene)nickel in a nonpolar solvent such as benzene. The complexes are usually deep red crystalline, air-sensitive solids that can be stored in the absence of air for at least several years. In polar solvents such as DMF, they are generally reactive toward a wide range of organic halides, reacting to replace the halide in the substrate with the allyl group originally on nickel.[1] Under more severe conditions, some (π-allyl)nickel halide complexes react with ketones or aldehydes to produce homoallylic alcohols.[2] In relation to ongoing studies directed toward the synthesis of heterocycles by palladium-catalyzed cyclizations of amino olefins,[3-6] a number of diene-containing substrates were required. Although a number of new methods for the introduction of pentadienyl and hexadienyl groups into organic substrates have been recently reported,[7-9] none offered viable approaches to the desired substrates. Thus, we synthesized four new (π-allyl)nickel halide complexes containing an additional double bond and studied their reactions with organic halides and carbonyl compounds.

Results and Discussion

Preparation of (π-Allyl)nickel Halide Complexes

Complex **1** was prepared in 76% isolated yield on a 10-g scale by the reaction of a mixture of 1-bromo-2,5-hexadiene and 3-bromo-1,5-hexadiene with nickel carbonyl in benzene at 70 °C. This stable red crystalline solid was a typical (π-allyl)nickel halide complex in both its physical and chemical characteristics. In that regard, complex **1** is similar to other nonconjugated, unsaturated (π-allyl)nickel halide complexes such as those containing π-geranyl ligands.[10]

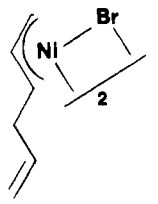

1

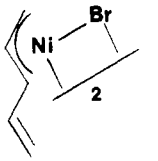

2

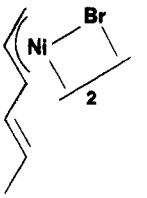

3

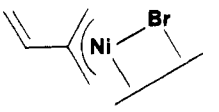

4

(1) For reviews concerning the preparation and reactions of (π-allyl)nickel halides see: (a) M. F. Semmelhack and P. Helquist, *Org. Synth.* **52**, 115 (1972); (b) M. F. Semmelhack, *Org. React.*, **19**, 115 (1972); (c) R. Baker, *Chem. Rev.*, **73**, 787 (1973); (d) L. S. Hegedus, *J. Organomet. Chem. Libr.*, 1, 329 (1976).

(2) (a) E. J. Corey and M. F. Semmelhack, *J. Am. Chem. Soc.*, **89**, 2755 (1967); (b) L. S. Hegedus, S. D. Wagner, E. L. Waterman, and K. Siirala-Hansen, *J. Org. Chem.*, **40**, 593 (1975).

(3) D. E. Korte, L. S. Hegedus, and R. K. Wirth, *J. Org. Chem.*, **42**, 1329 (1977).

(4) L. S. Hegedus, G. F. Allen, J. J. Bozell, and E. L. Waterman, *J. Am. Chem. Soc.*, **100**, 5800 (1978).

(5) L. S. Hegedus, G. F. Allen, and D. J. Olsen, *J. Am. Chem. Soc.*, **102**, 3583 (1980).

(6) L. S. Hegedus, P. M. Winton, and S. Varaprath, *J. Org. Chem.*, **46**, 2215 (1981).

(7) For the Lewis acid catalyzed reactions of dienylsilanes with electrophiles see: A. Hosomi, M. Saito, and H. Sakurai, *Tetrahedron Lett.*, **21**, 3783 (1980).

(8) For an approach to the isoprene synthon see: S. R. Wilson, L. R. Phillips, and K. J. Natalie, Jr., *J. Am. Chem. Soc.*, **101**, 3340 (1979).

(9) C. A. Henrick, *Tetrahedron*, **33**, 1845 (1977).

0276-7333/82/2301-0259$01.25/0

Table I. Reactions of (π-Allyl)nickel Halide Complexes 1-4 With Organic Halides

complex	halide	product	yield,[a] %
1	PhI	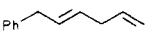	91
	PhCH=CHBr	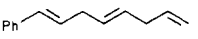	96
	PhCH=CHCH$_2$Br	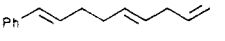	52
	cyclohexyl I	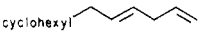	63
	n-C$_6$H$_{13}$I	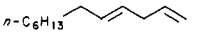	51
	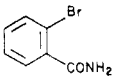	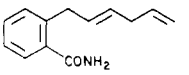	60
	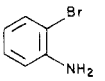	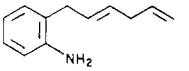	51
2	PhI	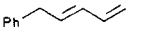	45[b]
	PhCH=CHBr	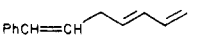	69[b]
	PhCH=CHCH$_2$Br	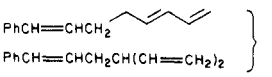	28[b]
3	PhI	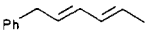	46
	PhCH=CHBr	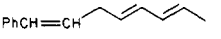	60[b]
	PhCH=CHCH$_2$Br	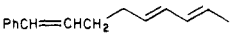	23
4	PhI	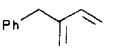	46
	PhCH=CHBr	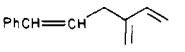	50
	PhCH=CHCH$_2$Br	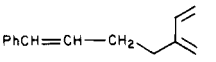	52

[a] Reported yields are for isolated, purified products, based on the substrate halide as a limiting reagent. [b] Based on NMR integration and VPC analysis; crude product contaminated with tetraenes from self-coupling of allyl groups.

Complex **4** was best prepared by the reaction of 2-(bromomethyl)-1,3-butadiene with bis(cyclooctadiene)-nickel in benzene at 0 °C. Under these conditions a 74% isolated yield of this stable, red crystalline material was obtained. Attempts to prepare this complex from nickel carbonyl always resulted in lower yields of impure materials. The starting bromide was available in overall 53% yield from isoprene, by using a modification of a published procedure reported to proceed in only 11% yield.[11] Complex **4** was also a typical (π-allyl)nickel complex, and its NMR spectrum indicated no interaction of the cross-conjugated double bond with the metal.

In contrast, complexes **2** and **3** were much less tractable and have not been isolated and purified. Reaction of the requisite dienic bromides either with nickel carbonyl at 40 °C or with bis(cyclooctadiene)nickel at 0 °C led to initial formation of the deep red color indicative of formation of a (π-allyl)nickel halide complex followed by a fading of this color with concommitant deposition of nickel bromide. From these reactions, only self-coupling products (dimers) were obtained. The reaction of these allylic halides with nickel carbonyl in the absence of the solvent produced a deed red sticky solid, insoluble in organic solvents ranging from benzene to DMF. Thus, these complexes could not be isolated and purified. However, it was clear that they were being formed, and a procedure for their generation and subsequent reaction in situ was developed.

Reactions of Complexes 1-4 with Organic Substrates. The results of the reactions of complexes **1-4** with a variety of organic halides are summarized in Table I. Complex **1** was the most generally useful, reacting with aryl, vinyl, allyl, and saturated alkyl halides to introduce the nonconjugated 1,4-hexadienyl side chain in fair to excellent yield. Complexes **2-4** were considerably less general in their reactions.

Because of their instability complexes **2** and **3** were generated in situ by reaction of the allylic halide with bis(cyclooctadiene)nickel in THF at −30 °C followed by addition of the substrate. The reaction was stirred at 0 °C until the red color of the (π-allyl)nickel halide complexes had disappeared. Reactions run at temperatures in excess of 0 °C resulted in preferential decomposition of the nickel complex. Because of this instability only the most reactive of substrates (aryl iodides, vinyl, and allyl

(10) E. J. Corey, M. F. Semmelhack, and L. S. Hegedus, *J. Am. Chem. Soc.*, **90**, 2416 (1968).
(11) R. C. Krug and T. F. Yen, *J. Org. Chem.*, **21**, 1082 (1956).

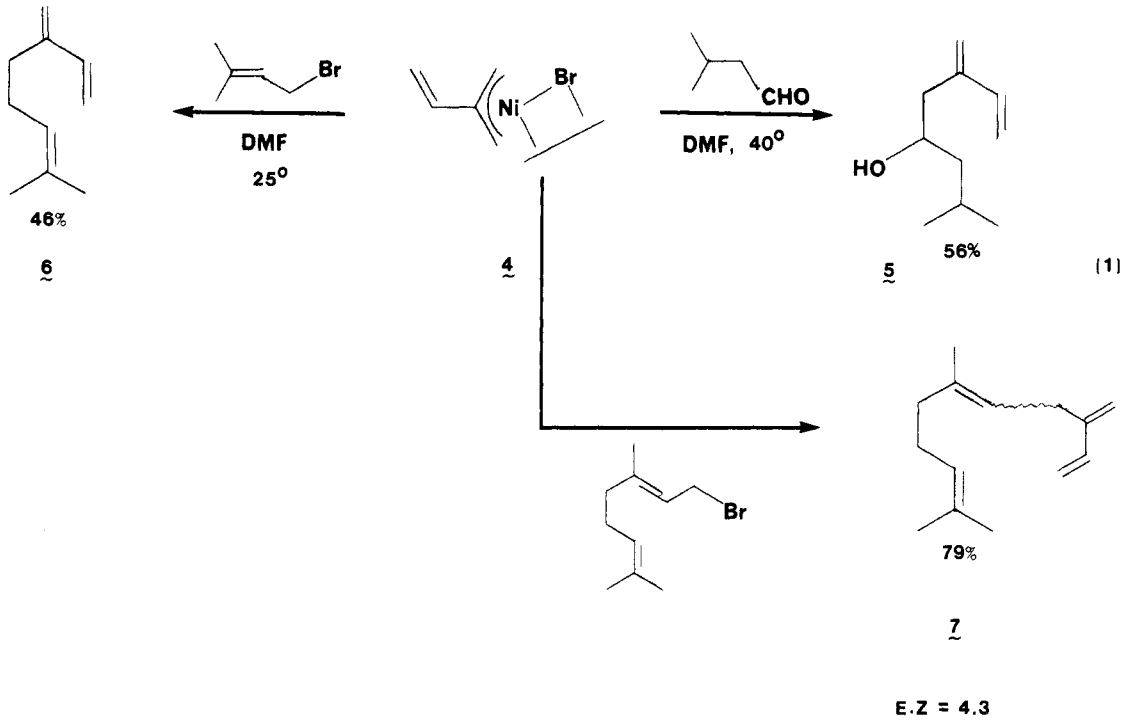

bromides) were successfully allylated. The reaction with cinnamyl bromide suffered from the usual allyl–allyl interchange resulting in the formation of all possible coupling products, hence lowering the yield of the desired cross-coupled product.[10] Other substrates, including ketones and aldehydes, lacked sufficient reactivity to undergo allylation at temperatures below which complex decomposition occurred.

Complex 4 reacted with aryl, vinyl, and allyl halides to introduce the isoprenyl group into these substrates. This complex was used to synthesize three terpenoid compounds, myrcene, β-farnesene, and tagetol (eq 1). These results demonstrate three interesting features of complex 4. The formation of tagetol (5) indicates that 4 is sufficiently stable to survive the gentle heating necessary to effect reactions with aldehydes. This stands in direct contrast to the behavior of complexes 2 and 3. The reaction with isoprenyl bromide to form myrcene in 63% yield indicates that allyl–allyl exchange does not occur to a significant extent and that cross coupling to allylic halides with this complex is an efficient process. This is confirmed in the cross coupling with geranyl bromide to form β-farnesene in high yield. This reaction is particularly interesting in light of the fact that the reaction of (π-geranyl)nickel bromide with isoprenyl bromide gave β-farnesene in only 20% yield, with an *E*:*Z* ratio of 0.8.[12] Clearly the reaction depends on the exact nature of the (π-allyl)nickel halide complex involved, and complex 4 appears to be an attractive reagent for the introduction of the isoprenyl group in the synthesis of terpenes.

In summary, complexes 1–4 offer a method to introduce diene-containing units into a variety of substrates, particularly organic halides. Although in some instances, the yields are rather low, the procedure only involves one step and may prove to be more efficient than multistep approaches.

Experimental Section

General Data. Infrared (IR) spectra were recorded on a Beckman Model 4200 spectrophotometer. Proton NMR spectra were determined on a Varian T-60 or EM-360A spectrometer. All the chemical shifts are reported in parts per million (δ) downfield from internal tetramethylsilane. Liquid chromatography was carried out at moderate pressures (40–80 psi) with either 15 × 250 mm or 15 × 1000 mm columns using Woelm type 206 silica gel. Preparative layer chromatography was carried out by using 20 × 20 cm plates coated with EM laboratories 60 PF-254 silica gel. Gas chromatography was done by using Bendix gas chromatograph 2300. Dry tetrahydrofuran (THF) and benzene were obtained by distillation from sodium. Dimethylformamide (DMF) was distilled over calcium hydride and under reduced pressure. Hexane was distilled over lithium aluminum hydride (LAH).

Preparation of π-Allylnickel Halide Complexes. (π-1-(2-Propenyl)allyl)nickel Bromide (1). This complex was prepared by the procedure of Semmelhack[1a] from *nickel carbonyl* (*Toxic*! *EXTREME Caution*!) (20 mL) and a mixture of 1-bromo-2,5-hexadiene and 3-bromo-1,5-hexadiene[13] (8 g) in benzene (200 mL) at 65–70 °C for 1 h. The product was recrystallized from hexane at −78 °C to give 8.3 g (77%) of the desired complex as a red, crystalline air-sensitive solid. Anal. Calcd for $C_{12}H_{18}Br_2Ni_2$: Ni, 26.70. Found: Ni, 26.30. In spite of repeated purification and careful sample preparations, the NMR spectrum of this complex was always very broad and ill-defined.

(π-2-Vinylallyl)nickel Bromide (4). This complex was obtained as a red, crystalline air-sensitive solid in 74% yield by allowing bis(1,5-cyclooctadiene)nickel(0) (1.42 g, 5.16 mmol) to react with 2-(bromomethyl)-1,3-butadiene[11] (0.75 g, 5.16 mmol) in benzene (75 mL) at 0 °C for 1 h and purifying the product by recrystallization from hexane following the general procedure.[1b] NMR (C_6D_6): δ 1.40 (s, 2, anti, CH), 2.80 (s, 2, syn, CH), 4.90 (d, J = 12 Hz, 1, cis, CH=CH_2), 5.18 (d, J = 20 Hz, 1, trans, CH=CH_2), 6.16 (d of d, J's = 12, 20 Hz, 1, CH=CH$_2$). Anal. Calcd for $C_{10}H_{14}Br_2Ni_2$: Ni, 28.52; Br, 38.87. Found: Ni, 28.39; Br, 38.47.

Reaction of Complex 1 with (a) Iodobenzene. Iodobenzene (0.33 g, 0.64 mmol) in 3 mL of DMF was added to the solution of the nickel complex (0.36 g, 0.82 mmol) in 10 mL of DMF and the mixture stirred at room temperature for 24 h. After the usual isolation (partitioning between dilute HCl and ether)[1b] the product was purified by preparative layer chromatography on silica gel developing with petroleum ether (R_f 0.6) to yield 0.24 g (91%) of 6-phenyl-1,4-hexadiene. NMR (CCl_4): δ 2.8 (t, J = 5 Hz, 2, =CCH$_2$C=), 3.3 (d, J = 5 Hz, 2, ArCH$_2$), 4.8–5.1 (m, 2, =CH$_2$), 5.5 (m, 3, CH=), 7.1 (m, 5, ArH). Mass spectrum: m/e 158 (M^+, parent ion). Anal. ($C_{12}H_{14}$): C, H.

(12) M. F. Semmelhack, Ph.D. Thesis, Harvard University, 1967. See also ref 1b, p 191.

(13) J. C. H. Hwa and H. Sims, "Organic Syntheses"; Coll. Vol. V, Wiley, New York, 1973, p 608.

(b) Cyclohexyl Iodide. The reaction was carried out in the usual manner using 0.47 g (1.10 mmol) of the nickel complex and 0.46 g (2.14 mmol) of cyclohexyl iodide in 10 mL of DMF. After the reaction was stirred at room temperature for 4 days, isolation in the usual manner, followed by evaporative distillation at 70 °C (4mmHg), yielded 0.22 g (62.6%) of a colorless oil. NMR ($CDCl_3$): δ 0.6–1.8 (m, 11, cyclohexyl-H), 1.8–2.0 (m, 2, CH_2C=), 2.8 (m, 2, =CCH_2C=), 4.8–5.3 (m, 2, C=CH_2), 5.4–6.2 (m, 2, CH=). Anal. ($C_{12}H_{20}$): C, H.

(c) 2-Bromobenzamide. 2-Bromobenzamide (3.25 g, 16.2 mmol) dissolved in 10 mL of DMF was treated with 4.2 g (9.5 mmol) of the nickel complex in 60 mL of DMF and stirred at room temperature for 7 days. The crude product was isolated following the usual procedure and purified by medium-pressure liquid chromatography (4:1 ether/hexane) to obtain the pure product (1.95 g, 60%) as a white crystalline solid: mp 98–100 °C. NMR ($CDCl_3$): δ 2.8 (t, J = 5 Hz, 2, =CCH_2C=), 3.6 (d, J = 5 Hz, 2, $ArCH_2$), 4.8–5.2 (m, 2, =CH_2), 5.4–6.2 (m, 3, CH=), 6.5 (br, 2, NH), 7.1–7.7 (m, 4, ArH). IR (KBr): 3375 (NH), 1650 (C=O), 1620 (C=O), 1595, 1575 cm^{-1}. Anal. ($C_{13}H_{15}NO$): C, H, N.

(d) 2-Bromoaniline. The nickel complex (0.43 g, 1.0 mmol) in 15 mL of DMF was treated with 0.25 g (1.50 mmol) of 2-bromoaniline dissolved in 2 mL of DMF. The reaction mixture was stirred at room temperature for 5 days. After standard isolation, the crude brown oil, purified by preparative layer chromatography on silica gel developing with chloroform (R_f 0.54), gave the product as a pale yellow liquid (0.13 g, 51%). NMR ($CDCl_3$): δ 2.75 (m, 2, =CCH_2C=), 3.15 (m, 2, $ArCH_2$), 3.45 (s, 2, NH_2), 4.75–5.2 (m, 2, =CH_2), 5.35–6.2 (m, 3, CH=), 6.3–7.1 (m, 4, ArH). IR (neat): 3470 (NH), 3390 (NH) cm^{-1}. Anal. ($C_{12}H_{15}N$): C, H, N. Mass spectrum: m/e 173 (M^+, parent ion).

(e) β-Bromostyrene. To 0.87 g (1.97 mmol) of the complex dissolved in 10 mL of DMF was added *trans*-β-bromostyrene (0.36 g, 1.97 mmol), and the mixture was stirred for 3 days at room temperature. The usual isolation followed by medium-pressure liquid chromatography (MPLC) on silica gel eluting with hexane gave 0.350 g (96%) of the product as a colorless oil. NMR (CCl_4): 2.8 (br m, 4, CH_2), 4.8–5.2 (m, 2, =CH_2), 5.35–5.9 (m, 3, =$C_{4,5,7}H$), 6.2 (t, J = 5 Hz, 1, =C_2H), 6.35 (d, J = 16 Hz, 1, C_1H), 7.26 (s, 5, ArH). Anal. ($C_{14}H_{16}$): C, H.

(f) 1-Iodohexane. Reaction of the complex (1.10 g, 2.5 mmol) with 1-iodohexane (0.53 g, 2.5 mmol) for 3 days at room temperature followed by the usual isolation and evaporative distillation gave the pure product (0.21 g, 50.6%) whose NMR spectrum was identical with that previously reported.[14]

(g) Cinnamyl Bromide. The complex (0.68 g, 1.53 mmol) was treated with *trans*-cinnamyl bromide (0.30 g, 1.53 mmol) in THF (10 mL) and stirred at room temperature for 3 days. After the usual isolation procedure, purification by medium-pressure liquid chromatography on silica gel eluted with hexane gave a colorless oil in 52% yield (0.16 g). NMR (CCl_4): δ 2.1–2.43 (m, 4, CH_2CH_2), 2.7 (m, 2, CCH_2C=), 4.71–5.2 (m, 2, =CH_2), 5.2–5.9 (m, 3, =CH), 6.1 (t, 1, J = 4 Hz, PhCHC*H*), 6.16 (d, J = 16 Hz, 1, PhC*H*=CH), 7.14 (s, 5, ArH). Anal. ($C_{15}H_{18}$): C, H.

General Procedure for the Reaction of Complex 2 with Halides. Bis(1,5-cyclooctadiene)nickel was dissolved in THF (20 mL/mmol) under an argon atmosphere. It was cooled to −30 °C, and 1-bromo-2,4-pentadiene was added while stirring the mixture rapidly. This was immediately followed by the rapid addition of the substrate, either as a neat liquid or as a solution in THF. The reaction mixture was kept initially at this temperature for 4 h and then at −20 °C for 1 h. It was then warmed to 0 °C and kept at this temperature until the red color disappeared. After the mixture was warmed to room temperature, water (5 mL) was added to dissolve the nickel salts, and THF was removed under vacuum. The product was extracted with ether, washed with water, followed by brine, dried ($MgSO_4$), and concentrated. The same general procedure was used in the reactions of complex 3 with halides.

Reaction of Complex 2 with (a) Iodobenzene. Reaction of the complex formed from 1.21 g (4.4 mmol) of bis(1,5-cyclooctadiene)nickel and 1-bromo-2,4-pentadiene (0.65 g, 4.4 mmol) with iodobenzene (0.45 g, 2.2 mmol) in THF in the manner described above gave, after purification by MPLC on silica gel eluted with hexane, 0.23 g of a colorless oil containing 45% (based on NMR) of 1-phenyl-2,4-pentadiene.[15] A sample of pure material was collected by preparative GLC (10 ft 10% Carbowax, 20M 110 °C, 3.8 min). NMR (CCl_4): δ 3.4 (d, J = 6 Hz, 2, $ArCH_2$), 4.8–6.6 (m, 5, =CH, =CH_2), 7.16 (s, 5, ArH). Anal. ($C_{11}H_{12}$): C, H.

(b) β-Bromostyrene. Reaction of $Ni(COD)_2$ (1.88 g, 6.82 mmol), 1-bromo-2,4-pentadiene (1.0 g, 6.82 mmol), and *trans*-β-bromostyrene (0.624 g, 3.41 mmol) in THF gave after the usual isolation and MPLC separation (silica gel, hexane) 0.70 g of an oil containing 69% of the product (based on NMR). Pure product was obtained by preparative GLC (10 ft 10% Carbowax, 20M 180 °C, 8 min). NMR (CCl_4): δ 2.96 (t, J = 5 Hz, 2, CH_2), 4.8–5.3 (m, 2, =CH_2), 5.53–6.4 (m, 3, =CH), 6.2 (t, J = 5 Hz, 1, PhCH=C*H*), 6.3 (d, J = 16 Hz, 1, PhC*H*=CH), 7.26 (s, 5, ArH). Mass spectrum: m/e 170 (M^+, parent ion). Anal. ($C_{13}H_{14}$): C, H.

(c) Cinnamyl Bromide. The procedure was slightly modified. To $Ni(COD)_2$ (1.68 g, 6.1 mmol) dissolved in THF (10 mL) was added triphenylphosphine dissolved in THF (1.50 g, 5.7 mmol). After 0.25 h, 1-bromo-2,4-pentadiene (0.90 g, 6.12 mmol) was added. The mixture was warmed to 25 °C and cinnamyl bromide (0.60 g, 3.06 mmol) was added. The isolation, after 3 days, following a partial separation (MPLC, silica gel, hexane) gave 410 mg of an oil containing 28% (by NMR) of the product as a 1:1 mixture of trienes. The mixture was separated by preparative GLC (10 ft 10% Carbowax, 150 °C; retention time, 12 min) to afford the pure compounds. NMR (CCl_4) (1-phenyl-1,5,7-octatriene): 2.2 (m, 4, CH_2CH_2), 4.8–5.36 (m, 2, =CH_2), 5.66–6.56 (m, 4, =CH), 6.3 (d, J = 16 Hz, 1, PhC*H*=CH), 7.23 (s, 5, ArH). Anal. ($C_{14}H_{16}$): C, H. NMR (CCl_4) (1-phenyl-4-vinyl-1,5-hexadiene): 2.5 (t, J = 6 Hz, 2, CH_2), 3.06–3.53 (m, 1, CH), 4.8–6.5 (m, 8, =CH_2, =CH), 7.23 (s, 5, ArH). Anal. ($C_{14}H_{16}$): C, H.

Reaction of Complex 3 with (a) Iodobenzene. Reaction of $Ni(COD)_2$ (1.16 g, 4.21 mmol), 1-bromo-2,4-hexadiene (0.68 g, 4.21 mmol), and iodobenzene (0.43 g, 2.1 mmol) gave, as described for complex **2** above after routine isolation procedures and purification (MPLC, silica gel, hexane) 0.15 g (46%) of pure product[16] as a colorless oil. NMR (CCl_4): δ 1.75 (d, J = 6 Hz, 3, CH_3), 3.33 (d, J = 6 Hz, 2, CH_2), 5.0–6.33 (m, 4, =CH), 7.2 (s, 5, ArH).

(b) β-Bromostyrene. Treatment of $Ni(COD)_2$ (1.31 g, 4.76 mmol) with 1-bromo-2,4-hexadiene (0.77 g, 4.76 mmol) and *trans*-β-bromostyrene (0.44 g, 2.38 mmol) in THF followed by isolation in the usual manner and the purification on silica gel by MPLC eluting with hexane gave an oil (520 mg) containing the product (60% based on NMR). It was separated by preparative GLC (10 ft 10% Carbowax, 180 °C, retention time, 9 min). NMR (CCl_4): δ 1.7 (d, J = 6 Hz, 3, CH_3), 2.9 (t, J = 6 Hz, 2, CH_2), 5.2–6.6 (m, 5, =CH_2), 6.3 (d, J = 16 Hz, 1, α-H, PhC*H*=CH), 7.15 (s, 5, ArH). Mass spectrum: m/e 184 (M^+, parent ion). Anal. ($C_{14}H_{16}$): C, H.

(c) Cinnamyl Bromide. The modified procedure involving the use of triphenylphosphine is analogous to that reported earlier for the synthesis of 1-phenyl-1,5,7-octatriene. Thus reaction of $Ni(COD)_2$ (1.30 g, 4.7 mmol), 1-bromo-2,4-hexadiene (0.764 g, 4.7 mmol), cinnamyl bromide (0.47 g, 2.37 mmol), and triphenylphosphine (1.24 g, 4.7 mmol) yielded the product (110 mg, 23%) as an oil after separation by MPLC (silica gel, hexane). NMR (CCl_4): δ 1.66 (d, J = 6 Hz, 3, CH_3), 2–2.5 (m, 4, CH_2), 4.7–6.4 (m, 6, =CH), 7.2 (s, 5, ArH). Mass spectrum: m/e 198 (M^+, parent ion). Anal. ($C_{15}H_{18}$): C, H.

Reactions of Complex 4 with (a) Iodobenzene. The nickel complex (0.40 g, 1.09 mmol) cooled to −30 °C was dissolved in 10 mL of DMF also cooled to the same temperature. To the resulting solution was added iodobenzene (0.22 g, 1.09 mmol), and the mixture was warmed to room temperature and stirred for 1 day. The usual isolation followed by purification by medium-pressure liquid chromatography (hexane) gave 72 mg (46%) of the pure product[17] as a colorless oil. NMR (CCl_4): δ 3.5 (s, 2, $ArCH_2$), 4.8–5.4 (m, 4, =CH_2), 6.4 (dd, J = 10 and 16 Hz, 1, =CH),

(14) A. Alexakis, G. Cahiez, and J. F. Normant, *Synthesis*, 826 (1979).

(15) A. V. Dombrovskii, *Dokl. Akad. Nauk SSSR*, 111, 827 (1956).

(16) H. J. Reich, S. K. Shah, and F. Chow, *J. Am. Chem. Soc.*, 101, 6648 (1979).

(17) G. Wittig and H. Duerr, *Justus Liebigs Ann. Chem.* 672, 55 (1964).

7.2 (s, 5, ArH). Anal. ($C_{11}H_{12}$): C, H.

(b) β-Bromostyrene. To the nickel complex (0.97 g, 2.63 mmol) cooled to −30 °C was added the solution of *trans*-β-bromostyrene (0.43 g, 2.36 mmol) in DMF (10 mL) also cooled to −30 °C. the mixture was warmed to room temperature and stirred for 2 days. The isolation in the usual manner followed by separation on silica gel by MPLC with hexane as eluant gave 0.20 g (49.8%) of the desired product as a colorless oil. NMR (CCl_4): δ 3.06 (dd, J = 4 Hz, 2, CH_2), 4.93–5.4 (m, 4, =CH_2), 6.2–6.6 (m, 2, =CH), 6.4 (dd, J = 10 and 16 Hz, 1, PhCHC*H*), 7.2 (s, 5, ArH). Anal. ($C_{13}H_{14}$): C, H. Mass spectrum: m/e 170 (M^+, parent ion).

(c) Cinnamyl Bromide. The reaction of the nickel complex (0.738 g, 1.78 mmol) with cinnamyl bromide (0.35 g, 1.78 mmol) in THF (20 mL) was carried out in a fashion similar to that described above. Purification by MPLC on silica gel using hexane for elution gave 52% (0.17 g) of the desired product. NMR (CCl_4): δ 2.4 (m, 4, CH_2), 4.8–5.35 (m, 4, =CH_2), 5.6–6.8 (m, 3, =CH), 7.25 (s, 5, ArH). Mass spectrum: m/e 184 (M^+, parent ion).

Synthesis of Myrcene (6). To the freshly prepared nickel complex (0.62 g, 1.5 mmol) dissolved in THF (15 mL) was added 1-bromo-3-methyl-2-butene (0.34 g, 2.26 mmol) rapidly via a syringe. After being stirred for 20 h at room temperature, the mixture was filtered to remove the brownish yellow solid which was repeatedly washed with pentane. The filtrate was washed with water to remove THF and dried over $MgSO_4$. Pentane was removed by distillation to obtain an oil (0.25 g) containing 63% of myrcene.[18] Preparative layer chromatography on silica gel developing with hexane (R_f 0.51) gave the pure product (0.13 g, 46%) in all respects identical with the authentic material.

β-Farnesene. With use of 0.26 g (0.62 mmol) of the nickel complex and 0.20 g (0.93 mmol) of *trans*-geranyl bromide, the reaction was carried out as in the case of myrcene. Isolation and purification by the procedure similar to that described for myrcene gave 0.15 g (78.5%) of the product mixture of (*E*)- and (*Z*)-β-farnesene in the ratios of 81.3 and 18.6, respectively (calculated based on GLC). NMR and IR spectra of the product were as reported for β-farnesene.[19]

Tagetol. The nickel complex (0.85 g, 2.0 mmol) and isovaleraldehyde (0.27 g, 3.1 mmol) were allowed to react in THF at room temperature for 20 h and at 40 °C for 6 h. The reaction mixture was treated with 1 mL of water and diluted with 20 mL of ether. The organic layer was separated, washed with brine, dried ($MgSO_4$), and concentrated under rotary evaporator to obtain a yellow oil which was purified by preparative layer chromatography (Si gel, 2:1 hexane:ether, R_f 0.58) (yield, 0.27 g (56%)). ^1H NMR and IR spectra were identical with that of tagetol.[20]

Preparation of Allylic Bromides. The allylic bromides for the synthesis of complexes **1–3**, 1-bromo-2,5-hexadiene,[13] 1-bromo-2,4-pentadiene,[21] and 1-bromo-2,4-hexadiene,[21] were synthesized by published procedures. The 2-(bromomethyl)-1,3-butadiene required for complex **4** was synthesized from 3-methyl-2,5-dihydrothiophene 1,1-dioxide (from isoprene and SO_2)[22] by the following procedure.

3-(Bromomethyl)-2,5-dihydrothiophene 1-Oxide (13). Freshly distilled methylene chloride (400 mL) was added to a mixture containing 35 g (0.26 mol) of 3-methyl-2,5-dihydrothiophene 1,1-dioxide and 47.2 g (0.26 mol) of recrystallized *N*-bromosuccinimide and 3 g of benzoyl peroxide. The mixture was stirred and heated at gentle reflux in an oil bath kept at 50 °C. The reaction flask was simultaneously irradiated with light from 500-W tungsten bulb to hasten the reaction. The reaction was followed by TLC on silica gel developing with ethyl acetate. Once all the NBS had been consumed, the flask was cooled to 25 °C and the solution filtered to remove the succinimide (25.0 g, 86.2%). The solvent was removed under vacuum and the product recrystallized from 95% ethanol (41.0 g, 73.0%); mp 87–88 °C (lit.[22] 87–88 °C). ^1H NMR (CCl_4): δ 6.0 (m, 1, =CH), 4.03 (s, 2, CH_2Br), 3.83 (s, 4, CH_2SO_2).

The (**14**) 2-(bromomethyl)-2,5-dihydrothiophene 1,1-dioxide (3.1 g) was placed in a short-path distillation apparatus. At a reduced pressure of 1mmHg the flask was immersed rapidly in an oil bath at 180 °C. No radical scavanger was added to the distillation flask. The product (1.56 g, 72%) was collected in a flask and cooled in Dry Ice/2-propanol bath. ^1H NMR (CCl_4): δ 4.26 (s, 2, CH_2Br), 5.4 (m, 4, =CH), 6.5 (m, 1, =CH).

Acknowledgment. Support for this research under Grant 1R01 GM26178-01 from the National Institutes of Health is gratefully acknowledged.

Registry No. **1**, 79483-21-9; **2**, 79483-22-0; **3**, 79483-23-1; **4**, 79483-24-2; **5**, 35628-05-8; **6**, 123-35-3; **7**-(*E*), 502-60-3; **7**-(*Z*), 28973-97-9; **13**, 79482-77-2; **14**, 31554-48-0; iodobenzene, 591-50-4; cyclohexyl iodide, 626-62-0; 2-bromobenzamide, 4001-73-4; 2-bromoaniline, 615-36-1; *trans*-β-bromostyrene, 588-72-7; 1-iodohexane, 638-45-9; 1-bromo-3-methyl-2-butene, 870-63-3; *trans*-geranyl bromide, 6138-90-5; isovaleraldehyde, 590-86-3; *trans*-cinnamyl bromide, 26146-77-0; 6-phenyl-1,4-hexadiene, 79482-78-3; 6-cyclohexyl-1,4-hexadiene, 79482-79-4; 2-(2,5-hexadienyl)benzamide, 76916-63-7; 2-(2,5-hexadienyl)aniline, 76916-50-2; 1-phenyl-1,4,7-octatriene, 79482-80-7; 1,4-dodecadiene, 79482-81-8; 9-phenyl-1,4,8-nonatriene, 79482-82-9; 5-bromo-1,3-pentadiene, 1001-93-0; 5-phenyl-1,3-pentadiene, 1007-52-9; 7-phenyl-1,3,6-heptatriene, 79482-83-0; 1-phenyl-1,5,7-octatriene, 79482-84-1; 1-phenyl-4-vinyl-1,5-hexadiene, 79482-85-2; 6-phenyl-2,4-hexadiene, 79482-86-3; 8-phenyl-2,4,7-octatriene, 79482-87-4; 9-phenyl-2,4,8-nonatriene, 79482-88-5; 3-methylene-4-phenyl-1-butene, 16079-66-6; 3-methylene-6-phenyl-1,5-hexadiene, 79482-89-6; 3-methyl-7-phenyl-1,6-heptadiene, 79482-90-9; 3-methyl-2,5-dihydrothiophene 1,1-dioxide, 1193-10-8; nickel tetracarbonyl, 13463-39-3; bis(1,5-cyclooctadiene)nickel (0), 1295-35-8; 6-bromo-1,4-hexadiene, 5903-38-8; 3-bromo-1,5-hexadiene, 53737-88-5; 2-(bromomethyl)-1,3-butadiene, 23691-13-6; 1-bromo-2,4-hexadiene, 63072-78-6.

(18) B. M. Mitzner, E. T. Theimer, L. Steinbeck, and J. Wolt, *J. Org. Chem.*, **30**, 646 (1964).
(19) S. Tanaka, A. Yasuda, H. Yamamoto, and H. Nozaki, *J. Am. Chem. Soc.*, **97**, 3251 (1975).
(20) C. A. Reece, J. O. Rodin, R. G. Brownlee, W. G. Duncan, and R. M. Silverstein, *Tetrahedron*, **24**, 4249 (1968).
(21) K. Mori, *Tetrahedron*, **30**, 3807 (1974).
(22) R. L. Frank and R. P. Seven, "Organic Syntheses", Coll. Vol. III, Wiley, New York, 1955, p 499.

Metal Complexes of Severely Crowded Molecules. Synthesis, Structure, and Reactivities of the $M(CO)_3$ (M = Cr, Mo, and W) Complexes of Octamethylnaphthalene

John W. Hull, Jr., and Wayne L. Gladfelter*

Department of Chemistry, University of Minnesota, Minneapolis, Minnesota 55455

Received July 7, 1981

The preparations of the metal tricarbonyl complexes (Cr, Mo, and W) of octamethylnaphthalene (OMN) are described. The structure of the chromium complex was determined by single-crystal X-ray crystallography [$P\bar{1}$ space group, $Z = 2$, $a = 9.326$ (4) Å, $b = 13.992$ (3) Å, $c = 7.919$ (2) Å, $\alpha = 95.44$ (2)°, $\beta = 115.00$ (3)°, $\gamma = 76.40$ (2)°]. The chromium tricarbonyl fragment is π bound to one the six-membered rings. The distortions of the metal-complexed OMN differ very little from the structure of the free ligand. The thermal and photochemical reactions of the Cr complex with phosphorus donor ligands differed. Photolysis of $(OMN)Cr(CO)_3$ in the presence of triphenylphosphine produces purple $(OMN)Cr(CO)_2PPh_3$, while heating $(OMN)Cr(CO)_3$ in neat trimethyl phosphite generates $Cr(CO)_3[P(OCH_3)_3]_3$. Maleic anhydride reacts with $(OMN)Cr(CO)_3$ to give two isomers resulting from a Diels–Alder addition to the free ring. The stereochemistry of one of the isomers was determined by X-ray crystallography [$P2_1/c$ space group, $Z = 4$, $a = 16.219$ (6) Å, $b = 9.284$ (3) Å, $c = 16.718$ (6) Å, $\beta = 118.07$ (3)°] and was found to result from attack of maleic anhydride on the side of the ring opposite the metal atom. The two isomers differ in the orientation (exo and endo) of the anhydride group with respect to the aromatic ring. A comparison of the equilibrium constants for the free ligand and the complex in the Diels–Alder reaction shows an enhancement of over 2 orders of magnitude for the metal complex. The difference is attributed to the increased strength of interaction of the metal with the planar ring of the cycloaddition product.

Introduction

When substituents are placed in the peri positions of naphthalene, a molecular distortion ensues caused by nonbonding repulsive forces between these groups. By changing the substituents, it has been possible to change both the magnitude and even the mode of the distortions.[1] At the extremes, two types are found. The first involves an in-plane bend of the C1– and/or the C8–substituent bond, I. The second involves a displacement of the sub-

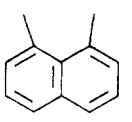

I

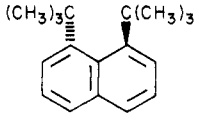

II

stituents above and below the mean plane of the naphthalene ring, II. 1,8-Dimethylnaphthalene exhibits an in-plane distortion[2] while larger groups such as bis(trimethylelement) (C, Ge, and Sn) force the out-of-plane distortion to occur.[3-7] The structural details of many of these compounds have been examined by X-ray crystallography[2,3,5,8-10] and evaluated by using force field calculations.[3,5,7] Molecules of the second type have the additional interesting feature of chirality. The barriers for enantiomerization are typically too low to allow observation for all but the bulkiest groups such as $[(CH_3)_3Z]_2$, where Z = C, Ge, and Sn. Although the value of $\Delta G^{\ddagger}$ for Z = C is estimated to be greater than 24 kcal/mol,[4] the measured value for 1,8-bis(trimethylgermyl)-4-(methoxymethyl)-naphthalene is 7.5 ± 0.1 kcal/mol at −122 °C.[7]

Octamethylnaphthalene (OMN) fits into a subclass of these systems in which both sets of peri positions are substituted. After its synthesis[11] in 1953, a single-crystal X-ray crystallographic study showed[12] that unlike 1,8-dimethylnaphthalene, OMN distorts in an out-of-plane fashion. This study also suggested that the structure is that shown in III, but this was later questioned after a

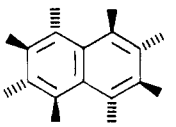

III

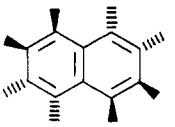

IV

study of octachloronaphthalene revealed[13] that the chloro substituents are distorted in a pairwise fashion, IV. Hart and co-workers recently published[14] an efficient synthesis of OMN and upon reinvestigating the X-ray crystallographic analysis indeed found that the molecule has the structure shown in IV.[15]

The effect of metal complexation of arenes on the conformation of the ligand itself recently was examined by Mislow and co-workers[16] in the chromium tricarbonyl complex of hexaethylbenzene. In solution and the solid-state structure of $(\eta^6\text{-}C_6Et_6)Cr(CO)_3$ the methyls are pos-

(1) Balasubramaniyan, V. *Chem. Rev.* **1966**, *66*, 567.
(2) Bright, D.; Maxwell, I. E.; deBoer, J. *J. Chem. Soc., Perkin Trans. 2* **1973**, 2101.
(3) Handal, J.; White, J. G.; Franck, R. W.; Yuh, Y. H.; Allinger, N. L. *J. Am. Chem. Soc.* **1977**, *99*, 3345.
(4) Anderson, J. E.; Franck, R. W.; Mandella, W. L. *J. Am. Chem. Soc.* **1972**, *94*, 4608.
(5) Blount, J. F.; Cozzi, F.; Damewood, J. R., Jr.; Iroff, L. D.; Sjöstrand, U.; Mislow, K. *J. Am. Chem. Soc.* **1980**, *102*, 99.
(6) Anet, F. A. L.; Donovan, D.; Sjöstrand, U.; Cozzi, F.; Mislow, K. *J. Am. Chem. Soc.* **1980**, *102*, 1748.
(7) Hounshell, W. D.; Anet, F. A. L.; Cozzi, F.; Damewood, J. R., Jr.; Johnson, C. A.; Sjöstrand, U.; Mislow, K. *J. Am. Chem. Soc.* **1980**, *102*, 5941.
(8) Einspuhr, H.; Robert, J. B.; Marsh, R. E.; Roberts, J. D. *Acta Crystallogr., Sect. B* **1973**, *B29*, 1611.
(9) Robert, J. B.; Sherfinski, J. S.; Marsh, R. E.; Roberts, J. D. *J. Org. Chem.* **1974**, *39*, 1152.
(10) Herbstein, F. H. *Acta Crystallogr., Sect. B* **1979**, *B35*, 1661.
(11) Abadir, J. B.; Cook, J. W.; Gibson, D. T. *J. Chem. Soc.* **1953**, 8.
(12) Donaldson, D. M.; Robertson, J. M. *J. Chem. Soc.* **1953**, 17.
(13) Gafner, G.; Herbstein, F. H. *Nature (London)* **1963**, *200*, 130.
(14) Hart, H.; Teuerstein, A. *Synthesis* **1979**, 693.
(15) Hart, H., personal communication.
(16) Hunter, G.; Iverson, D. J.; Mislow, K.; Blount, J. F. *J. Am. Chem. Soc.* **1980**, *102*, 5942.

0276-7333/82/2301-0264$01.25/0

itioned alternatively above and below the plane of the arene. Upon substitution of only one carbonyl with triphenylphosphine all the methyls were forced to the side of the ring which was opposite that of the metal.

We have initiated a study of the interaction of transition metals with severely crowded naphthalenes and report here our results on the synthesis, structure, and reactivity of (octamethylnaphthalene)tricarbonylmetal (M = Cr, Mo, and W) complexes.

Experimental Section

General Information. ^1H NMR spectra were obtained on Varian Models CFT-20 and XL-100, as well as a Bruker 270 MHz instrument. Infrared spectra were obtained on a Beckman Model 4250. All solvents were freshly distilled over sodium benzophenone ketyl under nitrogen atmosphere unless stated otherwise. All metal hexacarbonyls were purchased from Strem Chemical Co. Octamethylnaphthalene[14] and $(CH_3CN)_3M(CO)_3$ (M = Mo, W)[17,18] were prepared by using literature procedures. All elemental analysess were obtained from Galbraith Laboratories.

(Octamethylnaphthalene)tricarbonylchromium(0). Hexacarbonylchromium (2.1 g, 9.6 mmol) and OMN (2.3 g, 9.6 mmol) were placed into a 250-mL round-bottom flask, and dry di-*n*-butyl ether (125 mL) was distilled into the reaction flask, followed by 7 mL of dry tetrahydrofuran (THF). After being fitted with a reflux condenser, the system was stirred, flushed with N_2, and refluxed. After 24 h the solution was cooled, filtered through a 2-cm layer of silica gel placed on a glass frit, and then rinsed with a few milliliters of benzene. The solvent was removed on a rotary evaporator with a 90 °C water bath to yield a dark red solid. Recrystallization in benzene/hexane yielded dark red crystals (52%) which are stable to air. Anal. Calcd for $C_{21}H_{24}CrO_3$: C, 67.00; H, 6.44. Found: C, 67.07; H, 6.61.

(Octamethylnaphthalene)tricarbonylmolybdenum(0). Tris(acetonitrile)tricarbonylmolybdenum (0.44 g, 1.5 mmol) was weighed into a Schlenk tube in an inert-atmosphere glovebox. Octamethylnaphthalene (0.42 g, 1.8 mmol) and dried, deoxygenated hexane (20 mL) were added. A condenser was attached to the Schlenk tube, and refluxing was maintained for 12 h, with constant magnetic stirring. The solution was filtered hot under N_2, leaving insoluble (OMN)$Mo(CO)_3$ as an orange, slightly air-sensitive solid on the filter (ca. 30% yield). Recrystallization in dry, deoxygenated CH_2Cl_2/hexane yielded bright orange crystals. Anal. Calcd for $C_{21}H_{24}MoO_3$: C, 60.00; H, 5.76. Found: C, 60.15; H, 5.85.

(Octamethylnaphthalene)tricarbonyltungsten(0). Tris(acetonitrile)tricarbonyltungsten (1.14 g, 2.91 mmol) and OMN (0.91 g, 3.78 mmol) were refluxed in 40 mL of dry hexane under nitrogen atmosphere for 8 days. After heating was stopped, the solution was filtered through a glass frit, followed by a hexane rinse. The filter flask was then changed, and the solid mass on the frit was rinsed repeatedly with methylene chloride to wash out bright red (OMN)$W(CO)_3$. The solid obtained after evaporation was recrystallized in dry, degassed CH_2Cl_2/hexane to give bright orange-red crystals (0.26 g, 18% yield). Anal. Calcd for $C_{21}H_{24}O_3W$: C, 49.63; H, 4.76. Found: C, 49.45; H, 4.79.

(Octamethylnaphthalene)dicarbonyl(triphenylphosphine)chromium(0). (Octamethylnaphthalene)tricarbonylchromium (0.27 g, 0.72 mmol) and triphenylphosphine (0.56 g, 2.15 mmol, recrystallized from ethanol) were irradiated in 30 mL of dry hexane in a Schlenk tube with a Hanovia ultraviolet lamp for 8 h. The heat from the lamp was allowed to reflux the reaction miture, and good stirring was maintained under a N_2 atmosphere. The dark violet solution was filtered hot through a glass frit and rinsed with hexane to obtain 0.15 g (34%) of a violet solid which is stable to air. Recrystallization in dry, degassed CH_2Cl_2/hexane yielded large, dark violet crystals. Anal. Calcd for $C_{38}H_{39}CrPO_2$: C, 74.74; H, 6.44. Found: C, 75.00; H, 6.56.

Tricarbonyltris(trimethyl phosphite)chromium. (Octamethylnaphthalene)tricarbonylchromium (30.5 mg, 0.08 mmol) was warmed to 70 °C in 2 mL of trimethyl phosphite under a nitrogen atmosphere. After being stirred for 2 h, the solution was cooled in an ice bath. Octamethylnaphthalene crystallized from the solution and was filtered off, after which trimethyl phosphite was removed by vacuum distillation. The resulting light-colored solid was rinsed with cold hexane, dried under vacuum, and obtained in 57% yield as a moderately air-sensitive solid. Infrared analysis indicated the presence of predominantly the facial isomer.[19]

[1,4,5,6-Tetramethyl-7,8-(tetramethylbenzo)bicyclo-[2.2.2]octa-5,7-diene-2,3-dicarboxylic anhydride]tricarbonylchromium ([OMN·MA]$Cr(CO)_3$). (Octamethylnaphthalene)tricarbonylchromium (601 mg, 1.6 mmol) and maleic anhydride (783 mg, 8.0 mmol) were placed into a 25-mL round-bottom flask; a reflux condensor fitted with a gas stopcock was attached and the system was repeatedly evacuated and flushed with nitrogen on a Schlenk line. Dry benzene (15 mL, distilled over CaH_2) was added quickly by syringe through the top of the condensor. The dark red solution was allowed to reflux under a nitrogen atmosphere with magnetic stirring for 21 h, by which time the color had lightened considerably to orange-red. The solution was cooled to room temperature and the benzene evaporated leaving a red-yellow solid, which was completely redissolved in about 10 mL of dry THF. Hexane was then added to the cloud point, and the flask was cooled in a freezer. The first crop of yellow crystals (206 mg) consisted of mainly the exo isomer. A second crop (174 mg) obtained from the mother liquor consisted of mainly the endo isomer. After the second crop was isolated, the yellow filtrate was washed with two or three small portions of water to remove excess maleic anhydride, dried over $MgSO_4$, and reduced in volume. An additional 198 mg of yellow crystals consisting of mostly endo isomer was obtained, giving a total isolated yield of 578 mg (76%). Complete separation of isomers was readily accomplished on a silica gel column, eluted with 3/1 hexane/ethyl acetate. The exo isomer eluted fairly rapidly, followed by the much slower endo isomer. Recrystallization in THF/hexane afforded completely pure (OMN·MA)$Cr(CO)_3$ as the single isomers by the HPLC analysis. The final exo/endo ratio is 2.3. Anal. Calcd for $C_{25}H_{26}CrO_6$: C, 63.29; H, 5.52. Found: C, 64.11; H, 5.73.

1,4,5,6-Tetramethyl-7,8-(tetramethylbenzo)bicyclo[2.2.2]-octa-5,7-diene-2,3-dicarboxylic Anhydride (OMN·MA). A. From Octamethylnaphthalene. Octamethylnaphthalene (584.6 mg, 2.43 mmol) and reagent grade maleic anhydride (7.15 g, 73.0 mmol) were placed into a 50-mL round-bottom flask, and 25 mL of benzene was added. The solution turned immediately to a bright red color due to formation of the charge-transfer complex. The solution was refluxed with magnetic stirring for 65 h, after which the solvent was evaporated to give a yellow solid. Water was added to the flask with stirring to dissolve excess maleic anhydride. Diethyl ether was added, and the contents were transferred to a separatory funnel. The organic layer was extracted twice with water and then evaporated to a white solid. Recrystallization in methylene chloride/hexane afforded 486 mg (59%) of both exo and endo isomers in a ratio of 7:1.

B. From (Octamethylnaphthalene–maleic anhydride)-tricarbonylchromium. The readily separated (OMN·MA)Cr-$(CO)_3$ isomers can be treated to obtain the corresponding OMN·MA adducts as single isomers.[20] Thus, a single isomer of (OMN·MA)$Cr(CO)_3$ was irradiated in THF in the presence of oxygen with a Hanovia ultraviolet quartz lamp in a round-bottom flask with magnetic stirring. The flask was cooled with a rapid stream of air to prevent any retro-Diels–Alder reaction from occurring. After 6–8 h of irradiation, the resulting cloudy green solution was filtered through a glass frit containing a layer of diatomaceous earth, and the clear, colorless solution was evaporated to a white solid. Recrystallization in THF/hexane afforded a single isomer of pure (OMN·MA) adduct in essentially quantitative yield from (OMN·MA)$Cr(CO)_3$.

HPLC Analysis of Diels–Alder and Retro-Diels–Alder Reactions. High-pressure liquid chromatography was performed with a Waters Associates M-45 solvent delivery system equipped with a Rheodyne 7125 injector and Beckman 153 UV analytical detector. A Waters Associates 30-cm μPorasil silica column af-

(17) King, R. B. *J. Organomet. Chem.* **1967**, *8*, 139.
(18) Tate, D. L.; Knipple, W. R.; Aigl, J. M. *Inorg. Chem.* **1962**, *1*, 433.
(19) Mathieu, R.; Lenzi, M.; Poilblanc, R. *Inorg. Chem.* **1970**, *9*, 2030.
(20) Jaouen, G. *Ann. New York Acad. Sci.* **1977**, *295*, 59.

Table I. Data for the X-ray Diffraction Study of (OMN)Cr(CO)$_3$

Crystal Parameters

crystal system = triclinic	V = 910 (1) Å^3
space group = $P\bar{1}$	Z = 2
a = 9.326 (4) Å	calcd density = 1.37 g cm^{-3}
b = 13.992 (3) Å	temp = 22 °C
c = 7.919 (2) Å	abs coeff = 6.73 cm^{-1}
α = 95.44 (2)°	formula = $C_{21}H_{24}CrO_3$
β = 115.00 (3)°	
γ = 76.40 (2)°	

Measurement of Intensity Data

diffractometer = Enraf-Nonius CAD4
radiation = Mo Kα (λ = 0.710 69 Å)
monochrometer = graphite crystal
scan speed = variable, see text
scan range = $0° \leq 2\theta \leq 50°$
reflections measd = $\pm h, \pm k, +l$
check reflections = {0,8,0}, {6,0,0}, {3,3,−3}; measured every 1.5 h
reflections collected = 3221 unique reflections; 2665 with $I > 2.5\sigma(I)$
p = 0.05
R = 2.9%
R_w = 4.4%

forded baseline separation of reaction components, eluting with a 4/1 hexane/ethyl acetate solvent mixture (MCB glass distilled, filtered through 5 μm glass frit prior to use) at a rate of 3.0 mL/min (1500 psi). Stock solutions of OMN, OMN·MA (each isomer), (OMN)Cr(CO)$_3$, and (OMN·MA)Cr(CO)$_3$ (each isomer) in THF were injected at various concentrations to determine standard concentration curves from peak heights and peak areas.

A. Chromium Complexes. One-milliliter solutions of the complexes in benzene were prepared as in the (OMN·MA)Cr(CO)$_3$ synthesis. Contact of dissolved substrates with oxygen and moisture was scrupulously avoided. A typical run was as follows. (OMN)Cr(CO)$_3$ (10.8 mg, 0.029 mmol) and maleic anhydride (14.1 mg, 0.143 mmol) were refluxed in 1.0 mL of benzene under N_2 with magnetic stirring for 26 h. Benzene was evaporated on a rotary evaporator, and the solid was redissolved in 1.0 mL of dry THF for HPLC analysis. (The adducts are more soluble in THF at room temperature and stable when exposed to the atmosphere for a short period of time.)

For the retro-Diels–Alder reaction, each isomer of (OMN·MA)Cr(CO)$_3$ was refluxed in benzene under N_2, covering the oil bath system with foil to minimize exposure to light. Product analysis was carried out by HPLC at various time intervals up to 74 h.

B. Noncomplexed Ligands. No special precautions were used to avoid contact of the substrates with oxygen. A typical Diels–Alder reaction was as follows. Octamethylnaphthalene (36.1 mg, 0.15 mmol) and maleic anhydride (73.6 mg, 0.75 mmol) were refluxed in 1.0 mL of benzene and analyzed by HPLC (in 1.0 mL of THF as with the chromium complexes above) at various time intervals up to 66 h.

A typical retro-Diels–Alder reaction was as follows. OMN·MA (single isomer, 10.0 mg, 0.030 mmol) and maleic anhydride (11.6 mg, 0.12 mmol) were refluxed in 1.0 mL of benzene and analyzed by HPLC at various intervals up to 116 h.

Collection and Reduction of the X-ray Data. Suitable red crystals of (OMN)Cr(CO)$_3$ (A) grown from solutions of benzene and hexane were mounted on a glass fiber. Yellow crystals of (OMN·MA)Cr(CO)$_3$ (B) were grown in CH_2Cl_2/hexane mixtures. A suitable crystal was mounted inside a N_2-filled capillary since slow decomposition occurred in the presence of both air and light. The crystals were centered and indexed by the Enraf-Nonius CAD4-SDP peak search, centering, and indexing programs.[21] The

Table II

Crystal Parameters

crystal system = monoclinic	V = 2221 (3) Å^3
space group = $P2_1/c$	Z = 4
a = 16.219 (6) Å	calcd density = 1.42 g cm^{-3}
b = 9.284 (3) Å	formula = $C_{25}H_{26}CrO_6$
c = 16.718 (6) Å	temp = 22 °C
β = 118.07 (3)°	abs coeff = 5.80 cm^{-1}

Measurement of Intensity Data

diffractometer = Enraf-Nonius CAD4
radiation = Mo Kα (λ = 0.710 69 Å)
monochrometer = graphite crystal
scan speed = variable, see text
scan range = $0° \leq 2\theta \leq 50°$
reflections measd = $+h, +k, \pm l$
check reflections = {8,0,0}, {−2,−4,−1}, {0,2,6}; measured approximately every 150 reflections
reflections collected = 4319 unique reflections; 2013 with $I > 2.5\sigma(I)$
p = 0.03
R = 0.048
R_w = 0.048

Scheme I

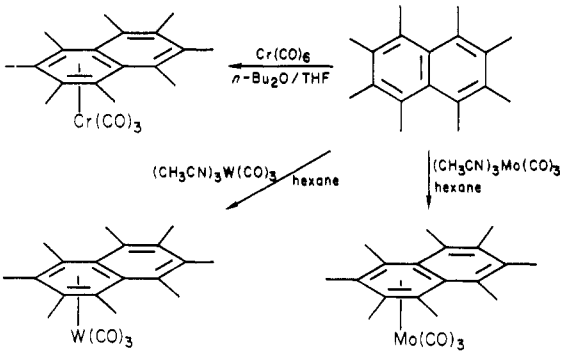

crystal systems were determined as triclinic for A and monoclinic for B. The centrosymmetric space group $P\bar{1}$ was chosen for A and eventually verified by successful refinement of the structure. The systematic absences in B uniquely identified the space group as $P2_1/c$. Summaries of the crystal data are presented in Tables I and II. Background counts were measured at both ends of the scan range by using a ω–2θ scan, equal at each side to one-fourth of the scan range of the peak. In this manner, the total duration of measured background is equal to half of the time required for the peak scan. The three check reflections in both A and B showed no decay during the course of data collection. In both structures the data intensity cutoff was set at $I > 2.5\sigma I$, which led to a total of 2665 reflections of A and 2013 reflections for B.[22] These were corrected for Lorrentz, polarization, and background effects but not for absorption.

Solution and Refinement of the Structure. The structures were solved by conventional heavy-atom techniques. The chromium atoms were located by a Patterson synthesis. Subsequent structure factor and difference Fourier calculations revealed the positions of the remaining nonhydrogen atoms.[23] After several

(21) All calculations were carried out on PDP 8A and 11/34 computers using the Enraf-Nonius CAD 4-SDP programs. This crystallographic computing package is described in: Frenz, B. A. In "Computing in Crystallography"; Schenk, H., Olthof-Hazekamp, R., van Koningsveld, H., Bassi, G. C., Eds.; Delft University Press: Delft, Holland, 1978; pp 64–71. Also "CAD 4 and SDP Users Manual"; Enraf-Nonius: Delft, Holland, 1978.

(22) The intensity data were processed as described: "CAD 4 and SDP Users Manual"; Enraf-Nonius: Delft, Holland, 1978. The net intensity $I = (K/\mathrm{NPI})(C - 2B)$, where $K = 20.1166x$ (attenuator factor); NPI = ratio of fastest possible scan rate to scan rate for the measurement, C = total count, and B = total background count. The standard deviation in the net intensity is given by $\mu^2(I) = (K/\mathrm{NPI})^2[C + 4B + (pI)^2]$, where p is a factor used to down weight intense reflections. The observed structure factor amplitude F_o is given by $F_o = (1/Lp)^{1/2}$, where Lp = Lorentz and polarization factors. The $\sigma(I)$'s were converted to the estimated errors in the relative structure factors $\sigma(F_o)$ and $\sigma(F_o) = {}^1/_2(\sigma(I)/I)F_o$.

(23) The function minimized was $\sum w(|F_o| - |F_c|)^2$, where $w = 1/\sigma^2(F_o)$. The unweighted and weighted residuals are defined as $R = (\sum||F_o| - |F_c||)/\sum|F_o|$ and $R_w = [(\sum w(|F_o| - |F_c|))^2/(\sum w|F_o|)^2]^{1/2}$. The error in an observation of unit weight is $[\sum w(|F_o| - |F_c|)^2/(\mathrm{NO} - \mathrm{NV})]^{1/2}$, where NO and NV are the number of observations and variables, respectively.

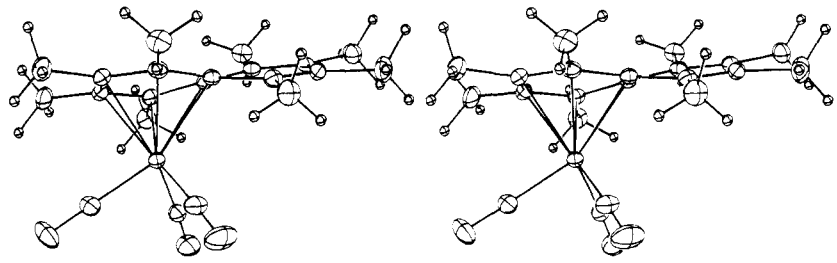

Figure 1. Stereoview of $(OMN)Cr(CO)_3$.

cycles of full-matrix least-squares refinement the difference Fourier calculations revealed the positions of every hydrogen atom in A and many of them in B. The remaining hydrogen atom positions in B could be calculated by using 1.0 Å for the C–H bond distance and $B(H) = B(C) + 1.0$ for the isotropic temperature factor. In the final least squares cycles the hydrogen atom parameters were not refined for B. However, in A both the position and isotropic temperature factors of every hydrogen were refined and were observed to converge normally. The values of the atomic scattering factors used in the calculations were taken from the usual tabulation,[24] and the effects of anomalous dispersion were included for the nonhydrogen atoms. The hydrogen atom scattering factors were taken from Cromer and Ibers' list.[25] Tables III and IV list the final positional and thermal parameters for the structures.

Results

Synthesis of $M(CO)_3$ Complexes. Scheme I shows the routes to the group 6 metal tricarbonyl complexes of OMN. The reactions proceed in moderate yields, with the exception of tungsten. These arene complexes are highly crystalline and relatively stable to air in the solid state but decompose in solution in the presence of oxygen. The order of air stability in solution is Cr > W > Mo, with the Cr complex stable over a period of hours and the Mo complex decomposing within minutes in the absence of an inert atmosphere. The spectroscopic properties of these and of all the compounds studied are given in Table V. The ^1H NMR spectra of the OMN complexes deserve comment. Although these structures are unsymmetric and should give rise to eight resonances, only four are observed. This is evidence that OMN is undergoing rapid ring flipping as shown.

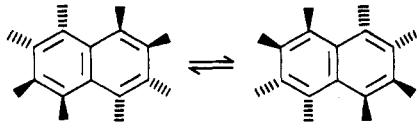

This result is not at all surprising, but it does experimentally confirm that octamethylnaphthalene can undergo this type of fluxional process. Due to the higher symmetry of OMN itself this rearrangement is undetectable. Attempts to "freeze" the motion of the complexes were not successful even at −100 °C by using a 270-MHz spectrometer. The variable-temperature work did show a substantial temperature dependence of the chemical shifts of every OMN complex.

Description of the Structure of $(OMN)Cr(CO)_3$. Figure 1 is a stereoview showing the overall structure of $(OMN)Cr(CO)_3$. The OMN ligand is bound to the $Cr(CO)_3$ group in the expected η^6 fashion. The structure of the OMN ligand is the same as that in its uncomplexed form,[15] which corresponds to the chiral point group D_2. The labeling is shown in Figure 2.

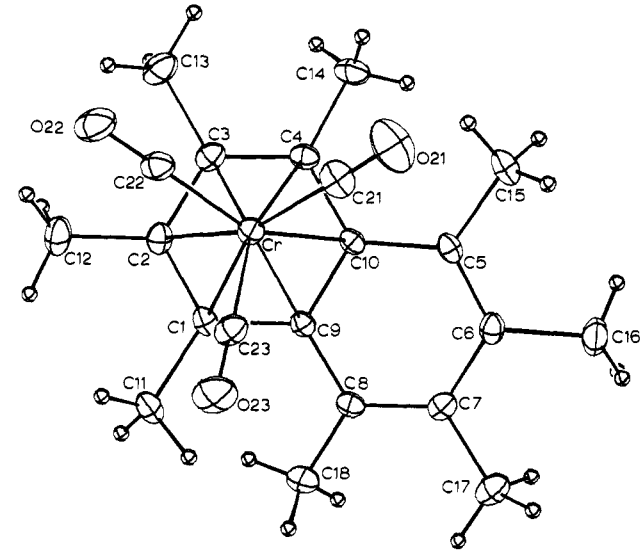

Figure 2. Atom labels for $(OMN)Cr(CO)_3$.

Due to the repulsive interactions principally involving the peri-methyl groups, the naphthalene ring system is severely distorted. These distortions are reflected in the bond distances and angles both within the ring and involving the methyls as well. One of the largest single effects of the distortions involves the expansion of the C1/4–C9/10–C8/5 angle to an average of 123.8 (2)°. The internal angles about C9/10 split the difference caused by this increase and average 118.1 (5)°. The remaining internal angles in the ring show no effect of the distortion and average 120.3 (7)°. The central C9–C10 bond distance is elongated to 1.440 (2) Å compared to 1.416 Å in OMN. As mentioned below this difference can be attributed to the metal. The C9/10/10/9–C1/4/5/8–C11/14/15/18 angles increase with the overall average being 121.0 (5)°. The distortions within these molecules are often best described by the various torsion angles. The twist about the C9–C10 bond is 19.3°, as measured by comparing the planes containing C1–C9–C10–C8 and C4–C9–C10–C5. The torsion angles C11/18/14/15–C1/8/4/5–C9/9/10/10–C8/1/5/4 average to 20 (1)° which reflects the additional distortion of the peri-methyl groups further out of the plane. A summary of distances and angles is given in Tables VI and VII.

We were able to locate and refine the positions and isotropic temperature factors of each of the methyl hydrogens. This now allows us to consider the orientation of the methyls as well as to probe the H–H interactions which are indeed causing the distortions. Both sets of peri-methyl groups are oriented as schematically shown in V. This orientation is similar to that of the methyl groups found in the 1,8-bis(trimethylstannyl)- and 1,8-bis(trimethylgermanyl)naphthalene[5] but differs from that observed in the *tert*-butyl derivative which exhibits the

(24) Cromer, D. T.; Waber, J. T. "International Tables for X-ray Crystallography"; Kynoch Press: Birmingham, England, 1974; Vol. IV, Table 2.2.4. Cromer, D. T. *Ibid.* Table 2.3.1.
(25) Cromer, D. T.; Ibers, J. A., in ref 24.

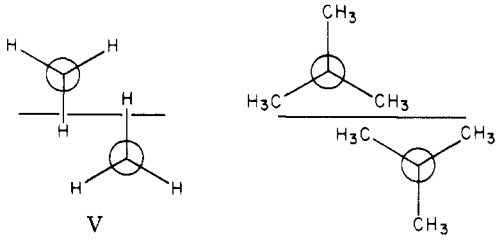

V VI

idealized geometry,[3] VI. It would appear that in the less crowded compounds the former geometry is preferred.

Further examination shows that between the peri-methyl groups, two H–H contacts per methyl group are less than the van der Waals contact (~2.5 Å). As far as the remaining methyl groups, there is one short contact between each.

The distances each atom is displaced from the mean plane consisting of C1 through C10 are shown in Figure 3. This, along with the facts mentioned above, indicates that the $Cr(CO)_3$ group has no effect on the mode of distortion and only a small effect on the magnitude of these distortions. The most notable effects are the increases of the bond distances C1–C2, C3–C4, and C9–C10. These, of course, are the carbon–carbon bonds containing the most double-bond character. The increase averages about 0.03 Å compared to OMN itself, which is similar to the increase observed in (naphthalene)$Cr(CO)_3$,[26] and can be attributed to the filled metal π-type orbitals interacting with empty π^* orbitals.

A consideration of the Cr–C(arene) interaction shows a set of five distances with an average of 2.25 (2) Å. The Cr–C9 distance is exceptionally long at 2.406 (2) Å. (Naphthalene)$Cr(CO)_3$ also shows two sets of bond distances, however, they are symmetric with respect to the mirror plane. The Cr–C9 and Cr–C10 values average 2.32 (2) Å, while the remaining four bonds are 2.20 (1) Å. This phenomenon appears to be a general structural feature for $Cr(CO)_3$ complexes of polynuclear aromatics.[27] The difference observed in (OMN)$Cr(CO)_3$ appears because the twist of the molecule forces C10 closer to the chromium. Another way of considering the chromium–arene interaction is as being partway between a planar arene system and a cyclohexadienyl complex. In $(\eta_5\text{-}C_6H_7)Mn(CO)_3$ (VII),

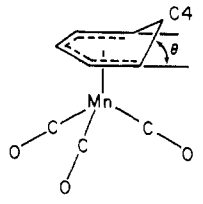

VII

the Mn–C4 bond distance is 2.76 Å.[28] Using the Cr–C9 distance of 2.409 (2) Å and the average of 2.25 (2) Å for the remaining five Cr–C distances, (OMN)$Cr(CO)_3$ is approximately one-third of the way toward a cyclohexadienyl system. Another measure of this is the angle θ which is 42° in the Mn compound and 38.6° in $[(\eta^5\text{-}[(C_4H_7S_2)C_6H_6]Cr(CO)_3]^-$.[29] In (OMN)$Cr(CO)_3$ the dihedral angle between the average plane comprised of C1–C2–C3–C4–C10 and C1–C9–C10 is 17.5°.

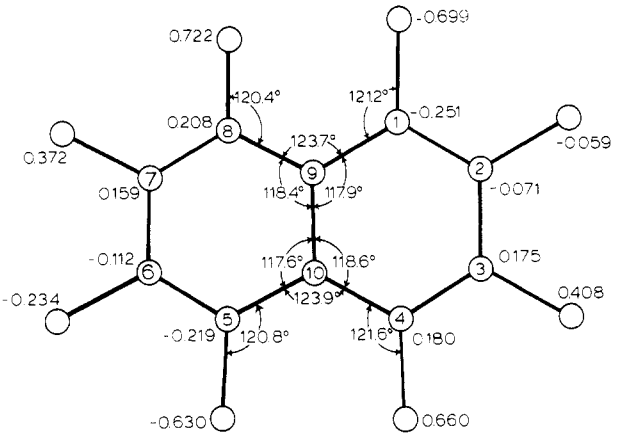

Figure 3. View of OMN ligand illustrating some of the effects of the molecular distortions. The fractional value beside each carbon is the distance below (+) or above (–) the average plane described by the ring carbons (C1–C10). The Cr atom is located above the C1-containing ring. The values for C9 and C10 are –0.031 and –0.033, respectively.

Description of the Structure of (*exo*-OMN·Ma)-$Cr(CO)_3$. A stereoview with selected labels is shown in Figure 4. The aromatic ring in the structure is planar and binds the $Cr(CO)_3$ group. The carbon–carbon bond distances around the ring are normal for (arene)tricarbonylchromium species. The average is 1.42 (2) Å, however, two of these, C9–C1 and C4–C10, are slightly longer at 1.445 (5) and 1.439 (5) Å, respectively. This could result from the crowding discussed below or possibly because C9 and C10 are involved in a bicyclic ring system. The $Cr(CO)_3$ is located symmetrically below the aromatic ring. The carbonyls, oriented in a staggered configuration, exhibit normal metal–carbon and carbon–oxygen parameters. The six Cr–C(arene) bonds are essentially equal and average 2.23 (2) Å.

The interesting feature of the structure centers around the distortions caused by the crowding between the methyl groups C18–C11 and C14–C15. Carbons C5 and C8 are now the two bridgehead atoms in the bicyclooctadiene ring system. The methyls (C15 and C18) are clearly tilted away from the aromatic ring methyls. This is easily seen by comparing the angles C9–C8–C18 and C10–C5–C15 which are 120.3 (3)° and 119.9 (4)°, respectively, with the angles C7–C8–C18 and C6–C5–C15 of 112.6 (4)° and 110.9 (4)°. The aromatic methyl groups in the 1- and 4-positions also reflect this crowding, as measured by the angles C9–C1–C11 or 122.8 (4)° and C10–C4–C14 of 123.4 (4)°. It is interesting that in this structure, however, the distortions are of the in-plane type. Specific distances and angles are presented in Tables VIII and IX.

Metal-Centered Reactivity of (OMN)$Cr(CO)_3$. The reactions of (OMN)$Cr(CO)_3$ with group 5 donors is dependent on the conditions. When dissolved in trimethyl phosphite and warmed to 70 °C for 2.0 h, complete displacement of OMN occurred (eq 1). Photolysis of

$$(OMN)Cr(CO)_3 + P(OCH_3)_3(\text{excess}) \xrightarrow[2.0\ h]{70\ ^\circ C} OMN + [P(OCH)_3]_3Cr(CO)_3 \quad (1)$$

(OMN)$Cr(CO)_3$ leads, however, to a different product. Purple crystals of (OMN)$Cr(CO)_2(PPh_3)$ can be obtained in reasonable yield by Pyrex-filtered UV irradiation of a hexane solution of (OMN)$Cr(CO)_3$ and PPh_3 (eq 2)

$$(OMN)Cr(CO)_3 + PPh_3 \xrightarrow{h\nu} CO + (OMN)Cr(CO)_2PPh_3 \quad (2)$$

(26) Kunz, V.; Nowacki, W. *Helv. Chim. Acta* **1967**, *50*, 1052.
(27) Cais, M.; Kaftory, M.; Kohn, D. H.; Tatrasky, D. *J. Organomet. Chem.* **1979**, *184*, 103.
(28) Churchhill, M. R.; Scholer, F. R. *Inorg. Chem.* **1969**, *8*, 1950.
(29) Semmelhack, M. F.; Hall, H. T., Jr.; Farina, R.; Yoshifuji, M.; Clark, G.; Bargar, T.; Hirotsu, K.; Clardy, J. *J. Am. Chem. Soc.* **1979**, *101*, 3535.

Table III. Positional and Thermal Parameters and Their Estimated Standard Deviations for (OMN)Cr(CO)$_3$[a]

atom	x	y	z	B(1,1)	B(2,2)	B(3,3)	B(1,2)	B(1,3)	B(2,3)
Cr	0.17527 (3)	0.18144 (2)	0.31747 (4)	0.01066 (3)	0.00393 (1)	0.01146 (4)	−0.00225 (4)	0.00809 (6)	0.00034 (4)
O21	−0.0875 (2)	0.1487 (2)	0.4138 (3)	0.0217 (2)	0.01500 (16)	0.0346 (3)	−0.0100 (3)	0.0318 (4)	0.0109 (4)
O22	0.3233 (2)	−0.0317 (1)	0.3949 (3)	0.0257 (3)	0.00414 (8)	0.0274 (4)	−0.0040 (3)	0.0034 (6)	0.0011 (3)
O23	0.3679 (2)	0.2117 (1)	0.7229 (2)	0.0265 (3)	0.00846 (11)	0.0125 (3)	−0.0060 (3)	0.0061 (5)	−0.0022 (3)
C21	0.0116 (3)	0.1629 (2)	0.3741 (3)	0.0152 (3)	0.00743 (13)	0.0174 (3)	−0.0045 (3)	0.0127 (5)	0.0042 (4)
C22	0.2643 (2)	0.0508 (1)	0.3654 (3)	0.0153 (3)	0.00482 (10)	0.0146 (3)	−0.0050 (3)	0.0058 (5)	−0.0008 (3)
C23	0.2913 (2)	0.2016 (1)	0.5659 (3)	0.0164 (3)	0.00442 (10)	0.0155 (3)	−0.0030 (3)	0.0125 (4)	−0.0001 (3)
C4	0.0171 (2)	0.2176 (1)	0.0119 (2)	0.0122 (2)	0.00436 (9)	0.0118 (3)	−0.0048 (2)	0.0064 (4)	0.0006 (3)
C3	0.1645 (2)	0.1568 (1)	0.0260 (2)	0.0157 (3)	0.00439 (10)	0.0123 (3)	−0.0026 (3)	0.0123 (4)	−0.0008 (3)
C2	0.3160 (2)	0.1810 (1)	0.1492 (2)	0.0124 (2)	0.00507 (10)	0.0136 (3)	−0.0005 (3)	0.0135 (4)	0.0009 (3)
C1	0.3169 (2)	0.2684 (1)	0.2507 (2)	0.0088 (2)	0.00512 (10)	0.0130 (3)	−0.0024 (2)	0.0089 (3)	0.0014 (3)
C9	0.1663 (2)	0.3402 (1)	0.2155 (2)	0.0086 (2)	0.00447 (9)	0.0100 (2)	−0.0029 (2)	0.0065 (3)	0.0007 (3)
C8	0.1589 (2)	0.4423 (1)	0.2686 (2)	0.0112 (2)	0.00449 (9)	0.0108 (3)	−0.0042 (2)	0.0061 (4)	0.0007 (3)
C7	0.0160 (2)	0.5010 (1)	0.2621 (2)	0.0142 (3)	0.00409 (9)	0.0107 (3)	−0.0016 (3)	0.0083 (4)	0.0011 (3)
C6	−0.1256 (2)	0.4619 (1)	0.2011 (2)	0.0104 (2)	0.00526 (11)	0.0128 (3)	0.0012 (3)	0.0083 (4)	0.0020 (3)
C5	−0.1279 (2)	0.3686 (1)	0.1332 (2)	0.0082 (2)	0.00547 (10)	0.0130 (3)	−0.0020 (2)	0.0058 (4)	0.0022 (3)
C10	0.0166 (2)	0.3076 (1)	0.1196 (2)	0.0090 (2)	0.00423 (9)	0.0103 (3)	−0.0031 (2)	0.0052 (3)	0.0012 (3)
C14	−0.1368 (3)	0.1961 (2)	−0.1421 (3)	0.0162 (3)	0.00620 (12)	0.0169 (4)	−0.0089 (3)	0.0038 (6)	−0.0029 (4)
C13	0.1657 (3)	0.0634 (2)	−0.0871 (3)	0.0237 (4)	0.00555 (12)	0.0189 (4)	−0.0033 (4)	0.0176 (6)	−0.0058 (4)
C12	0.4727 (3)	0.1140 (2)	0.1597 (3)	0.0163 (3)	0.00745 (15)	0.0226 (4)	0.0033 (4)	0.0218 (5)	−0.0011 (4)
C11	0.4781 (2)	0.2858 (2)	0.4001 (3)	0.0089 (2)	0.00706 (13)	0.0199 (4)	−0.0034 (3)	0.0077 (5)	0.0008 (4)
C18	0.2993 (2)	0.4895 (2)	0.3026 (3)	0.0148 (3)	0.00561 (11)	0.0196 (4)	−0.0083 (3)	0.0104 (5)	−0.0004 (3)
C17	0.0067 (3)	0.6077 (2)	0.3220 (3)	0.0219 (4)	0.00442 (11)	0.0212 (4)	−0.0019 (3)	0.0173 (6)	−0.0009 (4)
C16	−0.2775 (3)	0.5292 (2)	0.2082 (3)	0.0128 (3)	0.00811 (17)	0.0238 (5)	0.0035 (4)	0.0131 (6)	−0.0030 (5)
C15	−0.2771 (2)	0.3274 (2)	0.0863 (3)	0.0097 (2)	0.00798 (15)	0.0265 (4)	−0.0047 (3)	0.0136 (5)	0.0009 (4)

atom	x	y	z	B, Å	atom	x	y	z	B, Å
H14A	−0.110 (2)	0.170 (2)	−0.241 (3)	4.5 (5)	H18A	0.368 (2)	0.451 (2)	0.246 (3)	4.2 (5)
H14B	−0.176 (3)	0.158 (2)	−0.111 (3)	5.5 (6)	H18B	0.367 (2)	0.494 (2)	0.432 (3)	4.5 (5)
H14C	−0.219 (3)	0.253 (2)	−0.188 (3)	5.7 (6)	H18C	0.259 (3)	0.553 (2)	0.249 (3)	4.9 (5)
H13A	0.170 (3)	0.075 (2)	−0.200 (4)	6.8 (7)	H17A	−0.031 (3)	0.618 (2)	0.426 (4)	7.5 (8)
H13B	0.247 (3)	0.011 (2)	−0.012 (3)	6.6 (7)	H17B	−0.073 (3)	0.651 (2)	0.222 (3)	6.7 (7)
H13C	0.065 (3)	0.038 (2)	−0.135 (4)	7.6 (8)	H17C	0.106 (3)	0.630 (2)	0.374 (4)	7.6 (8)
H12A	0.569 (4)	0.133 (2)	0.257 (4)	8.9 (9)	H16A	−0.356 (5)	0.499 (3)	0.153 (5)	12.3 (12)
H12B	0.474 (3)	0.100 (2)	0.055 (4)	8.0 (8)	H16B	−0.275 (3)	0.551 (2)	0.326 (3)	6.4 (7)
H12C	0.485 (3)	0.042 (2)	0.206 (4)	6.9 (7)	H16C	−0.297 (3)	0.603 (2)	0.146 (4)	7.4 (8)
H11A	0.460 (2)	0.331 (1)	0.505 (3)	3.9 (5)	H15A	−0.251 (2)	0.257 (1)	0.094 (3)	3.8 (5)
H11B	0.548 (3)	0.312 (2)	0.349 (3)	5.8 (6)	H15B	−0.364 (3)	0.350 (2)	−0.035 (3)	4.9 (6)
H11C	0.540 (2)	0.225 (2)	0.468 (3)	4.8 (5)	H15C	−0.318 (3)	0.345 (2)	0.169 (3)	5.0 (5)

[a] The form of the anisotropic thermal parameter is $\exp[-(B(1,1)h^2 + B(2,2)k^2 + B(3,3)l^2 + B(1,2)hk + B(1,3)hl + B(2,3)kl)]$.

Table IV. Positional and Thermal Parameters and Their Estimated Standard Deviations for (OMN·MA)Cr(CO)$_3$[a]

atom	x	y	z	B(1,1)	B(2,2)	B(3,3)	B(1,2)	B(1,3)	B(2,3)
Cr	0.26705 (5)	0.05532 (9)	0.04080 (4)	0.00329 (3)	0.00776 (9)	0.00303 (2)	0.0002 (1)	0.00323 (3)	−0.0016 (1)
O19	0.2410 (2)	−0.0841 (4)	−0.2901 (2)	0.0104 (2)	0.0142 (6)	0.0047 (1)	−0.0020 (6)	0.0096 (2)	0.0026 (5)
O20	0.3219 (2)	−0.2541 (4)	−0.1904 (2)	0.0047 (1)	0.0128 (5)	0.0045 (1)	−0.0046 (5)	0.0058 (2)	−0.0027 (5)
O22	0.3674 (2)	−0.4426 (4)	−0.0971 (2)	0.0054 (2)	0.0136 (6)	0.0087 (2)	0.0055 (6)	0.0081 (2)	0.0038 (7)
O23	0.0964 (2)	0.2388 (4)	−0.0492 (2)	0.0059 (2)	0.0144 (6)	0.0089 (2)	0.0091 (6)	0.0075 (3)	0.0040 (6)
O24	0.3547 (3)	0.2783 (5)	0.1851 (3)	0.0089 (3)	0.0302 (8)	0.0100 (2)	−0.0056 (8)	0.0063 (4)	−0.0256 (7)
O25	0.1863 (2)	−0.0735 (5)	0.1512 (2)	0.0104 (2)	0.0200 (7)	0.0090 (2)	0.0131 (6)	0.0154 (2)	0.0143 (6)
C1	0.3597 (3)	−0.1335 (5)	0.0574 (2)	0.0030 (2)	0.0083 (7)	0.0025 (2)	0.0012 (6)	0.0028 (2)	−0.0000 (6)
C2	0.4100 (3)	−0.0068 (5)	0.0642 (3)	0.0025 (2)	0.0088 (7)	0.0031 (2)	−0.0007 (6)	0.0026 (3)	−0.0023 (6)
C3	0.3753 (3)	0.0994 (5)	−0.0045 (3)	0.0028 (2)	0.0073 (7)	0.0033 (2)	−0.0004 (6)	0.0030 (2)	−0.0012 (6)
C4	0.2862 (3)	0.0826 (5)	−0.0810 (3)	0.0036 (2)	0.0072 (7)	0.0035 (2)	0.0004 (6)	0.0040 (2)	−0.0007 (6)
C5	0.1386 (3)	−0.0914 (5)	−0.1717 (3)	0.0034 (2)	0.0076 (7)	0.0023 (2)	0.0005 (7)	0.0005 (3)	−0.0006 (6)
C6	0.0774 (3)	−0.1564 (6)	−0.1336 (3)	0.0025 (2)	0.0100 (7)	0.0041 (2)	0.0003 (7)	0.0020 (3)	−0.0032 (7)
C7	0.1155 (3)	−0.2628 (5)	−0.0742 (3)	0.0038 (2)	0.0100 (7)	0.0036 (2)	−0.0033 (7)	0.0042 (3)	−0.0044 (6)
C8	0.2160 (3)	−0.2992 (5)	−0.0518 (3)	0.0032 (2)	0.0073 (6)	0.0024 (2)	−0.0007 (6)	0.0028 (2)	−0.0006 (6)
C9	0.2721 (3)	−0.1559 (5)	−0.0238 (2)	0.0029 (2)	0.0060 (6)	0.0019 (1)	−0.0002 (6)	0.0027 (2)	−0.0014 (5)
C10	0.2337 (2)	−0.0467 (5)	−0.0896 (2)	0.0025 (2)	0.0064 (6)	0.0023 (1)	0.0002 (7)	0.0020 (2)	−0.0001 (6)
C11	0.3987 (3)	−0.2394 (6)	0.1347 (3)	0.0048 (3)	0.0119 (8)	0.0033 (2)	−0.0018 (8)	0.0012 (4)	0.0025 (7)
C12	0.5051 (3)	0.0174 (6)	0.1457 (3)	0.0041 (2)	0.0122 (9)	0.0043 (2)	−0.0022 (8)	0.0016 (4)	−0.0012 (8)
C13	0.4344 (3)	0.2294 (6)	0.0044 (3)	0.0043 (2)	0.0079 (7)	0.0065 (3)	−0.0018 (8)	0.0041 (4)	−0.0001 (8)
C14	0.2518 (3)	0.2028 (6)	−0.1510 (3)	0.0058 (3)	0.0084 (7)	0.0045 (2)	−0.0009 (8)	0.0037 (4)	0.0033 (7)
C15	0.0834 (3)	0.0178 (6)	−0.2465 (3)	0.0048 (3)	0.0108 (9)	0.0044 (3)	0.0020 (8)	−0.0001 (4)	0.0028 (8)
C16	−0.0180 (3)	−0.0957 (6)	−0.1601 (4)	0.0041 (2)	0.0132 (10)	0.0092 (3)	0.0010 (8)	0.0058 (4)	−0.0017 (9)
C17	0.0700 (3)	−0.3418 (7)	−0.0271 (3)	0.0053 (2)	0.0162 (9)	0.0055 (2)	−0.0064 (8)	0.0072 (3)	−0.0032 (8)
C18	0.2531 (3)	−0.4332 (6)	0.0080 (3)	0.0063 (2)	0.0068 (6)	0.0046 (2)	−0.0024 (8)	0.0052 (3)	0.0002 (7)
C19	0.2424 (3)	−0.1739 (6)	−0.2393 (3)	0.0056 (2)	0.0098 (7)	0.0023 (2)	−0.0024 (8)	0.0031 (3)	−0.0037 (6)
C20	0.1679 (3)	−0.2188 (5)	−0.2135 (3)	0.0035 (2)	0.0093 (7)	0.0025 (2)	−0.0009 (7)	0.0023 (3)	−0.0018 (6)
C21	0.2121 (3)	−0.3398 (5)	−0.1463 (3)	0.0034 (2)	0.0071 (6)	0.0031 (2)	−0.0032 (6)	0.0037 (2)	−0.0023 (6)
C22	0.3084 (3)	−0.3574 (5)	−0.1378 (3)	0.0047 (2)	0.0080 (7)	0.0041 (2)	−0.0019 (7)	0.0051 (3)	−0.0032 (6)
C23	0.1632 (3)	0.1673 (6)	−0.0122 (3)	0.0044 (2)	0.0089 (7)	0.0055 (2)	0.0010 (7)	0.0058 (3)	−0.0011 (7)
C24	0.3201 (3)	0.1918 (7)	0.1290 (3)	0.0050 (3)	0.0181 (10)	0.0052 (2)	−0.0024 (9)	0.0043 (4)	−0.0105 (8)
C25	0.2176 (3)	−0.0251 (6)	0.1077 (3)	0.0055 (2)	0.0117 (8)	0.0046 (2)	0.0068 (7)	0.0067 (3)	0.0050 (7)

atom	x	y	z	B, Å^2	atom	x	y	z	B, Å^2
H11A	0.4375 (0)	−0.1953 (0)	0.1875 (0)	4.8000 (0)	H15B	0.1245 (0)	0.0492 (0)	−0.2761 (0)	5.7000 (0)
H11B	0.3470 (0)	−0.2847 (0)	0.1442 (0)	4.8000 (0)	H15C	0.0270 (0)	−0.0301 (0)	−0.2956 (0)	5.7000 (0)
H11C	0.4346 (0)	−0.3183 (0)	0.1246 (0)	4.8000 (0)	H16A	−0.0523 (0)	−0.0852 (0)	−0.2284 (0)	5.6000 (0)
H12A	0.5625 (0)	0.0273 (0)	0.1250 (0)	4.9000 (0)	H16B	−0.0561 (0)	−0.1628 (0)	−0.1418 (0)	5.6000 (0)
H12B	0.5038 (0)	0.1067 (0)	0.1790 (0)	4.9000 (0)	H16C	−0.0153 (0)	0.0008 (0)	−0.1316 (0)	5.6000 (0)
H12C	0.5202 (0)	−0.0674 (0)	0.1889 (0)	4.9000 (0)	H17A	0.0000 (0)	−0.3320 (0)	−0.0625 (0)	4.2000 (0)
H13A	0.4570 (0)	0.2773 (0)	0.0625 (0)	4.3000 (0)	H17B	0.0862 (0)	−0.4461 (0)	−0.0202 (0)	4.2000 (0)
H13B	0.4911 (0)	0.2002 (0)	−0.0016 (0)	4.3000 (0)	H17C	0.0899 (0)	−0.2991 (0)	0.0351 (0)	4.2000 (0)
H13C	0.3978 (0)	0.3016 (0)	−0.0437 (0)	4.3000 (0)	H18A	0.2500 (0)	−0.4180 (0)	0.0625 (0)	4.0000 (0)
H14A	0.1875 (0)	0.2227 (0)	−0.1680 (0)	4.4000 (0)	H18B	0.2150 (0)	−0.5212 (0)	−0.0232 (0)	4.0000 (0)
H14B	0.2879 (0)	0.2956 (0)	−0.1259 (0)	4.4000 (0)	H18C	0.3202 (0)	−0.4533 (0)	0.0236 (0)	4.0000 (0)
H14C	0.2558 (0)	0.1773 (0)	−0.2074 (0)	4.4000 (0)	H20	0.1055 (0)	−0.2500 (0)	−0.2695 (0)	3.1000 (0)
H15A	0.0625 (0)	0.1113 (0)	−0.2305 (0)	5.7000 (0)	H21	0.1680 (0)	−0.4434 (0)	−0.1660 (0)	3.0000 (0)

[a] The form of the anisotropic thermal parameter is $\exp[-B(1,1)h^2 + B(2,2)k^2 + B(3,3)l^2 + B(1,2)hk + B(1,3)hl + B(2,3)kl)]$.

Table V. Spectroscopic Properties of OMN Derivatives

compd	color	ν_{CO}, cm^{-1}	^1H NMR δ[c]	ref
(OMN)Cr(CO)$_3$	red	1956 s, 1891 m, 1876 m (hexane)	2.62 (6 H), 2.58 (6 H), 2.38 (6 H), 2.33 (6 H)	*a*
(OMN)Mo(CO)$_3$	yellow	1942 s, 1858 s (CH_2Cl_2)	2.60 (6 H), 2.54 (6 H), 2.43 (6 H), 2.31 (6 H)	*a*
(OMN)W(CO)$_3$	orange	1940 s, 1843 s (CH_2Cl_2)	2.70 (6 H), 2.54 (6 H), 2.51 (6 H), 2.32 (6 H)	*a*
(OMN)Cr(CO)$_2$(PPh$_3$)	purple	1855 s, 1791 m (CH_2Cl_2)	7.19 (m, 15 H), 2.36 (6 H), 2.22 (6 H), 2.20 (6 H) 2.12 (6 H)	*a*
(*endo*-OMN·MA)Cr(CO)$_3$	yellow	1955 (s), 1877 m, 1776 w (CH_2Cl_2)	3.06 (2 H), 2.53 (6 H), 2.22 (6 H), 2.18 (6 H), 1.83 (6 H)	*b*
(*exo*-OMN·MA)Cr(CO)$_3$	yellow	1955 (s), 1877 m, 1776 w (CH_2Cl_2)	3.02 (2 H), 2.43 (6 H), 2.21 (6 H), 2.18 (6 H), 1.88 (6 H)	*b*
endo-OMN·MA	white	1857 w, 1778 s (Nujol)	3.13 (2 H), 2.50 (6 H), 2.23 (6 H), 2.20 (6 H), 1.74 (6 H)	*b*
exo-OMN·MA	white	1857 w, 1770 s (Nujol)	2.97 (2 H), 2.40 (6 H), 2.25 (6 H), 2.15 (6 H), 1.77 (6 H)	*b*

[a] Spectrum obtained in CD_2Cl_2 at 270 MHz. [b] Spectrum obtained in $CDCl_3$ at 80 MHz. [c] All resonances are singlets unless otherwise noted.

Table VI. Interatomic Distances for (OMN)Cr(CO)$_3$

atoms	dis, Å	atoms	dis, Å
Cr-C21	1.840 (2)	C6-C16	1.525 (3)
Cr-C22	1.824 (2)	C7-C17	1.518 (3)
Cr-C23	1.833 (2)	C8-C18	1.516 (2)
Cr-C1	2.230 (2)	C11-H11A	1.04 (2)
Cr-C2	2.229 (2)	C11-H11B	1.04 (3)
Cr-C3	2.264 (2)	C11-H11C	0.97 (3)
Cr-C4	2.270 (2)	C12-H12A	0.98 (4)
Cr-C9	2.406 (2)	C12-H12B	0.84 (3)
Cr-C10	2.257 (2)	C12-H12C	1.07 (3)
C21-O21	1.156 (3)	C13-H13A	0.95 (3)
C22-O22	1.154 (2)	C13-H13B	0.96 (3)
C23-O23	1.158 (2)	C13-H13C	0.99 (3)
C1-C2	1.399 (3)	C14-H14A	0.93 (3)
C2-C3	1.435 (3)	C14-H14B	0.82 (3)
C3-C4	1.400 (3)	C14-H14C	0.95 (3)
C4-C10	1.452 (2)	C15-H15A	0.96 (2)
C9-C10	1.440 (2)	C15-H15B	0.98 (3)
C5-C6	1.365 (3)	C15-H15C	0.88 (3)
C6-C7	1.424 (3)	C16-H16A	0.87 (4)
C7-C8	1.374 (3)	C16-H16B	0.95 (3)
C8-C9	1.444 (2)	C16-H16C	1.13 (3)
C1-C9	1.455 (2)	C17-H17A	1.01 (3)
C5-C10	1.457 (2)	C17-H17B	0.96 (3)
C1-C11	1.527 (2)	C17-H17C	0.96 (3)
C2-C12	1.513 (3)	C18-H18A	0.97 (2)
C3-C13	1.513 (3)	C18-H18B	0.96 (3)
C4-C14	1.514 (2)	C18-H18C	0.94 (3)
C5-C15	1.519 (3)		

Table VII. Selected Bond Angles for (OMN)Cr(CO)$_3$

atoms	angle, deg	atoms	angle, deg
C21-Cr-C22	87.32 (9)	Cr-C21-O21	177.7 (2)
C21-Cr-C23	88.45 (9)	Cr-C22-O22	178.6 (2)
C22-Cr-C23	86.80 (8)	Cr-C23-O23	177.9 (2)
C21-Cr-C1	155.79 (9)	Cr-C1-C11	120.2 (1)
C21-Cr-C2	158.55 (8)	Cr-C2-C12	130.3 (1)
C21-Cr-C3	121.47 (8)	Cr-C3-C13	130.0 (2)
C21-Cr-C4	95.77 (8)	Cr-C4-C14	139.4 (2)
C21-Cr-C9	120.14 (8)	Cr-C9-C8	143.3 (1)
C21-Cr-C10	94.00 (8)	Cr-C10-C5	122.4 (1)
C22-Cr-C1	116.59 (8)	C1-C2-C3	119.7 (2)
C22-Cr-C2	89.19 (8)	C2-C3-C4	120.9 (2)
C22-Cr-C3	88.82 (8)	C3-C4-C10	119.9 (2)
C22-Cr-C4	114.03 (7)	C4-C10-C9	118.6 (2)
C22-Cr-C9	152.42 (8)	C4-C10-C5	123.9 (2)
C22-Cr-C10	151.44 (7)	C10-C9-C1	117.9 (2)
C23-Cr-C1	89.15 (7)	C10-C9-C8	118.4 (1)
C23-Cr-C2	112.49 (8)	C1-C9-C8	123.7 (1)
C23-Cr-C3	149.52 (8)	C9-C8-C7	120.0 (2)
C23-Cr-C4	158.86 (7)	C8-C7-C6	120.3 (2)
C23-Cr-C9	95.83 (7)	C7-C6-C5	121.6 (2)
C23-Cr-C10	121.74 (7)	C2-C1-C9	120.2 (2)
C1-Cr-C2	36.57 (7)	C6-C5-C10	119.7 (2)
C2-Cr-C3	37.24 (7)	C5-C10-C9	117.6 (2)
C3-Cr-C4	35.99 (7)	C9-C1-C11	121.2 (2)
C4-Cr-C10	37.42 (6)	C9-C8-C18	120.4 (2)
C10-Cr-C9	35.78 (5)	C2-C1-C11	118.6 (2)
C9-Cr-C1	36.33 (6)	C7-C8-C18	118.9 (2)
C1-C2-C12	120.8 (2)	C10-C4-C14	121.6 (2)
C3-C2-C12	119.4 (2)	C10-C5-C15	120.8 (2)
C2-C3-C13	119.0 (2)	C3-C4-C14	117.6 (2)
C4-C3-C13	120.1 (2)	C6-C5-C15	119.4 (2)
C7-C6-C16	117.6 (2)		
C5-C6-C16	120.8 (2)		
C6-C7-C17	118.9 (2)		
C8-C7-C17	120.8 (2)		

Octamethylnaphthalene-Centered Reactivity of (OMN)Cr(CO)$_3$. (OMN)Cr(CO)$_3$ was found to undergo a Diels–Alder reaction with maleic anhydride. The isomeric compounds were conveniently separated by fractional crystallization from benzene/hexane solutions or by chromatography.

Both yellow crystalline products were shown by elemental and mass spectral analyses to have the formula $C_{25}H_{26}CrO_6$. ^1H NMR and infrared spectral studies further illustrated the similarities but gave no conclusive information allowing the assignment of the stereochemistry. Consideration of the reaction itself would give four possible products, VIII–XI (Scheme II). An X-ray structural analysis of one of the isomers proved that it had the stereochemistry illustrated by VIII. Decomplexation of the chromium from the ligand for each complex by photolysis under O_2 yielded the two separate isomers of OMN·MA. This result allows us to immediately eliminate X from consideration. We have no absolute proof which would allow differentiation between IX and XI as the second isomer, but the well-established steric directing effect of the Cr(CO)$_3$[20] makes attack of maleic anhydride from the opposite side of the OMN the only reasonable route. Therefore IX is assigned to the structure of the second isomer.

The Diels–Alder reaction of OMN itself was first reported in 1953.[11] The separation and assignment of the individual isomers was later made by Oku and co-workers[30] and was based on predicted shifts of the methine hydrogen. Our data show that the original stereochemical assignment of the OMN·MA isomers are reversed. From the X-ray structural analysis of (*exo*-OMN·MA)Cr(CO)$_3$ we know the stereochemistry. The oxidative removal of the Cr gives only one product which is the *exo*-OMN·MA having δ 2.97. Corresponding decomplexation of the (*endo*-OMN·MA)-Cr(CO)$_3$ gives only the endo product with δ 3.13.

(30) Oku, A.; Ohnishi, Y.; Mashio, F. *J. Org. Chem.* **1972**, *37*, 4264.

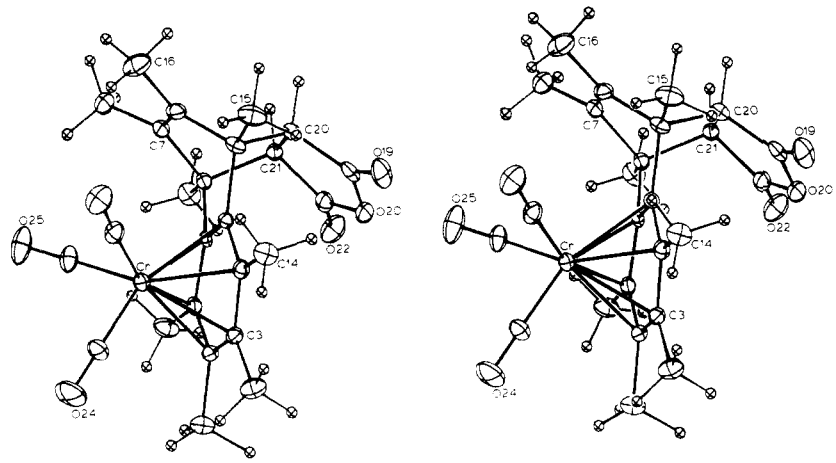

Figure 4. Stereoview and partial atom labels for (*exo*-OMN·MA)$Cr(CO)_3$. The basic OMN framework is numbered the same way as is (OMN)$Cr(CO)_3$. The anhydride portion consists of C19 through C22. This numbering sequence was adopted for simplicity in comparing the two structures and bears no resemblance to the usual nomenclature numbering sequence.

Table VIII. Bond Distances for (*exo*-OMN·MA)$Cr(CO)_3$

atoms	dist, Å	atoms	dist, Å
Cr-C23	1.816 (5)	C7-C6	1.329 (6)
Cr-C24	1.824 (5)	C6-C5	1.534 (5)
Cr-C25	1.816 (5)	C5-C10	1.563 (5)
Cr-C1	2.240 (4)	C8-C21	1.595 (5)
Cr-C2	2.238 (4)	C21-C20	1.511 (6)
Cr-C3	2.253 (4)	C21-C22	1.510 (6)
Cr-C4	2.214 (4)	C22-O22	1.179 (5)
Cr-C9	2.258 (4)	C22-O20	1.386 (5)
Cr-C10	2.199 (4)	O20-C19	1.376 (5)
C23-O23	1.168 (5)	C19-O19	1.183 (5)
C24-O24	1.159 (5)	C19-C20	1.519 (6)
C25-O25	1.156 (5)	C20-C5	1.558 (5)
C1-C2	1.405 (5)	C1-C11	1.506 (5)
C2-C3	1.414 (5)	C2-C12	1.520 (6)
C3-C4	1.418 (5)	C3-C13	1.504 (5)
C4-C10	1.439 (5)	C4-C14	1.520 (5)
C10-C9	1.408 (5)	C5-C15	1.529 (6)
C9-C1	1.445 (5)	C6-C16	1.503 (6)
C9-C8	1.554 (5)	C7-C17	1.500 (6)
C8-C7	1.529 (5)	C8-C18	1.531 (6)

Table IX. Bond Angles for (*exo*-OMN·MA)$Cr(CO)_3$

atoms	angle, deg	atoms	angle, deg
C23-Cr-C24	88.5 (2)	Cr-C1-C11	127.1 (3)
C23-Cr-C25	87.6 (2)	Cr-C2-C12	130.5 (3)
C24-Cr-C25	88.0 (2)	Cr-C3-C13	132.3 (3)
C23-Cr-C1	157.3 (2)	Cr-C4-C14	129.2 (3)
C23-Cr-C2	151.6 (2)	Cr-C9-C8	137.7 (3)
C23-Cr-C3	115.0 (2)	Cr-C10-C5	131.7 (3)
C23-Cr-C4	89.1 (2)	C2-C1-C9	118.2 (4)
C23-Cr-C9	119.8 (2)	C2-C1-C11	118.9 (4)
C23-Cr-C10	91.4 (2)	C9-C1-C11	122.8 (4)
C24-Cr-C1	114.2 (2)	C1-C2-C3	121.6 (4)
C24-Cr-C2	89.0 (2)	C1-C2-C12	120.2 (4)
C24-Cr-C3	90.0 (2)	C3-C2-C12	118.2 (4)
C24-Cr-C4	116.6 (2)	C2-C3-C4	120.2 (4)
C24-Cr-C9	151.7 (2)	C2-C3-C13	119.2 (4)
C24-Cr-C10	154.6 (2)	C4-C3-C13	120.6 (4)
C25-Cr-C1	93.6 (2)	C3-C4-C10	119.1 (4)
C25-Cr-C2	120.5 (2)	C3-C4-C14	117.5 (4)
C25-Cr-C3	157.2 (2)	C10-C4-C14	123.4 (4)
C25-Cr-C4	155.2 (2)	C5-C10-C9	112.7 (4)
C25-Cr-C9	93.6 (2)	C4-C10-C5	127.0 (4)
C25-Cr-C10	117.4 (2)	C4-C10-C9	120.0 (3)
C1-Cr-C2	36.6 (1)	C1-C9-C8	125.7 (4)
C2-Cr-C3	36.7 (1)	C10-C9-C1	120.6 (4)
C3-Cr-C4	37.0 (1)	C10-C9-C8	113.5 (3)
C4-Cr-C10	38.1 (1)	C10-C5-C15	119.9 (4)
C10-Cr-C9	36.8 (1)	C10-C5-C6	107.7 (3)
C9-Cr-C1	37.5 (1)	C10-C5-C20	102.2 (3)
Cr-C23-O23	177.6 (4)	C6-C5-C15	110.9 (4)
Cr-C24-O24	179.3 (5)	C6-C5-C20	106.4 (3)
Cr-C25-O25	178.5 (5)	C15-C5-C20	108.7 (3)
C7-C6-C16	123.5 (4)	C5-C6-C16	120.5 (4)
C6-C7-C17	125.7 (4)	C5-C6-C7	115.9 (4)
C6-C7-C8	114.6 (4)	C20-C21-C22	104.9 (3)
C8-C7-C17	119.7 (4)	C21-C22-O20	109.3 (4)
C7-C8-C18	112.6 (4)	C21-C22-O22	130.5 (5)
C7-C8-C9	106.9 (3)	O20-C22-O22	120.2 (4)
C7-C8-C21	105.6 (3)	C22-O20-C19	111.6 (4)
C9-C8-C18	120.3 (3)	O20-C19-O19	120.3 (5)
C9-C8-C21	104.3 (3)	O20-C19-C20	109.3 (4)
C18-C8-C21	106.0 (3)	O19-C19-C20	130.4 (5)
C8-C21-C20	110.2 (3)	C19-C20-C21	104.7 (4)
C8-C21-C22	112.0 (3)	C19-C20-C5	111.8 (4)
		C5-C20-C21	111.6 (3)

In order to obtain a more quantitative evaluation of the effect of the $Cr(CO)_3$ on the reactivity of OMN, we carefully monitored the reactions by using high-pressure liquid chromatography. The following two effects were explored. How does the rate of reaction differ? Further, does the $Cr(CO)_3$ change the equilibrium constant for the reaction?

After 66 h at 80 °C the estimates for the equilibrium are 6 and 1 for the exo and endo isomer, respectively. This is in reasonable agreement with previously reported measurement by Hart[31] and Oku and co-workers[30] (summarized in Table X). Although the exo isomer is thermodynamically favored, the less stable endo isomer is formed more rapidly in the initial stage of the reaction. The equilibrium composition is also approached from a mixture of either the endo or exo isomer and 4 equiv of maleic anhydride. Unfortunately, quantitative measurement of the retro-Diels–Alder reaction was prohibited by side reactions of the starting adducts apparently caused by the high initial concentrations of the adducts combined with the longer reaction times. This was a particularly difficult problem with the endo isomer.

Under identical conditions we found that (OMN)Cr-$(CO)_3$ reacted with MA at approximately the same rate as OMN did. There was, however, a substantial difference in the equilibrium constants for the reaction. The average values obtained from duplicate experiments were K(exo) = 870 (average of 880 and 860) and K(endo) = 390 (average of 400 and 380). The equilibrium again was approached by starting with each isomer, but the reaction was so slow it could not be accurately determined due to the small amount of decomposition from oxygen. It is interesting to note the exceptional thermal stability of the complexed

(31) Hart, H.; Oku, A. *J. Org. Chem.* **1972**, *37*, 4269.

Scheme II

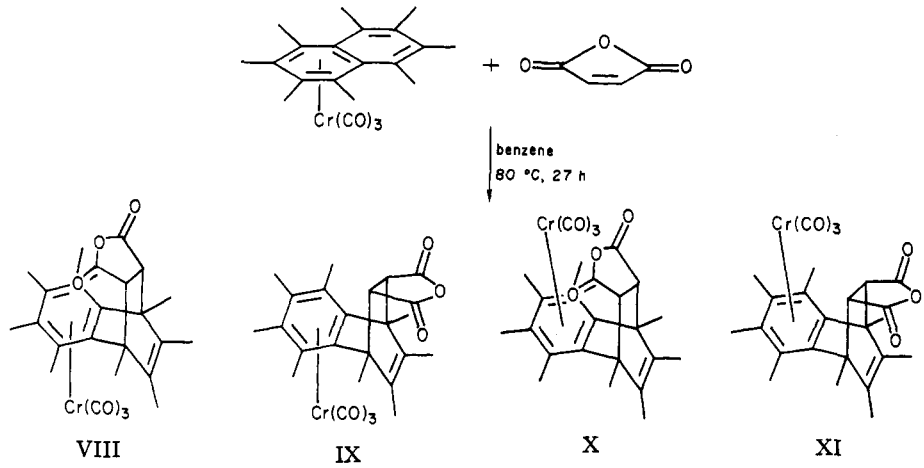

VIII IX X XI

Table X. Summary of Diels-Alder Reaction of OMN with Maleic Anhydride

ref	[OMN]/[MA]	temp, °C	solvent	time, h	initial [OMN], M	combined % yield	exo/endo
31	1	132		13.5	1	50.3	2.0
30	1	110	none	24		91	7.0
30	0.5	155	none	6		60	4.4
30 (retro-Diels-Alder)	0.5	155	none	6	0	80	4.4
this work	0.20	80		66	0.150	81	7.14

Diels–Alder adducts relative to the free ligand.

Discussion

Ligand Substitution Reactions. The reactions involving a direct change in the ligand environment around the metal depend on the conditions. Thermally, substitution of the OMN occurs with $P(OCH_3)_3$ to give $Cr(CO)_3[P(OCH_3)_3]_3$. Photolysis, however, leads to the replacement of a carbon monoxide ligand. This difference between ground- and excited-state reactivities has been previously observed and was attributed to the idea that a one-electron excitation will have a greater impact on a two-electron donor compared to a six-electron donor.[32]

Diels–Alder Reaction. Distorted molecules such as octamethylnaphthalene usually exhibit greater reactivity relative to the unperturbed counterparts. One of the principle goals of this work was to evaluate the effect of metal complexation on this already unusual reactivity. The reaction which was chosen for evaluation was the cycloaddition of maleic anhydride. Since the original synthesis of OMN,[11] it was known to undergo Diels–Alder reactions. The details of this reaction and of the reactions of most of the polymethylnaphthalenes have since been studied.[30,31]

The conditions used in our experiments allowed a straight-forward sampling procedure for monitoring the reactions by high-pressure liquid chromatography and decreased the likelihood of any thermal decomposition of the metal complexes. In all the reactions conducted in benzene, arene exchange was never observed. In fact, the only time we did observe this reaction was during an attempted preparative liquid chromatographic purification of $(OMN)Cr(CO)_3$. When the material was eluted through a silica gel column (200–400 μm) with benzene, a mixture of $(\eta^6\text{-}C_6H_6)Cr(CO)_3$ and $(OMN)Cr(CO)_3$ was obtained. Despite the differences in our experimental conditions with those previously studied (Table X), the results agree reasonably well.

The corresponding reaction of maleic anhydride with $(OMN)Cr(CO)_3$ shows a greater than 2 orders-of-magnitude increase in the equilibrium constant. The nature of this 3–4-kcal/mol difference in energy for the complexed vs. the uncomplexed reaction is simply attributed to the weakened Cr–ring bond in the starting material. As the molecular structures clearly illustrate, all the Cr–C distances are longer in $(OMN)Cr(CO)_3$ relative to the product. In other words, as we proceed from starting material to product the enhanced strength of the Cr–C(arene) interaction must be added to the overall energy change of the reaction. This increased interaction of the Cr with the arene is allowed as the ring becomes planar. Extension of this idea to other reactions is straightforward. Any reaction in which the steric crowding of the peri methyls is relieved, complexation of a metal to the free ring should push the reaction in the forward direction. We are particularly interested in exploiting this effect to assist in the hydrogenation of OMN. As shown, the addition of H_2 to the free ring at the peri positions will relieve the crowding in this molecule (eq 3).

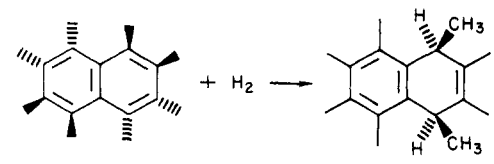

(3)

Acknowledgment is made to the Research Corp. and the University of Minnesota Graduate School for support of this research and to Du Pont Corp. for a Young Faculty Research Grant. We also gratefully acknowledge L. H. Pignolet and M. McGuiggan for assistance in the structural analyses and the NSF for partial support of our X-ray diffraction and structure-solving equipment (NSF Grant CHE 77-28505). We are grateful to H. Hart for commu-

(32) Geoffroy, G. L.; Wrighton, M. S. "Organometallic Photochemistry"; Academic Press: New York, 1979; p 79.

nicating his results prior to publication.

Registry No. (OMN)Cr(CO)$_3$, 79391-56-3; (OMN)Mo(CO)$_3$, 79391-57-4; (OMN)W(CO)$_3$, 79391-58-5; (OMN)Cr(CO)$_2$(PPh$_3$), 79391-59-6; (*endo*)-[OMN·MA]Cr(CO)$_3$, 79391-60-9; (*exo*)-[OMN·MA]Cr(CO)$_3$, 79434-50-7; (*endo*)-OMN·MA, 36744-72-6; (*exo*)-OMN·MA, 36744-73-7; Cr(CO)$_3$(P(OMe)$_3$)$_3$, 17764-72-6; Cr(CO)$_6$, 13007-92-6; (CH$_3$CN)$_3$Mo(CO)$_3$, 15038-48-9; (CH$_3$CN)$_3$W(CO)$_3$, 16800-47-8; MA, 108-31-6.

Supplementary Material Available: Listings of the observed and calculated structure factors used in the crystallographic analyses (21 pages). Ordering information is given on any current masthead page.

Further Studies on the Molecular Dynamics of the Four-Electron Bridging Carbonyl

John A. Marsella and Kenneth G. Caulton*

Department of Chemistry, Indiana University, Bloomington, Indiana 47405

Received July 14, 1981

Both $Mn_2(CO)_6(dpm)_2$, which contains only terminal carbonyls, and $Mn_2(CO)_5(dpm)_2$, which contains one μ:η^2 (four-electron donor) carbonyl, are shown to be fluxional by ^{13}C NMR spectroscopy. Scrambling in the hexacarbonyl occurs over both metal atoms with E_a = 10.2 kcal/mol and log A = 12.1, while that in pentacarbonyl involves only a wagging motion which results in disruption of the Dewar–Chatt portion of the four-electron donor carbonyl with E_a = 17.0 kcal/mol and log A = 15.0. By selective ^{31}P decoupling experiments, the chemical shift of the four-electron donor carbonyl is shown to fall in the chemical shift region normally attributed to terminal carbonyls. Coupling of ^{13}C to ^{31}P is small (<5 Hz) through the Dewar–Chatt portion of this type of carbonyl.

Introduction

The four-electron-donor carbonyl bridge, depicted formally as I, is an organometallic structural unit of relatively

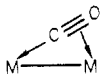

I

recent vintage. The first example, contained in $Mn_2(CO)_5(dpm)_2$, II (dpm = bis(diphenylphosphino)methane,

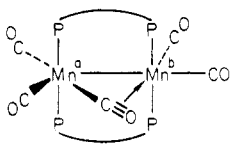

II

$Ph_2PCH_2PPh_2$), was reported in 1975 by Colton, Commons, and Hoskins.[1] The five carbonyls in this molecule are coplanar. Subsequent reports include $Cp_2NbMo(CO)_3Cp$,[2] $Cp_2Zr(OC)(OCMe)Mo(CO)Cp$,[3] and $(C_5Me_5)_2ZrCo(CO)_2(C_5H_5)$.[4] A cluster-bound analogue occurs in $HFe_4(CO)_{13}^-$, where one of the carbonyl ligands donates a total of four electrons to all four iron atoms in $Fe_4(CO)_{13}H^-$.[5] Finally an extreme example of carbonyl Lewis basicity is found in $Cp_3Nb_3(CO)_7$, where one CO ligand lies obliquely over the Nb_3 triangle and donates via the carbon lone pair and *both* filled C≡O π orbitals.[6]

Carbon monoxide assumes the μ_2:η^2 functionality in ligand-deficient situations; indeed, this structural unit is generally formed by thermal or photochemical processes which expel ligands (e.g., CO or CH_4). Since such ligand-deficient situations are precisely those found on lightly loaded metal surfaces, molecular examples of multipoint attachment of CO represent an important opportunity to examine the dynamics and reactivity of a catalytically relevant moiety by use of spectroscopic methods.

Several years ago, we reported the results of a ^{31}P NMR study of $Mn_2(CO)_5(dpm)_2$ which indicated that the migrational processes depicted in eq 1 (bridging dpm ligands

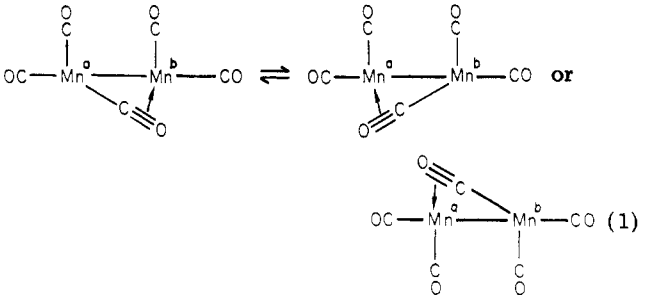

(1)

are omitted for simplicity) are *not* facile.[7] The observed inequivalence (at 30 °C) of the phosphorus nuclei attached to different manganese atoms allowed us to set a lower limit of 15.6 kcal/mol for the activation energy of eq 1. This result is compatible with the notion that multipoint carbonyl binding inhibits the characteristically facile migrations of two-electron donor carbonyls.

We were therefore somewhat surprised by our more recent result that *reorientation* of the six-electron donor carbonyl in $Cp_3Nb_3(CO)_7$ (eq 2) occurs with an activation energy, E_a, of 17 kcal/mol.[8] In order to examine this situation more critically, we have returned to perhaps the

(1) (a) Commons, C. J.; Hoskins, B. F. *Aust. J. Chem.* **1975**, *28*, 1663. (b) Colton, R.; Commons, C. J. *Ibid.* **1975**, *28*, 1673.
(2) Pasynskii, A. A.; Skripkin, Yu. V.; Eremenko, I. L.; Kalinnikov, V. T.; Aleksandrov, G. G.; Andrianov, V. G.; Struchkov, Yu. T. *J. Organomet. Chem.* **1979**, *165*, 49.
(3) Longato, B.; Norton, J. R.; Huffman, J. C.; Marsella, J. A.; Caulton, K. G. *J. Am. Chem. Soc.* **1981**, *103*, 209.
(4) Barger, P. T.; Bercaw, J. E. *J. Organomet. Chem.* **1980**, *201*, C39.
(5) Manassero, M.; Sanasoni, M.; Longoni, G. *J. Chem. Soc., Chem. Commun.* **1976**, 919.
(6) Herrmann, W. A.; Biersack, H.; Ziegler, M. L.; Weidenhammer, K.; Siegel, R.; Rehder, D. *J. Am. Chem. Soc.* **1981**, *103*, 1692.
(7) Caulton, K. G.; Adair, P. *J. Organomet. Chem.* **1976**, *114*, C11.
(8) Lewis, L. N.; Caulton, K. G. *Inorg. Chem.* **1980**, *19*, 3201.

0276-7333/82/2301-0274$01.25/0

nicating his results prior to publication.

Registry No. (OMN)Cr(CO)$_3$, 79391-56-3; (OMN)Mo(CO)$_3$, 79391-57-4; (OMN)W(CO)$_3$, 79391-58-5; (OMN)Cr(CO)$_2$(PPh$_3$), 79391-59-6; (*endo*)-[OMN·MA]Cr(CO)$_3$, 79391-60-9; (*exo*)-[OMN·MA]Cr(CO)$_3$, 79434-50-7; (*endo*)-OMN·MA, 36744-72-6; (*exo*)-OMN·MA, 36744-73-7; Cr(CO)$_3$(P(OMe)$_3$)$_3$, 17764-72-6; Cr(CO)$_6$, 13007-92-6; (CH$_3$CN)$_3$Mo(CO)$_3$, 15038-48-9; (CH$_3$CN)$_3$W(CO)$_3$, 16800-47-8; MA, 108-31-6.

Supplementary Material Available: Listings of the observed and calculated structure factors used in the crystallographic analyses (21 pages). Ordering information is given on any current masthead page.

Further Studies on the Molecular Dynamics of the Four-Electron Bridging Carbonyl

John A. Marsella and Kenneth G. Caulton*

Department of Chemistry, Indiana University, Bloomington, Indiana 47405

Received July 14, 1981

Both $Mn_2(CO)_6(dpm)_2$, which contains only terminal carbonyls, and $Mn_2(CO)_5(dpm)_2$, which contains one μ:η^2 (four-electron donor) carbonyl, are shown to be fluxional by ^{13}C NMR spectroscopy. Scrambling in the hexacarbonyl occurs over both metal atoms with E_a = 10.2 kcal/mol and log A = 12.1, while that in pentacarbonyl involves only a wagging motion which results in disruption of the Dewar–Chatt portion of the four-electron donor carbonyl with E_a = 17.0 kcal/mol and log A = 15.0. By selective ^{31}P decoupling experiments, the chemical shift of the four-electron donor carbonyl is shown to fall in the chemical shift region normally attributed to terminal carbonyls. Coupling of ^{13}C to ^{31}P is small (<5 Hz) through the Dewar–Chatt portion of this type of carbonyl.

Introduction

The four-electron-donor carbonyl bridge, depicted formally as I, is an organometallic structural unit of relatively

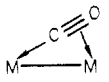

I

recent vintage. The first example, contained in $Mn_2(CO)_5(dpm)_2$, II (dpm = bis(diphenylphosphino)methane,

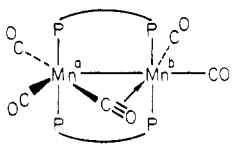

II

$Ph_2PCH_2PPh_2$), was reported in 1975 by Colton, Commons, and Hoskins.[1] The five carbonyls in this molecule are coplanar. Subsequent reports include $Cp_2NbMo(CO)_3Cp$,[2] $Cp_2Zr(OC)(OCMe)Mo(CO)Cp$,[3] and $(C_5Me_5)_2ZrCo(CO)_2(C_5H_5)$.[4] A cluster-bound analogue occurs in $HFe_4(CO)_{13}^-$, where one of the carbonyl ligands donates a total of four electrons to all four iron atoms in $Fe_4(CO)_{13}H^-$.[5] Finally an extreme example of carbonyl Lewis basicity is found in $Cp_3Nb_3(CO)_7$, where one CO ligand lies obliquely over the Nb_3 triangle and donates via the carbon lone pair and *both* filled C≡O π orbitals.[6]

Carbon monoxide assumes the μ_2:η^2 functionality in ligand-deficient situations; indeed, this structural unit is generally formed by thermal or photochemical processes which expel ligands (e.g., CO or CH_4). Since such ligand-deficient situations are precisely those found on lightly loaded metal surfaces, molecular examples of multipoint attachment of CO represent an important opportunity to examine the dynamics and reactivity of a catalytically relevant moiety by use of spectroscopic methods.

Several years ago, we reported the results of a ^{31}P NMR study of $Mn_2(CO)_5(dpm)_2$ which indicated that the migrational processes depicted in eq 1 (bridging dpm ligands

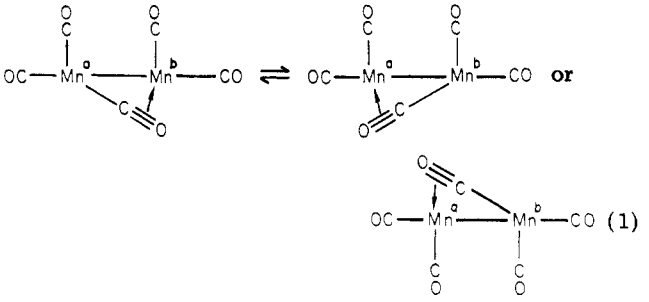

(1)

are omitted for simplicity) are *not* facile.[7] The observed inequivalence (at 30 °C) of the phosphorus nuclei attached to different manganese atoms allowed us to set a lower limit of 15.6 kcal/mol for the activation energy of eq 1. This result is compatible with the notion that multipoint carbonyl binding inhibits the characteristically facile migrations of two-electron donor carbonyls.

We were therefore somewhat surprised by our more recent result that *reorientation* of the six-electron donor carbonyl in $Cp_3Nb_3(CO)_7$ (eq 2) occurs with an activation energy, E_a, of 17 kcal/mol.[8] In order to examine this situation more critically, we have returned to perhaps the

(1) (a) Commons, C. J.; Hoskins, B. F. *Aust. J. Chem.* **1975**, *28*, 1663. (b) Colton, R.; Commons, C. J. *Ibid.* **1975**, *28*, 1673.
(2) Pasynskii, A. A.; Skripkin, Yu. V.; Eremenko, I. L.; Kalinnikov, V. T.; Aleksandrov, G. G.; Andrianov, V. G.; Struchkov, Yu. T. *J. Organomet. Chem.* **1979**, *165*, 49.
(3) Longato, B.; Norton, J. R.; Huffman, J. C.; Marsella, J. A.; Caulton, K. G. *J. Am. Chem. Soc.* **1981**, *103*, 209.
(4) Barger, P. T.; Bercaw, J. E. *J. Organomet. Chem.* **1980**, *201*, C39.
(5) Manassero, M.; Sanasoni, M.; Longoni, G. *J. Chem. Soc., Chem. Commun.* **1976**, 919.
(6) Herrmann, W. A.; Biersack, H.; Ziegler, M. L.; Weidenhammer, K.; Siegel, R.; Rehder, D. *J. Am. Chem. Soc.* **1981**, *103*, 1692.
(7) Caulton, K. G.; Adair, P. *J. Organomet. Chem.* **1976**, *114*, C11.
(8) Lewis, L. N.; Caulton, K. G. *Inorg. Chem.* **1980**, *19*, 3201.

0276-7333/82/2301-0274$01.25/0

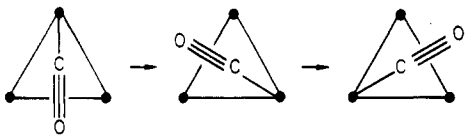

(2)

• = $CpNb(CO)_2$

simplest example, $Mn_2(CO)_5(dpm)_2$. This time, we have examined the migrating nuclei directly using ^{13}C NMR. This provides information which complements, but does not duplicate, our earlier ^{31}P NMR study. Of equal importance, this study yields unexpected information about the spectroscopic characteristics of the four-electron donor carbonyl.

Experimental Section

The compound $Mn_2(CO)_5(dpm)_2$ was synthesized according to the published procedure.[1b] Carbon-13 enrichment was achieved by stirring a suspension of the complex under 0.5 atm of enriched ^{13}CO (70%) at 140 °C in a mixture of xylenes for 3 days. The resulting orange solution was then degassed, and heating was continued for 1 day under 1 atm of N_2 (closed system) to yield enriched $Mn_2(CO)_5(dpm)_2$ as a red precipitate. From the orange filtrate was obtained enriched $Mn_2(CO)_6(dpm)_2$. The purity and identity of these two complexes were confirmed by ^{31}P NMR spectroscopy.[7]

NMR spectra were obtained on a Varian XL 100 spectrometer operating at 25.206 MHz for carbon and equipped with ^{31}P decoupling capability. Methylene chloride solvent was used for all spectra obtained at 30 °C and below. For high-temperature spectra (>30 °C), 1,2-dichloroethane was used. Samples were approximately 50% enriched, based on the relative intensities of the μ-CO bands at 1645 (^{12}CO) and 1605 cm^{-1} (^{13}CO) of $Mn_2(CO)_5(dpm)_2$. NMR solutions were approximately 30 mM in manganese complex and 10 mM in $Cr(acac)_3$. None of the spectra showed significant broadening by the quadrupolar manganese nuclei. Temperatures were measured by means of a thermometer inserted into the sample probe.

Dynamic NMR spectra were simulated with the program DNMR.[8] Activation parameters for $Mn_2(CO)_6(dpm)_2$ were derived from spectra in the range −55 to −20 °C, while those for the pentacarbonyl employed spectra in the range 5 to 75 °C. These parameters were evaluated from a least-squares fit of the derived rate constants.

Results

The poor solubility of $Mn_2(CO)_5(dpm)_2$ necessitates ^{13}CO enrichment in order to obtain reliable data on ligand migration. This enrichment was effected by taking advantage of the equilibrium[9] in eq 3. The forward and

$$Mn_2(CO)_5(dpm)_2 + CO \rightleftharpoons Mn_2(CO)_6(dpm)_2 \quad (3)$$

reverse steps of this reaction have been carried out at 25 and 140 °C, respectively.[1,7] The enrichment proceeds by the agitation of $Mn_2(CO)_5(dpm)_2$ under ^{13}CO at 140 °C in xylene.

The $^{13}C\{^1H\}$ NMR spectrum of $Mn_2(CO)_5(dpm)_2$ in the carbonyl region at −52 °C consists of a complex series of overlapping resonances (Figure 1a). The coupling to phosphorus represents an obstacle to assigning the spectrum. We therefore recorded the *broad-band* ^{31}P-decoupled ^{13}C spectrum (Figure 1d). While no proton decoupling was employed, this caused no significant broadening of the carbonyl resonances. The $^{13}C\{^{31}P\}$ NMR spectrum of $Mn_2(CO)_5(dpm)_2$ at −52 °C shows a closely spaced cluster of five lines in the region from 240 to 225 ppm. None of these lines is due to $Mn_2(CO)_6(dpm)_2$ impurity (see below).

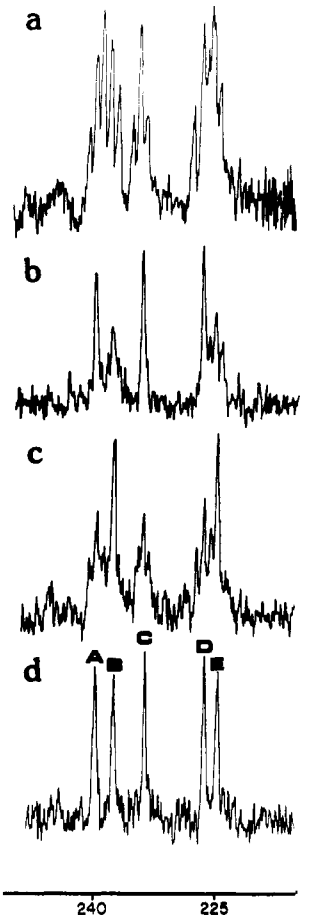

Figure 1. Carbonyl region ^{13}C NMR spectra of $Mn_2(CO)_5(dpm)_2$ at −52 °C. (a) No ^{31}P decoupling. (b) Selective decoupling of the 75.9-ppm ^{31}P resonance. (c) Selective decoupling of the 59.5-ppm ^{31}P resonance. (d) Broad-band ^{31}P decoupling.

While this spectrum is in accord with the solid-state structure, it is remarkable in that the four-electron donor carbonyl exhibits a chemical shift in the "terminal carbonyl region" and not further downfield in the region typical of normal μ_2:η^1 bridging carbonyls.[10]

Selective ^{31}P decoupling experiments make it possible to assign most of this spectrum. Irradiation of the 75.9-ppm ^{31}P resonance frequency (i.e., with the 59.5-ppm phosphorus nuclei coupling to carbon) leaves two of the carbonyl signals (B and E) as triplets (Figure 1b). These carbonyls are therefore assigned as bonded to Mn^b in II. Irradiation of the other (59.5 ppm) phosphorus frequency yields triplet patterns for lines A, C, and D. Thus, no carbon couples significantly to both types of phosphorus. These lines are then assigned to carbonyls bonded to Mn^a;[11,12] one of these three is then the resonance of the four-electron-donor carbonyl. This permits the conclusion that carbon in the μ_2:η^2-CO structural unit couples selectively to the phosphorus to which it dative bonds through carbon but that coupling to phoshorus through the π-donor orbital is small (<5 Hz).

The course of the ligand migration process is best observed in the completely ^{31}P decoupled spectrum (Figure

(9) $Mn_2(CO)_5(dpm)_2$ adds *p*-$CH_3C_6H_4NC$ irreversibly in refluxing xylene, subsequently displacing CO to give (μ-η^1:η^2-$CH_3C_6H_4NC$)Mn_2-$(dpm)_2(CO)_4$. Benner, L. S.; Olmstead, M. M.; Balch, A. L. *J. Organomet. Chem.* **1977**, *159*, 289.

(10) Todd, L. J.; Wilkinson, J. R. *J. Organomet. Chem.* **1974**, *77*, 1.

(11) This assignment of resonances A, C, and D to carbons bound to Mn^a in II is not arbitrary, nor is it based simply on arguments about the magnitude of J(P–C). The nature of the nuclear permutation deduced under Discussion uniquely leads to this assignment.

(12) These experiments also indicate that the 75.9-ppm phosphorus nuclei are bonded to Mn^a and the 59.5-ppm phoshorus nuclei reside on Mn^b.

Table I. Carbonyl Ligand ^{13}C Chemical Shifts in $Mn_2(CO)_5(dpm)_2$

resonance	chemical shift (ppm)
A	239.8
B	237.5
C	233.8
D	226.8
E	224.9
(A + C)[a]	237.4
(B + E)[a]	231.5

[a] Observed position above coalescence temperature.

2). As the temperature is raised, resonances A, B, C, and E (see Figure 1d for labels) broaden and *selectively* coalesce, while resonance D remains sharp. The selective character of the coalescence lies in the fact that lines A, B, C, and E coalesce to *two* lines. On the basis of the averaged chemical shifts, we can show that lines A and C merge to one line, while B and E merge to a second line. Differential line broadening is evident in the spectra in the range 30–75 °C, but this is caused by the fact that resonances A and C are separated by a smaller gap (133 Hz at −75 °C, 152 Hz at −30 °C) than B and E (320 Hz) (see Table I).

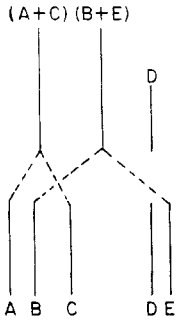

Line-shape analysis (see below) shows that a single kinetic process (one rate constant) is sufficient to reproduce this differential line broadening.

By +75 °C, resonances A and C have coalesced to a singlet (broad band ^{31}P decoupled) which is nearly as sharp as (unchanged) resonance D. The slower coalescence of lines B and E leaves their merged resonance broader at +75 °C. The coalesced pattern approximates the expected 2:2:1 intensity ratios for the assignment (reading upfield) (A + C), (B + E), and D. Selective ^{31}P decoupling at +75 °C permits independent confirmation of the above conclusion that, within any pair of interchanging carbonyls, the two nuclei are bound to the same metal atom. Thus, decoupling at the 75.9-ppm ^{31}P frequency broadens only the central resonance (relative to the broad-band ^{31}P-decoupled spectrum), which was assigned as B + E (both on Mn^b). Decoupling at the 59.5-ppm phosphorus resonance yields triplets for the resonance assigned as (A + C) and D (both on Mn^a); the (B + E) resonance is unaffected. The connectivity and site-exchange required of these data are contained in the following: [Mn^a: P(75.9 ppm); (A + C); D] [Mn^b: P(59.5 ppm); (B + E)].

For a number of reasons, it was deemed useful to examine the ^{13}C NMR of $Mn_2(^{13}CO)_6(dpm)_2$ (III).[1b] Curi-

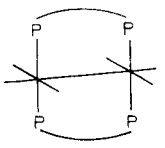

III

ously, the $^{13}C\{^1H\}$ spectrum of this compound at 30 °C shows only a quintet resonance in the carbonyl region (δ 232.5), due to coupling to phosphorus (J = 10.3 Hz). Both the single apparent chemical shift and the apparently equivalent coupling to all four phosphorus nuclei speak for a fluxional molecule. No single structural alternative to III could account for these observations. At −75 °C, the $^{13}C\{^{31}P\}$ NMR spectrum of $Mn_2(CO)_6(dpm)_2$ consists of two resonances, 234.8 and 226.5 ppm, of relative intensity approximately 2:1. In the phosphorus-coupled spectrum, each resonance is broadened ($\nu_{1/2}$ = 30 Hz) sufficiently to be consistent with unresolved coupling to ^{31}P; the $^{13}C\{^{31}P\}$ broad-band NMR spectrum at −75 °C (Figure 3) is considerably sharper ($\nu_{1/2}$ = 10 Hz).[13] This confirms that

Figure 2. Variable-temperature ^{13}C NMR spectra (carbonyl region) of $Mn_2(CO)_5(dpm)_2$ under conditions of broad-band ^{31}P decoupling.

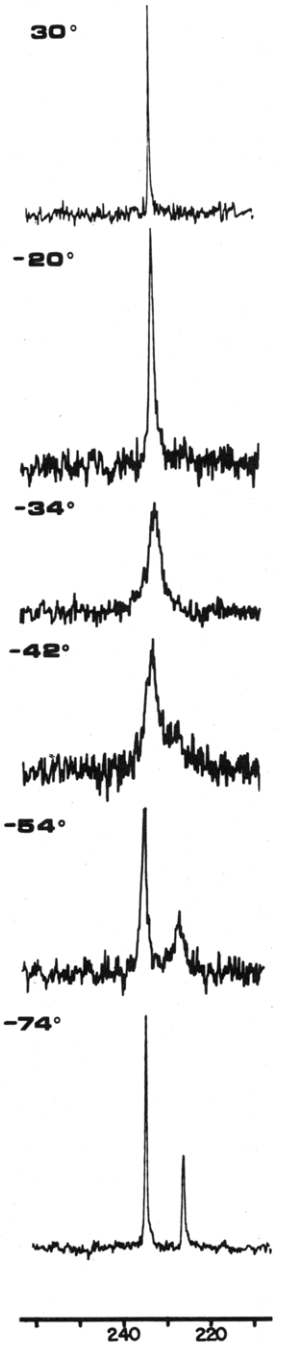

Figure 3. Variable-temperature ^{13}C NMR spectra (carbonyl region) of $Mn_2(CO)_6(dpm)_2$ under conditions of broad-band ^{31}P decoupling.

$Mn_2(CO)_6(dpm)_2$ exhibits global intramolecular carbonyl scrambling and provides a useful standard for the energetics of the rearrangement of the four-electron donor carbonyl. In retrospect, it is clear that CO scrambling between the two inequivalent sites in $Mn_2(CO)_6(dpm)_2$ is essential to the *random* enrichment which we seek in eq 3.

Discussion

We have detected a facile intramolecular (P–C coupling is retained) rearrangement of the four-electron-donor carbonyl in $Mn_2(CO)_5(dpm)_2$. The rearrangement is of limited, not global, scope: it does not result in equivalence of the two metal atoms in the molecule, and in this regard it is consistent with our earlier ^{31}P NMR results.[7] The rearrangement creates a time-averaged molecular mirror plane containing the metal–metal bond and the four phosphorus nuclei but no mirror plane relating the two metal atoms. Furthermore, the data show clearly that, during the progress of the rearrangement, *no* carbonyl ligand migrates to a terminal position on the second metal (for example, see Scheme I). All such processes would lead to quintets due to ^{31}P coupling.

Scheme I

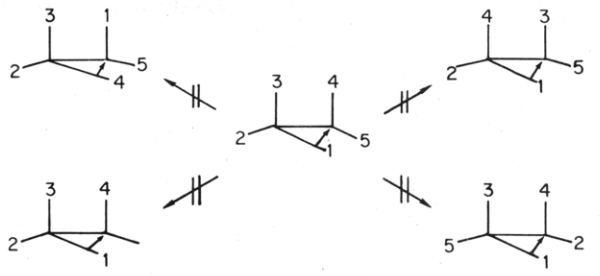

Scheme II

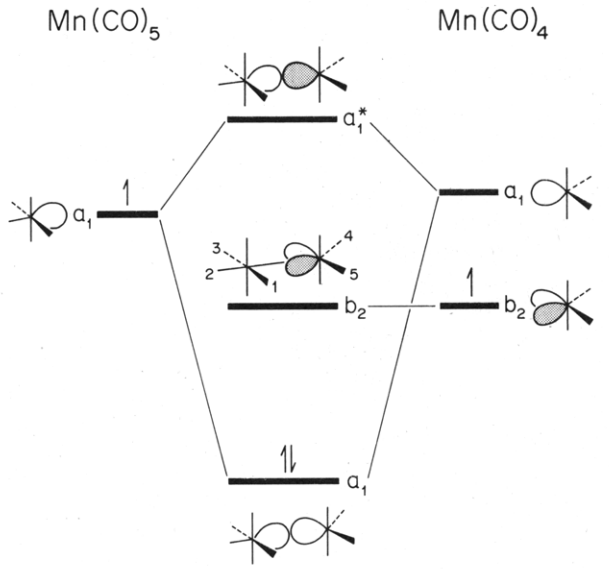

The limited character of the fluxional behavior of II contrasts with the global migration observed in $Fe_2(CO)_5[(EtO)_2POP(OEt)_2]_2$.[14] The structure of the iron complex differs from that of II in that it contains a symmetrical bridging carbon monoxide ligand. The very facile process (coalescence temperature ~ −108 °C) in the symmetrically bridged iron complex involves all CO's moving to *both* metal centers.

The simplest mechanism which accomplishes the observed coalescence is the limited but concerted wagging process shown in eq 4 and Figure 4. This mechanism

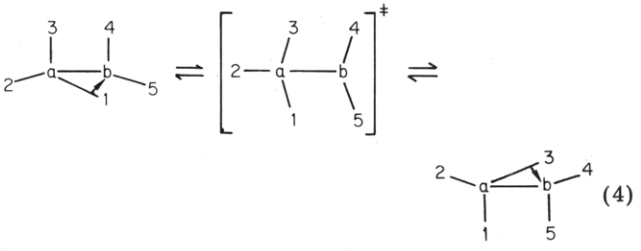

(4)

(13) The room-temperature $^{13}C\{^{31}P\}$ spectrum is considerably sharper, with $\nu_{1/2} \sim 3$ Hz. At −75 °C, the fluxional processes are not completely frozen, and the resulting broadening (or viscosity broadening) prevents resolution of P–^{13}C coupling.

(14) Cotton, F. A.; Haines, R. J.; Hanson, B. E.; Sekutowski, J. C. *Inorg. Chem.* **1978**, *17*, 2010.

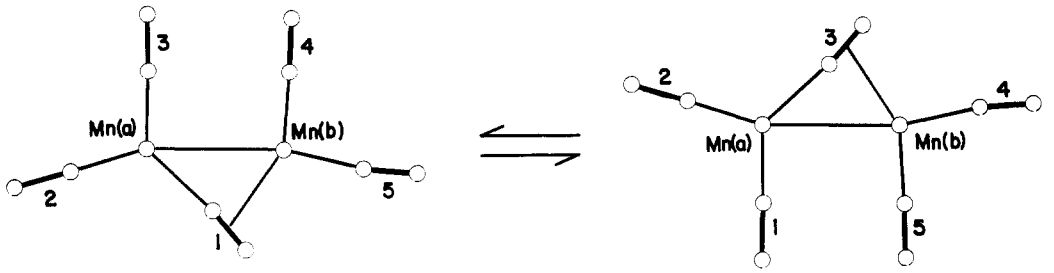

Figure 4. ORTEP drawings of the fluxional motion occurring in $Mn_2(CO)_5(dpm)_2$.

equivalences the two carbonyls bound to Mn^b, as is required by the phosphorus-coupled ^{13}C NMR data. It also requires that resonances A and C are due to environments 3 and 1, *or the reverse*; a unique assignment cannot be made with the available data, but this has no influence on the conclusions drawn. Most importantly, the temperature invariance of resonance D (now assigned to environment 2) arises in an unusual (but not unique) manner. While this quasi-axial carbonyl undergoes a spatial movement (Figure 4), it remains in an equivalent environment after such rearrangement and, therefore, exhibits no lifetime broadening.

The rearrangement mechanism in eq 4 appears to sacrifice the CO π-donor portion of the four-electron donor unit during the process. The proposed transition state has a geometry similar to that of $Re_2Cl_5(dpm)_2$.[15] It is not possible to achieve an 18-electron configuration at Mn^b by drawing a Mn=Mn double (covalent) bond in this structure. However, this transition state might reasonably employ bond making concurrent with bond breaking (IV).

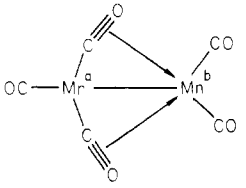

IV

Such behavior is wholly analogous to that shown in the ground-state structure of $Cp_2V_2(CO)_5$[16] (V), where the net

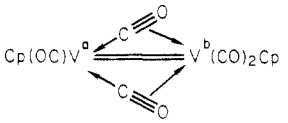

V

result of two "semibridging" carbonyls is the formal donation of a total of only two electrons to V^b. It is this proposed compensatory nature of the rearrangement in $Mn_2(CO)_5(dpm)_2$ which lowers the activation energy of an otherwise unfavorable 18-electron → 16-electron transformation. Line-shape analysis of the observed spectra gives an E_a of 10.2 kcal/mol (log A = 12.1) for $Mn_2(CO)_6(dpm)_2$ and E_a = 17.0 kcal/mol (log A = 15.0) for $Mn_2(CO)_5(dpm)_2$. Consequently, rearrangement of the four-electron-donor carbonyl is found to cost only 6.8 kcal/mol more than that of a more conventional carbonyl complex. Combining the frontier orbitals of the fragments $Mn(CO)_5$ and $Mn(CO)_4$,[17] as shown in Scheme II, reveals that the LUMO of the C_{2v} $Mn_2(CO)_9$ transition state resides on the $Mn(CO)_4$ fragment and is of the proper symmetry (b_2) to accept from one filled π orbital of each of the two carbonyls in question. The requisite empty orbital is thus available for the interaction depicted in IV. Comparison of the activation energy in $Mn_2(CO)_5(dpm)_2$ with that in $Fe_2(CO)_5[(EtO)_2POP(OEt)_2]_2$ is also warranted since the b_2 orbital of this proposed intermediate is filled in the latter compound. The iron compound exhibits intramolecular carbonyl exchange at over 10^3 s^{-1} at 100 °C. The difference in ground-state structure tends to frustrate any more detailed comparison, however.

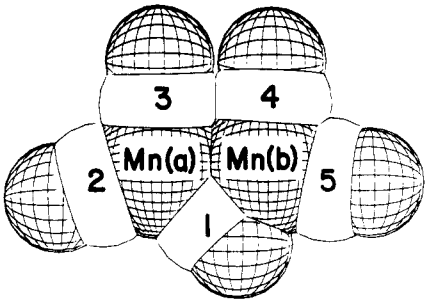

Figure 5. Space-filling scale model of the $Mn_2(CO)_5$ unit in $Mn_2(CO)_5(dpm)_2$.

Figure 5 shows a scale view of the $Mn_2(CO)_5$ plane with all atoms drawn at their van der Waals radii. This space-filling model reveals that the clockwise motion of the four-electron-donor carbonyl which initiates the rearrangement in eq 4 will displace all other carbonyls in the direction shown. The synchronous motion of all five carbonyls is assured in particular by the close contact between carbonyls 3 and 4, which flank the metal–metal bond on different metal atoms.

The carbonyl migration in $Mn_2(CO)_6(dpm)_2$ is most readily accomplished by the merry-go-round mechanism shown in eq 5. Our DNMR result shows that the bridged

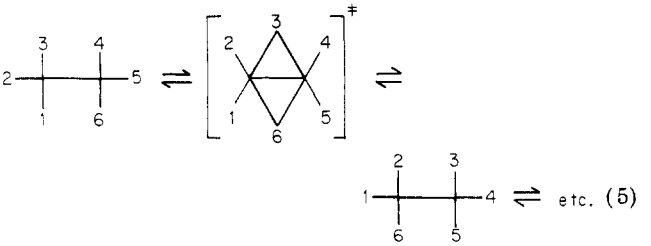

carbonyl complex lies less than or equal to 10.2 kcal/mol above the all-terminal ground state. While carbonyls symmetrically bridging two manganese atoms are rare, an example has been reported recently.[18] The key question, and the origin of our surprise at the fluxionality of $Mn_2(CO)_6(dpm)_2$, is why this compound differs so much from $Mn_2(CO)_{10}$, which appears stereochemically rigid at 30 °C by ^{13}C NMR and up to 130 °C by ^{17}O NMR.[19] We suggest

(15) Cotton, F. A.; Shive, L. W.; Stults, B. R. *Inorg. Chem.* **1976**, *15*, 2239.
(16) Huffman, J. C.; Lewis, L. N.; Caulton, K. G. *Inorg. Chem.* **1980**, *19*, 2755. Lewis, L. N.; Caulton, K. G. *Ibid.* **1980**, *19*, 1840.
(17) Elian, M.; Hoffmann, R. *Inorg. Chem.* **1975**, *14*, 1058.
(18) Lewis, L. N.; Huffman, J. C.; Caulton, K. G. *Inorg. Chem.* **1980**, *19*, 1246.

that conformational differences around the Mn–Mn single bond contribute to this difference.[20] $Mn_2(CO)_{10}$ is staggered. $Mn_2(CO)_6(dpm)_2$ is, of course, eclipsed. While this has not been established crystallographically for $Mn_2(CO)_6(dpm)_2$, the $Ph_2PCH_2PPh_2$ linkage is too short to span a staggered metal–metal bond 2.9–3.0 Å long. Eclipsed conformations are found in $Re_2Cl_5(dpm)_2$,[15] $Mo_2Cl_4(dpm)_2$,[21a] and the many M–M single bonded species $M_2(dpm)_2X_n$ (M = Rh, Pt, Pd).[21b] An interesting corollary of this argument is that the $Ph_2PCH_2CH_2PPh_2$-bridged analogue, $Mn_2(CO)_6(dppe)_2$, is predicted to have a higher barrier to carbonyl scrambling. $Re_2Cl_4(dppe)_2$,[22] $Mo_2Br_2(Ph_2PCH_2CH_2AsPh_2)$,[23] and $W_2Cl_4(dppe)_2$[24] are all staggered.

Although we believe the steric consequences of the phosphine bridge to be the most important consideration, it should be noted that the stereochemical rigidity of $Os_3(CO)_{12}$ is diminished upon phosphine substitution. Thus, $Os_3(CO)_{12}$ is only fluxional above 100 °C, while $Os_3(CO)_{11}P(Et)_3$ (VI) shows two-center carbonyl fluxionality at room temperature (eq 6).[20] On the other hand,

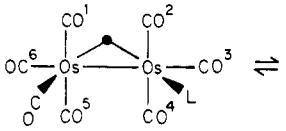

VI

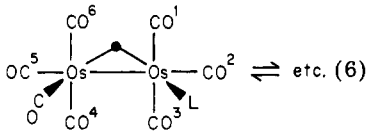

• = $Os(CO)_4$; L = $P(C_2H_5)_3$

axial $Mn_2(CO)_9(PPh_3)$, like $Mn_2(CO)_{10}$, is rigid.[19c]

Conclusion

Fluxional processes operate in both $Mn_2(CO)_6(dpm)_2$ and $Mn_2(CO)_5(dpm)_2$. These are in contrast to the nonfluxional nature of the parent carbonyl complex. The chemical shift of the μ_2 carbonyl in $Mn_2(CO)_5(dpm)_2$ is in the "normal" terminal carbonyl region. This result is consistent with the observation of resonances at 229.9 and 227.8 ppm for the two carbonyl ligands in $Cp_2Zr(\mu\text{-}C(O)Me)(\mu\text{-}CO)Mo(CO)Cp$[3] and suggests that ^{13}C NMR is *not* diagnostic of four-electron donor carbonyl ligands. Coupling constants from phoshorus to the carbonyl carbons in $Mn_2(CO)_n(dpm)_2$ (n = 5, 6) are in the range of values (9–25 Hz) observed previously for cis geometry.[10] Carbon in the four-electron donor carbonyl exhibits little coupling through metals to which the C–O π-donor bond is formed. This is a feature which it shares with the typical Dewar–Chatt bond to ethylene in $Os(PPh_3)_2NO(CO)C_2H_4^+$ ($J_{P\text{-}CO}$ is observed, while $J_{P\text{-}C_2H_4}$ is unresolved).[25]

At the beginning of this paper, we proposed that the four-electron bridging carbonyl might be a common structural unit on lightly loaded metal surfaces. In all probability, just such an example already exists in the literature. A study[26] of Mn_2 dimers in CO-doped low-temperature matrices has produced a species of composition Mn_2CO which exhibits a stretching frequency of 1683 cm^{-1}. We suggest that this is not simply a carbon-bonded bridging carbonyl but rather a four-electron donor, I. The generality of this binding mode makes it an attractive model for studies of dissociative chemisorption of CO.

Acknowledgment. This work was supported by NSF Grants CHE 77-10059 and 80-06331 and by the Lubrizol Foundation (fellowship to John A. Marsella). We thank Robert Addleman, Deon Osman, and Karen Klebofski for making the ^{31}P decoupling experiments possible. We thank the M. H. Wrubel Computing Center and Dr. John Huffman for help in obtaining the figures from data available through the Cambridge Crystallographic Data Center files.

Registry No. $Mn_2(CO)_5(dpm)_2$, 56665-73-7; $Mn_2(CO)_6(dpm)_2$, 57403-90-4.

(19) (a) Hickey, J. P.; Wilkinson, J. R.; Todd, L. J. *J. Organomet. Chem.* **1979**, *179*, 159. (b) Aime, S.; Milone, L.; Osella, D.; Hawkes, G. E.; Randall, G. W. *Ibid.* **1979**, *178*, 171. (c) Kump, R. L.; Todd, L. J. *Ibid.* **1980**, *194*, C43.

(20) The importance of coplanarity in facile carbonyl scrambling has been noted: Band, E.; Muetterties, E. L. *Chem. Rev.* **1978**, *78*, 639, and references cited therein.

(21) (a) Abbott, E. H.; Bose, K. S.; Cotton, F. A.; Hall, W. T.; Sekutowski, J. C. *Inorg. Chem.* **1978**, *17*, 3240. (b) For a summary of known structures, see: Olmstead, M. M.; Lindsay, C. H.; Benner, L. S.; Balch, A. L. *J. Organomet. Chem.* **1979**, *179*, 289.

(22) Cotton, F. A.; Stanley, G. G.; Walton, R. A. *Inorg. Chem.* **1978**, *17*, 2099.

(23) Cotton, F. A.; Fanwick, P. E.; Fitch, J. W.; Glicksman, H. D.; Walton, R. A. *J. Am. Chem. Soc.* **1979**, *101*, 1752.

(24) Cotton, F. A.; Felthouse, T. R.; Lay, D. G. *J. Am. Chem. Soc.* **1980**, *102*, 1431.

(25) Segal, J. A.; Johnson, B. F. G. *J. Chem. Soc., Dalton Trans.* **1975**, 677.

(26) Huber, H.; Kündig, E. P.; Ozin, G. A.; Poë, A. J. *J. Am. Chem. Soc.* **1975**, *97*, 308.

Carbanions from α-Phenylthio Boronic Esters as Synthetic Intermediates

Donald S. Matteson* and Karl H. Arne

Department of Chemistry, Washington State University, Pullman, Washington 99164

Received July 8, 1981

(Phenylthio)methaneboronic acid (1) was easily prepared from (phenylthio)methyllithium and trimethyl borate and was converted to boronic esters **2**. The pinacol ester **2b** was efficiently deprotonated by lithium diisopropylamide in tetrahydrofuran/ether/hexane to yield the lithio derivative **3** as its THF complex, an isolable though air-sensitive solid. Evidence was also obtained that **1** was C-lithiated as well as B-butylated by excess butyllithium. Reaction of **3** with primary alkyl halides yielded pinacol 1-(phenylthio)alkane-1-boronates **5**, which could also be deprotonated with LDA and reacted with alkyl halides to introduce a second alkyl group. Reaction of **3** or lithiated **5** with carboxylic esters has efficiently yielded α-phenylthio ketones **9**, providing a uniquely general and regiospecific synthesis of this useful class of compounds. With aldehydes and ketones, **3** or lithiated **5** behaves as Wittig reagents to provide high yields of enethiol ethers **12**. Reaction of **3** or lithiated **5** with ethylene oxide resulted in a mixture of pinacol (hydroxyalkyl)boronic ester (**15**) and cyclic boronic half ester (**16**). Pinacol bromo(phenylthio)methaneboronate (**18**) was prepared by bromination of **3**. Phenylmagnesium bromide converted **18** to pinacol phenyl(phenylthio)methaneboronate (**20**), but this type of transformation failed with cyclohexylmagnesium bromide or butyllithium. Conversion of pinacol 2-phenyl-1-(phenylthio)ethane-1-boronate (**5b**) to the 2-phenyl-1-iodoethane-1-boronate (**22**) was accomplished with methyl iodide and sodium iodide in DMF. Conversion of the difficultly hydrolyzable pinacol boronic ester group of **5b** to a diethanolamine ester (**7**) was also accomplished.

Introduction

Carbanions stabilized by adjacent boron have recently been generated by deprotonation of sterically hindered organoboron compounds with hindered lithium dialkylamides[1-4] and show promise as intermediates for organic synthesis. Prior to these discoveries, boron-substituted carbanions were accessible only through deboronation of compounds having three or four boronic ester groups[5,6] or two boronic ester and one or two group 4 metal substituents on the same carbon[7] or through deprotonation of carboranes[8] or a borabenzene anion precursor.[9] None of these earlier routes could provide carbanions at low enough cost to be considered for general synthetic organic purposes. The substantial improvement in synthetic practicality provided by the deprotonation of *gem*-diboronic esters[2] immediately suggested the possibility that pairing boron with another carbanion-stabilizing element might lead to some new and useful synthetic operations. The obvious choice of a second element was sulfur.

Deprotonation of organosulfur compounds has become a widely used route to carbanions for synthetic purposes. Examples include thioanisole,[10,11] dithiane,[12] cyclopropyl phenyl sulfide,[13] dimethyl sulfide,[14] $PhSCH_2SiMe_3$,[15] CH_3OCH_2SPh,[16] $CH_3SCH_2PO(OEt)_2$,[17] and $PhSCH_2CH(CH_3)_2$.[18] We expected that reaction of a suitable sulfur-substituted carbanion with trimethyl borate would lead to a sulfur-substituted boronic acid, which could be converted to a variety of boronic ester derivatives. With sufficient steric hindrance by the boronic ester group to prevent attack on boron by a sterically hindered lithium dialkylamide,[2] deprotonation of the carbon flanked by boron and sulfur would be expected.

Results

Synthesis of (Phenylthio)methaneboronic Esters. Treatment of (phenylthio)methyllithium[10] with trimethyl borate followed by aqueous workup efficiently yielded (phenylthio)methaneboronic acid (**1**), which was easily

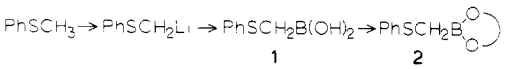

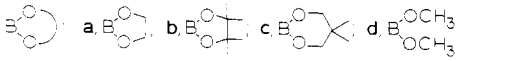

converted to (phenylthio)methaneboronic esters (**2**) by standard methods. This very simple route to **2** is easily operable on a 1-mol scale, and involves less effort and potential hazard than the preparation of *gem*-diboronic esters.[6]

Deprotonation–Methylation Studies. Exploration to find conditions suitable for deprotonation of (phenylthio)methaneboronic esters (**2**) was aided by proton NMR

(1) Preliminary communication: Matteson, D. S.; Arne, K. *J. Am. Chem. Soc.* **1978**, *100*, 1325–1326.
(2) (a) Matteson, D. S.; Moody, R. J. *J. Am. Chem. Soc.* **1977**, *99*, 3196–3197. (b) Matteson, D. S.; Moody, R. J. *Organometallics* **1982**, *1*, 0000–0000.
(3) (a) Rathke, M. W.; Kow, R. *J. Am. Chem. Soc.* **1972**, *94*, 6854–6856. (b) Kow, R.; Rathke, M. W. *J. Am. Chem. Soc.* **1973**, *95*, 2715–2716.
(4) Subsequent to our preliminary communication:[1] (a) Mendoza, A.; Matteson, D. S. *J. Org. Chem.* **1979**, *44*, 1352–1354. (b) Matteson, D. S.; Majumdar, D. *J. Chem. Soc., Chem. Commun.* **1980**, 39–40. (c) Wilson, J. W. *J. Organomet. Chem.* **1980**, *186*, 297–300.
(5) Matteson, D. S.; Moody, R. J. *J. Org. Chem.* **1980**, *45*, 1091–1095.
(6) (a) Matteson, D. S.; Hagelee, L. A. *J. Organomet. Chem.* **1975**, *93*, 21–32. (b) Matteson, D. S. "Gmelins Handbuch der Anorganischen Chemie", 8th ed., New Supplement Series; Niedenzu, K.; Buschbeck, K.-C., Eds.; Springer-Verlag: Berlin, 1977; Vol. 48, Part 16, pp 37–72. (c) Matteson, D. S. *Synthesis* **1975**, 147–158.
(7) (a) Matteson, D. S.; Larson, G. L. *J. Organomet. Chem.* **1973**, *57*, 225–230. (b) Matteson, D. S.; Wilcsek, R. J. *Ibid.* **1973**, *57*, 231–242. (c) Matteson, D. S.; Jesthi, P. K. *Ibid.* **1976**, *110*, 25–37.
(8) Grimes, R. N. "Carboranes"; Academic Press: New York, 1970; pp 66–68.
(9) Ashe, A. J., III; Shu, P. *J. Am. Chem. Soc.* **1971**, *93*, 1804–1805.
(10) Corey, E. J.; Seebach, D. *J. Org. Chem.* **1966**, *31*, 4097–4099.
(11) Corey, E. J.; Jautelat, M. *Tetrahedron Lett.* **1968**, 5787–5788.
(12) House, H. O. "Modern Synthetic Reactions", 2nd ed., W. A. Benjamin: Menlo Park, CA, 1972; pp 731–733.
(13) (a) Trost, B. M.; Keeley, D. E.; Bogdanowicz, M. J. *J. Am. Chem. Soc.* **1973**, *95*, 3068–3070. (b) Trost, B. M.; Keeley, D. E.; Arndt, H. C.; Rigby, J. H.; Bogdanowicz, M. M. *Ibid.* **1977**, *99*, 3080–3087.
(14) Peterson, D. J. *J. Org. Chem.* **1967**, *32*, 1717–1720.
(15) Carey, F. A.; Court, A. S. *J. Org. Chem.* **1972**, *37*, 939–943.
(16) Trost, B. M.; Miller, C. H. *J. Am. Chem. Soc.* **1975**, *97*, 7182–7183.
(17) Corey, E. J.; Schulman, J. I. *J. Org. Chem.* **1970**, *35*, 777–780.
(18) Dolak, T. M.; Bryson, T. A. *Tetrahedron Lett.* **1977**, 1961–1964.

0276-7333/82/2301-0280$01.25/0

Table I. Exploration of Conditions for Deprotonation of Pinacol (Phenylthio)methaneboronate (2b) and Methylation to Pinacol 1-(Phenylthio)ethane-1-boronate (4)

deprotonation conditions							products, % yields[a]		
base	equiv	other	equiv	solvent	T, °C	time, h	4	2b	$PhSCH_3$
LiTMP[b]	1			THF	25	5	70	15	10
LiTMP	1	DABCO[c]	1	THF	25	5	85	15	0
LiTMP	1	HMPA[d]	1	THF	25	21	45	45	5
LiTMP	1			ether	25	7	70	30	0
LiTMP	1	DABCO	1	ether	25	7	70	30	0
LiNRR'[e]	1			isooctane	−10	0.5	60	35	0
LiNRR'[e]	1.2	TMEDA[f]	1.2	THF	0	3	85	15	0
LDA[g]	1.2	TMEDA	1.2	THF	0	3	85	15	0
LiO-*t*-Bu	1	DABCO	2	THF	0	21	0	60	25
$LiCPh_3$	1			THF	25	14	0	100	0

[a] Estimated from the proton NMR spectrum. Where total is less than 100%, other products were present, including $PhSCH_2CH_3$. [b] Lithium 2,2,6,6-tetramethylpiperidide. [c] 1,4-Diazabicyclo[2.2.2]octane. [d] Hexamethylphosphoramide. [e] R = cyclohexyl, R' = isopropyl. [f] 1,2-Bis(dimethylamino)ethane. [g] Lithium diisopropylamide.

analysis of the products. After each trial set of conditions for deprotonation of **2**, methyl iodide was added and allowed to react ~2 h at 20–25 °C, the mixture was worked up with aqueous acid, and the organic product was analyzed by proton NMR for $PhSCH_3$, SCH_2B, $SCH(CH_3B$, and SCH_2CH_3, each of which gave distinctive signals at 60 MHz.

The first attempts at deprotonation were made with the ethylene glycol ester **2a** and all failed totally. Bases tried included lithium 2,2,6,6-tetramethylpiperidide (LiTMP), *n*- and *tert*-butyllithium, and lithium *tert*-butoxide in tetrahydrofuran (THF). Additives, including hexamethylphosphoramide (HMPA), 1,4-diazabicyclo[2.2.2]-octane (DABCO), or 1,2-bis(dimethylamino)ethane (TMEDA), did not help. The major product was always recovered (phenylthio)methaneboronic acid (**1**), often with lesser amounts of thioanisole ($PhSCH_3$) and sometimes ethyl phenyl sulfide ($PhSCH_2CH_3$). Thus, it appeared that these bases coordinate with the relatively unhindered boron atom of **2a** to form tetrahedral borates, which in some cases deboronate to a small extent to form $PhSCH_2Li$.

Successful deprotonation was immediately achieved with the sterically hindered pinacol ester **2b**. Pinacol lithio

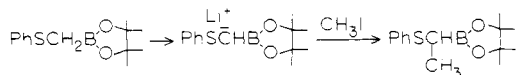

2b 3 4

(phenylthio)methaneboronate (**3**) often precipitated from concentrated THF solutions and was readily methylated in situ to form pinacol 1-(phenylthio)ethane-1-boronate (**4**). Results are summarized in Table I. It may be noted that yields of **4** were generally good and not very sensitive to the base or conditions. The only failures encountered with the bases tested were with lithium *tert*-butoxide and triphenylmethyllithium.

Since lithium diisopropylamide (LDA) led to as high yields of **4** as any of the bases tested and is convenient and inexpensive, it was chosen for all further work. In some of the reactions where **3** was used in situ to be described in the remainder of this article, TMEDA was included as a lithium ion complexing agent, but its relevance is highly doubtful for reasons to be pointed out in the following section on the isolation of **3**. Early results seemed to indicate that the use of TMEDA or DABCO improved the yields of **4** somewhat, and this impression was reinforced by the finding in concurrent work that TMEDA was absolutely essential in the deprotonation of propanediol methanediboronate.[2]

Deprotonation of other (phenylthio)methaneboronic esters (**2**) was examined briefly, with LiTMP used as base and THF as solvent. Yields of methylated product from the 2,2-dimethyl-1,3-propanediol ester (**2c**) were 55–60% and yields from the dimethyl ester **2d**, zero. The propanediol ester[19] gave 45–50%. Thus, the steric hindrance to base attack at boron provided by the pinacol ester group appears to be essential.

An altogether different approach to deprotonation was explored briefly with some success. Treatment of (phenylthio)methaneboronic acid (**1**) with 3 equiv of *n*-butyl-

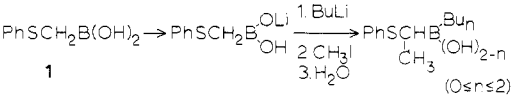

1

lithium in THF, with or without TMEDA, followed by methyl iodide resulted in 90% methylation, estimated by NMR. However, this C-methylation was incorporated into a mixture of B-butylated products. Less butyllithium gave less C-methylation and less B-butylation, and one equivalent yielded none of either. Attempts to deprotonate **1** with 3 equiv of LDA, sodium hydride, or lithium hydride led to no methylated product. The known deprotonation of carboxylate salts[20] provides a sort of precedent for the deprotonation of **1**. We were discouraged from further work on this system by the need for such a large excess of butyllithium and the inherent problem of dealing with a mixture of alkylborane products, even though the PhSCH(R)–B group of interest is common to all of them.

Isolation of Pinacol Lithio(phenylthio)methaneboronate (3). The precipitation of **3** during successful deprotonations of **2b** had been noted, and therefore the isolation and characterization of **3** were undertaken. The best yields of **3** precipitated from a mixture of THF, ether, and petroleum ether, and after the solid was collected under argon in a Schlenk apparatus and washed with additional solvent mixture, 80–85% yields of **3** as the monotetrahydrofuran complex were routinely obtained. Though this material is highly hygroscopic and sensitive to air, it yielded a satisfactory elemental analysis, and a solution in pyridine-d_5 showed the correct proton NMR spectrum for **3** (probably as an adduct with the solvent) with 1 mol of THF. If protected from air, solid **3**·THF appeared stable indefinitely.

Not all of the factors involved in the preparation of **3** are understood, and on a few occasions the precipitate proved fine or gummy and did not filter as rapidly as usual, with yields reduced to 60–70%. This problem was not

(19) Mendoza, A.; Matteson, D. S. *J. Organomet. Chem.* **1978**, *156*, 149–157.
(20) Creger, P. L. *J. Am. Chem. Soc.* **1967**, *89*, 2500–2501.

Table II. Alkylation of Pinacol Lithio(phenylthio)methaneboronate (3) with Alkyl Halides, RX, To Yield Pinacol 1-(Phenylthio)alkane-1-boronates 4 and 5

RX	method[a]	product	yield,[b] %
CH_3I	A	4	83[c]
CH_3I	B	4	84
n-C_4H_9Br	A	5a	80[c]
n-C_4H_9Br	B	5a	88
n-C_4H_9Cl	A	5a	76[c]
n-C_4H_9I	A	5a	79[c]
$(CH_3)_3CCH_2CH(CH_3)CH_2CH_2Br$	A	5c	58
$PhOCH_2CH_2Br$	A	5d	71
$PhCH_2Br$	A	5b	50–57
$PhCH_2Br$	B	5b	75[d]
$(CH_3)_2CHBr$	B	5e[e]	40[e]

[a] Method A is without isolation of 3, B is with isolation of 3, see text. [b] Distilled product. [c] Yield contained in a mixture with 10–12% of unconverted 2b. [d] We thank Abel Mendoza for this result. [e] Mixed with equal amount of 2b, not obtained pure.

frequent, and insufficient attention to excluding moisture is suspected. The presence or absence of TMEDA in the reaction mixture reproducibly showed no effect whatever on the yield of isolated 3, and TMEDA was not incorporated into the precipitate. Products prepared from isolated 3 were generally very pure and free from any unreacted boronic ester 2b.

Alkylations. As soon as the methylation studies had established that pinacol (phenylthio)methaneboronate (2b) could be deprotonated by LDA and the resulting lithio derivative 3 methylated in situ, alkylations with other primary halides were tried and found to yield pinacol 1-(phenylthio)alkane-1-boronates 5. Results are summarized in Table II, "method A". It was later found that filtering and washing the precipitated lithio derivative 3 before alkylation led to improved yields and purities of 5, as shown in Table II, "method B". Isolation of 3 was crucial to obtaining a pure sample of the methylation product 4.

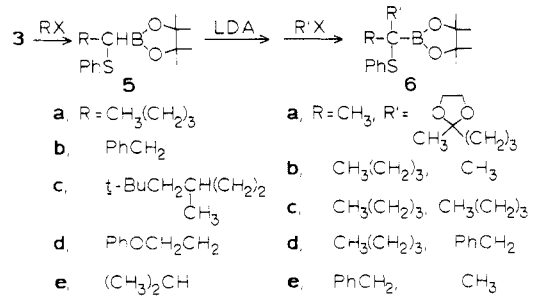

Even with isolated 3, secondary halides gave poor results. Isopropyl bromide yielded a 45/55 mixture of 5 and starting material 2b according to NMR analysis. 2-Pentyl bromide yielded only 10% of 5; 2-pentyl tosylate yielded 30–50% of 5.

Selected alkylation products (4, 5a, 5b) were tested for the possibility of a second deprotonation and alkylation. Deprotonation was readily accomplished with LDA in THF (without TMEDA). The lithio derivatives were all soluble in the reaction medium and were readily alkylated in situ to yield the dialkylated (phenylthio)methaneboronic esters 6, summarized in Table III. Little if any of the starting material 5 remained unconverted.

Hydrolysis and Oxidation of Pinacol Esters. Typical unhindered boronic esters hydrolyze immediately on contact with water, but pinacol boronic esters do not. Their unusual stability permits chromatography, extraction, handling in air, and general treatment as stable organic compounds. The only inconvenience comes when it is time to run a carbon–boron bond-breaking reaction. For this purpose, it became desirable to find a way to cleave the pinacol efficiently from the boron.

Table III. Alkylation of Pinacol 1-(Phenylthio)alkane-1-boronates 4 and 5 by Deprotonation with LDA and Treatment with Alkyl Halides, R'X

boronic ester	R	R'X	product	bp, °C (torr)	yield, %
4	CH_3	$CH_3C(O_2C_2H_4)$-$(CH_2)_3Cl$	6a	174 (0.3)	71[a]
5a	n-Bu	CH_3I	6b	136 (0.1)	70
5a	n-Bu	n-BuBr	6c	150 (0.2)	67
5a	n-Bu	$PhCH_2Br$	6d	184 (0.5)	78
5b	$PhCH_2$	CH_3I	6e	160 (0.2)	77

[a] Reaction time 12 h, yield only 48% after 3 h.

Many pinacol boronic esters form rapidly at 20 °C from pinacol hydrate and the boronic acids, and the reverse process can be very slow only if the equilibrium constant for esterification is very high. Equilibria, including water/ether partitioning, appeared to be the major problem in a series of explorations of the hydrolysis of pinacol (phenylthio)methaneboronate (2b) by aqueous methanol containing aluminum chloride, phosphoric acid, or boric acid and ethanolamine, followed by dilution and extraction, all of which yielded 50–70% of boronic acid (1). Turning to a more sterically hindered and more relevant example, treatment of pinacol 1-(phenylthio)-2-phenylethane-1-boronate (5b) with methanol, boric acid, and ethanolamine followed by water/ether partitioning and crystallization from moist dichloromethane/petroleum ether yielded only 45% of the presumed boronic acid. Boiling 5b a few minutes in 2 M sulfuric acid in 1:1 water/tetramethylene sulfone, conditions vigorous enough to cause pinacol rearrangement, led to 58% of the presumed boronic acid, not enough for a good synthetic process.

Diethanolamine forms stable, crystalline, chelated esters with boronic acids.[21] Treatment of 5b with diethanolamine in 2-propanol/ether resulted in crystallization of analytically pure diethanolamine ester 7 (79–83%). This

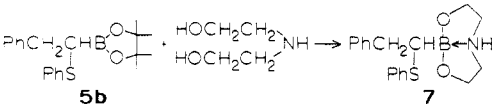

solves the hydrolysis problem in principle, since diethanolamine esters are readily hydrolyzed by cold dilute acid, as was illustrated by the conversion of 2b to the diethanolamine ester (not characterized) to the boronic acid 1 in 70% overall yield. A more recent related example of diethanolamine ester hydrolysis has been reported.[22]

For oxidation of 5 to aldehyde equivalents, it is best to bypass the hydrolysis problem by using the facile reaction of 5 with N-chlorosuccinimide in methanol buffered with triethylamine, which yields monothioacetals or acetals.[19]

Several attempts to oxidize dialkylated (phenylthio)methaneboronic esters 6 to ketones have failed. For example, 6c was not attacked by sodium perborate[5] or hydrogen peroxide and sodium acetate[23] at 25 °C, and refluxing overnight with alkaline sodium perborate resulted mainly in protodeboronation to 5-(phenylthio)nonane ac-

(21) Letsinger, R. L.; Skoog, I. J. Am. Chem. Soc. 1955, 77, 2491–2494.
(22) Matteson, D. S.; Ray, R. J. Am. Chem. Soc. 1980, 102, 7590–7591.
(23) Yamamoto, S.; Shiono, M.; Mukaiyama, T. Chem. Lett. 1973, 961–962.

cording to NMR evidence. *N*-Chlorosuccinimide in methanol[19] failed to attack **6d** even after extended reflux.

α-Phenylthio Ketones from Esters. By analogy to the acylation of carbanions from 1,1-diboronic esters with carboxylic esters to form ketones,[2] it was anticipated that acylation of the carbanions from 1-(phenylthio)alkane-1-boronic esters **2b**, **4**, and **5** with carboxylic esters would

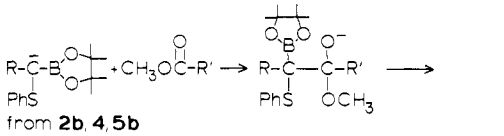

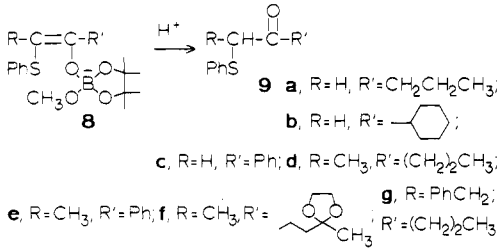

proceed by way of a postulated enol borate intermediate (**8**) to provide an efficient regiospecific synthesis of α-phenylthio ketones **9**, which are known to be useful synthetic intermediates.[24] These reactions worked very well, as shown in Table IV. Analogous acylation of **3** with succinic anhydride yielded the γ-keto acid **10**, and lithiated **5a** with γ-butyrolactone formed the γ-hydroxy ketone **11**.

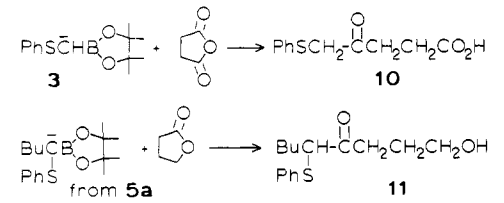

Enethiol Ethers from Aldehydes and Ketones. Again by analogy to 1,1-diboronic ester chemistry,[2] it was expected that the carbanions derived from **2b**, **4**, and **5** would undergo Wittig type condensation with aldehydes and ketones, with elimination of boron to form enethiol ethers **12**. These reactions were also successful, as shown

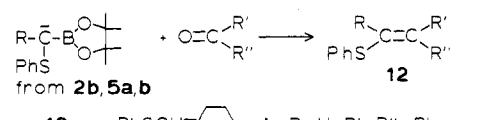

12a = PhSCH= ; **b**, R = H, R' = R'' = Ph;

c, R = H, R', R'' = Ph, $(CH_2)_2CH_3$; **d**, R = $CH_3(CH_2)_3$, R', R'' = H, $(CH_2)_5CH_3$; **e**, R = $CH_3(CH_2)_3$, R', R'' = H, ; **12f** =

in Table V. On the basis of NMR spectra, it appeared that mixtures of *Z* and *E* isomers were obtained where possible. The reaction of lithiated **4** with methyl levulinate showed the expected preference for carbanion attack at the ketone group but provided a minor surprise in the total hydrolysis of the methyl ester. Perhaps an intermediate lactone (**13**) is formed, which undergoes elimination to form the salt of the isolated carboxylic acid (**14**). The major isomer of **14** crystallized, leaving an apparent mixture of isomers in the mother liquor.

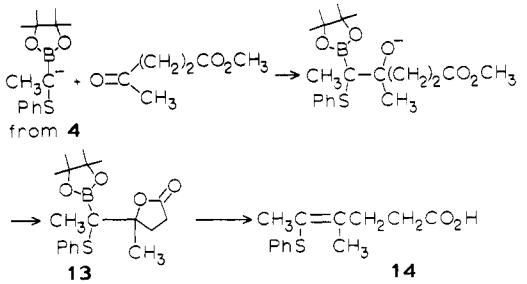

Epoxide Openings. Reaction of **3** or lithiated **5a** with

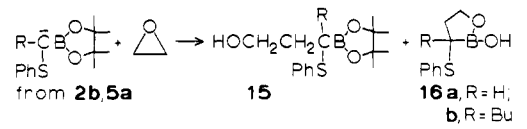

ethylene oxide occurred readily enough, but product isolation was complicated by partial hydrolysis of the initially formed pinacol boronic ester (**15**) to form a cyclic boronic half ester (**16**), which was the product isolated in each case. The investigation was not pursued to find a way to control the reaction to produce either pure **15** or pure **16**. However, reaction of **3** with cyclohexene oxide produced a single product (**17**), in which the hydroxyl group is not in a position to cyclize to the boronic ester group.

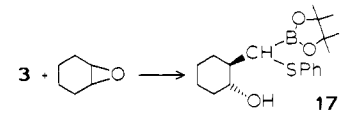

Bromination. Isolation of the lithium salt **3** and bromination at −78 °C in ether yielded pinacol bromo(phenylthio)methaneboronate (**18**), which could be purified on a small scale by molecular distillation. Treatment of crude **18** with phenylmagnesium bromide was expected to yield a *B*-phenyl borate complex (**19a**), which would rearrange to pinacol (phenylthio)phenylmethaneboronate (**20**) if it followed well-established precedent.[26,27] However, the yield of **20** was only 57% of impure material. A major byproduct based on NMR evidence was the cleavage product, pinacol phenylboronate (**21a**) (35%). When **18** was treated with butyllithium or cyclohexylmagnesium bromide, no alkyl migration product analogous to **20** could be detected, only the cleavage product **21b** or **21c** mixed with unidentified byproducts. Thus, the hope of establishing a synthetic route to 1-(phenylthio)alkane-1-boronic esters **5** not accessible by alkylation of **3** was not realized. However, an indirect route to this goal involving some analogous chemistry has been found more recently.[28]

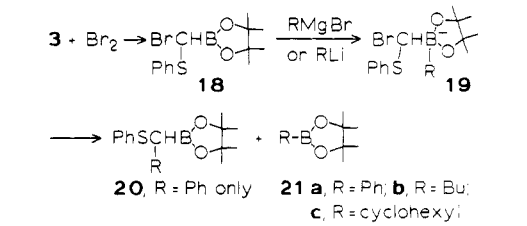

(24) Trost, B. M.; Salzmann, T. N.; Hiroi, K. *J. Am. Chem. Soc.* **1976**, *98*, 4887–4902.

(25) (a) Kenney, W. J.; Walsh, J. A.; Davenport, D. A. *J. Am. Chem. Soc.* **1961**, *83*, 4019–4022. (b) Delisle, A. *Ber. Dtsch. Chem. Ges.* **1889**, *22*, 306–309.

(26) Matteson, D. S.; Mah, R. W. H. *J. Am. Chem. Soc.* **1963**, *85*, 2599–2603.

(27) Brown, H. C.; De Lue, N. R.; Yamamoto, Y.; Maruyama, K.; Kasahara, T.; Murahashi, S.; Sonoda, A. *J. Org. Chem.* **1977**, *42*, 4088–4092.

(28) Matteson, D. S.; Majumdar, D. *J. Am. Chem. Soc.* **1980**, *102*, 7588–7590.

Table IV. Acylation of Lithiated Pinacol 1-(Phenylthio)alkane-1-boronates, $RCLi(SPh)BO_2C_2Me_4$, by Esters or an Anhydride To Yield α-Phenylthio Ketones, $RCH(SPh)COR'$, 9, 10, and 11

boronic ester	R	acylating agent $R'CO_2CH_3$ or other	product[a]	yield, %
2b	H	$CH_3(CH_2)_2CO_2CH_3$[b]	9a	82
2b	H	c-$C_6H_{11}CO_2CH_3$	9b	80
2b	H	$PhCO_2CH_3$[c]	9c[d]	75
2b	H	succinic anhydride	10[e]	74
4	CH_3	$CH_3(CH_2)_2CO_2CH_3$[f]	9d	81
4	CH_3	$PhCO_2CH_3$	9e	86
4	CH_3	$CH_3C(O_2C_2H_4)(CH_2)_2CO_2CH_3$[g]	9f[h]	66
5a	n-Bu	butyrolactone[i]	11	50
5b	$PhCH_2$	$CH_3(CH_2)_2CO_2CH_3$	9g[j]	82

[a] Isolated by preparative TLC as analytically pure oils, except as noted. [b] Added dropwise over 30 min period at 35 °C. [c] Reacted with isolated 3. [d] From aqueous ethanol, mp 53–54 °C (lit.[25] mp 53–54 °C). [e] From ether, mp 78–79 °C. [f] Added at −78 °C. Addition at 0 °C yielded only 63%. [g] Impurity present by NMR, may have lowered yield of 9f. [h] Omitted washing with acid in order to preserve ketal. [i] Added dropwise at 40 °C, probably not optimum conditions. [j] Distilled, bp 161–163 °C (0.2 torr).

Table V. Wittig Condensation of Pinacol 1-Lithio-1-(phenylthio)alkane-1-boronates, $RCLi(SPh)BO_2C_2Me_4$, with Aldehydes or Ketones, $R'COR''$, To Yield Enethiol Ethers, $R'R''C{=}C(SPh)R$, 12 and 14

boronic ester	R	aldehyde or ketone	product	bp, °C (torr)	yield, %
2b	H	cyclohexanone	12a	110 (0.2)[a]	71
2b	H	PhCOPh	12b	cryst[b]	71
2b	H	$PhCOCH_2CH_2CH_3$	12c[c]	130 (0.1)	82
5a	n-Bu	$CH_3(CH_2)_5CHO$[d]	12d[c]	116 (0.1)	86
5a	n-Bu	c-$C_6H_{11}CHO$	12e[c]	136–139 (0.1)	84
4	CH_3	$CH_3COCH_2CH_2CO_2CH_3$	14[e]	cryst[e]	61
5b	$PhCH_2$	cyclopentanone	12f	156–158 (0.25)	81

[a] Lit.[15] bp 133 °C (1.1 torr). [b] From aqueous ethanol, mp 68–70 °C (lit.[10] mp 71 °C). [c] Mixture of E and Z isomers. [d] A 20% excess was used. [e] Note that the product is a free carboxylic acid. One isomer crystallized first from ether/petroleum ether, mp 83–85 °C. The second crop was a mixture of geometric isomers.

An α-Iodo Boronic Ester. 1-(Phenylthio)alkanes are readily converted to 1-iodoalkanes by methyl iodide and sodium iodide in dimethylformamide.[11] When pinacol 1-(phenylthio)-2-phenylethane-1-boronate (**5b**) was subjected to the reported conditions, a low yield of pinacol 1-iodo-2-phenylethane-1-boronate (**22**) was obtained together with the 2-phenyletheneboronate (**23**). Reducing the temperature to 25 °C and extending the time to 3 days yielded mainly **22**, though analytical purity was not achieved. The structure of **22** was proved by replacement of the halide with phenylmagnesium bromide[26] followed by oxidation of the resulting pinacol 1,2-diphenylethaneboronate with sodium perborate[5] to yield 1,2-diphenylethanol.

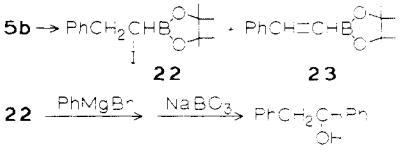

Previous syntheses of α-halo boronic esters had been laborious[29] or restricted to α-branched carbon chains and other special structural types.[30] The method described here has been extended to provide the most convenient synthesis of iodomethaneboronic esters known to date.[31] However, for other general purposes this approach has been superseded by the recently developed homologation of boronic esters with dichloromethyllithium to yield α-chloro boronic esters.[22,28]

Discussion

Our results show that pinacol (phenylthio)methaneboronate (**2b**) by way of its lithio derivative (**3**) can furnish a highly versatile connecting carbon for synthetic purposes. It is possible to classify **3** as a formyl anion equivalent, but **3** can also function as a Wittig reagent and, in the reaction with esters, as a new type of reagent entirely, a self-protecting source of $PhSCH_2^-$ for converting RCO_2CH_3 to $RCOCH_2SPh$ without further reaction of the ketone. Since **3** can be alkylated and the resulting 1-(phenylthio)alkane-1-boronic esters **5** can be lithiated and undergo a similar range of reactions, convergent syntheses can be designed in which two major fragments are ultimately joined to the central carbon provided by **3**.

Alkylation of **3** provides an efficient conversion of R–X to R–CHO by way of the monothioacetal $R–CH(SPh)OCH_3$ or acetal $R–CH(OCH_3)_2$.[19] There are a number of other good routes from R–X to R–CHO, including the well-known use of dithiane[12] and the use of a methanediboronic ester.[2] The route most closely related to that based on **3**, and perhaps the most competitive from the standpoint of efficiency and convenience, is that based on alkylation of lithiated $PhSCH_2SiMe_3$.[32] The use of **3** to convert R–X to $R–CH(SPh)OCH_3$ takes on added interest in view of the recent report that monothioacetals can be reduced to α-lithioalkyl methyl ethers, $R–CHLiOCH_3$.[33] A simpler alternative, described explicitly only in the case of alkylation by an allylic halide, might be the use of lithiated $PhSCH_2OCH_3$ to provide the monothioacetal directly.[16] The most useful application of the alkylation of **3** is likely to be to provide 1-(phenylthio)alkane-1-boronic esters **5** as synthetic intermediates for further carbon–carbon connections. Although this route to **5** is restricted to primary alkyl halides R–X, the general availa-

(29) Matteson, D. S.; Jesthi, P. K. *J. Organomet. Chem.* **1976**, *114*, 1–7.
(30) (a) Matteson, D. S. *Intra-Sci. Chem. Rep.* **1973**, *7*, 147–143. (b) Matteson, D. S. *Acc. Chem. Res.* **1970**, *3*, 186–193. (c) Brown, H. C.; De Lue, N. R.; Yamamoto, Y.; Maruyama, K. *J. Org. Chem.* **1977**, *42*, 3252–3254.
(31) Matteson, D. S.; Majumdar, D. *J. Organomet. Chem.* **1979**, *170*, 259–264.
(32) Kocienski, P. J. *Tetrahedron Lett.* **1980**, *21*, 1559–1562.
(33) Cohen, T.; Matz, J. R. *J. Am. Chem. Soc.* **1980**, *102*, 6900–6902.

bility of α-chloro boronic esters R–CHCl–$B(OR')_2$ by homologation of R–$B(OR')_2$ has made it possible to synthesize analogues of **5** containing branched alkyl groups R.[28]

The unique and most promising feature of α-phenylthio boronic ester chemistry is the condensation of **3** or lithiated **5** with carboxylic esters to yield α-phenylthio ketones **9**. The synthetic utility of this class of compounds has been demonstrated by Trost and co-workers.[24] However, the usual preparative route involves treatment of an enolate with diphenyl disulfide[24] and is therefore not regiospecific for unsymmetrical ketones. Our new route to **9** is regiospecific by nature and assembles the carbon skeleton in the same operation.

The boronic ester group provides vital activation and protection during the synthesis of **9**, even though it is lost in the process. It appears that the normal mode of reaction of (phenylthio)methyllithium, $PhSCH_2Li$, with carboxylic esters, R–CO_2CH_3, is double addition to form the carbinol, R–$C(OH)(CH_2SPh)_2$.[34] If the carboxyl group is sterically hindered, as in $(CH_3)_3CCO_2CH_3$ or poly(methyl methacrylate), it is possible to obtain the alkyl (phenylthio)methyl ketone, R–$COCH_2SPh$, in good yield at the cost of consuming two mols of the lithium reagent, the intermediate which protects the ketone being R–COCHLiSPh.[35] The α-phenylthio ketone has also been obtained from the reaction of lithiated isobutyl phenyl sulfide with methyl benzoate, though not in good yield.[18] Lithiation of higher homologues of $PhSCH_3$ requires special conditions,[18] and it is not clear from the published report whether this lithiation will work with any alkyl groups other than isobutyl or 2-methylalkyl. Thus, the general access to alkyl groups provided by deprotonation of **5** is significant, as is the comsumption of only 1 mol of **5** in the reaction to produce **9**.

As in the analogous reactions of propanediol lithiomethanediboronate with carboxylic esters,[2] we postulate that reactions of **3** or lithiated **5** with esters stop at the ketone stage because of rapid rearrangement of the initial adducts to stable boron enolates (**8**). Although the existence of **8** has not been proved and a few attempts to trap such an intermediate by alkylation have been inconclusive, **8** should be thermodynamically stable. Boron–oxygen bonds are 30–40 kcal/mol stronger than boron–carbon bonds if the boron is tricoordinate,[36] and on the basis of measured pK values,[37] coordination to methoxide will have a negligible effect. The exothermicity will be slightly diminished as a result of converting a keto structure B—C—C=O to an enol C=C—O—B. Intramolecular 1,3-suprafacial shift of boron is symmetry forbidden by the Woodward–Hoffmann rules if the boron is kept firmly tetracoordinate by the basicity of the ligands, but expulsion of alkoxide to provide a vacant orbital voids the symmetry restriction, and it seems likely that this or some other mechanism for formation of **8** will have a low activation energy.

The use of **3** or lithiated **5** as α-substituted Wittig reagents in condensations with aldehydes or ketones to produce enethiol ethers **12** also has considerable synthetic potential. Enethiol ethers can be unmasked to aldehydes or ketones, though the conditions are somewhat vigorous.[38] Allylic oxidation of enethiol ethers is a useful synthetic operation.[39] A prostaglandin synthesis utilizes enethiol ethers prepared by means of the Wittig reagent $PhSCH{=}PPh_3$.[40]

Our results suggest that α-phenylthio boronic esters may be the best reagents yet found for the Wittig route to enethiol ethers, but there are alternatives to consider. Yields from $PhSCHLiSiMe_3$,[15] $PhSCH{=}PPh_3$, or $BuSCH{=}PPh_3$[41] appear to average somewhat lower than ours, and $RSC(CH_3){=}PPh_3$[41] is definitely inferior to lithiated **5**. Unprotected hydroxyl groups in sugars are tolerated by $PhSCH{=}PPh_3$,[42] a feature which our reagents cannot match. The phosphonate $CH_3SCHLiPO(OEt)_2$ can also undergo Wittig reactions but shows a tendency to promote aldol condensations.[17]

The reaction of ethylene oxide with **3** or **5a** appeared to proceed in high yield, but the mixture of **15** and **16** produced is a nuisance from a synthetic point of view. Presumably, this reaction could be adjusted to provide a single product if there were sufficient incentive. However, the silicon analogue of **3**, $PhSCHLiSiMe_3$, already gives high yields of pure products with epoxides.[32]

The use of an α-phenylthio boronic ester **5** as a source of RCHLiSPh by deboronation has been reported elsewhere.[4a] The temperature required was high enough to require immediate trapping of the anion, which was efficiently accomplished with methyl iodide, but further investigation did not seem warranted.

Other possible applications of α-(phenylthio)alkaneboronic ester chemistry remain to be explored. The inertness of the dialkylated series **6** discouraged us from trying to develop a ketone synthesis based on these compounds. However, new opportunities to make **6** may arise as a consequence of other recent synthetic developments,[22,28] and possibilities remain for oxidative or reductive cleavage of either the boron or the sulfur. Conjugate addition of **3** to α,β-unsaturated ketones and esters and conversion of **5** to α-phenylthio aldehydes have been accomplished recently and will be reported elsewhere.[43]

It may be concluded that α-phenylthio boronic esters are easily prepared and handled, that they are capable of undergoing some unique transformations, and that they are highly promising reagents for organic synthesis.

Experimental Section

General. Reactions were run under argon or nitrogen. Tetrahydrofuran (THF) and diethyl ether (ether) were distilled from sodium benzophenone ketyl. Other anhydrous solvents and reagents were distilled from calcium hydride. Butyllithium was 2 M in hexane, checked by titration with isopropyl alcohol with 1,10-phenanthroline as indicator.[44] Proton NMR spectra were recorded at 60 MHz with a Varian EM-360 instrument and are referred to internal tetramethylsilane.[45] Infrared spectra were recorded with a Beckman IR-5 or IR-18A. Glassware was dried at 130 °C for 1 h and flushed with argon during assembly. Extensive use was made of "Airless Ware" Schlenk type glassware from Kontes Glass Corp. Syringes and needles were used to transfer liquids. Elemental analyses were by Galbraith Laboratories, Knoxville, TN.

(34) Sowerby, R. L.; Coates, R. M. *J. Am. Chem. Soc.* **1972**, *94*, 4758–4759.
(35) Bourguignon, J. J.; Galin, J. C. *Macromolecules* **1977**, *10*, 804–813.
(36) Finch, A.; Gardner, P. J. "Progress in Boron Chemistry"; Brotherton, R. J.; Steinberg, H., Eds.; Pergamon Press: Oxford, 1970; Vol. 3, pp 177–210.
(37) Matteson, D. S.; Allies, P. G. *J. Organomet. Chem.* **1973**, *54*, 35–50.
(38) Mura, A. J., Jr.; Majetich, G.; Grieco, P. A.; Cohen, T. *Tetrahedron Lett.* **1975**, 4437–4440.
(39) Trost, B. M.; Tanigawa, Y. *J. Am. Chem. Soc.* **1979**, *101*, 4413–4416.
(40) Vlattas, I.; Lee, A. O. *Tetrahedron Lett.* **1974**, 4451–4454.
(41) Mukaiyama, T.; Fukuyama, S.; Kumamoto, T. *Tetrahedron Lett.* **1969**, 3787–3790.
(42) Bestmann, H. J.; Angerer, J. *Tetrahedron Lett.* **1969**, 3665–3666.
(43) Ray, R.; Matteson, D. S., manuscript in preparation.
(44) Watson, S. C.; Eastham, J. F. *J. Organomet. Chem.* **1967**, *9*, 165–168.
(45) Recent recalibration of this instrument has indicated that all δ values were 2.7% too large (δ 0.2 at δ 7.5) at the time these measurements were made. A few spectra taken on a JEOL MH-100 also have yielded slightly smaller δ values than those tabulated.

Table VI. Physical Properties of Pinacol 1-(Phenylthio)alkane-1-boronates 4 and 5 from Alkylation of Pinacol (Phenylthio)methaneboronate (2b)

		NMR ($CDCl_3$),[a] δ				C		H		B		S	
compd	bp, °C (torr)	SCHB	R	CCH_3	C_6H_5S	calcd	found	calcd	found	calcd	found	calcd	found
4	125-127 (0.7)	2.99 q	1.36 d	1.20	7.50	63.65	63.41	8.01	8.09	4.09	3.95	12.14	12.05
5a	115-120 (0.1)	2.80 t	0.9 m, 1.5 m	1.21	7.42	66.67	66.74	8.89	8.97	3.53	3.45	10.47	10.42
5b	140-145 (0.05)	3.10 s	3.10 s, 7.35	1.14	7.35	70.59	70.72	7.41	7.42	3.18	3.08	9.42	9.57
5c	160-165 (0.3)	2.82 t	0.91 s (*t*-Bu), 0.6-1.9 m	1.23	7.47	70.20	70.44	9.91	10.01	2.87	2.85	8.52	8.49
5d	146-150 (0.1)	3.05 t	2.26 m, 4.16 t, 6.8-7.7 m	1.21	6.8-7.7	68.11	68.24	7.35	7.25	2.92	2.85	8.66	8.77
5e	115-117 (0.2)	2.63 d	1.1 obscured	1.17	7.3	not purified							

[a] Correct integrals were obtained (except for 5e). The pinacol CCH_3 appeared as a singlet and the C_6H_5S as a multiplet.

(Phenylthio)methaneboronic Acid (1). (Phenylthio)methyllithium was prepared by a modification of the published procedure[10] from thioanisole (1 mol) and 1,2-bis(dimethylamino)ethane (TMEDA) (1 mol) in THF (700 mL) treated with butyllithium (1 mol) at or below 20 °C and kept 1 h at 20 °C. The solution was cooled with a −78 °C bath and stirred during the dropwise addition of trimethyl borate (1.3 mol) over a period of 1 h. Stirring was continued overnight as the mixture warmed to 20 °C. The mixture was partially concentrated under vacuum, and the residue was treated with 130 mL of 85% phosphoric acid and 100 g of ice and the mixture then extracted with ether (3 × 300 mL). The organic phase was washed with water and concentrated under vacuum. The residue was recrystallized from moist ether/petroleum ether to yield 77–94% of 1 in two crops, mp 109–110 °C. Excessive drying of 1 should be avoided.[46] NMR (CD_3SOCD_3): δ 2.25 (s, 2, SCH_2B), 3.5 (s, 15 Hz wide at half height, 2, OH), 7.34 (m, 5, C_6H_5). Anal. Calcd for $C_7H_9BO_2S$: C, 50.04; H, 5.40; B, 6.43; S, 19.08. Found: C, 49.95; H, 5.52; B, 6.40; S, 18.99.

Ethylene Glycol (Phenylthio)methaneboronate (2a). Equimolar amounts of ethylene glycol and 1 were heated in benzene to distil the benzene–water azeotrope, the solution was concentrated, and the residue was crystallized from ether/petroleum ether, yielding 85% of 2, mp 65–66.5 °C. NMR ($CDCl_3$): δ 2.51 (s, 2, SCH_2B), 4.25 (s, 4, OCH_2), 7.26 (m, 5, C_6H_5). Anal. Calcd for $C_9H_{11}BO_2S$: C, 55.70; H, 5.71; B, 5.57; S, 16.52. Found: C, 55.70; H, 5.91; B, 5.70; S, 16.70.

Pinacol (Phenylthio)methaneboronate (2b). Pinacol or pinacol hydrate (1 mol) and 1 (1 mol) were stirred in ether (1 L) until the solids dissolved and two liquid phases remained. The phases were separated, the ether phase was washed with a little water and dried over magnesium sulfate, and **2b** was distilled: bp 105–108 °C (0.1 torr); 89–97%. **2b** may be kept indefinitely as a liquid, but cooling a pure sample to −78 °C and scratching induced crystallization; mp 33–36 °C. NMR ($CDCl_3$): δ 1.17 (s, 12, CCH_3), 2.38 (s, 2, SCH_2B), 7.30 (m, 5, C_6H_5). Anal. Calcd for $C_{13}H_{19}BO_2S$: C, 62.42; H, 7.66; B, 4.32; S, 12.82. Found: C, 62.65; H, 7.82; B, 4.14; S, 12.62.

2,2-Dimethyl-1,3-propanediol (Phenylthio)methaneboronate (2c). The azeotrope was distilled from an equimolar mixture of 2,2-dimethyl-1,3-propanediol and 1 in toluene, and **2c** was distilled: bp 108–112 °C (0.3 torr); 87%. NMR ($CDCl_3$): δ 0.90 (s, 6, CCH_3), 2.36 (s, 2, SCH_2B), 3.64 (s, 4, OCH_2), 7.13–7.65 (m, 5, C_6H_5). Anal. Calcd for $C_{12}H_{17}BO_2S$: C, 61.04; H, 7.26; B, 4.58; S, 13.58. Found: C, 60.88; H, 7.36; B, 4.62; S, 13.34.

Dimethyl (Phenylthio)methaneboronate (2d). A 10% solution of 1 in 2,2-dimethoxypropane was distilled slowly to remove the esterification byproducts, acetone, and methanol, and **2d** was distilled: bp 85–88 °C (0.5 torr); 88%. NMR ($CDCl_3$): δ 2.37 (s, 2, SCH_2B), 3.62 (s, 6, OCH_3), 7.15–7.8 (m, 5, C_6H_5). Anal. Calcd for $C_9H_{13}BO_2S$: C, 55.13; H, 6.68; B, 5.51; S, 16.35. Found: C, 55.30; H, 6.77; B, 5.51; S, 16.45.

Pinacol Lithio(phenylthio)methaneboronate (3). Butyllithium (15 mmol) in hexane was added dropwise to diisopropylamine (15.7 mmol) in THF (5 mL) stirred at 0 °C in a 100-mL Schlenk flask. A solution of pinacol (phenylthio)methaneboronate (**2b**) (15 mmol) in THF (5 mL) was added rapidly dropwise, yielding a white precipitate. Ether (10 mL) and light petroleum ether (10 mL) were added to complete precipitation. After 1 h of stirring at 0 °C, the mixture was cooled with a −78 °C bath and filtered. The collected **3** was washed with chilled (0 °C) ether and dried under vacuum (0.1 torr) 4 h at 25 °C, yield 80–85% as the complex with 1 mol of THF. Rigorous exclusion of air was maintained in all operations with **3**. NMR (pyridine-d_5): δ 1.20 (s, 12, CCH_3), 1.7 (m, 4, OCH_2CH_2), 2.18 (s, 1, SCHB), 3.8 (m, 4, OCH_2CH_2), 7.55 (m, 5, C_6H_5). Anal. Calcd for $C_{17}H_{26}BLiO_3S$: C, 62.21; H, 7.98; B, 3.29; Li, 2.11; S, 9.77. Found: C, 62.34; H, 7.89; B, 3.26; Li, 2.09; S, 9.62.

Alkylation of Pinacol (Phenylthio)methaneboronate (2b). Method A. A solution of 5 mmol of diisopropylamine and 12 mmol of TMEDA in 50 mL of THF was treated with 5 mmol of butyllithium at 0 °C followed by 5 mmol of **2b**. After 1 h at 0 °C the mixture was treated with 5 mmol of the selected alkyl halide and stirred at 20 °C 6–16 h. The mixture was treated with excess cold 10% phosphoric acid, and the product (**4** or **5**) was extracted with ether and distilled. Yields are listed in Table II. Physical properties are summarized in Table VI. **Method B.** Pinacol lithio(phenylthio)methaneboronate (**3**) was isolated as described in the preceding paragraph and transferred under argon to a reaction vessel with the aid of THF (2–5 mL/mmol of **3**). The slurry was stirred at 0 °C, 1 equiv of alkyl halide was added, and stirring was continued 2–12 h at 20–25 °C. Excess cold 10% phosphoric acid was added, and the product (**4** or **5**) was extracted with ether and distilled. Yields are summarized in Table II and physical properties in Table VI.

Deprotonation of Pinacol 1-(Phenylthio)alkane-1-boronates 4, 5, and 2b. Butyllithium (5 mmol) was added to diisopropylamine (5 mmol) in THF (20–25 mL) with stirring at 0 °C. The selected pinacol 1-(phenylthio)alkane-1-boronate (**4**, **5**, or **2b**) (5 mmol) was injected from a syringe, either through a wide-bore needle or with the aid of a few milliliters of THF to reduce the viscosity. The mixture was stirred at least 2 h at 0 °C before use. Longer times up to 20 h gave the same results. Shorter times were not tried, except that **2b** yields **3** rapidly.

Alkylation of Deprotonated 4 and 5 to Pinacol α-(Phenylthio)alkaneboronates (6). Deprotonation of **4** or **5** was carried out as described in the preceding paragraph. The selected alkyl halide (5 mmol) was added and the mixture was kept 2–4 h at room temperature. Aqueous 10% phosphoric acid was then added and the product (**6**) was extracted with ether and distilled. Yields and boiling points are recorded in Table III and proton NMR and analytical data in Table VII.

Acylation–Deboronation of Deprotonated 2b, 4, and 5 to α-Phenylthio Ketones 9, 10, and 11. Deprotonation of **2b**, **4**, or **5** was carried out in the usual manner (1-mmol scale) and 0.8 equiv of the selected methyl ester, anhydride, or lactone was injected at 0 °C. After 6–16 h at room temperature, the mixture was concentrated under vacuum. The residue was dissolved in pentane and washed with 3 M sodium hydroxide (30 mL for 1-mmol scale), 10% phosphoric acid (30 mL), and water (30 mL). The product (**9**, **11**) was purified by chromatography on a silica gel plate with pentane/ether (20:1 or 10:1) as solvent. Yields are listed in Table IV, where some exceptions to the general procedure are also noted. The acid **10** was isolated by extraction from ether into aqueous sodium bicarbonate, which on acidification pre-

(46) Boronic acids may become air sensitive if dried to the point of boronic anhydride formation but are stable on storage if moist. Commercial samples of butaneboronic acid and others usually contain some water as a preservative.

Table VII. Proton NMR and Analytical Data for Pinacol α-(Phenylthio)alkaneboronates (6) Derived from Pinacol (Phenylthio)methaneboronate (2b) by Two Alkylations

	NMR ($CDCl_3$),[a] δ				C		H		B		S	
compd	R	R′	CCH_3	C_6H_5S	calcd	found	calcd	found	calcd	found	calcd	found
6a	CH_3 1.2 s[b]	1.23,[b] 1.5, 3.87 s	1.18	7.2-7.8	64.28	64.04	8.48	8.30	2.76	2.78	8.17	8.29
6b	Bu 0.9, 1.5 m	CH_3 1.24 s	1.19	7.3-7.7	67.50	67.46	9.13	9.10	3.38	3.47	10.01	10.26
6c	Bu 0.9, 1.5 m	Bu 0.9, 1.5 m	1.20	7.3-7.7	69.60	69.81	9.74	9.67	2.98	2.77	8.85	8.91
6d	Bu 0.9, 1.5 m	2.93 d, 3.11 d, 7.4[c]	1.16	7.3-7.7	73.85	73.74	6.97	7.17	2.77	2.54	8.21	7.96
6e	CH_3 1.17 s	2.86 d, 3.31 d, 7.4[c]	1.21, 1.23	7.3-7.9	71.19	71.38	7.68	7.78	3.05	3.35	9.05	8.85

[a] Correct integrals were obtained. Pinacol CCH_3 was a singlet, except that **6e** showed two closely spaced singlets. PhS appeared as a multiplet. [b] R′ is $CH_3C(O_2C_2H_4)(CH_2)_3$. One CH_3 appears at δ 1.23 on the side of the pinacol CCH_3; the other is obscured. [c] R′ is benzyl. The CH_2 appears as an AB pattern, J = 14 Hz and the C_6H_5 as a single peak in the midst of the PhS multiplet.

Table VIII. Proton NMR and Analytical Data for α-Phenylthio Ketones, RCH(SPh)COR′, 9, 10, and 11

	NMR ($CDCl_3$),[a] δ				C		H		S	
compd	R	CHSPh[b]	COCH of R′	other R′	calcd	found	calcd	found	calcd	found
9a	H 3.72 s	3.72 s	2.58 t	CH_2 1.65 m, CH_3 0.87 t	68.00	68.26	7.26	7.02	16.50	16.31
9b	H 3.79 s	3.79 s	2.7 m	$(CH_2)_5$ 1.2-1.9 m	71.75	71.61	7.74	7.69	13.68	13.38
9d	CH_3 1.41 d	3.85 q	2.63 t	CH_2 1.6 m, CH_3 0.90 t	69.19	69.40	7.74	7.77	15.39	15.10
9e	CH_3 1.48 d	4.61 q	none	Ph 7.2-7.7, 8.0-8.2 m	74.34	74.14	5.82	5.98	13.23	13.07
9f	CH_3 1.42 d	3.85 m	2.76 m	1.99 m, 3.95 s, 1.32 s[c]	64.26	64.51	7.19	7.36	11.44	11.23
9g[d]	C_6H_5 7.15 s[b] CH_2 3.03 m	3.82 t	2.30 m	CH_2 1.46 m, CH_3 0.80 t	76.01	76.43	7.09	6.92	11.27	11.14
10	H 3.79 s	3.79 s	2.85 m	2.85 m, CO_2H 7.8 s	58.91	59.15	5.39	5.50	14.30	14.33
11	Bu 0.85, 1.5 m	3.65 m	2.67 m	1.85 m, 3.65 m[e]	67.63	68.04	8.32	8.34	12.04	12.22

[a] Satisfactory integrals were obtained. [b] The SC_6H_5 absorption was a single peak near δ 7.4 in all cases, except for **9g**, the spectrum of which was redetermined after the instrument was recalibrated, δ 7.25. [c] Peaks for CH_2, $C(O_2C_2H_4)$, CH_3, respectively. [d] IR: (C=O, 1700 cm^{-1}. [e] Peaks for CH_2, CH_2O, respectively, OH obscured.

Table IX. Proton NMR and Analytical Data for Enethiol Ethers, PhSCR=CR′R″, 12 and 14

	NMR ($CDCl_3$),[a] δ			C		H		S	
compd	R	R′	R″	calcd	found	calcd	found	calcd	found
12c	H 6.36, 6.57[b]	Ph 7.4	CH_2 2.6 m, CH_2 1.4 m, CH_3 0.88 m	80.26	80.07	7.13	7.20	12.60	12.73
12d[c]	Bu 0.9, 1.3 m 2.2 m	H 5.83 m[c]	$(CH_2)_5$ 1.3 m, 2.2 m, CH_3 0.9 m	78.20	78.30	10.21	10.14	11.60	11.56
12e[d]	Bu 0.85, 1.4 m	H 5.78, 5.91 s	$(CH_2)_5$ 1.3-1.7, CH 2.7 m	78.77	78.66	9.55	9.71	11.68	11.53
12f	C_6H_5 7.33 s CH_2 3.63 s	CH_2 1.78, 2.58 m		81.38	81.47	7.19	7.31	11.43	11.23
14	CH_3 2.02 s	CH_3 2.05 s	$(CH_2)_2$ 2.61 s CO_2H 12.0 s	66.07	66.08	6.82	6.83	13.57	13.57

[a] Satisfactory integrals were obtained. The PhS peak appeared as a singlet at δ 7.35-7.45. [b] The two C=CH peaks of approximately equal size imply two geometric isomers. [c] Spectrum taken after recalibration of NMR instrument, PhS at δ 7.17. The C=CH absorption appears as two overlapping triplets 2 Hz apart, perhaps resulting from two geometric isomers in nearly equal amounts.

cipitated some **10**, the remainder being recovered by extraction with ether. Proton NMR and analytical data for the new compounds are listed in Table VIII.

Enethiol Ethers 12 and 14 from Deprotonated Boronic Esters 2b, 4, and 5 and Aldehydes or Ketones. The deprotonation of **2b**, **4**, or **5** was carried out in the usual manner (5-mmol scale). The mixture was cooled to −78 °C before the aldehyde or ketone (4–5 mmol) was injected, then allowed to warm slowly to 20 °C, and stirred 12–16 h. Pentane (50 mL) was added, and the mixture was extracted successively with 3 M sodium hydroxide (50 mL), 10% phosphoric acid (50 mL), and water. The organic phase was concentrated, and the product **12** was distilled or recrystallized. The acidic product **14** was found on acidification of the sodium hydroxide extract, and was purified by way of extraction into sodium bicarbonate. Recrystallization from ether/petroleum ether yielded 26% of **14** and 35% of a second crop containing **14** and its geometric isomer according to NMR analysis. Yields and boiling or melting points are summarized in Table V and proton NMR and analytical data for the new compounds in Table IX. NMR spectra in agreement with the published data were obtained for **12a**[15] and **12b**.[10]

2-Hydroxy-3-(phenylthio)-1,2-oxaborolane (16a). Deprotonation of **2b** (50 mmol) was carried out in the usual manner. The mixture was cooled to −78 °C, and ethylene oxide (57 mmol) was introduced by distillation through a double-ended needle. The mixture was allowed to warm slowly to 20 °C, stirred 16 h, concentrated, and treated with ether and 10% phosphoric acid. Analysis of the ether extract by NMR indicated a mixture of pinacol 3-hydroxy-1-(phenylthio)propane-1-boronate (**15a**) and its hydrolysis product (**16a**), which was refluxed overnight with boric acid (6 g) and sodium borate (6 g) in water (50 mL) in an attempt to complete the hydrolysis. Crystallization from ether/petroleum ether, with repetition of the hydrolysis on the mother liquor to produce a second crop, yielded 39% of **16a**, mp 104–106 °C. NMR ($CDCl_3$): δ 1.98 (m, CCH_2C), 2.35 (m, SCHB), 4.01 (m, CH_2O), 5.3 (br, OH), 7.29 (m, C_6H_5). Anal. Calcd for $C_9H_{11}BO_2S$: C, 55.70; H, 5.71; B, 5.57; S, 16.52. Found: C, 55.68; H, 5.64; B, 5.39; S, 16.73.

3-Butyl-2-methoxy-3-(phenylthio)-1,2-oxaborolane (Methyl Ester of 16b). The procedure used to make **16a** was followed

with **5a** in place of **2b**, up to the point where a mixture of **15b** and **16b** was first obtained. Attempted separation of the pinacol by steam distillation resulted in distillation of all of the product. Chromatography on silica yielded a fraction which appeared to be largely **16b** by NMR analysis. This was converted to the methyl ester of **16b** by treatment with 2,2-dimethoxypropane and distillation: bp 115 °C (0.4 torr); 15%. NMR ($CDCl_3$): δ 0.91 (m, 3, CH_3), 1.1–2.2 (m, 8, CCH_2C), 3.57 (s, 3, OCH_3), 4.2 (m, 2, CH_2O), 7.3–7.8 (m, 5, C_6H_5). Anal. Calcd for $C_{14}H_{21}BO_2S$: C, 63.65; H, 8.01; B, 4.09; S, 12.14. Found: C, 63.73; H, 8.09; B, 3.97; S, 12.13.

Pinacol (*trans*-2-Hydroxycyclohexyl)(phenylthio)methaneboronate (17). The lithium salt **3** (12 mmol) in THF (20 mL) was treated with cyclohexene oxide (12 mmol) at 0 °C and stirred 20 h at 25 °C. The solution was concentrated, water (75 mL) was added, and the product **17** was extracted into ether, washed with water, and isolated by concentration under vacuum as a viscous oil (diastereoisomers probable), 91%, analytically pure. NMR ($CDCl_3$): δ 1.22 (s, 12, CCH_3), 0.9–2.4 (m, 9, $(CH_2)_4CH$), 2.83 (d, 1, SCHB), 3.33 (s, 1, OH), 3.65 (br, 1, CHOH), 7.43 (s, 5, C_6H_5). NMR (CD_3OD): δ 1.20, 1.25 (s, s, 12, CCH_3), 0.9–2.4 (m, 9, $(CH_2)_4CH$), 2.83 (d, 1, SCHB), 3.46 (br, 1, CHOD), 5.3 (s, CD_3OH), 7–7.4 (m, 5, C_6H_5). Anal. Calcd for $C_{19}H_{29}BO_3S$: C, 65.52; H, 8.39; B, 3.10; S, 9.21. Found: C, 65.66; H, 8.15; B, 3.17; S, 9.48. Further evidence in support of structure **17** was obtained by *N*-chlorosuccinimide oxidation in methanol[19] to the dimethyl ketal, which was converted to *trans*-2-hydroxycyclohexanecarboxaldehyde 2,4-dinitrophenylhydrazone, which was characterized only by 100-MHz proton NMR (CD_3SOCD_3 + CD_3OD): δ 1.3 (m, 6, $(CH_2)_3$), 1.8 (m, 3, CHCOH), 3.43 (unresolved m, 25–30 Hz wide at a half-height, 1, CHOD), 3.9 (CD_3OH), 7.92, 8.36, 8.91 (m, 1 each, $C_6H_3(NO_2)_2$), 8.02 (d, J = 5 Hz, 1, N=CHCH). The broad CHOH absorption of **17** and the derived 2,4-DNP is characteristic of trans-2-substituted cyclohexanols.[47]

Pinacol Bromo(phenylthio)methaneboronate (18). The lithiated boronic ester **3** was isolated (12 mmol), and a suspension in ether (60 mL) was stirred at −78 °C during the dropwise addition of just enough bromine (10.3 mmol) to produce a persistent yellow color. The mixture was warmed to 20 °C and concentrated under vacuum. The residue was taken up in 25 mL of petroleum ether, and the precipitated lithium bromide was filtered. Concentration under vacuum yielded a residue of **18**. A small sample was purified by molecular distillation at 140–170 °C (0.1–0.5 torr). NMR ($CDCl_3$): δ 1.25 (s, 12, CCH_3), 5.03 (s, 1, SCHBrB), 7.47 (m, 5, C_6H_5). Anal. Calcd for $C_{13}H_{18}BBrO_2S$: C, 47.45; H, 5.51; B, 3.29; Br, 24.28; S, 9.74. Found: C, 47.61; H, 5.49; B, 3.41; Br, 24.03; S, 9.60.

Pinacol Phenyl(phenylthio)methaneboronate (20). The bromination of **3** was carried out as described in the preceding paragraph, and with the mixture still at −78 °C, an equivalent amount of phenylmagnesium bromide was added. After 16 h at 20 °C, the mixture was concentrated and worked up with 10% phosphoric acid and ether. Distillation yielded pinacol phenylboronate (**21a**), bp 90–110 °C (0.25 torr), 33% identified by NMR, and pinacol phenyl(phenylthio)methaneboronate (**20**), bp 145–150 °C (0.2 torr), 57%. NMR ($CDCl_3$): δ 1.26 (s, 12, CCH_3), 4.06 (s, 1, PhCH(SPh)B), 7.36 (m, 10, C_6H_5). Anal. $C_{19}H_{23}BO_2S$: C, 69.95: H, 7.11; B, 3.31% S, 9.83. Found: C, 69.45; H, 7.13; B, 3.09; S, 11.71.

Pinacol 1-Iodo-2-phenylethane-1-boronate (22). A solution of 3.40 g (10 mmol) of **5b**, 2 g of sodium iodide, and 7 mL of methyl iodide in 25 mL of dimethyl formamide was kept in the dark at 20–25 °C for 66 h. Ether (100 mL) and pentane (100 mL) were added, and the mixture was washed with water (3 × 100 mL). Distillation yielded 84% of **22**, not analytically pure even after redistribution, bp 98–99 °C (0.05 torr). 100-MHz NMR ($CDCl_3$): δ 1.20 (s, 12, CCH_3), 3.24 (m, 3, CH_2CH), 7.24 (s, 5, C_6H_5). Anal. Calcd for $C_{14}H_{20}BIO_2$: C, 46.97; H, 5.63; B, 3.02; I, 35.45. Found: C, 49.83; H, 5.76; B, 2.78; I, 33.22. Although the presence of pinacol 2-phenylethene-1-boronate (**23**) was not evident in the NMR spectrum, when the reaction of **5b** with methyl iodide was carried out with heating according to the model procedure,[11] the major product was **23** as indicated by the characteristic vinylic proton doublet near δ 5.6.[2,7c]

1,2-Diphenylethanol. Treatment of **22** in THF at −78 °C with 1 equiv of phenylmagnesium bromide was followed by standing at 20 °C overnight, workup with acid and ether, and oxidation with alkaline sodium perborate 2 days at 20 °C, which yielded the theoretical amount of 1,2-diphenylethanol. The NMR spectrum was identical with that of an authentic sample prepared from benzaldehyde and phenylmagnesium bromide, except that the crude sample contained about 3% pinacol. Recrystallization from ethanol/water yielded 52%.

Diethanolamine 2-Phenyl-1-(phenylthio)ethane-1-boronate (7). A solution of 2.5 mmol of the pinacol ester **5b** in 10 mL of ether was mixed with a solution of 2.7 mmol of diethanolamine in 5 mL of 2-propanol at 20 °C. After 1–3 days the crystalline **7** was collected: 82–83%: mp 190–192 °C. Anal. Calcd for $C_{18}H_{22}BNO_2S$: C, 66.07; H, 6.78; B, 3.30; N, 4.28; S, 9.80. Found: C, 65.92; H, 6.84; B, 3.46; N, 4.28; S, 9.44.

Deprotonation of (Phenylthio)methaneboronic Acid (1). Butyllithium (15 mmol) was added to a solution of **1** (5 mmol) in THF (30 mL) at −78 °C. The mixture was allowed to warm to 20 °C, then cooled to −78 °C and treated with methyl iodide (15 mmol), warmed to 20 °C for 2 h, treated with 10% phosphoric acid, extracted with ether, and concentrated. NMR analysis of the residue indicated that the ratio of $SCH(CH_3)B$ to SCH_2B groups was about 9:1 and that there was a large proportion of material which contained one or two *B*-butyl groups.

Acknowledgment. We thank the National Science Foundation for support, Grants MPS 75-19557, CHE 77-11283, and CHE-8025229.

Registry No. **1**, 67975-88-6; **2a**, 72824-03-4; **2b**, 66080-23-7; **2c**, 79121-30-5; **2d**, 79121-31-6; **3**, 66080-26-0; **4**, 66080-24-8; **5a**, 66080-25-9; **5b**, 66080-30-6; **5c**, 66080-29-3; **5d**, 66080-32-8; **5e**, 79121-32-7; **6a**, 66080-33-9; **6b**, 66080-34-0; **6c**, 66080-35-1; **6d**, 66080-36-2; **6e**, 79121-33-8; **7**, 79121-12-3; **9a**, 38793-73-6; **9b**, 79121-34-9; **9c**, 16222-10-9; **9d**, 66080-38-4; **9e**, 28403-86-3; **9f**, 66080-39-5; **9g**, 79121-35-0; **10**, 66080-37-3; **11**, 66080-40-8; **12a**, 33521-88-9; **12b**, 13112-46-4; **12c** (*E*), 79121-36-1; **12c** (*Z*), 79121-37-2; **12d**, 79121-38-3; **12e** (*E*), 79121-39-4; **12e** (*Z*), 79121-40-7; **12f**, 79121-41-8; **14**, 79121-42-9; **15a**, 79121-43-0; **16a**, 66080-42-0; **16b**, Me ester, 79121-44-1; **17**, 66080-41-9; **18**, 79121-45-2; **20**, 79121-46-3; **21a**, 24388-23-6; **22**, 79121-47-4; **23**, 78782-27-1; CH_3I, 74-88-4; *n*-BuBr, 109-65-9; *n*-BuCl, 109-69-3; *n*-BuI, 542-69-8; $(CH_3)_3CCH_2CH(CH_3)CH_2CH_2Br$, 50915-80-5; $PhOCH_2CH_2Br$, 589-10-6; $PhCH_2Br$, 100-39-0; $(CH_3)_2CHBr$, 75-26-3; $CH_3C(O_2C_2H_4)(CH_2)_3Cl$, 5978-08-5; $CH_3(CH_2)_2CO_2CH_3$, 623-42-7; c-$C_6H_{11}CO_2CH_3$, 4630-82-4; $PhCO_2CH_3$, 93-58-3; succinic anhydride, 108-30-5; $CH_3C(O_2C_2H_4)(CH_2)_2CO_2CH_3$, 35351-33-8; butyrolactone, 96-48-0; cyclohexanone, 108-94-1; PhCOPh, 119-61-9; $PhCOCH_2CH_2CH_3$, 495-40-9; $CH_3(CH_2)_5CHO$, 111-71-7; c-$C_6H_{11}CHO$, 2043-61-0; $CH_3COCH_2CH_2CO_2CH_3$, 624-45-3; cyclopentanone, 120-92-3; *trans*-2-hydroxycyclohexanecarboxaldehyde 2,4-dinitrophenylhydrazone, 79121-48-5; (phenylthio)methyllithium, 13307-75-0; trimethyl borate, 121-43-7.

(47) Bhacca, N. S.; Williams, D. H. "Application of NMR Spectroscopy in Organic Chemistry"; Holden-Day: San Francisco, 1964; pp 77–80.

Reactions of (Silylamino)phosphines with Ketones and Aldehydes[1,2]

David W. Morton and Robert H. Neilson*

Department of Chemistry, Texas Christian University, Fort Worth, Texas 76129

Received July 21, 1981

(Silylamino)phosphines including $(Me_3Si)_2NPMe_2$ (1), $Me_2\overline{SiCH_2CH_2SiMe_2}NPMe_2$ (2), and $Me_3SiN(R)PMe_2$ (3, R = *t*-Bu; 4, R = Me) react smoothly with carbonyl compounds in dichloromethane via nucleophilic attack by phosphorus and [1,4]-silyl migration from nitrogen to oxygen. Thus, treatment of phosphine 1 with saturated ketones and aldehydes affords high yields of the new *N*-silylphosphinimines $Me_3SiN{=}PMe_2{-}CRR'{-}OSiMe_3$ (**5a–h**). Similarly, 2 reacts with acetone to form the 8-membered ring product $Me_2\overline{SiCH_2CH_2SiMe_2N{=}PMe_2CMe_2{-}O}$ (**6**). With α,β-unsaturated carbonyl compounds, 1,4 addition occurs to yield the acyclic (from 1) or 10-membered cyclic (from 2) silyl enol ethers $Me_3SiN{=}PMe_2CHRCH{=}CR'OSiMe_3$ [**7**, R = R′ = H; **8**, R = R′ = Me; **9**, R, R′ = $(-CH_2-)_3$] and $Me_2\overline{SiCH_2CH_2SiMe_2N{=}PMe_2CH_2CH{=}CMeO}$ (**10**). The (*N*-alkyl-*N*-silylamino)phosphines 3 and 4 also react with carbonyl compounds, but, except for $t\text{-BuN}{=}PMe_2C(CF_3)_2OSiMe_3$ (**11**), the products are phosphine oxides $O{=}PMe_2{-}CRR'{-}OSiMe_3$ (**13**, R = H, R′ = Me; **14**, R = R′ = Me; **15**, R = H, R′ = Ph). Phosphine 3 reacts with methyl vinyl ketone to afford the unstable phosphinimine $t\text{-BuN}{=}PMe_2CH_2CH{=}CMeOSiMe_3$ (**16**). Proton, ^{13}C, and ^{31}P NMR spectroscopic data for this new series of compounds are reported.

Introduction

Recent studies of (silylamino)phosphines such as $(Me_3Si)_2NPMe_2$ have shown them to be easily prepared reagents which exhibit a rich and interesting derivative chemistry. Specifically there are three potential modes of reactivity in such systems: (a) nucleophilic attack by phosphorus; (b) nucleophilic attack by nitrogen; (c) electrophilic attack by silicon.

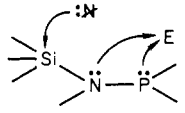

:N = nucleophile; E = electrophile

We have previously observed that a combination of pathways a and c is operative in the attempted synthesis of oxide (eq 1)[3] or ylide (eq 2)[4] derivatives. In both cases, the isolated products are the isomeric *N*-silylphosphinimines resulting from [1,3]-silyl migrations. Similarly, the bromination of (silylamino)phosphines (eq 3)[5] involves reaction at both phosphorus and silicon to afford the *P*-bromophosphinimines which are important intermediates in the synthesis of alkyl-substituted phosphazene polymers.[6,7]

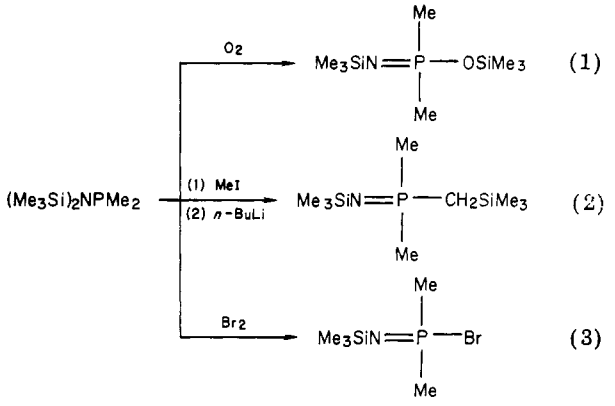

The findings have led us into a more extensive investigation of the reactivity of (silylamino)phosphines especially toward electrophilic organic substrates. A preliminary study[8] has shown that treatment of $(Me_3Si)_2NPMe_2$ with either acetone or hexafluoroacetone gives high yields of novel phosphinimines (eq 4). These observations were

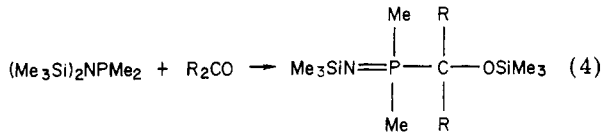

R = Me, CF_3

contrasted with the general lack of reactivity of phosphines with ketones[9] and with the oxidative reaction of $(CF_3)_2CO$ with $(Me_3Si)_2NPF_2$ to give the cyclic phosphorane[10]

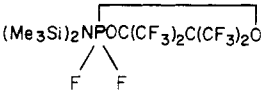

We report here some results of a more detailed study in which a representative series of (silylamino)phosphines were treated with a variety of aldehydes and ketones including α,β-unsaturated systems. The reactions of (silylamino)phosphines with other types of organic compounds will be reported in subsequent papers.

(1) Presented in part at the International Conference on Phosphorus Chemistry, Durham, NC, June 1981; Abstr. 176.
(2) Taken in part from the Ph.D. Dissertation of D. W. Morton, Texas Christian University, Fort Worth, TX, 1981.
(3) Neilson, R. H.; Wisian-Neilson, P.; Wilburn, J. C. *Inorg. Chem.* **1980**, *19*, 413.
(4) Wilburn, J. C.; Neilson, R. H. *Inorg. Chem.* **1979**, *18*, 347.
(5) Wisian-Neilson, P.; Neilson, R. H. *Inorg. Chem.* **1980**, *19*, 1875.
(6) Wisian-Neilson, P.; Neilson, R. H. *J. Am. Chem. Soc.* **1980**, *102*, 2848.
(7) Neilson, R. H.; Wisian-Neilson, P. *J. Macromol. Sci., Chem.* **1981**, *A16*, 425.
(8) Neilson, R. H.; Goebel, D. W. *J. Chem. Soc., Chem. Commun.* **1979**, 769.
(9) Emsley, J.; Hall, D. "The Chemistry of Phosphorus"; Halsted Press: New York, 1976; Chapter 4.
(10) Gibson, J. A.; Röschenthaler, G.-V.; Schmutzler, R. *J. Chem. Soc., Dalton Trans.* **1975**, 918.

0276-7333/82/2301-0289$01.25/0

Table I. Preparative and Analytical Data for New *N*-Silylphosphinimines

	preparative			analytical[a]	
compd	rx time	% yield	bp, °C (mm)	% C	% H
5a	<1 min	89	39-40 (0.2)	33.97 (34.10)	6.40 (6.24)
5b	42 h	88	51-53 (1.2)	47.18 (47.27)	11.05 (10.82)
5c	1.5 h	91	50 (0.3)	45.25 (45.24)	10.60 (10.63)
5d	6 h	69	80-82 (0.01)	54.94 (55.00)	9.47 (9.23)
5e[b]	2 h	72	62 (0.07) (mp 48-51)		
5f	4.3 h	66	57 (0.01)	42.35 (42.08)	9.41 (9.31)
5g[c]	1 h				
5h	48 h	67	56-57 (0.01)	52.90 (52.62)	10.96 (10.72)
6[c]	2 h				
7	<1 min	61	57-58 (0.01)	47.72 (47.61)	10.37 (10.17)
8	<1 min	91	45 (0.01)	49.28 (49.44)	10.47 (10.37)
9	36 h	69	79 (0.02)	52.82 (52.95)	10.14 (10.16)
10[c]	<1 min				
11	<1 min	81	43-45 (0.3)	38.86 (38.81)	6.49 (6.51)
13	4 h	69	54-56 (0.02) (mp 43-44)	43.01 (43.27)	9.66 (9.86)
14	65 h	76	46-47 (0.01)	46.37 (46.13)	10.40 (10.16)
15	1 h	66	99-101 (0.02) (mp 73-74)	56.47 (56.22)	8.30 (8.26)
16[c]	<1 min	42	60 (0.02)		

[a] Calculated values in parentheses. [b] Insufficient purity for elemental analysis. [c] Elemental analysis prevented by thermal instability.

Results and Discussion

The reactions of carbonyl compounds with [bis(trimethylsilyl)amino]dimethylphosphine (**1**), its cyclic analogue **2**, and the (*N*-alkyl-*N*-silylamino)phosphines **3** and **4** were studied in this work.

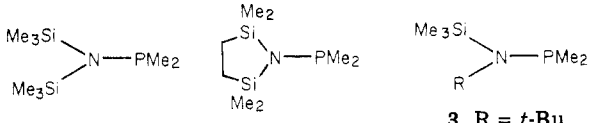

1 **2** **3**, R = *t*-Bu; **4**, R = Me

(Disilylamino)phosphines. When 1 equiv of the aldehyde or ketone was added to a dichloromethane solution of the phosphine **1** at 0 °C (or room temperature in some cases), a spontaneous, sometimes very exothermic, reaction ensued (eq 5). Solvent removal and fractional distillation

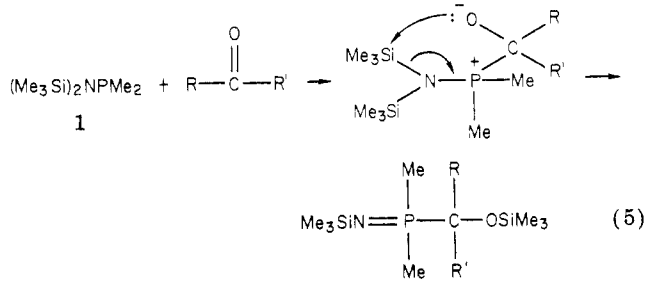

(5)

5a, R = CF_3, R′ = CF_3
b, R = R′ = Me
c, R = Me, R′ = H
d, R = Ph, R′ = H
e, R = Me, R′ = C(O)Me
f, R = Me, R′ = CH_2Cl
g, R = R′ = CH_2Cl
h, R = R′ = $-CH_2(CH_2)_3CH_2-$

generally afforded high yields of the novel *N*-silylphosphinimines **5** which apparently result from nucleophilic attack by phosphorus on the carbonyl carbon followed by a [1,4]-silyl migration from nitrogen to oxygen.

The reaction conditions, yields, and physical properties of these phosphinimines are summarized in Table I. Structural characterization of the products was readily accomplished by ^1H, ^{13}C, and ^{31}P NMR spectroscopy, and these data are collected in Table II. The progress of the reaction was conveniently monitored by ^1H NMR spectroscopy which clearly showed the formation of nonequivalent Me_3Si groups as well as the characteristic increase of the P–C–H coupling constant for the PMe_2 protons.[3-5]

Upon treatment of the (disilylamino)phosphine **2** with acetone, ring expansion to the 8-membered cyclic phosphinimine **6** occurred (eq 6). Compound **6** is a white, waxy

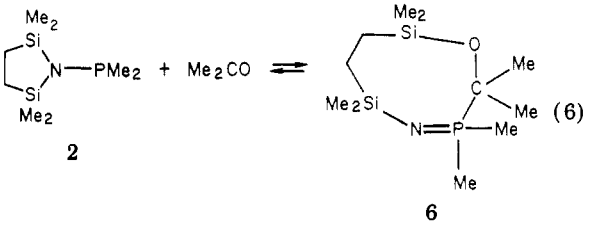

2 **6** (6)

solid which, on heating above ca. 65 °C, decomposed cleanly to the starting phosphine **2** and acetone. Due to this thermal instability, it was not possible to obtain an analytically pure sample of **6**. Nevertheless, its formation as virtually the only reaction product is clearly shown by ^1H, ^{13}C, and ^{31}P NMR spectroscopy (Table II).

The reasons for the reversibility of eq 6 are not clear although it is possible that the 8-membered ring may adopt a conformation which places the siloxy silicon atom in close proximity to the nitrogen, thus facilitating Si–N bond formation. In this context, it is interesting to note that the more rigid 7-membered cyclic phosphinimine[4] (eq 7) is a stable compound which shows no tendency to revert back to its precursor.

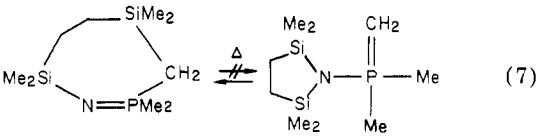

(7)

In spite of its thermal instability, the exclusive formation of the ring-expanded product **6** (eq 6) does have mechanistic implications. In this case certainly, and perhaps in the others (eq 5), the silyl shift from nitrogen to oxygen must occur by an *intramolecular* pathway. Otherwise, acyclic oligomers would have been produced.

The reaction times in Table I show the expected trends in reactivity of aldehydes and ketones. For example, the reaction with acetaldehyde is much faster than the reaction with acetone. The fluoro- and chloro-substituted acetones

also react substantially faster than acetone itself, undoubtedly due to the enhanced electrophilicity of the haloacetones. These qualitative observations are consistent with a mechanism in which attack by phosphorus on the carbonyl carbon is the rate-determining step.

A few other features of this general reaction (eq 5) are worthy of note. First, another possible mode of reactivity for the chloroacetones might have been attack by phosphorus on the CH_2Cl carbon to give a phosphonium salt; however, products resulting from this pathway were not observed. Second, in the case of biacetyl, reaction with phosphine **1** occurred at only one of the carbonyl groups to yield **5e** even if an excess of **1** was employed.

Third, the compounds **5f** and **5g** derived from chloroacetone and 1,3-dichloroacetone, respectively, are an interesting pair with regard to their spectral and physical properties. As indicated in Table I, compound **5f** is distillable and can be purified by careful fractionation to remove any unreacted chloroacetone. The diastereotopic protons of the chloromethyl group give rise to an ABX pattern (X = ^{31}P) in which the upfield half is clearly split into quartets with a coupling constant of 0.4 Hz. This coupling is assigned as a ^4J between one of the CH_2 protons and those of the CH_3 group attached to the chiral carbon. Compound **5g** was prepared in order to observe the ABX pattern without this long-range coupling. Indeed, spectra of the crude product **5g** were obtained with the desired result. Attempted distillation of **5g**, however, brought about elimination of Me_3SiCl and the bulk of the material solidified into a white mass. Complete characterization of the solid was not accomplished, but the NMR data are consistent with the formation of oligomers of the type $[-N{=}PMe_2{-}C(OSiMe_3)(CH_2Cl)CH_2-]_x$.

Similar reactions of α,β-unsaturated carbonyl compounds with (silylamino)phosphines were studied to determine whether the addition would proceed in a 1,2 or 1,4 manner. The carbonyl compounds investigated were methyl vinyl ketone, acrolein, and 2-cyclohexen-1-one. In each case, 1,4 addition was the observed result (eq 8), leading to the formation of *N*-silylphosphinimines **7–9** containing silyl enol ether functional groups.

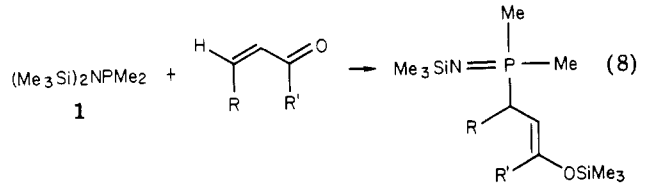

(8)

7, R = R′ = H
8, R = H, R′ = Me
9, R = R′ = $-CH_2CH_2CH_2-$

The product of the acrolein reaction **7** is obtained as a mixture of isomers in a ratio of approximately 80% *Z* and 20% *E*. These two configurations were distinguished in the ^1H NMR spectrum by the magnitudes of the vinylic coupling constants: 5.75 Hz for the cis protons of **7**(*Z*) and 11.91 Hz for the trans protons of **7**(*E*). The product ratio was estimated from the ^{13}C NMR spectrum by using the relative intensities of the corresponding vinylic and allylic carbon signals.

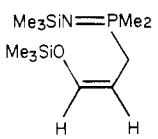

7 (*Z*)

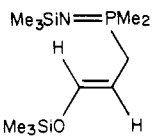

7 (*E*)

Molecular models of the intermediate enolates (eq 9)

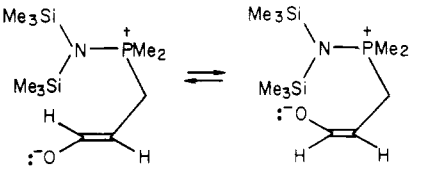

(9)

E *Z*

show that an intramolecular [1,6]-silyl migration is more easily accomplished when the configuration is *Z*, thus giving rise to the more abundant product **7**(*Z*). The *E* isomer may be formed by an intramolecular silyl migration in the enolate with *E* configuration, although the transition state for such a process has a rather strained geometry. Alternatively, it is possible that **7**(*E*) is formed by an *intermolecular* silyl shift, as in the case of the reaction of **1** with 2-cyclohexen-1-one (eq 10).

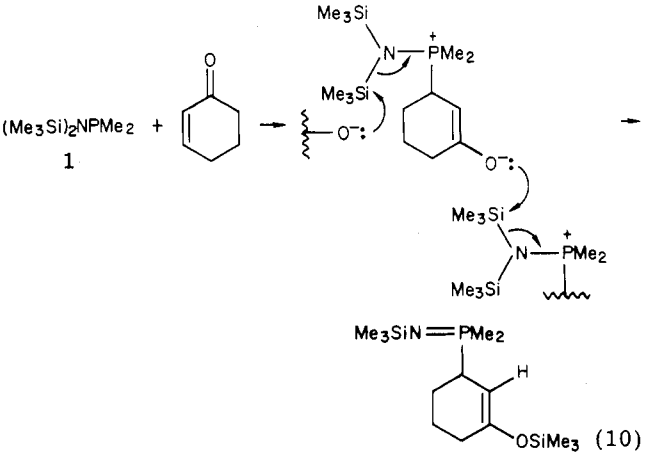

(10)

9

It is interesting to note that the reaction of **1** with acrolein (and with methyl vinyl ketone) occurs almost instanteously, but the reaction with 2-cyanohexen-1-one requires about 38 h for completion. This marked contrast in reaction times (and molecular models) strongly suggests that the formation of **9** occurs via an *intermolecular* silyl migration as shown in eq 10.

Methyl vinyl ketone reacts (eq 8) as rapidly with phosphine **1** as does acrolein. In this case, however, only a single silyl enol ether **8** is obtained. Although the actual configuration is uncertain, the rapidity of the reaction suggests an intramolecular silyl shift which would favor formation of the *Z* isomer.

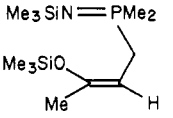

8 (*Z*)

The cyclic (silylamino)phosphine **2** also reacted with methyl vinyl ketone (eq 11), and the reaction progress was

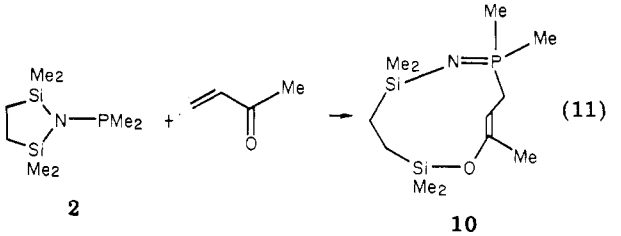

(11)

2 **10**

monitored by NMR spectroscopy. If methyl vinyl ketone

Table II. NMR Spectroscopic Data[a]

compd	signal	^{1}H NMR δ	^{1}H NMR J_{PH}	^{1}H NMR J_{HH}	^{13}C NMR δ	^{13}C NMR J_{PC}	^{31}P NMR δ
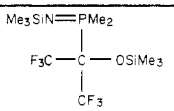 **5a**	Me_3SiN	0.07	0.4		3.51	3.1	7.76
	Me_3SiO	0.34			1.14		
	Me_2P	1.60	12.6		17.77	72.6	
	$(F_3C)_2C$				79.84[b]	70.8	
	F_3C				123.10[b]		
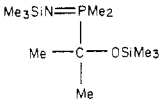 **5b**	Me_3SiN	−0.02	0.4		4.16	3.1	20.93
	Me_3SiO	0.17			2.40		
	Me_2P	1.30	12.6		12.97	65.3	
	Me_2C	1.41	12.6		24.02	5.5	
	Me_2C				73.54	96.4	
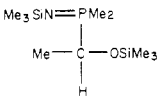 **5c**	Me_3SiN	−0.03	0.4		3.96	3.1	17.41
	Me_3SiO	0.28			−0.08		
	MeP	1.39	12.3		11.67	64.1	
	MeP	1.45	12.3		15.57	66.5	
	MeC	1.49	15.0	6.8	16.41	2.4	
	HC	3.94	4.8	6.8	68.24	93.4	
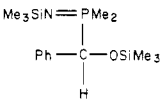 **5d**	Me_3SiN	−0.04	0.4		3.86	3.7	15.06
	Me_3SiO	0.15			−0.12		
	MeP	1.17	12.6		12.26	61.0	
	MeP	1.45	12.6		16.08	69.6	
	HC	4.73	10.7		75.90	87.9	
	Ph	7.18-7.44			126.82	3.7	
					127.45	5.5	
					127.47		
					137.34	0.6	
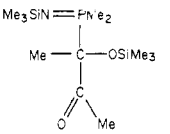 **5e**	Me_3SiN	0.03	0.4		3.84	3.1	15.62
	Me_3SiO	0.21			2.14		
	MeP	1.27	12.6	0.6	13.90	66.5	
	MeP	1.39	12.2	0.6	14.23	62.9	
	PC*Me*	1.69	14.3		20.21		
	PCMe				84.54	83.6	
	PCC*Me*	2.35			28.34		
	PCCMe				207.85	3.9	
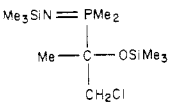 **5f**	Me_3SiN	0.00[c]	0.4		3.96	3.1	18.73
	Me_3SiO	0.24			2.27		
	MeP	1.32	12.2	0.5	14.01	64.7	
	MeP	1.35	12.3	0.5	14.42	63.5	
	PC*Me*	1.59	13.3	0.4	19.35	4.3	
	PCMe				75.71	93.4	
	C*H*Cl	3.91	4.8	11.5			
				0.4			
	C*H*Cl	4.06	6.4	11.5			
	CH_2Cl				51.15	16.5	
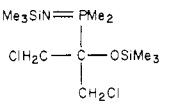 **5g**	Me_3SiN	0.03	0.4		3.96	3.1	15.44
	Me_3SiO	0.29			2.27		
	Me_2P	1.47	12.0		16.81	63.5	
	PCH_2	3.9	9.0	11.6	46.74	11.0	
	PCH_2	4.10	9.4	11.6			
	PCH_2				78.17	91.6	
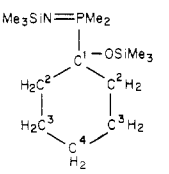 **5h**	Me_3SiN	−0.03	0.4		4.32	2.9	17.84
	Me_3SiO	0.20			2.79		
	Me_2P	1.27	12.0		13.61	61.5	
	C^1				76.64	96.7	
	C^2H_2	1.60-1.83			30.93	5.9	
	C^3H_2	1.60-1.83			21.18	9.8	
	C^4H_2	1.60-1.83			25.40		
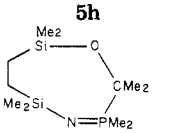 **6**	Me_2SiN	−0.09	0.4		1.97	5.5	20.50
	Me_2SiO	0.07			0.49		
	$SiCH_2$	0.61[d]			11.09		
	Me_2P	1.29	12.0		13.26	65.3	
	Me_2C	1.34	13.4		25.30	8.5	
	Me_2C				73.62	83.0	
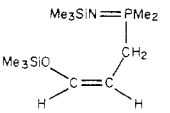 **7 (*Z*)**	Me_3SiN	0.03	0.4		3.61	3.7	8.16
	Me_3SiO	0.20			−1.10		
	Me_2P	1.35	12.8		16.91	67.8	
	PCH_2	2.50	16.1	7.9	29.73	65.9	
				1.2			
	PC*CH*	4.47	4.8	7.9	100.59	8.6	
				5.7			
	PCC*CH*	6.25	4.9	5.7	139.69	11.0	
				1.2			

Table II (*Continued*)

compd	signal	^{1}H NMR δ	^{1}H NMR J_{PH}	^{1}H NMR J_{HH}	^{13}C NMR δ	^{13}C NMR J_{PC}	^{31}P NMR δ
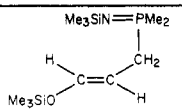 7(*E*)	Me_3SiN	0.03	0.4		3.61	3.7	5.84
	Me_3SiO	0.20			−1.10		
	Me_2P	1.35	12.8		16.91	67.8	
	PCH_2	2.29	14.9	8.1	32.91	67.8	
				1.2			
	PC*C*H	4.92	5.5	11.9	101.78	7.9	
				8.1			
	PCC*C*H	6.20	4.8	11.9	142.09	13.4	
				1.2			
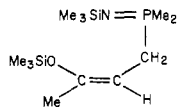 8	Me_3SiN	−0.03	0.4		4.00	4.3	12.13
	Me_3SiO	0.21			0.71		
	Me_2P	1.24	12.3		17.38	68.4	
	PCH_2	2.30	15.6	7.5	31.54	65.31	
	PC*C*H	4.32	5.4	7.5	98.50	8.6	
				<0.4			
	PCCC*Me*	1.78	5.4	<0.4	22.32	2.9	
	PCC*C*Me				149.24	11.6	
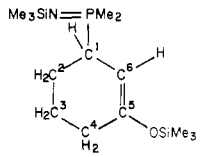 9	Me_3SiN	0.04[e]	0.4		3.84	3.1	12.33
	Me_3SiO	0.21			−0.12		
	Me_2P	1.28	11.4		15.15	67.1	
	HC^1	2.2-2.7			38.94	71.4	
	H_2C^2	1.2-2.1			22.13	<0.6	
	H_2C^3	1.2-2.1			21.77	10.4	
	H_2C^4	1.2-2.1			29.16	2.4	
	C^5				152.67	11.6	
	HC^6	4.90	8.7	5.6	99.43	5.5	
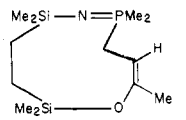 10(*Z*)	Me_2SiN	0.03[e]	0.4		1.67	4.9	11.17
	Me_2SiO	0.26			−0.73		
	CH_2SiN	0.39-0.90			11.05	4.3	
	CH_2SiO	0.39-0.90			7.51		
	Me_2P	1.40	12.0		18.13	70.2	
	PCH_2	2.42	12.3	7.9	31.09	62.9	
	PC*C*H	4.35	4.9	7.9	96.77	9.8	
				1.0			
	PCCC*Me*	1.88	5.4	1.0	22.15	3.1	
	PCC*C*Me				150.17	11.0	
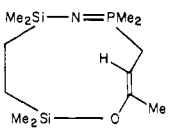 10(*E*)	Me_2SiN	0.04[e]	0.4		1.01	3.1	5.84
	Me_2SiO	0.20			−1.95		
	CH_2SiN	0.39-0.90			11.05	4.3	
	CH_2SiO	0.39-0.90			9.26		
	Me_2P	1.34	12.0		17.16	67.8	
	PCH_2	2.42	12.3	7.9	31.09	66.5	
	PC*C*H	4.44	4.9	7.9	97.42	8.6	
				1.0			
	PCCC*Me*	1.83	5.7	1.0	22.15	2.4	
	PCC*C*Me				148.97	11.6	
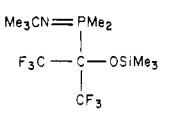 11	Me_3Si	0.34			0.90		−4.90
	Me_3C	1.18			34.74	10.4	
	Me_3C				51.52	5.5	
	Me_2P	1.60	11.5		17.30	72.0	
	$(F_3C)_2C$				79.49[f]	67.8	
	F_3C				123.03[f]		
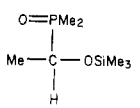 13	Me_3Si	0.03			−1.42		47.49
	MeP	1.23	12.4	0.4	8.75	66.5	
	MeP	1.28	12.8	0.4	11.66	67.1	
	*Me*C	1.25	14.5	6.9	15.13	1.8	
	HC	3.83	5.5	6.9	65.22	91.6	
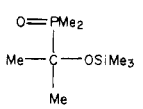 14	Me_3Si	0.04			1.01		52.16
	Me_2P	1.24	12.6		9.34	65.9	
	Me_2C	1.34	13.2		22.52	5.5	
	Me_2C				70.84	95.8	
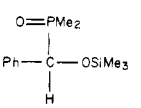 15	Me_3Si	0.06			−1.18		46.02
	MeP	1.11	12.8		9.71	67.1	
	MeP	1.40	12.8		12.26	67.1	
	HC	4.93	10.2		72.91	86.1	
	Ph	7.10-7.43			125.22	4.3	
					126.64	3.1	
					127.00	1.8	
					135.63	1.6	

Table II (*Continued*)

compd	signal	^{1}H NMR δ	^{1}H NMR J_{PH}	^{1}H NMR J_{HH}	^{13}C NMR δ	^{13}C NMR J_{PC}	^{31}P NMR δ
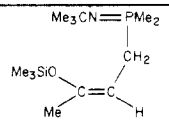 16	Me_3Si	0.16			1.42[g]		ca. 12[g,h]
	Me_3C	1.10			36.73	11.6	
	Me_3C				52.06	6.1	
	Me_2P	1.22	12.0		18.33	64.1	
	PCH_2	2.32	14.9	7.8	32.97	62.3	
	PC*C*H	4.35	5.4	7.8	101.07	7.3	
				0.6			
	PCCC*Me*	1.74	4.5	0.6	23.13	1.8	
	PCCC*Me*				149.05	10.4	

[a] Chemical shifts downfield from Me_4Si for ^{1}H and ^{13}C spectra and from H_3PO_4 for ^{31}P spectra; coupling constants in Hz. Solvents: ^{1}H, CH_2Cl_2; ^{13}C and ^{31}P, $CDCl_3$. [b] J_{CF} = 289.9 Hz, J_{CCF} = 28.5 Hz. [c] Benzene solution used for ^{1}H NMR. [d] $\bar{\nu}$ for AA'BB' pattern. [e] Benzene/$CDCl_3$ solution used for ^{1}H NMR. [f] J_{CF} = 289.5 Hz, J_{CCF} = 28.1 Hz. [g] Benzene-d_6 solution used for ^{13}C and ^{31}P NMR. [h] Spectrum recorded on partially decomposed sample.

was slowly added to a dichloromethane solution of **2** at either −78 or 0 °C and if the ^{1}H NMR spectrum was obtained immediately, then the PMe_2 group appears as a doublet at δ 1.33. As several hours pass, however, a new doublet at δ 1.27 begins to appear, eventually replacing the one at δ 1.33. A similar phenomenon occurs in the ^{31}P NMR spectra: an initial signal at δ 11.17 being slowly replaced by one at δ 5.84. Comparison of these ^{31}P chemical shifts with those of **7** (*Z*, δ 8.16, and *E*, δ 5.84) suggests that, in the reaction of **2** with methyl vinyl ketone, initially a product with *Z* configuration was formed, which slowly converted to the *E* isomer. Unfortunately, it was not possible to distill either of these compounds without substantial decomposition to unidentified products. Consequently their characterization is based upon NMR spectral data (Table II).

(*N*-Alkyl-*N*-silylamino)phosphines. The *tert*-butyl derivative **3** reacted spontaneously with hexafluoroacetone as expected to form the phosphinimine **11** (eq 12), but it

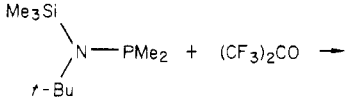

3

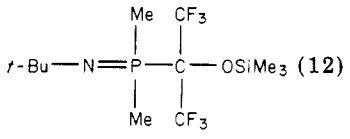

(12)

11

was unreactive toward acetone even after several months. Phosphine **3** does, however, react with acetaldehyde to form phosphine oxide **13** in high yield (eq 13, 14) rather

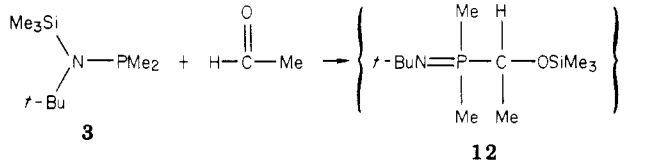

3 **12** (13)

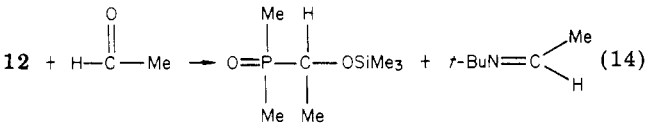

(14)

13

than the phosphinimine **12**. If only 1 equiv of acetaldehyde was added to **3**, only the phosphine oxide **13**, the imine *t*-BuN=CHMe, and unreacted phosphine **3** could be detected by ^{1}H NMR. It is concluded that the *N*-*tert*-butylphosphinimine **12**, which was never observed by ^{1}H NMR, reacts faster with the aldehyde than does the phosphine **3**. Similar reactivity trends have been observed by Pudovik and co-workers for some related Si–N–P systems.[11-13]

In contrast to **3**, the *N*-methyl analogue **4** does react with acetone to form the phosphine oxide **14**. Phosphine **4** also reacts with benzaldehyde to yield **15** (eq 15).

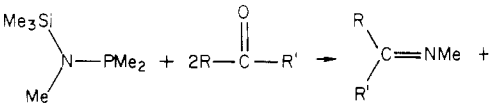

4

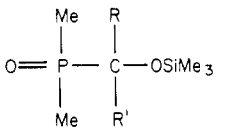

(15)

14, R = R′ = Me
15, R = H, R′ = Ph

Generally, the reactions of the *N*-alkyl phosphines **3** and **4** with α,β-unsaturated carbonyl compounds gave somewhat less straightforward results. Phosphine **3** reacted with 1 equiv of methyl vinyl ketone to yield the 1,4-addition product **16** (eq 16), a compound which is stable in

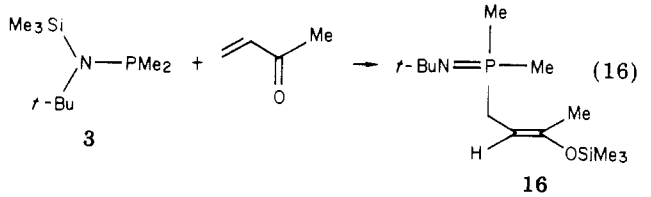

3 **16** (16)

the reaction mixture and for a short time after distillation. A freshly distilled sample of **16**, however, decomposed on standing for several hours to an unidentified dark brown substance.

Phosphine **4** also reacts vigorously with methyl vinyl ketone, but, unlike **3**, the products are unidentifiable. Presumably, the *N*-methyl analogue of **16** is formed initially, but this compound must be even less stable than **16**. Due to these instability problems, the reactions of **3** and **4** with other α,β-unsaturated carbonyl compounds were not investigated.

(11) Pudovik, M. A.; Medevdeva, M. D.; Kibardina, L. K.; Pudovik, A. N. *J. Gen. Chem. USSR (Engl. Trnsl.)* **1975**, *45*, 924.
(12) Pudovik, M. A.; Kibardina, L. K.; Medvedeva, M. D.; Pestova, T. A.; Kharlampidi, Kh. E.; Pudovik, A. N. *J. Gen. Chem. USSR (Engl. Transl.)* **1976**, *46*, 1878.
(13) Pudovik, M. A.; Kibardina, L. K.; Medvedeva, M. S.; Pudovik, A. N. *Bull. Acad. Sci. USSR, Div. Chem. Sci.* **1979**, *28*, 1022.

Conclusion

(Silylamino)phosphines generally react smoothly with carbonyl compounds via nucleophilic attack by phosphorus with subsequent silyl migration to oxygen. This process is a convenient synthetic route to new *N*-silylphosphinimines or phosphine oxides which contain Me_3SiO-functionalized organic substituents.

Experimental Section

Materials and General Procedures. The (silylamino)phosphines were prepared according to the published procedures.[4,14] Acetone, acetaldehyde, benzaldehyde, cyclohexanone, and dichloromethane were obtained from commerical sources, distilled, and stored over molecular sieves prior to use. Acrolein was distilled and used immediately. Other reagents were used as obtained without further purification. All reactions were performed under an atmosphere of dry nitrogen with reagents being transferred by syringe. Proton NMR spectra were obtained on Varian EM390 or JEOL MH-100 spectrometers. Carbon-13 and ^{31}P NMR spectra were obtained on a JEOL FX-60 spectrometer operating in the FT mode. Elemental analyses were performed by Schwarzkopf Microanalytical Laboratories, Woodside, NY.

Reactions of (Silylamino)phosphines with Aldehydes and Ketones. Typically, the phosphine (ca. 10–20 mmol) was dissolved in CH_2Cl_2 (ca. 10–15 mL) in a 25-mL flask equipped with a magnetic stirrer and an adapter with a gas-inlet side arm and a rubber septum. The carbonyl compound was then added via syringe to the stirred phosphine solution. Some reagents (see below) required addition at 0 °C to moderate the exothermic reaction. The progress of the reactions was monitored by ^1H NMR spectroscopy, and Table I lists the times by which disappearance of the starting phosphine was observed to be complete. Reaction times of <1 min indicate that the reaction is very rapid at 0 °C. Upon completion of the reaction, solvent was removed under reduced pressure, and the product was purified by fractional distillation (Table I).

In the above procedure, the reagents added at room temperature were acetone, cyclohexanone, and 2-cyclohexen-1-one. Those added at 0 °C were acetaldehyde, benzaldehyde, chloroacetone, dichloroacetone (as a CH_2Cl_2 solution), acrolein, and methyl vinyl ketone.

In the synthesis of the 10-membered ring **10**, the *Z* isomer was favored if methyl vinyl ketone was slowly swept into the reaction mixture at 0 °C under a stream of nitrogen.

In the syntheses of **5a** and **11**, hexafluoroacetone was introduced as a gas into an evacuated flask containing the phosphine, without solvent, which was being stirred at 0 °C. An exothermic reaction ensued in which only 1 equiv of hexafluoroacetone was consumed. Products were then purified by fractional distillation (Table I).

Acknowledgment. We thank The Robert A. Welch Foundation and the U.S. Army Research Office for generous financial support of this research.

Registry No. **1**, 63744-11-6; **2**, 68437-96-7; **3**, 68437-82-1; **4**, 68437-84-3; **5a**, 72805-01-7; **5b**, 72805-03-9; **5c**, 79200-64-9; **5d**, 79200-65-0; **5e**, 79200-66-1; **5f**, 79200-67-2; **5g**, 79200-68-3; **5h**, 79200-69-4; **6**, 79200-70-7; **7**(*Z*), 79200-71-8; **7**(*E*), 79200-72-9; **8**, 79200-73-0; **9**, 79200-74-1; **10**(*Z*), 79200-75-2; **10**(*E*), 79200-76-3; **11**, 72805-02-8; **13**, 79215-35-3; **14**, 79200-77-4; **15**, 79200-78-5; **16**, 79200-79-6; hexafluoroacetone, 684-16-2; acetone, 67-64-1; acetaldehyde, 75-07-0; benzaldehyde, 100-52-7; biacetyl, 431-03-8; chloroacetone, 78-95-5; dichloroacetone, 534-07-6; cyclohexanone, 108-94-1; methyl vinyl ketone, 78-94-4; acrolein, 107-02-8; 2-cyclohexen-1-one, 930-68-7.

(14) Wilburn, J. C. Ph.D. Dissertation, Duke University, Durham, NC, 1978.

A Double Michaelis–Arbuzov Rearrangement Involving $(\eta^5\text{-}C_5H_5)CoI_2(CO)$ and $P(OCH_3)_3$. Formation of the Cobalt "Supersandwich" Complex

D. K. Towle,[1a] S. J. Landon,[1a] T. B. Brill,*[1a] and T. H. Tulip*[1b]

Department of Chemistry, University of Delaware, Newark, Delaware 19711, and the Central Research and Development Department, E. I. du Pont de Nemours and Company, Experimental Station, Wilmington, Delaware 19898

Received July 15, 1981

The reaction of $(\eta^5\text{-}C_5H_5)CoI_2(CO)$ with $P(OR)_3$, R = CH_3 and C_2H_5, yields different products depending on the amount of phosphite and on conditions employed. By stoichiometric ligand substitution, $(\eta^5\text{-}C_5H_5)CoI_2[P(OCH_3)_3]$ is produced. However, with excess $P(OCH_3)_3$ a double Michaelis–Arbuzov reaction occurs to yield $(\eta^5\text{-}C_5H_5)Co[P(O)(OCH_3)_2]_2[P(OCH_3)_3]$ (**3**) with formation of CH_3I. Complex **3**, isolatable in both the anhydrous and monohydrated form, is converted to the cobalt supersandwich $(\eta^5\text{-}C_5H_5)_2Co_3[P(O)(OCH_3)_2]_6$ by pyrolysis or by the addition of anhydrous $CoCl_2$. The nature of **3** has been verified by a single-crystal X-ray diffraction study at −100 °C. It crystallizes as a monohydrate in space group C_{2h}^5—$P2_1/c$ with four formula units in a cell of dimensions a = 7.872 (1) Å, b = 15.105 (2) Å, c = 16.517 (2) Å, and β = 91.819 (1)°. Least-squares refinement of a data set containing 3238 reflections having $F_o^2 > 3\sigma(F_o^2)$ converged to conventional agreement indices (on F) of R = 0.031 and R_w = 0.034. The spectral, structural, and reactivity details of the complex, apparently unique in its formation via a double Michaelis–Arbuzov reaction, are discussed.

Introduction

The Michaelis–Arbuzov rearrangement, as illustrated in reaction 1, results in the production of a phosphonate

$$RX + P(OR')_3 \rightarrow P(O)R(OR')_2 + R'X \qquad (1)$$

species by alkyl transfer to phosphorus in a reaction between an alkyl halide and a trialkyl phosphite.[2-4] Analogous transformations which occur when certain organotransition-metal halides such as $CpFeX(CO)_2$,[5,6] CpNiX-

(1) (a) University of Delaware. (b) E. I. du Pont de Nemours and Co., Contribution No. 2952.

(2) Michaelis, A.; Kaehne, R. *Chem. Ber.* **1898**, *31*, 1048–55.
(3) Arbuzov, A. E. *Zh. Russ. Fiz.-Khim. O-va.* **1906**, *38*, 687.
(4) Harvey, R. G.; DeSombre, E. R. *Top. Phosphorus Chem.* **1964**, *1*, 57.

0276-7333/82/2301-0295$01.25/0

Conclusion

(Silylamino)phosphines generally react smoothly with carbonyl compounds via nucleophilic attack by phosphorus with subsequent silyl migration to oxygen. This process is a convenient synthetic route to new *N*-silylphosphinimines or phosphine oxides which contain Me_3SiO-functionalized organic substituents.

Experimental Section

Materials and General Procedures. The (silylamino)phosphines were prepared according to the published procedures.[4,14] Acetone, acetaldehyde, benzaldehyde, cyclohexanone, and dichloromethane were obtained from commerical sources, distilled, and stored over molecular sieves prior to use. Acrolein was distilled and used immediately. Other reagents were used as obtained without further purification. All reactions were performed under an atmosphere of dry nitrogen with reagents being transferred by syringe. Proton NMR spectra were obtained on Varian EM390 or JEOL MH-100 spectrometers. Carbon-13 and ^{31}P NMR spectra were obtained on a JEOL FX-60 spectrometer operating in the FT mode. Elemental analyses were performed by Schwarzkopf Microanalytical Laboratories, Woodside, NY.

Reactions of (Silylamino)phosphines with Aldehydes and Ketones. Typically, the phosphine (ca. 10–20 mmol) was dissolved in CH_2Cl_2 (ca. 10–15 mL) in a 25-mL flask equipped with a magnetic stirrer and an adapter with a gas-inlet side arm and a rubber septum. The carbonyl compound was then added via syringe to the stirred phosphine solution. Some reagents (see below) required addition at 0 °C to moderate the exothermic reaction. The progress of the reactions was monitored by ^1H NMR spectroscopy, and Table I lists the times by which disappearance of the starting phosphine was observed to be complete. Reaction times of <1 min indicate that the reaction is very rapid at 0 °C. Upon completion of the reaction, solvent was removed under reduced pressure, and the product was purified by fractional distillation (Table I).

In the above procedure, the reagents added at room temperature were acetone, cyclohexanone, and 2-cyclohexen-1-one. Those added at 0 °C were acetaldehyde, benzaldehyde, chloroacetone, dichloroacetone (as a CH_2Cl_2 solution), acrolein, and methyl vinyl ketone.

In the synthesis of the 10-membered ring **10**, the *Z* isomer was favored if methyl vinyl ketone was slowly swept into the reaction mixture at 0 °C under a stream of nitrogen.

In the syntheses of **5a** and **11**, hexafluoroacetone was introduced as a gas into an evacuated flask containing the phosphine, without solvent, which was being stirred at 0 °C. An exothermic reaction ensued in which only 1 equiv of hexafluoroacetone was consumed. Products were then purified by fractional distillation (Table I).

Acknowledgment. We thank The Robert A. Welch Foundation and the U.S. Army Research Office for generous financial support of this research.

Registry No. **1**, 63744-11-6; **2**, 68437-96-7; **3**, 68437-82-1; **4**, 68437-84-3; **5a**, 72805-01-7; **5b**, 72805-03-9; **5c**, 79200-64-9; **5d**, 79200-65-0; **5e**, 79200-66-1; **5f**, 79200-67-2; **5g**, 79200-68-3; **5h**, 79200-69-4; **6**, 79200-70-7; **7**(*Z*), 79200-71-8; **7**(*E*), 79200-72-9; **8**, 79200-73-0; **9**, 79200-74-1; **10**(*Z*), 79200-75-2; **10**(*E*), 79200-76-3; **11**, 72805-02-8; **13**, 79215-35-3; **14**, 79200-77-4; **15**, 79200-78-5; **16**, 79200-79-6; hexafluoroacetone, 684-16-2; acetone, 67-64-1; acetaldehyde, 75-07-0; benzaldehyde, 100-52-7; biacetyl, 431-03-8; chloroacetone, 78-95-5; dichloroacetone, 534-07-6; cyclohexanone, 108-94-1; methyl vinyl ketone, 78-94-4; acrolein, 107-02-8; 2-cyclohexen-1-one, 930-68-7.

(14) Wilburn, J. C. Ph.D. Dissertation, Duke University, Durham, NC, 1978.

A Double Michaelis–Arbuzov Rearrangement Involving $(\eta^5\text{-}C_5H_5)CoI_2(CO)$ and $P(OCH_3)_3$. Formation of the Cobalt "Supersandwich" Complex

D. K. Towle,[1a] S. J. Landon,[1a] T. B. Brill,*[1a] and T. H. Tulip*[1b]

Department of Chemistry, University of Delaware, Newark, Delaware 19711, and the Central Research and Development Department, E. I. du Pont de Nemours and Company, Experimental Station, Wilmington, Delaware 19898

Received July 15, 1981

The reaction of $(\eta^5\text{-}C_5H_5)CoI_2(CO)$ with $P(OR)_3$, R = CH_3 and C_2H_5, yields different products depending on the amount of phosphite and on conditions employed. By stoichiometric ligand substitution, $(\eta^5\text{-}C_5H_5)CoI_2[P(OCH_3)_3]$ is produced. However, with excess $P(OCH_3)_3$ a double Michaelis–Arbuzov reaction occurs to yield $(\eta^5\text{-}C_5H_5)Co[P(O)(OCH_3)_2]_2[P(OCH_3)_3]$ (**3**) with formation of CH_3I. Complex **3**, isolatable in both the anhydrous and monohydrated form, is converted to the cobalt supersandwich $(\eta^5\text{-}C_5H_5)_2Co_3[P(O)(OCH_3)_2]_6$ by pyrolysis or by the addition of anhydrous $CoCl_2$. The nature of **3** has been verified by a single-crystal X-ray diffraction study at −100 °C. It crystallizes as a monohydrate in space group C_{2h}^5—$P2_1/c$ with four formula units in a cell of dimensions a = 7.872 (1) Å, b = 15.105 (2) Å, c = 16.517 (2) Å, and β = 91.819 (1)°. Least-squares refinement of a data set containing 3238 reflections having $F_o^2 > 3\sigma(F_o^2)$ converged to conventional agreement indices (on F) of R = 0.031 and R_w = 0.034. The spectral, structural, and reactivity details of the complex, apparently unique in its formation via a double Michaelis–Arbuzov reaction, are discussed.

Introduction

The Michaelis–Arbuzov rearrangement, as illustrated in reaction 1, results in the production of a phosphonate

$$RX + P(OR')_3 \rightarrow P(O)R(OR')_2 + R'X \qquad (1)$$

species by alkyl transfer to phosphorus in a reaction between an alkyl halide and a trialkyl phosphite.[2-4] Analogous transformations which occur when certain organotransition-metal halides such as $CpFeX(CO)_2$,[5,6] CpNiX-

(1) (a) University of Delaware. (b) E. I. du Pont de Nemours and Co., Contribution No. 2952.

(2) Michaelis, A.; Kaehne, R. *Chem. Ber.* **1898**, *31*, 1048–55.
(3) Arbuzov, A. E. *Zh. Russ. Fiz.-Khim. O-va.* **1906**, *38*, 687.
(4) Harvey, R. G.; DeSombre, E. R. *Top. Phosphorus Chem.* **1964**, *1*, 57.

0276-7333/82/2301-0295$01.25/0

Table I. Summary of NMR Data[a]

	^1H		$^{31}P\{^1H\}$		$^{13}C\{^1H\}$	
	δ[b]	J_{HP}[c]	δ[d]	J_{HP}[c]	δ[b]	J_{CP}[c]
$CpCoI_2[P(OMe)_3]$ (2)						
C_5H_5	5.30	0.8 (d)			87.17	
$P(OCH_3)_3$	3.87	10.7 (d)	132.5		56.53	8.2 (d)
$CpCo[P(O)(OMe)_2]_2[P(OMe)_3]$ (3)						
C_5H_5	5.26				90.40	
$P(OCH_3)_3$	3.84	11.2 (d)	148.9	134 (t)	54.12	7.9 (d)
$P(O)(OCH_3)_2$	3.71	9.5, 2.0 (vt)	95.2	134 (d)	51.33	4.0 (d)

[a] Measured in $CDCl_3$. [b] Ppm downfield from $SiMe_4$. [c] Hz (multiplicity). [d] Ppm downfield from H_3PO_4.

$[P(OMe)_3]$[7] (X = halide), and $CpReBr_2(CO)_2$[8] are substituted for the alkyl halide lead to monophosphonate metal complexes. Several other variations which involve organometallic complexes have been reported.[9-11]

In the course of studies on the substitution chemistry of $CpCoI_2(CO)$ (1) we have found that while a simple exchange to yield $CpCoI_2[P(OMe)_3]$ (2) results from the reaction of 1 with 1 equiv of trimethyl phosphite, treatment with excess $P(OMe)_3$ produces a complex, $CpCo[P(O)(OMe)_2]_2[P(OMe)_3]$ (3), derived from an unprecedented double Michaelis–Arbuzov reaction. Because such transformations have not been previously reported, we have explored the systematics of this reaction as well as those of a series of novel related transformations. We find that complexes 1, 2, and 3 are transformed by various pathways into the trinuclear cobalt "supersandwich" $Cp_2Co_3[P(O)(OMe)_2]_6$ (4).[12] In contrast to previous syntheses these reactions proceed under mild conditions and involve air-stable reactants.

We report herein the results of our investigations into the substitution chemistry of complex 1, the formation of complex 3 via a double Michaelis–Arbuzov rearrangement, which includes a single-crystal X-ray diffraction study of 3 itself, and the facile preparation of the cobalt supersandwich complex.

Results and Discussion

Synthesis and Reactions. $(\eta^5\text{-}C_5H_5)CoI_2(CO)$ (1) reacts with $P(OMe)_3$ to yield a variety of products depending on reaction stoichiometry, temperature, and solvent. Figure 1 summarizes some of the transformations described below. As previously demonstrated by Heck[13] and King[14] the carbonyl group of complex 1 is highly labile. When 1 equiv of $P(OMe)_3$ is added to 1 in CH_2Cl_2 at ambient temperature, a gradual color change from violet to brown ensues with evolution of a gas (presumably CO). The brown-black monophosphite derivative is isolated as the sole metal-containing product of the reaction. Although complexes of the form $CpCoI_2L$, where L = N or P donor ligand, are well-known, complex 2 has not been previously reported. As indicated in Table I, which contains a summary of NMR data, the ^{31}P NMR spectrum of complex 2 consists of a broad absorption centered at δ 132.5 which is characteristic of a P(III) nucleus coordinated to a first-row element.[15] The ^1H NMR spectrum contains a C_5H_5 doublet at δ 5.30 and a methyl resonance centered at δ 3.87 of appropriate intensities (5:9). $^3J_{HP}$ for the Cp and methyl signals are 0.8 and 10.7 Hz, respectively. The ^{13}C NMR spectrum of complex 2 exhibits a cyclopentadienyl carbon resonance at δ 87.17 and a methyl carbon doublet centered at δ 56.53 ($^2J_{CP}$ = 8.2 Hz).

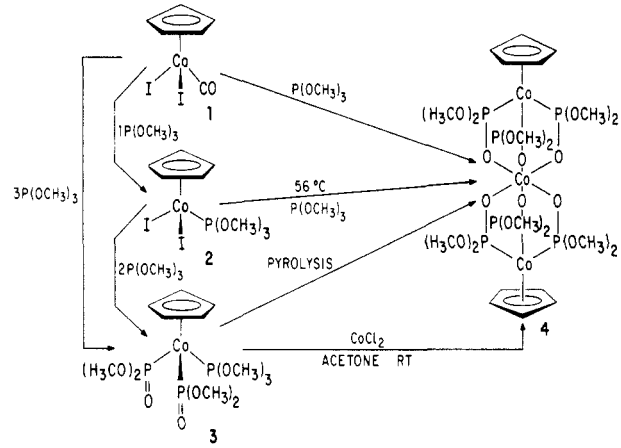

Figure 1. Reaction scheme of interconversions of complexes 1–4.

The addition of 3 or more equiv of $P(OMe)_3$ to complex 1 (CH_2Cl_2, 25 °C) causes a marked decolorization of the solution from deep violet to yellow which is complete within a matter of minutes. A bright yellow air-stable crystalline product is readily isolated. However, we observed different products depending upon solvent pretreatment and the extent of atmospheric exposure during workup. One product melts reproducibly at 108 °C while the other melts at 145 °C. On the basis of ^1H, ^{13}C, and ^{31}P NMR spectroscopies, both complexes appeared to have the formula $(\eta^5\text{-}C_5H_5)Co[P(O)(OCH_3)_2]_2[P(OCH_3)_3]$. While the complex clearly contains Co(III), the various spectra do not unequivocably distinguish the two likely bonding modes: $MOP(OMe)_2$[16] and $M[P(O)(OMe)_2]$.[5,7-10,17,18] We subsequently found (vide infra) that the two complexes are the anhydrous and monohydrated forms of complex 3. The anhydrous form melts at 108 °C and is quite hygroscopic, although it is otherwise stable to atmospheric exposure. The monohydrate is neither air nor moisture sensitive and has the higher, 145 °C, melting point, undoubtedly because of lattice stablization afforded by the intermolecular hydrogen bonding of the water molecules.

(5) Haines, R. J.; DuPreez, A. L.; Marais, I. L. *J. Organomet. Chem.* **1971**, *28*, 405–13.
(6) Abbreviations: $\eta^5\text{-}C_5H_5$, Cp; CH_3, Me; C_2H_5, Et.
(7) Clemens, J.; Neukomm, H.; Werner, H. *Helv. Chim. Acta* **1974**, *57*, 2000–2010.
(8) King, R. B.; Reimann, R. H. *Inorg. Chem.* **1976**, *15*, 179–83.
(9) Neukomm, H.; Werner, H. *J. Organomet. Chem.* **1976**, *108*, C26–8.
(10) Klaui, W.; Neukomm, H. *Org. Magn. Reson.* **1977**, *10*, 126–31.
(11) King, R. B.; Diefenbach, S. P. *Inorg. Chem.* **1979**, *18*, 63–8.
(12) Harder, V.; Dubler, E.; Werner, H. *J. Organomet. Chem.* **1974**, *71*, 427–33.
(13) Heck, R. F. *Inorg. Chem.* **1965**, *4*, 855–7; **1968**, *7*, 1513–16.
(14) King, R. B. *Inorg. Chem.* **1966**, *5*, 82–7.
(15) Nixon, J. F.; Pidcock, A. *Annu. Rev. NMR Spectrosc.* **1969**, *2*, 345–422.
(16) (a) Stelling, O. *Z. Phys. Chem., Stoechiom. Verwandschaftsl.* **1925**, *117*, 161–74, 194–208. (b) Daasch, L. W. *J. Am. Chem. Soc.* **1958**, *80*, 5301–3. (c) Smith, T. D. *J. Inorg. Nucl. Chem.* **1960**, *15*, 95–8.
(17) Haines R. J.; Nolte, C. R. *J. Organomet. Chem.* **1970**, *24*, 725–36.
(18) Howell, J. A. S.; Rowan, A. J. *J. Chem. Soc., Dalton Trans.* **1980**, 1845–51.

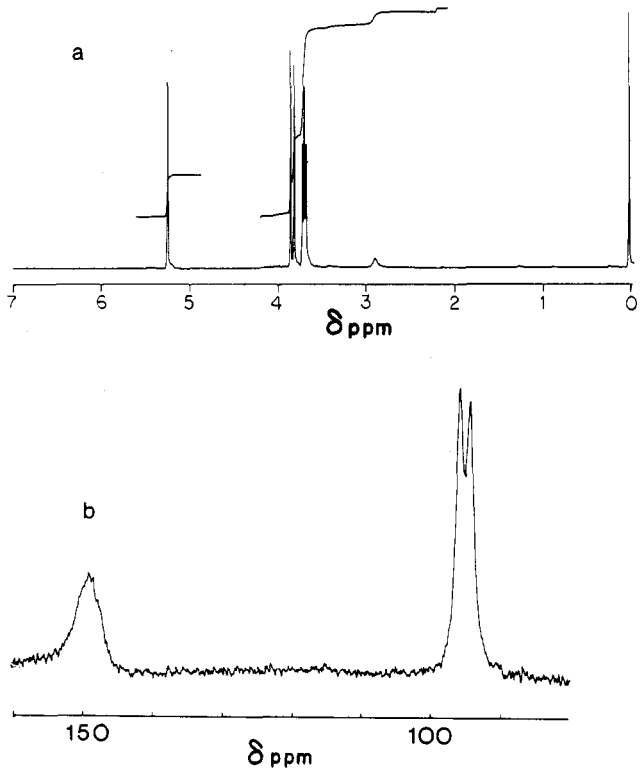

Figure 2. ^1H (a) and ^{31}P $\{^1H\}$ (b) NMR spectra of $CpCo[P(O)(OMe)_2]_2[P(OMe)_3]$ (3).

The use of rigorously anhydrous conditions yields the anhydrous form, but if no special precautions are exercised, the hydrated form often results.

The essential structural features of complex 3 are established by its NMR spectra, as listed in Table I. The ^{31}P NMR spectrum, as shown in Figure 2, consists of a broad, partially resolved triplet at δ 148.9 and a doublet centered at δ 95.29 ($^2J_{PP}$ = 134.4 Hz) arising from the phosphite and phosphonate phosphorus nuclei, respectively. The integrated intensities conform to the expected 1:2 ratio. Coupling with the ^{59}Co quadrupole moment may give rise to the broadened phosphite signal. The observed chemical shifts are in accord with those previously reported for $P(OMe)_3$ and $P(O)(OMe)_2$ ligands bound to transition metals.[17-19] Compare the shifts for complex 3 with those of $CpMo[P(O)(OMe)_2](CO)_2[P(OMe)_3]$,[17] δ 188.0 and 115.0, and $CpRu[P(O)(OMe)_2](CO)[P(OMe)_3]$,[18] δ 160 and 110 [$P(OMe)_3$ and $P(O)(OMe)_2$ signals, respectively, in each case]. Free trimethyl phosphite exhibits a resonance at δ 141[20] while nonmetallic phosphonates give rise to signals in the range δ 0–30.[21] Thus the change in chemical shift upon complexation is smaller for $P(OMe)_3$ than for the $-P(O)(OMe)_2$ group.

The ^1H NMR spectrum of complex 3, as shown in Figure 2, contains a C_5H_5 resonance, a $P(OCH_3)_3$ doublet centered at δ 3.84, and a triplet at δ 3.71, in the expected 5:9:12 ratio of integrated intensities. The triplet resonance arises from the phosphate methyl protons. The observed splitting is invariant at 90, 220, and 250 MHz, and thus inequivalent $P(O)(OMe)_2$ groups, which could produce an apparent triplet, are precluded. Rather, the triplet signal is the AA′ portion of a $A_6XX'A'_6$ spectrum in which the phosphonate methyl protons are virtually coupled to both phosphonate phosphorus nuclei. The observed second-order spectrum results from a large coupling between the X and X′ (phosphonate phosphorus) nuclei. We have successfully simulated the observed pattern by using 2.0 and 9.5 Hz for $^5J_{HP}$ and $^3J_{HP}$, respectively. Variation of $^2J_{PP}$ between 100 and 150 Hz has negligible effect on the simulated pattern. The ^1H NMR parameters of complex 3 are entirely those reported for $CpCoX[P(O)(OMe)_2][P(OMe)_3]$, where X = I and CH_3.[10]

The cyclopentadienyl carbon nuclei give rise to a singlet at δ 90.40 while complex patterns centered at δ 54.12 and 51.33 are observed for the phosphite and phosphonate carbon atoms, respectively.

The formation of complex 3 is related to the classical Michaelis–Arbuzov transformation of a phosphite to a phosphonate by an alkyl halide reagent. The reaction occurs by initial addition of the alkyl halide to the phosphite to form a phosphonium salt which subsequently rearranges to yield a trialkyl phosphonate and the alternative alkyl halide.[2-4] In the reaction of complex 1, $CpCoI_2(CO)$, with trimethyl phosphite the CpCoXI group, where X = I or $P(O)(OMe)_2$, may function analogously to the alkyl group of the alkyl halide as it coordinates a $P(OMe)_3$ molecule. In the presence of excess trimethyl phosphite, the reaction proceeds with successive liberation of two molecules of CH_3I via a double Michaelis–Arbuzov reaction as shown in equ 2. The required byproduct

$$CpCoI_2(CO) + 3P(OMe)_3 \rightarrow CpCo[P(O)(OMe)_2]_2[P(OMe)_3] + 2MeI + CO \quad (2)$$

methyl iodide is readily observed in the yellow reaction mixture by ^1H NMR spectroscopy. In the mechanism described above the final phosphite to coordinate should remain unchanged.

The formation of complex 3 via the Michaelis–Arbuzov rearrangement is not unlike reactions which occur when $CpNiX[P(OMe)_3]$(X = halide,[7] $CpFeCl(CO)_2$,[5] or $CpReBr_2(CO)_2$[8] react with trimethyl phosphite to produce organometallic monophosphonate complexes and alkyl halides. Note that in the case of $CpReBr_2(CO)_2$ only one Br atom is replaced by a phosphonate group. Apparently the steric requirements of the complex dictate the extent of phosphonate-for-halide replacement.

The formation of ethyl analogues of complexes 2 and 3 result from the treatment of complex 1 with triethyl phosphite. Complete transformation of complex 1 to $CpCo[P(O)(OEt)_2]_2[P(OEt)_3]$ proceeds at a rate slower than that of the trimethyl phosphite reaction, possibly because of the lower volatility of ethyl vs. methyl iodide. The physical and spectral properties of the ethyl derivatives are entirely in accord with those of the methyl congeners, complexes 2 and 3.

Complexes 1, 2, and 3 are readily converted to the trinuclear cobalt "supersandwich" complex $Cp_2Co_3[P(O)(OMe)_2]_6$ (4). Complex 4 was initially prepared by Harder, Dubler, and Werner,[12] whose synthesis involved heating cobaltacene with $P(OCH_3)_3$ or $HP(O)(OCH_3)_2$ in a sealed tube at 140–150 °C for several days. Complexes 1, 2, and 3 are transformed into 4 under much less vigorous conditions. Heating $CpCoI_2(CO)$ (1) with excess $P(OMe)_3$ in CH_2Cl_2 produces a small amount of complex 4, probably by the sequence 1 → 2 → 3 → 4 as depicted in Figure 1. When $CpCo[P(O)(OMe)_2]_2[P(OMe)_3]$ (3) is refluxed in acetone with 3 equiv of $P(OMe)_3$, the trinuclear complex is produced in 50% yield. Complex 4 is also formed (70% yield) from the reaction of complex 3 with 0.5 molar equiv of $CoCl_2$. Note that Michaelis–Arbuzov rearrangements are required for these reactions to proceed but are not

(19) Mabich, W.; Janta, R. *Angew. Chem., Int. Ed. Engl.* **1978**, *17*, 211-2.
(20) Van Wazer, J. R. *Top. Phosphorus Chem.* **1967**, *5*, 227-457.
(21) Emsley, J. W.; Feeney, J.; Sutcliffe, L. H. "High Resolution Nuclear Magnetic Resonance"; Pergammon Press: New York, 1966: Vol. II, p 1006.

Table II. Selected Distances (Å) and Angles (Deg) in $CpCo[P(O)(OMe)_2]_2[P(OMe)_3]\cdot H_2O$

Distances

Co-P(1)	2.196 (1)	P(1)-O(3)	1.618 (2)	O(6)-C(4)	1.439 (3)
Co-P(2)	2.202 (1)	P(2)-O(4)	1.492 (3)	O(7)-C(5)	1.441 (3)
Co-P(3)	2.151 (1)	P(2)-O(5)	1.598 (2)	O(8)-C(6)	1.456 (3)
Co-C(10)	2.093 (2)	P(2)-O(6)	1.613 (2)	O(9)-C(7)	1.438 (3)
Co-C(11)	2.094 (2)	P(3)-O(7)	1.572 (2)	C(10)-C(11)	1.414 (3)
Co-C(12)	2.077 (2)	P(3)-O(8)	1.583 (2)	C(10)-C(14)	1.417 (3)
Co-C(13)	2.103 (2)	P(3)-O(9)	1.596 (2)	C(11)-C(12)	1.410 (3)
Co-C(14)	2.112 (2)	O(2)-C(1)	1.437 (3)	C(12)-C(13)	1.427 (3)
P(1)-O(1)	1.487 (2)	O(3)-C(2)	1.428 (3)	C(13)-C(14)	1.410 (3)
P(1)-O(2)	1.614 (2)	O(5)-C(3)	1.422 (3)	O-H(1)	0.75 (3)
				O-H(2)	0.80 (4)
O(1)···H(2)	2.03 (4)	O(4)···H(1)	2.03 (3)		

Angles

P(1)-Co-P(2)	91.87 (2)	O(7)-P(3)-O(8)	101.20 (9)	P(2)-O(5)-C(3)	123.7 (2)
P(1)-Co-P(3)	93.50 (2)	O(7)-P(3)-O(9)	99.15 (9)	P(2)-O(6)-C(4)	118.1 (2)
P(2)-Co-P(3)	95.67 (2)	O(8)-P(3)-O(9)	106.52 (9)	P(3)-O(7)-C(5)	126.5 (2)
Co-P(1)-O(1)	120.77 (7)	P(1)-O(2)-C(1)	118.16 (1)	P(3)-O(8)-C(6)	121.4 (2)
Co-P(1)-O(2)	104.45 (6)	P(1)-O(3)-C(2)	120.9 (2)	P(3)-O(9)-C(7)	123.0 (2)
Co-P(1)-O(3)	110.31 (7)	O(1)-P(1)-O(2)	110.94 (9)	C(11)-C(10)-C(14)	108.1 (2)
Co-P(2)-O(4)	116.77 (7)	O(1)-P(1)-O(3)	109.23 (9)	C(10)-C(11)-C(12)	108.3 (2)
Co-P(2)-O(5)	113.51 (7)	O(2)-P(1)-O(3)	98.86 (9)	C(11)-C(12)-C(13)	107.6 (2)
Co-P(2)-O(6)	103.50 (6)	O(4)-P(2)-O(5)	108.70 (9)	C(12)-C(13)-C(14)	108.1 (2)
Co-P(3)-O(7)	122.47 (7)	O(4)-P(2)-O(6)	110.89 (9)	C(13)-C(14)-C(10)	107.9 (2)
Co-P(3)-O(8)	107.35 (7)	O(5)-P(2)-O(6)	102.48 (10)	H(1)-O-H(2)	109 (3)
Co-P(3)-O(9)	118.09 (6)				
P(1)-O(1)···H(2)	144 (1)	P(2)-O(4)···H(1)	136 (1)		
O(1)···H(2)-O	169 (4)	O(4)···H(1)-O	171 (3)		

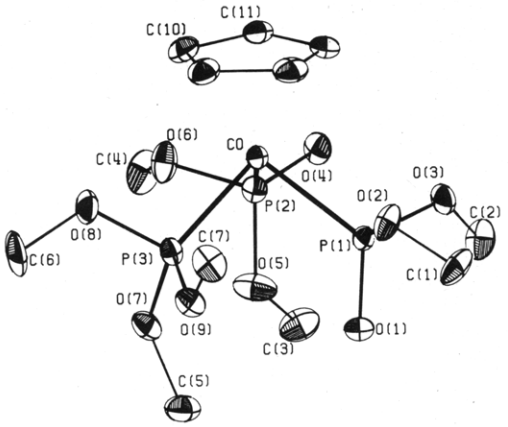

Figure 3. A perspective view of $CpCo[P(O)(OMe)_2]_2[P(OMe)_3]\cdot H_2O$ (**3**). The vibrational ellipsoids are drawn at the 50% level here and in subsequent figures. The water molecule and the hydrogen atoms have been omitted for clarity. Atom labels are included.

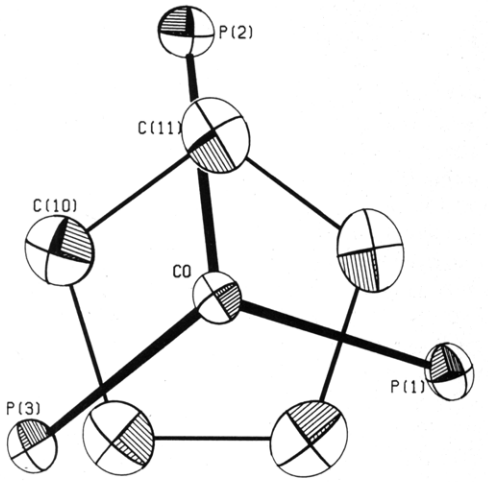

Figure 4. A perspective view normal to the cyclopentadienyl plane.

necessary in the following transformation. A solid sample of $CpCo[P(O)(OMe_2]_2[P(OMe)_3]$ (**3**) is smoothly converted to $Cp_2Co_3[P(O)(OMe)_2]_6$ (**4**) by simply heating the mononuclear complex above its melting point. The anhydrous form of complex **3** melts at 108 °C and then recrystallizes as the yellow "supersandwich" complex. A gas, presumably a mixture of trimethyl phosphite and a cyclopentadiene-derived product, possibly dicyclopentadiene, is evolved as the complex solidifies. Although the volatile products were not completely characterized, the pyrolysis reaction appears to be a shown in reaction 3. The hydrated form of

$$3CpCo[P(O)(OMe)_2]_2[P(OMe)_3] \rightarrow Cp_2Co_3[P(O)(OMe)_2]_6 + 3P(OMe)_3 + 0.5C_{10}H_{10} \quad (3)$$

3 melts at 145 °C and remains a liquid up to approximately 170 °C. At this temperature gas evolution is observed and the material solidifies as yellow crystals. The yield of complex **4** from these thermolysis reactions is approximately 70–80%. The reaction of the hydrated form of complex **3** to **4** appears to be a thermal dehydration followed by the transformation shown in reaction 3.

Description of the Structure of $CpCo[P(O)(OMe)_2]_2[P(OMe)_3]\cdot H_2O$ (3). The crystal structure of **3** consists of the packing of four molecules linked by hydrogen-bound water molecules. The molecules are well separated, having no significant close intermolecular contacts other than those associated with the bridging water molecule. Bond distances and angles are compiled in Table II. Figure 3 contains a representation of the unsolvated molecule and includes the atom labels which are used in this discussion. The piano stool conformation of the molecule is emphasized in the depiction of the inner coordination sphere shown in Figure 4. The intermolecular hydrogen bonding involving the water of hydration is illustrated in Figure 5.

The observed molecular structure confirms the spectroscopic characterization of complex **3** described above. The molecule contains a Co(III) center surrounded by an unremarkable η^5-cyclopentadienyl ring, a trimethyl phosphite ligand, and two phosphorus-bound dimethyl phosphonate groups. As shown in Figures 3 and 4 the

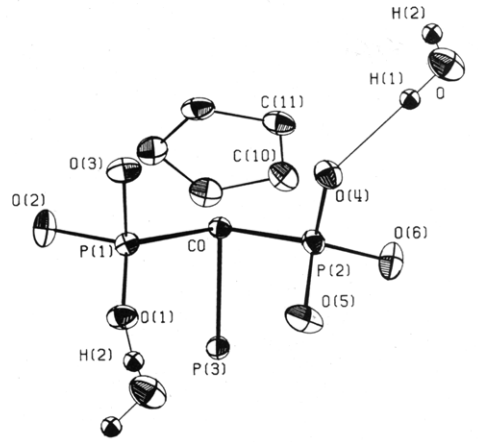

Figure 5. A perspective view of the molecule showing the molecule of hydration. A number of atoms have been omitted for clarity. Two water molecules have been included to illustrate the intermolecular hydrogen bonding.

coordination geometry is pseudooctahedral with the η^5-C_5H_5 ligand occupying three facial sites. The P–Co–P angles approximate the octahedral value as they range from 91.9 to 95.7 (2)°. The water molecule of complex **3** bridges the unique phosphonate oxygen atoms of adjacent molecules. At 2.773 and 2.828 (3) Å, the O–O separations of the hydrogen-bonding fragments are normal as are the near linear (ca. 170°) but unsymmetrical O–H···O arrays.[22] These latter values are based upon refined hydrogen atom positions. Although these atoms were readily located and refined smoothly, the derived O–H bond distances, 0.75 (3) and 0.80 (4) Å, are substantially shorter than expected. In the absence of neutron diffraction data, these values must be regarded with caution.

Only a few complexes which incorporate a phosphonate ligand have been structurally characterized.[23-29] The best comparisons can be drawn between the structural parameters of complex **3** and those of $CpCr[P(O)(OMe)_2](CO)_2[P(OMe)_3]$ (**5**), the only other structurally characterized complex which contains both phosphonate and phosphite ligands.[23] In both complexes the M–P(phosphite) separations (2.267 (3) and 2.151 (1) Å, Cr and Co) are shorter than the respective M–P(phosphonate) distances, 2.360 (3) and 2.199 (1) Å. These differences must be electronic in origin because the steric demand of $P(O)(OMe)_2$ and $P(OMe)_3$ ligands appear comparable. The phosphonate phosphorus atom should be a much poorer σ donor than its phosphite counterpart on the basis of the former atom's higher oxidation state. This σ term apparently dictates the M–P bond length but contributions from π withdrawal must also be present. Preliminary NQR experiments reveal that complex **3** closely resembles the cobalt(I) species $CpCo(CO)_2(HgCl_2)$ and indicate that the phosphonate ligand may be similar to carbon monoxide in its donor–acceptor properties.[30] Thus, in complex **5** competition between the CO and $P(O)(OMe)_2$ ligands accentuates the M–P bond length difference with respect to that of complex **3**, in which analogous π competition is absent. The longer metal-bonding radius and the presence of an additional ligand in the Cr complex undoubtedly also contribute to the observed differences between complexes **3** and **5**.

The observed orientation of the P=O vectors in complex **3** probably results from hydrogen-bonding considerations rather than from bonding requirements within the complex itself. The P=O bond distances, at 1.487 and 1.492 (2) Å, are only marginally longer than that reported for the Cr complex **5**, 1.478 (6) Å, despite the absence of hydrogen bonding in the latter complex. There is, in fact, only a minor deviation in this separation in coordinated phosphonate groups, regardless of secondary oxygen interaction. These distances range from 1.44 (7) to 1.53 (2) Å, for $HgCl[P(O)(OEt)_2]$[28] and $Os_5C(H)[OP(OMe)OP(OMe)_2](CO)_{13}$,[25] respectively. The mercury complex shows a strong O—Hg interaction while an osmium atom is clearly oxygen bound in the carbide cluster. Of the reported phosphonate complex structures only the Cr complex **5** exhibits no secondary oxygen interactions although its P=O separation is bracketted by values of the oxygen-coordinated complexes.

Table III. Summary of X-ray Diffraction Data

complex	$(\eta^5\text{-}C_5H_5)Co[P(O)(OCH_3)_2]_2[P(OCH_3)_3]\cdot H_2O$
formula	$C_{12}H_{28}CoO_{10}P_3$
fw	484.21
a, Å	7.872 (1)
b, Å	15.105 (2)
c, Å	16.517 (2)
β, deg	91.819 (1)
V, Å^3	1963.0 (8)
Z	4
ρ_{calcd}, g cm^{-3}	1.638
space group	C_{2h}^5—$P2_1/c$ (no. 14)
cryst dimens, mm	0.20 × 0.26 × 0.26
temp, °C	−100
radiatn	Mo Kα (0.710 69 Å) from graphite monochromator
μ, cm^{-1}	12.01
transmissn factors	0.928–0.993; av 0.967
2θ limits, deg	4.0–55.0
total no. of observns	4496
unique data, $F_o^2 > 3\sigma(F_o^2)$	3238
final no. of variables	243
R	0.031
R_w	0.034
error in observn of unit wt	1.54 electrons

Experimental Section

All solvents were of reagent grade, or better, and were used as received. Alkyl phosphites were obtained from ROC-RIC and were used without further purification. The complex $CpCo(CO)_2$ was obtained from Pressure Chemical and used as received.

^1H, $^{13}C\{^1H\}$, and $^{31}P\{^1H\}$ NMR spectra were recorded on a Bruker WM-250 spectrometer. $CDCl_3$ was the solvent for all NMR spectra. ^1H and ^{13}C chemical shifts are reported relative to $SiMe_4$ (δ 0.0) while ^{31}P shifts are referenced downfield to 85% H_3PO_4 (external). ^1H NMR spectra were simulated by using an ITRCL program.

Mass spectra were obtained by using a Du Pont 21-492B mass spectrometer. Microanalyses were performed by MicroAnalysis, Wilmington, DE. All melting points were obtained by using a

(22) Hamilton, W. C.; Ibers, J. A. "Hydrogen Bonding in Solids"; W. A. Benjamin: New York, 1968.
(23) Goh, L.-Y.; D'Aniello, M. J., Jr.; Slater, S.; Muetterties, E. L.; Tavanaiepour, I.; Chang, M. I.; Fredrich, M. F.; Day, V. W. *Inorg. Chem.* **1979**, *18*, 192–7.
(24) Bruce, M. I.; Howard, J.; Nowell, I. W.; Shaw, G.; Woodward, P. *J. Chem. Soc. D* **1972**, 1041–2.
(25) Orpen, A. G.; Sheldrick, G. M. *Acta Crystallog. Sect. B* **1978**, *B34*, 1992–4.
(26) Fernandez, J. M.; Johnson, B. F. G.; Lewis, J.; Raithby, P. R.; Sheldrick, G. M. *Acta Crystallogr. Sect. B* **1978**, *B34*, 1994–7.
(27) Southern, T. G.; Dixneuf, P. H.; LeMarouille, J. Y.; Grandjean, D. *Inorg. Chem. Acta* **1978**, *31*, L415–6.
(28) Bennett, J.; Pidcock, A.; Waterhouse, C. R.; Coggon, P.; McPhail, A. T. *J. Chem. Soc. A.* **1970**, 2094–9.
(29) Mather, G. G.; Pidcock, A. *J. Chem. Soc., Dalton Trans.* **1973**, 560–2.
(30) Brill, T. B.; Landon, S. J.; Towle, D. K., submitted for publication.

Table IV. Positional and Thermal Parameters for the Atoms of $CpCo[P(O)(OMe)_2]_2[P(OMe)_3]\cdot H_2O$

Atom	x	y	z	B(1,1)	B(2,2)	B(3,3)	B(1,2)	B(1,3)	B(2,3)
Co	0.28602(4)	0.27488(2)	0.06806(2)	1.17(1)	1.26(1)	1.06(1)	-0.06(1)	0.03(1)	-0.02(1)
P(1)	0.06417(9)	0.31511(5)	0.14915(4)	1.42(2)	1.30(2)	1.05(2)	-0.10(2)	0.14(2)	-0.02(2)
P(2)	0.34397(9)	0.15612(5)	0.14112(4)	1.38(2)	1.49(3)	1.38(2)	0.16(2)	-0.11(2)	0.08(2)
P(3)	0.11228(9)	0.21012(5)	-0.01581(4)	1.48(2)	1.41(3)	1.29(2)	0.11(2)	-0.15(2)	-0.17(2)
O(1)	-0.0635(2)	0.2362(1)	0.1628(1)	1.62(7)	2.09(8)	2.11(8)	-0.57(7)	0.37(6)	-0.18(7)
O(2)	0.0223(2)	0.4103(1)	0.1130(1)	2.46(8)	1.75(8)	1.59(7)	0.73(7)	0.61(6)	0.46(7)
O(3)	0.1652(2)	0.3465(1)	0.2357(1)	2.40(8)	2.28(8)	1.12(7)	-0.61(7)	-0.01(6)	-0.20(7)
O(4)	0.4417(2)	0.1699(1)	0.2169(1)	1.84(8)	2.38(9)	1.37(7)	0.08(7)	-0.26(6)	0.06(7)
O(5)	0.1807(3)	0.0971(1)	0.1584(1)	2.19(8)	2.84(9)	2.68(9)	-0.89(8)	-0.68(7)	1.49(7)
O(6)	0.4465(3)	0.0942(1)	0.0606(1)	3.16(9)	1.99(8)	1.67(7)	1.06(8)	0.11(7)	0.04(7)
O(7)	0.0366(2)	0.1150(1)	0.0008(1)	1.90(8)	1.35(7)	2.31(8)	-0.09(7)	-0.21(7)	-0.14(7)
O(8)	0.2108(2)	0.1927(1)	-0.0984(1)	2.15(8)	2.92(9)	1.27(7)	0.14(8)	0.05(6)	-0.63(7)
O(9)	-0.0589(2)	0.2606(1)	-0.0419(1)	1.64(7)	1.68(8)	1.91(7)	0.11(7)	-0.58(6)	0.20(7)
O	0.7759(3)	0.1368(2)	0.2078(1)	1.85(8)	3.57(10)	3.00(9)	-0.30(8)	-0.22(8)	1.23(8)
C(1)	-0.1103(4)	0.4334(2)	0.1364(2)	2.3(1)	2.1(1)	2.8(1)	0.81(10)	1.09(10)	0.4(1)
C(2)	0.1413(4)	0.2955(2)	0.3071(2)	3.3(1)	2.6(1)	1.2(1)	0.35(11)	0.03(10)	0.3(1)
C(3)	0.1546(4)	0.0552(2)	0.2331(2)	2.4(1)	2.4(1)	3.1(1)	-0.21(11)	0.42(11)	0.9(1)
C(4)	0.5120(4)	0.0108(2)	0.1108(2)	3.8(1)	1.9(1)	2.8(1)	1.15(12)	0.79(12)	0.3(1)
C(5)	-0.1228(4)	0.0967(2)	0.0376(2)	2.2(1)	1.8(1)	3.3(1)	-0.54(10)	0.02(11)	0.0(1)
C(6)	0.1260(4)	0.1342(2)	-0.1676(2)	3.6(1)	3.6(1)	1.6(1)	0.39(13)	-0.45(11)	-1.2(1)
C(7)	-0.0616(4)	0.3502(2)	-0.0715(2)	2.7(1)	2.0(1)	2.0(1)	0.31(11)	-0.46(10)	0.3(1)
C(10)	0.5052(4)	0.2657(2)	0.0000(2)	1.6(1)	2.3(1)	1.9(1)	-0.12(10)	0.00(8)	0.1(1)
C(11)	0.5465(3)	0.3009(2)	0.0825(2)	1.3(1)	2.4(1)	2.0(1)	-0.45(9)	0.08(9)	0.1(1)
C(12)	0.4509(4)	0.3746(2)	0.1071(2)	1.9(1)	2.4(1)	2.0(1)	-1.07(10)	0.56(9)	-0.5(1)
C(13)	0.3542(4)	0.4052(2)	0.0381(2)	1.9(1)	1.5(1)	3.0(1)	-0.27(10)	0.09(10)	0.4(1)
C(14)	0.3674(4)	0.3486(2)	-0.0275(2)	2.0(1)	2.5(1)	1.7(1)	-0.51(11)	0.22(9)	0.5(1)
H(1)	0.603(4)	0.140(2)	0.200(2)	3.4(8)					
H(2)	0.855(5)	0.171(3)	0.245(2)	5.2(10)					

THE FORM OF THE ANISOTROPIC THERMAL PARAMETER IS:

$EXP[-1/4(B(1,1)\ h^2 a^{*2} + \ldots + 2\ k\ l\ B(2,3)\ b^*\ c^*)]$.

Melt-Temp heating block and are not corrected. The molecular weight determination was made with an Hitachi Perkin-Elmer 115 vapor pressure osmometer, using CH_2Cl_2 solutions referenced to a calibration curve prepared with standard solutions of benzil.

$CpCoI_2(CO)$ was prepared according to standard literature methods.[13,14]

1:1 Reaction, $CpCoI_2(CO) + P(OMe_3)$. $CpCoI_2[P(OMe)_3]$ (2). Trimethyl phosphite (0.3 mL, 2.48 mmol) was added dropwise, as CH_2Cl_2 solution, to a 50-mL solution of 1, $CpCoI_2(CO)$ (1.0 g, 2.48 mmol), in the same solvent. Gas evolution occurred immediately, with a concomitant color change from dark purple to dark brown. After the solution was left standing for 60 min, 30 mL of heptane was added and the methylene chloride removed under reduced pressure at 25 °C to yield 0.90 g (73%) of brown, air-stable crystals of $CpCoI_2[P(OMe)_3]$ (2). The complex decomposes above 140 °C without melting and is soluble in polar organic solvents but insoluble in hydrocarbons or diethyl ether. Anal. Calcd for $C_8H_{16}CoO_3I_2P$: C, 19.07; H, 3.18; P, 6.15. Found: C, 18.92; H, 3.04; P, 6.10. Mass spectrum: 375.2, $[CpCoI[P(OMe)_3]]^+$; 251.0, $[CpCoI]^+$.

1:3 Reaction, $CpCoI_2(CO) + P(OMe)_3$. $CpCo[P(O)(OMe)_2]_2[P(OMe)_3]$ (3). A solution of $P(OMe)_3$ (0.61 mL, 5.04 mmol) in 20 mL of methylene chloride was added dropwise to a solution of 0.67 g (1.68 mmol) of complex 1 in the same solvent (150 mL). After approximately 20 min, a color change from purple to bright yellow, with accompanying gas evolution, was complete. Filtration, after the mixture was stirred for several hours, removed a small amount of brown residue. An orange oil resulted from evaporation of the solvent at 25 °C and reduced pressure. Extraction of this oil with 50 mL of acetone dissolved 3 and left a small amount of $Cp_2Co_3[P(O)(OMe)_2]_6$ (4), as an insoluble product. Addition of 100 mL of xylene to the acetone solution, followed by slow evaporation at 25 °C, produced 0.33 g (43%) of $CpCo[P(O)(OMe)_2]_2[P(OMe)_3]\cdot H_2O$ (3) as yellow needles, which were washed with hexane (2 × 50 mL) and dried in the air; mp 145 °C. Anal. Calcd for $C_{12}H_{28}CoO_{10}P_3$: C, 29.77; H, 5.83. Found: C, 29.78; H, 6.16. Mol. weight: calcd, 473.24; found, 453. The complex is soluble in acetone, CH_2Cl_2, and other polar organic solvents but insoluble in aliphatic hydrocarbons.

The melting point varied between 108 and 145 °C, depending upon the degree of hydration of this compound. The anhydrous form of 3 can be prepared by taking precautions to work with dry solvents and in a dry atmosphere. The melting point of anhydrous 3 is 108 °C. Intermediate melting points are believed to result from intermediate stages of hydration.

$Cp_2Co_3[P(O)(OMe)_2]_6$ (4). Method A. A mixture of complex 1 (0.50 g, 1.24 mmol) and trimethyl phosphite (0.15 mL, 1.24 mmol) in 30 mL of acetone was stirred for 1 h at ambient temperature. An additional 0.30 mL of $P(OMe)_3$ (3.72 mmol total) was then added. The resulting solution was degassed by N_2 purge

and subsequently refluxed for 2 h. The yellow brown solid which formed on cooling was shown to be a mixture of the desired product and cobalt oxide. Extraction with CH_2Cl_2 yielded a yellow solution from which 0.23 g (58%) of $Cp_2Co_3[P(O)(OMe)_2]_6$ (4) was isolated on concentration. The complex was identified by comparison of its spectral features, including mass spectrum, with those previously reported.[12]

Method B. A solid sample (0.040 g, 0.086 mmol) of $CpCo[P(O)(OMe)_2]_2[P(OMe)_3]$ (3) in a 5-mm o.d. tube was slowly heated in an oil bath. The complex melted at 138 °C and vigorous bubbling immediately ensued. Crystallization occurred at 145 °C but the sample was heated to 170 °C to ensure complete reaction. After the yellow solid cooled to room temperature and was washed with acetone to remove unreacted starting material, 0.022 g (0.026 mmol, 79%) of complex 4 was collected.

Method C. A mixture of anhydrous $CoCl_2$ (0.012 g, 0.09 mmol) and 3 (0.083 g, 0.18 mmol) was dissolved in 10 mL of acetone at ambient temperature. Yellow crystals of the product resulted within 30 min. After the solution was left standing overnight, 0.030 g (0.09 mmol, 35% based on Co) of yellow crystals of complex 4 was collected.

X-ray Data Collection and Structure Solution and Refinement. Crystals of $CpCo[P(O)(OMe)_2]_2[P(OMe)_3]\cdot H_2O$ (3) suitable for diffraction studies were obtained by slowly evaporating a 1:1 benzene–xylene solution. The crystal chosen was encapsulated in a glass capillary under an atmosphere of N_2. Preliminary photographic investigations indicated the crystal system, space group, and approximate cell dimensions. These and other crystallographic data are summarized in Table III. The crystal was then placed on a Syntex P3 diffractometer and shown to be suitable for diffraction on the basis of ω scans which showed the peak width at half-height to be ca. 0.16° at −100 °C. The cell parameters were then refined on the basis of 48 computer-centered reflections chosen from diverse regions of reciprocal space.

Intensity data were collected by using the ω-scan technique (variable scan range, 4.0–10.0° min^{-1}; total background time equals scan time). The intensities of four standard reflections were measured every 200 reflections. No significant deviations in the intensities of these standards were observed. The intensities of several reflections were measured at 10° increments about the diffractor vector. Empirical corrections for absorption thereby derived were subsequently applied. The data were processed by using counting statistics and a p value of 0.02 to derive standard deviations.[31]

The solution and refinement of the structure were carried out on a PDP-11 computer using local modifications of programs supplied by the Enraf-Nonius Corp.[32] The cobalt and phosphorus atoms were located by direct methods (Multan series). The positions of the remaining nonhydrogen atoms were obtained by the usual combination of structure factor and Fourier synthesis calculations and full-matrix least-squares refinements. In the least-squares refinements, the function minimized was $\sum w(|F_o| - |F_c|)^2$, where $|F_o|$ and $|F_c|$ are respectively the observed and calculated structure amplitudes and where $w = 1/\sigma^2(F_o)$. The atomic scattering factors were taken from the compilations of Cromer and Waber.[33a] Anomalous dispersion terms used were those of Cromer.[33b] After convergence of the nonhydrogen portion of the molecule in which the atoms were allowed to vibrate anisotropically, the hydrogen atoms were located in a difference Fourier synthesis. The hydrogen atoms of the water molecule were included as isotropic bodies in subsequent refinements in order to elaborate the hydrogen bonding in which they are involved. The remainder of the hydrogen atoms were placed in idealized positions by using a C–H distance of 0.95 Å and included as fixed contributions ($B_H = 4.0$). Least-squares refinement then converged to values of $R = 0.031$ and $R_w = 0.034$ where $R = \sum||F_o| - |F_c||/\sum|F_o|$ and $R_w = [\sum w(|F_o| - |F_c|)^2/\sum wF_o]^{1/2}$. A number of peaks on the order of 0.3 e $Å^{-3}$ remain in a final difference Fourier synthesis.

The final positional and thermal parameters of the refined atoms appear in Table IV. Tables of hydrogen atom positions and structure amplitudes (observed and calculated) are available.[34,35]

Acknowledgment. T.H.T. wishes to thank Mr. L. Lardear for skilled technical assistance. T.B.B. thanks Dr. R. Crecely for help with the NMR spectra.

Registry No. 1, 12012-77-0; 2, 79018-67-0; $3\cdot H_2O$, 79255-76-8; 4, 59113-93-8.

Supplementary Material Available: A table of idealized hydrogen atom positions and a listing of the observed and calculated structure amplitudes (25 pages). Ordering information is given on any current masthead page.

(31) Corfield, P. W. R.; Doedens, R. J.; Ibers, J. A. *Inorg. Chem.* **1967**, *6*, 197–204.

(32) Frenz, B. A. "The Enraf-Nonius CAD4 SDP—A Realtime System for Concurrent X-ray Data Collection and Crystal Structure Determinations", In "Computing in Crystallography"; Schenk, H., Olthof-Hazelhamp, R., Van Koningsveld, H., Bassi, G. C., Eds.; Delft University Press: Delft, Holland, 1978; pp 64–71.

(33) "International Tables for X-ray Crystallography"; Kynoch Press: Birmingham, England, 1974; Vol. IV: (a) Table 2.2B; (b) Table 2.3.1.

(34) See paragraph at end of paper regarding supplementary material.

(35) After acceptance of this paper we became aware of a report of 3 [Werner, H., Juthani, B. (*J. Organomet. Chem.* **1981**, *209*, 211)] prepared by a somewhat different route.

Preparation and Structural Characterization of the Isostructural Dichromium(II) and Dimolybdenum(II) Complexes, $M_2(O_2CCH_3)_2[o\text{-}(NMe_2)C_6H_4CH_2]_2$, Containing Two Four Atom Bridging Ligands and Surprisingly Short M≡M Quadruple Bonds

F. Albert Cotton* and Graham N. Mott

Department of Chemistry, Texas A&M University, College Station, Texas 77843

Received July 23, 1981

The title compounds have been prepared in good yields by reactions of $Cr_2(O_2CCH_3)_4$ and $Mo_2(O_2CCH_3)_4$ with $Li[o\text{-}(NMe_2)C_6H_4CH_2]$ in THF. Although the molecules of the two compounds are isostructural, each compound was obtained in a different crystal form. For $Cr_2(O_2CCH_3)_2[o\text{-}(NMe_2)C_6H_4CH_2]_2$: space group, *Pbca* with $a = 12.478$ (2) Å, $b = 19.048$ (2) Å, $c = 9.795$ (2) Å, $V = 2328$ (1) Å^3, and $Z = 4$. The molecules reside on inversion centers and all of the ligands are bridging. With the $Me_2NC_6H_4CH_2$ ligands oppositely oriented, the inversion center is the only symmetry element possessed by the molecule. The phenyl ring planes make dihedral angles of 55.0° with the central $Cr_2C_2N_2$ plane. The Cr–Cr distance is in the "supershort" range, viz., 1.870 (1) Å. The molybdenum compound crystallizes in space group $P2_1/c$ with $a = 8.577$ (2) Å, $b = 8.685$ (1) Å, $c = 15.663$ (2) Å, $\beta = 101.72$ (1)°, $V = 1142$ (1) Å^3, and $Z = 2$. The molecular structure is qualitatively the same as that of the chromium homologue with an Mo–Mo distance of 2.065 (1) Å, which is among the shortest Mo–Mo quadruple bond distances known, and the dihedral angle corresponding to the one quoted above is 57.6°.

Introduction

Several years ago Manzer[1] studied the ability of the isomeric chelating ligands **1** and **2** to improve the stability

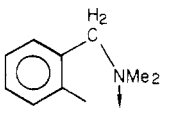

1

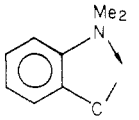

2

of M–C σ bonds in organometallic compounds of the early transition elements. He found that significant enhancements of stability did occur for mononuclear complexes of Ti^{III}, V^{III}, and Cr^{III}. Whether the increased stability is entirely a result of the chelate effect is not certain since the bulky NMe_2 groups may contribute by sterically restricting the reactivity of the M–C bonds. Whatever may be the detailed explanation for the stabilization effect, the empirical fact that there is such an effect prompted us to examine the usefulness of these ligands in preparing stable organo derivatives of multiply bonded dimetal units such as Cr_2^{4+} and Mo_2^{4+}.

We have previously reported our studies of the reactions of the lithium derivative of **1** with $Cr_2(O_2CCH_3)_4$[2] and $Mo_2(O_2CCH_3)_4$.[3] All of the products obtained contained the chelating form of **1** but with chromium no simple compound of Cr_2^{4+} was obtained. With Mo_2^{4+} we did get the expected tetrakis-chelate species, albeit with a few unexpected structural details.

We turned then to ligand **2**, which we thought would be even more likely to give products that (1) would retain the M_2^{4+} units and (2) would contain four chelating bidentate ligands. As we show in this report, expectation 1 proved correct but 2 has not been fulfilled. Ligand **2** assumes a bidentate bridging role with respect to the Cr_2^{4+} and Mo_2^{4+} species. Moreover, expectation 2 was unfulfilled also in that no more than two of these ligands could be induced to enter the products as replacements for acetate groups. Finally, the products, $M_2(O_2CCH_3)_2[o\text{-}(NMe_2)C_6H_4CH_2]_2$, both have very short M–M quadruple bonds.

For convenience in subsequent discussions in this paper, we shall use DMAB as a code for the *o*-(dimethylamino)benzyl ligand.

Experimental Section

All preparations and other operations were carried out under a dry and oxygen-free argon atmosphere, using standard Schlenk techniques. Solvents were dried and purged of molecular oxygen by distillation from sodium–potassium amalgam. $Li[o\text{-}(NMe_2)C_6H_4CH_2]$ was prepared by a literature procedure.[1]

Preparation of $Cr_2(O_2CCH_3)_2[o\text{-}(NMe_2)C_6H_4CH_2]_2$. The (*o*-(dimethylamino)benzyl)lithium reagent (0.83 g, 5.8 mmol) was dissolved in 30 mL of THF. Dichromium tetraacetate (1.0 g, 2.9 mmol) was added and the resulting dark orange solution stirred overnight. The amorphous precipitate of lithium acetate was removed by filtration, and the resultant solution was cooled to −10 °C to afford orange-red, air-sensitive crystals. Yield: 0.95 g (64%).

Preparation of $Mo_2(O_2CCH_3)_2[o\text{-}(NMe_2)C_6H_4CH_2]_2$. The molybdenum compound was prepared in a similar manner to that for the chromium compound using 1.0 g (2.3 mmol) of dimolybdenum tetraacetate and 0.66 g (4.6 mmol) of the benzyllithium reagent. After filtration the dark yellow THF solution was reduced to a volume of about 10 mL. Overnight cooling at −10 °C afforded bright yellow, air-stable crystals. Yield: 1.1 g (80%).

Several attempts were made to replace all four acetate moieties with $o\text{-}(NMe_2)C_6H_4CH_2$ groups, first by using a 1:4 dimetal tetraacetate to $o\text{-}(NMe_2)C_6H_4CH_2Li$ ratio at room temperature and then a tenfold excess of ligand with refluxing for several days in THF, but in no case was there evidence for the introduction of more than two of the DMAB ligands.

Collection and Reduction of X-ray Data. Suitable crystals of the title compounds were transferred to capillaries and sealed under a stream of argon by using epoxy cement. The crystallographic studies were conducted in the same manner for both compounds. Crystallographic data are collected in Table I. The crystal class, cell dimensions, and space groups were established in a routine manner by examination on an Enraf-Nonius CAD-4 diffractometer, operating at room temperature, and the same

(1) Manzer, L. E. *J. Am. Chem. Soc.* **1978**, *100*, 8068.
(2) Cotton, F. A.; Mott, G. N. *Organometallics* **1982**, 1, 38.
(3) Cotton, F. A.; Mott, G. N. *Inorg. Chem.* **1981**, *20*, 3896.

0276-7333/82/2301-0302$01.25/0

Table I. Crystallographic Data and Data Collection Procedures

	$Cr_2O_4N_2C_{22}H_{30}$ (1)	$Mo_2O_4N_2C_{22}H_{30}$ (2)
M	490.49	578.38
space group	$Pbca$	$P2_1/c$
a, Å	12.478 (2)	8.5766 (17)
b, Å	19.048 (2)	8.6849 (9)
c, Å	9.795 (2)	15.6631 (20)
β, deg	90.00	101.723 (14)
V, Å^3	2328 (1)	1142 (1)
Z	4	2
ρ_{calcd}, g/cm^3	1.399	1.68
μ (Mo Kα), cm^{-1}	7.177	6.687
cryst size, mm	0.35 × 0.30 × 0.30	0.15 × 0.20 × 0.20
diffractometer	Enraf Nonius CAD-4	
radiation	graphite-monochromated Mo Kα ($\lambda(\alpha)$ = 0.710 73 Å)	
collection range	$+h,+k,+l$; $0 < 2\theta \leq 50°$	$+h,+k,\pm l$; $0 < 2\theta \leq 50°$
aperture width, mm	1.50 + 1.0 tan θ	1.50 + 1.0 tan θ
prescan rejection limit	2.0	2.0
max counting time, s	30	30
prescan acceptance limit	0.02	0.02
X-ray exposure time, h	24	16
no. of unique data	2035	1993
no. of data with $I \geq 3\sigma(I)$	1363	1505
p	0.05	0.05
no. of variables	184	184
R_1	0.033	0.023
R_2	0.043	0.031
esd	1.29	0.97
largest shift/error ratio	0.01	0.05
largest peak, e/Å^3	0.43	0.24

instrument was then used to collect intensity data. The centering, autoindexing, and data collection procedures have been described previously.[4] The intensity data were collected to $2\theta = 50°$ by using the ω–2θ method and a scan range determined by $\Delta\omega = (0.54 + 0.35 \tan \theta)°$ for the Cr compound and $\Delta\omega = (0.50 + 0.35 \tan \theta)°$ for the Mo compound with a 25% extension at either end for background determination in each case. The data were monitored by measuring three standard reflections every 100 reflections. Only the reflections having intensities, I, greater than $3\sigma(I)$ were retained as observed and, after correction for Lorentz and polarization effects, were used to solve and refine the structures. With $\mu < 8$ cm^{-1} for both compounds no absorption corrections were deemed necessary.

Solution and Refinement of the Structures. $Cr_2(O_2CCH_3)_2[o\text{-}(NMe_2)C_6H_4CH_2]_2$. This compound crystallizes in the space group $Pbca$ with each molecule residing on an inversion center and half of the molecule constituting the asymmetric unit. The structure was solved by Patterson and Fourier methods and refined[5] by the full-matrix least-squares procedure. The position of the chromium atom was obtained through a three-dimensional Patterson synthesis. Three cycles of isotropic least-squares refinement gave values of $R_1 = 0.41$ and $R_2 = 0.50$ where the R_i are defined as follows: $R_1 = \sum(||F_o| - |F_c||)/\sum|F_o|$; $R_2 = [\sum w(|F_o| - |F_c|)^2/\sum w(|F_o|)^2]^{1/2}$. Subsequent least-squares cycles and difference Fourier maps located all nonhydrogen atoms, and after anisotropic refinement the discrepancy indices were $R_1 = 0.045$ and $R_2 = 0.063$. Hydrogen atoms were then located at all expected positions except for those of the acetate ion, but these three were introduced at calculated positions. With inclusion of the hydrogen atoms, the refinement proceeded to convergence at $R_1 = 0.033$ and $R_2 = 0.043$.

(4) Bino, A.; Cotton, F. A.; Fanwick, P. E. *Inorg. Chem.* **1979**, *18*, 3558.
(5) All crystallographic computing was performed on a PDP 11/60 computer at the Molecular Structure Corp., College Station, TX, using a modified version of the Enraf-Nonius Structure Determination Package.

Table II. Positional Parameters and Their Estimated Standard Deviations for $Cr_2(O_2CCH_3)_2[o\text{-}(NMe_2)C_6H_4CH_2]_2$[a]

atom	x	y	z
Cr(1)	0.03741 (4)	0.05598 (5)	0.03132 (2)
O(1)	−0.1529 (2)	−0.1064 (2)	0.0361 (1)
O(2)	−0.0627 (2)	0.0223 (2)	0.1114 (1)
N	−0.1567 (2)	0.0607 (3)	−0.0933 (1)
C(1)	−0.1387 (3)	−0.0590 (3)	0.0969 (2)
C(2)	−0.2149 (3)	−0.0993 (5)	0.1547 (2)
C(3)	−0.0441 (3)	0.2359 (3)	0.0039 (2)
C(4)	−0.0533 (2)	0.2701 (3)	−0.0713 (2)
C(5)	−0.0011 (3)	0.3851 (4)	−0.0995 (2)
C(6)	−0.0039 (3)	0.4161 (4)	−0.1700 (2)
C(7)	−0.0578 (3)	0.3339 (4)	−0.2162 (2)
C(8)	−0.1087 (3)	0.2195 (4)	−0.1907 (2)
C(9)	−0.1068 (2)	0.1862 (3)	−0.1201 (2)
C(10)	−0.2611 (13)	0.0950 (4)	−0.0583 (2)
C(11)	−0.1795 (3)	−0.0407 (4)	−0.1483 (2)
H(3A)	−0.104 (2)	0.231 (3)	0.023 (1)
H(3B)	−0.008 (3)	0.308 (3)	0.028 (1)
H(5)	0.033 (2)	0.437 (3)	−0.072 (1)
H(6)	0.026 (3)	0.479 (3)	−0.188 (2)
H(7)	−0.058 (3)	0.361 (4)	−0.266 (2)
H(8)	−0.147 (2)	0.168 (3)	−0.220 (1)
H(10A)	−0.251 (2)	0.166 (3)	−0.018 (1)
H(10B)	−0.310 (3)	0.131 (4)	−0.095 (2)
H(10C)	−0.291 (3)	0.012 (4)	−0.038 (1)
H(11A)	−0.228 (3)	−0.010 (4)	−0.187 (2)
H(11B)	−0.206 (3)	−0.123 (3)	−0.123 (1)
H(11C)	−0.116 (3)	−0.062 (3)	−0.177 (2)

[a] Estimated standard deviations in the least significant digits are shown in parentheses.

Table III. Positional Parameters and Their Estimated Standard Deviations for $Mo_2(O_2CCH_3)_2[o\text{-}(NMe_2)C_6H_4CH_2]_2$[a]

atom	x	y	z
Mo(1)	0.07968 (3)	0.09014 (3)	0.01345 (2)
O(1)	0.2533 (2)	−0.0262 (3)	−0.0386 (1)
O(2)	0.0855 (3)	−0.2236 (3)	−0.0666 (1)
N	0.0378 (3)	0.2430 (3)	−0.1133 (2)
C(1)	0.2201 (4)	−0.1614 (5)	−0.0666 (2)
C(2)	0.3457 (5)	−0.2502 (5)	−0.0989 (3)
C(3)	−0.2065 (4)	−0.0021 (5)	−0.1417 (2)
C(4)	−0.2464 (4)	0.1654 (4)	−0.1478 (2)
C(5)	−0.4057 (4)	0.2130 (5)	−0.1625 (2)
C(6)	−0.4508 (5)	0.3663 (6)	−0.1663 (3)
C(7)	−0.3370 (5)	0.4774 (5)	−0.1562 (3)
C(8)	−0.1771 (5)	0.4381 (4)	−0.1404 (2)
C(9)	−0.1323 (4)	0.2838 (4)	−0.1352 (2)
C(10)	0.0914 (4)	0.1768 (5)	−0.1895 (2)
C(11)	0.1445 (5)	0.3730 (4)	−0.0818 (3)
H(3A)	−0.293 (4)	−0.056 (4)	−0.153 (2)
H(3B)	−0.140 (4)	−0.025 (4)	−0.179 (2)
H(5)	−0.468 (4)	0.129 (4)	−0.159 (2)
H(6)	−0.552 (4)	0.382 (4)	−0.173 (2)
H(7)	−0.363 (4)	0.568 (4)	−0.152 (2)
H(8)	−0.103 (3)	0.505 (4)	−0.132 (2)
H(10A)	0.200 (4)	0.351 (4)	0.327 (2)
H(10B)	0.080 (4)	0.257 (5)	0.266 (2)
H(10C)	0.038 (5)	0.423 (5)	0.291 (3)
H(11A)	0.100 (4)	0.417 (4)	0.957 (3)
H(11B)	0.246 (4)	0.329 (4)	0.929 (2)
H(11C)	0.142 (4)	0.454 (4)	0.867 (2)

[a] Estimated standard deviations in the least significant digits are shown in parentheses.

$Mo_2(O_2CCH_3)_2[o\text{-}(NMe_2)C_6H_4CH_2]_2$. This compound crystallizes in the space group $P2_1/c$, again with the molecule on an inversion center and half of the molecule per asymmetric unit. The position of the molybdenum atom was located through a Patterson synthesis. Three cycles of isotropic least-squares refinement gave values of $R_1 = 0.29$ and $R_2 = 0.38$. Subsequent least-squares cycles and difference Fourier maps located all atoms

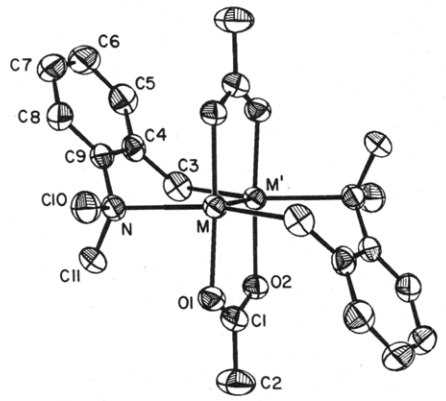

Figure 1. The molecular structure of the $Cr_2(O_2CCH_3)_2[o\text{-}(NMe_2)C_6H_4CH_2]_2$ molecule. The structure of the molybdenum homologue is virtually identical and the same atom numbering scheme applies to both molecules.

Table IV. Bond Distances (Å) for the $M_2(O_2CCH_3)_2[o\text{-}(NMe_2)C_6H_4CH_2]_2$ Molecules

	M = Cr	M = Mo
M(1)-M(1)′	1.870 (1)	2.065 (1)
-O(1)	1.992 (2)	2.097 (2)
-O(2)	2.000 (2)	2.127 (2)
-N	2.217 (2)	2.355 (3)
-C(3)	2.101 (3)	2.217 (4)
O(1)-C(1)	1.261 (4)	1.265 (5)
O(2)-C(1)	1.268 (4)	1.274 (5)
N-C(9)	1.469 (3)	1.473 (4)
-C(10)	1.502 (4)	1.479 (5)
-C(11)	1.472 (4)	1.473 (5)
C(1)-C(2)	1.508 (4)	1.494 (6)
C(3)-C(4)	1.474 (4)	1.493 (6)
-H(3A)	0.83 (3)	0.87 (4)
-H(3B)	0.95 (4)	0.92 (4)
C(4)-C(5)	1.408 (4)	1.401 (5)
-C(9)	1.409 (4)	1.405 (5)
C(5)-C(6)	1.378 (5)	1.385 (7)
-H(5)	0.85 (3)	0.91 (4)
C(6)-C(7)	1.369 (6)	1.359 (8)
-H(6)	0.80 (4)	0.86 (4)
C(7)-C(8)	1.376 (5)	1.386 (6)
-H(7)	0.98 (3)	0.82 (4)
C(8)-C(9)	1.385 (4)	1.392 (6)
-H(8)	0.88 (3)	0.85 (4)
C(10)-H(10A)	1.05 (3)	0.95 (4)
-H(10B)	1.00 (4)	0.89 (5)
-H(10C)	0.97 (4)	1.00 (5)
C(11)-H(11A)	1.00 (4)	0.87 (5)
-H(11B)	0.99 (4)	0.94 (5)
-H(11C)	0.97 (4)	1.07 (4)

except for the acetate methyl hydrogen atoms. These were introduced at calculated positions and their contributions included in F_c values, but they were not refined. With all hydrogen atoms included refinement converged at $R_1 = 0.023$ and $R_2 = 0.031$.

The final atomic positional parameters for the chromium and molybdenum compounds are listed in Tables II and III, respectively. Tables of thermal vibration parameters and positional parameters for the hydrogen atoms that were included at calculated positions but not refined are available as supplementary material.

Results and Discussion

Figure 1 shows the molecular structure for the chromium compound and the numbering scheme for the atoms. This drawing will also serve to represent the molybdenum compound since the only differences are slight changes in some internuclear distances and the atom numbering schemes are parallel. This is possible, even though the crystals are different, because in each case the molecules reside on crystallographic inversion centers. The bond lengths and bond angles are listed in Tables IV and V for both compounds.

Table V. Bond Angles (Deg) for the $M_2(O_2CCH_3)_2[o\text{-}(NMe_2)C_6H_4CH_2]_2$

	M = Cr	M = Mo
M(1)-M(1)′-O(1)	95.45 (6)	92.75 (7)
-O(2)	94.49 (7)	91.55 (7)
-N	111.88 (7)	105.92 (7)
-C(3)	95.2 (1)	96.1 (1)
O(1)-M(1)-O(2)	169.97 (8)	175.62 (9)
-N	89.18 (9)	86.7 (1)
-C(3)	89.0 (1)	86.0 (1)
O(2)-M(1)-N	85.87 (9)	91.3 (1)
-C(3)	91.5 (1)	94.4 (1)
N-M(1)-C(3)	125.9 (1)	157.1 (1)
M(1)-O(1)-C(1)	113.6 (2)	117.0 (2)
M(1)-O(2)-C(1)	113.8 (2)	116.4 (3)
M(1)-N-C(9)	109.4 (2)	107.8 (2)
-C(10)	117.4 (2)	116.2 (3)
-C(11)	99.3 (2)	99.9 (2)
C(9)-N-C(10)	109.5 (3)	111.2 (3)
-C(11)	113.6 (3)	114.4 (3)
C(10-N-C(11)	107.4 (3)	107.1 (3)
O(1)-C(1)-O(2)	122.4 (3)	122.2 (4)
-C(2)	119.1 (3)	118.0 (4)
O(2)-C(1)-C(2)	118.5 (3)	119.8 (4)
M(1)-C(3)-C(4)	118.0 (2)	117.3 (3)
-H(3A)	106 (2)	104 (3)
-H(3B)	106 (2)	104 (2)
C(4)-C(3)-H(3A)	112 (2)	110 (3)
-H(3B)	109 (2)	110 (3)
H(3A)-C(3)-H(3B)	105 (3)	111 (4)
C(3)-C(4)-C(5)	121.1 (3)	120.0 (4)
-C(9)	123.0 (3)	124.1 (4)
C(5)-C(4)-C(9)	115.7 (3)	115.8 (4)
C(4)-C(5)-C(6)	122.5 (4)	123.0 (5)
-H(5)	119 (2)	109 (3)
C(6)-C(5)-H(5)	119 (2)	127 (3)
C(5)-C(6)-C(7)	120.6 (4)	119.3 (5)
-H(6)	125 (3)	115 (3)
C(7)-C(6)-H(6)	114 (3)	126 (3)
C(6)-C(7)-C(8)	118.7 (4)	120.5 (5)
-H(7)	118 (2)	119 (4)
C(8)-C(7)-H(7)	124 (2)	120 (4)
C(7)-C(8)-C(9)	121.7 (4)	119.9 (5)
-H(8)	120 (2)	123 (3)
C(9)-C(8)-H(8)	119 (2)	117 (3)
N-C(9)-C(4)	117.4 (2)	119.1 (3)
-C(8)	121.8 (3)	119.6 (4)
C(4)-C(9)-C(8)	120.8 (3)	121.3 (4)
N-C(10)-H(10A)	112 (2)	109 (3)
-H(10B)	107 (2)	112 (3)
-H(10C)	109 (2)	112 (3)
H(10A)-C(10)-H(10B)	111 (3)	109 (4)
-H(10C)	108 (2)	103 (4)
H(10B)-C(10)-H(10C)	110 (3)	111 (4)
N-C(11)-H(11A)	116 (2)	104 (3)
-H(11B)	106 (2)	104 (3)
-H(11C)	113 (2)	110 (2)
H(11A)-C(11)-H(11B)	113 (3)	126 (4)
-H(11C)	97 (3)	107 (4)
H(11B)-C(11)-H(11C)	111 (3)	106 (3)

The molecular structure, common to both compounds even though they adopt different crystal packing patterns, is a neat and simple one, as can be clearly seen in Figure 1. The $M_2(O_2CCH_3)_2$ portion of the molecules forms a planar unit which has D_{2h} symmetry within the experimental errors. There are no significant inequalities among the M–O and C–O bond lengths. On either side of this plane the two DMAB ligands are placed so that all symmetry elements of D_{2h} are annulled except for the inversion center. The carbon atom of each DMAB ligand is trans to the nitrogen atom of the other one.

A ligand of the type of DMAB has a predilection to function as a chelating ligand with the coordinated metal

atom lying in the mean plane of the ring and the two donor atoms. In this configuration the substituents on each of the donor atoms are directed away from those on the other one. In order for the ligand-to-metal bonds to be directed towards two separate metal atoms, as they are here, it is necessary to rotate the Me_2N and H_2C groups around the ring–N and ring–C bonds, thus giving rise to the considerable dihedral angles (55.0° in the Cr compound and 57.6° in the Mo compound) between the M_2CN plane and the CC_6H_4N plane. This leads also to a relatively close approach of one of the NMe_2 methyl groups to one of the CH_2 hydrogen atoms (for M = Mo, Cr, H(3B)–H(10C) = 1.914 and 2.066 Å, respectively), and it is this which tends to disfavor the bridging role for this ligand. However, contrary to our initial expectation, this factor does not have the decisive role and the bridging arrangement is adopted. Very probably if it were not for the fact that one of the two groups that are forced to be close together is only a hydrogen atom, the bridging arrangement would not be tolerable. For example, the *diars* ligand, 1,2-bis(dimethylarsino)benzene, or others of that sort, presumably could not fulfill a bridging role.

The larger dihedral angle (57.6°) mentioned above for the molybdenum compounds as compared to that (55.0°) for the chromium compound can be attributed to the greater separation of the two molybdenum atoms.

An examination of the internal dimensions of the structure does not suggest that there would be any powerful steric opposition to the accommodation of four DMAB ligands around the M_2^{4+} unit, although one can, perhaps, envision minor steric problems. Thus, one remains uncertain as to why the formation of the $M_2(DMAB)_4$ molecules does not occur, even under forcing conditions.

The fact that the two $M_2(O_2CCH_3)_2(DMAB)_2$ compounds are molecularly isostructural but crystallize differently is mildly suprising but not alarming. Because of the selectively unequal changes in certain bond lengths and not others, the two molecules are not congruent. Thus, the M–M distances differ by ca. 0.20 Å, the various M-ligand distances differ by only 0.10–0.14 Å, and the intraligand distances are essentially unchanged. Also, the different dihedral angles between the DMAB ligand plane and the central CNMMCN plane, 55.0° in the chromium compound and 57.6° in the molybdenum compound, could also make a small difference in the energy of any given packing arrangement.

For $Mo_2(O_2CCH_3)_2(DMAB)_2$ it is interesting to compare the metal–ligand bond lengths with those found in $Mo_2[o\text{-}(CH_2NMe_2)C_6H_4]_4$, containing the ligand **1**, which is isomeric to DMAB, **2**. We noted in that earlier case[3] that the difference between the Mo–C (2.18 Å) and Mo–N (2.43 Å) distances was remarkably large and that this seemed to be due mainly to the fact that the Mo–N bonds were unusually long. The present results confirm these observations. Here we find an Mo–C bond length about 0.04 Å longer than in the previous case, but that can be attributed to the change from an sp^2 carbon atom to an sp^3 carbon atom. In the present case, we find an Mo–N bond length about 0.075 Å shorter than before. Even so, the difference between the Mo–C and Mo–N distances in the present case, 0.138 (5) Å, is quite large; it may be compared with the conventional difference in tetrahedral single-bond radii for C and N, which is 0.07 Å in the *other direction*. Evidently, the amine donor bond is weak compared to the Mo–C bond.

The structure of $Cr_2(O_2CCH_3)_2(DMAB)_2$ invites comparison with that of $Cr_2(O_2CCH_3)(o\text{-}(t\text{-}Bu)OC_6H_4)_2$, which is the only other dichromium compound known with a supershort Cr–Cr bond that contains two carboxyl ligands.[6] The two structures are very similar in all the dimensions of the central portions of the molecules. Designating the two molecules A and B in the above order for convenience, we note that the Cr–O(acetate) distances, 1.996 (3) Å in A and 1.996 (2) Å in B, are identical and the Cr–C distances, 2.101 (3) Å in A and 2.064 (3) Å in B, differ by an amount that is about equal to the difference in covalent radii for sp^3 and sp^2 carbon atoms. The Cr–Cr distance in B, 1.862 (1) Å, is scarcely different from that found here for A, viz., 1.870 (1) Å. We have here another example of the fact that the retention of as many as two carboxylate ligands is not incompatible with the existence of a supershort Cr–Cr bond. It is also interesting that for A, even more than for B, the axial positions do not appear to be so severely hindered by the bridging ligands that coordination of the THF molecules available in the preparation is sterically impossible. Instead, the indication seems to be that the $Cr_2(O_2CCH_3)_2(DMAB)_2$ molecule simply has insufficient affinity for axial ligands to attract and hold the available THF molecules.

Acknowledgment. We thank the National Science Foundation for financial support and Dr. Brian W. S. Kolthammer for assistance with the crystallography.

Registry No. 1, 79803-01-3; 2, 79803-02-4; $Cr_2(O_2CCH_3)_4$, 15020-15-2; $Mo_2(O_2CCH_3)_4$, 14221-06-8.

Supplementary Material Available: Tables of structure factors for both compounds and tables of thermal parameters and positions of nonrefined hydrogen atoms (16 pages). Ordering information is given on any current masthead page.

(6) Cotton, F. A.; Millar, M. *Inorg. Chem.* **1978**, *17*, 2014.

Ligand-Substitution Processes in Tetranuclear Carbonyl Clusters. 5. A Kinetic and Infrared Investigation of ^{13}CO Incorporation into $Co_4(CO)_9(\mu\text{-}CO)_3$ and Its Monosubstituted Derivatives

Donald J. Darensbourg,* Bradley Scott Peterson, and Raymond E. Schmidt, Jr.

Department of Chemistry, Tulane University, New Orleans, Louisiana 70118

Received July 22, 1981

A kinetic investigation of carbon monoxide exchange processes in the parent tetranuclear cobalt carbonyl cluster, $Co_4(CO)_{12}$, and its monosubstituted analogues $Co_4(CO)_{11}L$ (where L = phosphorus donor ligand) is reported. The $Co_4(CO)_{11}L$ derivatives were concluded to be isostructural on the basis of ν(CO) infrared and ^{13}C NMR spectroscopy aided by X-ray structural analysis of a representative species. The carbonyl-exchange reactions were monitored by infrared spectroscopy in the ν(CO) bridging region employing ^{13}C-labeled carbon monoxide, which has allowed as well for a detailed vibrational analysis of the ν(CO) stretching vibrations for the bridging carbonyl ligands. The activation parameters for CO dissociation in $Co_4(CO)_{12}$ and $Co_4(CO)_{11}P(OEt)_3$ were determined to be $\Delta H^* = 24.9 \pm 1.9$ and 27.5 ± 3.3 kcal/mol, and $\Delta S^* = 2.9 \pm 5.9$ and 11.0 ± 10.2 eu, respectively. Although there was no significant effect on the rate parameters for dissociative CO substitution in the tetranuclear cluster upon replacement of CO by a ligand of comparable spatial requirements (e.g., $P(OMe)_3$ or $P(OEt)_3$), dissociative CO loss was enhanced when the cluster substrate contained sterically more demanding ligands. A summary of comparative kinetic results in the stepwise phosphine or phosphite substitutional processes in $Co_4(CO)_{12}$ and $Ir_4(CO)_{12}$ species is included.

Introduction

Dissociation of a neutral ligand from low-valent metal centers, thus providing a vacancy in the coordination sphere of the metal, pervades the mechanistic literature as a principal occurrence prior to substrate binding in catalytic processes involving transition-metal complexes.[1] Kinetic investigations of representative metal complexes furnish vital information pertinent to an understanding of the influences of the various steric and electronic factors which govern ligand-substitution processes. To date much is known concerning these substitution processes in low-valent mononuclear metal carbonyl derivatives, including the reactivity of and ligand mobility in the unsaturated intermediates afforded en route to product formation.[2]

On the other hand our knowledge of the similar intricacies pertaining to ligand-substitution processes in metal clusters, the homogeneous role models for metal surfaces in both chemisorption and catalytic processes,[3-5] is just beginning to emerge. Indeed it would be fair to characterize detailed kinetic investigation in metal-cluster chemistry as a rather untested area of chemical research. These comments are not intended to detract from the many fine contributions which are presently in the chemical literature,[6-10] but their purpose is to emphasize the importance of continuing vigorous efforts in these directions.

Our attentions have been centered on displacement reactions involving dissociative loss of carbon monoxide and phosphorus donor ligands in tetranuclear metal carbonyl cluster derivatives of the group 8 metals, Co, Rh, and Ir.[7-10] Special emphasis has been placed on discernment of steric effects attributable to prior substitution by phosphorus donor ligands on subsequent ligand-substitution processes. Herein we report the kinetic and activation parameters for ^{13}CO exchange reactions with the parent dodecacarbonyl, $Co_4(CO)_9(\mu\text{-}CO)_3$ (eq 1).[8] These observations are employed

$$Co_4(CO)_{12} + n^{13}CO \rightleftharpoons Co_4(CO)_{12-n}(^{13}CO)_n + n^{12}CO \quad (1)$$

as a basis for comparison with analogous data in monosubstituted derivatives, $Co_4(CO)_8(\mu\text{-}CO)_3L$, where L is a phosphine or phosphite ligand of varying steric and electronic character (eq 2). This methodology (i.e., measurement of ^{13}CO exchange rates) minimizes the incoming ligand's associative term which often prevails in the rate expression for ligand-substitution processes where L is the entering ligand.[6a,d,g] Hence, more accurate evaluation of the dissociative CO rate parameters is achievable.

$$Co_4(CO)_{11}L + n^{13}CO \rightleftharpoons Co_4(CO)_{11-n}(^{13}CO)_nL + n^{12}CO \quad (2)$$

(1) Henrici-Olivé, G.; Olivé, S. "Coordination and Catalysis"; Verlag Chemie: New York, 1977.

(2) A short listing of some of the published work in this area includes the following: (a) Angelici, R. J. *Organomet. Chem. Rev.* **1968**, *3*, 173. (b) Werner, H. *Angew. Chem., Int. Ed. Engl.* **1968**, *7*, 930. (c) Brown, D. A. *Inorg. Chim. Acta Rev.* **1967**, *1*, 35. (d) Hyde, C. L.; Darensbourg, D. J. *Inorg. Chem.* **1973**, *12*, 1286. (e) Dobson, G. R. *Acc. Chem. Res.* **1976**, *9*, 300. (f) Lichtenberger, D. L.; Brown, T. L. *J. Am. Chem. Soc.* **1978**, *100*, 366, and other members of this series of papers. (g) Kelly, J. M.; Hermann, H.; Koerner, von Gustorf, E. *J. Chem. Soc., Chem. Commun.* **1973**, 105. (h) Darensbourg, D. J.; Graves, A. H. *Inorg. Chem.* **1979**, *18*, 1257. (i) Dobson, G. R. *Inorg. Chem.* **1980**, *19*, 1413.

(3) Muetterties, E. L. *Bull. Soc. Chim. Belg.* **1975**, *84*, 959.

(4) Muetterties, E. L. *Bull. Soc. Chim. Belg.* **1976**, *85*, 451.

(5) Muetterties, E. L. *Science (Washington, D.C.)* **1977**, *196*, 839.

(6) Some of the published reports dealing with this subject from other laboratories include the following: (a) Karel, K. J.; Norton, J. R. *J. Am. Chem. Soc.* **1974**, *96*, 6812. (b) Malik, S. K.; Poë, A. *Inorg. Chem.* **1978**, *17*, 1484. (c) Bor, G.; Dietler, U. K.; Pino, P.; Poë, A. *J. Organomet. Chem.* **1978**, *154*, 301. (d) Sonnenberger, D.; Atwood, J. D. *Inorg. Chem.* **1981**, *20*, 3243. (e) Candlin, J. P.; Shortland, A. C. *J. Organomet. Chem.* **1969**, *16*, 289. (f) Malik, S. K.; Poë, A. *Inorg. Chem.* **1979**, *18*, 1241. (g) Stuntz, G. F.; Shapley, J. R. *J. Organomet. Chem.* **1981**, *213*, 389.

(7) Darensbourg, D. J.; Incorvia, M. J. *J. Organomet. Chem.* **1979**, *171*, 89.

(8) Darensbourg, D. J.; Incorvia, M. J. *Inorg. Chem.* **1980**, *19*, 2585.

(9) Darensbourg, D. J.; Incorvia, M. J. *Inorg. Chem.* **1981**, *20*, 1911.

(10) Darensbourg, D. J.; Baldwin-Zuschke, B. J. *Inorg. Chem.*, in press.

0276-7333/82/2301-0306$01.25/0

Experimental Section

$Co_4(CO)_{12}$ and all phosphorus donor ligands were obtained from Strem Chemicals, Inc., and were used without further purification. Hexane and heptane were distilled over sodium under a nitrogen atmosphere. Carbon monoxide (93.3 atom % ^{13}CO) was obtained from Prochem, B.O.C. Ltd., London.

Preparation of $Co_4(CO)_{11}L$ Compounds. The monosubstituted cobalt cluster carbonyls $Co_4(CO)_{11}L$ (L = $(MeO)_3P$, $(EtO)_3P$, $(o\text{-}CH_3C_6H_4O)_3P$, PEt_3, and $AsPh_3$) were all prepared in a completely analogous manner.[11] Reactions were carried out with Schlenkware under an inert atmosphere.

An equimolar mixture (2 mmol) of $Co_4(CO)_{12}$ and ligand was stirred at ambient temperature in 75 mL of hexane for 4–5 h, at which point the solution was reduced to approximately 3–4 mL. The sample was then chromatographed by using flash chromatography to remove any unreacted $Co_4(CO)_{12}$ utilizing nitrogen pressure.[12] This procedure drastically reduces the amount of time the sample spends on the column, as the entire separation could be accomplished in approximately 10 min. The column (40 cm × 20 mm) was packed with silica gel (60–200 mesh) by using a hexane slurry. Eluting the sample with hexane removed the unreacted $Co_4(CO)_{12}$, and the desired product was obtained by eluting with a 20% (v/v) toluene–hexane solvent mixture.

Preparation of ^{13}CO-Enriched $Co_4(CO)_{11}L$ Compounds. Samples of $Co_4(CO)_{11-n}(^{13}CO)_nL$ for ^{13}C NMR investigations were synthesized and purified as described above from enriched $Co_4(CO)_{12}$ (prepared from $Co_4(CO)_{12}$ under an atmosphere of ^{13}CO at 40 °C for 24 h). Alternatively, ^{13}CO incorporation was achieved by direct CO exchange with $Co_4(CO)_{11}L$ at 40 °C for ~1 day, followed by purification by column chromatography. This latter procedure is not applicable for the ^{13}CO enrichment of $Co_4(CO)_{11}L$ derivatives where L is a labile ligand (e.g., L = PPh_3 or $AsPh_3$).

Kinetic Measurements of ^{13}CO-Exchange Reactions. A 100-ml Schlenk flask, containing the preweighed sample, was fitted with a rubber septum secured by copper wire and was evacuated under vacuum. The flask was then equilibrated in a constant-temperature bath, and an atmosphere (760 torr) of ^{13}CO (93.3 atom % ^{13}C) was introduced into it. Heptane (15 mL, distilled over sodium) was then syringed into the flask. The reaction flask was agitated to effect sample dissolution (~15 s), and the timer was started immediately thereafter. Samples (~0.7 mL) were withdrawn at noted time intervals with a hypodermic syringe for infrared analysis.

Infrared Measurements and Vibrational Analysis. The infrared spectra were recorded in 1.0-mm matched NaCl sealed cells on a Perkin-Elmer 283B spectrophotometer equipped with an Infrared Data Station. Spectra recorded for the ^{13}CO-exchange reactions were the average of four (added repetitively) scanned spectra employing the PECDS software package provided by Perkin-Elmer. The spectra were calibrated against a water-vapor spectrum below 2000 cm^{-1} and against a CO spectrum above 2000 cm^{-1}.

Initial CO stretching force constants for the bridging CO region in the $Co_4(CO)_{11}L$ derivatives were obtained by altering the parameters computed for the parent, $Co_4(CO)_{12}$, species.[8] That is, both F_{CO} values in $Co_4(CO)_{11}L$ were slightly lowered relative to that in $Co_4(CO)_{12}$, with the F_{CO} parameter corresponding to the two CO groups bridging the cobalt atom bearing the unique substituent being lowered to the greater extent. The trial force constants were refined by use of the ^{13}CO frequency data and an iterative computer program that adjusts a set of force constants common to a group of isotopically substituted molecules to give simultaneously a least-squares fit between the observed and calculated frequencies for all the molecules. The trial force constants were refined to reproduce the observed ^{12}CO and ^{13}CO vibrations to within an average of ≤0.8 cm^{-1}.

^{13}C NMR Measurements. The ^{13}C NMR spectra were recorded on a JEOL FX60 operated at 15.03 MHz with an internal deuterium lock. Samples were run in either $CDCl_3$ or CD_2Cl_2 solvents in 10-mm tubes. Spectra were determined by employing a sweep width of 4000 Hz (16K data block) with an acquisition time of 2 s, a pulse repetition rate of 5 s, and a flip angle of 30°.

(11) This is a modification of that previously reported: Cetini, G.; Gambino, O.; Rossetti, R.; Stanghellini, P. L. *Inorg. Chem.* **1968**, *7*, 609.
(12) Still, W. C.; Kahn, M.; Mitra, A. *J. Org. Chem.* **1978**, *43*, 2923.

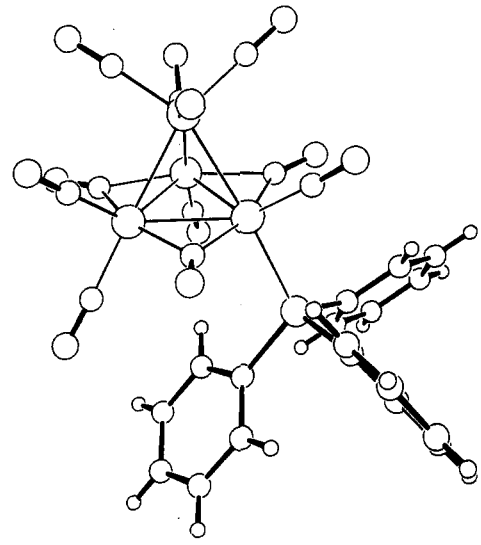

Figure 1. Perspective ORTEP drawing of the $Co_4(CO)_{11}[PPh_3]$ molecule (taken from ref 9).

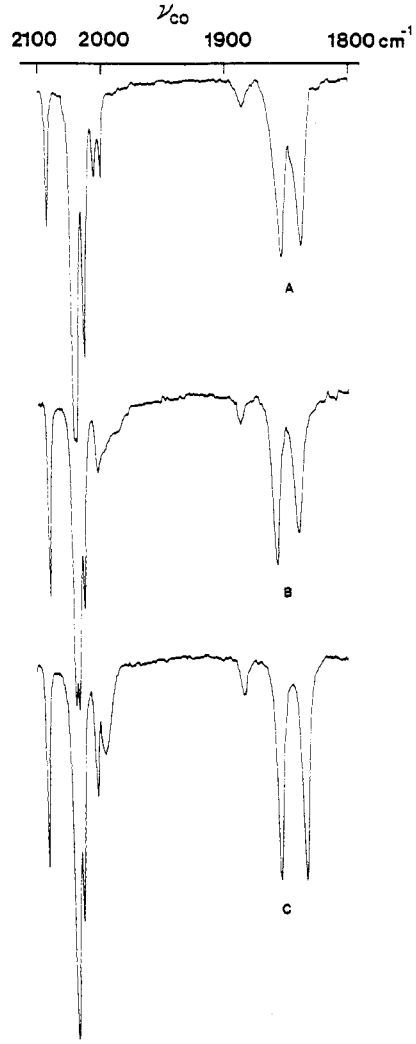

Figure 2. Infrared spectra in $\nu(CO)$ region in heptane solution. (A) $Co_4(CO)_{11}P(OEt)_3$; (B) $Co_4(CO)_{11}PPh_3$; (C) $Co_4(CO)_{11}PEt_3$.

Results and Discussion

The salient features of the solid-state structure of $Co_4(CO)_{11}PPh_3$ are reiterated in Figure 1, where the triphenylphosphine ligand is seen to occupy an axial coordination site in the tetranuclear cluster.[9] The solution

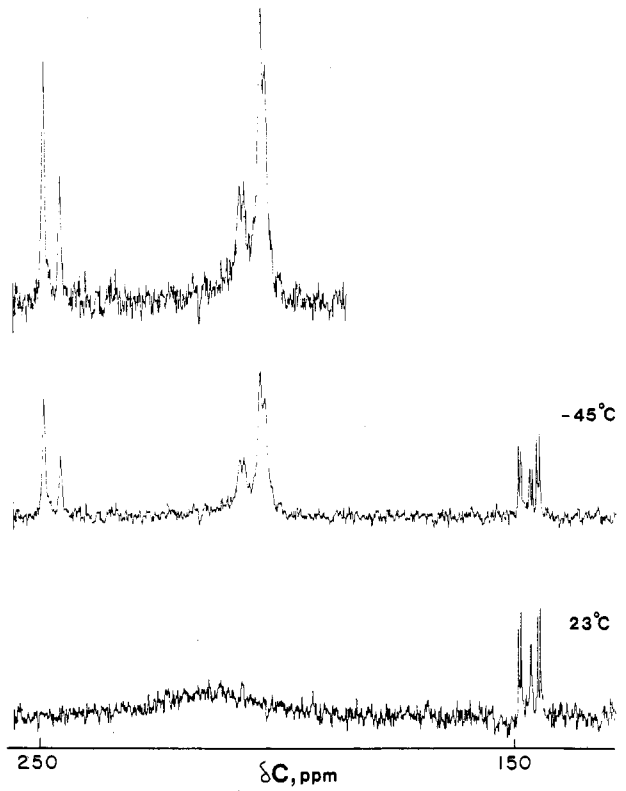

Figure 3. ^{13}C FT NMR spectrum of $Co_4(CO)_{11}PPh_3$ in $CDCl_3$ at −45 °C and ambient temperature.

Table I. ^{13}C Chemical Shifts (Ppm) in $Co_4(CO)_{11}L$

	L			
	PPh_3[a]	PEt_3[b]	$P(OMe)_3$[c]	CO[d]
bridging	249.8	249.2	248.2	
	245.8	245.7	245.6	243.1
equatorial	202.1	201.3	198.0	
	201.0	199.7	197.2	
axial	197.1	196.7	196.1	195.9
apical	195.9		193.7	191.9

[a] Spectrum determined in $CDCl_3$ at −45 °C (see Figure 3 3). [b] Spectrum determined in CD_2Cl_2 at −69 °C. [c] Taken from ref 13. [d] Taken from: Evans, J.; Johnson, B. F. G.; Lewis, J.; Matheson, T. W. *J. Am. Chem. Soc.* 1975, *97*, 1245.

structure of this derivative, as evinced by ν(CO) infrared and ^{13}C NMR spectroscopy, is consistent with this formulation (see Figure 2B and 3). Brown and co-workers[13] have reported the low-temperature ^{13}C NMR spectrum for $Co_4(CO)_{11}P(OMe)_3$ which displays a very close resemblance to that noted here for the PPh_3 analogue (Table I). The most distinguishing feature in both these spectra lies in the bridging CO region (most downfield peaks) where two carbon resonances in relative intensity ratio 1:2 are observed, with the two bridging CO groups bonded to the basal cobalt atom bearing the phosphorus ligand being more downfield as anticipated.[14] Assignment of the terminal carbon resonances are on a more tenuous basis. Quadrupole broadening by the ^{59}Co nucleus prohibits the observation of ^{13}C–P coupling in the ^{13}C NMR spectra of these derivatives. If we assume the generally observed trend of an upfield shift of carbonyl carbon peaks with decreasing metal–carbon interaction, as revealed by the M–C bond distances, the peak assignments are as listed in Table I. This designation is congruous with that made by Stuntz and Shapley[15] for $Ir_4(CO)_{11}PPh_2Me$.

Table II. Infrared Spectra in the ν(CO) Region of $Co_4(CO)_{11}L$ Derivatives[a]

L	ν(CO), cm^{-1}
PEt_3	2086, 2040, 2030, 2006, 1996, 1885, 1856, 1836
PPh_3	2084, 2044, 2039, 2029, 2006, 1993, 1881, 1854, 1835
$AsPh_3$	2085, 2046, 2041, 2031, 2007, 1995, 1881, 1853, 1834
$P(OMe)_3$	2091, 2051, 2046, 2032, 2017, 2003, 1889, 1858, 1843
$P(OEt)_3$	2089, 2048, 2044, 2030, 2013, 2001, 1887, 1857, 1841
$P(Otolyl)_3$	2090, 2049, 2042, 2033 2011, 2002, 1885, 1856, 1844

[a] Measured in heptane solution, accurate to ±2 cm^{-1}.

Table III. Rate Data for CO-Exchange Processes in $Co_4(CO)_{11}L$ Species[a]

L	temp, °C	$k \times 10^4$, s^{-1} [b]
CO	40.0	3.27 ± 0.20
	43.0	5.10 ± 0.26
	45.0	6.10 ± 0.15
	45.0	5.53 ± 0.08
	52.0	14.5 ± 0.35
	56.0	24.5 ± 3.8
	56.0	23.5 ± 3.0
$P(OEt)_3$	35.0	1.50 ± 0.14
	37.5	2.05 ± 0.14
	40.0	3.37 ± 0.13
	45.0	6.79 ± 0.41
	50.0	12.1 ± 1.6
PEt_3	35.0	8.87 ± 0.61
	40.0	15.6 ± 0.62

[a] Determined in heptane solution under an atmosphere of ^{13}CO. [b] Error limits for rate constants represent 95% confidence limits.

Table II contains the ν(CO) spectra for a series of $Co_4(CO)_{11}L$ derivatives where L is varied over a wide range of donor/acceptor ratios,[16] and Figure 2 further illustrates the great deal of conformity evident in these spectra. Hence, the spectral data strongly suggest that all the $Co_4(CO)_{11}L$ species are isostructural, with the lowest energy isomer being that in which the unique ligand (L) resides at an axial location. Therefore, variations in the reactivity of these $Co_4(CO)_{11}L$ derivatives may be ascribed only to changes in the electronic and/or steric character of the ligand (L), and not to structural variations in the clusters.

We have previously reported a rough estimate for the rate of CO dissociation in the parent $Co_4(CO)_{12}$ species as determined by ^{13}CO incorporation at ambient temperature.[8] It is of utmost importance to more accurately quantify the rate parameters associated with dissociative CO loss in the dodecacarbonyl derivative in order to make meaningful comparisons with the corresponding values obtained as a function of substitution with electron-donor ligands at the metal centers. Table III lists the rate constants for ^{13}CO exchange with the substrate $Co_4(CO)_{12}$ as a function of temperature. These rate constants were measured by employing the ν(CO) vibrational modes in the bridging CO region as described in our previous publication[8] and were calculated by assuming three dissociative CO ligands in $Co_4(CO)_{12}$.[17] This procedure is based on

(13) Cohen, M. A.; Kidd, D. R.; Brown, T. L. *J. Am. Chem. Soc.* **1975**, *97*, 4408.
(14) Todd, L. J.; Wilkinson, J. R. *J. Organomet. Chem.* **1974**, *77*, 1.
(15) Stuntz, G. F.; Shapley, J. R. *J. Am. Chem. Soc.* **1977**, *99*, 607.
(16) Bodner, G. M.; May, M. P.; McKinney, L. E. *Inorg. Chem.* **1980**, *19*, 1951.

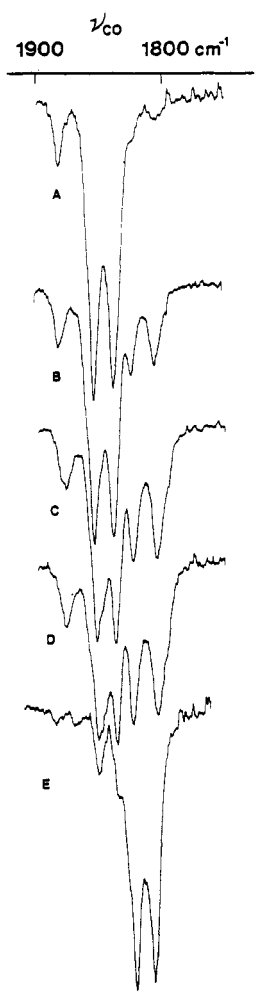

Figure 4. Time-dependent infrared spectra in the ν(CO) bridging region for the exchange reaction between $Co_4(CO)_{11}P(OEt)_3$ and ^{13}CO at 40 °C. (A) Spectrum after 5 min; (B) Spectrum after 52 min; (C) Spectrum after 119 min; (D) Spectrum after 185 min; (E) Spectrum at "infinity" reading.

the fact that intramolecular CO rearrangement is fast relative to the CO dissociation process. No observable variations in the rate of ^{13}C incorporation were noted for CO pressures ranging from 380 to 1140 torr.

Reaction 3 has been demonstrated to be strongly dependent on the nature of the incoming ligand (L), with measurable rates by conventional techniques being possible only when L is isotopically labeled carbon monoxide.[8]

$$Co_4(CO)_{12} + L \rightarrow Co_4(CO)_{11}L + CO \qquad (3)$$

Similar ^{13}CO exchange rate data were determined in the monosubstituted $Co_4(CO)_{11}L$ species. This procedure of obtaining rate data for CO dissociation eliminates the incoming ligand's associative term which is often dominant in the rate expression for ligand-substitution processes.

The infrared traces in the ν(CO) bridging region observed during the incorporation of ^{13}CO into $Co_4(CO)_{11}P(OEt)_3$ are depicted in Figure 4. For the $Co_4(CO)_{12}$ complex it has previously been demonstrated that the interaction force constants between terminal and bridging CO groups may be considered as being zero.[9,18] By using this assumption in the $Co_4(CO)_{11}L$ derivatives, it should be possible to analyze their spectra in the ν(CO) bridging region (Figure 4) in terms of progressive formation of *only* five ^{13}CO-substituted cluster fragments in addition to the starting all-^{12}CO species (see Figure 5). This is indeed found to be the case, for the spectral band assignments compiled in Tables IV and V were computed by employing a restricted CO force field involving only the bridging CO ligands. Table VI lists comparative CO stretching force constants for the bridging CO groups in $Co_4(CO)_{11}L$ species where L varies in donor/acceptor ratio from that of PEt_3

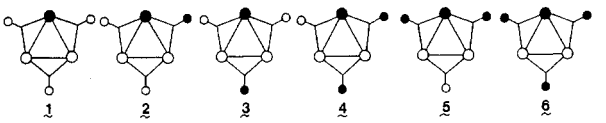

Figure 5. Possible isotopic species involving the bridging CO ligands in $Co_4(CO)_{11}L$.

Table IV. Calculated and Observed CO Stretching Frequencies in the Bridging Region of $Co_4(CO)_{11}P(OEt)_3$[a]

molecule	ν(CO), cm^{-1} obsd[b]	ν(CO), cm^{-1} calcd[c]	symmetry
all-^{12}CO, 1	1879.4	1879.3	A′
	1849.7	1849.0	A′
	1834.3	1835.0	A″
mono-^{13}CO, 2		1878.8	A
	1843.0	1843.3	A
	1801.3	1800.2	A
mono-^{13}CO, 3		1853.1	A′
	1833.4	1833.4	A′
		1835.0	A″
di-^{13}CO, 4		1846.9	A
	1833.4	1833.6	A
		1800.0	A
di-^{13}CO, 5		1878.3	A′
	1808.2	1808.8	A′
	1798.8	1794.1	A″
all-^{13}CO, 6	1838.3	1837.4	A′
	1807.4	1807.9	A′
	1794.6	1794.1	A″

[a] Spectra were recorded in heptane solution. [b] The observed frequencies are accurate to ±1.0 cm^{-1}. [c] The CO stretching force field arrived at in this computation is summarized in Table VI. Average error in calculated frequencies = 0.5 cm^{-1} or 0.029%.

Table V. Calculated and Observed CO Stretching Frequencies in the Bridging Region of $Co_4(CO)_{11}PEt_3$[a]

molecule	ν(CO), cm^{-1} obsd[b]	ν(CO), cm^{-1} calcd[c]	symmetry
all-^{12}CO, 1	1876.6	1872.8	A′
	1848.4	1848.6	A′
	1827.2	1827.6	A″
mono-^{13}CO, 2		1868.8	A
	1841.8	1842.7	A
	1796.2	1796.5	A
mono-^{13}CO, 3	1862.8	1861.8	A′
	1819.6	1818.1	A′
		1827.6	A″
di-^{13}CO, 4		1851.7	A
	1819.6	1819.0	A
	1796.2	1795.8	A
di-^{13}CO, 5		1865.8	A′
	1814.1	1814.2	A′
	1787.4	1786.9	A″
all-^{13}CO, 6		1831.1	A′
	1806.9	1807.4	A′
	1787.4	1786.9	A″

[a] Spectra were recorded in heptane solution. [b] The observed frequencies are accurate to ±1.0 cm^{-1}. [c] The CO stretching force field arrived at in this computation is summarized in Table VI. Average error in calculated frequencies = 0.8 cm^{-1} or 0.044%.

(17) Because of the accuracy with which these parameters are measured, no correction for the fact that 93.3 atom % ^{13}C-labeled carbon monoxide was employed in these investigations.

(18) Bor, G.; Sbrignadello, G.; Noack, K. *Helv. Chim. Acta* **1975**, *58*, 815.

Table VI. Comparative Bridging CO Stretching Force Constants in $Co_4(CO)_{11}L$ Derivatives

	force constant, mdyn/Å[a]			
L	F_{CO} (1)	F_{CO} (2)	$F_{CO,CO}$ (1)	$F_{CO,CO}$ (2)
CO	14.23_2		0.17_4	
$P(OEt)_3$	13.71_1	14.23_6	0.07_1	0.11_6
PEt_3	13.71_5	14.01_4	0.12_6	0.22_9

[a] F_{CO} (1) (bridging to Co atom bearing L) and $F_{CO,CO}$ (1) (both interacting CO groups bound to Co atom bearing L).

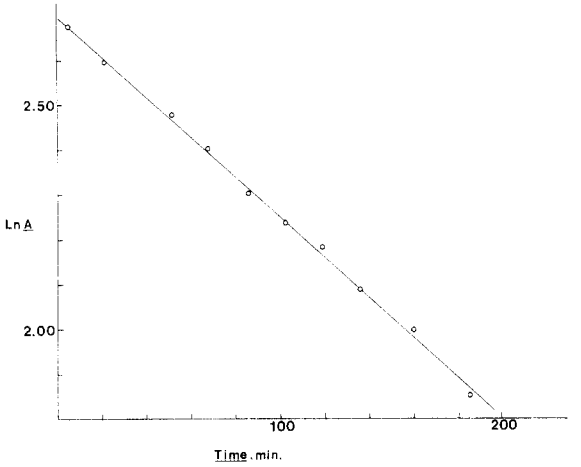

Figure 6. First-order rate plot for the disappearance of substrate for the reaction of $Co_4(CO)_{11}P(OEt)_3$ with ^{13}CO in heptane at 40 °C. $k_{obsd} = 7.49 \times 10^{-5}$ s^{-1}, which when multiplied by 9 and divided by 2 affords $k = 3.37 \times 10^{-4}$ s^{-1}. Because reactions were monitored in the ν(CO) bridging region, and hence incorporation of ^{13}CO at the eight terminal CO positions goes unnoticed, the k_{obsd} must be multiplied by the factor 9, i.e., there are nine positions which among the single incoming ^{13}CO ligand may distribute itself. Division of k_{obsd} by the factor 2 arises from the assumption that there is selective dissociation of one of the two axial CO groups.

to CO. As is apparent in Table VI these vibrational parameters indicate some increase in electron density, which is passed on to the CO groups, at the metal atom bearing the phosphine substituent. On the other hand, the carbonyl ligand bridging unsubstituted cobalt atoms appears to be unaffected. A similar conclusion can be reached from ^{13}C NMR data, where the CO group bridging unsubstituted cobalt atoms has a carbon resonance resembling that of the bridging CO groups in $Co_4(CO)_{12}$.[13]

Table III presents the kinetic parameters for CO-exchange processes in the monosubstituted $Co_4(CO)_{11}L$ derivatives, where L = $P(OEt)_3$ and PEt_3. The rate constants were calculated by assuming two dissociative CO ligands in $Co_4(CO)_{11}L$. Figures 6 and 7 contain representative plots of the data employed in computing rate constants and activation parameters for dissociative CO loss in these cobalt cluster species. Comparative rate constants and activation parameters for the system investigated herein, as well as those previously reported,[7,8] are collected in Table VII. Attempts at measuring the rate of ^{13}CO incorporation into the PPh_3 and $AsPh_3$ analogues were hampered by the more facile reaction involving donor-ligand replacement (eq 4), where the $AsPh_3$ ligand was observed to dissociate more rapidly than PPh_3.

$$Co_4(CO)_{11}L + {}^{13}CO \rightarrow Co_4(CO)_{11}({}^{13}CO) + L \quad (4)$$

At high pressures of carbon monoxide, declusterification of $Co_4(CO)_{12}$ to afford $Co_2(CO)_8$ is proposed to proceed via a mechanism involving $Co_4(CO)_{13}$, which is formed by the breaking of one Co–Co bond with concomitant formation

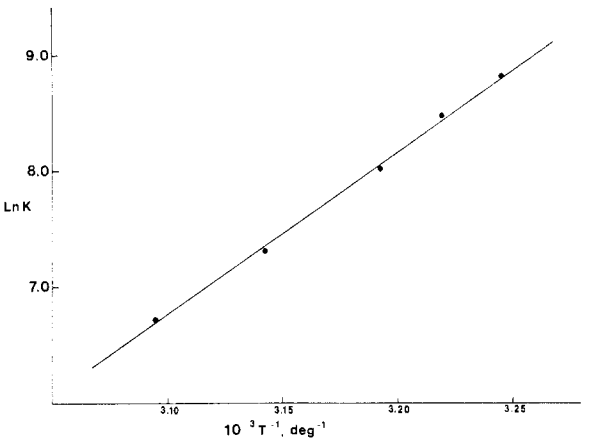

Figure 7. Arrhenius plot of $-\ln k$ vs. $1/T$ for the CO exchange reaction of $Co_4(CO)_{11}P(OEt)_3$ with ^{13}CO in heptane.

Table VII. Comparative Rate and Activation Parameters for Carbon Monoxide Displacement in $Co_4(CO)_{11}L$

L	cone angle,[a] deg	10^4k, s^{-1} [b]	ΔH^* [c]	ΔS^* [c]
$P(OMe)_3$ [d]	107	2.03 (1.00)	26.8 ± 1.0	8.2 ± 3.5
CO	~95	3.27 (1.61)	24.9 ± 1.9	2.9 ± 5.9
$P(OEt)_3$	109	3.37 (1.66)	27.5 ± 3.3	11.0 ± 10.2
PEt_3	132	15.6 (7.68)	*e*	*e*
$P(OMe)_3$ [f]	107	4.77 (2.35)	27.1 ± 1.1	10.7 ± 3.7

[a] Taken from: Tolman, C. A. *Chem. Rev.* **1977**, *77*, 313. [b] Relative rate data are listed in parentheses. Reactions were carried out at 40.0 °C. [c] Error limits for activation parameters represent 95% confidence limits. [d] Taken from ref 8 where the incoming ligand employed was PPh_3. [e] These parameters were not measured in this instance. [f] Taken from ref 8 for CO displacement in $Co_4(CO)_{10}[P(OMe)_3]_2$ where $P(OMe)_3$ was the incoming ligand employed.

of a Co–CO bond and a repositioning of one bridging CO ligand.[6c] In this connection it is noteworthy that the kinetic parameters, coupled with the absence of dimer production under the mild temperature and CO pressure of this study, strongly argue against the formation of an intermediate or transition state of this type for these CO-exchange reactions. That is, CO exchange is a lower energy process than declusterification (as shown, e.g., in eq 5 where $\text{rate}_1 > \text{rate}_2$).

$$Co_4(CO)_{12} + n^{13}CO \underset{}{\overset{\text{rate}_1}{\rightleftharpoons}} Co_4(CO)_{12-n}({}^{13}CO)_n + n^{12}CO \xrightarrow{\text{rate}_2} Co_2(CO)_8 \quad (5)$$

A slightly revised relative order of reactivity for dissociative CO substitutional processes in $Co_4(CO)_{12}$ with progressive substitution of $P(OMe)_3$ is provided in Table VII and eq 6. These data dramatically illustrate the

$$Co_4(CO)_{12} \xrightarrow{1.00} Co_4(CO)_{11}P(OMe)_3 \xrightarrow{0.62} Co_4(CO)_{10}[P(OMe)_3]_2 \xrightarrow{1.46} Co_4(CO)_9[P(OMe)_3]_3 \quad (6)$$

absence of an effect on the rate parameters for CO loss in the Co_4 cluster with successive replacement of CO by the small, good π-acceptor $P(OMe)_3$ ligand. However, there is a small, yet significant, increase in the rate of dissociative CO loss as L is altered in the $Co_4(CO)_{11}L$ derivatives, increasing in the order $P(OMe)_3 < P(OEt)_3 < PEt_3$. Unfortunately, our efforts to extend these investigations to sterically more demanding ligands, e.g., PPh_3, was prohibited by the ready loss of the ligand L. More extensive

studies of the rate of dissociative CO loss in Ir_4 cluster species as a function of the phosphorus donor ligand indicate the spatial requirements of these ligands to be a major consideration in determining these rates.[10,19] Similar, more pronounced, arguments should apply in the Co_4 systems reported upon herein and are indeed consistent with the rate constant vs. cone-angle data summarized in Table VII.[20]

If steric acceleration is a governing factor in the enhancement of the rate of CO loss as the size of the phosphorus donor ligand increases in these $Co_4(CO)_{11}L$ derivatives, then the coordination site of the CO group which is dissociated must be in rather close proximity to the phosphorus ligand. Crystallographically defined models reveal this to be either the equatorial CO group on the phosphorus-bearing cobalt atom or one of the two axial CO groups.[21] X-ray structural results show these latter CO groups to be slightly more weakly bound than the equatorial CO ligand of the Co–P moiety,[9] hence making them more likely candidates for dissociation. Nevertheless, CO loss at the metal center which bears the phosphorus donor ligand with a concomitant facile CO migration leading to unsaturation at an adjacent metal site cannot be ruled out.[22-24] Unfortunately, because of intramolecular ligand rearrangements in the substrate molecule, which occur on a time scale faster than dissociative ligand loss, definitive answers to questions of this type will go unresolved.

In light of the prominence of steric effects in substitutional processes in metal carbonyl clusters, a consideration of importance in any general discussion of progressive rate enhancement for dissociative CO loss with ligand substitution must take account of structural differences. For example, in the cobalt complex containing the small trimethyl phosphite ligands, $Co_4(CO)_{10}[P(OMe)_3]_2$, the two phosphite ligands occupy axial sites[9] whereas in $Ir_4(CO)_{10}[PPh_3]_2$ and $Rh_4(CO)_{10}[PPh_3]_2$ the phosphine ligands are found in both axial and equatorial positions,[25,26] apparently as a result of spatial requirements.

The enormous rate acceleration for CO dissociation observed during the stepwise phosphine substitution of $Ir_4(CO)_{12}$ to give $Ir_4(CO)_9[PPh_3]_3$ is often regarded as being supportive evidence that electronic interactions can be transmitted from neighboring metal atoms to the active catalytic center in a cluster. Such a conclusion is arrived at by neglecting steric factors. Indeed, our work,[19,27] as well as that of others,[28] demonstrates that this observation is not a general one for a wide range of phosphorus donor ligands. It is our contention that a sizable contribution to the rate acceleration for stepwise substitution in the Ir_4 system arises from sterically induced dissociation.

Acknowledgment. The financial support of the National Science Foundation through Grant CHE 80-09233 is greatly appreciated.

Registry No. $Co_4(CO)_{12}$, 17786-31-1; $Co_4(CO)_{11}(PEt_3)$, 79664-00-9; $Co_4(CO)_{11}(PPh_3)$, 12336-57-1; $Co_4(CO)_{11}(AsPh_3)$, 12336-56-0; $Co_4(CO)_{11}(P(OMe)3)$, 56277-17-9; $Co_4(CO)_{11}(P(OEt)_3)$, 79664-01-0; $Co_4(CO)_{11}(P(o\text{-tolyl})_3)$, 79664-02-1.

(19) Darensbourg D. J.; Baldwin-Zusche, B. J. "Abstracts of Papers", 181st National Meeting of the American Chemical Society, Atlanta, GA, March 1981; American Chemical Society: Washington, D.C., 1981; INOR 190.

(20) As evident in Table VII the rates of CO dissociation in the closely related $Co_4(CO)_{11}L$ derivatives, where L = $P(OMe)_3$ and $P(OEt)_3$, are quite similar. An important difference, however, is that the incoming ligand was PPh_3 for the $Co_4(CO)_{11}P(OMe)_3$ rate study and ^{13}CO for the corresponding $Co_4(CO)_{11}P(OEt)_3$ investigation. These observations would support the conclusion that the measured rate constants are dissociative in character. It also argues strongly against a mechanism involving phosphorus ligand dissociation (eq 4) followed by rapid intramolecular rearrangement of the incorporated ^{13}CO and replacement of CO by the phosphorus ligand via the reverse of eq 4.

(21) This is the assumption employed in the derivation of the specific rate constants as computed from k_{obsd} (see Table III).

(22) Atwood, J. D.; Brown, T. L. *J. Am. Chem. Soc.* **1976**, *98*, 3160.

(23) Darensbourg, M. Y.; Atwood, J. L.; Burch, R. R., Jr.; Hunter, W. E.; Walker, N. *J. Am. Chem. Soc.* **1979**, *101*, 2631.

(24) Darensbourg, D. J.; Burch, R. R., Jr.; Darensbourg, M. Y. *Inorg. Chem.* **1978**, *17*, 2677.

(25) Albano, V.; Bellon, P.; Scatturin, V. *Chem. Commun.* **1967**, 730.

(26) Heaton, B. T.; Longhetti, L.; Mingos, D. M. P.; Briant, C. E.; Minshall, P. C.; Theobald, B. R. C.; Garlaschelli, L.; Sartorelli, U. *J. Organomet. Chem.* **1981**, *213*, 333.

(27) Darensbourg, D. J.; Baldwin-Zuschke, B. J., Tenth International Conference on Organometallic Chemistry, Toronto, Canada, August 1981, p 25.

(28) Sonnenberger, D. C.; Atwood, J. D., Tenth International Conference on Organometallic Chemistry, Toronto, Canada, August 1981, p 24.

Reaction of 1-Alkyl-1,1′-diphosphaferrocene Monoanions with Acyl Chlorides. Synthesis and Zwitterionic Structure of Stable λ^3,λ^5-Diphosphaferrocenes

Bernard Deschamps,[1a] Jean Fischer,[1b] François Mathey,*[1a] André Mitschler,[1b] and Louis Ricard[1b]

Laboratoire CNRS-SNPE, BP No. 28, 94320 Thiais, and Laboratoire de Cristallochimie, ERA 08, Institut le Bel, Université Louis Pasteur, 67070 Strasbourg Cedex, France

Received August 19, 1981

Reaction of *tert*-butyllithium with 3,3′,4,4′-tetramethyl-1,1′-diphosphaferrocene (1) affords the 1-*tert*-butyl P anion **2a** which reacts in situ with acyl chlorides to give the corresponding stable 1-*tert*-butyl-1-acyl-1,1′-diphosphaferrocenes **4** (acyl = MeCO) and **5** (acyl = PhCO). The X-ray crystal structure analysis of **5** shows that the pentavalent phosphorus atom is not bonded to iron and that these λ^3,λ^5-diphosphaferrocenes are better represented as (η^5-phospholyl)(η^4-phospholium)iron zwitterions. The rather short Fe···λ^5-P distance (2.565 Å) nevertheless indicates a strong through-space interaction which seems to be responsible for the unusual stability of these species. Pyrolysis of **5** under vacuum at 170 °C affords diphosphaferrocene **1**, 1-*tert*-butylphosphole **7**, probably through a migration of the benzoyl group from phosphorus to iron, and 1′-phenyl-1-phosphaferrocene **8**, by a mechanism certainly related to a phosphole to cyclopentadiene conversion described earlier.

Following their discovery in 1978, improved synthetic procedures have increased the availability of 1,1′-diphosphaferrocenes. The 3,3′,4,4′-tetramethyl derivative **1** is now available on a kilogram scale. This has allowed us to launch a thorough investigation of their chemistry which has revealed many unique features for compounds of this type. Thus, they are acylated,[3] formylated,[3] and carboxylated to the ring carbons through electrophilic substitutions in strict analogy to ferrocenes. On the contrary, reactive alkyl halides liberate the phosphole rings through alkylation at phosphorus.[4] Similarly, their phosphorus lone pairs behave as donors and will coordinate to an additional metal center.[4] In another vein, preliminary electrochemical studies[5] have shown that 1,1′-diphosphaferrocenes are reversibly oxidized to 1,1′-diphosphaferricinium ions less readily than ferrocenes. Finally, in a previous paper,[6] we demonstrated that alkyllithiums attacked these species at phosphorus to give monoanions such as **2**, but we were unable to isolate the expected λ^3,λ^5-diphosphaferrocenes **3** by alkylation of **2**. The search for stable species such as **3** is the subject of this paper.

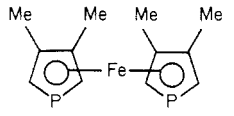

1

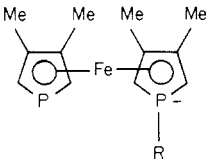

2a, R = *t*-Bu

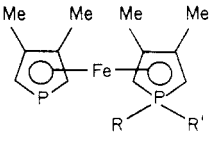

3

Results and Discussion

Synthesis. In our preliminary experiments we reacted **2a** with methyl iodide and benzyl bromide. In both cases, after the usual workup, we recovered the starting diphosphaferrocene **1** because of spontaneous reductive elimination of the two alkyl groups on the λ^5-phosphorus of **3**. Similar reductive eliminations from λ^5-phosphorus have been previously reported for λ^5-phosphorins[7] but only at high temperature (≃300 °C). We then sought to improve the stability of the desired λ^3,λ^5-diphosphaferrocenes by replacing the alkyl P substituents by other groups. Thus, we discovered that the reaction of **2a** with acetyl and benzoyl chlorides afforded the stable compounds **4** and **5** which were purified by column chromatography on silica gel. We attributed to them a partly zwitterionic structure

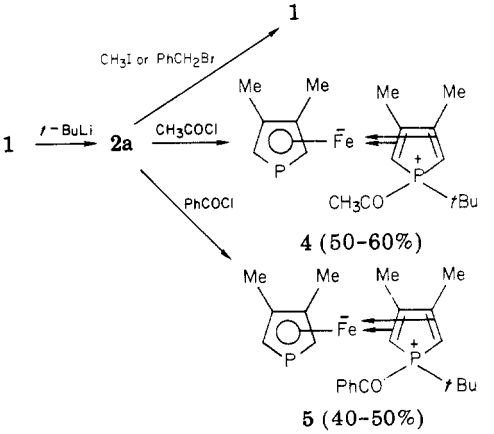

on the basis of the X-ray crystal structure analysis of **5** (vide infra). These compounds show numerous interesting spectral features. First, their mass spectra indicate a tendency to loose the λ^5-P substituents, producing the starting diphosphaferrocene **1**. Indeed, in both cases the *m/e* 278 peak (1) is the base peak. It also seems quite clear that the main decomposition path involves the primary departure of the *tert*-butyl group in both cases. Accordingly, the structure of **5** shows that the *t*-Bu–P bond is

(1) (a) Laboratoire CNRS-SNPE. (b) Institut Le Bel.
(2) G. De Lauzon, F. Mathey, and M. Simalty, *J. Organomet. Chem.*, **156**, C33 (1978).
(3) G. De Lauzon, B. Deschamps, J. Fischer, F. Mathey, and A. Mitschler, *J. Am. Chem. Soc.*, **102**, 994 (1980).
(4) G. De Lauzon, B. Deschamps, and F. Mathey, *Nouv. J. Chim.*, **4**, 683 (1980).
(5) P. Tordo, personal communication.
(6) B. Deschamps, J. Fischer, F. Mathey, and A. Mitschler, *Inorg. Chem.*, **20**, 3252 (1981).
(7) G. Märkl, *Phosphorus Sulfur*, **3**, 77 (1977).

0276-7333/82/2301-0312$01.25/0

longer and weaker (1.876 Å) than the PhCO–P bond (1.858 Å). The ^{1}H NMR spectra also give some insight into the electronic structure of these compounds. Indeed, the *tert*-butyl groups of **4** and **5** are very shielded: **4**, δ(*t*-Bu) 0.70 ($CDCl_3$); **5** δ(*t*-Bu) 0.72 (CD_2Cl_2). These values can be compared to that recorded for a normal phospholium salt such as **6**: δ(*t*-Bu) 1.38 ($CDCl_3$). This shielding seems to indicate the presence of a direct through-space interaction between Fe^- and P^+–*t*-Bu, partly "neutralizing" the positive charge on phosphorus. Consistent with this suggestion, it should be stressed that the λ^5-phosphorus of **4** and **5** resonates at high field but in the low part of the range normally associated with the pentacoordinate species: −2.4 ppm ($CDCl_3$) for **4** and −8.5 ppm (C_6D_6) for **5** vs. +50.3 ppm ($CDCl_3$) for **6**.

Another curious feature has been noted for the ^{1}H NMR spectrum of **5**. Whereas the *t*-Bu signal appears as one sharp doublet, all other methyl or CH groups of the phosphole rings give rise to two equal and independent signals (we have checked that this is not due to J(H–P) couplings). This doubling does not occur in the spectrum of **4**. The X-ray crystal structure of **5** gives a clue for explaining this phenomenon. Indeed, the phenyl ring of the benzoyl group crosses the plane of the λ^3-phospholyl moiety, and the distance between the λ^3-phosphorus (P_1) and the plane of the phenyl (PL_4) is very short (0.60 Å). Thus the rotation of the λ^5-phospholyl ring about the ring Fe vector is very probably hindered, with P_2 only oscillating between the verticals of C_2 and P_1 (see Figure 1) due to P_1 and Me–C_2 interactions with the phenyl ring. Thus the two sides of both phosphole rings become inequivalent and the λ^3-phospholyl C_1H is very shielded: δ(C_1H in **5**) 2.85 vs. δ 3.01 (C_4H in **5**), 3.31 (λ^3-phospholyl CH in **4**), and 3.71 (CH in **1**). The short distance between P_1 and PL_4 also explains why it is impossible to attack the second phosphorus atom of **5** even with a great excess of *tert*-butyllithium and benzoyl chloride to obtain a product similar to **11** which was described in our previous paper[6] when using MeI instead of PhCOCl. Finally it must be noted that, in the ^{13}C NMR spectra, the carbonyl carbons of **4** and **5** appear in the normal region with a very strong ^1J(C–P) coupling similar to what was noted in acylphosphonium zwitterions.[8] δ(CO in **4**) 186.2 (^1J(C–P) = 90.3 Hz ($CDCl_3$)), δ(CO in **5**) 175.2 (^1J(C–P) = 100.4 Hz (C_6D_6)).

In view of the mass spectral data of **5**, we wanted to determine if **5** would regenerate **1** upon pyrolysis. At 170 °C under vacuum, **5** decomposed and indeed gave some λ^3,λ^3-diphosphaferrocene **1** but also yielded two other unexpected products **7** and **8**. The structure of **7** was

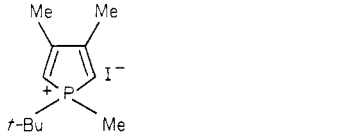

6

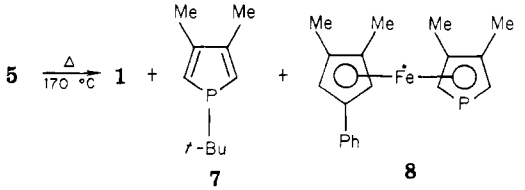

7 **8**

established by comparing its ^{1}H and ^{31}P NMR spectra with those of an authenticated sample[9] and by converting it into its P sulfide which was analyzed (correct melting point and ^{1}H NMR spectrum). The mechanism for the formation of **7** probably includes a migration of the benzoyl group from phosphorus to iron followed by the decomplexation of the tervalent phosphole.

The structure of **8** was established by mass, ^{1}H NMR, and ^{31}P NMR spectroscopy. Since **8** was not very stable, it was difficult to obtain a perfectly correct C, H, Fe, and P analysis as with other monophosphaferrocenes. Nevertheless, the experimental ratio Fe/P was found to be 1.01. Moreover, in the mass spectrum (70 eV, 80 °C), the molecular peak (m/e 336) was also the base peak as usual for these species.[10] No other peak exceeded a 6% intensity. The ^{31}P spectrum ($CDCl_3$) showed a very shielded phosphorus at δ(^{31}P(**8**)) −75 as expected. The ^{1}H NMR spectrum was also in perfect agreement with the proposed formula. Although **8** was only obtained in 13% yield, the two-step conversion of a diphosphaferrocene into a monophosphaferrocene (**1** → **5** → **8**) remains noteworthy. The mechanism for this pyrolysis is certainly complicated, but previous work in our laboratory throws some light on this problem. Indeed, we have established the sequence shown in eq 1.[11] There is an obvious relationship between this

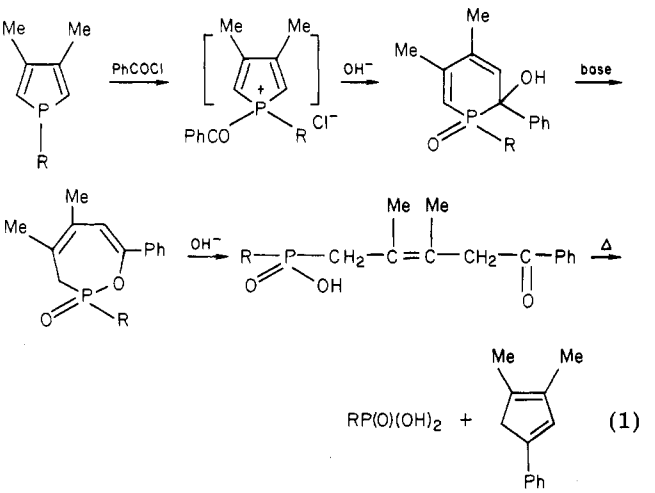

(1)

sequence which converts an acylphospholium salt into a substituted cyclopentadiene and the formation of **8** from **5**, although, according to preliminary experiments (thermolysis of **5** in the presence of hydrated basic alumina), it does not seem that OH^- anions are necessary in the present case.

Crystal Structure of 5

$C_{23}H_{30}FeOP_2$ (**5**): monoclinic, space group $P2_1/n$, a = 17.564 (6) Å, b = 12.254 (4) Å, c = 10.346 (4) Å, β = 96.39 (2)°, Z = 4. Atomic coordinates and thermal parameters with their estimated standard deviations are listed in Tables I and II. Intermolecular contacts less than 3 Å are given in Table III.

The crystal structure of **5** consists of discrete molecules in which an iron atom is sandwiched between two phosphole rings. The individual molecules are linked only by hydrogen bonds and van der Waals type interactions.

Figure 1 shows an ORTEP[12] plot of a molecule together with the labeling scheme used. Hydrogen atoms are omitted for clarity, and the other atoms are represented

(8) R. Appel and M. Montenarh, *Chem. Ber.*, **110**, 2368 (1977).

(9) F. Mathey, *Tetrahedron*, **28**, 4171 (1972).
(10) F. Mathey, *J. Organomet. Chem.*, **139**, 77 (1977).
(11) F. Mathey, *Tetrahedron*, **29**, 707 (1973); *Bull. Soc. Chim. Fr.*, 2783 (1973).
(12) C. K. Johnson, Report ORNL 3794, Oak Ridge, Tenn., 1965.

Table III. Intermolecular Contacts (Å) Less Than 3 Å and Intermolecular Contacts around P2 Less Than 3.5 Å

A···B		equiv positns[a]
C3···H1C15	2.82	1/001
C9···HC21	3.00	2/101
C12···HC21	3.00	2/101
O···HC10	2.75	2/011
O···HC19	2.78	2/011
C20···H2C6	2.98	2/001
C21···H3C11	2.70	2/000
C21···H2C12	2.93	2/000
H1C5···H1C16	2.96	2/011
H1C5···H2C16	2.90	2/001
H2C5···H3C14	2.99	2/001
H1C6···HC20	2.89	2/100
H2C6···H1C15	2.91	1/001
H2C6···HC20	2.70	2/100
H1C11···H1C16	2.64	1/001
H2C12···HC22	2.52	2/101
H2C14···HC23	2.66	2/001
H2C15···H3C16	2.86	1/001
H3C15···HC21	2.77	2/101
H3C15···HC22	2.73	2/001
H3C15···HC23	2.66	2/001
H2C16···HC20	2.99	2/011
P2···C18	2.938 (9)	
P2···C19	3.277 (9)	
P2···HC19	2.90	

[a] The relative coordinates of the atom in column A are listed in Table I. The atoms in column B have their atom atomic parameters specified by *I*/*uvw* which denotes how the parameters can be derived from the corresponding atoms in the crystal unit: $1, x, y, z; \bar{1}, \bar{x}, \bar{y}, \bar{z}; 2, {}^1/_2 + x, {}^1/_2 - y, {}^1/_2 + z; \bar{2}, {}^1/_2 - x, {}^1/_2 + y, {}^1/_2 - z$. *u*, *v*, and *w* code a lattice transition as $u\vec{a} + v\vec{b} + w\vec{c}$.

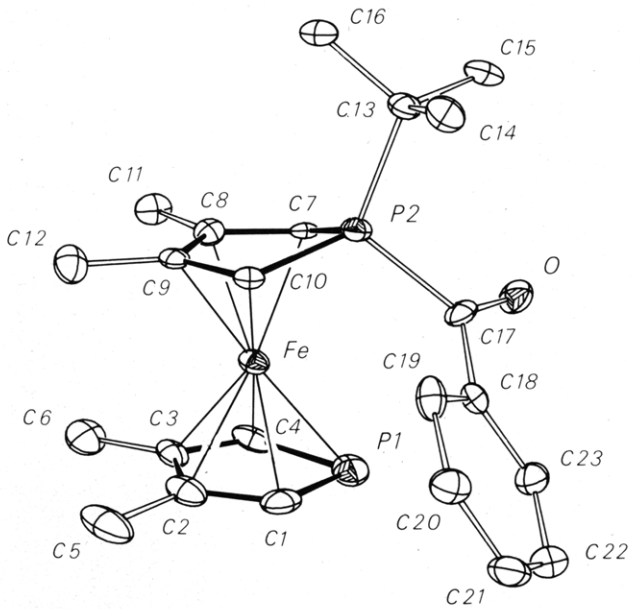

Figure 1.

by their ellipsoids of thermal motion scaled to enclose 50% of the electron density. Figure 2 shows the projection of one phosphole ring on the plane of the other. Table IV gives selected bond lengths (Å), angles (deg), and average values. Table V gives the least-squares planes of interest.

The key point to be discussed here is the bonding mode of the λ^5-phospholyl moiety with the iron atom. The Fe···P_2 distance [2.565 (2) Å] is clearly outside of the normal length range associated with phosphorus–iron bonds. Indeed, one of the longest previously determined Fe···P bonds was found in the structure of t-$Bu_3P{\rightarrow}Fe(CO)_4$: 2.364 (1) Å.[13] Thus, the structure is certainly partly

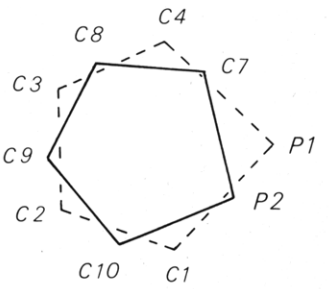

Figure 2.

Table IV. Selected Bond Lengths (Å) and Angles (Deg) with Their Estimated Standard Deviation

Bond Lengths

Fe-P1	2.289 (3)	C7-C8	1.41 (1)
Fe-C1	2.042 (8)	C8-C9	1.41 (1)
Fe-C2	2.075 (9)	C9-C10	1.43 (1)
Fe-C3	2.089 (8)	av C-C	1.418 (6)
Fe-C4	2.092 (7)		
av Fe-C	2.074 (4)	C8-C11	1.51 (1)
		C9-C12	1.52 (1)
Fe-P2	2.565 (2)	P2-C13	1.876 (7)
Fe-C7	2.078 (7)	P2-C17	1.858 (8)
Fe-C8	2.018 (7)	C13-C14	1.53 (1)
Fe-C9	2.011 (7)	C13-C15	1.53 (1)
Fe-C10	2.087 (8)	C13-C16	1.52 (1)
P1-C1	1.74 (1)	C17-O	1.217 (9)
P1-C4	1.76 (1)	C17-C18	1.52 (1)
av P-C	1.752 (7)	C18-C19*	1.40 (1)
		C19-C20*	1.39 (1)
C1-C2	1.39 (1)	C20-C21*	1.38 (1)
C2-C3	1.39 (1)	C21-C22*	1.37 (1)
C3-C4	1.42 (1)	C22-C23*	1.38 (1)
av C-C	1.402 (7)	C23-C18*	1.40 (1)
		av C-C*	1.388 (4)
C2-C5	1.52 (1)		
C3-C6	1.50 (1)		
P2-C7	1.746 (8)		
P2-C10	1.763 (8)		
av P-C	1.754 (6)		

Bond Angles

C1-P1-C4	87.1 (4)	C7-C8-C11	123.0 (7)
P1-C1-C2	115.8 (7)	C10-C9-C12	120.6 (7)
P1-C4-C3	114.3 (7)	C9-C8-C11	124.7 (7)
av P-C-C	115.0 (5)	C8-C9-C12	126.9 (7)
		C7-P2-C13	117.1 (3)
C1-C2-C3	111.6 (9)	C10-P2-C13	118.3 (3)
C4-C3-C2	111.0 (9)	C13-P2-C17	105.6 (3)
av C-C-C	111.3 (6)	C7-P2-C17	108.8 (4)
		C10-P2-C17	116.2 (4)
C1-C2-C5	125 (1)	P2-C17-O	116.4 (6)
C3-C2-C5	123 (1)	P2-C17-C18	120.2 (7)
C4-C3-C6	123.3 (9)		
C2-C3-C6	125.5 (9)		
C7-P2-C10	90.5 (4)		
P2-C7-C8	110.6 (6)		
P2-C10-C9	109.0 (6)		
av P-C-C	109.8 (4)		
C7-C8-C9	112.3 (7)		
C10-C9-C8	112.4 (7)		
av C-C-C	112.3 (5)		

zwitterionic as represented in formula **5**. Nevertheless, both the folding of the λ^5-phospholyl ring around the C_7–C_{10} axis (20.8°) and the Fe···P_2 distance are much smaller than those in other known η^4-complexed λ^5-phosphole rings such as in **9**, **10**, and **11**. Thus, it is quite

(13) J. Pickardt, L. Rösch, and H. Schumann, *J. Organomet. Chem.*, **107**, 241 (1976).
(14) K. Yasufuku, A. Amada, K. Aoki, and H. Yamazaki, *J. Am. Chem. Soc.*, **102**, 4363 (1980).

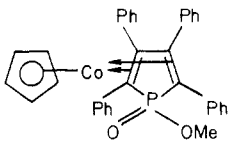

9[14] (folding 30.3°)

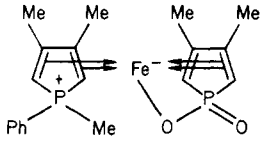

10[6] (folding 34.3° (P^+ moiety), Fe···P^+ = 2.732 (1) Å)

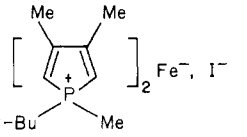

11[6] (folding 31°, Fe···P = 2.688 (1) Å)

clear that there is a rather strong through-space interaction between iron and the P_2 phosphorus in agreement with what has been suggested on the basis of ^1H and ^{31}P NMR spectroscopy, such that **5** is probably best represented as a bond–no bond resonance hybrid.

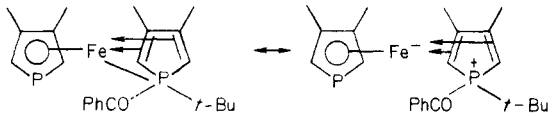

5

This through-space interaction is probably responsible for the stability of these compounds. The question then is how can an acyl group facilitate such an Fe···P interaction whereas it does not exist in compounds with only alkyl or aryl groups on phosphorus. A direct interaction between the iron atom and the carbonyl carbon being excluded [Fe···C = O 3.17 Å], we suggest that the acyl group increases the positive charge on phosphorus, thus creating a stronger Coulombic attraction between iron and P_2 phosphorus. As a whole the λ^5-phospholyl becomes more electron attracting and, consequently, the λ^3-phospholyl–iron bond is weakened as monitored by Fe···P_1 [2.289 (3) Å] and Fe···PL_1 [1.670 (1) Å] distances (see Table V) which are abnormally long when compared with other (η^5-phospholyl)iron complexes.[3,15] Due to this longer Fe···PL_1 distance, the λ^3-phospholyl ring is now strictly planar whereas it is significantly folded (0.67–3.84°) around its Cα–Cα' axis in **1**.[3] Finally, the endo position of the acyl group explains why it migrates easily to iron in the thermal decomposition of **5**. This facile migration of the benzoyl group between phosphorus and iron together with the lack of steric control on the relative positions of *tert*-butyl and benzoyl groups (according to the structural data the *tert*-butyl group could not interact strongly with the λ^3-phospholyl ring if it were endo) suggests that the initial attack of benzoyl chloride onto **2a** takes place at iron.

Experimental Section

NMR spectra [chemical shifts in parts per million from internal Me_4Si for ^1H and ^{31}C and from H_3PO_4 (external reference) for ^{31}P; δ positive for downfield shifts in all cases] were recorded for proton on a Bruker WP 80 instrument at 80 MHz and on a Varian XL 100 A instrument at 100 MHz and for carbon and phosphorus on a Bruker WP 80 instrument at 20.15 and 32.44 MHz, respectively. We thank Mrs. M. J. Pouet and M. P. Simonnin (ENSCP Laboratory) for the ^{31}P decoupled proton spectra. Mass spectra were recorded on a MS 30 AEI spectrometer at 70 eV.

(15) F. Mathey, A. Mitschler, and R. Weiss, *J. Am. Chem. Soc.*, **99**, 3537 (1977).

Table V. Significant Mean Planes

no.		dist,[a] Å	equations[b]	χ^2
PL1	P1°	−0.002 (3)	$a = -0.0334$, $b = 0.0958$,	14
	C1°	0.023 (9)	$c = -0.9948$, $d = -10.9740$	
	C2°	−0.015 (8)		
	C3°	−0.003 (8)		
	C4°	0.014 (8)		
	C5	−0.151 (10)		
	C6	−0.088 (10)		
	Fe	1.670 (1)		
PL2	P2°	0	$a = -0.3315$, $b = 0.3688$,	0
	C7°	0	$c = -0.8684$, $d = -6.3009$	
	C10°	0		
PL3	C7°	−0.002 (7)	$a = -0.0723$, $b = 0.1461$,	0
	C8°	0.003 (8)	$c = -0.9866$, $d = -7.5108$	
	C9°	−0.003 (7)		
	C10°	0.002 (8)		
	P2	0.439 (2)		
	Fe	−1.629 (1)		
	C11	0.017 (9)		
	C12	0.049 (9)		
PL4	C18°	0.000 (9)	$a = 0.5620$, $b = -0.4703$,	4
	C19°	−0.008 (9)	$c = -0.6805$, $d = -4.1348$	
	C20°	0.013 (9)		
	C21°	−0.012 (10)		
	C22°	0.002 (10)		
	C23°	0.003 (9)		
	C17	0.021 (8)		
	O	0.457 (6)		
	P2	−0.602 (2)		
	P1	−2.964 (3)		

Dihedral Angles

PL1/PL2 = 24.5° PL2/PL3 = 20.8°
PL1/PL3 = 3.7°

[a] Atom labels marked with a degree sign are used for computing the mean plane. [b] Least-squares planes are computed according to D. M. Blow, *Acta Crystallogr.*, 13, 168 (1960).

All reactions were carried out under argon. Chromatographic separations were performed on a silica gel column (70–230 mesh Merck).

(η^4-1-*tert*-Butyl-1-benzoyl-3,4-dimethylphospholium)(η^5-3,4-dimethylphospholyl)iron (5). To a stirred solution of 3,3′,4,4′-tetramethyl-1,1′-diphosphaferrocene (**1**)[3] (1.39 g, 5×10^{-3} mol) in THF (100 cm^3) was added at −80 °C 5×10^{-3} mol of *t*-BuLi in pentane. After 30 min, 0.5 cm^3 (5×10^{-3} mol) of freshly distilled benzoyl chloride was added to this solution. After 1 h, the reaction mixture was allowed to come to room temperature. The THF was evaporated and the residue was chromatographed with ether. The green fraction was rechromatographed with ether–pentane (10–90): $R_f \approx 0.5$; yield 0.9–1.1 g (40–50%); mp 205 °C dec (ether–pentane at low temperature); ^1H NMR (CD_2Cl_2) δ 0.72 (d, ^3J(H–P) = 14 Hz, 9 H, *t*-Bu), 1.27 (m, 2 H, CH–P_2), 1.60 and 1.77 (2s, 3 + 3 H, Me–C_3 and Me–C_9), 1.97 and 2.01 (2s, 3 + 3 H, Me–C_2 and Me–C_3), 2.85 (d, ^2J(H–P) = 36 Hz, 1 H, H–C_1), 3.01 (d, ^2J(H–P) = 36 Hz, 1 H, H–C_4), 7.6 (m, 3 H, Ph meta and para), 8.2 (m, 2 H, Ph ortho); ^{31}P NMR (C_6D_6) δ −8.5 and −63.7 (J(P–P) = 2.5 Hz); IR (KBr) ν(CO) 1592–1612 cm^{-1}; mass spectrum (70 eV, 180 °C), *m/e* 440 (M, 17%), 383 (M − *t*-Bu, 13%), 355 (383 − CO, 21%), 2 78 (**1**, 100%). In ether solution, **5** shows an absorption at 740 mm in the visible part of the spectrum which is not present in the spectra of either **1** or **4**; this absorption is probably responsible for the green color of **5** whereas **1** and **4** are red.

(η^4-1-*tert*-Butyl-1-acetyl-3,4-dimethylphospholium)(η^5-3,4-dimethylphospholyl)iron (4). The procedure is the same as above except with 0.35 cm^3 (5×10^{-3} mol) of acetyl chloride: $R_f \approx 0.6$; yield 0.9–1.1 g (50–60%); red crystals; mp 80 °C; ^1H NMR ($CDCl_3$) δ 0.70 (d, ^3J(H–P) = 13.7 Hz, 9 H, *t*-Bu), 1.07 (d, ^2J(H–P) = 23.9 Hz, 2 H, CH–P–λ^5), 1.77 (s, 6 H, Me), 1.97 (d, J = 0.9 Hz, 6 H, Me), 2.82 (dd, J = 4.9 and 1.5 Hz, 3 H, Me–CO), 3.31 (d, ^2J(H–P) = 35.9 Hz, 2 H, CH–P–λ^3); ^{31}P NMR ($CDCl_3$) δ −2.4 and −65.5 (J(P–P) $\simeq$ 0 Hz); IR (KBr) ν(CO) 1650 cm^{-1}; mass spectrum (70 eV, 200 °C), *m/e* 378 (M, 13%), 335 (M − COMe, 1%), 321

(M - t-Bu, 11%), 306 (321 - Me, 4%), 293 (321 - CO, 5%), 278 (1, 100%).

Thermolysis of 5

1 (0.5 g) is thermolyzed at 170 °C in a Büchi GKR 50 tubular furnace under vacuum. 7 distils slowly: yield 0.07 g (36%); $\delta(^{31}P(7))$ 24.1 ($CDCl_3$) (lit.[9] 27.5 ppm ($CDCl_3$)), correct ^1H NMR spectrum. P sulfide of 7 (through reaction with S_8 in benzene): mp 156 °C (lit.[9] 160 °C); correct ^1H NMR spectrum and C, H, and P elemental analysis.

The residue of the thermolysis is recovered in hexane and chromatographed after filtration of the insoluble products (hexane–benzene (90–10)). The first red band is 1 and the second red band 8: yield 0.05 g (13%); ^1H NMR ($CDCl_3$) δ 1.77 (s, 6 H, Me), 1.88 (s, 6 H, Me), 3.22 (d, ^2J(H–P) = 36 Hz, 2 H, CH–P), 4.37 (s, 2 H, CH of the Cp ring), 7.10 (m, 5 H, Ph).

X-ray Data Collection and Processing

Suitable single crystals of 5 were obtained by recrystallization in a mixture of CH_2Cl_2–pentane at −20 °C. Preliminary crystal data of 5 were determined by a systematic search in reciprocal space using a Philips PW1100/16 automatic diffractometer and Cu Kα radiations; crystals of 5 are monoclinic. The lattice parameters were refined at 18 ± 2 °C by using 25 high-angle reflections evenly distributed in reciprocal space and standard Philipps programs.[16] Final results are as follows: a = 17.564 (6) Å, b = 12.254 (4) Å, c = 10.346 (4) Å, β = 96.39 (2)°, V = 2213 Å.^{3} With four molecules of $C_{23}H_{30}FeOP_2$ per unit cell (mol wt 440.29), ρ_{calcd} = 1.32 g·cm^{-3}, and ρ_{obsd}(measured by flotation in an aqueous KI solution) = 1.30 ± 0.02 g·cm^{-3}. The space group is $P2_1/n$ (C_h^5), F_{000} = 928, and μ = 69.87 cm^{-1}.

A parallelepiped crystal of dimensions 0.26 × 0.11 × 0.10 mm was related in a Lindemann glass capillary and mounted on a rotation-free goniometer head. All quantitative data were obtained from a Philips PW1100/16 four-circle diffractometer controlled by a P852 computer using graphite-monochromated Cu Kα radiation and the standard software. Intensity data were collected by using the flying $\theta/2\theta$ step–scan technique with a scan rate of 0.020° s^{-1}, a total scan width of [1.20 + (Cu Kα_1,α_2 splitting)]°, and a step width of 0.050°. An attenuator was inserted in the diffracted beam whenever the scan count exceeded 60 000 counts·s^{-1}. The intensities of three standard reflections were monitored throughout the data collection at intervals of 2 h; they did not vary by more than 2% during the entire data collection period. All 3194 hkl and $hk\bar{l}$ independent reflections within 0.045° < sin θ/λ < 0.544° were recorded. The raw step–scan data were converted to intensities by using the Lehman–Larson algorithm[17] which were then corrected for Lorentz, polarization, and absorption factors, the latter being computed by numerical integration[18] (transmission factors between 0.2596 and 0.4226). For each reflection, the estimated variance from counting statistics was $\sigma^2(I) = \sigma^2_{count} + (pI)^2$.

For all computations the Enraf-Nonius SDP/V17 package[19] was used on a PDP 11/60 computer.

The structure was solved by using direct methods; the most probable phase set of MULTAN[20] was the correct one, and the E map permitted the location of all nonhydrogen atoms. A difference map computed at the end of isotropic refinement revealed electron density close to the computed positions for hydrogen atoms. These were included in all subsequent calculations with anisotropic temperature factors of 8 Å and with their computed coordinates using a C–H distance of 0.95 Å, but they were not refined.

Atomic coordinates and individual anisotropic thermal parameters for all nonhydrogen atoms were refined by full-matrix least squares minimizing $\sum w(|Fo| - |Fc|)^2$ and using 1457 independent reflections having $F^2 \geq 3\sigma(F^2)$ with p = 0.08. Refinement converged to $R_1 = \sum||Fo| - |Fc||/\sum|Fo| = 0.061$ and $R_2 = (\sum w||Fo| - |Fc||^2/\sum w|Fo|^2)^{1/2} = 0.077$. The standard deviation of a unit weight observation was 1.55.

Registry No. 1, 67887-86-9; 4, 79664-03-2; 5, 79664-04-3; 6, 38066-27-2; 7, 38066-25-0; 7 sulfide, 38066-26-1; 8, 79664-05-4.

Supplementary Material Available: Tables of atomic coordinates and thermal parameters (Tables I and II) and a listing of observed and calculated structure factors (×10) (Table VI) (12 pages). Ordering information is given on any current masthead page.

(16) "Computer Controlled Single Crystal X-ray Diffractometer PW1100, Users manual", N.V. Philips Gloeilampenfabricken, Eindhoven, The Netherlands, 1974.

(17) M. S. Lehmann and F. K. Larsen, *Acta Crystallogr., Sect. A*, **A30**, 580 (1974).

(18) W. R. Busing "Crystallographic Computing", F. R. Ahmed, Ed., Munksgaard, Copenhagen, 1970, p 319.

(19) B. A. Frenz, "Computing in Crystallography", H. Schenk, R. Olthof-Hazenkamp, H. Van Konigsveld, and G. C. Bassi, Eds.; Delft University Press, Delft, Holland, 1978, p 64.

(20) G. Germain, P. Main, and M. M. Woolfson, *Acta Crystallogr., Sect. B* **B26**, 274 (1970); *Acta Crystallogr., Sect. A* **A27**, 368 (1971).

Aluminum Chloride Catalyzed Skeletal Rearrangement of Permethylated Cyclic Polysilanes

Mitsuo Ishikawa,*[1a] Makoto Watanabe,[1a] Jun Iyoda,[1b] Haruhiko Ikeda,[1a] and Makoto Kumada*[1a]

Department of Synthetic Chemistry, Faculty of Engineering, Kyoto University, Kyoto 606, and Government Industrial Research Institute, Osaka, Ikeda, Osaka 563, Japan

Received September 30, 1981

The aluminum chloride catalyzed skeletal rearrangement of mono- and bicyclic polysilanes has been investigated. Treatment of dodecamethylcyclohexasilane with a catalytic amount of aluminum chloride in refluxing cyclohexane gave (trimethylsilyl)nonamethylcyclopentasilane. Isomerization of both (trimethylsilyl)undecamethylcyclohexasilane and (pentamethyldisilanyl)nonamethylcyclopentasilane in the presence of aluminum chloride in benzene afforded 1,1-bis(trimethylsilyl)octamethylcyclopentasilane in high yields. Similar rearrangement of tetradecamethylbicyclo[2.2.2]octasilane gave 1-(trimethylsilyl)-undecamethylbicyclo[2.2.1]heptasilane as the sole product. Under identical conditions, *trans*-octadecamethylbicyclo[4.4.0]decasilane and bi(nonamethylcyclopentsilanyl) were both converted into an equilibrium mixture consisting of 1,4-bis(trimethylsilyl)dodecamethylbicyclo[2.2.2]octasilane, 1,4,7-tris(trimethylsilyl)nonamethylbicyclo[2.2.1]heptasilane, and a small amount of an unidentified isomer.

Introduction

The chemistry of organopolysilanes constitutes one of the most active areas of current research.[2-6] Recently, we have shown that the permethylated linear and branched-chain polysilanes undergo skeletal rearrangement in the presence of a catalytic amount of aluminum chloride to give the branched polysilanes bearing at least one tris(trimethylsilyl)silyl moiety.[7] For instance, the reaction of tetradecamethylhexasilane with a catalytic amount of aluminum chloride in refluxing benzene leads to the formation of 2,2-bis(trimethylsilyl)octamethyltetrasilane quantitatively but not 2,3-bis(trimethylsilyl)octamethyltetrasilane. The latter compound can also be transformed into 2,2-bis(trimethylsilyl)octamethyltetrasilane under similar conditions.

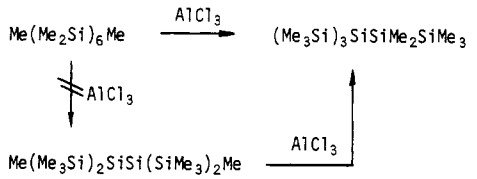

In order to obtain further information concerning the skeletal rearrangement of catenated silicon compounds, we have examined the behavior of some permethylated mono- and bicyclic polysilanes toward a catalytic amount of aluminum chloride.[8a]

Results and Discussion

Monocyclic Polysilanes. In 1969, we found that when a mixture of trimethylsilyl-substituted compounds such as α,ω-bis(trimethylsilyl)alkanes or some lower homologues of permethylated polysilanes with a large excess of trimethylchlorosilane was refluxed gently in the presence of a catalytic amount of aluminum chloride, the respective chlorodimethylsilyl compounds were formed in excellent yields, together with tetramethylsilane.[8b] As an extention of this method, preparation of the chloro-substituted cyclohexasilane was attempted by refluxing a mixture of dodecamethylcyclohexasilane (1) with a large excess of trimethylchlorosilane in the presence of aluminum chloride in a flask fitted with a fractional distillation column. Three molar equivalents of tetramethylsilane gradually distilled out. At this point, the distillation of the residue gave a solid compound which was gas chromatographically homogeneous. On the basis of the elemental analysis of the product, this compound had three chlorine atoms in the molecule.[9] In order to learn whether the six-membered ring remained unchanged during the methyl–chlorine exchange reaction, we treated the resulting chloro compound with methylmagnesium bromide in ethyl ether (Scheme I). The mass spectrum of the methylated product showed a parent peak at m/e 348, corresponding to the calculated molecular weight of $Me_{12}Si_6$. However, its proton NMR spectrum showed complicated resonances consisting of six lines. The proton-decoupled ^{29}Si NMR spectrum displayed four resonances at −10.1, −36.1, −40.9, and −83.2 ppm upfield from tetramethylsilane, assignable to a silicon atom

Scheme I

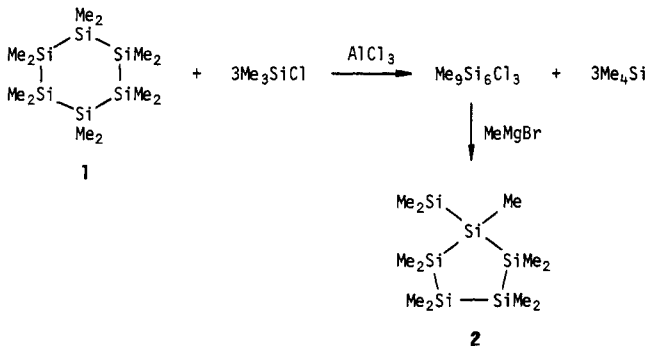

(1) (a) Kyoto University. (b) Government Industrial Research Institute.
(2) Hengge, E. *Top. Curr. Chem.* **1974**, *51*.
(3) Kumada, M. *J. Organomet. Chem.* **1975**, *100*, 127.
(4) West, R.; Carberry, E. *Science (Washington, D. C.)* **1975**, *189*, 179.
(5) West, R.; Barton, T. *J. Chem. Educ.* **1980**, *57*, 165, 334.
(6) (a) Ishikawa, M.; Kumada, M. *Rev. Silicon, Germanium, Tin Lead Compd.* **1979**, *4*, 7. (b) Ishikawa, M.; Kumada, M. *Adv. Organomet. Chem.* **1981**, *19*, 51.
(7) Ishikawa, M.; Iyoda, J.; Ikeda, H.; Kotake, K.; Hashimoto, T.; Kumada, M. *J. Am. Chem. Soc.* **1981**, *103*, 4845.
(8) (a) Ishikawa, M.; Kumada, M. *J. Chem. Soc. D* **1969**, 567. (b) Ishikawa, M.; Kumada, M.; Sakurai, H. *J. Organomet. Chem.* **1970**, *23*, 63.
(9) The ^1H NMR spectrum of the product shows complicated multiplet lines indicating that the product consists of a mixture of several isomers.

0276-7333/82/2301-0317$01.25/0

Scheme II

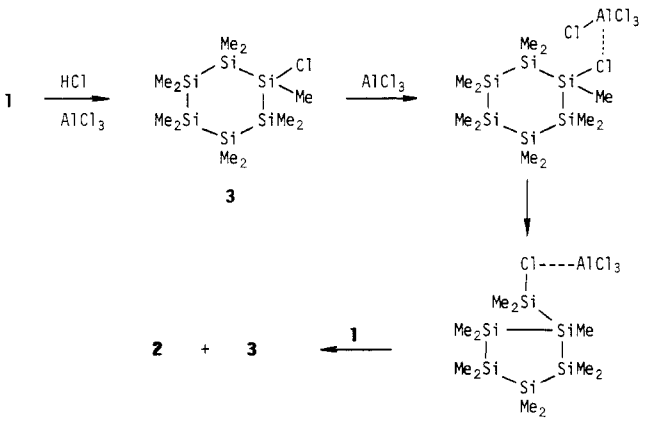

of the trimethylsilyl group, two different bis(silyl)-substituted silicon atoms, and a tris(silyl)-substituted silicon atom, respectively.[7] These results clearly indicate that the compound is in agreement with the structure of (trimethylsilyl)nonamethylcyclopentasilane (**2**).

To establish whether or not trimethylchlorosilane was involved in the isomerization, **1** alone was treated with a catalytic amount of anhydrous aluminum chloride in cyclohexane. At room temperature, no reaction occurred over a period of 25 h,[10] while in refluxing temperature, **1** was readily converted into **2** in high yield (better than 90%). In our previous paper,[7] it was shown that the rearrangement of the permethylated linear polysilane proceeded via formation of a trace of an internal chloropolysilane by the reaction of the starting compound with aluminum chloride, either by itself or in association with hydrogen chloride present in a trace amount in the reaction system. It seems likely that the present isomerization also involves the initial formation of the chloro compound. Indeed, the aluminum chloride catalyzed reaction of **1** always produced a small amount of a compound having the same retention time as chloroundecamethylcyclohexasilane (**3**) in the early stages of the reaction. Treatment of **3** prepared by an independent route[11] with a catalytic amount of aluminum chloride in cyclohexane at room temperature afforded the rearranged product (chlorodimethylsilyl)nonamethylcyclopentasilane[12] (**4**) quantitatively. We think that, in the reaction of **1** in cyclohexane, the rate of methyl–chlorine exchange producing chlorocyclohexasilane **3** is very slow at room temperature, but, in refluxing cyclohexane, **3** may be formed readily.[13] As a result, **3** thus formed undergoes ring contraction by the action of aluminum chloride to give **4**. The aluminum chloride catalyzed methyl–chlorine exchange between **4** and the starting compound **1** completes a catalytic cycle to afford the final product **2** and the chloro compound **3** (Scheme II):

In contrast to the cyclohexane–methylcyclopentane isomerization catalyzed by aluminum halides, in which the formation of the six-membered ring is favored,[14] equilibrium in the present system lies far to the formation of silacyclopentasilane **2**. Only a trace amount of **1** in the equilibrium mixture can be detected by VPC analysis.

Scheme III

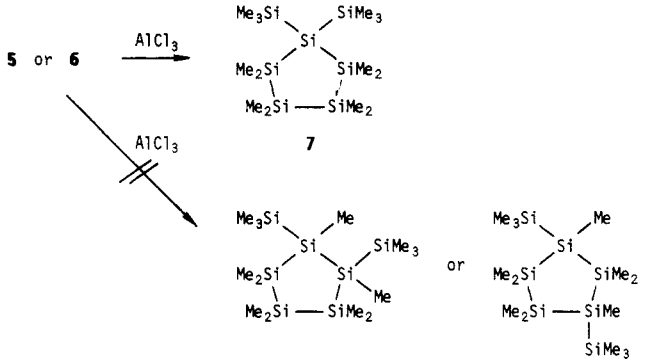

We next prepared a trimethylsilyl-substituted cyclohexasilane and a pentamethyldisilanyl-substituted cyclopentasilane and investigated their behavior toward aluminum chloride.

For the preparation of the former compound we utilized the redistribution reaction (we reported previously[15]) of decamethylcyclopentasilane by the action of a catalytic amount of a silyllithium in THF to give dodecamethylcyclohexasilane. In the silyllithium-catalyzed redistribution reaction, formation of the six-membered ring is much more favored than that of the five-membered ring. Thus, the redistribution of **2** was carried out in the presence of a catalytic amount of (phenyldimethylsilyl)lithium in THF. The product was identified as (trimethylsilyl)undecamethylcyclohexasilane (**5**) by the ^{29}Si NMR spectroscopic study.

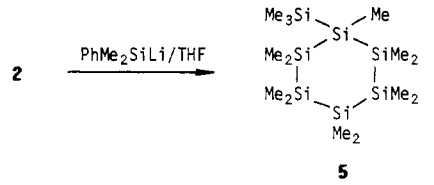

The synthesis of (pentamethyldisilanyl)nonamethylcyclopentasilane (**6**) was accomplished, in 49% yield, by sodium–potassium alloy condensation of (chlorodimethylsilyl)nonamethylcyclopentasilane **4** with trimethylchlorosilane in a hydrocarbon solvent.

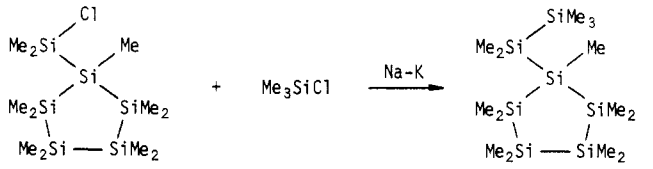

Both compounds **5** and **6** were readily converted into the most highly branched isomer 1,1-bis(trimethylsilyl)octamethylcyclopentasilane (**7**) as the sole product when treated with the aluminum chloride catalyst in boiling benzene (Scheme III). No 1,2- or 1,3-bis(trimethylsilyl)octamethylcyclopentasilane was observed in the reaction mixture. The structure of **7** was established by ^{29}Si NMR spectroscopic analysis as shown in Table I. The proton resonances at δ (ppm) 0.14 (12 H, s, Me_2Si), 0.19 (18 H, s, Me_3Si), and 0.26 (12 H, s, Me_2Si) were also consistent with the proposed structure.

In the five-membered ring system, no skeletal contraction to the four-membered ring was observed. Thus, when decamethylcyclopentasilane [15–17] was treated with a cata-

(10) In benzene, **1** was converted into **2** at room temperature.
(11) Ishikawa, M.; Kumada, M. *Synth. Inorg. Met.-Org. Chem.*, **1971**, *1*, 191.
(12) Ishikawa, M.; Kumada, M. *Synth. Inorg. Met. Org. Chem.* **1971**, *1*, 229.
(13) Monitoring the progress of the reaction by VPC revealed that a trace of compound whose retention time was identical with that of **4** always appeared in the early stage of the reaction and remained throughout.
(14) Pines, H.; Hoffman, E. *Friedel–Crafts Relat. React.* **1964**, *2* (Part II), 1211.
(15) Kumada, M.; Ishikawa, M.; Sakamoto, S.; Maeda, S. *J. Organomet. Chem.* **1969**, *17*, 223.

Table I. ^{29}Si Chemical Shifts for Permethylated Mono- and Bicyclic Polysilanes (Ppm in $CDCl_3$)

compd[a]	chem shifts					
	[a]Si	[b]Si	[c]Si	[d]Si	[e]Si	[f]Si
	−42.1 (−41.8[b]) −41.9[c]					
	−10.1	−36.2	−40.9	−83.2		
	−7.7	−31.8	−40.5	−132.4		
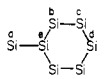	−9.4	−38.8	−40.9	−42.3	−82.2	
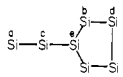	−15.3	−34.9	−38.5	−41.3	−80.4	
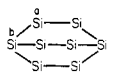	−40.0	−91.6				
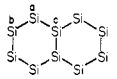	−39.4	−44.9	−82.2			
	−39.6	−46.2	−80.7			
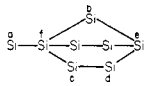	−5.1	−25.1	−33.3	−39.1	−71.8	−128.9
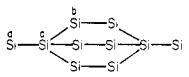	−6.0	−38.1	−129.8			
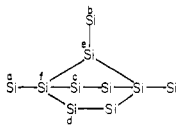	−5.5	−9.4	−28.5	−31.7	−74.0	−122.9

[a] All methyl groups are omitted. [b] In benzene. [c] Reference 22.

lytic amount of aluminum chloride under the same conditions as above, no change was observed; the starting compound was recovered almost quantitatively. Similar treatment of chlorononamethylcyclopentasilane[12] only resulted in recovery of the starting chlorocyclopentasilane.

Bicyclic Polysilanes. To study the behavior of bicyclic polysilanes toward aluminum chloride, we prepared tetradecamethylbicyclo[2.2.2]octasilane (**9**), octadecamethylbicyclo[4.4.0]decasilane (**10**), and bi(nonamethylcyclopentasilanyl) (**12**). Compounds **9** and **10** were first prepared by West and Indrikson[18] using Na/K condensation of $MeSiCl_3$ and Me_2SiCl_2. We carried out a similar condensation with lithium metal in the presence or absence of (phenyldimethylsilyl)lithium in THF. Two types of the bicyclic polysilanes **9** and **10** were obtained, in addition to cyclohexasilane **1** (Scheme IV). Although the yields of the products somewhat fluctuated in several runs, **1** (35–42% yield), **9** (3–5% yield), and **10** (3-7% yield) were always obtained. Compounds **9** and **10** could be isolated by recrystallization, after distillation of the reaction mixture, followed by sublimation under reduced pressure. The mass spectrum of **9** showed a parent peak at m/e 434, corresponding to the calculated molecular weight of

Scheme IV

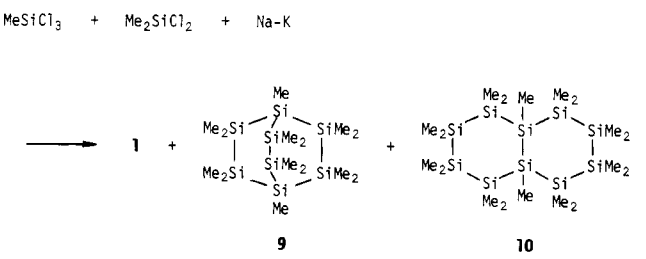

$Me_{14}Si_8$. The proton chemical shifts of this compound were identical with those reported by West et al.[18] Its ^{29}Si NMR spectrum was also consistent with that of the proposed structure.

With the assumption that the conformational concepts associated with decalin may be extended to our compound **10**, the methyl groups on the two juncture silicon atoms in two fused cyclohexasilyl rings may be cis or trans. In several runs, however, only one isomer could be obtained from the reaction mixture. The proton-decoupled ^{29}Si NMR spectrum showed three resonances at −39.4, −44.9, and −82.2 ppm, the first two being assignable to two kinds of bis(silyl)-substituted silicon atoms and the last one to a tris(silyl)-substituted silicon atom. In the case of decalin, the presence of three different kinds of carbon atoms for both cis and trans isomers is shown by the ^{13}C NMR spectroscopic study.[19] In the bicyclo[4.4.0]decasilane,

(16) Carberry, E.; West, R. *J. Am. Chem. Soc.* **1969**, *91*, 5440.
(17) Matsumura, K.; Brough, L. F.; West, R. *J. Chem. Soc., Chem. Commun.* **1978**, 1092.
(18) West, R.; Indrikson, A. *J. Am. Chem. Soc.* **1972**, *94*, 6110.

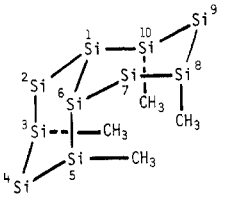

Figure 1. The skew interactions between four methyl groups on the silicon atoms in the 3-, 5-, 8-, and 10-positions.

however, examination of molecular models indicates that the four methyl groups at the 3-, 5-, 8-, and 10-positions in the cis isomer must experience significant skew interactions (Figure 1), whereas in the trans isomer no methyl-methyl interference is present. For this reason, we assign our compound to the trans isomer.

Bi(nonamethylcyclopentasilanyl) (**12**) was prepared in a 65% yield by the condensation of chlorononamethylcyclopentasilane (**11**) with sodium–potassium alloy in benzene.

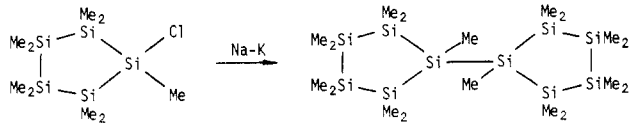

11 **12**

The ^1H and ^{29}Si NMR and mass spectrometric analyses of **12** were wholly consistent with those of the proposed structure.

In the aluminum chloride catalyzed isomerization of **9** in refluxing benzene, a single product was obtained quantitatively. The ^{29}Si NMR spectrum of this compound showed six resonances at −5.1, −25.1, −33.3, −39.1, −71.8, and −128.9 ppm. The signal at −5.1 ppm can be assigned to the silicon atom of the trimethylsilyl group and the signals at −25.1, −33.3, and −39.1 ppm to three different bis(silyl)-substituted silicon atoms. The two signals at −71.8 and −128.9 ppm are due to the tris(silyl)-substituted silicon atom and the tetrakis(silyl)-substituted silicon atom, respectively. Therefore we conclude that the compound is 1-(trimethylsilyl)undecamethylbicyclo[2.2.1]heptasilane (**13**).

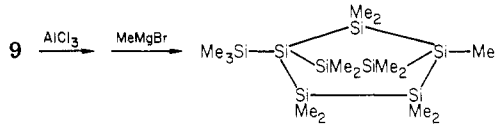

13

Compound **10** underwent readily skeletal rearrangement in the presence of aluminum chloride in refluxing benzene. In contrast to the isomerization of **9**, VPC analysis of the product showed two peaks having an area ratio of 23:77. The products could readily be isolated by preparative VPC. In a previous review article,[3] we described the rearranged products to be spiro compounds, octamethylspiro[4.5]-decasilane and trimethylsilyl-substituted pentadecamethylspiro[4.4]nonasilane. This structural assignment has turned out to be erroneous. Careful studies of mass and ^1H and ^{29}Si NMR data indicate that they must be bicyclic compounds. The ^{29}Si NMR spectrum of the minor product displays three resonances at −5.9, −38.0, and −129.8 ppm, assignable respectively to the silicon atom of the trimethylsilyl group, bis(silyl)-substituted silicon, and tetrakis(silyl)-substituted silicon atoms. Its proton NMR spectrum indicates two signals at δ (ppm) 0.25 and 0.29, having a ratio of 1:2. These results strongly indicate that this compound is 1,4-bis(trimethylsilyl)dodecamethylbicyclo[2.2.2]octasilane (**14**).

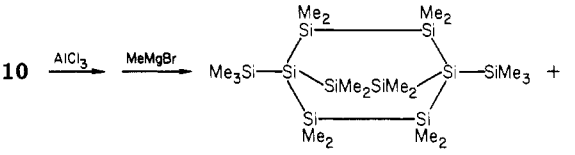

14

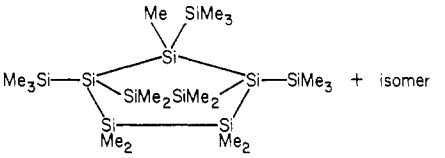

15

The ^{29}Si NMR spectrum of the product corresponding to the major peak on a VPC column indicated that it was a mixture consisting of at least two isomers. All attempts to isolate these compounds in a pure form by preparative VPC using various columns were unsuccesful. However, the main product which is estimated to be more than 60% from the ^{29}Si NMR spectrum of the mixture (see Table I) could be tentatively assigned to 1,4,7-tris(trimethylsilyl)nonamethylbicyclo[2.2.1]heptasilane (**15**).

Interestingly, the isomerization of **12** under similar conditions afforded the same result as that of compound **10**. The ^{29}Si NMR and mass spectral data of the isolated products, **14** and a mixture of isomers, were identical with those of the products obtained from isomerization of **10**.

Experimental Section

General Procedure. ^1H NMR spectra were determined with a JEOL Model JNM-MH-100 spectrometer in carbon tetrachloride using cyclohexane as an internal standard. ^{29}Si NMR spectra were determined with a JEOL Model JNM-PFT-100 spectrometer in deuteriochloroform using tetramethylsilane as an internal standard. Mass spectra were measured on a JEOL Model JMS-D300 equipped with a JMA-2000 data processing system. An Aerograph Model 90-P gas chromatograph with a thermal conductivity detector was used for separating compound **14** and isomers.

Materials. Decamethylcyclopentasilane,[12] chlorononamethylcyclopentasilane,[12] dodecamethylcyclohexasilane,[20] and chloroundecamethylcyclohexasilane[11] were prepared as reported in the literature. Cyclohexane and benzene were dried over lithium aluminum hydride and distilled just before use. Anhydrous aluminum chloride was sublimed before use. Trimethylchlorosilane was distilled just before use.

Reaction of Dodecamethylcyclohexasilane (1) with Trimethylchlorosilane in the Presence of $AlCl_3$. In a 100-mL flask fitted with a 1.0 × 30 cm fractional distillation column, packed with glass helices, was placed a mixture of 10 g (0.029 mol) of **1**, 50 g (0.46 mol) of trimethylchlorosilane, and 0.5 g (3.8 mmol) of anhydrous aluminum chloride. The flask was heated to gentle reflux. Tetramethylsilane, bp 26–28 °C, soon began to distill. After ca. 4 h, 7.5 g (99% yield) of tetramethylsilane was collected. The temperature of the flask was then increased to distill about 30 g of trimethylchlorosilane. At this stage, 5 mL of dry acetone was added to the flask for the purpose of deactivating the catalyst. The residue of the flask was distilled under reduced pressure to give 9.2 g (77% yield) of a semisolid: bp 132–133 °C (1 mm). Anal. Calcd for $C_9H_{27}Cl_3Si_6$: Cl, 25.93. Found: Cl, 25.37.

Methylation of $C_9H_{27}Cl_3Si_6$. To a solution of methylmagnesium bromide prepared from 4.8 g (0.2 mol) of magnesium and 24 g (0.25 mol) of methyl bromide in 100 mL of ethyl ether

(19) Pretsch, E.; Clerc, T.; Seibl, J.; Simon, W. "Tabellen zur Strukturaufklärung Organischer Verbindungen mit Spectroskopischen Methoden"; Springer-Verlag, Berlin, Heidelberg, New York, 1976.

(20) Gilman, H.; Tomasi, R. A. *J. Org. Chem.* **1963**, *28*, 1651.

was added 15 g (0.037 mol) of $C_9H_{27}Cl_3Si_6$ in 50 mL of ether while cooling the mixture with ice. The mixture was refluxed for 10 h and then hydrolyzed with dilute hydrochloric acid. The organic layer was washed with water until neutral and dried over potassium carbonate. The solvent ether was distilled off, and the residue was fractionally distilled to give 11 g (86% yield) of **2**: bp 111–112 °C (2 mm); mp 62–63 °C; mass spectrum, *m/e* 348; UV (C_6H_{12}) 236 nm (ε 9500), 262 (1600), 282 (1300); ^1H NMR δ (ppm) 0.048 (3 H, s, MeSi), 0.143 (6 H, s, s, 2MeSi), 0.147 (6 H, s, 2MeSi), 0.151 (9 H, s, Me_3Si), 0.195 (6 H, s, 2MeSi), 0.202 (6 H, s, 2MeSi). Anal. Calcd for $C_{12}H_{36}Si_6$: C, 41.30; H, 10.40. Found: C, 41.54; H, 10.19.

Isomerization of 1. In a 100-mL flask fitted with a reflux condenser was placed 10 g (0.029 mol) of **1** and 0.5 g (3.8 mmol) of aluminum chloride in 50 mL of cyclohexane. The mixture was refluxed for 3 h. At this stage, VPC analysis of the mixture showed that the starting **1** was completely transformed into **2**. The mixture was hydrolyzed with water. The organic layer was separated and the water layer was extracted with ether. The organic layer and the ether extracts were combined, washed with water, and dried over potassium carbonate. The solvents were evaporated, and the residue was distilled under reduced pressure to give 9.2 g (92% yield) of white crystals: bp 112–115 °C (2 mm). The ^1H NMR, IR, and mass spectral data of the crystals were indentical with those of an authentic sample.

Isomerization of Chloroundecamethylcyclohexasilane (3). A mixture of 5.0 g (0.014 mol) of **3** and 0.2 g (1.5 mmol) of aluminum chloride in 30 mL of cyclohexane was stirred at room temperature for 1 h. At this point, VPC analysis of the mixture showed that the starting **3** was completely transformed into **4**. Acetone (3 mL) was then added to the mixture. The solvent cyclohexane was evaporated, and the residue of the flask was distilled under reduced pressure to give 4.8 g (96% yield) of **4**: mp 97–98 °C (in a sealed capillary). All spectral data were identical with those of an authentic sample.[11]

Preparation of (Trimethylsilyl)undecamethylcyclohexasilane (5). In a 300-mL flask fitted with a reflux condenser was placed 45 g (0.13 mol) of **2** in 150 mL of dry THF. To this was added a (phenyldimethylsilyl)lithium–tetrahydrofuran solution prepared from 3 g (0.018 mol) of phenyldimethylchlorosilane and 1 g (0.14 mol) of lithium in 50 mL of THF. The mixture was stirred for 6 days at room temperature and then hydrolyzed with water. The organic layer was separated, washed until neutral, and dried over potassium carbonate. After evaporation of the solvent, the reaction mixture was fractionally distilled under reduced pressure to give 19 g (36% yield) of **5**: bp 136–138 °C (2 mm); mp 133–134 °C after recrystallization from ethanol; mass spectrum, *m/e* 406; UV (C_6H_{12}) 232 nm (ε 14 600), 256 (5800). Anal. Calcd for $C_{14}H_{42}Si_7$: C, 41.30; H, 10.40. Found: C, 41.28; H, 10.34.

Preparation of (Pentamethyldisilanyl)nonamethylcyclopentasilane (6). In a 1-L three-necked flask fitted with a condenser, a stirrer, and a dropping funnel was placed a charge of sodium-potassium alloy prepared from 82 g (2.1 mol) of potassium and 9 g (0.14 mol) of sodium in 200 mL of xylene. To this was added slowly a mixture of 216 g (2.0 mol) of trimethylchlorosilane and 60 g of crude (chlorodimethylsilyl)nonamethylcyclopentasilane[21] (contaminated with 9% of **1**, 6% of **2**, and 20% of polychlorosilacyclopentasilane) in 200 mL of dry benzene at the temperature of 40–50 °C. After the addition of the chlorosilanes was completed, the mixture was warmed to 60–80 °C for 8 h. The mixture was hydrolyzed in the usual way. Fractional distillation afforded 18 g (49% yield) of **6** as a colorless liquid: bp 134–136 °C (3 mm); mass spectrum, *m/e* 406. Anal. Calcd for $C_{14}H_{42}Si_7$: C, 41.30; H, 10.40. Found: C, 41.51; H, 10.29.

Isomerization of 5. A mixture of 8.0 g (0.020 mol) of **5** and 0.5 g (3.8 mmol) of anhydrous aluminum chloride in 30 mL of dry benzene was stirred for 2.5 h at room temperature and then refluxed for 10 min. The mixture was hydrolyzed with water and dried over potassium carbonate. Distillation under reduced pressure gave 6.9 g (86% yield) of white crystals which sublimed at 80–135 °C (2 mm): mp 248–249 °C (in a sealed capillary) after crystallization from ethanol; mass spectrum, *m/e* 406; UV (C_6H_{12}) 237 nm (ε 9200), 280.5 (1800); ^1H NMR δ (ppm) 0.14 (12 H, s, Me_2Si), 0.19 (18 H, s, Me_3Si), 0.26 (12 H, s, Me_2Si). Anal. Calcd for $C_{14}H_{42}Si_7$: C, 41.30; H, 10.40. Found: C, 41.08; H, 10.42.

Isomerization of 6. A mixture of 3.0 g (7.4 mmol) of **6** and 0.3 g (2.3 mmol) of aluminum chloride in 15 mL of dry benzene was refluxed for 2 h. To this was added 5 mL of a methylmagnesium bromide–ether solution (2.3 M) at room temperature. The mixture was then refluxed for 5 h and hydrolyzed with water. Distillation of the reaction mixture afforded 2.5 g (83% yield) of **7**. All spectral data of **7** were identical with those of the sample obtained from isomerization of **5**.

Condensation of Methyltrichlorosilane and Dimethyldichlorosilane with Lithium. In a 1-L three-necked flask fitted with a reflux condenser, a stirrer, and a dropping funnel was placed 36 g (5.2 mol) of finely cut lithium in 400 mL of dry THF. To this was slowly added a mixture of 194 g (1.5 mol) of dimethyldichlorosilane and 75 g (0.5 mol) of methyltrichlorosilane dissolved in 200 mL of tetrahydrofuran at room temperature over a period of 10 h. When approximately 100 mL of the chlorosilanes was added to the lithium, dark brown color appeared. After completion of the addition of the chlorosilanes, the mixture was stirred for 40 h at room temperature. At this point, the lithium metal was completely consumed. The mixture was then refluxed for 8 h, and ca. 200 mL of the solvent was distilled off. The remainder was hydrolyzed with water, the solvent was evaporated, and the residue was distilled under reduced pressure to give 30 g (36% yield) of **1** boiling over a range of 100–145 °C (2 mm) and 45 g of a semicrystalline solid boiling at 145–220 °C (2 mm). The latter fraction was recrystallized from acetone to give 22 g of white crystals consisting of **1**, **9** and **10**. The crystals were sublimed first at 65–75 °C (1 mm) to give 5 g (5.6% yield) of **1** and second at 85–90 °C (1 mm) to give 3.6 g (3.3% yield) of **9**. The residue was recrystallized from acetone to give 6.0 g (4.4% yield) of **10**. For **9**: mp >300 °C (in a sealed capillary) (lit.[18] mp >340 °C); mass spectrum, *m/e* 434; UV (C_6H_{12}) 245 nm (ε 4300); ^1H NMR δ (ppm) 0.13 (6 H, s, MeSi), 0.22 (36 H, s, Me_2Si). For **10**: mp 187–189 °C; mass spectrum, *m/e* 550; UV (C_6H_{12}) 253 nm (ε 25 200), 284 (9300); ^1H NMR δ (ppm) 0.14 (12 H, s, Me_2Si), 0.15 (12 H, s, Me_2Si), 0.19 (6 H, s, MeSi), 0.26 (24 H, s, Me_2Si). Anal. Calcd for $C_{12}H_{54}Si_{10}$: C, 39.20; H, 9.87. Found: C, 39.35; H, 9.93.

Preparation of Bi(nonamethylcyclopentasilanyl) (12). In a 500-mL three-necked flask was placed a sodium–potassium alloy prepared from 0.6 g (0.026 mol) of sodium and 3.3 g (0.08 mol) of potassium in 50 mL of dry heptane. To this was added 20 g (0.064 mol) of chlorononamethylcyclopentasilane in 100 mL of dry benzene at the temperature of 60–70 °C over a period of 1 h. The mixture was refluxed for 10 h and then hydrolyzed in the usual way. Distillation of the mixture under reduced pressure gave 11.5 g (65% yield) of **12**: bp 180–183 °C (3 mm); mp 117–118 °C after recrystallization from ethanol; mass spectrum, *m/e* 550; UV (C_6H_{12}) 225 nm (ε 39 200), 249.5 (30 000), 296 (6400); ^1H NMR δ (ppm) 0.14 (12 H, s, Me_2Si), 0.15 (12 H, s, Me_2Si), 0.19 (24 H, s, Me_2Si), 0.26 (6 H, s, MeSi). Anal. Calcd for $C_{18}H_{54}Si_{10}$: C, 39.20; H, 9.87. Found: C, 39.05; H, 10.06.

Isomerization of 9. A mixture of 2.0 g (4.6 mmol) of **9** contaminated with a small amount of **1** and 0.2 g (1.5 mmol) of aluminum chloride in 10 mL of benzene was relfuxed for 2 h. To this was slowly added 5 mL of a methylmagnesium bromide–ether solution (2.3 M) and 5 mL of dry THF. The mixture was refluxed for 10 h and then hydrolyzed with water. After evaporation of the solvents, the residue was distilled under reduced pressure to give 1.8 g (90% yield) of **13**. Pure **13** was isolated by preparative VPC: mp >300 °C; mass spectrum, *m/e* 434; ^1H NMR δ (ppm) 0.20 (3 H, s, MeSi), 0.22 (15 H, s, Me_3Si and Me_2Si), 0.24 (6 H, s, Me_2Si), 0.28 (12 H, s, Me_2Si), 0.35 (6 H, s, Me_2Si). Anal. Calcd for $C_{14}H_{42}Si_8$: C, 38.64; H, 9.37. Found: C, 38.36; H, 9.40.

Isomerization of 10. A mixture of 3 g (5.5 mmol) of **10** and 0.3 g (2.3 mmol) of aluminum chloride in 30 mL of benzene was stirred at room temperature for 7 h. At this point, 5 mL of acetone was added to the mixture. The mixture was distilled under reduced pressure to give 2.9 g of white crystals. They were dissolved in THF, and a methylmagnesium bromide–ether solution (2.0 M) was added to the solution. The mixture was refluxed for 20 h and then hydrolyzed with water. The solvent was evaporated, and the residue was distilled to give 2.7 g of white crystals. VPC

(21) A mixture obtained from the reaction of **1** with trimethylchlorosilane in the presence of $AlCl_3$ was used without further purification.[12]

(22) Stanislawski, D. A.; West, R. *J. Organomet. Chem.* **1981**, *204*, 295.

analysis of the distillate showed two peaks having an area ratio of 27:73. The two peaks were separated by preparative VPC. For **14**: mp 146–147 °C; mass spectrum, *m/e* 550; UV 241 nm (ε 18000); ^{1}H NMR δ (ppm) 0.25 (18 H, s, Me_3Si), 0.29 (36 H, s, Me_2Si). Anal. Calcd for $C_{18}H_{54}Si_{10}$: C, 39.20; H, 9.87. Found: C, 38.99; H, 9.93. For **15** (mixture of isomers): mp 150–151 °C; mass spectrum, *m/e* 550. Anal. Calcd for $C_{18}H_{54}Si_{10}$: C, 39.20; H, 9.87. Found: C, 39.41; H, 10.01.

Isomerization of 12. A mixture of 3 g (5.5 mmol) of **12** and 0.4 g (3.0 mmol) of aluminum chloride in 50 mL of benzene was stirred at room temperature for 10 h. Acetone (5 mL) was added to the mixture, and the solvent was distilled off. The residue of the flask was distilled under reduced pressure to give 2.8 g of white crystals. Methylation of the product using methylmagnesium bromide followed by distillation under reduced pressure afforded 2.6 g of crystals. VPC analysis of the distillate showed two peaks having an area ratio of 27:73. All spectral data for **14** and a mixture of isomers separated by preparative VPC were identical with those obtained from isomerization of **10**.

Acknowledgment. The cost of this research was defrayed partly by a Grant-in-Aid for Scientific Research by the Ministry of Education to which our thanks are due. We also express our appreciation to Toshiba Silicon Co., Ltd., and Shin-etsu Chemical Co., Ltd., for a gift of organochlorosilanes.

Registry No. 1, 4098-30-0; **2**, 23118-85-6; **3**, 23118-87-8; **4**, 23118-86-7; **5**, 57171-38-7; **6**, 79769-57-6; **7**, 79769-58-7; **9**, 30314-60-4; **10**, 37249-28-8; **11**, 23118-89-0; **12**, 79769-59-8; **13**, 79769-60-1; **14**, 79769-61-2; **15**, 79769-62-3; $AlCl_3$, 7446-70-0; Me_3SiCl, 75-77-4; $PhMe_2SiCl$, 768-33-2; Me_2SiCl_2, 75-78-5; $MeSiCl_3$, 75-79-6.

Metal-Catalyzed Reactions of Allylazirines

Taeko Izumi and Howard Alper*[1]

Department of Chemistry, University of Ottawa Ottawa, Ontario, Canada K1N 9B4

Received September 14, 1981

Tetrakis(triphenylphosphine)palladium(0) and certain other palladium(0) compounds catalyze the conversion of 2-allylazirines to pyridines and pyrroles. The reaction is sensitive to the atmosphere in which it is conducted, as well as to the pressure. The use of other catalysts (e.g., molybdenum and rhodium carbonyls) for the ring opening of 2-allylazirines is also described. A mechanism, involving a key common intermediate, is proposed for the formation of pyridines and pyrroles.

Photochemical and thermal reactions of the three-membered ring heterocycles, azirines, have been investigated in considerable detail.[2] Metal complexes can induce some synthetically useful transformations of azirines under exceedingly mild conditions.[3] One example is the molybdenum hexacarbonyl induced intramolecular cycloaddition of 3-phenyl-2-substituted-2*H*-azirines (**1**) to

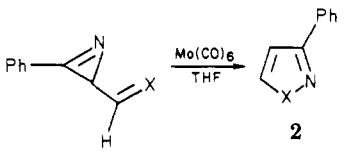

1, X = O, NR **2**

five-membered ring heterocycles. This reaction occurs at room temperature, affording **2** in fine yields.[4] The synthesis of β-lactams (**4**) by the tetrakis(triphenylphosphine)palladium(0)-catalyzed carbonylation of azirines (**3**) is another noteworthy reaction.[3] 2-Allyl-substituted 2*H*-azirines undergo interesting thermal and photochemical reactions. For instance, when 2-allyl-2-methyl-3-phenyl-2*H*-azirine (**5**) was heated in a sealed tube for 180

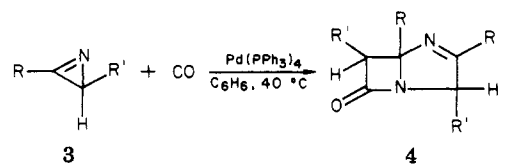

3 **4**

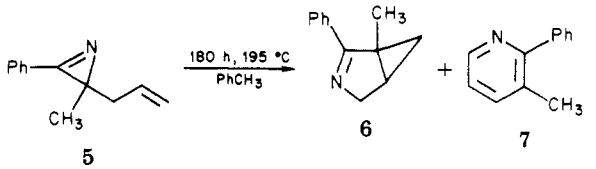

5 **6** **7**

h at 195 °C, the 3-azabicyclo[3.1.0]hex-3-ene **6** was obtained in 90% yield and 3-methyl-2-phenylpyridine (**7**) was formed in 10% yield. *Partial* conversion of **6** to **7** occurred on extended heating (195 °C, 85 h).[5] In contrast, irradiation of **5** proved to be very facile (15 min, λ > 250 nm) leading to the quantitive formation of **8**.[6] The irradiation process likely occurs by carbon–carbon bond cleavage of **5**, while there is good evidence for carbon–nitrogen bond cleavage in the thermolysis of allylazirines.

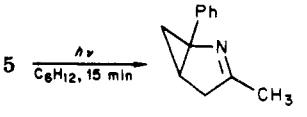

8

This paper describes the interesting metal-catalyzed chemistry of allylazirines. Since it is probable that the molybdenum- and palladium-catalyzed reactions of simple

(1) E.W.R. Steacie Fellow, 1980–1982.
(2) For a review see: Nair, V.; Kim, K. H. *Heterocycles* **1977**, *7*, 353.
(3) Alper, H.; Perera, C. P.; Ahmed, F. R. *J. Am. Chem. Soc.* **1981**, *103*, 1289 and references cited therein.
(4) Alper, H.; Prickett, J. E.; Wollowitz, S. *J. Am. Chem. Soc.* **1977**, *99*, 4330.
(5) Padwa, A.; Carlsen, P. H. J. *J. Org. Chem.* **1978**, *43*, 2029. Padwa, A.; Carlsen, P. H. J. *Tetrahedron Lett.* **1978**, 433.
(6) Padwa, A.; Carlsen, P. H. J., *J. Am. Chem. Soc.* **1977**, *99*, 1514.

0276-7333/82/2301-0322$01.25/0

analysis of the distillate showed two peaks having an area ratio of 27:73. The two peaks were separated by preparative VPC. For **14**: mp 146–147 °C; mass spectrum, *m/e* 550; UV 241 nm (ε 18000); ^{1}H NMR δ (ppm) 0.25 (18 H, s, Me_3Si), 0.29 (36 H, s, Me_2Si). Anal. Calcd for $C_{18}H_{54}Si_{10}$: C, 39.20; H, 9.87. Found: C, 38.99; H, 9.93. For **15** (mixture of isomers): mp 150–151 °C; mass spectrum, *m/e* 550. Anal. Calcd for $C_{18}H_{54}Si_{10}$: C, 39.20; H, 9.87. Found: C, 39.41; H, 10.01.

Isomerization of 12. A mixture of 3 g (5.5 mmol) of **12** and 0.4 g (3.0 mmol) of aluminum chloride in 50 mL of benzene was stirred at room temperature for 10 h. Acetone (5 mL) was added to the mixture, and the solvent was distilled off. The residue of the flask was distilled under reduced pressure to give 2.8 g of white crystals. Methylation of the product using methylmagnesium bromide followed by distillation under reduced pressure afforded 2.6 g of crystals. VPC analysis of the distillate showed two peaks having an area ratio of 27:73. All spectral data for **14** and a mixture of isomers separated by preparative VPC were identical with those obtained from isomerization of **10**.

Acknowledgment. The cost of this research was defrayed partly by a Grant-in-Aid for Scientific Research by the Ministry of Education to which our thanks are due. We also express our appreciation to Toshiba Silicon Co., Ltd., and Shin-etsu Chemical Co., Ltd., for a gift of organochlorosilanes.

Registry No. 1, 4098-30-0; **2**, 23118-85-6; **3**, 23118-87-8; **4**, 23118-86-7; **5**, 57171-38-7; **6**, 79769-57-6; **7**, 79769-58-7; **9**, 30314-60-4; **10**, 37249-28-8; **11**, 23118-89-0; **12**, 79769-59-8; **13**, 79769-60-1; **14**, 79769-61-2; **15**, 79769-62-3; $AlCl_3$, 7446-70-0; Me_3SiCl, 75-77-4; $PhMe_2SiCl$, 768-33-2; Me_2SiCl_2, 75-78-5; $MeSiCl_3$, 75-79-6.

Metal-Catalyzed Reactions of Allylazirines

Taeko Izumi and Howard Alper*[1]

Department of Chemistry, University of Ottawa Ottawa, Ontario, Canada K1N 9B4

Received September 14, 1981

Tetrakis(triphenylphosphine)palladium(0) and certain other palladium(0) compounds catalyze the conversion of 2-allylazirines to pyridines and pyrroles. The reaction is sensitive to the atmosphere in which it is conducted, as well as to the pressure. The use of other catalysts (e.g., molybdenum and rhodium carbonyls) for the ring opening of 2-allylazirines is also described. A mechanism, involving a key common intermediate, is proposed for the formation of pyridines and pyrroles.

Photochemical and thermal reactions of the three-membered ring heterocycles, azirines, have been investigated in considerable detail.[2] Metal complexes can induce some synthetically useful transformations of azirines under exceedingly mild conditions.[3] One example is the molybdenum hexacarbonyl induced intramolecular cycloaddition of 3-phenyl-2-substituted-2*H*-azirines (**1**) to

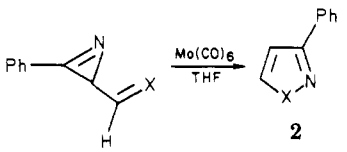

1, X = O, NR **2**

five-membered ring heterocycles. This reaction occurs at room temperature, affording **2** in fine yields.[4] The synthesis of β-lactams (**4**) by the tetrakis(triphenylphosphine)palladium(0)-catalyzed carbonylation of azirines (**3**) is another noteworthy reaction.[3] 2-Allyl-substituted 2*H*-azirines undergo interesting thermal and photochemical reactions. For instance, when 2-allyl-2-methyl-3-phenyl-2*H*-azirine (**5**) was heated in a sealed tube for 180

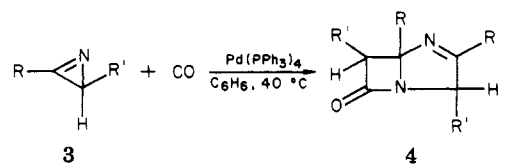

3 **4**

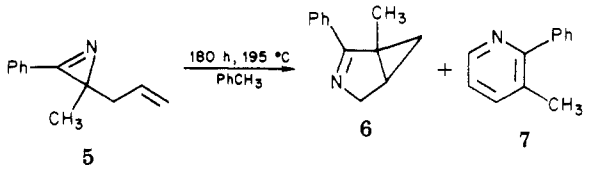

5 **6** **7**

h at 195 °C, the 3-azabicyclo[3.1.0]hex-3-ene **6** was obtained in 90% yield and 3-methyl-2-phenylpyridine (**7**) was formed in 10% yield. *Partial* conversion of **6** to **7** occurred on extended heating (195 °C, 85 h).[5] In contrast, irradiation of **5** proved to be very facile (15 min, λ > 250 nm) leading to the quantitive formation of **8**.[6] The irradiation process likely occurs by carbon–carbon bond cleavage of **5**, while there is good evidence for carbon–nitrogen bond cleavage in the thermolysis of allylazirines.

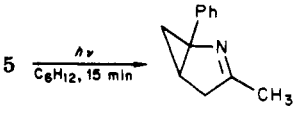

8

This paper describes the interesting metal-catalyzed chemistry of allylazirines. Since it is probable that the molybdenum- and palladium-catalyzed reactions of simple

(1) E.W.R. Steacie Fellow, 1980–1982.
(2) For a review see: Nair, V.; Kim, K. H. *Heterocycles* **1977**, *7*, 353.
(3) Alper, H.; Perera, C. P.; Ahmed, F. R. *J. Am. Chem. Soc.* **1981**, *103*, 1289 and references cited therein.
(4) Alper, H.; Prickett, J. E.; Wollowitz, S. *J. Am. Chem. Soc.* **1977**, *99*, 4330.
(5) Padwa, A.; Carlsen, P. H. J. *J. Org. Chem.* **1978**, *43*, 2029. Padwa, A.; Carlsen, P. H. J. *Tetrahedron Lett.* **1978**, 433.
(6) Padwa, A.; Carlsen, P. H. J., *J. Am. Chem. Soc.* **1977**, *99*, 1514.

0276-7333/82/2301-0322$01.25/0

Table I. Products Obtained from the Cleavage of Allylazirines

azirine	reaction atmosphere	catalyst	product	yield, %
5	N_2	$Pd(PPh_3)_4$	7	18
			9	20
	CO_2	$Pd(PPh_3)_4$	7	70
			9	trace
	CO_2	$Pd(dba)_2$	7	12
	CO_2	$Pd(dba)_2$, diphos	9	14
	CO_2	$Pd(diphos)_2$	...	...
	CO_2	$Mo(CO)_6$	...	...
10	CO_2	$Pd(PPh_3)_4$	11	18
			12	10
13	N_2	$Pd(PPh_3)_4$	14	30[a]
			15	33[b]
	CO_2	$Pd(PPh_3)_4$	14	19
			15	24
	CO_2	$Pd(dba)_2$	14	12
			15	30
	CO_2	$Rh_6(CO)_{16}$	14	6
			15	8
16	CO_2	$Pd(PPh_3)_4$	17	45
			18	14
			19	12
	CO_2	$Mo(CO)_6$	19	30

[a] New compound. Anal. Calcd for $C_{14}H_{15}N$: C, 85.24; H, 7.66; N, 7.10. Found: C, 85.04; H, 8.02; N, 6.83. [b] New compound. Anal. Calcd for $C_{14}H_{13}N$: C, 86.12; H, 6.63; N, 7.17. Found: C, 86.05; H, 6.27; N, 6.81.

azirines (see above) proceed via carbon–nitrogen bond cleavage of the azirine, such cleavage in the case of allylazirines would generate metal-complexed allyl-substituted vinylnitrenes. As reported herein, not only does the metal complex have an influence on the reaction course, as compared with the thermal process, but also the atmosphere used for the reaction is important as well.

Results and Discussion

Exposure of **5** to a catalytic amount of tetrakis(triphenylphosphine)palladium(0) [10:1 ratio of **5**:$Pd(PPh_3)_4$] in benzene at 50 °C gave 3,5-dimethyl-2-phenylpyrrole (**9**) in 20% yield and 3-methyl-2-phenylpyridine (**7**) in 18% yield, with the remainder being recovered starting material. Use of acetone as the reaction solvent gave **7** in the same yield but only a small amount (3.5%) of **9**.

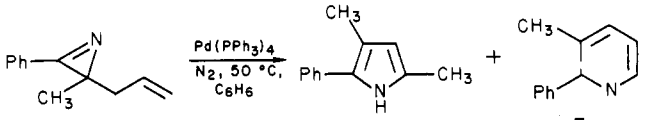

5 **9** **7**

Although a variety of azirines can be carbonylated to β-lactams by using $Pd(PPh_3)_4$, allylazirines such as **5** were unreactive in the presence of carbon monoxide and the palladium catalyst. Use of carbon dioxide as the reaction atmosphere proved more fruitful, as **5** was converted to 3-methyl-2-phenylpyridine (**7**) in 70% yield, with only a trace of the pyrrole formed. Other palladium catalysts such as bis(dibenzylideneacetone)palladium(0) and (1,2-bis(diphenylphosphino)ethane)palladium(0) were of little use as catalysts for these reactions (Table I). Compounds **7** and **9**, as well as the products of the reactions of other allyl azirines, were identified by comparison of spectral data (Table II) with those for authentic materials (when available).

Reaction of 2-allyl-3-methyl-2-phenyl-2*H*-azirine (**10**), an isomer of **5**, with $Pd(PPh_3)_4$ under carbon dioxide afforded 2,5-dimethyl-3-phenylpyrrole (**11**) and 2-methyl-3-phenylpyridine (**12**). However, the product yields obtained in this reaction were in the same range as those realized for **7** and **9** in the reaction of **5** under nitrogen.

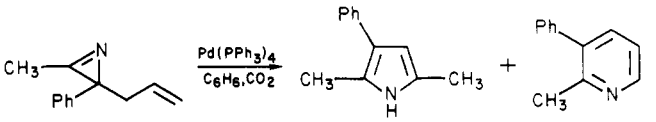

10 **11** **12**

In the case of a diallylazirine, 2,2-diallyl-3-phenyl-2*H*-azirine (**13**), the expected pyrrole (**14**) and pyridine (**15**) derivatives were obtained in somewhat higher yields by using CO_2 rather than a nitrogen atmosphere for the $Pd(PPh_3)_4$-catalyzed reaction. Both products were also obtained using $Pd(dba)_2$ as the catalyst.

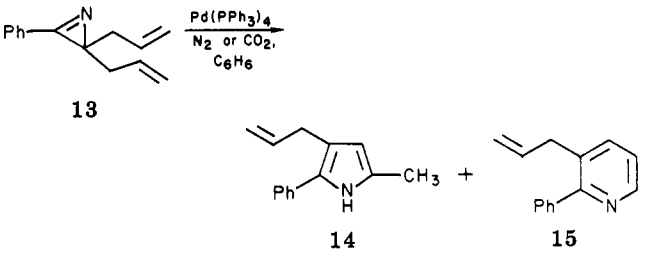

13 **14** **15**

The behavior of a monoallylazirine, lacking any other substituent at the 2-position, toward $Pd(PPh_3)_4$ was also examined. 2-Allyl-3-phenyl-2*H*-azirine (**16**) was prepared from 1-phenyl-4-penten-1-one by a modified Neber reaction. The $Pd(PPh_3)_4$-catalyzed reaction of **16** afforded 2-phenylpyridine in 45% yield, together with small amounts of the expected 2-methyl-5-phenylpyrrole (**18**) and a compound assigned structure **19** on the basis of spectral data (e.g., ^{13}C shows two different allyl groups).

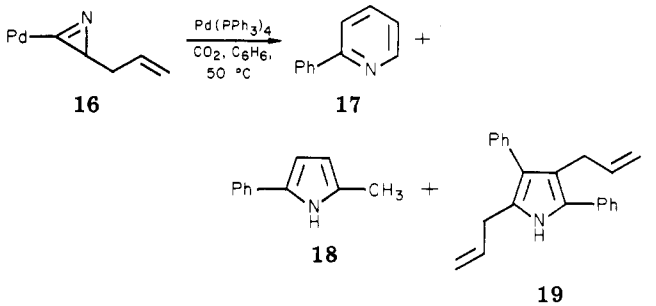

16 **17** **18** **19**

Pressure does have an effect on the reaction, since it results in the formation of pyridines in fine yields. For example, the yield of 2-phenylpyridine (**17**) increased from 45 to 75% when the reaction of **16** was repeated at 24.5 atm for 20 h at 50 °C. Raising the temperature to 80 °C resulted in the formation of **17** in essentially the same yield (77%). Pyrroles (**18**, **19**) were not isolated from any of the reactions effected at elevated pressures. They were also small amounts of products possibly resulting from reaction of the azirine with carbon dioxide,[7] since they exhibited carbonyl absorption in the infrared region at 1740–1750 cm^{-1}. However, all attempts to isolate these byproducts in analytically pure form failed.

A number of other metal complexes were used as catalysts for the cleavage of allylazirines. While **14** and **15** were obtained in poor yields by exposure of the diallylazirine **13** to hexarhodium hexadecacarbonyl (50 °C, 1 atm of

(7) For an example of the reaction of small ring compounds with CO_2, see: Inoue, Y.; Hibi, T.; Satake, M.; Hashimoto, H. *J. Chem. Soc., Chem. Commun.* **1979**, 982.

Scheme I

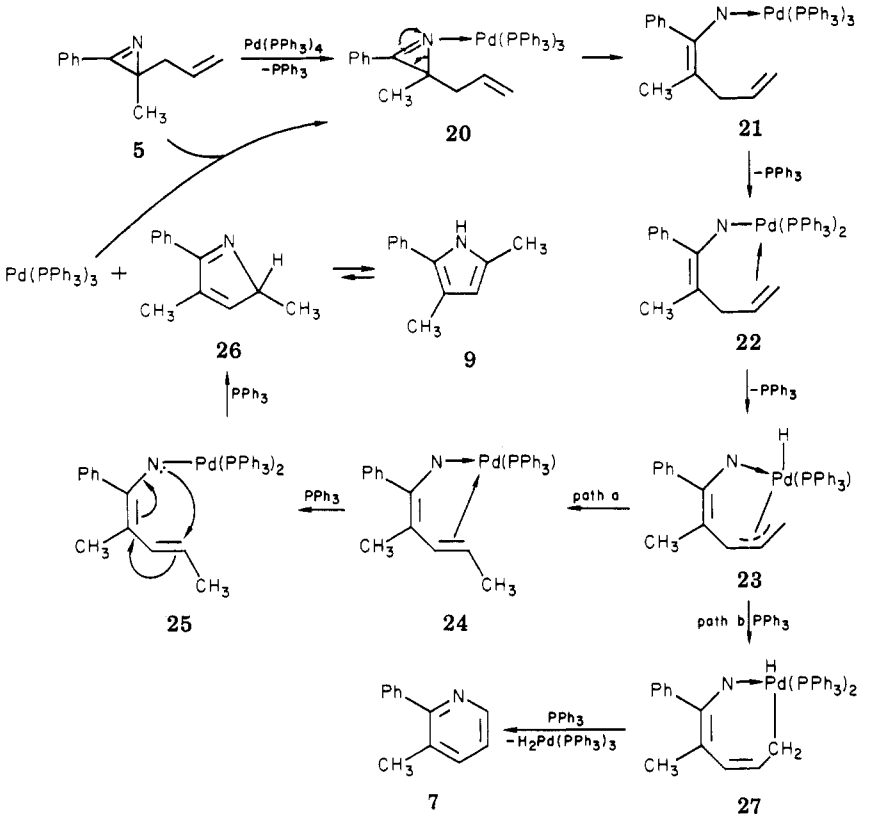

CO_2), no reaction occurred by using chlorodicarbonylrhodium(I) dimer, tetrakis(triphenylphosphine)platinum, or molybdenum hexacarbonyl as the catalyst. While the molybdenum complex was also ineffective for other 2-allyl-2-substituted-azirines (e.g., **5**), it did effect the conversion of **16** to the pyrrole **19** in 30% yield.

The formation of pyridines and pyrroles from allylazirines can be rationalized by the pathways outlined in Scheme I (illustrated for **5**). Coordination of the azirine nitrogen to palladium (**20**) would weaken the carbon–nitrogen single bond, the cleavage of which would generate **21**. Unlike simple nitrene–metal complexes, compound **21** has an allylic group and binding of the double bond of the allyl unit to palladium is conceivable (**22**). The palladium hydride **23**, formed on allylic hydrogen abstraction, can react by two (or more) pathways. Delivery of the hydride to the least substituted terminal carbon of the allyl unit would give **24** and then **25** (with PPh_3—path a). Cyclization and decomplexation would afford **26** and $Pd(PPh_3)_3$. The latter can then react with additional azirine **5** to regenerate **20**, completing the catalytic cycle, while **26** would readily isomerize to the pyrrole **9**. Complex **25** is of the same structural type as the intermediate formed on metal-induced cleavage of a vinylazirine such as (*E*)-3-phenyl-2*H*-azirine-2-acrylate.[4]

Instead of hydrogen transfer from palladium to the organic ligand, **23** can experience $\pi \rightarrow \sigma$ allyl conversion giving **27** (path b). Dehydrogenation and elimination from **27** would result in the formation of the pyridine **7** and $Pd(PPh_3)_2H_2$ which, with readdition of PPh_3 (previously disassociated), would give $Pd(PPh_3)_3$ and hydrogen. It is also possible that, in the presence of PPh_3, **27** eliminates $Pd(PPh_3)_3$ and hydrogen directly.

What is the function of carbon dioxide in these reactions? Carbon dioxide may react with the azirine complex **20** formed initially (or **21**), the resultant bound CO_2 affecting the ease of cleavage of the three-membered ring or the complexation of the allylic double bond to palladium. Alternatively, CO_2 may react with $Pd(PPh_3)_3$ to form **28**, the latter exhibiting different reactivity than $Pd(PPh_3)_3$ toward the azirine. It is not clear why there is greater selectivity for pyridine formation (i.e., path b) at elevated pressures of carbon dioxide.

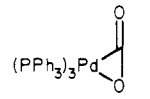

28

In conclusion, $Pd(PPh_3)_4$ can catalyze the conversion of allylazirines to pyridines and pyrroles under gentle conditions, with the reaction atmosphere and pressure used being of importance.

Experimental Section

General Remarks. Infrared determinations were made by using a Unicam SP-1100 spectrometer, equipped with a calibration standard. Proton magnetic resonance spectra were recorded on a Varian T-60 or HA-100 spectrometer, and a Varian FT-80 spectrometer, operating in the fully and partially decoupled modes, was used for carbon magnetic resonance spectra. Mass spectra were run on a Varian MS902 spectrometer. Melting point determinations were made by using a Fisher-Johns apparatus. Elemental analyses were carried out by Canadian Microanalytical Service, Vancouver, Canada.

Tetrakis(triphenylphosphine)palladium(0)[8] and bis(dibenzylideneacetone)palladium(0)[9] were synthesized following literature procedures. Molybdenum and rhodium carbonyls, as well as tetrakis(triphenylphosphine)platinum and chlorodicarbonylrhodium(I) dimer, were commercial products (Strem Chemicals, Inc.).

Solvents were purified and dried by standard methods. Reactions at elevated pressures of carbon dioxide were run in a Parr reactor.

(8) Coulson, D. R. *Inorg. Synth.* **1972**, *13*, 121.
(9) Takahashi, Y.; Ito, E.; Sakai, S.; Ishii, Y. *J. Chem. Soc. D* **1970**, 1065.

Table II. Pertinent Spectral Data for the Reaction Products

compd	IR ν, cm^{-1}	^1H NMR, δ [a]	MS, *m/e*
7	1592, 1577	2.30 (s, 3 H, CH_3), 7.05-7.60 (m, 7 H, H4, H5, Ph), 8.53 (dd, 1 H, H6, J_{H5-H6} = 5 Hz, J_{H4-H6} = 1 Hz)	169
9	3480, 1530	2.14 (s, 3 H, CH_3), 2.20 (s, 3 H, CH_3), 5.75 (d, 1 H, CH, J = 3 H), 7.10-7.40 (m, 6 H, Ph and NH)	171
11	3460, 1515	2.13 (s, 3 H, CH_3), 2.25 (s, 3 H, CH_3), 5.99 (d, 1 H, CH_2, J = 3 Hz), 7.10-7.40 (m, 6 H, Ph and NH)	171
12	1578, 1561	2.48 (s, 3 H, CH_3), 7.00-7.50 (m, 7 H, H4, H5, Ph), 8.45 (dd, 1 H, H6, J_{H6-H5} = 5 Hz, J_{H6-H4} = 1.5 Hz)	169
14	3380, 1515	2.30 (s, 3 H, CH_3), 3.33 (d, 2 H, CH_2, J = 6 Hz), 5.10 (m, 2 H, CH_2=), 5.83 (m, 1 H, CH=), 5.93 (d, 1 H, J = 3 Hz, CH), 7.17-7.65 (m, 6 H, Ph and NH)	197
15	1650, 1590, 1575	3.35 (d, 2 H, CH_2, J = 6 Hz), 4.92 (m, 2 H, CH_2=), 6.00 (m, 1 H, CH=), 7.00-7.65 (m, 7 H, Ph, H4, H5), 8.55 (dd, 1 H, H6, J_{H5-H6} = 5 Hz, J_{H4-H6} = 1.5 Hz)	195
17	1578, 1570, 1562	7.00-8.00 (m, 8 H, Ph, H3-H5), 8.61 (m, 1 H, H6)	155
18	3380, 1515	2.27 (s, 3 H, CH_3), 5.88 (t, 1 H, H3), 6.35 (t, 1 H, H4), 7.1-7.5 (m, 8 H, Ph), 7.80 (s (br), 1 H, NH)	157
19 [b]	3380, 1523	3.20 (m, 4 H, CH_2), 4.95 (m, 4 H, CH_2=), 5.80 (m, 2 H, CH=), 7.22 (m, 10 H, Ph), 7.80 (s (br), 1 H, NH)	299

[a] $CDCl_3$ with Me_4Si as internal standard. [b] ^{13}C NMR ($CDCl_3$) δ 29.28 (CH_2), 30.85 (CH_2), 115.03 (CH_2=), 125.98, 126.11, 126.41, 126.64, 127.87, 128.02, 128.30, 128.66, 129.28, 130.06, 133.48, 138.07 (aromatic and heterocyclic carbons), 135.92 (CH=), 138.70 (CH=).

Azirines Literature procedures were used to prepare 2-allyl-2-methyl-3-phenyl-2*H*-azirine (**5**) and 2-allyl-3-methyl-2-phenyl-2*H*-azirine (**10**).[6]

2,2-Diallyl-3-phenyl-2*H*-azirine (**13**) was prepared by a modified Neber reaction in which 4-benzoyl-1,6-heptadiene was treated with dimethylhydrazine according to the general procedure of Padwa and Carlsen.[6] The required 4-benzoyl-1, 6-heptadiene was synthesized by the following procedure. To a slurry of sodium hydride (0.1 mol) in dimethyl sulfoxide (100 mL) was added acetophenone (0.1 mol) at 25–35 °C. Allyl bromide (1 mol) was then added dropwise at 35 °C. The reaction mixture, after stirring for 3 h, was poured into ice water (200 mL) and extracted with ether. Removal of the ether followed by distillation at 85–87 °C (0.2 mm) afforded 4-benzoyl-1,6-heptadiene in 69% yield.

13: bp 88–90 °C (0.3mm); IR (neat) 1745 (C=N), 1655 (C=C) cm^{-1}; ^1H NMR ($CDCl_3$) δ 2.45 (d, 2 H, J = 6 Hz, CH_2), 2.50 (d, 2 H, J = 6 Hz, CH_2), 5.00 (m, 4 H, CH_2=), 5.80 (m, 2 H, CH=), 7.50 (m, 5 H, Ph); mass spectrum, *m/e* 197 (M^+).

Anal. Calcd for $C_{14}H_{15}N$: C, 85.24; H, 7.66; N, 7.10. Found: C, 84.97; H, 7.84; N, 7.16.

2-Allyl-3-phenyl-2*H*-azirine (**16**) was prepared from 1-phenyl-4-penten-1-one[10] by a modified Neber reaction.[6]

16: bp 42–46 °C (0.07 mm); IR (neat) 1732 (C=N), 1638 (C=C) cm^{-1}; ^1H NMR ($CDCl_3$) δ 2.31 (m, 3 H, CH (ring) and CH_2), 5.08 (m, 2 H, CH_2=), 5.80 m, 1 H, CH=), 7.60 (m, 5 H, Ph); ^{13}C NMR ($CDCl_3$) δ 31.38 (saturated carbon of azirine), 37.77 (CH_2), 116.58 (CH_2=), 125.71 (quaternary carbon of phenyl group), 129.06, 129.29, 132.80 (other phenyl carbons), 135.23 (CH=), 171.48 (C=N); mass spectrum, *m/e* 157 (M^+).

Anal. Calcd for $C_{11}H_{11}N$: C, 84.04; H, 7.05; N, 8.91. Found: C, 84.10; H, 6.94; N, 8.10.

General Procedure for the $Pd(PPh_3)_4$-Catalyzed Reaction of 2-Allylazirines. Carbon dioxide (or nitrogen) was bubbled, for 10–30 min, through a dry benzene (40 ml) solution containing $Pd(PPh_3)_4$ (1.0 mmol). The allylazirine (10.0 mmol) in benzene (10 ml) was added, and the reaction mixture was then stirred at 50 °C under CO_2 or N_2. After no further conversion occurred (followed by thin-layer and/or gas chromatography), the solvent was removed by rotary evaporation and the products were separated by column chromatography with silica gel. The pyrrole was eluted with hexane (any recovered azirine was eluted after the pyrrole), and the pyridine was eluted by using 10% hexane–ethylacetate.

This procedure, using a Parr reactor, was applied to reactions effected at elevated pressures of carbon dioxide.

The reactions using other palladium complexes as well as different metal catalysts were run in a manner identical with that described for $Pd(PPh_3)_4$.

Acknowledgment. We are grateful to the Natural Sciences and Engineering Research Council for support of this work.

Registry No. **5**, 56434-95-8; **7**, 10273-90-2; **9**, 3274-53-1; **10**, 59175-18-7; **11**, 3771-60-6; **12**, 3256-89-1; **13**, 79815-47-7; **14**, 79815-48-8; **15**, 79815-49-9; **16**, 79815-50-2; **17**, 1008-89-5; **18**, 3042-21-5; **19**, 79815-51-3; $Pd(PPh_3)_4$, 14221-01-3; $Pd(dba)_2$, 32005-36-0; $Pd(dba)_2$diphos, 79827-24-0; $Pd(diphos)_2$, 31277-98-2; $Mo(CO)_6$, 13939-06-5; $Rh_6(CO)_{16}$, 28407-51-4.

(10) Marvell, E. N.; Li, T. H. C. *J. Am. Chem. Soc.* **1978**, *100*, 883.

Structure of Bis(cyclopropyl)bis(dimethylphenylphosphine)platinum(II), *cis*-Pt(CHCH$_2$CH$_2$)$_2$[P(CH$_3$)$_2$(C$_6$H$_5$)]$_2$. Relationship between Structural and $^1J(^{195}Pt-^{31}P)$ Data and Position of Cyclopropyl Group in Trans-Influence Series

Nancy L. Jones and James A. Ibers*

Department of Chemistry, Northwestern University, Evanston, Illinois 60201

Received June 8, 1981

The structure of *cis*-bis(cyclopropyl)bis(dimethylphenylphosphine)platinum(II), *cis*-Pt(CHCH$_2$CH$_2$)$_2$(PMe$_2$Ph)$_2$, has been determined crystallographically at −133 (2) °C and consists of discrete molecules of the neutral complex. The complex crystallizes from pentane in the triclinic space group C_i^1-$P\bar{1}$ with two formula units in a unit cell of dimensions a = 11.055 (3) Å, b = 11.457 (3) Å, c = 9.897 (2) Å, α = 112.46 (1)°, β = 96.43 (1)°, γ = 67.73 (1)°. The structure was solved from Patterson and electron density maps. Full-matrix least-squares refinement has led to a final value of the R index on F^2 of 0.068 based on 8749 reflections and 226 variables. The conventional R index on F for those 7210 reflections having $F_o^2 > 3\sigma(F_o^2)$ is 0.039. This complex of Pt(II) possesses nearly square-planar geometry, P(1)–Pt–P(2) = 94.86 (4)°, C(1)–Pt–C(4) = 89.91 (18)°. The cyclopropyl rings are equilateral with average C–C distances of 1.506 (13) Å and C–C–C angles of 60.00 (80)°. Some important molecular parameters are Pt–C(1) = 2.086 (4) Å, Pt–C(4) = 2.070 (4) Å, Pt–P(1) = 2.302 (1) Å, and Pt–P (2) = 2.291 (1) Å. Examination of the structural and $^{31}P\{^1H\}$ NMR data and comparison of these data with those of other Pt(II) complexes suggest placement of the cyclopropyl group in the trans-influence series between metallocycloalkanes and alkyl groups, such as methyl and neopentyl.

Introduction

Recently much interest has focused on metal-assisted rearrangements of cyclopropanes to olefins.[1] Transition-metal σ-cyclopropyl complexes may be intermediates in these rearrangements. Since no simple σ-bound cyclopropyl transition-metal complexes had previously been characterized structurally[2,3] and few such complexes had been synthesized,[4] we undertook a crystallographic study of *cis*-Pt(CHCH$_2$CH$_2$)$_2$[P(CH$_3$)$_2$(C$_6$H$_5$)]$_2$[5] to investigate the effect of the metal on the C–C bonding within the cyclopropyl rings. We combined the structural results with $^{31}P\{^1H\}$ NMR data in an attempt to determine the trans influence of the cyclopropyl group. The results of the NMR study and our low temperature structure determination are reported here.

Experimental Section

The complex *cis*-Pt(CHCH$_2$CH$_2$)$_2$(PMe$_2$Ph)$_2$ was prepared by the method of Phillips and Puddephatt[5] by reacting *cis*-PtCl$_2$(PMe$_2$Ph)$_2$ with 2 equiv of cyclopropyllithium in dry, deaerated diethyl ether under an atmosphere of dinitrogen. Workup included addition of water to the ethereal suspension, evaporation of the solvent from the ether layer, and extraction of the residue into pentane. The ^1H NMR spectrum [(C_6D_6 solution, room temperature) δ(PhP) 6.95 (m), δ(MeP) 1.28 (d, $^2J + {}^4J$(PH) 7.7 Hz), δ(C$_3$H$_5$) 0.97 (m) ppm], the melting point (104 °C), and elemental analysis (calcd for $C_{22}H_{32}P_2Pt$: C, 47.74; H, 5.83; P, 11.19. Found: C, 47.56; H, 5.95; P, 11.18) agree with those reported in the literature.[5] The $^{31}P\{^1H\}$ NMR spectrum (C_6D_6 solution, room temperature) is consistent with the equivalence of the two phosphine ligands (s, −16.6 ppm downfield from external 85% H_3PO_4, J(Pt–P) = 1770 Hz).

Colorless crystals suitable for diffraction study were grown by slow evaporation of a pentane solution of *cis*-Pt(CHCH$_2$CH$_2$)$_2$(PMe$_2$Ph)$_2$. Preliminary precession photographic data taken at room temperature from a crystal mounted in air revealed no symmetry, other than the trivial center of symmetry. A Delaunay reduction of the cell constants did not reveal any hidden symmetry. The density, 1.62 (1) g/cm^3, measured by flotation of the crystals in aqueous $ZnCl_2$, may be compared with the density of 1.716 g/cm^3 calculated for two molecules of *cis*-Pt(CHCH$_2$CH$_2$)$_2$(PMe$_2$Ph)$_2$ in the low temperature cell.

A colorless crystal, described by faces {100}, {10$\bar{3}$}, ($\bar{1}$5$\bar{2}$), and ($\bar{2}$5$\bar{3}$), cut from a larger crystal, was mounted on a four-circle, computer-controlled Picker FACS-1 diffractometer.[6] Throughout the data collection the crystal was continuously bathed in a stream of cold (−133 (2) °C) dinitrogen gas.[7] Somewhere between −135 and −157 °C the crystals undergo an irreversible, destructive phase transition. Cell constants at −133 °C were obtained as described elsewhere[8] by a least-squares refinement of 18 centered reflections in the range 30° < 2θ (Mo Kα_1) < 32°. The cell constants are a = 11.055 (3) Å, b = 11.457 (3) Å, c = 9.897 (2) Å, α = 112.46 (1)°, β = 96.43 (1)°, γ = 67.73 (1)°, V = 1071 Å^3.

The θ–2θ scan technique was used to collect intensity data in shells of 2θ. Stationary-counter, stationary-crystal background counts of 10 s were measured at the beginning and end of each scan. For reflections having $I < 3\sigma(I)$, the reflection was rescanned and each background recounted for 20 s. The results of the two scans and two backgrounds were then combined. Six strong reflections were remeasured every 100 reflections during the course of the data collection. Their intensities decreased from the initial

(1) For a recent review, see: Bishop, K. C., III *Chem. Rev.* **1976**, *76*, 461–486.
(2) Attig, T. G.; Ziegler, R. J.; Brock, C. P. *Inorg. Chem.* **1980**, *19*, 2315–2320.
(3) Binger, P.; Doyle, M. J.; McMeeking, J.; Kruger, C.; Tsay, Y.-H. *J. Organomet. Chem.* **1977**, *135*, 405–414.
(4) (a) Cutler, A.; Fish, R. W.; Giering, W. P.; Rosenblum, M. *J. Am. Chem. Soc.*, **1972**, *94*, 4354–4355. (b) Brown, J. M.; Mertis, K. *J. Chem. Soc., Perkin Trans. 2*, **1973**, 1993–2001. (c) Periasamy, M. P.; Walborsky, H. M. *J. Am. Chem. Soc.* **1975**, *97*, 5930–5931. (d) Nuzzo, R. G.; McCarthy, T. J.; Whitesides, G. M., *J. Am. Chem. Soc.* **1981**, *103*, 3404–3410.
(5) Phillips, R. L.; Puddephatt, R. J. *J. Chem. Soc., Dalton Trans.* **1978**, 1732–1735.
(6) The disk-oriented diffractometer control program is from: Lenhert, P. G. *J. Appl. Crystallogr.* **1975**, *8* 568–570.
(7) Huffman, J. C. Ph.D. Thesis, Indiana University, 1974.
(8) Corfield, P. W.; Doedens, R. J.; Ibers, J. A. *Inorg. Chem.* **1967**, *6*, 197–204.

0276-7333/82/2301-0326$01.25/0

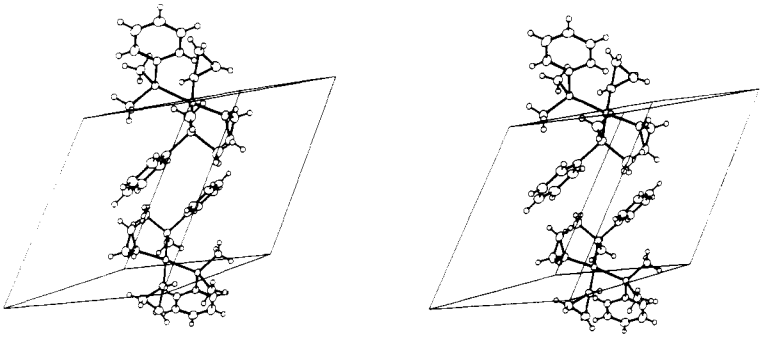

Figure 1. Stereoview of the unit cell of *cis*-Pt(CHCH$_2$CH$_2$)$_2$(PMe$_2$Ph)$_2$. Vibrational ellipsoids are drawn at the 50% probability level, except for hydrogen atoms which have been drawn artificially small.

measured intensities by an average of approximately 2%, and a correction for this decrease was made. Other parameters relevant to the data-collection process are listed in Table I.

Solution and refinement of the structure were carried out by procedures standard in this laboratory.[9] The position of the platinum atom was derived from an origin-removed sharpened Patterson map, on the assumption that the space group is the centrosymmetric one, C_i^1-$P\bar{1}$. This choice was confirmed ultimately by the successful refinement of the structure. Positions for the nonhydrogen atoms were obtained from Fourier and difference Fourier syntheses interspersed with structure-factor calculations and cycles of least-squares refinement. The function minimized was $\sum w(|F_o| - |F_c|)^2$, where $|F_o|$ and $|F_c|$ are, respectively, the observed and calculated structure amplitudes and where $w = 4F_o^2/\sigma^2(F_o^2)$. Atomic scattering factors were taken from the usual tabulation.[10] Initial refinements were on F and utilized only one-fourth of those reflections having $F_o^2 > 3\sigma(F_o^2)$. Refinement was continued until the conventional R index was 0.08. At this stage of refinement anomalous dispersion terms were included for the Pt and two P atoms;[10] in addition an absorption correction[9] was made. Atoms were now assigned an anisotropic model for their thermal motion. One cycle of least-squares refinement on one-third of those reflections having $F_o^2 > 3\sigma(F_o^2)$ yielded values for R and R_w on F of 0.044 and 0.049, respectively. On a resultant difference electron density map hydrogen atoms appeared with peak heights in the range 1.2 to 0.7 e/Å^3. These hydrogen atoms were placed in idealized locations (C–H 0.95 Å), each was given an isotropic thermal parameter B 1.0 Å^2 greater than that of its attached carbon atom, and all were held fixed during subsequent refinement. The function $\sum w(F_o^2 - F_c^2)^2$, where $w = 1/\sigma^2(F_o^2)$, was minimized in the final cycle of least-squares refinement, which involved 226 variables and 8749 observations (including those for which $F_o^2 < 0$). This refinement converged to values of R and R_w (on F_o^2) of 0.068 and 0.082, respectively, to an error in an observation of unit weight of 1.34 electrons^2, and for those reflections having $F_o^2 > 3\sigma(F_o^2)$ to values of the conventional R and R_w indices on $|F_o|$ of 0.039 and 0.040, respectively. The final difference electron density map is essentially featureless with the highest peak (4.2 eÅ^{-3}) near the Pt atom. This height may be compared with that of about 22 eÅ^{-3} for a typical C atom on an earlier electron density map. Analysis of R indices as a function of Miller indices, F_o^2, and setting angles revealed no unexpected trends. The final positional and thermal parameters of all atoms are listed in Table II. Table III lists values of $10|F_o|$ and $10|F_c|$;[11] a negative entry for $|F_o|$ indicates $F_o^2 < 0$.

Description of the Structure

The crystal structure consists of discrete molecules of *cis*-Pt(CHCH$_2$CH$_2$)$_2$[P(CH$_3$)$_2$(C$_6$H$_5$)]$_2$. The crystal packing is shown in Figure 1. The shortest intermolecular interaction is calculated to be 2.33 Å between two hydrogen atoms, H(1)C(5) and HC(11). The shortest Pt···H(cyclopropyl) distance is 2.46 Å [Pt–HC(4)], beyond the range of a metal–hydrogen interaction.

Figure 2 is a drawing of an individual molecule. Figure 3 is a drawing of the inner coordination sphere and displays some pertinent bond distances and angles. Bond angles and lengths are listed in Table IV. The coordination

Table I. Summary of Crystal Data and Intensity Collection for *cis*-Pt(CHCH$_2$CH$_2$)$_2$(P(CH$_3$)$_2$(C$_6$H$_5$))$_2$

compound	*cis*-Pt(CHCH$_2$CH$_2$)$_2$(PMe$_2$Ph)$_2$
formula	$C_{22}H_{32}P_2Pt$
formula wt	553.54 amu
a	11.055 (3) Å
b	11.457 (3) Å
c	9.897 (2) Å
α	112.46 (1)°
β	96.43 (1)°
γ	67.73 (1)°
V	1071 Å^3
Z	2
ρ_{calcd}	1.716 g/cm^3 (−133 °C)
ρ_{obsd}	1.62 (1) g/cm^3 (23 °C)
space group	C_i^1-$P\bar{1}$
crystal dimensions	0.28 × 0.45 × 0.23 mm along direct crystal axes
crystal shape	approximated as a 6-sided prism with major faces {100}, {10$\bar{3}$}, ($\bar{1}$5$\bar{2}$), ($\bar{2}$5$\bar{3}$)
crystal vol	0.0096 mm^3
temp	−133 °C[a]
radiation	graphite-monochromated Mo Kα, λ(Mo Kα$_1$) 0.7093 Å
linear absorption coefficient	67.6 cm^{-1}
transmission factors	0.197 – 0.449
receiving aperture	5.5 × 5.5 mm; 32 cm from crystal
take-off angle	3.1°
scan speed	2.0° in 2θ/min
2θ limits	3.5° < 2θ < 68.0°
scan range	1.1° below Kα$_1$ to 0.9° above Kα$_2$
background counts	10 s at each end of scan with rescan option[b]
unique data used in final refinement[c]	8749 ±h,±k,+l
unique data, $F_o^2 > 3\sigma(F_o^2)$	7210
final number of variables	226
R (on F_o^2, all data)	0.068
R_w (on F_o^2, all data)	0.082
R (on F_o for $F_o^2 > 3\sigma(F_o^2)$)	0.039
error in observation of unit weight	1.34 electrons^2

[a] See ref 7. [b] See ref 6. [c] This includes reflections with $F_o^2 < 0$.

(9) See, for example: Waters, J. M.; Ibers, J. A. *Inorg. Chem.* **1977**, *16*, 3273–3277.
(10) Cromer, D. T.; Waber, J. T. "International Tables for X-ray Crystallography"; Kynoch Press: Birmingham, England, 1974; Vol. IV, Table 2.2A and 2.3.1. For hydrogen atoms, see: Stewart, R. F.; Davidson, E. R.; Simpson, W. T. *J. Chem. Phys.* **1965**, *42*, 3175–3186.
(11) See paragraph at end of paper regarding supplementary material.

Table II. Positional and Thermal Parameters for the Atoms of *cis*-Pt($\overline{CHCH_2CH_2}$)$_2$($P(CH_3)_2(C_6H_5)$)$_2$

ATOM	X[A]	Y	Z	B_{11}[B] OR B, $Å^2$	B_{22}	B_{33}	B_{12}	B_{13}	B_{23}
PT	-0.244346(14)	-0.020781(15)	0.058603(16)	38.81(12)	35.00(13)	43.24(15)	-17.10(9)	8.61(9)	6.62(10)
P(1)	-0.386480(95)	0.10418(10)	0.25977(11)	41.95(81)	40.19(87)	51.5(11)	-15.27(69)	10.74(73)	10.12(80)
P(2)	-0.10739(10)	-0.17290(11)	0.15716(12)	41.74(84)	47.58(97)	60.3(12)	-14.68(73)	1.95(78)	11.52(88)
C(1)	-0.36162(42)	0.11943(42)	-0.03290(48)	63.6(39)	50.6(38)	66.2(49)	-25.0(31)	-4.3(35)	26.7(37)
C(4)	-0.11878(38)	-0.12322(43)	-0.12412(46)	48.6(32)	54.8(40)	62.9(46)	-21.8(29)	12.8(30)	6.2(36)
C(2)	-0.36054(47)	0.26292(45)	0.02034(55)	75.2(45)	52.4(40)	87.1(60)	-25.3(34)	3.2(41)	22.7(41)
C(3)	-0.31777(52)	0.16587(49)	-0.13438(53)	100.8(53)	69.6(46)	72.9(55)	-36.9(41)	13.9(43)	24.9(42)
C(5)	-0.09980(45)	-0.26127(48)	-0.23490(49)	64.1(43)	69.0(47)	69.2(48)	-22.5(37)	22.7(36)	2.0(39)
C(6)	-0.15565(44)	-0.14133(47)	-0.28064(46)	75.2(41)	76.6(45)	58.2(43)	-39.1(35)	13.2(33)	8.8(36)
C(7)	-0.42452(45)	0.01790(46)	0.36154(52)	64.5(43)	53.4(43)	72.7(56)	-22.2(35)	16.6(39)	17.7(41)
C(8)	-0.55135(35)	0.20778(41)	0.23004(49)	42.0(29)	59.1(38)	81.8(52)	-14.0(27)	5.8(31)	19.2(36)
C(9)	-0.33264(38)	0.22972(38)	0.40367(42)	46.8(34)	39.3(34)	55.3(40)	-12.9(28)	11.2(29)	7.5(31)
C(10)	-0.22429(39)	0.25361(42)	0.37944(46)	49.9(34)	48.7(39)	59.0(45)	-17.2(30)	7.1(31)	13.1(35)
C(11)	-0.18359(42)	0.34919(46)	0.48928(53)	56.5(38)	54.9(45)	72.6(58)	-24.5(34)	-1.5(38)	19.8(43)
C(12)	-0.25038(51)	0.42113(49)	0.62293(52)	79.6(53)	53.1(46)	76.9(51)	-30.9(41)	-4.9(41)	4.6(40)
C(13)	-0.35784(58)	0.39913(57)	0.64852(59)	100.8(61)	74.5(58)	83.3(62)	-42.0(50)	37.2(48)	-23.7(49)
C(14)	-0.39870(49)	0.30318(53)	0.54074(54)	76.9(48)	73.3(54)	78.4(55)	-39.9(42)	30.4(41)	-11.4(44)
C(15)	-0.33689(46)	-0.09244(48)	0.32520(50)	62.9(43)	66.9(47)	82.1(50)	-29.4(37)	-19.2(37)	23.4(40)
C(16)	0.03939(47)	-0.30643(52)	0.05362(57)	49.9(43)	74.9(52)	100.9(62)	-6.2(39)	10.9(41)	18.5(46)
C(17)	-0.17752(38)	-0.27373(39)	0.20341(44)	47.2(34)	37.2(34)	56.9(42)	-7.2(27)	1.5(30)	9.8(32)
C(18)	-0.26083(45)	-0.32864(44)	0.10592(50)	59.9(42)	52.6(41)	75.0(50)	-21.5(34)	-12.6(36)	21.4(37)
C(19)	-0.31268(47)	-0.40993(49)	0.13507(58)	62.9(45)	58.3(47)	111.2(65)	-28.4(38)	-10.3(43)	21.8(46)
C(20)	-0.28546(46)	-0.43469(43)	0.26364(52)	66.4(44)	48.2(39)	104.2(54)	-16.8(33)	14.3(39)	20.8(38)
C(21)	-0.20580(51)	-0.37858(49)	0.36255(53)	88.0(52)	64.0(47)	77.2(54)	-24.0(40)	10.3(42)	25.5(42)
C(22)	-0.15178(45)	-0.29980(43)	0.33202(48)	77.4(43)	62.6(39)	61.2(48)	-30.8(34)	-10.8(36)	20.7(36)
HC1	-0.444	0.109	-0.046	3.2					
H1C2	-0.438	0.339	0.042	3.8					
H2C2	-0.295	0.284	0.089	3.8					
H1C3	-0.227	0.127	-0.165	4.0					
H2C3	-0.370	0.182	-0.212	4.0					
HC4	-0.145	-0.096	-0.089	3.1					
H1C5	-0.014	-0.324	-0.270	3.7					
H2C5	-0.154	-0.336	-0.231	3.7					
H1C6	-0.245	-0.111	-0.304	3.5					
H2C6	-0.136	-0.129	-0.343	3.5					
H1C7	-0.502	0.079	0.422	3.7					
H2C7	-0.440	-0.059	0.295	3.7					
H3C7	-0.355	-0.007	0.421	3.7					
H1C8	-0.604	0.244	0.316	3.3					
H2C8	-0.548	0.278	0.205	3.3					
H3C8	-0.587	0.151	0.152	3.3					
HC10	-0.176	0.201	0.289	3.2					
HC11	-0.111	0.369	0.471	3.5					

ATOM	X	Y	Z	B, $Å^2$
HC12	-0.222	0.488	0.594	4.0
HC13	-0.405	0.451	0.742	4.7
HC14	-0.475	0.289	0.557	4.2
H1C15	0.029	-0.159	0.353	3.7
H2C15	0.000	-0.036	0.309	3.7
H3C15	-0.103	-0.038	0.400	3.7
H1C16	0.016	-0.368	-0.029	4.2
H2C16	0.089	-0.267	0.024	4.2
H3C16	0.092	-0.353	0.115	4.2
HC18	-0.282	-0.311	0.019	3.6
HC19	-0.367	-0.448	0.067	4.0
HC20	-0.323	-0.490	0.281	3.7
HC21	-0.187	-0.395	0.449	4.0
HC22	-0.096	-0.263	0.401	3.4

[A] ESTIMATED STANDARD DEVIATIONS IN THE LEAST SIGNIFICANT FIGURE(S) ARE GIVEN IN PARENTHESES IN THIS AND ALL SUBSEQUENT TABLES. [B] THE FORM OF THE ANISOTROPIC THERMAL ELLIPSOID IS: $\exp[-(B_{11}h^2+B_{22}k^2+B_{33}l^2+2B_{12}hk+2B_{13}hl+2B_{23}kl)]$. THE QUANTITIES GIVEN IN THE TABLE ARE THE THERMAL COEFFICIENTS $\times 10^4$.

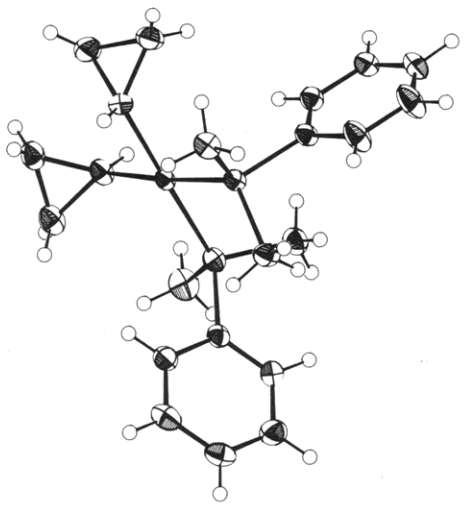

Figure 2. Drawing of an individual molecule of *cis*-Pt($\overline{CHCH_2CH_2}$)$_2$(PMe_2Ph)$_2$.

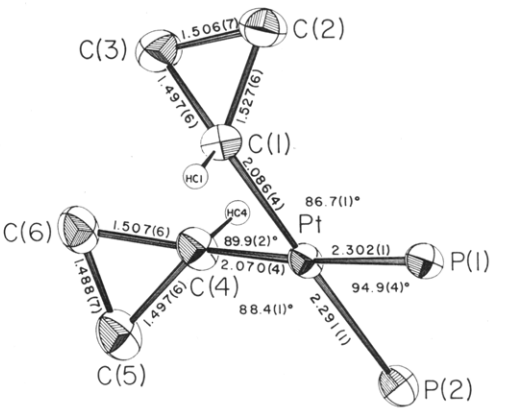

Figure 3. Coordination sphere of *cis*-Pt($\overline{CHCH_2CH_2}$)$_2$-(PMe_2Ph)$_2$ with some bond distances and angles.

about the Pt atom is essentially planar. The average deviation of the Pt, two P, and two C atoms attached to the Pt center from the best-weighted least-squares plane is 0.033 Å. The maximum deviation is that of atom C(4) (0.083 Å). Angles around the Pt atom are distorted from 90°. The angle P(1)–Pt–C(1) also differs slightly from the angle P(2)–Pt–C(4), 86.69 (13)° and 88.45 (13)°, respectively. The Pt–P(1) and Pt–P(2) bond distances, 2.302 (1)

Table IV. Selected Distances (Å) and Angles (Deg) in *cis*-Pt(CHCH$_2$CH$_2$)$_2$(P(CH$_3$)$_2$(C$_6$H$_5$))$_2$

Bond Distances		
Pt-P(1)	2.302 (1)	2.296 (8)[a]
Pt-P(2)	2.291 (2)	
Pt-C(1)	2.086 (4)	2.078 (11)
Pt-C(4)	2.070 (4)	
C(1)-C(2)	1.527 (6)	1.506 (13)
C(2)-C(3)	1.506 (7)	
C(3)-C(1)	1.497 (6)	
C(4)-C(5)	1.508 (6)	
C(5)-C(6)	1.488 (7)	
C(6)-C(4)	1.507 (6)	
P(1)-C(7)	1.827 (5)	1.823 (5)
P(1)-C(8)	1.823 (4)	
P(1)-C(9)[b]	1.829 (4)	
P(2)-C(15)	1.818 (4)	
P(2)-C(16)	1.821 (5)	
P(2)-C(17)[b]	1.819 (4)	
C(9)-C(10)	1.389 (5)	1.387 (8)
C(10)-C(11)	1.392 (6)	
C(11)-C(12)	1.378 (7)	
C(12)-C(13)	1.372 (7)	
C(13)-C(14)	1.387 (7)	
C(14)-C(9)	1.402 (6)	
C(17)-C(18)	1.397 (6)	
C(18)-C(19)	1.383 (7)	
C(19)-C(20)	1.384 (7)	
C(20)-C(21)	1.379 (7)	
C(21)-C(22)	1.386 (6)	
C(22)-C(17)	1.391 (6)	
Bond Angles		
P(1)-Pt-P(2)	94.86 (4)	
C(1)-Pt-C(4)	89.91 (18)	
P(1)-Pt-C(1)	86.69 (13)	
P(1)-Pt-C(4)	175.89 (13)	
P(2)-Pt-C(1)	177.36 (12)	
P(2)-Pt-C(4)	88.45 (13)	
C(2)-C(1)-C(3)	59.73 (30)	60.00 (80)
C(1)-C(2)-C(3)	59.13 (29)	
C(1)-C(3)-C(2)	61.14 (30)	
C(5)-C(4)-C(6)	59.15 (30)	
C(4)-C(5)-C(6)	60.41 (30)	
C(4)-C(6)-C(5)	60.45 (30)	
Pt-P(1)-C(7)	119.68 (15)	
Pt-P(1)-C(8)	116.83 (15)	
Pt-P(1)-C(9)	113.38 (13)	
Pt-P(2)-C(15)	112.68 (16)	
Pt-P(2)-C(16)	119.55 (19)	
Pt-P(2)-C(17)	116.78 (13)	
C(7)-P(1)-C(8)	100.12 (21)	
C(8)-P(1)-C(9)	102.05 (18)	
C(7)-P(1)-C(9)	102.18 (20)	
C(15)-P(2)-C(16)	100.70 (22)	
C(16)-P(2)-C(17)	100.04 (22)	
C(15)-P(2)-C(17)	104.76 (21)	
C(14)-C(9)-C(10)	118.51 (36)	120.00 (98)
C(9)-C(10)-C(11)	120.26 (39)	
C(10)-C(11)-C(12)	120.38 (40)	
C(11)-C(12)-C(13)	120.11 (41)	
C(12)-C(13)-C(14)	120.17 (47)	
C(13)-C(14)-C(9)	120.55 (43)	
C(22)-C(17)-C(18)	117.86 (39)	
C(17)-C(18)-C(19)	120.62 (43)	
C(18)-C(19)-C(20)	120.68 (42)	
C(19)-C(20)-C(21)	119.34 (43)	
C(20)-C(21)-C(22)	120.10 (44)	
C(21)-C(22)-C(17)	121.37 (39)	

[a] The estimated standard deviation given in parentheses is the larger of that calculated for an individual observation on the assumption that the values averaged are from the same population or of that calculated from the inverse lease-squares matrix. [b] Atoms C(9)-C(14) and C(17)-C(22) constitute the phenyl rings.

and 2.291 (1) Å, respectively, differ slightly, the P atom attached through the longer bond being trans to the C atom attached through the shorter Pt–C bond [2.070 (4) vs. 2.086 (4) Å]. The differences in the Pt–P bond lengths may be caused by steric crowding. The Pt-C(1) and Pt-C(4) bond lengths are typical for Pt–C σ bonds. The C–C bond lengths within the cyclopropyl rings do not differ significantly. Similarly, the C–C–C bond angles are also equal. There does not appear to be any orbital overlap between the phosphine phenyl rings and the cyclopropyl rings.

The platinum σ-cyclopropyl complex [2,3-bis(methoxycarbonyl)-1-methylcyclopropyl]bis(triphenylphosphine)-platinum(II) tetrafluoroborate (A), studied by Attig, Zie-

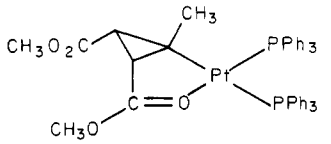

A

gler, and Brock,[2] contains a functionalized cyclopropyl ring. The oxygen atom of one ester group interacts with the platinum center, causing the ring to be distorted. Thus direct comparison of that structure with the present one is impossible. The structural characterization of the nickel σ-cyclopropyl complex α,α'-bipyridyl-5-nickela-3,3,7,7-tetramethyl-*trans*-tricyclo[4.1.0.0^{2,4}]heptane (B), carried

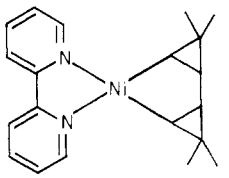

B

out by Binger et al.,[3] has revealed functionalized cyclopropyl rings constrained by a C–C bond between the rings. No distortion of the rings is apparent. The cyclopropyl rings are equilateral with an average C–C bond distance of 1.52 Å and an average C–C–C bond angle of 60°.

Upon comparison with Pt–P bond lengths (Table V) in other compounds,[12-20] we can place the σ-bound cyclopropyl group (Pt–P 2.302 (1) and 2.291 (1) Å) in the trans-influence series between metallocycloalkanes and alkyl groups, such as methyl and neopentyl groups.[21] A comparison of the $^1J(^{195}Pt-^{31}P)$ coupling constant (1770 Hz) with the coupling constants of other alkyl(bis(tertiary

(12) Manojlović-Muir, L.; Muir, K. W.; Solomun, T.; Meek, D. W.; Peterson, J. L. *J. Organomet. Chem.* **1978**, *146*, C26-C28.
(13) Crociani, B.; Nicolini, M.; Clemente, D. A.; Bandoli, G. *J. Organomet. Chem.* **1973**, *49*, 249–256.
(14) Gee, R. J. D.; Powell, H. M. *J. Chem. Soc. A* **1971**, 1956–1960.
(15) Bresciani-Pahor, N.; Plazzotta, M.; Randaccio, L.; Bruno, G.; Ricevuto, V.; Romeo, R.; Belluco, U. *Inorg. Chim. Acta* **1978**, *31*, 171–175.
(16) Howard, J.; Woodward, P. *J. Chem. Soc., Dalton Trans.* **1973**, 1840–1843.
(17) Ibers, J. A.; DiCosimo, R.; Whitesides, G. M. *Organometallics* **1982**, *1*, 13.
(18) Yarrow, D. J.; Ibers, J. A.; Lenarda, M.; Graziani, M. *J. Organomet. Chem.* **1974**, *70*, 133–145.
(19) Bielfeld, C. G.; Eick, H. A.; Grubbs, R. H. *Inorg. Chem.* **1973**, *12*, 2166–2170.
(20) Barker, G. K.; Green, M.; Howard, J. A. K.; Spencer, J. L.; Stone, F. G. A. *J. Chem. Soc., Dalton Trans.* **1978**, 1839–1847.
(21) The electron-withdrawing groups, —C≡N and —CH=CH$_2$, present in the metallocyclic compounds, *cis*-Pt(C(CN)$_2$CH$_2$C(CN)$_2$)-(PPh$_3$)$_2$ and *cis*-Pt(CH(CHCH$_2$)(CH$_2$)$_2$CH(CHCH$_2$))(PMe$_3$)$_2$, may bring about Pt–P bond lengths longer than those present in the unsubstituted platinum metallocycles.

Table V. Selected Pt-P Bond Distances in Other Complexes, *cis*-$PtXY(PR_3)_2$

X	Pt-P (trans to X), Å	Y	PR_3	ref
CH_3	2.327 (1)	$PMe_2(C_6F_5)$	$PMe_2(C_6F_5)$	12
C_6H_5	2.330 (20)	$PbPh_3$	PPh_3	13
C_6H_5	2.317 (5)	$GePh_3OH$	PEt_3	14
$CH_3C_6H_5$	2.320 (9)	Cl	PEt_3	15
C_6F_5	2.326 (7)	Cl	PEt_3	15
$CH(CF_3)_2$	2.310 (7)	F	PPh_3	16
CF_3	2.326 (1)	X	$PMe_2(C_6F_5)$	12
$CH_2C(CH_3)_3$	2.322 (1)	X	PEt_3	17
$CHCH_2CH_2$	2.302 (1), 2.291 (1)	X	PMe_2Ph	this work
$C(CN)_2CH_2C(CN)_2$	2.314 (2), 2.291 (2)		PPh_3	18
$CH_2C(CH_3)_2CH_2$	2.287 (1), 2.282 (2)		PEt_3	17
$CH_2(CH_2)_2CH_2$	2.279 (5), 2.285 (6)		PPh_3	19
$CH(CHCH_2)(CH_2)_2CH(CHCH_2)$	2.294 (2), 2.306 (2)		PMe_3	20

Table VI. Selected $^1J(^{195}Pt-^{31}P)$ Coupling Constants for Complexes *cis*-$PtXY(PR_3)_2$[a]

X	^1J(Pt-P(trans to X)), Hz	Y	^1J(Pt-P(trans to Y)), Hz	PR_3	ref
C_6H_5	1577	Cl	4138	PEt_3	22
C_6H_5	1705	X		PEt_3	22
2,4,6-$C_6H_2(CH_3)_3$	1603	Br	4234	PEt_3	22
$CH(CH_2)_3CH_2$	1616	X		PEt_3	4d
$CH_2C(CH_3)_3$	1638	X		PEt_3	23
$CH(CH_2)_2CH_2$	1647	X		PEt_3	4d
CH_3	1719	Cl	4179	PEt_3	22
CH_3	1856	X		PEt_3	22
CH_3	1865	$PMe_2(C_6F_5)$	2822	$PMe_2(C_6F_5)$	12
$CHCH_2CH_2$	1770	X		PMe_2Ph	this work
$CHCH_2CH_2$	1790	X		PEt_3	4d
$CH_2C(CH_3)_2CH_2$	1868			PEt_3	23
Cl	3454	$P(Bu\text{-}n)_3$	2270	$P(Bu\text{-}n)_3$	22

[a] No correction has been made to account for the different phosphine groups or different NMR solvents used.

phosphine))platinum(II) compounds[4d,12,22,23] (Table VI) supports this placement of the σ-bound cyclopropyl group in the trans-influence series, although more data are needed. Interpretation of these data indicates that the cyclopropyl group tends to weaken the bond trans to itself (i.e., lengthen the Pt–P bond) by an inductive effect. The ^1J(Pt-P) coupling constant depends mainly on the covalency and s character of the Pt–P bond, as determined by the inductive effect of the group trans to the phosphine.[24] The Cl^- ligand is considered to be low in the trans-influence series[25] and Pt–P bond lengths trans to the Cl^- ligand are shorter than the bond lengths we report here. For example, the Pt–P bond lengths reported for *cis*-$PtCl_2[PMe_2(C_6F_5)]_2$ are 2.231 (1) and 2.240 (1) Å and a ^1J(Pt–P) coupling constant of 3586 Hz is also reported.[12] The phenyl group is placed high in the trans-influence series, and this is reflected in the low ^1J(P–P) coupling constants measured[22] (1577 and 1705 Hz for Pt(II)–phenyl complexes) and the lengthening of the Pt–P bond in *cis*-$Pt(C_6H_5)(GePh_2OH)(PEt_3)_2$ to 2.317 (5) Å.[14] The ^1J(Pt–P) value of 1770 Hz for *cis*-$Pt(CHCH_2CH_2)_2(PMe_2Ph)_2$ reported here fits in nicely between that of 1638 Hz for *cis*-$Pt[CH_2C(CH_3)_3]_2(PEt_3)_2$ and a ^1J(Pt–P) of 1868 Hz for $Pt[CH_2C(CH_3)_2CH_2](PEt_3)_2$.[23]

Acknowledgment. This research was supported by the National Science Foundation (Grant CHE80-09671). We thank Johnson-Matthey, Inc., Malvern, PA., for the generous loan of platinum. We thank Professor G. M. Whitesides for informing us of his results prior to publication.

(22) Allen, F. H.; Pidcock, A. *J. Chem. Soc. A* **1968**, 2700–2704.
(23) Foley, P.; DiCosimo, R.; Whitesides, G. M. *J. Am. Chem. Soc.* **1980**, *102*, 6713–6725.
(24) Mason, R.; Meek, D. W. *Angew. Chem., Int. Ed. Engl.* **1978**, *17*, 183–194.
(25) Appleton, T. G.; Clark, H. C.; Manzer, L. E. *Coord. Chem. Rev.* **1973**, *10*, 335–422.

Registry No. *cis*-$Pt(CHCH_2CH_2)_2(PMe_2Ph)_2$, 64522-77-6; *cis*-$PtCl_2(PMe_2Ph)_2$, 15393-14-3.

Supplementary Material Available: Table III, listing of $10|F_o|$ vs. $10|F_c|$ values (30 pages). Ordering information is given on any current masthead page.

Intramolecular π Coordination in γ-Phenylpropylmercurials

William Kitching,* Gregory M. Drew, and Vincent Alberts

Department of Chemistry, University of Queensland, Brisbane, Australia

Received August 12, 1981

The ^{13}C and ^{199}Hg nuclear magnetic resonance spectra of series of 3-(*p*-substituted-phenyl)-2-methoxypropylmercuric chlorides and 3-(*p*-substituted-phenyl)-2-methyl-2-methoxypropylmercuric chlorides have been obtained. Variations in spectral parameters with the para substituent, solvent, concentration, and temperature are fully in accord with the conclusion that γ-phenylpropylmercuric halides exist (in poorly donor solvents) largely as intramolecular π complexes. Spectral comparisons for *n*-butyl-, 3-phenylpropyl-, and 3-(cyclopropyl)propylmercuric chlorides indicate that the π-donor ability of the 3-cyclopropyl group is insignificant.

Introduction

Some years ago Kiefer and co-workers reported extensive ^1H NMR data for certain 3-aryl-2-methyl-2-methoxypropylmercuric derivatives in which the 3-aryl group was, in the main, a para-substituted phenyl group.[1-3] Variations in the degree of magnetic inequivalence displayed by the methylene protons, and the four-bond ^{199}Hg–CH_3 coupling constant strongly indicated a chelate effect involving the π system of the 3-aryl group. Changing the para substituent from methoxy to trifluoromethyl induced changes explicable in terms of stronger donor action by the *p*-anisyl group. More classical approaches such as temperature, solvent, and concentration changes produced the anticipated variations in the ^1H NMR spectra, and the conformation permitting Hg–arene interaction (A) agreed

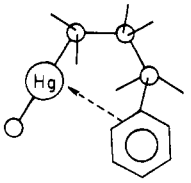

A

with the crystal structure[1] of 3-(*p*-methoxyphenyl)-2-methyl-2-methoxypropylmercuric chloride.

We have reported the ^{13}C and ^{199}Hg NMR spectra of several classes of organomercurials and developed conclusions concerning some of the determinants of ^{13}C–^{199}Hg coupling and ^{199}Hg chemical shifts.[4-8] If γ-phenylpropylmercuric chlorides did indeed possess a clear-cut (1–2 kcal/mol) conformational energy minimum, it appeared that the ^{13}C and ^{199}Hg NMR parameters should follow certain trends if our previous generalizations on these matters were valid. We have, therefore, obtained the ^{13}C and ^{199}Hg NMR spectra of two series of oxymercurials: 3-(*p*-substituted-phenyl)-2-methoxypropylmercuric chlorides and 3-(*p*-substituted-phenyl)-2-methyl-2-methoxypropylmercuric chlorides. The unsubstituted 3-phenylpropylmercuric chloride has also been examined, along with 3-(cyclopropyl)propyl and *n*-butylmercuric chlorides. Effects of para substituents on the spectra, as well as solvent, concentration, and temperature changes, have been evaluated.

Results and Discussion

Compounds. The mercurials I and II were prepared in a standard way by methoxymercuration (mercuric acetate in methanol) followed by treatment with aqueous sodium chloride (eq 1, 2). Some of the mercurials were

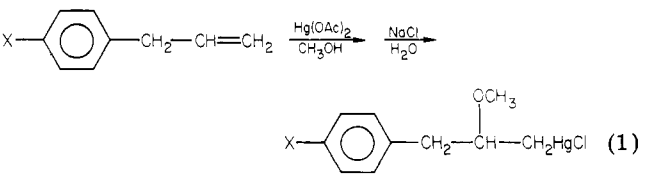

I, X = H, OCH_3, CF_3

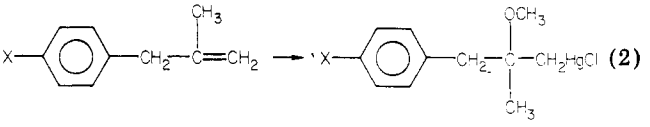

II, X = H, CH_3, OCH_3, CF_3

crystalline, while others were viscous oils.

3-Phenylpropylmercuric chloride was synthesized from the bromide, which in turn was obtained from the reaction of mercuric bromide and 3-phenylpropylmagnesium bromide. Condensation of cyclopropylcarbinyl bromide with diethyl sodiomalonate followed by hydrolysis and decarboxylation provided 3-(cyclopropyl)propanoic acid which was reduced to the alcohol. Bromination (PBr_3/ether) yielded the bromide which was converted to the bromomercurial via the Grignard reagent in the normal way. The bromomercurial was metathesized with a slight excess of silver acetate, and the acetatomercurial was converted to the chloromercurial which was fully characterized. The constitutions of the mercurials follow from the syntheses, the ^1H, ^{13}C, and ^{199}Hg spectra, and from the analyses of the crystalline derivatives.

^{13}C Spectra. Examination of series I was conducted initially to establish that significant changes in the vicinal ^{13}C–^{199}Hg coupling occurred, as the substituent and concentration varied. The data are in Table I and confirm variations in $^3J_{^{13}C-^{199}Hg}$ of such a magnitude that further measurements were warranted.

The important aspect of the date in Table I is the variation of the ^{199}Hg coupling to C_3 (*vic* coupling), particularly with substituent. Thus an increase of some 21 Hz is observed when R is changed from OCH_3 to CF_3, with R = H exhibiting an intermediate value. A small decrease (~3 Hz) is also observed when the concentration is reduced from 0.4 M to 0.2 M for R = OCH_3. These changes encouraged examination of series II oxymercurials, the series studied initially (by ^1H NMR) by Kiefer and co-

(1) Kiefer, E. F.; Waters, W. L.; Carlson, D. A. *J. Am. Chem. Soc.* **1968**, *90*, 5127.
(2) Kiefer, E. F.; Gericke, W. *J. Am. Chem. Soc.* **1968**, *90*, 5131.
(3) Kiefer, E. F.; Gericke, W.; Amimoto, S. T. *J. Am. Chem. Soc.* **1968**, *90*, 6246.
(4) Kitching, W.; Praeger, D.; Doddrell, D.; Anet, F. A. L.; Krane, J. *Tetrahedron Lett.* **1975**, 759.
(5) Anet, F. A. L.; Krane, J.; Kitching, W.; Doddrell, D.; Praeger, D. *Tetrahedron Lett.* **1974**, 3255.
(6) Barron, P. F.; Doddrell, D.; Kitching, W. *J. Organomet. Chem.* **1977**, *139*, 369.
(7) Kitching, W.; Drew, G. M.; Adcock, W.; Abeywickrema, A. *J. Org. Chem.* **1981**, *46*, 2252.
(8) Kitching, W.; Drew, G. M. *J. Org. Chem.* **1981**, *46*, 2695.

0276-7333/82/2301-0331$01.25/0

Table I. ^{13}C NMR Data[a] for

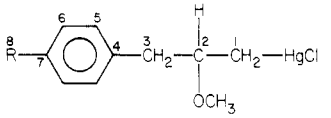

R	solvent	carbon number 1	2	3	4	5	6	7	8	OCH_3
H	$CDCl_3$ (0.4 M)	34.87 (1546.7)	78.0	42.0 (73.3)	137.4	129.0	129.7	127.2		56.2
OCH_3	$CDCl_3$ (0.4 M)	34.2	80.0	40.8 (70.3)	129.1	130.6	114.7	159.0	55.4	56.0
	$CDCl_3$ (0.2 M)	34.2 (1551.1)	80.0	40.7 (67.4)	129.1	130.6	114.7	159.1	55.5	56.0
CF_3	$CDCl_3$ (0.4 M)	35.8 (1555.2)	79.8	42.6 (91.6)	141.7	130.0	125.7 [3.7]	129.2 [27.1]	123.6 [271.8]	56.2

[a] Chemical shifts (ppm) relative to internal Me_4Si. Values in parentheses are ^{13}C-^{199}Hg couplings (Hz), and values in brackets are ^{13}C-^{19}F couplings (Hz).

Table II. ^{13}C NMR Data[a,b] for

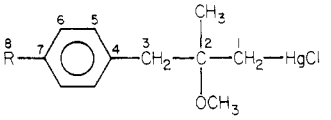

R	solvent	carbon number 1	2	3	4	5	6	7	8	CH_3	OCH_3
H	$CDCl_3$ (0.4 M)	41.9 (1612.6)	77.8	44.8 (61.5)	137.7	128.7	130.3	127.1		27.1 (198.6)	49.5
	$CDCl_3$-pyridine[c] (0.4 M)	41.0 (1656.6)	77.4	44.7 (73.3)	137.4	128.0	129.8	126.4		26.5 (186.1)	48.9
OCH_3	$CDCl_3$ (0.2 M)	41.4 (1608.9)	78.0	43.8 (54.2)	129.7	131.2	114.6	159.2	55.5	27.0 (208.1)	49.5
	$CDCl_3$ (0.4 M)	41.4 (1611.1)	77.9	43.8 (55.7)	129.6	131.2	114.6	159.2	55.4	27.0 (208.1)	49.5
	$CDCl_3$ (0.6 M)	41.4 (1613.3)	77.9	43.8 (56.4)	129.6	131.2	114.5	159.1	55.4	27.0 (207.4)	49.4
	$CDCl_3$-pyridine[c] (0.4 M)	40.5 (1699.1)	77.4	43.7 (65.9)	129.2	130.7	113.8	158.5	54.7	26.4 (195.6)	48.6
CH_3	$CDCl_3$ (0.4 M)	41.5 (1614.8)	77.8	44.2 (55.7)	137.3	130.2	129.7	134.6	21.1	27.1 (206.6)	49.5
	$CDCl_3$-pyridine[c] (0.4 M)	40.6 (1657.3)	77.3	44.2 (66.9)	136.3	129.7	128.9	134.2	20.5	26.5 (194.2)	48.9
CF_3	$CDCl_3$ (0.4 M)	42.5 (1587.0)	77.8	45.3 (79.1)	141.9	130.7	125.3 [4.4]	129.4 [32.3]	124.1 [271.8]	27.1 (181.7)	49.6
	$CDCl_3$-pyridine[c] (0.4 M)	41.0 (1667.6)	77.3	45.2 (92.3)	141.7 [1.4]	130.2	124.7 [3.6]	127.5 [33.0]	123.7 [271.8]	26.5 (165.6)	48.9

[a] Chemical shifts (ppm) are relative to internal Me_4Si. [b] Values in parentheses are ^{13}C-^{199}Hg couplings (Hz), and values in brackets are ^{13}C-^{19}F couplings (Hz). [c] $CDCl_3$-pyridine refers to 80:20 by volume

workers.[1,2] The full listing of the ^{13}C data for series II is listed in Table II.

The series II oxymercurials have the advantageous feature that two vicinal ^{199}Hg–^{13}C couplings (to C_3 and CH_3) can be measured. The salient features of the data in Table II are the following: (a) For 0.4 M solutions in $CDCl_3$, the *vic* ^{13}C–^{199}Hg coupling to C_3 is ~55 Hz for donor R groups (OCH_3, CH_3) and increases to 79 Hz for R = CF_3, with R = H exhibiting an intermediate value (61.5 Hz). In contrast, the *vic* coupling to CH_3 is ca. 207 Hz for R = OCH_3, CH_3, 199 Hz for R = H, and 182 Hz for R = CF_3. (b) For 0.4 M solutions, in 80:20 $CDCl_3$:pyridine, a significant increase in all *vic* couplings to C_3 occurs (compared with data for $CDCl_3$ solutions), whereas significant reductions occur in ^3J to CH_3. The variations with R are comparable with the changes observed for $CDCl_3$ solvent. (c) For R = OCH_3, concentration changes from 0.2 to 0.6 M ($CDCl_3$) induce slight increases in ^3J (of C_3) but a marginal decrease in ^3J to CH_3.

We also examined the effect of temperature on the ^{13}C spectra of the *p*-anisyl derivative, and the results are shown in Table III.

The chief feature to emerge from this study is the reduction in ^3J to C_3 (55.7 → 50.6 Hz) with decreasing temperature, but the increase (208 → 223.7 Hz) in ^3J to CH_3.

The large difference in the ^3J values to C_3 and CH_3 in these systems (~50–90 Hz compared with 180–210 Hz) is particularly noteworthy, as are the changes in these couplings with substituent and the less pronounced but significant variations with concentration, solvent, and temperature. We have demonstrated previously that *vic* ^{199}Hg–^{13}C coupling is strongly dihedral-angle dependent, of the Karplus type.[4,5] For example, in alkylmercuric chlorides, couplings of ca. 75 and 275 Hz are associated with dihedral angles of ca. 60° and 180°, respectively, although a β-methoxy group may have a slight effect on these couplings. It is quite clear, then, that in the present series the average dihedral angle between ^{199}Hg and C_3 and

Table III. ^{13}C NMR Data[a,b] for

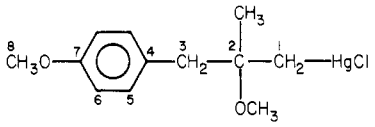

temp, K	carbon number 1	2	3	4	5	6	7	8	CH_3	OCH_3
303	41.4 (1611.1)	77.9	43.8 (55.7)	129.6	131.2	114.6	159.2	55.4	27.0 (208.1)	49.5
274	41.4 (1615.6)	77.8	43.6 (53.5)	129.6	131.2	114.5	159.1	55.4	27.0 (210.3)	49.5
233	41.2 (1631.7)	77.6	42.6 (50.6)	129.3	131.1	114.2	158.8	55.4	27.0 (223.7)	49.6

[a] Values in parentheses are ^{13}C–^{199}Hg couplings (Hz). Chemical shifts in ppm. [b] 0.4 M in $CDCl_3$.

Table IV. ^{199}Hg Chemical Shifts[a] for 2-Methoxy-3-phenylpropylmercuric Chloride

p-$RC_6H_4CH_2CH(OCH_3)CH_2HgCl$, R =	conditions 0.2 M $CDCl_3$	0.4 M $CDCl_3$	0.4 M (80:20) $CDCl_3$-pyridine	0.3 M (65:35) $CDCl_3$-pyridine
OCH_3	174.0	172.3	177.3	180.6
H		168.1	175.1	178.7
CF_3		157.9	173.5	180.3
p-$RC_6H_4CH_2C(CH_3)(OCH_3)CH_2HgCl$, R =	0.2 M $CDCl_3$	0.4 M $CDCl_3$	0.6 M $CDCl_3$	0.4 M (80:20) $CDCl_3$-pyridine
OCH_3	154.5	154.4	154.2	158.2
CH_3		154.6		157.9
H		149.1		154.5
CF_3		149.1		156.8

[a] Positive values are to lower field. Chemical shifts in ppm.

between ^{199}Hg and CH_3 must be quite different and approach ~60° and 160–170°, respectively. The variations in *vic* couplings with a para substituent cannot be attributed to any direct interaction (of the substituent) with the coupling ^{13}C and ^{199}Hg nuclei as the substituent is simply too remote from them. Rather, the (average) dihedral angle changes (as evidenced by changes in ^3J) must be associated with a change in conformational equilibria, regulated by the donor ability of the aryl group. The responses listed above to the classical tests for intramolecular interaction (concentration, temperature, etc.) favor this conclusion.

Kiefer and co-workers[1,2] argued that an equilibrium of the form shown in eq 3 was primarily responsible for the spectral variations they observed. K_f should be larger as

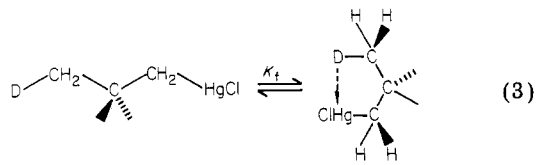

(3)

donor ability increased (e.g., electron-donating para substituents) and also at lower concentrations where competition from intermolecular coordination would diminish. On the other hand, addition of sufficient external donor, e.g., a strongly coordinating solvent, would reduce the requirement for the chelate effect and reduce K_f. Variation of the ^{13}C parameters with temperature verifies the existence of a preferred conformation, the nature of which can be reasonably inferred if the "spectral characteristics" of one limiting conformation are available.

To discuss our data (^3J values) in terms of the model above, it is necessary to decide the preferred conformations for both the chelated and open arrangements, so that dihedral angles can be estimated. The favored open and chelated arrangements are shown in eq 4.

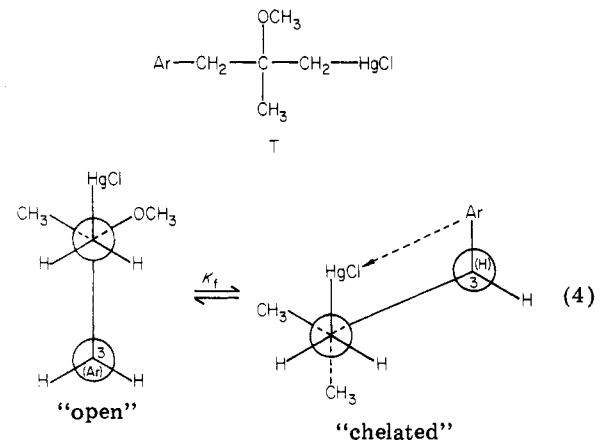

(4)

Notice that the dihedral angles between Hg and CH_3 are 180° in the "chelated" form and 60° in the open form, but 60° to C_3 in the chelated form and 180° in the open form. Thus an overwhelming predominance of chelated form should be characterized by ^3J values of ca. 200–230 Hz to CH_3 and ca. 50 Hz to C_3. (These values are adjusted downwards slightly for the suppressing effect of β-methoxy substitution on ^3J.)[4] As K_f is reduced by various changes, $^3J(CH_3)$ should decline and $^3J(C_3)$ increase, given the dihedral angle changes associated with the open ⇌ chelated interconversion.

The ^3J values listed in Table II are in accord with this analysis and vary in the anticipated way with para substituent. Thus K_f should be larger for p-CH_3 and p-OCH_3 and smallest for p-CF_3. At lower concentrations, K_f should be larger and accompanied by a decline in $^3J(C_3)$ but an

Table V. ^{13}C and ^{199}Hg NMR Data[a] for R-$\overset{3}{C}H_2\overset{2}{C}H_2\overset{1}{C}H_2HgCl$ (all 0.4 M in $CDCl_3$)

R	temp, °C	carbon position 1	2	3	other		^{199}Hg shift, ppm
CH_3	room	33.06 (1439.7)	30.49 (85)	27.83 (176.6)	13.47		159.7
CH_3	0	33.2 (1429)	30.5 (85)	27.9 (174.4)	13.5		158.3
C_6H_5	room	30.1 (1488)	29.4 (91.6)	38.7 (134)	140.6 (ipso) 128.6 (*o*) 128.9 (*m*) 126.6 (*p*)		191.7
	0	30.0 (1491)	29.4 (93)	35.4 (131.1)			192.8
	−40	29.9 (1504)	29.4 (95.3)	38.2 (129.2)			193.8
c-C_3H_5	room	32.83 (1442.6)	28.44 (85.7)	39.29 (163.4)	10.28	4.60	161.0
	0	32.92 (1447.8)	28.44 (85.7)	39.29 (164.9)	10.28	4.57	159.5
	−40	33.12 (1462.4)	28.47 (87.2)	39.24 (168.5)	10.25	4.51	156.3

[a] Values in parentheses are ^{13}C–^{199}Hg couplings (Hz). Chemical shifts in ppm.

increase in $^3J(CH_3)$. The effects of lower temperature for the *p*-OCH_3 derivative are confirmatory, with a significant reduction in $^3J(C_3)$ and increase (208 → 223.7 Hz) in $^3J(CH_3)$ as required for increasing K_f. It is very likely that for the *p*-OCH_3 case at 233 K ($^3J_{CH_3}$ = 223 Hz) a limiting value of ^3J is attained, with the chelated conformer essentially exclusive. Assuming the ^3J values for the *p*-OCH_3 case at 233 K are close to the limiting values, then for $\varphi = 60°$, $J \sim 50$ Hz, and for $\varphi = 180°$, $J \sim 230$ Hz. It is then possible to calculate the free energy difference between open and chelated forms as being ca. 1.3 kcal/mol, a value close to the rough estimate of Kiefer.[1] The addition of pyridine (20% by volume) would be expected to quench to a significant degree, intramolecular coordination, and this is confirmed by the increase in $^3J(C_3)$ and decrease in $^3J(CH_3)$ for all cases.

^{199}Hg Spectra. The relative ^{199}Hg shifts for both series of oxymercurials are assembled in Table IV.

For series I, it is clear that the *p*-anisyl compound has the lowest field ^{199}Hg resonance, some 14 ppm removed from that of the *p*-CF_3 derivative. Granted that intramolecular coordination is more important for the *p*-anisyl derivative, it may have been thought that its ^{199}Hg resonance should have been at higher field. However ^{199}Hg is one nucleus, for which *increased* electron density appears to result in *low-field* shifts.[7,8] Thus the order of ^{199}Hg shifts is agreeable with the conclusion of enhanced π coordination in the *p*-anisyl compound. Increasing amounts of the coordinating pyridine cause shifts to lower field (increased electron density at Hg) and a substantial compression in the range of ^{199}Hg shifts from ~14 ppm for 0.4 M $CDCl_3$ solutions to ~2 ppm for the 65:35 $CDCl_3$–pyridine system. This is expected for a much reduced population of the π-coordinated arrangement, and in the limit, the ^{199}Hg shifts for the three derivatives should be almost identical. Changing the concentration from 0.4 M → 0.2 M should increase K_f, with a move to lower field as observed. Considerations of the same type apply to series II, although the range of shifts is smaller. Again the resonance for the *p*-CF_3 compound is to higher field of *p*-OCH_3 (by ~5 ppm). All resonances are affected by pyridine (move to lower field), with the range of shifts (OCH_3, CF_3) being reduced to ~1.4 ppm. The general behavior of the ^{199}Hg shifts is in accord with the conclusion that π coordination is more pronounced for anisyl and increases with dilution and can be quenched by the addition of a superior ligand such as pyridine.

In view of the frequent comparisons between phenyl and cyclopropyl as π-donor groups, we decided to compare the ^{13}C and ^{199}Hg spectral characteristics of *n*-butyl-, 3-phenylpropyl-, and 3-(cyclopropyl)propylmercuric chlorides to determine if the γ-cyclopropyl group could function as a π donor toward -HgCl, as phenyl evidently does.

The ^{13}C and ^{199}Hg data are shown in Table V.

Vicinal ^{199}Hg–^{13}C coupling constants (^3J) have been reported[4] for the compounds RCH_2CH_2HgCl, where R = CH_3, CH_3CH_2, *i*-$(CH_3)_2CH$, and *t*-Bu and ^3J = 190, 183, 212, 227 Hz, respectively. In the (reasonable) absence of any specific interaction with the alkyl (R) groups, the moderately increasing ^3J values may be associated with an increased population of the rotamer A, with dihedral

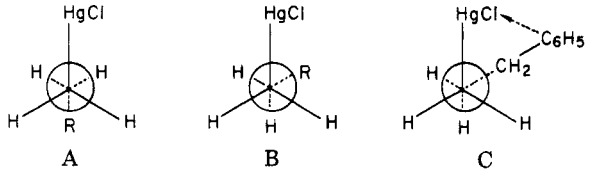

angle 180°. For $J \approx 200$ Hz, it may be calculated that the populations of A and B are ca. 60–70% and 40–30%, respectively. If we accept that the steric size of benzyl is no smaller than that of methyl,[9] the quite low value (~130 Hz) of ^3J for the 3-phenylpropylmercurial at first seems anomalous as it corresponds to ~70–75% population of the *gauche* B (R = $CH_2C_6H_5$). However it is in C (B with R = $CH_2C_6H_5$) that the π-donor ability of phenyl towards -HgCl can be exercised. We conclude that in 3-phenylpropylmercuric chloride at room temperature (in $CDCl_3$) the favored conformation is that one stabilized by a Hg–phenyl π interaction. This conclusion is supported by the ^{199}Hg shift (ca. 190 ppm the lowest field position of all observed in this study), some 30 ppm to low field of the signal for the *n*-butyl compound under identical conditions.

Regarding the 3-cyclopropyl compound, there is a clear similarity between its ^{199}Hg shifts (~160 ppm) and *vic* ^{199}Hg–^{13}C couplings (~165 Hz) and those of the *n*-butyl derivative (~160 ppm and ~175 Hz). However, these data are quite different from those (discussed above) for the corresponding phenyl compound and permit the conclusion that π-donor action by the 3-cyclopropyl group is insignificant. This is supported by the trends in the *vic* ^{13}C–^{199}Hg couplings and ^{199}Hg shifts (for this compound) with temperature, as both are in the wrong direction for a favored π interaction. The magnitudes of *vic* ^1H–^{199}Hg coupling constants also indicate a greater population of the *gauche* rotamer (see C) for the phenyl compound than for *n*-butyl or the 3-cyclopropyl derivative. The (average) *vic* $^3J_{^{199}Hg-^1H}$ are 312 (phenyl), 274 (*n*-butyl), and 278 Hz (cyclopropyl), requiring a greater average dihedral angle between HgCl and the C_2 protons, in the phenyl derivative. The essential lack of π-donor action by the 3-cyclopropyl

(9) Whitesides, G. M.; Sevenair, J. P.; Goetz, R. W. *J. Am. Chem. Soc.* **1967**, *89*, 1135.

group toward -HgCl is not surprising when the radial and energy characteristics of the appropriate orbitals are considered. Some of the expected consequences of arene–mercury coordination have been discussed previously.[1,2]

Experimental Section

Compounds. The oxymercurials were synthesized in a standard oxymercuration sequence as described below for the *p*-methoxy derivative:

3-(*p*-Methoxyphenyl)-2-methylpropene (1.23 g, 7.6 mmol) in methanol (~7 mL) was added to mercuric acetate (2.44 g, 7.7 mmol) in methanol (15 mL) and acetic acid (4 drops), and the mixture was stirred for 1 h (no yellow precipitate with aqueous sodium hydroxide). This solution was filtered into an aqueous sodium chloride solution (~0.6 M) to produce the chloromercurial as an oil, which was crystallized from aqueous methanol as fine white crystals (1.74 g, 54%), mp 75.5–76 °C. Anal. Calcd for $C_{12}H_{17}ClHgO_2$: C, 33.56; H, 3.96. Found: C, 33.77; H, 4.07.

3-(*p*-(Trifluoromethyl)phenyl)-2-methyl-2-methoxypropylmercuric chloride was obtained similarly, mp 83–84 °C. Anal. Calcd for $C_{12}H_{14}ClF_3HgO$: C, 30.83; H, 3.00. Found: C, 30.99; H, 3.15.

3-(*p*-Methylphenyl)-2-methyl-2-methoxypropylmercuric chloride had mp 78.9–79 °C. Anal. Calcd for $C_{12}H_{17}ClHgO$: C, 34.86; H, 4.12. Found: C, 34.87; H, 4.31.

The remaining members of the 2-methyl series of oxymercurials and all members of the parent series were viscous oils which could not be crystallized. However, the method of synthesis and ^1H, ^{13}C, and ^{199}Hg NMR spectra confirm the assigned structures.

3-Phenylpropylmercuric chloride was obtained via the Grignard reagent of 3-phenylpropyl bromide and mercuric bromide. Treatment with silver acetate provided a solution of the acetatomercurial which was filtered into aqueous sodium chloride. The resulting chloromercurial was recrystallized from ethanol–hexane, mp 51–52 °C; ^1H NMR (100 MHz; $CDCl_3$) δ 7.4 (5 H, m, phenyl), 2.8 (2 H, t, CH_2(benzylic)), 2.12 (2 H, p, CH_2–CH_2Hg; $J_{^{199}Hg-^1H}$ = 312 Hz), 2.0 (2 H, t (distorted), CH_2Hg, $J_{^{199}Hg-^1H}$ = 200 Hz) (all $J_{^1H-^1H} \approx 7$ Hz). Anal. Calcd for $C_9H_{11}HgCl$: C, 30.41; H, 3.10. Found: C, 30.47; H, 3.19.

***n*-Butylmercuric chloride** was prepared analogously and had mp 126–126.5 °C. Anal. Calcd for C_4H_9HgCl: C, 16.38; H, 3.07. Found: C, 16.47; H, 3.11. The 300-MHz ^1H spectrum ($CDCl_3$) showed resonances at δ 2.11 (t, $J \sim 7$ Hz, CH_2HgCl, $J_{^{199}Hg-^1H}$ = 197 Hz), 1.73 (p, $J \sim 7$ Hz, CH_2–CH_2Hg, $J_{^{199}Hg-^1H}$ = 274 Hz), 1.42 (sextet, $J \sim 7$ Hz, CH_3CH_2), and 0.96 (t, $J \sim 7$ Hz, CH_3).

3-(Cyclopropyl)propylmercuric chloride was obtained by treating the Grignard reagent from 3-(cyclopropyl)propyl bromide (see below) with mercuric bromide, followed by conversion to the acetate and precipitation of the chloride, which was recrystallized from ethanol; mp 78.5–79 °C. Anal. Calcd for $C_6H_{11}HgCl$: C, 22.56; H, 3.45. Found: C, 22.59, H. 3.46. The 300-MHz ^1H NMR spectrum ($CDCl_3$ solvent) exhibited the following: δ 1.31 (q, $J \sim 7$ Hz, c-$C_3H_5CH_2$), 1.86 (p, $J \sim 7$ Hz, CH_2–CH_2; $J_{^{199}Hg-^1H}$ = 278 Hz), 2.10 (t, $J \sim 7$ Hz, CH_2Hg; $J_{^{199}Hg-^1H}$ = 195 Hz), and the cyclopropyl resonances of δ 0.05 (2 H), 0.45 (2 H), and 0.70 (1 H). The ^{13}C and ^{199}Hg NMR shifts are discussed in the text.

3-(Cyclopropyl)propyl bromide was obtained by brominating (phosphorus tribromide in ether) the alcohol. The bromide (bp 59 °C (22 mm)) exhibited ^1H NMR absorptions centered at δ 3.5 (t, CH_2Br) and (1–2.3, *m* 4 H) CH_2–CH_2) and the characteristic cyclopropyl resonances.

NMR Spectra. ^{13}C spectra were obtained for the indicated concentrations and solvents (see text) on a JEOL FX-100 spectrometer at 25.04 MHz. ^{199}Hg spectra were obtained on the same spectrometer modified for multinuclear observation (17.822 MHz), and 10-mm tubes were employed. The ^{199}Hg shifts in Tables IV and V are relative to the highest field data point, and more positive shifts are to lower field. More discussion of the experimental details is presented elsewhere.[7] ^1H spectra were obtained at 100 or 300 MHz for $CDCl_3$ solutions.

Summary

Examination of the ^{13}C and ^{199}Hg NMR spectra of certain 3-(*p*-substituted-phenyl)-2-methoxypropylmercuric chlorides strongly supports the view that in poorly coordinating solvents, these mercurials exist largely as intramolecular π complexes. The study further illustrates the use of ^{13}C–^{199}Hg vicinal coupling constants in conformational analysis and sheds further light on the factors affecting ^{199}Hg shifts.

Acknowledgment. We gratefully acknowledge the support of the Australian Research Grants Committee.

Registry No. I (X = H), 79663-94-8; I (X = OCH_3), 79663-95-9; I (X = CF_3), 79663-96-0; II (X = H), 4175-60-4; II (X = CH_3), 79663-97-1; II (X = OCH_3), 4175-61-5; II (X = CF_3), 21388-54-5; 3-phenylpropylmercuric chloride, 41408-75-7; *n*-butylmercuric chloride, 543-63-5; 3-(cyclopropyl)propylmercuric chloride, 79663-98-2; 3-phenylpropene, 300-57-2; 3-(*p*-methoxyphenyl)propene, 140-67-0; 3-(*p*-trifluoromethylphenyl)propene, 1813-97-4; 3-phenyl-2-methylpropene, 3290-53-7; 3-(*p*-methylphenyl)-2-methylpropene, 40296-92-2; 3-(*p*-methoxyphenyl)-2-methylpropene, 20849-82-5; 3-(*p*-trifluoromethylphenyl)-2-methylpropene, 53482-96-5; 3-phenylpropyl bromide, 637-59-2; 3-(cyclopropyl)propyl bromide, 78300-38-6.

Redox Chemistry of Hexakis(phenyl isocyanide) Complexes of Molybdenum and Tungsten: The Synthesis of the Seven-Coordinate Cations $[M(CNPh)_7]^{2+}$ and Their Electrochemistry and Substitution Reactions

Douglas D. Klendworth, Warren W. Welters, III, and Richard A. Walton*

Department of Chemistry, Purdue University, West Lafayette, Indiana 47907

Received August 3, 1981

The reactions of the quadruply bonded tungsten complexes $W_2(mhp)_4$ and $W_2(dmhp)_4$ (mhp and dmhp are the anions of 2-hydroxy-6-methylpyridine and 2,4-dimethyl-6-hydroxypyrimidine, respectively) with excess phenyl isocyanide lead to reductive cleavage of the metal–metal bond and the formation of $W(CNPh)_6$. Oxidation of $M(CNPh)_6$ (M = Mo or W) with Ag^+ in the presence of free phenyl isocyanide yields the first examples of seven-coordinate, homoleptic aryl isocyanide complexes of molybdenum(II) and tungsen(II), $[M(CNPh)_7](PF_6)_2$. Oxidation of $M(CNPh)_6$ is also observed with I_2 and $NOPF_6$, reactions which yield $[M(CNPh)_6I]^+$ and $[M(NO)(CNPh)_5]PF_6$, respectively. The reactions of $[M(CNPh)_7]^{2+}$ (M = Mo or W) with a variety of mono- or bidentate phosphines generate seven-coordinate mixed-ligand cations of the types $[M(CNPh)_6(PR_3)]^{2+}$, $[M(CNPh)_5(PR_3)_2]^{2+}$, $[M(CNPh)_5(dppm)]^{2+}$, and $[M(CNPh)_5(dppe)]^{2+}$, where dppm = bis(diphenylphosphino)methane and dppe = 1,2-bis(diphenylphosphino)ethane. The cyclic voltammograms of these seven coordinate complexes are characterized by a single one-electron oxidation between +0.9 and +1.5 V and an irreversible two-electron reduction close to −1.0 V. Reduction of $[M(CNPh)_7]^{2+}$ with magnesium regenerates the six-coordinate homoleptic complexes $M(CNPh)_6$. Spectroscopic characterization of these complexes have included measurement of their ^1H NMR, IR, and electronic absorption spectra.

Introduction

The fission of metal–metal multiple bonds by π-acceptor ligands such as CO and NO and alkyl and aryl isocyanides is well documented.[1-10] One of the interesting features within this class of ligand induced cleavage reactions is the difference which exists between alkyl and aryl isocyanides in their reactions toward quadruply bonded dinuclear complexes such as $Cr_2(O_2CCH_3)_4$,[5] $Mo_2(O_2CCH_3)_4$,[6] and $W_2(mhp)_4$ (mhp is the anion of 2-hydroxy-6-methylpyridine).[7] In the case of alkyl isocyanides, nonreductive cleavage yields the seven-coordinate cations $[M(CNR)_7]^{2+}$ (where M = Mo or W; R = CH_3, CMe_3, or C_6H_{11}), whereas for aryl isocyanide, reductive cleavage has been found to produce the six-coordinate complexes $M(CNAr)_6$ (where M = Cr or Mo). The formation of $Cr(CNPh)_6$ and $Mo(CNPh)_6$ by this latter procedure constitutes the most convenient synthetic route to these complexes.

In spite of the strong tendency for reductive cleavage to occur in the presence of ArNC ligands, it seemed to us that this should not preclude the formation of salts containing the seven-coordinate phenyl isocyanide cations $[M(CNPh)_7]^{2+}$. Following our discovery of a convenient preparation of $W(CNPh)_6$ we have now devised routes to $[Mo(CNPh)_7](PF_6)_2$ and $[W(CNPh)_7](PF_6)_2$ through the oxidation of $M(CNPh)_6$ in the presence of excess phenyl isocyanide. In the present report we describe these results along with details of the spectroscopic and electrochemical properties of these new compounds and their substitution chemistry. Preliminary details of certain of these results have been reported previously.[8]

Experimental Section

Starting Materials. The following compounds were prepared by standard literature procedures: $Mo(CNPh)_6$,[6] $W_2(mhp)_4$,[11] $W_2(dmhp)_4$,[12] and PhNC.[13] All monodentate and bidentate phosphines, 2-hydroxy-6-methylpyridine (Hmhp), 2,4-dimethyl-6-hydroxypyrimidine (Hdmhp), and other reagents and solvents were obtained from commercial sources. Solvents were of the highest purity commercially available and were used without further purification with the exception of acetone, which was dried over $CaSO_4$, and tetrahydrofuran, which was distilled from sodium benzophenone. Potassium hexafluorophosphate was recrystallized from aqueous solution. Tetra-*n*-butylammonium hexafluorophosphate (TBAH) was obtained by reacting tetra-*n*-butylammonium iodide with KPF_6 in hot water. The product was recrystallized from aqueous ethanol and dried in vacuo.

Reaction Procedures. All reactions were carried out in a nitrogen atmosphere, and all solvents were deoxygenated prior to use by purging with N_2 gas.

A. Preparation of $W(CNPh)_6$ from Quadruply Bonded Tungsten(II) Complexes. (i) $W_2(dmhp)_4$ (dmhp Is the Anion of 2,4-Dimethyl-6-hydroxypyrimidine). A quantity of $W_2(dmhp)_4$ (0.60 g, 0.70 mmol) was added with stirring to 25 mL of methanol which was cooled to −20 °C in a dry ice bath. To this was added an excess (10:1) of phenyl isocyanide. The resulting reaction mixture was stirred for 1 h and filtered and the resulting red solid washed sparingly with ethanol. The product was then dissolved in benzene and the solution passed through an alumina

(1) Hertzer, C. A.; Myers, R. E.; Brant, P.; Walton, R. A. *Inorg. Chem.* **1978**, *17*, 2383.
(2) Nimry, T.; Urbancic, M. A.; Walton, R. A. *Inorg. Chem.* **1979**, *18*, 691.
(3) Brant, P.; Cotton, F. A.; Sekutowski, J. C.; Wood, T. E.; Walton, R. A. *J. Am. Chem. Soc.* **1979**, *101*, 6588.
(4) Wood, T. E.; Deaton, J. C.; Corning, J.; Wild, R. E.; Walton, R. A. *Inorg. Chem.* **1980**, *19*, 2614.
(5) Malatesta, L.; Sacco, A.; Ghielmi, S. *Gazz. Chim. Ital.* **1952**, *82*, 516.
(6) Mann, K. R.; Cimolino, M.; Geoffroy, G. L.; Hammond, G. S.; Orio, A. A.; Albertin, G.; Gray, H. B. *Inorg. Chim. Acta* **1976**, *16*, 97.
(7) Mialki, W. S.; Wild, R. E.; Walton, R. A. *Inorg. Chem.* **1981**, *20*, 1380.
(8) Klendworth, D. D.; Welters, W. W., III; Walton, R. A. *J. Organomet. Chem.* **1981**, *213*, C13.
(9) Girolami, G. S.; Anderson, R. A. *J. Organomet. Chem.* **1979**, *182*, C43.
(10) Cotton, F. A.; Darensbourg, D. J.; Kolthammer, B. W. S. *J. Organomet. Chem.* **1981**, *217*, C14.
(11) Cotton, F. A.; Fanwick, P. E.; Niswander, R. H.; Sekutowski, J. C. *J. Am. Chem. Soc.* **1978**, *100*, 4725.
(12) Cotton, F. A.; Niswander, R. H.; Sekutowski, J. C. *Inorg. Chem.* **1979**, *18*, 1152.
(13) Weber, W. P.; Gokel, G. W. *Tetrahedron Lett.* **1972**, 1637.

0276-7333/82/2301-0336$01.25/0

column using benzene as the eluant. This procedure was carried out in the dark to avoid photodecomposition. The solvent was removed under a stream of N_2, and red crystals of the complex were isolated; yield 0.30 g (27%). Anal. Calcd for $C_{42}H_{30}N_6W$: C, 62.85; H, 3.76. Found: C, 63.09; H, 3.80.

(ii) $W_2(mhp)_4$ (mhp Is the Anion of 2-Hydroxy-6-methylpyridine). A quantity of $W_2(mhp)_4$ (0.421 g, 0.52 mmol) was reacted by using a procedure analogous to that described in A(i); yield 0.24 g (29%). The resulting red crystals had the same spectroscopic properties as those of the sample of $W(CNPh)_6$ prepared in A(i).

B. Oxidation Reactions of $Mo(CNPh)_6$. (i) $[Mo(NO)(CNPh)_5]PF_6$. A quantity of $Mo(CNPh)_6$ (0.2 g, 0.28 mmol) was dissolved in 30 mL of freshly distilled tetrahydrofuran. Slightly more than a stoichiometric amount of $NOPF_6$ (0.06 g, 0.34 mmol) was added to the stirred solution via a side arm addition tube. The color of the solution changed immediately from bright red to dark purple. A small volume (10 mL) of deoxygenated hexane was then added to the reaction vessel. The dark purple solid which formed was collected, washed well with diethyl ether, and dried in vacuo; yield 0.20 g(90%). Anal. Calcd for $C_{35}H_{25}F_6MoN_6OP$: C, 53.44; H, 3.21; N, 10.69. Found: C, 53.11; H, 3.45; N, 10.78.

After removal of the dark purple product by filtration, the filtrate was taken to dryness. Recrystallization of the residue from acetone–diethyl ether yielded a small quantity of $[Mo(CNPh)_7](PF_6)_2$ as fine yellow needles; yield 0.029 g (9%). Anal. Calcd for $C_{49}H_{35}F_{12}MoN_7P_2$: C, 53.12; H, 3.19; N, 8.85. Found: C, 53.32; H, 3.41; N, 8.59. A higher yield synthesis of this complex is described in B(iv).

(ii) $[Mo(CNPh)_6I]PF_6$. A dichloromethane solution of iodine (0.180 g, 0.71 mmol) was added dropwise to a stirred dichloromethane solution of $Mo(CNPh)_6$ (0.5 g, 0.70 mmol). The color of the solution changed gradually from bright red to orange during this addition. Potassium hexafluorophosphate (0.25 g, 1.36 mmol) dissolved in acetone was then added to the reaction vessel. The solvent was removed under a stream of N_2, and the resulting solid residue was dissolved in benzene. Upon the addition of petroleum ether bright orange crystals separated. The product was washed well with water, 2-propanol, and diethyl ether and dried in vacuo; yield 52%. Anal. Calcd for $C_{42}H_{30}F_6IMoN_6P$: C, 51.13; H, 3.07; N, 8.52. Found: C, 50.89; H, 3.31; N, 8.34.

(iii) $[Mo(CNPh)_6I]BPh_4$. This complex was prepared in a manner similar to that of its analogous PF_6^- salt, except that an acetone solution of $NaBPh_4$ (0.4 g, 1.17 mmol) was added following the iodine oxidation. The addition of an excess of diethyl ether induced precipitation of the desired product. The orange solid was recrystallized from acetone–diethyl ether, washed well with ethanol and diethyl ether, and dried in vacuo; yield 79%. Anal. Calcd for $C_{66}H_{50}BIMoN_6$: C, 68.28; H, 4.35; N, 7.24. Found: C, 68.38; H, 4.35; N, 7.26.

(iv) $[Mo(CNPh)_7](PF_6)_2$. A mixture of $Mo(CNPh)_6$ (0.30 g, 0.42 mmol), $AgNO_3$ (0.17 g, 1.0 mmol), and KPF_6 (0.17 g, 0.92 mmol) was added to a 100-mL round-bottom flask followed by 25 mL of acetone and immediately thereafter 0.5 mL of phenyl isocyanide. The contents of the reaction flask were stirred at room temperature for 3 h in the dark. The reaction mixture was then filtered and diethyl ether added to the filtrate until precipitation of a yellow crystalline solid occurred. This was filtered off and washed successively with water, 2-propanol, and diethyl ether. Recrystallization was carried out by dissolving the product in acetone followed by the careful addition of diethyl ether; yield 0.33 g (71%). Anal. Calcd for $C_{49}H_{35}F_{12}MoN_7P_2$: C, 53.12; H, 3.19; N, 8.85. Found: C, 53.32; H, 3.32; N, 8.78.

Workup of the reaction filtrate afforded a small quantity of the nitrosyl derivative $[Mo(NO)(CNPh)_5]PF_6$ (yield less than 10%). Proof of its identity as the same complex as that prepared in B(i) was established by its spectroscopic and electrochemical properties.

C. Oxidation Reactions of $W(CNPh)_6$. (i) $[W(NO)(CNPh)_5]PF_6$. A quantity of $W(CNPh)_6$ (0.2 g, 0.249 mmol) was dissolved in 30 mL of acetone and a solution of $NOPF_6$ (0.044 g, 0.25 mmol) in acetone or dichloromethane (15 mL) added dropwise. This mixture was stirred for 45 min and diethyl ether than added to precipitate the purple product; yield 0.161 g (74%). Anal. Calcd for $C_{35}H_{25}F_6N_6OPW$: C, 48.07; H, 2.88; N, 9.61. Found: C, 47.92; H, 2.87; N, 9.50.

(ii) $[W(CNPh)_6I]BPh_4$. A quantity of $W(CNPh)_6$ (0.20 g, 0.249 mmol) was dissolved in dichloromethane (30 mL). To this stirred solution was added dropwise a dichloromethane solution containing iodine (0.063 g, 0.248 mmol). A similar procedure was followed to that described in B(iii); yield 0.217 g (70%). Anal. Calcd for $C_{66}H_{50}BIN_6W$: C, 63.47; H, 4.04. Found: C, 63.67; H, 4.21.

(iii) $[W(CNPh)_7](PF_6)_2$. A mixture of $W(CNPh)_6$ (0.700 g, 0.87 mmol), powdered $AgNO_3$ (0.30 g, 1.77 mmol), KPF_6 (0.33 g, 1.79 mmol), and phenyl isocyanide (~0.3 mL) was reacted in 30 mL of acetone in an analogous procedure to that described in B(iv); yield 0.72 g (69%). Anal. Calcd for $C_{49}H_{35}F_{12}N_7P_2W$: C, 49.24; H, 2.92; N, 8.20. Found: C, 49.06; H, 3.04; N, 7.95.

Workup of the reaction filtrate in a manner similar to B(iv) afforded a small crop of purple $[W(NO)(CNPh)_6]PF_6$ (yield <10%). Its identity as the same complex as that prepared in C(i) was established by its spectroscopic and electrochemical properties.

D. Interconversions between $[Mo(CNPh)_6X]PF_6$ (X = Halide) and $[Mo(CNPh)_7](PF_6)_2$. (i) The Preparation of $[Mo(CNPh)_6Cl]PF_6$. A mixture of $[Mo(CNPh)_6I]PF_6$ (0.28 g, 0.28 mmol) and LiCl (0.20 g, 4.7 mmol) was stirred and heated in ethanol for 20 min. The contents of the reaction flask were then cooled and filtered, and an orange solid was collected. This was washed several times with diethyl ether; yield 0.10 g (40%). The product was identified by its spectroscopic and electrochemical properties.

With an analogous procedure, the chloro derivative $[Mo(CNPh)_6Cl]PF_6$ was also prepared by the reaction of $[Mo(CNPh)_7](PF_6)_2$ with LiCl; yield 72%.

(ii) The Conversion of $[Mo(CNPh)_6Cl]PF_6$ to $[Mo(CNPh)_7](PF_6)_2$. A mixture of $[Mo(CNPh)_6Cl]PF_6$ (0.1 g, 0.11 mmol), KPF_6 (0.40 g, 2.2 mmol), and phenyl isocyanide (0.3 mL, 3.2 mmol) was stirred in ethanol at room temperature for 6 h. During this period the solution color changed from a yellow-orange to green. A yellow solid (0.10 g) was isolated upon filtering the reaction mixture and was washed successively with water, 2-propanol, and diethyl ether and dried in vacuo; yield 81%. Its identity as a pure sample of $[Mo(CNPh)_7](PF_6)_2$ was confirmed by using infrared spectroscopy and cyclic voltammetry.

E. Reactions of $[Mo(CNPh)_7](PF_6)_2$ with Phosphines and Phosphites. (i) $[Mo(CNPh)_5(P\text{-}n\text{-}Pr_3)_2](PF_6)_2$. To a stirred slurry of $[Mo(CNPh)_7](PF_6)_2$ (0.18 g, 0.16 mmol) in ethanol was added tri-*n*-propylphosphine (0.6 mL, 3.0 mmol) under a nitrogen atmosphere. The solution was stirred at room temperature for 96 h, and the canary yellow solid was collected by filtration. The solid was washed well with diethyl ether and dried in vacuo. Recrystallization was accomplished by using an acetone–diethyl ether mixture; yield 0.058 g (30%). Anal. Calcd for $C_{53}H_{67}F_{12}MoN_5P_4$: C, 52.09; H, 5.53; N, 5.73. Found: C, 51.55; H, 4.94; N, 5.73.

(ii) $[Mo(CNPh)_5(PEt_3)_2](PF_6)_2$. Ethanol (30 mL) was added to $[Mo(CNPh)_7](PF_6)_2$ (0.30 g, 0.27 mmol), and the resulting solution was stirred and treated with an excess of triethylphosphine (0.50 mL, 3.4 mmol). When the solution was heated to just below boiling its color changed from yellow to dark brown. After 20 min the reaction mixture was cooled to room temperature and filtered. A canary yellow solid was collected, washed well with diethyl ether, and dried in vacuo. The product was recrystallized from an acetone–diethyl ether mixture; yield 0.20 g (65%). Anal. Calcd for $C_{47}H_{55}F_{12}MoN_5P_4$: C, 49.61; H, 4.88; N, 6.16. Found: C, 49.44; H, 4.78; N, 5.84.

(iii) $[Mo(CNPh)_5(PEt_2Ph)_2](PF_6)_2$. This complex was prepared in a manner similar to E(i); yield 83%. Anal. Calcd for $C_{55}H_{55}F_{12}MoN_5P_4$: C, 53.53; H, 4.50; N, 5.68. Found: C, 52.88; H, 4.70; N, 5.52.

(iv) $[Mo(CNPh)_5(PEtPh_2)_2](PF_6)_2$. This complex was prepared by using a procedure analogous to that used in E(ii). The yellow complex was recrystallized from an acetone–diethyl ether mixture; yield 60%. Anal. Calcd for $C_{63}H_{55}F_{12}MoN_5P_4$: C, 56.89; H, 4.18; N, 5.27. Found: C, 56.83; H, 4.04; N, 5.40.

(v) $[Mo(CNPh)_6(PPh_3)](PF_6)_2$. This monodentate phosphine derivative was prepared by reacting $[Mo(CNPh)_7](PF_6)_2$ (0.32 g, 0.29 mmol) with triphenylphosphine (0.40 g, 1.52 mmol). The reactants were dissolved in tetrahydrofuran and refluxed with stirring for 6 h. The color of the solution changed quickly from orange to a brilliant red and then more slowly to an orange-brown.

After the mixture was cooled to room temperature, the product was precipitated from solution as orange crystals by the addition of diethyl ether; yield 71%. Anal. Calcd for $C_{60}H_{45}F_{12}MoN_6P_3$: C, 56.88; H, 3.59; N, 6.63. Found: C, 56.61; H, 3.73; N, 6.35.

(vi) $[Mo(CNPh)_5(P(OEt)_3)_2](PF_6)_2$. This yellow complex was obtained by a procedure analogous to that used in E(v); yield 60%. ^1H NMR spectroscopy confirmed the stoichiometry of the complex.

(vii) $[Mo(CNPh)_5(dppe)](PF_6)_2$. $[Mo(CNPh)_7](PF_6)_2$ (0.19 g, 0.17 mmol) was reacted with 1,2-bis(diphenylphosphino)ethane (0.25 g, 0.63 mmol) in 25 mL of absolute ethanol under reflux conditions. The solution color changed from yellow to orange as the reaction progressed. After a 30-min reflux period the heat was removed and the reaction vessel allowed to cool to room temperature. Filtration yielded an orange solid which was washed well with diethyl ether and dried in vacuo; yield 55%. Anal. Calcd for $C_{61}H_{49}F_{12}MoN_5P_4$: C, 56.36; H, 3.81; N, 5.39. Found: C, 55.93; H, 4.42; N, 5.54.

(viii) $[Mo(CNPh)_5(dppm)](PF_6)_2$. This complex was prepared by combining $[Mo(CNPh)_7](PF_6)_2$ and bis(diphenylphosphino)methane in 30 mL of absolute ethanol. The solution was refluxed and stirred for 1 h. During this time the solution color changed from yellow to orange to a dark orange-brown. The reaction mixture was cooled to room temperature and filtered to yield an orange solid. The product was washed well with diethyl ether and dried in vacuo; yield 0.32 g (59%). Anal. Calcd for $C_{60}H_{47}F_{12}MoN_5P_4$: C, 56.04; H, 3.69; N, 5.45. Found: C, 55.84; H, 3.60; N, 5.48.

F. Reactions of $[W(CNPh)_7](PF_6)_2$ with Phosphines. (i) $[W(CNPh)_5(PEt_3)_2](PF_6)_2$. A quantity of $[W(CNPh)_7](PF_6)_2$ (0.19 g, 0.16 mmol) was reacted with triethylphosphine (0.6 mL, 4.06 mmol) by using a procedure analogous to that described in E(ii); yield 0.15 g (77%). The purity and stoichiometry of the compound were confirmed by using cyclic voltammetry and ^1H NMR spectroscopy.

(ii) $[W(CNPh)_5(PEtPh_2)_2](PF_6)_2$. A procedure analogous to that used in E(iv) was employed; yield 75%. The purity and stoichiometry of the compound were confirmed using cyclic voltammetry and ^1H NMR spectroscopy.

(iii) $[W(CNPh)_6(PPh_3)](PF_6)_2$. The reaction between $[W(CNPh)_7](PF_6)_2$ (0.2 g, 0.17 mmol) and triphenylphosphine (0.2 g, 0.76 mmol) was performed in a manner analogous to that described in E(v), except the reaction was carried out for 7 days; yield 0.163 g (72%). This complex can be recrystallized from acetone–diethyl ether mixtures. Anal. Calcd for $C_{60}H_{45}F_{12}N_6P_3W$: C, 53.19; H, 3.34. Found: C, 51.99; H, 3.30.

(iv) $[W(CNPh)_5(dppe)](PF_6)_2$. Using a procedure analogous to that used in the preparation of E(vii) yielded this complex as bright orange needles; yield 58%. Anal. Calcd for $C_{61}H_{49}F_{12}N_5P_4W$: C, 52.78; H, 3.56. Found: C, 52.24; H, 3.45.

G. Reduction of the Seven-Coordinate Molybdenum(II) and Tungsten(II) Species $[M(CNPh)_7](PF_6)_2$ to $M(CNPh)_6$. (i) $Mo(CNPh)_6$. The reduction of $[Mo(CNPh)_7](PF_6)_2$ to $Mo(CNPh)_6$ was accomplished by stirring a mixture of the starting material (1.0 mmol) with magnesium metal (2.0 mmol) (activated with 1,2-dibromoethane) in tetrahydrofuran. As the reaction progressed, the solution changed color from yellow to a dark brown. After the contents of the reaction vessel had been stirred for several hours, they were filtered and absolute ethanol was added to the filtrate. This precipitated the complex $Mo(CNPh)_6$; yield 80%. The identity of this complex was confirmed by a comparison of its spectroscopic and electrochemical properties with those of an authentic sample.

(ii) $W(CNPh)_6$. A procedure analogous to that in G(i) was used although it was essential that only a stoichiometric amount of the magnesium reducing agent was used. After complete reduction of the $[W(CNPh)_7](PF_6)_2$, the reaction mixture was added to an alumina column and eluted with deoxygenated benzene. Exposure to light was minimized during the entire process. The solvent was slowly removed from the orange eluate under a stream of N_2. The red crystalline solid was collected, washed with ethanol, and dried in vacuo; yield 0.3 g (70%). Its identity was confirmed by its spectroscopic and electrochemical properties.

H. Reduction Reactions of $[Mo(CNPh)_5(dppe)](PF_6)_2$ and $[Mo(CNPh)_5(PEtPh_2)_2](PF_6)_2$. The procedures used for reducing these two complexes were essentially the same so details are reported only for the dppe derivative. Magnesium metal (0.09 g, 3.7 mmol) (40 mesh) was added to a three-neck round bottom flask under a nitrogen atmosphere. Freshly distilled tetrahydrofuran (30 mL) was added via a cannula followed by 1,2-dibromoethane (0.15 mL, 1.7 mmol). After this mixture was stirred for 15 min, a second aliquot of 1,2-dibromoethane was added producing an immediate effervescence, thereby signaling the activation of the magnesium surface. The complex $[Mo(CNPh)_5dppe](PF_6)_2$ (0.225 g, 0.196 mmol) was added via a side arm addition tube and the resulting mixture stirred at room temperature in the dark for 4 h. The reaction mixture was then chromatographed on alumina and the orange band eluted by using benzene. The chromatography was conducted under oxygen-free conditions with minimal exposure to direct light. The orange eluate was collected from the column and the solvent removed under a stream of N_2. The resulting oil was treated with ethanol to help separate the red crystalline solid which was collected on a sintered frit and dried in vacuo; yield 0.089 g (50%). The product, which was very air sensitive, was formulated as $Mo(CNPh)_4(dppe)$ by using IR and ^1H NMR spectroscopy and cyclic voltammetry. A similar procedure when used to reduce $[Mo(CNPh)_5(PEtPh_2)_2](PF_6)_2$ afforded a red oil which we were unable to crystallize. This was characterized by using IR and ^1H NMR spectroscopy but the presence of contaminants precluded a definitive structural assignment.

Physical Measurements. Infrared spectra (4000–400 cm^{-1}) were recorded as Nujol mulls between KBr plates on a Beckman IR-12 spectrophotometer. Electronic absorption spectra were recorded on dichloromethane solutions using a Varian series 634 spectrophotometer. Nuclear magnetic resonance spectra were recorded in acetone-d_6 with tetramethylsilane (Me_4Si) as an internal reference using a Perkin-Elmer R-32 90 MHz NMR spectrometer.

Electrochemical measurements were made on dichloromethane and acetonitrile solutions containing 0.2 M tetra-*n*-butylammonium hexafluorophosphate (TBAH) as supporting electrolyte. $E_{1/2}$ values (taken as $(E_{p,a} + E_{p,c})/2$) are referenced to the saturated potassium chloride calomel electrode (SCE) at 22 ± 2 °C and are uncorrected for junction potentials. Cyclic voltammetry experiments were performed by using a BioAnalytical Systems Inc. Model CV-1A instrument in conjunction with a Hewlett-Packard Model 7035B x-y recorder. Potential control for coulometric experiments was maintained with a potentiostat purchased from BioAnalytical Systems Inc. Values of n, where n is the total number of equivalents of electrons transferred in exhaustive electrolysis at constant potentials, were calculated after measuring the total area under current vs. time curves for the complete reaction. The reactions were judged to be complete when the current had fallen below 1% of the initial value. Alternatively, values of n could be estimated by comparing the peak currents with the ferrocene–ferricinium couple with those arising from an equimolar solution of the complex of interest. All voltammetric measurements were made at a platinum bead electrode in solutions deaerated into a stream of dry nitrogen.

Elemental microanalyses were performed by Dr. C. S. Yeh of the Purdue University microanalytical laboratory.

Results and Discussion

As a consequence of our studies on the cleavage reactions of dinuclear complexes containing metal–metal multiple bonds, we have been able to develop a new synthetic route to $W(CNPh)_6$. The reductive cleavage of $W_2(dmhp)_4$ (dmhp is the anion of 2,4-dimethyl-6-hydroxypyrimidine) and $W_2(mhp)_4$ (mhp is the anion of 2-hydroxy-6-methylpyridine) by phenyl isocyanide proceeds in a yield of ca. 30% which, while rather low, is still superior to that reported in existing procedures.[6,14] Furthermore, our method is convenient and quick and would seem, at least for the time being, to offer the easiest route to $W(CNPh)_6$. Thus, it is clear that like chromium and molybdenum

(14) Yamamoto, Y. *Coord. Chem. Rev.* **1980**, *32*, 193 and references therein.

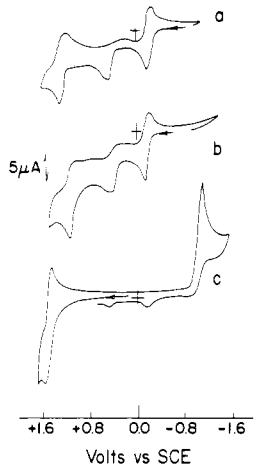

Figure 1. Cyclic voltammograms in 0.2 M tetra-*n*-butylammonium hexafluorophosphate–dichloromethane of (a) Mo(CNPh)$_6$, (b) W(CNPh)$_6$, and (c) [Mo(CNPh)$_7$](PF$_6$)$_2$. Sweep rates for a and b are 200 mV/s and for c 300 mV/s, respectively.

quadruply bonded species, tungsten complexes containing the W_2^{4+} core are no exception to the general rule that alkyl and aryl isocyanides bring about facile cleavage of the metal–metal bond.[15]

Electrochemical and Chemical Oxidations of M(CNPh)$_6$ (M = Mo or W). With a ready source of W(CNPh)$_6$ and the availability of Mo(CNPh)$_6$ through the related reductive cleavage of $Mo_2(O_2CCH_3)_4$, we have carried out a study of the redox chemistry of these two homoleptic zerovalent metal complexes. Surprisingly, the electrochemical properties of these two complexes have not previously been reported, although photoredox reactions have been shown to occur when chloroform solutions of M(CNPh)$_6$ (M = Cr, Mo or W) are irradiated at 436 nm.[16,17] The resulting photo-oxidation products are the seven-coordinate cations [M(CNPh)$_6$Cl]$^+$. With the more sterically hindered M(CNIph)$_6$ derivatives (Iph = 2,6-diisopropylphenyl) photooxidation terminates at the [M(CNIph)$_6$]$^+$ stage.[16,17]

In contrast to the well-defined electrochemical processes which characterize the cyclic voltammograms for the chromium(0) aryl isocyanide derivatives Cr(CNAr)$_6$ (corresponding to the redox sequence [Cr]$^{3+}$ ← [Cr]$^{2+}$ ← [Cr]$^+$ ← [Cr]^0),[18] the CV's of Mo(CNPh)$_6$ and W(CNPh)$_6$ are significantly more complex (Figure 1). With 0.2 M Bu_4NPF_6 as supporting electrolyte, dichloromethane solutions of Mo(CNPh)$_6$ exhibit a reversible one-electron oxidation (n = 1.0 ± 0.1 by coulometry) at $E_{1/2}$ = −0.19 V vs. SCE. With switching potentials of +0.3 and −0.8 V, this couple is characterized by $i_{p,c}/i_{p,a} = 1$ and $E_{p,a} - E_{p,c} \simeq 60$ mV and the $i_p/v^{1/2}$ ratio was found to be constant for sweep rates (v) between 50 and 400 mV/s, in accord with diffusion control. A second oxidation at $E_{p,a}$ = +0.48 V vs. SCE (v = 200 mV/s) is irreversible and is followed by a chemical step in which an unidentified product ($E_{1/2}$ = +1.28 V vs. SCE) is formed (i.e., by an EEC mechanism). In the case of W(CNPh)$_6$ the corresponding oxidations are at $E_{1/2}$ = −0.18 V and $E_{p,a}$ = +0.44 V. However, the chemical product which is formed following the oxidation to [W(CNPh)$_6$]$^{2+}$ is characterized by a less reversible couple ($E_{p,a}$ = +1.16 V, $i_{p,c}/i_{p,a} \ll 1$) than is the case with the analogous molybdenum system (Figure 1).[19]

Bulk electrolysis of the Mo(CNPh)$_6$ solution at +0.6 V (i.e., positive of the irreversible oxidation) produced a lemon yellow solution whose CV displayed an oxidation wave at $E_{1/2}$ = +1.41 V and an irreversible reduction at $E_{p,c}$ = −1.12 V. In addition, another couple at $E_{1/2} \simeq 1.0$ V showed that a second product was present which, on the basis of peak currents, was obviously a minor component of the system. From these results it was apparent that the chemical product ($E_{1/2} \simeq$ +1.2 V) which forms following the electrochemical oxidation of M(CNPh)$_6$ to [M(CNPh)$_6$]$^{2+}$ (Figure 1a) is itself sufficiently unstable that it cannot be obtained by bulk electrolysis. From a consideration of the known electrochemical properties of the seven-coordinate homoleptic alkyl isocyanide complexes [Mo(CNR)$_7$](PF$_6$)$_2$,[7] we felt that the species responsible for the electrochemical processes at $E_{1/2}$ = +1.41 V and $E_{p,c}$ = −1.12 V could be the seven-coordinate phenyl isocyanide cation [Mo(CNPh)$_7$]$^{2+}$.[20] Accordingly, we carried out a series of reactions aimed at the chemical oxidation of M(CNPh)$_6$ (M = Mo or W) to [M(CNPh)$_7$]$^{2+}$.

When $NOPF_6$ is added to a stirred solution of Mo(CNPh)$_6$ in tetrahydrofuran, there is an immediate color change from bright red to dark purple. Addition of hexane to the solution precipitates dark purple [Mo(NO)(CNPh)$_5$]PF$_6$ in very high yield. A comparable oxidation of W(CNPh)$_6$ produced the analogous [W(NO)(CNPh)$_5$]PF$_6$. By a careful workup of the filtrate from the reaction between Mo(CNPh)$_6$ and $NOPF_6$, we isolated a small crop of yellow needles which analyzed as the desired seven-coordinate complex [Mo(CNPh)$_7$](PF$_6$)$_2$. To optimize the yield of the latter complex, the presence of a mild oxidant, an excess of phenyl isocyanide, and an excess of hexafluorophosphate anion were judged to be necessary. Upon treating an acetone solution of Mo(CNPh)$_6$ with $AgNO_3$, KPF_6, and PhNC, we obtained [Mo(CNPh)$_7$](PF$_6$)$_2$ in 71% yield.[21] A comparable procedure was found to convert W(CNPh)$_6$ to [W(CNPh)$_7$](PF$_6$)$_2$ in yields close to 70%.

Undoubtedly, there are a variety of other oxidation procedures which will give similar results. However, the only other method we investigated involved the iodine oxidation of dichloromethane solutions of M(CNPh)$_6$. This afforded the orange cations [M(CNPh)$_6$I]$^+$ which could be crystallized as their PF_6^- or BPh_4^- salts. These new species are members of the class of molecules of the type [M(CNR)$_6$X]Y (X = halide, $SnCl_3^-$, or CN^-; Y = halide, PF_6^-, BPh_4^-, etc.) which was first prepared by Lippard and coworkers[22-24] and whose chemistry has been subsequently

(15) Walton, R. A. *ACS Symp. Ser.* **1981**, *No. 155*, p 207.
(16) Mann, K. R.; Gray, H. B.; Hammond, G. S. *J. Am. Chem. Soc.* **1977**, *99*, 306.
(17) Gray, H. B.; Mann, K. R.; Lewis, N. S.; Thich, J. A.; Richman, R. M. *Adv. Chem. Ser.* **1978**, *No. 168*, 44.
(18) Treichel, P. M.; Firsich, D. W.; Essenmacher, G. P. *Inorg. Chem.* **1979**, *18*, 2405.

(19) The chemical product which is formed on the time scale of the cyclic voltammetry experiment and which is characterized by $E_{1/2}$ = +1.28 V in the case of Mo(CNPh)$_6$ and $E_{p,a}$ = +1.16 V for W(CNPh)$_6$ is not the mixed chloride–isocyanide species [M(CNPh)$_6$Cl]$^+$. Although this latter ion could conceivably be formed through reaction of [M(CNPh)$_6$]$^{2+}$ with the CH_2Cl_2 solvent, separate studies on the CV of authentic [Mo(CNPh)$_6$Cl]$^+$ have shown that the [Mo(CNPh)$_6$Cl]$^{+,2+}$ couple has an $E_{1/2}$ value of +0.99 V vs. SCE (see Table I).
(20) Our reasoning ran as follows. Since the $E_{1/2}$ value for the [Mo(CNR)$_7$]$^{2+,3+}$ couple (R = CH_3, CMe_3, or C_6H_{11}) is ≃+1.1 V vs. SCE, we would expect an $E_{1/2}$ value for [Mo(CNPh)$_7$]$^{2+,3+}$ which is appreciably greater than +1.1 V since PhNC is a better π acceptor than RNC and thus less able to stabilize the 3+ state. Paralleling this trend we would also anticipate that reduction of [Mo(CNPh)$_7$]$^{2+}$ would occur more readily than [Mo(CNR)$_7$]$^{2+}$. This expectation is realized by the appearance of a reduction wave at E_p = −1.1 V in the CV of the product which emanates from the irreversible electrochemical oxidation of Mo(CNPh)$_6$.
(21) Workup of the filtrate yielded a small crop of [Mo(NO)(CNPh)$_5$]PF$_6$ which is presumably formed through a secondary reaction involving reduction of the excess nitrate ion which is present.
(22) Lam, C. T.; Novotny, M.; Lewis, D. L.; Lippard, S. J. *Inorg. Chem.* **1978**, *17*, 2127.
(23) Giandomenico, C. M.; Dewan, J. C.; Lippard, S. J. *J. Am. Chem. Soc.* **1981**, *103*, 1407.

investigated quite extensively.[23-26] Accordingly, we have not carried out a detailed study of these cations other than noting the following two relevant points. First, reaction of $[Mo(CNPh)_6I]PF_6$ with the chloride ion results in halide exchange and the formation of $[Mo(CNPh)_6Cl]PF_6$. Second, reaction of the chloride complex with excess phenyl isocyanide produces $[Mo(CNPh)_7]^{2+}$, behavior which resembles that noted by Lippard[22,23,25] for the analogous alkyl isocyanide species (eq 1). Accordingly, we see here a close correspondence between the reaction chemistry of the analogous alkyl and aryl isocyanide derivatives.

$$[Mo(CNR)_6X]^+ + RNC \rightleftarrows [Mo(CNR)_7]^{2+} + X^- \quad (1)$$

The identity of $[Mo(CNPh)_7](PF_6)_2$ as a genuine example of seven-coordinate molybdenum(II) has been established by a crystal structure determination, details of which will be reported elsewhere.[27]

A comparison of the CV of a dichloromethane solution of an authentic sample of $[Mo(CNPh)_7](PF_6)_2$ (Figure 1c) with the CV's of the solutions which are formed following the exhaustive electrolysis (at +0.6 V) of $Mo(CNPh)_6$ confirmed that this seven-coordinate cation is indeed present as a major product following the electrochemical oxidation of $Mo(CNPh)_6$. In addition to the one-electron oxidation $[Mo(CNPh)_7]^{2+} \rightarrow [Mo(CNPh)_7]^{3+} + e^-$ ($E_{1/2}$ = 1.41 V), there is an irreversible two-electron reduction at $E_{p,c}$ = −1.12 V in the CV of $[Mo(CNPh)_7](PF_6)_2$. The waves at $E_{p,a}$ = −0.18 V and $E_{p,a}$ = +0.44 V (Figure 1c) are due to the formation of $Mo(CNPh)_6$ following this reduction. This particular aspect of the redox chemistry of $[Mo(CNPh)_7](PF_6)_2$ and related species will be dealt with more fully later in the discussion. One final point of interest concerning a comparison between the CV's of $[Mo(CNPh)_7](PF_6)_2$ and the electrolyzed $Mo(CNPh)_6$ solutions is the presence of the additional couple at $E_{1/2} \simeq$ +1.0 V in the latter. We have ascertained that this is due to the formation of small amounts of $[Mo(CNPh)_6Cl]^+$ ($E_{1/2}$ = +0.99 V vs. SCE) through reaction of $[Mo(CNPh)_7]^{2+}$ with chloride ion which is generated at the auxiliary electrode and diffuses to the working electrode compartment.[28]

Acetonitrile solutions of $[Mo(CNPh)_7](PF_6)_2$ (0.2 M in Bu_4NPF_6) display similar electrochemical processes to those in dichloromethane (Table I), except that the oxidation at +1.4 V is now irreversible, no doubt due to reaction of $[Mo(CNPh)_7]^{3+}$ with the acetonitrile solvent. A dichloromethane solution of $[W(CNPh)_7](PF_6)_2$ displays very similar electrochemical behavior to that of its molybdenum analogue, with the reversible one-electron oxidation at $E_{1/2}$ = +1.32 V and the irreversible two-electron reduction at $E_{p,c}$ = −1.02 V vs. SCE (Table I).

The important features in the IR, ^1H NMR, and electronic absorption spectra of the complexes $[M(CNPh)_7](PF_6)_2$ (M = Mo or W), $[Mo(CNPh)_6X]PF_6$ (X = Cl or I), $[W(CNPh)_6I]BPh_4$, and $[M(NO)(CNPh)_5]PF_6$ (M = Mo or W) are presented by Table II and in all cases clearly serve to confirm the identity of these diamagnetic complexes through the similarity of their spectral properties to those of their alkyl isocyanide analogues $[M(CNR)_7]^{2+}$,[3,22,24] $[M(CNR)_6X]^+$,[22,24] (M = Mo or W; X = Cl or I), and $[Mo(NO)(CNR)_5]^+$.[29] The most noteworthy difference is the higher ν(NO) and lower ν(CN) frequencies in the IR spectra of $[M(NO)(CNPh)_5]^+$ (Table II) compared to those of the alkyl isocyanide derivatives $[Mo(NO)(CNR)_5]^+$.[29] This may be a further reflection of the better π-acceptor capabilities of PhNC relative to RNC.

Table I. Voltammetric Half-Wave Potentials for Phenyl Isocyanide Complexes of Molybdenum(II) and Tungsten(II)[a]

complex	$E_{1/2}$(ox)[b]	$E_{p,c}$(red)[b,c]
$[Mo(CNPh)_7](PF_6)_2$	+1.41	−1.12
	+1.40[d]	−1.06[d]
$[W(CNPh)_7](PF_6)_2$	+1.32	−1.02
$[Mo(NO)(CNPh)_5]PF_6$	+0.86	−1.72
	+1.02[d]	−1.43[d]
$[W(NO)(CNPh)_5]PF_6$	+0.85	−1.67
$[Mo(CNPh)_6Cl]PF_6$	+0.99	−1.44
$[Mo(CNPh)_6I]PF_6$	+1.06	−1.38
$[Mo(CNPh)_5(PEt_3)_2](PF_6)_2$	+1.27	−1.19
$[Mo(CNPh)_5(P\text{-}n\text{-}Pr_3)_2](PF_6)_2$	+1.28	−1.22
$[Mo(CNPh)_5(PEt_2Ph)_2](PF_6)_2$	+1.29	−1.08
$[Mo(CNPh)_5(PEtPh_2)_2](PF_6)_2$	+1.30	−1.03
$[Mo(CNPh)_6(PPh_3)](PF_6)_2$	+1.43	−1.05
[Mo(CNPh)$_5$(dppm)](PF$_6$)$_2$	+1.31	−0.90
[Mo(CNPh)$_5$(dppe)](PF$_6$)$_2$	+1.34	−1.04
$[Mo(CNPh)_5(P(OEt)_3)_2](PF_6)_2$	+1.43	−1.18
$[W(CNPh)_5(PEt_3)_2](PF_6)_2$	+1.22	−1.14
$[W(CNPh)_5(PEtPh_2)_2](PF_6)_2$	+1.26	−1.04
[W(CNPh)$_5$(dppe)](PF$_6$)$_2$	+1.27	−1.12

[a] Measurements in CH_2Cl_2 with 0.2 M tetra-*n*-butylammonium hexafluorophosphate (TBAH) as supporting electrolyte unless stated otherwise. [b] Volts vs. SCE with a Pt-bead working electrode. [c] Values taken at a scan rate of 200 mV/s. [d] Measurements in CH_3CN.

The electrochemical properties of $[M(CNPh)_6X]^+$ (M = Mo or W) are similar to those of $[M(CNPh)_7]^{2+}$ in that the former complexes possess a reversible one-electron oxidation (n = 0.99 by coulometry for $[Mo(CNPh)_6I]PF_6$). However, the relevant $E_{1/2}$ values which characterize their CV's (Table I) are ~0.4 V less than those for the related oxidations of the homoleptic species, a trend which parallels that which has been found for the analogous pairs of alkyl isocyanide complexes $[M(CNR)_7]^{2+}$ vs. $[M(CNR)_6X]^{2+}$; the latter have $E_{1/2}$ values of $\simeq$ 1.1 and $\simeq$ 0.6 V, respectively.[7,28,30] The much lower electrode potentials of the halo derivatives (Table I) reflect the ability of halide ligands to better stabilize the higher oxidation states of molybdenum and tungsten in comparison to the phenyl isocyanide ligand.

The seven-coordinate aryl isocyanide complexes $[Mo(CNPh)_7](PF_6)_2$ and $[Mo(CNPh)_6X]PF_6$ (X = Cl or I) display three absorption bands in their electronic absorption spectra between 275 and 450 nm. These spectral features are reminiscent of those present in the related spectra of their alkyl isocyanide analogues[22,24] except that the absorptions for the alkyl isocyanide complexes occur at higher energies.

The 18-electron nitrosyl complexes $[M(NO)(CNPh)_5]PF_6$ exhibit electrochemical behavior which resembles qualitatively that of $[M(CNPh)_7]^{2+}$, namely, a one-electron oxidation (n = 0.92 by coulometry for M = Mo) and an irreversible reduction (Table I). The oxidation is much more accessible ($E_{1/2} \simeq$ +0.85 V vs. SCE) than that for either $[M(CNPh)_7]^{2+}$ or $[M(CNPh)_6X]^+$ but is strongly solvent dependent since an acetonitrile solution of [Mo-

(24) Giandomenico, C. M.; Hanau, L. H.; Lippard, S. J., submitted for publication.
(25) Lippard, S. J. *Prog. Inorg. Chem.* **1976**, *21*, 91.
(26) Corfield, P. W. R.; Baltusis, L. M.; Lippard, S. J. *Inorg. Chem.* **1981**, *20*, 922.
(27) Dewan, J. C.; Lippard, S. J. *Inorg. Chem.*, submitted for publication.
(28) Bell, A.; Klendworth, D. D.; Wild, R. E.; Walton, R. A. *Inorg. Chem.* **1981**, *20*, 4456.
(29) McCleverty, J. A.; Williams, J. *Trans. Met. Chem.* **1976**, *1*, 288.
(30) Detailed studies have been undertaken of the dependence of the $E_{1/2}$ values for the $[M(CNR)_6X]^{+,2+}$ couple upon the nature of R and X (private communication from Professor S. J. Lippard). These results and their significance will be discussed in detail in due course.

Table II. Selected Spectroscopic Properties of Phenyl Isocyanide Complexes of Molybdenum(II) and Tungsten(II)

complex	^{1}H chem shifts in δ [a]			IR absorptns ν(C≡N),[b] cm^{-1}	electronic absorptn spectra,[c] nm
	alkyl	P(CH$_2$)$_n$P	phenyl		
[Mo(CNPh)$_7$](PF$_6$)$_2$			7.75 br, 7.60 m	2180 sh, 2170 sh, 2140 s 2140 s[f]	425 (4.5), 310 (61.1), 290 sh
[W(CNPh)$_7$](PF$_6$)$_2$			~7.70 br	2210 vw, 2170 sh, 2120 vs 2130 vs[f]	420 (7.7), 320 (65.0), 295 sh
[Mo(NO)(CNPh)$_5$]PF$_6$				2192 w, 2108 s, 1678 m[g] 2190 vw,[f] 2170 vw,[f] 2110 s,[f] 1680 m, br[f,g]	520 (1.4), 368 sh, 352 (41.0)
[W(NO)(CNPh)$_5$]PF$_6$				2195 w, 2160 w, 2090 vs, 1660 m[g]	528 (1.8), 375 sh, 360 (42.2)
[Mo(CNPh)$_6$Cl]PF$_6$				2130 s, 2100 s	440 sh, 320
[Mo(CNPh)$_6$I]PF$_6$				2195 w, 2110 s	438 sh, ~315 br
[W(CNPh)$_6$I]BPh$_4$				2190 w, ~2100 vs, br	450 sh, 335 sh, 310
[Mo(CNPh)$_5$(PEt$_3$)$_2$](PF$_6$)$_2$	2.48 m, 1.40 p		7.68 m	2130 sh, 2105 sh, 2075 s 2160 w,[f] 2090 s[f]	
[Mo(CNPh)$_5$(P-*n*-Pr$_3$)$_2$](PF$_6$)$_2$	2.33 m, 1.81 br, 1.00 t		7.68 m	2164 w, 2082 s	436 sh, 350 sh ?, 328 sh, 309
[Mo(CNPh)$_5$(PEt$_2$Ph)$_2$](PF$_6$)$_2$	2.80 m, 1.30 p		7.86 br, 7.52 m	2160 w, 2125 sh, 2092 s 2168 w,[f] 2098 s[f]	440–430 sh, 390 sh, 352 sh, 328 sh, 310
[Mo(CNPh)$_5$(PEtPh$_2$)$_2$](PF$_6$)$_2$	3.16 m, 1.31 p		7.78 br, 7.52 m, 7.24 m	2170 w, 2100 s	~430 sh, 353 sh, 325 (39.9)
[Mo(CNPh)$_6$(PPh$_3$)](PF$_6$)$_2$			7.80 br, 7.58 m	2195 w, 2170 sh, 2115 s 2190 w,[f] 2124 s, br[f]	438 sh, 376 sh, 326 sh
[Mo(CNPh)$_5$(dppm)](PF$_6$)$_2$		5.39 t[d]	7.95 br, 7.54 m, 7.33 m	2178 m, 2140 m-s, 2095 s	462, 386 sh, 342, 300
[Mo(CNPh)$_5$(dppe)](PF$_6$)$_2$		3.49 d[e]	7.93 br, 7.57 m, 7.29 m	2178 m-w, ~2140 sh, 2100 s 2170 m-w,[f] 2108 s[f]	425 sh, 344 sh, 307
[Mo(CNPh)$_5$(P(OEt)$_3$)$_2$](PF$_6$)$_2$				2188 m-w, 2165 m, 2095 s	
[W(CNPh)$_5$(PEt$_3$)$_2$](PF$_6$)$_2$	2.52 m, 1.37 p		7.67 m	2170 w, 2085 s	
[W(CNPh)$_5$(PEtPh$_2$)$_2$](PF$_6$)$_2$	3.25 m, 1.31 m		7.79 br, 7.53 m, 7.22 br	2168 w, 2120 sh, 2090 s	432 sh, 337 sh, 312 (49.2)
[W(CNPh)$_5$(dppe)](PF$_6$)$_2$		3.56 d[e]	7.90 br, 7.52 m, 7.21 m	2175 w, 2080 s, br 2175 w,[f] 2100 s,[f]	425 sh, 350 sh, 312 (53.7)
[W(CNPh)$_6$(PPh$_3$)](PF$_6$)$_2$				2200 w, 2110 s	450 sh, 318 sh, 302

[a] All ^{1}H NMR spectra were recorded in acetone-d_6. Abbreviations are as follows: br = broad, d = doublet, m = multiplet, p = pentet, q = quartet, t = triplet. [b] IR spectra recorded as Nujol mulls unless stated otherwise (see footnote *f*). [c] Electronic absorption spectra recorded on dichloromethane solutions. ϵ_{max} values (M^{-1} cm^{-1} × 10^{-3}) when recorded are given in parentheses. [d] J_{CH_2-P} = 11 Hz. [e] J_{CH_2-P} = 22 Hz. [f] Data recorded in dichloromethane. [g] ν(NO).

$(NO)(CNPh)_5]PF_6$ (with 0.2 M Bu_4NPF_6 as supporting electrolyte) has a CV with $E_{1/2}(ox) = +1.02$ V and $E_{p,c}(red) = -1.43$ V vs. SCE. This solvent effect is under further study at this time.

Substitution Chemistry: Reactions with Tertiary Phosphines and Phosphites. The close resemblance between the substitution chemistry of $[M(CNR)_7]^{2+}$ and $[M(CNPh)_7]^{2+}$ is seen not only in the existence of equilibria of the type shown in eq 1 (vide supra), involving replacement of one RNC or PhNC ligand by halide, but also in the ready formation of mixed phosphine–isocyanide complexes through substitution of up to two isocyanide ligands (eq 2 and 3). These products are isoelectronic with their

$$[M(CNPh)_7]^{2+} + xPR_3 \rightarrow [M(CNPh)_{7-x}(PR_3)_x]^{2+} + x\text{PhNC} \quad (2)$$

M = Mo or W; PR_3 = PEt_3, $P(OEt)_3$, P-*n*-Pr_3, PEt_2Ph, $PEtPh_2$ or PPh_3; x = 1 or 2

$$[M(CNPh)_7]^{2+} + Ph_2P(CH_2)_nPPh_2 \rightarrow [M(CNPh)_5(Ph_2P(CH_2)_nPPh_2)]^{2+} + 2\text{PhNC} \quad (3)$$

M = Mo or W; n = 1 or 2

precursor complexes $[M(CNPh)_7]^{2+}$, as well as with their alkyl isocyanide congeners.[4,7] Only the reactions of triphenylphosphine with $[M(CNPh)_7]^{2+}$ produced monosubstituted products, i.e., $[M(CNPh)_6(PPh_3)]^{2+}$. Steric crowding rather than electronic factors may be responsible for these reactions terminating at the monosubstitution stage, since the reaction of $[Mo(CNPh)_7]^{2+}$ with triethyl phosphite $P(OEt)_3$, a weaker Lewis base than PPh_3, readily yields a disubstituted product.

In all instances the spectroscopic properties of the mixed phosphine–phenyl isocyanide complexes (Table II) bear the same close relationship to $[Mo(CNPh)_7]^{2+}$ as do those of the mixed phosphine–alkyl isocyanide derivatives to $[M(CNR)_7]^{2+}$. One notable feature is a shift in the most intense $\nu(C{\equiv}N)$ mode to lower energy upon substituting phosphine for PhNC (Table II), a trend which reflects the transfer of electron density into the π^* orbitals of PhNC upon coordination of the better σ-donor phosphine ligands. Integration of the phenyl and alkyl resonances in the ^1H NMR spectra gave values in accord with the proposed stoichiometries of the complexes.

The electrochemical properties of the mixed-ligand complexes were studied by using the cyclic voltammetry technique. All complexes exhibited an accessible oxidation. The appropriate voltammetric half-wave potentials for all of the seven-coordinate complexes of the types $[M(CNPh)_5(PR_3)_2](PF_6)_2$, where M = Mo or W and PR_3 = PEt_3, P-*n*-Pr_3, PEt_2Ph, or $PEtPh_2$, $[M(CNPh)_5(dppm)](PF_6)_2$, and $[M(CNPh)_5(dppe)](PF_6)_2$ were substantially lower than the corresponding half-wave potentials for the homoleptic complexes $[M(CNPh)_7](PF_6)_2$. This reflects the greater ability of these phosphine ligands to stabilize the molybdenum(III) and tungsten(III) states in these complexes compared to the π-acceptor PhNC ligand. Note that with complexes containing the weaker bases PPh_3 and $P(OEt)_3$ the $E_{1/2}$ values (Table I) are comparable to those of $[M(CNPh)_7](PF_6)_2$.

For all the molybdenum(II) and tungsten(II) complexes, the current ratio $i_{p,c}/i_{p,a}$ for the one-electron couple was equal to unity (or very close to it) for sweep rates (v) between 50 and 400 mV/s, and plots of i_p vs. $v^{1/2}$ gave straight lines for sweep rates between 100 and 400 mV/s. The potential separation between the anodic and cathodic peaks ($\Delta E_p = E_{p,a} - E_{p,c}$) varied in the range from 67 to 112 mV for scan rates from 50 to 400 mV/s. From measurements on known reversible couples (e.g., ferrocene/ferricinium) using our experimental setup,[31] we believe that these electrochemical properties are best considered in a qualitative sense as being in accord with reversible electron transfer.

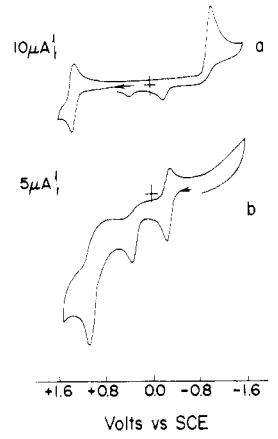

Figure 2. Cyclic voltammograms in 0.2 M tetra-*n*-butylammonium hexafluorophosphate–dichloromethane of $[Mo(CNPh)_5(PEt_2Ph)_2](PF_6)_2$ (a) before and (b) after reduction at −1.2 V. Sweep rates for a and b are 200 mV/s.

Like $[M(CNPh)_7]^{2+}$, each of the mixed phosphine–isocyanide complexes also exhibit an electrochemically irreversible reduction close to −1.0 V, the CV's showing that this reduction is followed by the formation of zerovalent mixed ligand complexes as evidenced by the appearance of characteristic waves ($E_{p,a} \simeq +0.4$ and −0.2 V) at the end of the first scan. This is shown in Figure 2a in the CV of $[Mo(CNPh)_5(PEt_2Ph)_2](PF_6)_2$, where the oxidations at $E_{p,a}$ = +0.36 and −0.24 V demonstrate that a molybdenum(0) species (vide infra) is formed following the two-electron reduction of the seven-coordinate molybdenum(II) complex. A similar phenomenon is seen in the CV of $[Mo(CNPh)_7](PF_6)_2$ (Figure 1c) where reduction leads to the formation of $Mo(CNPh)_6$. The chemical and electrochemical reductions of these mixed-ligand complexes and their homoleptic parents are dealt with further in the following section.

Reduction of Seven-Coordinate M(II) to Six-Coordinate M(0). As discussed in previous sections, all the seven-coordinate (phenyl isocyanide)molybdenum(II) and -tungsten(II) complexes, whether homoleptic, mixed halide–phenyl isocyanide, or mixed phosphine–phenyl isocyanide have cyclic voltammograms which display a two-electron reduction wave at ca. −1.0 V vs. SCE. Furthermore, these CV's display, on the return scan, product waves at ca. +0.4 and −0.2 V vs. SCE (see Figures 1c and 2a). Electrochemical reduction of $[M(CNPh)_7](PF_6)_2$ in dichloromethane yields solutions whose cyclic voltammograms are characteristic of $M(CNPh)_6$. The chemical reduction of $[M(CNPh)_7](PF_6)_2$ to $M(CNPh)_6$ in high yield was accomplished by using activated magnesium as the reducing agent (see Experimental Section).

Similar results were obtained upon carrying out the electrolytic reduction of $[Mo(CNPh)_5(PEt_2Ph)_2](PF_6)_2$ at a potential of −1.2 V. As shown in Figure 2b, the resultant orange solution has a CV which is characteristic of a phenyl isocyanide complex of molybdenum(0). The oxidations at $E_{p,a}$ = +0.36 V and $E_{1/2}$ = −0.28 V vs. SCE are clearly different from those of $Mo(CNPh)_6$ itself ($E_{1/2}$ = +0.48 V and $E_{p,a}$ = −0.19 V), thereby signifying that phosphine ligands must be present in the product. Upon carrying out

(31) Zietlow, T. C.; Klendworth, D. D.; Nimry, T.; Salmon, D. J.; Walton, R. A. *Inorg. Chem.* **1981**, *20*, 947.

the chemical reduction of $[Mo(CNPh)_5(PEtPh_2)_2](PF_6)_2$ using magnesium metal (alternatively, sodium can be used), we produced a red oil which proved difficult to characterize. However, the corresponding magnesium reduction of $[Mo(CNPh)_5(dppe)](PF_6)_2$ produced an air-sensitive red solid whose CV displayed oxidations at $E_{p,a}$ = +0.42 V and $E_{1/2}$ = −0.27 V vs. SCE as well as a couple at $E_{1/2}$ = +1.16 V which heralded the formation of a chemical product following the irreversible oxidation at +0.42 V. The IR spectrum of this complex (CH_2Cl_2 solution) had ν(C≡N) modes at 1955 (vs) and 1810 (sh) cm^{-1}, and its ^1H NMR spectrum (in CD_2Cl_2) displayed phenyl resonances at δ ~8.4 (br) and ~7.78 (m) and $-C_2H_4-$ resonances at δ 3.13 (d, J_{CH_2-P} = 20 Hz), the latter feature implying the presence of bidentate dppe. The most likely formulation for this unstable molecule is $Mo(CNPh)_4(dppe)$, based upon an integration of the above signals in the ^1H NMR spectrum.

These reduction reactions are of interest from two points of view. First, they provide an alternative strategy to that already available[32] for the synthesis of mixed phosphine–isocyanide complexes of molybdenum(0).[33] Second, the metal-based reductions of $[M(CNR)_7]^{2+}$ and $[M(CNR)_{7-x}(PR_3)_x]^{2+}$ proceed by a different mechanism from that which occurs in the zinc reduction of $[Mo(CNCMe_3)_6I]^+$.[26,34] The latter reduction leads to the reductive coupling of two adjacent isocyanide ligands to afford the $[Mo(CNCMe_3)_4(Me_3CNHCCNHCMe_3)]^+$ cation.[26,34] The factors which govern the latter reaction course are currently under further study.[35]

Acknowledgment. We thank the National Science Foundation (Grant CHE79-09233) for research support and Mr. David E. Wigley for invaluable experimental assistance. We are also very grateful to Professor S. J. Lippard for providing us with a preprint of ref 24 and for keeping us informed of his research progress in this area.

Registry No. $Mo(CNPh)_6$, 14154-60-0; $W(CNPh)_6$, 14128-11-1; $[Mo(NO)(CNPh)_5]PF_6$, 78653-92-6; $[Mo(CNPh)_7](PF_6)_2$, 78653-88-0; $[Mo(CNPh)_6I]PF_6$, 79721-63-4; $[Mo(CNPh)_6I]BPh_4$, 79721-64-5; $[W(NO)(CNPh)_5]PF_6$, 78653-94-8; $[W(CNPh)_6I]BPh_4$, 79721-66-7; $[W(CNPh)_7](PF_6)_2$, 78653-90-4; $[Mo(CNPh)_6Cl]PF_6$, 79721-70-3; $[Mo(CNPh)_5(P\text{-}n\text{-}Pr_3)_2](PF_6)_2$, 79734-82-0; $[Mo(CNPh)_5(PEt_3)_2](PF_6)_2$, 79734-84-2; $[Mo(CNPh)_5(PEt_2Ph)_2](PF_6)_2$, 79721-72-5; $[Mo(CNPh)_5(PEtPh_2)_2](PF_6)_2$, 79721-74-7; $[Mo(CNPh)_6(PPh_3)](PF_6)_2$, 79721-76-9; $[Mo(CNPh)_5(P(OEt)_3)_2](PF_6)_2$, 79721-78-1; $[Mo(CNPh)_5(dppe)](PF_6)_2$, 79721-80-5; $[Mo(CNPh)_5(dppm)](PF_6)_2$, 79734-86-4; $[W(CNPh)_5(PEt_3)_2](PF_6)_2$, 79721-82-7; $[W(CNPh)_5(PEtPh_2)_2](PF_6)_2$, 79721-84-9; $[W(CNPh)_6(PPh_3)](PF_6)_2$, 79721-86-1; $[W(CNPh)_5(dppe)](PF_6)_2$, 79721-88-3; $W_2(dmhp)_4$, 69351-88-8; $W_2(mhp)_4$, 67634-84-8.

(32) Pombeiro, A. J. L.; Chatt, J.; Richards, R. L. *J. Organomet. Chem.* **1980**, *190*, 297.
(33) Such complexes are invariably formed as oils, as we have also found, so that their characterization has been based mainly upon their NMR spectroscopic properties.[32]
(34) Lam, C. T.; Corfield, P. W. R.; Lippard, S. J. *J. Am. Chem. Soc.* **1977**, *99*, 617.
(35) Lippard, S. J., private communication.

Synthesis of Cyclic Aminooxo- and Dioxocarbenes from Carbonyl Ligands in Complexes of Iron and Manganese

Herbert Motschi and Robert J. Angelici*

Department of Chemistry and Ames Laboratory—U.S. DOE[1] Iowa State University, Ames, Iowa 50011

Received August 25, 1981

Electrophilic CO ligands in metal carbonyl complexes are converted to cyclic aminooxo- or dioxocarbene ligands by the following reactions: $M{-}C{\equiv}O^+ + H_3NCH_2CH_2Br^+ + 2B \rightarrow M{-}\overline{COCH_2CH_2NH}^+ + 2BH^+ + Br^-$; $M{-}C{\equiv}O^+ + HOCH_2CH_2Br + B \rightarrow M{-}\overline{COCH_2CH_2O}^+ + BH^+ + Br^-$. The base B used in these reactions is frequently NaH, but Et_3N and K_2CO_3 can also be successfully applied in certain cases. It is suggested that the reactions proceed by nucleophilic attack of the amine or alkoxide on a CO carbon atom to give a carbamoyl or alkoxycarbonyl intermediate, which cyclizes intramolecularly to yield the carbene products. One CO group in each of the following complexes has been observed to undergo one or both of these reactions: $FeCp(CO)_3^+$, $MnCp(NO)(CO)_2^+$, $MnCp(NO)(P(OPh)_3)(CO)^+$, $MnCp(NO)(CNC_6H_{11})(CO)^+$, and $Fe(CO)_5$. The reaction of $MnCp(NO)(CO)_2^+$ with $HOCH_2CH_2Br$ is the only one which leads to a dicarbene complex, $MnCp(NO)(\overline{COCH_2CH_2O})_2^+$. On the basis of studies of these and other metal carbonyl complexes, it appears that only CO groups that are sufficiently electropositive and have ν(CO) force constants equal to or greater than 17.0 mdyn/Å participate in these reactions. The amino group in $FeCp(CO)_2(\overline{COCH_2CH_2NH})^+$ is deprotonated by NaH or K_2CO_3 to give the imine complex $FeCp(CO)_2(\overline{COCH_2CH_2N})$ which reacts with $PdCl_2(NCMe)_2$ to yield the di-chloro-bridged dimer *sym*,-*trans*-$[FeCp(CO)_2(\overline{COCH_2CH_2N})Pd(\mu\text{-}Cl)Cl]_2$ in which the imine complexes are coordinated to the Pd(II) via their N atoms. Trends in the infrared and ^1H and ^{13}C NMR spectra of the complexes are discussed.

Introduction

Aliphatic amines react with electrophilic carbonyl ligands to give carbamoyl complexes (eq 1).[2,3] The reactivity

$$M{-}CO^+ + 2H_2NR \rightleftharpoons M{-}C(=O)NHR + RNH_3^+ \quad (1)$$

of a given CO ligand depends upon its electron density, which is reflected in its C–O stretching force constant.[4] Those CO ligands with force constants greater than approximately 17.2 mdyn/Å readily form carbamoyl com-

(1) Ames Laboratory is operated for the U.S. Department of Energy by Iowa State University under Contract No. W-7405-Eng-82. This research was supported by the Office of Basic Energy Sciences, Chemical Sciences Division.
(2) Angelici, R. J. *Acc. Chem. Res.* **1972**, *5*, 335.
(3) Behrens, H. *Adv. Organomet. Chem.* **1980**, *18*, 19.
(4) Angelici, R. J.; Blacik, L. J. *Inorg. Chem.* **1972**, *11*, 1754.

0276-7333/82/2301-0343$01.25/0

the chemical reduction of $[Mo(CNPh)_5(PEtPh_2)_2](PF_6)_2$ using magnesium metal (alternatively, sodium can be used), we produced a red oil which proved difficult to characterize. However, the corresponding magnesium reduction of $[Mo(CNPh)_5(dppe)](PF_6)_2$ produced an air-sensitive red solid whose CV displayed oxidations at $E_{p,a}$ = +0.42 V and $E_{1/2}$ = −0.27 V vs. SCE as well as a couple at $E_{1/2}$ = +1.16 V which heralded the formation of a chemical product following the irreversible oxidation at +0.42 V. The IR spectrum of this complex (CH_2Cl_2 solution) had ν(C≡N) modes at 1955 (vs) and 1810 (sh) cm^{-1}, and its ^1H NMR spectrum (in CD_2Cl_2) displayed phenyl resonances at δ ~8.4 (br) and ~7.78 (m) and $-C_2H_4-$ resonances at δ 3.13 (d, J_{CH_2-P} = 20 Hz), the latter feature implying the presence of bidentate dppe. The most likely formulation for this unstable molecule is $Mo(CNPh)_4(dppe)$, based upon an integration of the above signals in the ^1H NMR spectrum.

These reduction reactions are of interest from two points of view. First, they provide an alternative strategy to that already available[32] for the synthesis of mixed phosphine–isocyanide complexes of molybdenum(0).[33] Second, the metal-based reductions of $[M(CNR)_7]^{2+}$ and $[M(CNR)_{7-x}(PR_3)_x]^{2+}$ proceed by a different mechanism from that which occurs in the zinc reduction of $[Mo(CNCMe_3)_6I]^+$.[26,34] The latter reduction leads to the reductive coupling of two adjacent isocyanide ligands to afford the $[Mo(CNCMe_3)_4(Me_3CNHCCNHCMe_3)]^+$ cation.[26,34] The factors which govern the latter reaction course are currently under further study.[35]

Acknowledgment. We thank the National Science Foundation (Grant CHE79-09233) for research support and Mr. David E. Wigley for invaluable experimental assistance. We are also very grateful to Professor S. J. Lippard for providing us with a preprint of ref 24 and for keeping us informed of his research progress in this area.

Registry No. $Mo(CNPh)_6$, 14154-60-0; $W(CNPh)_6$, 14128-11-1; $[Mo(NO)(CNPh)_5]PF_6$, 78653-92-6; $[Mo(CNPh)_7](PF_6)_2$, 78653-88-0; $[Mo(CNPh)_6I]PF_6$, 79721-63-4; $[Mo(CNPh)_6I]BPh_4$, 79721-64-5; $[W(NO)(CNPh)_5]PF_6$, 78653-94-8; $[W(CNPh)_6I]BPh_4$, 79721-66-7; $[W(CNPh)_7](PF_6)_2$, 78653-90-4; $[Mo(CNPh)_6Cl]PF_6$, 79721-70-3; $[Mo(CNPh)_5(P\text{-}n\text{-}Pr_3)_2](PF_6)_2$, 79734-82-0; $[Mo(CNPh)_5(PEt_3)_2](PF_6)_2$, 79734-84-2; $[Mo(CNPh)_5(PEt_2Ph)_2](PF_6)_2$, 79721-72-5; $[Mo(CNPh)_5(PEtPh_2)_2](PF_6)_2$, 79721-74-7; $[Mo(CNPh)_6(PPh_3)](PF_6)_2$, 79721-76-9; $[Mo(CNPh)_5(P(OEt)_3)_2](PF_6)_2$, 79721-78-1; $[Mo(CNPh)_5(dppe)](PF_6)_2$, 79721-80-5; $[Mo(CNPh)_5(dppm)](PF_6)_2$, 79734-86-4; $[W(CNPh)_5(PEt_3)_2](PF_6)_2$, 79721-82-7; $[W(CNPh)_5(PEtPh_2)_2](PF_6)_2$, 79721-84-9; $[W(CNPh)_6(PPh_3)](PF_6)_2$, 79721-86-1; $[W(CNPh)_5(dppe)](PF_6)_2$, 79721-88-3; $W_2(dmhp)_4$, 69351-88-8; $W_2(mhp)_4$, 67634-84-8.

(32) Pombeiro, A. J. L.; Chatt, J.; Richards, R. L. *J. Organomet. Chem.* **1980**, *190*, 297.
(33) Such complexes are invariably formed as oils, as we have also found, so that their characterization has been based mainly upon their NMR spectroscopic properties.[32]
(34) Lam, C. T.; Corfield, P. W. R.; Lippard, S. J. *J. Am. Chem. Soc.* **1977**, *99*, 617.
(35) Lippard, S. J., private communication.

Synthesis of Cyclic Aminooxo- and Dioxocarbenes from Carbonyl Ligands in Complexes of Iron and Manganese

Herbert Motschi and Robert J. Angelici*

Department of Chemistry and Ames Laboratory—U.S. DOE[1] Iowa State University, Ames, Iowa 50011

Received August 25, 1981

Electrophilic CO ligands in metal carbonyl complexes are converted to cyclic aminooxo- or dioxocarbene ligands by the following reactions: $M{-}C{\equiv}O^+ + H_3NCH_2CH_2Br^+ + 2B \rightarrow M{-}\overline{COCH_2CH_2NH}^+ + 2BH^+ + Br^-$; $M{-}C{\equiv}O^+ + HOCH_2CH_2Br + B \rightarrow M{-}\overline{COCH_2CH_2O}^+ + BH^+ + Br^-$. The base B used in these reactions is frequently NaH, but Et_3N and K_2CO_3 can also be successfully applied in certain cases. It is suggested that the reactions proceed by nucleophilic attack of the amine or alkoxide on a CO carbon atom to give a carbamoyl or alkoxycarbonyl intermediate, which cyclizes intramolecularly to yield the carbene products. One CO group in each of the following complexes has been observed to undergo one or both of these reactions: $FeCp(CO)_3^+$, $MnCp(NO)(CO)_2^+$, $MnCp(NO)(P(OPh)_3)(CO)^+$, $MnCp(NO)(CNC_6H_{11})(CO)^+$, and $Fe(CO)_5$. The reaction of $MnCp(NO)(CO)_2^+$ with $HOCH_2CH_2Br$ is the only one which leads to a dicarbene complex, $MnCp(NO)(\overline{COCH_2CH_2O})_2^+$. On the basis of studies of these and other metal carbonyl complexes, it appears that only CO groups that are sufficiently electropositive and have ν(CO) force constants equal to or greater than 17.0 mdyn/Å participate in these reactions. The amino group in $FeCp(CO)_2(\overline{COCH_2CH_2NH})^+$ is deprotonated by NaH or K_2CO_3 to give the imine complex $FeCp(CO)_2(\overline{COCH_2CH_2N})$ which reacts with $PdCl_2(NCMe)_2$ to yield the di-chloro-bridged dimer *sym*,-*trans*-$[FeCp(CO)_2(\overline{COCH_2CH_2N})Pd(\mu\text{-}Cl)Cl]_2$ in which the imine complexes are coordinated to the Pd(II) via their N atoms. Trends in the infrared and ^1H and ^{13}C NMR spectra of the complexes are discussed.

Introduction

Aliphatic amines react with electrophilic carbonyl ligands to give carbamoyl complexes (eq 1).[2,3] The reactivity

$$M{-}CO^+ + 2H_2NR \rightleftharpoons M{-}C(=O)NHR + RNH_3^+ \quad (1)$$

of a given CO ligand depends upon its electron density, which is reflected in its C–O stretching force constant.[4] Those CO ligands with force constants greater than approximately 17.2 mdyn/Å readily form carbamoyl com-

(1) Ames Laboratory is operated for the U.S. Department of Energy by Iowa State University under Contract No. W-7405-Eng-82. This research was supported by the Office of Basic Energy Sciences, Chemical Sciences Division.
(2) Angelici, R. J. *Acc. Chem. Res.* **1972**, *5*, 335.
(3) Behrens, H. *Adv. Organomet. Chem.* **1980**, *18*, 19.
(4) Angelici, R. J.; Blacik, L. J. *Inorg. Chem.* **1972**, *11*, 1754.

0276-7333/82/2301-0343$01.25/0

plexes; those with force constants between approximately 16.5 and 17.2 mdyn/Å give reversible equilibrium mixtures of carbonyl reactant and carbamoyl product; and those with constants below 16.5 mdyn/Å show no evidence of carbamoyl formation.[2] Alkoxide ions (RO^-) show a similar reactivity although they have not been studied in as great detail.

The present investigation was designed to take advantage of carbonyl ligand reactivity in the synthesis of cyclic carbene complexes. Using amines and alkoxides with a good leaving group in the β-position, it was hoped that cyclization to the carbene would occur. With (2-bromoethyl)amine (and base B) and 2-bromoethoxide, the reactions would occur as shown in eq 2 and 3. Previously,

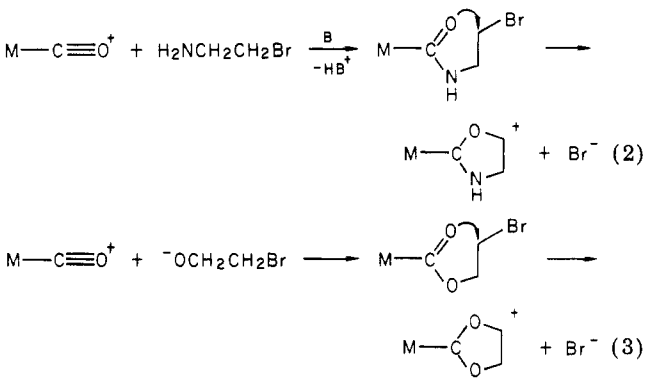

Stone and co-workers[5] showed that $Mn(CO)_6^+$ reacts with $HOCH_2CH_2Cl$ in the presence of Et_3N to give the alkoxycarbonyl complex, $Mn(CO)_5[C(=O)OCH_2CH_2Cl]$, which upon treatment with Ag^+ cyclizes to give the dioxocarbene, $Mn(CO)_5[\overline{COCH_2CH_2O}]^+$. The cyclization did not occur without assistance from Ag^+. In the present study, cyclization occurs spontaneously in both reactions 2 and 3. The generality of these reactions is explored, and the spectroscopic properties of the carbene products are reported.

Experimental Section

General Methods. Unless otherwise noted, reagent chemicals of the highest quality available were used without further purification. All reactions were performed under an N_2 atmosphere. Except for that of $Fe(CO)_4(\overline{COCH_2CH_2NH})$, product isolations were carried out in air atmosphere. Infrared spectra were recorded on Perkin Elmer 281, Beckman 4250, or IBM 98 (Fourier Transform) instrument; ^1H- and ^{13}C-NMR spectra were recorded on a JEOL FX-90Q spectrometer.

Starting Complexes. $[FeCp(CO)_3]CF_3SO_3$[6] and $[MnCp(NO)(CO)_2]PF_6$[7] were prepared by literature methods.

$[MnCp(NO)(CO)(L)]PF_6$ (L = CNC_6H_{11}, $P(OPh)_3$). These complexes were prepared by a modification of the method of Brunner and Schindler.[8] A solution (~0.25 M) of $[MnCp(NO)(CO)_2]PF_6$ (0.5 mmol) in CH_3CN was reacted with a solution (~0.25 M) of L (0.5 mmol) in CH_3CN for 2 h at room temperature. Evaporation to dryness was followed by extraction with 10 mL of CH_2Cl_2 and filtration through Celite. The filtrate was concentrated to about 3 mL, and the product was crystallized by adding diethyl ether. Yields: 74% for L = CNC_6H_{11}; 88% for L = $P(OPh)_3$.

Synthesis of Complexes. $[FeCp(CO)_2(\overline{COCH_2CH_2NH})]PF_6$. To a suspension of 240 mg (1.17 mmol) of $[BrCH_2CH_2NH_3]Br$ in 20 mL of CH_3CN was added 100 mg (2.1 mmol) of 50% NaH in oil. After being stirred for 5 min, the mixture was treated with 400 mg (1.13 mmol) of $[FeCp(CO)_3]CF_3SO_3$ and stirred for an additional 15 min. An excess of KPF_6 (~2 g) was added to exchange the anion, and the mixture was stirred for 5 min. The solvent was removed under reduced pressure, and the residue was treated with several small portions of ether until the washings were colorless. The dried residue was extracted with CH_2Cl_2 and filtered through $MgSO_4$. The yellow filtrate was concentrated until pale yellow needles started to appear. Further crystallization was induced by the addition of ether: yield 290 mg (65.3%); mp 132 °C. Anal. Calcd for $C_{10}H_{10}F_6FeNO_3P$: C, 30.56; H, 2.56; N, 3.56. Found: C, 30.62; H, 2.54; N, 3.61.

$[FeCp(CO)_2(\overline{COCH_2CH_2O})]PF_6$. To 200 mg (0.564 mmol) of $[FeCp(CO)_3]CF_3SO_3$ was added 1.5 mL (21 mmol) of $BrCH_2CH_2OH$. To this stirred mixture was added ~150 mg (3.1 mmol) of 50% NaH in oil in small portions. Vigorous H_2 evolution was observed, and the reaction flask was cooled in an ice bath. After 5 min, excess $BrCH_2CH_2OH$ was removed under reduced pressure. The residue was treated with 10 mL of CH_3CN, and excess KPF_6 (~2 g) was added. Filtration through Celite resulted in a red filtrate. Removal of the solvent was followed by washing of the residue with ether until the washings became colorless. The residue was extracted with CH_2Cl_2 and filtered through $MgSO_4$. The filtrate was concentrated, and pale yellow crystals of the product precipitated upon addition of ether: yield 134 mg (60.3%); mp 129 °C. Anal. Calcd for $C_{10}H_9F_6FeO_4P$: C, 30.48; H, 2.30. Found: C, 30.40; H, 2.33.

$[MnCp(NO)(CO)(\overline{COCH_2CH_2NH})]PF_6$. The same procedure as for $[FeCp(CO)_2(\overline{COCH_2CH_2NH})]PF_6$ was used. Starting with 350 mg (~1 mmol) of $[MnCp(NO)(CO)_2]PF_6$, 280 mg (71%) of orange crystalline product was obtained; mp 134 °C. Anal. Calcd for $C_9H_{10}F_6MnN_2O_3P$: C, 27.43; H, 2.56; N, 7.10. Found: C, 27.58; H, 2.61; N, 7.06.

$[MnCp(NO)(\overline{COCH_2CH_2O})_2]PF_6$. The same procedure as for $[FeCp(CO)_2(\overline{COCH_2CH_2O})]PF_6$ was followed. Starting with 100 mg (0.285 mmol) of $[MnCp(NO)(CO)_2]PF_6$, the yield of product was 94 mg (75%). Yellow needles were obtained from CH_2Cl_2/ether and yellow-orange cubes from CH_3CN/ether; mp 232 °C. Anal. Calcd for $C_{11}H_{13}F_6MnNO_5P$: C, 30.09; H, 2.98; N, 3.19. Found: C, 30.09; H, 2.99; N, 3.12.

$[MnCp(NO)(P(OPh)_3)(\overline{COCH_2CH_2NH})]PF_6$. Following the procedure for the preparation of $[FeCp(CO)_2(\overline{COCH_2CH_2NH})]PF_6$ and starting with 300 mg (0.474 mmol) of $[MnCp(NO)(CO)(P(OPh)_3)]PF_6$, 230 mg (72%) of the orange crystalline product was isolated; mp 64 °C. Anal. Calcd for $C_{26}H_{25}F_6MnN_2O_5P_2$: C, 46.17; H, 3.73; N, 4.14. Found: C, 46.05; H, 3.90; N, 4.05.

$[MnCp(NO)(P(OPh)_3)(\overline{COCH_2CH_2O})]PF_6$. To 100 mg (0.158 mmol) of $[MnCp(NO)(CO)(P(OPh)_3)]PF_6$ dissolved in 4 mL of CH_2Cl_2 was added 40 mg (0.32 mmol) of $BrCH_2CH_2OH$ and an excess of 50% NaH in oil. The reaction was followed in the IR, and a shift of the ν(NO) band and the simultaneous disappearance of the ν(CO) band were observed after 1 h. The resulting suspension was filtered and washed with CH_2Cl_2 through Celite. Upon removal of CH_2Cl_2 under vacuum, a yellow-orange oil resulted. The oil was washed with dry ether and stirred with hexanes; it slowly converted to a yellow powder; yield 61 mg (57%). Anal. Calcd for $C_{26}H_{24}F_6MnNO_6P_2$: C, 46.10; H, 3.57; N, 2.07. Found: C, 46.15; H, 3.60; N, 2.00.

$[MnCp(NO)(CNC_6H_{11})(\overline{COCH_2CH_2O})]PF_6$. Using the same procedure as for the preparation of $[MnCp(NO)(P(OPh)_3)(\overline{COCH_2CH_2O})]PF_6$ and starting with 50 mg of $[MnCp(NO)(CO)CNC_6H_{11})]PF_6$ and using a reaction time of 22 h, we isolated 50 mg (90%) of the product as a red-orange viscous oil at 25 °C; it solidified at about −20 °C. Anal. Calcd for $C_{15}H_{20}F_6MnN_2O_3P$: C, 37.83; H, 4.23; N, 5.88. Found: C, 38.43; H, 4.42; N, 6.07.

$Fe(CO)_4(\overline{COCH_2CH_2NH})$. To 305 mg (1.49 mmol) of finely ground $[BrCH_2CH_2NH_3]Br$ was added 3 mL of NEt_3 in a Schlenk tube. Following repeated evacuation and saturation with N_2 of the solution, 0.20 mL (1.49 mmol) of $Fe(CO)_5$ (toxic!) was added with a syringe. The mixture was stirred for about 2 h under N_2 at 25 °C. This was followed by distillation under vacuum at room

(5) Bowen, D. H.; Green, M.; Grove, D. M.; Moss, J. R.; Stone, F. G. A. *J. Chem. Soc., Dalton Trans.* **1974**, 1189.
(6) Quick, M. H., Angelici, R. J. *J. Organomet. Chem.* **1978**, *160*, 231.
(7) Connelly, N. G. *Inorg. Synth.* **1974**, *15*, 91.
(8) Brunner, H.; Schindler, H.-D. *J. Organomet. Chem.* **1969**, *19*, 135.

temperature of all NEt_3 and the small amount of unreacted $Fe(CO)_5$. The residue was treated with 25 mL of CaH_2-dried ether and the mixture stirred for 5 min. The resulting suspension was filtered through Celite into a connected Schlenk tube. All these manipulations were carried out in a closed system under an N_2 atmosphere. The pale yellow filtrate was concentrated until all ether was removed and a bright yellow oil resulted; yield 310 mg (87%). The compound is very air sensitive. Opening the Schlenk tube even under a stream of N_2 causes the color to change to orange within seconds. It was characterized by its infrared and ^1H and ^{13}C NMR spectra.

Deprotonation of $[FeCp(CO)_2(\overline{COCH_2CH_2NH})]PF_6$. Method A. Finely ground K_2CO_3 (~500 mg, ~4.5 mmol) was added to a mixture of 100 mg (0.254 mmol) of $[FeCp(CO)_2(\overline{COCH_2CH_2NH})]PF_6$ in 3 mL of CH_2Cl_2. After 1–2 days, an intensely yellow solution had formed together with a reddish brown precipitate. Removal under vacuum of CH_2Cl_2 was followed by extraction with ~20 mL of dry ether; the resulting suspension was filtered under $MgSO_4$. After the filtrate was evaporated to dryness, a yellow amorphous powder of $FeCp(CO)_2(\overline{COCH_2CH_2N})$ remained (~30 mg, 48%). The compound was extremely moisture sensitive and very soluble in common organic solvents. If opened to the atmosphere, it turned red and darkened within a few hours. In dilute solution (CH_2Cl_2, ether, hexanes) it can be kept for several hours without noticeable decomposition, whereas, in very concentrated solution, the formation of a red brown precipitate was observed in 4 h.

Method B. The yellow compound was also obtained by treating $[FeCp(CO)_2(\overline{COCH_2CH_2NH})]PF_6$ in CH_2Cl_2 with a large excess of 50% NaH in oil. After 2–3 h, the product was isolated together with some of the oil (from the NaH) which stabilized the complex.

$[FeCp(CO)_2(\overline{COCH_2CH_2N})PdCl(\mu\text{-}Cl)]_2$. A fresh sample of $FeCp(CO)_2(\overline{COCH_2CH_2N})$ prepared from 100 mg (0.254 mmol) of $[FeCp(CO)_2(\overline{COCH_2CH_2NH})]PF_6$ (method B) was dissolved in ~5 mL of CH_2Cl_2 to which 66 mg (0.255 mmol) of $PdCl_2(CH_3CN)_2$ was added. While the solution stirred for 30 min at 25 °C, its color turned orange-red and some brown precipitate formed. The suspension was filtered over $MgSO_4$, and the product was isolated as a brown-orange powder (30 mg, 28%) by concentration of the filtrate and addition of ether. It decomposed as a solid at 126 °C (turns black). The compound is moderately soluble in CH_2Cl_2 and CH_3CN, slightly soluble in ether, and insoluble in hexanes. In solution it is unstable and shows the same type of decomposition as $FeCp(CO)_2(\overline{COCH_2CH_2N})$. Anal. Calcd for $C_{20}H_{18}Cl_4Fe_2N_2O_6Pd_2$: C, 28.31; H, 2.14; N, 3.30. Found: C, 27.98; H, 2.23; N, 3.36.

Results and Discussion

Reactions of $FeCp(CO)_3^+$. This cation is known[9] to react with aliphatic amines and alkoxides to give carbamoyl and alkoxycarbonyl complexes. When $FeCp(CO)_3^+$ is added to a mixture of $H_3NCH_2CH_2Br^+$ and NaH, a CO group is rapidly converted to a carbene in 65% yield.

$$FeCp(CO)_3^+ + H_3\overset{+}{N}CH_2CH_2Br \xrightarrow[-2HB^+]{2B} FeCp(CO)_2\text{—}C(=O)\text{—}\overset{+}{N}H\text{—}CH_2\text{—}CH_2\text{—}O + Br^- \quad (4)$$

The metal complex cation is added last to the reaction mixture in order to avoid its reaction with the CH_3CN solvent. The most convenient base for this reaction is NaH in mineral oil, which presumably gives H_2 as the other product. However, the reaction also proceeds, but in lower yields, with K_2CO_3 and Et_3N in CH_2Cl_2 solvent. Some $[CpFe(CO)_2]_2$ is also formed as a byproduct in these reactions. There is no infrared evidence during the course of the reaction for a carbamoyl intermediate; it presumably cyclizes rapidly to the carbene ligand under the reaction conditions. Even in the presence of excess $H_3NCH_2CH_2Br^+$ and base, the conversion of a second CO ligand to a carbene does not occur. The lack of further reaction of $FeCp(CO)_2(\overline{COCH_2CH_2NH})^+$ is presumably due to the higher electron density on the CO carbons, as indicated by the $\nu(CO)$ force constant (16.76 mdyn/Å, Table I), which inhibits attack by an amine.

Treatment of $FeCp(CO)_3^+$ in liquid $HOCH_2CH_2Br$ with NaH rapidly gives the dioxocarbene in 60% yield.

$$FeCp(CO)_3^+ + HOCH_2CH_2Br \xrightarrow[-H_2]{NaH} FeCp(CO)_2\text{—}C(=O)\text{—}O\text{—}CH_2\text{—}CH_2\text{—}\overset{+}{O} + Br^- \quad (5)$$

There is no IR evidence for the presumed (eq 3) alkoxycarbonyl intermediate.

These aminooxo- and dioxocarbene complexes, as well as those described below, are characterized by their elemental analyses and infrared (Table I) and ^1H (Table II) and ^{13}C (Table III) NMR spectra. Except where indicated otherwise, all are stable in air for weeks in the solid state.

Reactions of $MnCp(NO)(CO)_2^+$. The known[10] reaction of $MnCp(NO)(CO)_2^+$ with aliphatic amines to give carbamoyl complexes suggests that one CO group in $MnCp(NO)(CO)_2^+$ could be converted to an aminooxocarbene upon reaction with $H_3NCH_2CH_2Br^+$ and base. Indeed, the carbene $MnCp(NO)(CO)(\overline{COCH_2CH_2NH})^+$ is isolated in 71% yield in this reaction when NaH is the base. An excess of base should be avoided because the carbene product is decomposed by strong bases (the same is true for $FeCp(CO)_2(\overline{COCH_2CH_2NH})^+$, vide infra). An excess of $H_3NCH_2CH_2Br^+$ and NaH does not give the dicarbene complex.

The cationic complex $MnCp(NO)(CO)_2^+$ has been reported[11] to react with methoxide ion to give the alkoxycarbonyl $MnCp(NO)(CO)(CO_2Me)$. The reaction of $MnCp(NO)(CO)_2^+$ with 2-bromoethanol and NaH gives a mixture of carbene products.

$$MnCp(NO)(CO)_2^+ + HOCH_2CH_2Br \xrightarrow[-H_2]{NaH} MnCp(NO)(CO)\text{—}C(=O)\text{—}O\text{—}CH_2\text{—}CH_2\text{—}\overset{+}{O} + MnCp(NO)\left(C(=O)\text{—}O\text{—}CH_2\text{—}CH_2\text{—}\overset{+}{O}\right)_2 \quad (6)$$

It appears that the dicarbene complex $MnCp(NO)(\overline{COCH_2CH_2O})_2^+$ is formed from the monocarbene by conversion of the last CO group into a carbene. Even using only 1 mol of $HOCH_2CH_2Br$/mol of $MnCp(NO)(CO)_2^+$ gave more dicarbene than monocarbene complex. This probably is due to the low solubility of the starting complex as compared to the monocarbene which could undergo the second reaction more readily. For this reason the monocarbene complex was not isolated in a pure form. The pure dicarbene was isolated from reactions in which $HOCH_2CH_2Br$ was used as the solvent.

That the CO in $MnCp(NO)(CO)(\overline{COCH_2CH_2O})^+$ is also converted into a carbene may be understood in terms

(9) Busetto, L.; Angelici, R. J. *Inorg. Chim. Acta* **1968**, *2*, 391.

(10) Busetto, L.; Palazzi, A.; Pietropaolo, D.; Dolcetti, G. *J. Organomet. Chem.* **1974**, *66*, 453.

(11) King, R. B.; Bisnette, M. B.; Fronzaglia, A. *J. Organomet. Chem.* **1966**, *5*, 341.

Table I. Infrared Frequencies Measured in CH_2Cl_2 Solvent

complex	ν(CO), cm^{-1}	k(CO)[a]	ν(NO), cm^{-1}	k(NO)[a]
$[FeCp(CO)_3]CF_3SO_3$	2120, 2065	17.60		
$[FeCp(CO)_2(COCH_2CH_2NH)]PF_6$	2060 s, 2015 s	16.76		
$FeCp(CO)_2(COCH_2CH_2N)$	2035 s, 1980 s	16.27		
$[FeCp(CO)_2(COCH_2CH_2N)PdCl(\mu\text{-}Cl)]_2$[b]	2043 s, 1996 s	16.47		
$[FeCp(CO)_2(COCH_2CH_2O)]PF_6$	2080 s, 2035 s	17.09		
$[MnCp(NO)(CO)_2]PF_6$	2125, 2075	17.80	1840	14.89
$[MnCp(NO)(CO)(COCH_2CH_2NH)]PF_6$	2047	16.92	1805	14.33
$[MnCp(NO)(CO)(COCH_2CH_2O)]^+$	2060	17.14	1820	14.57
$[MnCp(NO)(COCH_2CH_2O)_2]PF_6$			1790	14.09
$[MnCp(NO)(CO)(CNC_6H_{11})]PF_6$[c]	2060	17.14	1823	14.61
$[MnCp(NO)(CNC_6H_{11})(COCH_2CH_2O)]PF_6$[d]			1790	14.09
$[MnCp(NO)(P(OPh)_3)(CO)]PF_6$	2060	17.14	1827	14.68
$[MnCp(NO)(P(OPh)_3)(COCH_2CH_2NH)]PF_6$			1775	13.85
$[MnCp(NO)(P(OPh)_3)(COCH_2CH_2O)]PF_6$			1795	14.17
$Fe(CO)_5$	2000, 2023	17.0 ax 16.4 eq		
$Fe(CO)_4(COCH_2CH_2NH)$	2050 w, 2040 w, 1970 s, 1950 s, 1935 sh			

[a] mdyn/A. [b] In Nujol mull: ν(CO) at 2031 s, 1976 s cm^{-1}; ν(Pd-Cl) at 319 m, 336 s, 357 m cm^{-1}. In CsCl pellet: ν(CO) at 2038 s, 1984 s cm^{-1}; ν(Pd-Cl) at 330 s, 361 m cm^{-1}. [c] ν(CN) at 2210 cm^{-1}. [d] ν(CN) at 2190 cm^{-1}.

Table II. ^{1}H NMR Data[a]

complex	OCH_2	$NHCH_2$	NH	Cp
$[FeCp(CO)_2(COCH_2CH_2NH)]PF_6$[b]	4.60[c]	3.70[c]	9.5	5.30
$FeCp(CO)_2(COCH_2CH_2N)$[b]	3.75[c]	3.60[c]		5.00
$[FeCp(CO)_2(COCH_2CH_2N)PdCl(\mu\text{-}Cl)]_2$[b]	4.05[c]	3.59[c]		5.40
$[FeCp(CO)_2(COCH_2CH_2O)]PF_6$[b]	4.73			5.38
$[MnCp(NO)(CO)_2]PF_6$[d]				6.14
$[MnCp(NO)(CO)(COCH_2CH_2NH)]PF_6$[b]	4.62[c]	3.71[c]	9.1	5.44
$[MnCp(NO)(CO)(COCH_2CH_2O)]^+$[d]	5.13			5.95
$[MnCp(NO)(COCH_2CH_2O)_2]PF_6$[b]	4.65			5.35
	4.92[d]			5.60[d]
$[MnCp(NO)(CO)(CNC_6H_{11})]PF_6$[d]				5.88[e]
$[MnCp(NO)(CNC_6H_{11})(COCH_2CH_2O)]PF_6$[b]	4.71			5.35
$[MnCp(NO)(P(OPh)_3)(CO)]PF_6$[d]				5.67[e]
$[MnCp(NO)(P(OPh)_3)(COCH_2CH_2NH)]PF_6$[b]	4.40[c]	3.50[c]	8.7	4.90
$[MnCp(NO)(P(OPh)_3)(COCH_2CH_2O)]PF_6$[b]	4.55			5.00
$[Fe(CO)_4(COCH_2CH_2NH)]$[f]	3.19[c]	1.97[c]	5.96	

[a] Chemical shifts (δ) in parts per million downfield from tetramethylsilane. [b] In CD_3CN solvent. [c] See text for discussion of AA'BB' splitting of these protons. [d] In acetone-d_6 solvent. [e] Reference 8. [f] In C_6D_6 solvent.

of its relatively high ν(CO) force constant (17.14 mdyn/Å). In this system, the dioxocarbene ligand is not sufficiently electron donating to prevent alkoxide attack at the remaining CO group.

Reactions of $MnCp(NO)(L)(CO)^+$. The phosphite complex $MnCp(NO)(P(OPh)_3)(CO)^+$ reacts with $H_3NCH_2CH_2Br^+$ and NaH in CH_3CN at room temperature to give a 72% yield of the aminooxocarbene

Table III. ^{13}C NMR Data[a]

complex	C[b]	CO	OCH_2	$NHCH_2$	Cp
$[FeCp(CO)_2(\overline{COCH_2CH_2NH})]PF_6$[c]	221.5	212.1	74.2	47.0	88.7
	221.5[d]	212.5[d]	74.2[d]	47.0[d]	88.7[d]
$FeCp(CO)_2(\overline{COCH_2CH_2N})$[e]	183.7[f]	214.3	64.9	56.2	85.6
	[g]	[g]	66.5[c]	57.3[c]	88.0[c]
$[FeCp(CO)_2(COCH_2CH_2N)PdCl(\mu\text{-}Cl)]_2$[e]	193.6[f]	212.5	67.0	56.0	86.2
$[FeCp(CO)_2(\overline{COCH_2CH_2O})]PF_6$[c]	243.4	210.5	74.8		89.9
$[MnCp(NO)(CO)(\overline{COCH_2CH_2NH})]PF_6$[c]	224.2[h]	229.4	74.4	46.9	96.2
$[MnCp(NO)(\overline{COCH_2CH_2O})_2]PF_6$[c]	263.0		73.5		96.9
$[MnCp(NO)(CNC_6H_{11})(\overline{COCH_2CH_2O})]PF_6$[c]	[g]		73.9		96.1
$[MnCp(NO)(P(OPh)_3)(\overline{COCH_2CH_2NH})]PF_6$[c]	239.7[i]		73.6	46.6	94.9
$[MnCp(NO)(P(OPh)_3)(\overline{COCH_2CH_2O})]PF_6$[c]	263.6[j]		73.9		95.7
$Fe(CO)_4(\overline{COCH_2CH_2NH})$[e]	233.1	216.0	71.3	44.9	
$Fe(CO)_4(\overline{CNRCH_2CH_2NR})$[k]	213.2	217.4			
$Fe(CO)_4(\overline{COCR_2CR_2O})$[k]	251.2	215.3			

[a] Chemical shifts in parts per million downfield from Me_4Si. [b] Carbene C atom. [c] In CD_3CN solvent. [d] In 3 M HCl/D_2O. [e] In C_6D_6 solvent. [f] Uncertain assignment due to low signal to noise. [g] Not observed. [h] Assignment based on line broadening due to ^{14}N quadrupolar coupling. [i] d, $J(PMnC) = 44.4$ Hz. [j] d, $J(PMnC) = 40.0$ Hz. [k] Reference 16.

$MnCp(NO)(P(OPh)_3)(\overline{COCH_2CH_2NH})^+$. The reaction of $MnCp(NO)(P(OPh)_3)(CO)^+$ with $HOCH_2CH_2Br$ and NaH gives the analogous dioxocarbene $MnCp(NO)(P(OPh)_3)(\overline{COCH_2CH_2O})^+$ in 57% yield.

Since it is known[12] that certain isocyanide ligands undergo nucleophilic attack by alcohols and amines, a complex with both CO and CNR ligands was studied. The reaction of $MnCp(NO)(C{\equiv}N{-}C_6H_{11})(CO)^+$ with $HOCH_2CH_2Br$ and NaH leads exclusively to the dioxocarbene product $MnCp(NO)(CNC_6H_{11})(\overline{COCH_2CH_2O})^+$ in 90% yield.

Reaction of $Fe(CO)_5$. Pentacarbonyliron reacts with primary and secondary amines according to eq 7.[13,14] The

$$Fe(CO)_5 + 2H_2NR \rightleftharpoons Fe(CO)_4{-}C(=O)(NHR)^- + \overset{+}{N}H_3R \quad (7)$$

equilibrium lies to the right in polar solvents and to the left in nonpolar solvents. That carbamoyl formation occurs suggests that $Fe(CO)_5$ would yield an aminooxocarbene. Indeed, such a reaction does occur at 25 °C when Et_3N is used as the base and the solvent.

$$Fe(CO)_5 + \overset{+}{H_3}NCH_2CH_2Br \xrightarrow{Et_3N} Fe(CO)_4{-}C(O)(N)H + Br^- \quad (8)$$

The very air-sensitive carbene product does not form when K_2CO_3 is the base and the solvent is either CH_2Cl_2 or tetrahydrofuran (THF).

Acyclic aminooxocarbene complexes, e.g., $Fe(CO)_4[C(OEt)(NMe_2)]$,[15,16] have been prepared previously and have $\nu(CO)$ absorptions very similar to those (Table I) of the cyclic carbene complex reported here. As for the acyclic carbenes, the number and intensity of the $\nu(CO)$ bands do not allow one to assign unambiguously the carbene ligand to an axial or equatorial position in the $Fe(CO)_4(\overline{COCH_2CH_2NH})$ molecule. The equivalence of all four CO groups in the ^{13}C NMR spectrum (Table III) indicates that it is fluxional at room temperature.

Although cyclic dioxocarbene complexes $Fe(CO)_4(\overline{COCR_2CR_2O})$ have been reported,[17] there was no evidence for the formation of $Fe(CO)_4(\overline{COCH_2CH_2O})$ in reactions of $Fe(CO)_5$ with $HOCH_2CH_2Br$ and the bases K_2CO_3 or NaH.

Trends in Reactivity. Those metal carbonyl complexes which have been converted to aminooxocarbenes and/or dioxocarbenes as in eq 2 and 3 are as follows (their $\nu(CO)$ force constants are given in parentheses, see Table I): $MnCp(NO)(CO)_2^+$ (17.80 mdyn/Å), $FeCp(CO)_3^+$ (17.60), $MnCp(NO)(CO)(CNC_6H_{11})^+$ (17.14), $MnCp(NO)(CO)(P(OPh)_3)^+$ (17.14), $MnCp(NO)(CO)(\overline{COCH_2CH_2O})^+$ (17.14), and $Fe(CO)_5$ (17.0 axial, 16.4 equatorial). The $M(CO)_6$ complexes (M = Cr (16.49 mdyn/Å), Mo (16.52), or W (16.41)) did not yield carbenes; they are also known not to form carbamoyl complexes with amines. Likewise, $MnCp(CO)_3$ (15.6 mdyn/Å) did not react, and it is known[18] not to form carbamoyl complexes.

These results suggest that the tendency of a CO group to react according to eq 2 and 3 follows its ability to react with amines to give carbamoyl complexes. It appears that CO ligands with $\nu(CO)$ force constants equal to or greater than 17.0 mdyn/Å are likely to be converted into carbenes; those below 17.0 mdyn/Å are unlikely to react in this manner. That no reactions are observed for force constants below 17.0 mdyn/Å suggests that $H_2NCH_2CH_2Br$ is somewhat less reactive than primary aliphatic amines.

(12) Brown, F. J. *Prog. Inorg. Chem.* **1980**, *27*, 1 and references therein.
(13) Edgell, W. F.; Yang, M. T.; Bulkin, B. J.; Bayer, R.; Koizumi, N. *J. Am. Chem. Soc.* **1965**, *87*, 3080.
(14) Edgell, W. F.; Bulkin, B. J. *J. Am. Chem. Soc.* **1966**, *88*, 4839.
(15) Fischer, E. O.; Beck, H.-J.; Kreiter, C. G.; Lynch, J.; Müller, J.; Winkler, E. *Chem. Ber.* **1972**, *105*, 162.
(16) Schmetzer, J.; Daub, J.; Fischer, P. *Angew. Chem., Int. Ed. Engl.* **1975**, *14*, 487. Cardin, D. J.; Cetinkaya, B.; Cetinkaya, E.; Lappert, M. F.; Randall, E. W.; Rosenberg, E. *J. Chem. Soc., Dalton Trans.* **1973**, 1982.
(17) Daub, J.; Kappler, J. *J. Organomet. Chem.* **1974**, *80*, C4. Daub, J.; Erhardt, U.; Kappler, J.; Trautz, V. *Ibid.* **1974**, *69*, 423.
(18) Angelici, R. J.; Blacik, L. J. *Inorg. Chem.* **1972**, *11*, 1754.

This is understandable in view of the lower basicity (and probably nucleophilicity) of $H_2NCH_2CH_2Br$ ($pK_a \approx 8.49$)[19] as compared to that ($pK_a \approx 10.5$) for primary aliphatic amines. While other factors such as steric considerations and CO lability may affect carbene formation in specific complexes, the force constant appears to be a useful guideline for estimating reactivity.

Even though the general reactivity of $H_2NCH_2CH_2Br$ is consistent with its reaction according to eq 2, it should be noted that $H_2NCH_2CH_2Br$ cyclizes[20] readily to aziridine under conditions similar to those used in the reactions. Thus, some aziridine is likely to be present in the reaction solutions, and aziridine could be involved in the carbene formation. This possibility is being investigated.

In the reactions reported above, the 5-membered carbene ligand is formed. Attempts to generate 6-membered carbene ligands from $FeCp(CO)_3^+$ and $MnCp(NO)(CO)_2^+$ using $NH_3CH_2CH_2CH_2Br^+$ or $HOCH_2CH_2CH_2Br$ under the same conditions used to form the 5-membered carbenes gave no carbene formation. It appears that ring closure to the 6-membered carbene is less favorable.

Certain coordinated isocyanide ligands have been observed to undergo nucleophilic attack by amines and alcohols.[12] Some evidence[21] indicates that these reactions are slower than those occurring with CO groups, which may account for the conversion of only the CO group of $MnCp(NO)(CO)(CNC_6H_{11})^+$ to a carbene. However, we also did not observe the formation of carbene complexes in reactions of $H_3NCH_2CH_2Br^+$ or $HOCH_2CH_2Br$ with $MnCp(NO)(CNC_6H_{11})_2^+$ or *cis*-$PtCl_2(P(OPh)_3)(CNC_6H_{11})$. It is perhaps worth exploring these reactions further by using less bulky isocyanide ligands.

Spectroscopic Properties of the Carbene Complexes. Infrared Spectra. With ν(CO) force constants as a measure of the donor–acceptor properties of L in the $FeCp(CO)_2(L)^+$ complexes, it is evident (Table I) that the π-acceptor/σ-donor ratio of L decreases in the order (k-(CO) in parentheses): CO (17.60 mdyn/Å) > $\overline{COCH_2CH_2O}$ (17.09) > $\overline{COCH_2CH_2NH}$ (16.76). The same trend is found in the ν(CO) and ν(NO) force constants of the $MnCp(NO)(CO)(L)^+$ series of complexes. The stronger π-bonding ability of the nitrogen or its lower electronegativity as compared to those of oxygen accounts for the aminooxocarbene being a better donor ligand than the dioxocarbene.[22]

The π-acceptor/σ-donor ratio of both carbene ligands is clearly lower than that of CO. By comparing ν(CO) and ν(NO) force constants of the $MnCp(NO)(CO)L^+$ complexes, one can observe that the dioxocarbene ligand, $-\overline{COCH_2CH_2O}$ has electronic properties similar to those of $P(OPh)_3$ and $C{\equiv}N{-}C_6H_{11}$. Force constants (ν(CO)) of the $FeCp(CO)_2L^+$ complexes indicate that the aminooxocarbene ligand, $-\overline{COCH_2CH_2NH}$, has electronic properties similar to those of the dithiocarbene, $-C(SMe)_2$, and to PPh_3.[22]

^{1}H NMR Spectra. The ^{1}H NMR spectra (Table II) of all of the dioxocarbene ($-\overline{COCH_2CH_2O}$) complexes show a singlet for the carbene protons in the range δ 4.5–5.2. In the complexes $MnCp(NO)(L)(\overline{COCH_2CH_2O})^+$, the lowest field carbene resonance occurs for L = CO (δ 5.13), whereas those complexes with more strongly electron donating ligands (CNC_6H_{11}, $P(OPh)_3$, and $-\overline{COCH_2CH_2O}$) have resonances at higher field in the region of δ 4.55–4.71.

^{1}H NMR spectra of the aminooxocarbene complexes are somewhat more complicated. Although they appear to be close to that expected for an A_2B_2 spin system, they really represent AA′BB′ systems.

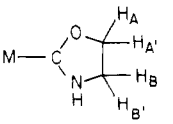

The AA′BB′ systems have been analyzed in detail in related organic ring systems such as:[23]

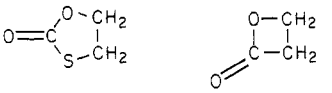

On the basis of assignments of protons in 2-oxazolines and related systems,[24,25] the methylene protons adjacent to the oxygen are assigned to the lower field resonances which are approximately 1-ppm downfield from those of the methylene protons adjacent to the nitrogen.

As for the dioxocarbene complexes, the methylene resonances of $MnCp(NO)(CO)(\overline{COCH_2CH_2NH})^+$ (δ 4.62, 3.71) are downfield from those in the electron-rich $MnCp(NO)(P(OPh)_3)(\overline{COCH_2CH_2NH})^+$ (δ 4.40, 3.50). The most upfield methylene resonances occur in the neutral complex $Fe(CO)_4(\overline{COCH_2CH_2NH})$ (δ 3.19, 1.97).

^{13}C NMR Spectra. The carbene carbon chemical shifts of the $-\overline{COCH_2CH_2NH}$ ligands occur in the range of 220–240 ppm, while those of the $-\overline{COCH_2CH_2O}$ occur at 240–263 ppm. In the acyclic carbene complexes $FeCp(CO)_2[C(XR)(YR)]^+$,[26] where X and Y = O, NH, S and/or Se, the carbene carbon chemical shifts depend upon the atoms bound to that carbon: $-C(NHR)_2$, 190–220 ppm; $-C(NHR)(OR)$, 220–230; $-C(OR)_2$, ~250; $-C(OR)(SR)$, $-C(SR)_2$, 280–310; $-C(SR)(SeR)$, ~320. The cyclic carbene complexes reported here also follow this trend. For example, in the $FeCp(CO)_2(carbene)^+$ and $Fe(CO)_4(carbene)$ complexes, the carbene carbon resonance of the $-\overline{COCH_2CH_2NH}$ compound is at approximately 20 ppm higher field than that of the analogous $-\overline{COCH_2CH_2O}$ compound. For the diaminocarbene $Fe(CO)_4(\overline{CNRCH_2CH_2NR})$[16] the carbene resonance (Table III) is 20 ppm still higher. The upfield shift caused by the nitrogen has been attributed to more π bonding in the C(carbene)–N bond than in the C(carbene)–O bond.[27] However, the difference between –OR and –NHR substituent effects in aliphatic hydrocarbons is also about 20 ppm.[25]

(19) Perrin, D. D. "Dissociation Constants of Organic Bases in Aqueous Solution"; Butterworths: London, 1965. Girault, G.; Rumpf, R. *C. R. Hebd. Seances Acad. Sci.* **1956**, *243*, 663.
(20) Dermer, O. C.; Ham, G. E. "Ethylenimine and Other Aziridines"; Academic Press: New York, 1969; p 11.
(21) Angelici, R. J.; Christian, P. A.; Dombek, B. D.; Pfeffer, G. A. *J. Organomet. Chem.* **1974**, *67*, 287.
(22) McCormick, F. B.; Angelici, R. J. *Inorg. Chem.* **1979**, *18*, 1231. McCormick, F. B.; Angelici, R. J. *J. Organomet. Chem.* **1981**, *205*, 79.
(23) Emsley, J. W.; Feeney, J.; Sutcliffe, L. H. "High Resolution Magnetic Resonance Spectroscopy"; Pergamon Press: New York, 1965; Vol. 1, p 347.
(24) Lambert, R. F.; Kristofferson, C. E. *J. Org. Chem.* **1965**, *30*, 3938.
(25) Pretsch, E.; Clerc, Th.; Seible, J.; Simon, W. In "Strukturaufklärung organischer Verbindungen"; Springer-Verlag: Berlin 1976.
(26) McCormick, F. B.; Angelici, R. J. *Inorg. Chem.* **1981**, *20*, 1111; **1981**, *20*, 1118.
(27) Cardin, D. J.; Cetinkaya, B.; Lappert, M. F. *Chem. Rev.* **1972**, *72*, 572.

Replacement of the CO in $MnCp(NO)(CO)(\overline{COCH_2CH_2NH})^+$ by $P(OPh)_3$ shifts the carbene resonance downfield from 224.2 to 239.7 ppm; a similar trend was observed for the $FeCp(CO)(L)[C(SMe)_2]^+$ carbene carbon.[22] The carbene resonance is essentially the same (~263 ppm) for both $MnCp(NO)(P(OPh)_3)(\overline{COCH_2CH_2O})^+$ and $MnCp(NO)(\overline{COCH_2CH_2O})_2^+$, which suggests that $P(OPh)_3$ and $-\overline{COCH_2CH_2O}$ have similar electronic properties, a conclusion that was also inferred from ν(CO) frequencies of the $MnCp(NO)(CO)(L)^+$ complexes.

Generation and Reactions of $FeCp(CO)_2(\overline{COCH_2CH_2N})$. This neutral imine complex can be produced by deprotonation of the aminooxocarbene in CH_2Cl_2 with K_2CO_3 or NaH.

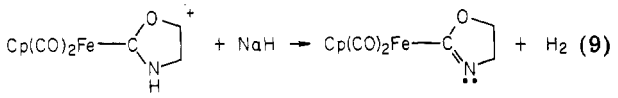

(9)

It is also generated as a small amount of side product in the synthesis of the carbene (eq 4). Its instability, which prevented its isolation as a pure compound, contrasts with the high stability of its precursor carbene. As expected for a deprotonation, the ν(CO) frequencies (2060, 2015 cm^{-1}) of the carbene decrease to 2035 and 1980 cm^{-1} in $FeCp(CO)_2(\overline{COCH_2CH_2N})$. In ^1H NMR studies, deprotonation causes a shift of the OCH_2 and NCH_2 protons from δ 4.60 and 3.70, respectively, in the carbene to δ 3.75 and 3.60 in the imine. While an upfield shift of these protons is expected, the greater shift of the OCH_2 protons is surprising inasmuch as the deprotonation occurred at the nitrogen. In ^{13}C NMR studies, the OCH_2 carbon of the carbene shifts upfield upon deprotonation from 74.2 to 64.9 ppm, while the NCH_2 carbon shifts downfield from 47.0 to 56.2 ppm.

The imine complex $FeCp(CO)_2(\overline{COCH_2CH_2N})$ can be dissolved in 3 M aqueous HCl, where it is protonated to give the carbene, which is stable in the solution for at least 3 weeks. The HCl does not cleave the Fe–C bond. In pure water the imine decomposes rapidly. The basicity of the imine nitrogen is demonstrated by its reaction with $NH_4^+PF_6^-$ in CH_2Cl_2 at −70 °C to give the carbene.

The coordinating ability of the imine nitrogen is seen in its reaction with $PdCl_2(NCMe)_2$.

$$2FeCp(CO)_2(\overline{COCH_2CH_2N}) + 2PdCl_2(NCMe)_2 \xrightarrow{25\ °C} sym,trans\text{-}[FeCp(CO)_2(\overline{COCH_2CH_2N})Pd(\mu\text{-}Cl)Cl]_2 \quad (10)$$

The product is formulated as a di-μ-Cl bridged sym,trans dimer based on elemental analyses and the three ν(Pd–Cl) absorptions at 319, 336, and 357 cm^{-1} in the infrared region.[28] The ν(CO) frequencies of the compound (Table I) occur between those of $FeCp(CO)_2(\overline{COCH_2CH_2NH})^+$ and $FeCp(CO)_2(\overline{COCH_2CH_2N})$, which indicates that the Pd(II) is a weaker Lewis acid toward the imine nitrogen than H^+. In fact, the dimer reacts within a few minutes with gaseous HCl bubbled into a CH_2Cl_2 solution of the dimer to protonate the imine and to give the carbene $FeCp(CO)_2(\overline{COCH_2CH_2NH})^+$ and $PdCl_4^{2-}$.

Acknowledgment. Partial funding for the JEOL FX-90Q NMR spectrometer was provided by an instrumentation grant from the National Science Foundation.

Registry No. $[FeCp(CO)_2(\overline{COCH_2CH_2NH})]PF_6$, 69532-52-1; $FeCp(CO)_2(\overline{COCH_2CH_2N})$, 79664-06-5; $[FeCp(CO)_2(\overline{COCH_2CH_2N})PdCl(\mu\text{-}Cl)]_2$, 79664-07-6; $[FeCp(CO)_2(\overline{COCH_2CH_2O})]PF_6$, 79664-09-8; $[MnCp(NO)(CO)(\overline{COCH_2CH_2NH})]PF_6$, 79664-11-2; $[MnCp(NO)(CO)(\overline{COCH_2CH_2O})]^+$, 79664-12-3; $[MnCp(NO)(\overline{COCH_2CH_2O})_2]PF_6$, 79664-14-5; $[MnCp(NO)(CO)(CNC_6H_{11})]PF_6$, 32982-02-8; $[MnCp(NO)(CNC_6H_{11})(\overline{COCH_2CH_2O})]PF_6$, 79664-16-7; $[MnCp(NO)(P(OPh)^3)(CO)]PF_6$, 32875-46-0; $[MnCp(NO)(P(OPh)_3)(\overline{COCH_2CH_2NH})]PF_6$, 79680-93-6; $[MnCp(NO)(P(OPh)_3)(\overline{COCH_2CH_2O})]PF_6$, 79664-18-9; $Fe(CO)_4(\overline{COCH_2CH_2NH})$, 79664-19-0; $[FeCp(CO)_3]CF_3SO_3$, 76136-47-5; $[MnCp(NO)(CO)_2]PF_6$, 31921-90-1.

(28) Adams, D. M.; Chandler, P. J. *J. Chem. Soc. A* **1969**, 588. Goodfellow, R. J.; Goggin, P. L.; Venanzi, L. M. *Ibid.* **1967**, 1897.

Tetraorganotellurium(IV) Derivatives. Crystal and Molecular Structure of Tetraphenyltellurium–Benzene (1/8), $(C_6H_5)_4Te\cdot{}^1/_8C_6H_6$

Cheryl S. Smith, Jung-Si Lee, Donald D. Titus,*[1a] and Ronald F. Ziolo*[1b]

Department of Chemistry, Temple University, Philadelphia, Pennsylvania 19122, and Xerox Corporation, Webster Research Center, Webster, New York 14580

Received July 28, 1981

The crystal and molecular structure of tetraphenyltellurium–benzene (1/8) has been determined by a single-crystal X-ray diffraction study. The results represent the first structural characterization of a tetraorgano derivative of a group 6 element. The compound crystallizes in the space group $P\bar{1}$ with eight molecules per unit cell. Lattice parameters (23 ± 1 °C) are as follows: a = 14.547 (5) Å, b = 21.687 (7) Å, c = 13.140 (6) Å, α = 101.93 (3)°, β = 93.39 (3)°, γ = 89.46 (3)°, and V = 4052 (2) Å^3. The structure was determined by Patterson and Fourier methods from automatic diffractometer data using filtered Mo Kα radiation. Refinement by the least-squares technique led to a conventional R factor (on F) of 0.074 for 7893 reflections having $F_o^2 < 3\sigma(F_o^2)$. Tetraphenyltellurium has a distorted, ψ-trigonal-bipyramidal geometry with the axial phenyl groups bending toward the equatorial groups. Mean angles are as follows: C_{eq}–Te–C_{eq} = 108.6°, C_{ax}–Te–C_{ax} = 168.7 (7)°, and C_{eq}–Te–C_{ax} = 86.7 (3)°. The equatorial Te–C distances are normal with a mean of 2.13 (0) Å. The axial Te–C distances are elongated and range from 2.27 (1) to 2.31 (1) Å. These distances are the longest primary Te–C bond distances known. It is suggested that the relative thermal stability of the R_nTeX_{4-n} (n = 2, 4) compounds relates, in part, to the stability of the long, axial $M^{\delta+}\cdots L^{\delta-}$ bond. The stereochemistry about Te in the four independent molecules is identical. Each molecule, however, is conformationally unique due to phenyl group orientations. Short intermolecular contacts are absent, giving tellurium a genuine fourfold configuration. The closest Te–Te approach is 4.803 (1) Å.

Introduction

Tetraphenyltellurium is a relatively stable solid that decomposes on heating to diphenyl telluride and biphenyl.[2,3] It is one of the few stable tetraorganochalcogen molecules known. The molecule shows the reactivity of an organometallic compound as seen in its reactions with CH_2Cl_2 and $CHCl_3$ to form $(C_6H_5)_3TeCl$.[4] Although no structural work on the tetraorganochalcogens has been reported, tetraphenyltellurium, as an AB_4E molecule, is expected to have a ψ-trigonal-bipyramidal geometry similar to that, for example, of $(CH_3)_2TeCl_2$[5] or of gas-phase $TeCl_4$.[6] In the solid state, however, the presence of intermolecular interactions gives tellurium(IV) a coordination number higher than that expected from the compound's stoichiometry.[7-9] For example, solid tellurium tetrachloride possesses six-coordinate tellurium and is a tetramer.[10] Similarly, $(CH_3)_2TeCl_2$ is more accurately described as having a distorted octahedral geometry with intermolecular bonding.[11] In general, intermolecular bonding leads to five- and six-coordinate distorted octahedral geometries in the R_nTeX_{4-n} (n = 0–3) compounds.[7,8,12] When n = 4 and R is C_6H_5, the situation is not as predictable. Although the indium and gallium phenyls exhibit short intermolecular contacts,[13] none is observed in trimethyltelluronium tetraphenylborate due to steric or electronic constraints.[14] To date, structural examples of a genuine four-coordinate solid-state tellurium(IV) species appear to be unknown.[15]

As part of a larger effort to study the stereochemistry and bonding in hypervalent tellurium compounds, we have determined the structure of tetraphenyltellurium by X-ray diffraction techniques.[17] This example serves as the first structural characterization of a tetraorgano derivative of a group 6 element. Structural examples of groups 3, 4, and 5 heavier element phenyls are known.[18]

Experimental Section

Tetraphenyltellurium was prepared from diphenyltellurium dichloride and phenyllithium by the method of Wittig and Fritz.[2] The product was crystallized at 10 °C from a 3:1 mixture of anhydrous diethyl ether and benzene. The crystal density was not measured.

A crystal coated with dry Nujol was mounted randomly in a glass capillary. Unit cell parameters were obtained from a least-squares analysis of 25 reflections. Tetraphenyltellurium–benzene (1/8) crystallizes in the triclinic system: a = 14.547 (5) Å, b = 21.687 (7) Å, c = 13.140 (6) Å, α = 101.93 (3)°, β = 92.39 (3)°, γ = 89.46 (3)°, V = 4052 (2) Å^3, d_{calcd} = 1.46 g/cm^3 for Z = 8. A Delaunay reduction of the cell revealed no hidden symmetry.

Intensity data were collected at Molecular Structure Corp.[19] on an Enraf-Nonius CAD4 automatic diffractometer using gra-

(1) (a) Temple University. (b) Xerox Corp.
(2) Wittig, G.; Fritz, H. *Justus Liebigs Ann. Chem.* **1952**, *577*, 39.
(3) Barton, D. H. R.; Glover, S. A.; Ley, S. V. *J. Chem. Soc. Chem. Commun.* **1977**, 266.
(4) Irgolic, K. J. "The Organic Chemistry of Tellurium"; Gordon and Breach: New York, 1974.
(5) Christofferson, G. D.; Sparks, R. A.; McCullough, J. D. *Acta Crystallogr.* **1958**, *11*, 782.
(6) Stevenson, D. P.; Schomaker, V. *J. Am. Chem. Soc.* **1940**, *62*, 1268. Beattie, I. R.; Bizri, O.; Blayden, H. E.; Brumbach, S. B.; Bukovszky, A.; Gilson, T. R.; Phillips, B. A. *J. Chem. Soc., Dalton Trans.* **1974**, 1747.
(7) Ziolo, R. F.; Titus, D. D. In "Proceedings of the 3rd International Symposium on Organic Selenium and Tellurium Chemistry"; Cagniant, D., Kirsch, G., Eds.; Université de Metz: Metz, France, 1979; pp 319–347.
(8) Alcock, N. W. *Adv. Inorg. Chem. Radiochem.* **1972**, *15*, 1.
(9) Zemann, J. *Monatsh. Chem.* **1971**, *102*, 1209.
(10) Buss, B.; Krebs, B. *Inorg. Chem.* **1971**, *10*, 2795.
(11) Ziolo, R. F.; Troup, J. M. *J. Am. Chem. Soc.*, in press.
(12) Bird, P. H.; Kumar, V.; Pant, B. C. *Inorg. Chem.* **1980**, *19*, 2487.
(13) Malone, J. F.; McDonald, W. S. *J. Chem. Soc. A* **1970**, 3362.
(14) Ziolo, R. F.; Troup, J. M. *Inorg. Chem.* **1979**, *18*, 2271.
(15) The possibility that $(C_6H_5)_2TeBr_2$[16] is an exception to this statement has not been ruled out. The Te–Br contact is at or near the van der Waals distance and the bromine is in a stereochemically significant position. A situation similar to that in $(CH_3)_2TeCl_2$[11] is expected.
(16) Christofferson, G. D.; McCullough, J. D. *Acta Crystallogr.* **1958**, *11*, 249.
(17) Presented in part at the Third International Symposium on Organic Selenium and Tellurium Compounds, Metz, France, July 9–12 1979.
(18) Wyckoff, R. W. G. "Crystal Structures", 2nd ed.; Interscience: New York, 1971; Vol. 6, Part 2.
(19) Molecular Structure Corp., 3304 Longmire Dr., College Station, TX 77840.

0276-7333/82/2301-0350$01.25/0

phite-monochromatized Mo Kα radiation. The prism used measured 0.3 × 0.3 × 0.35 mm. The width of half-height from ω scans was 0.2°.

A total of 11 940 independent reflections were collected by the θ–2θ scan technique in the range $0 < 2\theta$ (Mo Kα) < 47°. A takeoff angle of 5.6° was used with a counter aperture width of 2.0 mm. The incident-beam collimeter diameter was 2.0 mm and the crystal to detector distance 21 cm. A variable scan rate of 8–20°/min (in 2θ) was used with stationary-crystal stationary-counter background counts where scan time per background time equaled 2.0. The scan range was from 2θ (Mo $K\alpha_1$) − 0.7° to 2θ (Mo $K\alpha_2$) + 0.7°.

Intensities and standard deviations of intensities were calculated as described previously.[20] The factor, p, introduced to down-weight intense reflections was set to 0.05. Lorentz and polarization corrections were applied to the data. Extinction and absorption corrections were unnecessary. Psi scans of the relatively uniform prism showed less than 5% variation in transmission . The calculated linear absorption coefficient (Mo Kα), μ, is 15.2 cm^{-1}. Three representative reflections which were measured periodically showed a linear decrease in intensity with X-ray exposure. A total average decrease of 39% in the standard reflections was corrected for by a linear factor.

A data set consisting of the 4519 reflections with $2\theta < 40°$ (Mo Kα) was employed for solution and initial refinement of the structure. A sharpened Patterson map failed to yield unambiguous positions for the four independent tellurium atoms in the asymmetric unit. A structure factor calculation was carried out by assuming noncentrosymmetric $P\bar{1}$ symmetry with a single tellurium atom placed at the origin. A Fourier map phased on this basis was used in conjunction with the Patterson map to fix the relative positions of the Te atoms. Once these were established, the coordinates were transformed to the centrosymmetric space group $P\bar{1}$; all subsequent calculations employed this symmetry. A structure factor calculation based on the four tellurium atoms gave an $R\ (=\sum||F_o| - |F_c||/\sum|F_o|)$ value 0.459. Two cycles of least squares refinement and Fourier syntheses located all of the carbon atoms; with isotropic thermal parameters for all atoms, the R value stood at 0.061. At this point the data set was expanded to 7893 reflections, including all independent reflections having $F_o > 3\sigma(F_o)$. Because of the large number of parameters to be refined (413), each complete cycle of least squares was broken down into several smaller blocks. In view of the crystal decomposition during data collection, it seemed likely that the original values of $\sigma(F_o)$ were underestimated. A careful study of the goodness of fit, $[\sum w(F_o - F_c)^2/(\text{no. of reflections} - \text{no. of variables})]^{1/2}$, as the refinement progressed indicated that the standard deviations were too small by a factor of about 9.5. In subsequent calculations all values of $\sigma(F_o)$ were increased by this factor. Because of the prohibitive amount of computing time that would be required and because of the substantial decomposition of the crystal during data collection, anisotropic refinement of the model was not attempted. The hydrogen atoms were included as fixed contributions to the structure factors, assuming the normal ring geometry with C–H distances set at 0.95 Å. Refinement of the model was terminated with R at 0.074 and $R_w\ (=\sum w(|F_o| - |F_c|)^2/\sum w|F_o|^2)$ at 0.065. A few of the parameters shifted by more than their standard deviations in the last cycles. Most of the large shifts were associated with carbon atoms meta or para to the tellurium position, reflecting the weakness of the isotropic model for these atoms. An additional complete cycle of refinement was carried out in order to determine if better convergence could be achieved. Some shifts greater than σ (parameter) were again noted, while the values for R and R_w remained unchanged; there was no improvement in the derived bond distances and angles. A final difference Fourier map showed several large peaks (ca. 1.1 e/$Å^3$) within 0.4 Å of the tellurium atoms. No other peaks exhibited electron densities higher than 15% of the observed carbon atom densities.

Scattering factors were taken from the compilation of Hanson et al.;[21] those for Te were corrected for the real and imaginary components of anomalous dispersion by using the values of Cromer.[22] The programs used are listed in an earlier publication.[20] In the least-squares refinement the function minimized was $\sum w(|F_o| - |F_c|)^2$ where $w = \sigma^{-2}(F)$.

The final positional and thermal parameters for the atoms are given in Table I. The hydrogen atom parameters and the observed and calculated structure factors are available as supplementary material.

Results and Discussion

Tetraphenyltellurium–benzene (1/8) crystallizes in the triclinic system with eight molecules in the unit cell. The unique conformation of each of the four independent molecules is illustrated in Figure 1, and distances and angles about Te are given in Table II. With the possible exception of two C–Te2–C angles, the stereochemistry about tellurium in the four molecules is identical within experimental error.

In the solid state, tetraphenyltellurium has a distorted, pseudo-trigonal-bipyramidal (ψ-tbp) geometry, similar to that observed in $(CH_3)_2TeCl_2$.[5] The third equatorial site is presumably occupied by the Te(IV) lone pair as has been found in the X–X electron deformation density study of dimethyltellurium dichloride.[11] The mean value[23] of the equatorial C–Te–C angles in $(C_6H_5)_4Te$ is 108.6 (1.3)° and is the largest known for the R_2TeX_2 molecules.[24] In $(C_6H_5)_2TeBr_2$[16] and $(p\text{-}ClC_6H_4)_2TeI_2$,[25] for example, the C–Te–C angles are 96.3 (1.2) and 101.1 (1.0)°, respectively. Although no correlation is implied, we note that the large angle is in keeping with the trend of increasing size of the axial ligands, bromine, iodine, and phenyl. The axial phenyls bend toward the equatorial groups with the C–Te–C angles ranging from 167.9 (4) to 170.8 (4)°. Thus, the C_{eq}–Te–C_{ax} angles are all acute with an observed range of 84.2 (4) to 88.5 (4)°. The direction of bend of the axial angles is consistent with the predictions of the VSEPR model[26] and is like that observed in $(CH_3)_2TeCl_2$[5] but opposite to that observed in Br_2.[16] The deviation of the axial angles from the idealized value of 180° is matched only by that in $[CH_3CH(Cl)CH_2]_2TeCl_2$.[27] Unfortunately, it is not yet possible to distinguish between the steric and electronic factors that affect the equilibrium structure of the Te(IV) AB_4E molecules. Moreover, it is possible that the lone pair participates in the bonding as has been suggested in other instances.[10,26]

The Te–C distances in the molecule fall into two groups. The equatorial Te–C distances have a mean value of 2.13 (0) Å[23] and are identical with the sum of the covalent radii[28a] and to the Te–C distances found in the $(C_6H_5)_3Te^+$ ion.[14,20,29,30] In keeping with the salient feature of axial elongation in the trigonal-bipyramidal AB_4E molecules, the Te–C axial distances range from 2.27 (1) to 2.31 (1) Å and represent the longest primary Te–C bond distances known.[31] Their bond order[28b] of approximately 0.5 is

(20) Lee, J.-S.; Titus, D. D.; Ziolo, R. F. *Inorg. Chem.* **1977**, *16*, 2487.
(21) Hanson, H. P.; Herman, F.; Lea, J. D.; Skillman, S. *Acta Crystallogr.* **1964**, *17*, 1040.
(22) Cromer, D. T. *Acta Crystallogr.* **1965**, *18*, 17.
(23) The estimated variance of the mean is given in parentheses and is calculated as $[\sum(x\text{-}\bar{x})^2/(n(n-1))]^{1/2}$. "International Tables for X-Ray Crystallography", The Kynoch Press: Birmingham, England, 1972; Vol. II, p 89.
(24) For a comparison of the axial and equatorial angles about tellurium in the R_2TeX_2 molecules, see: Mancinelli, C. S.; Titus, D. D., Ziolo, R. F. *J. Organomet. Chem.* **1977**, *140*, 113.
(25) Chao, G. Y.; McCullough, J. D. *Acta Crystallogr.* **1962**, *15*, 887.
(26) Gillespie, R. J. *Can J. Chem.* **1961**, *39*, 318. Gillespie, R. J. *J. Chem. Educ.* **1970**, *47*, 18.
(27) Kobelt, D.; Paulus, E. F. *J. Organomet. Chem.* **1971**, *27*, C63.
(28) (a) Pauling, L. "The Nature of the Chemical Bond", 3rd ed.; Cornell University Press: Ithaca, 1960; p 224. (b) *Ibid.* p 255. (c) *Ibid.* p 260.
(29) Ziolo, R. F.; Extine, M. *Inorg. Chem.* **1980**, *19*, 2964.
(30) Titus, D. D.; Lee, J.-S.; Ziolo, R. F. *J. Organomet. Chem.* **1976**, *120*, 381.

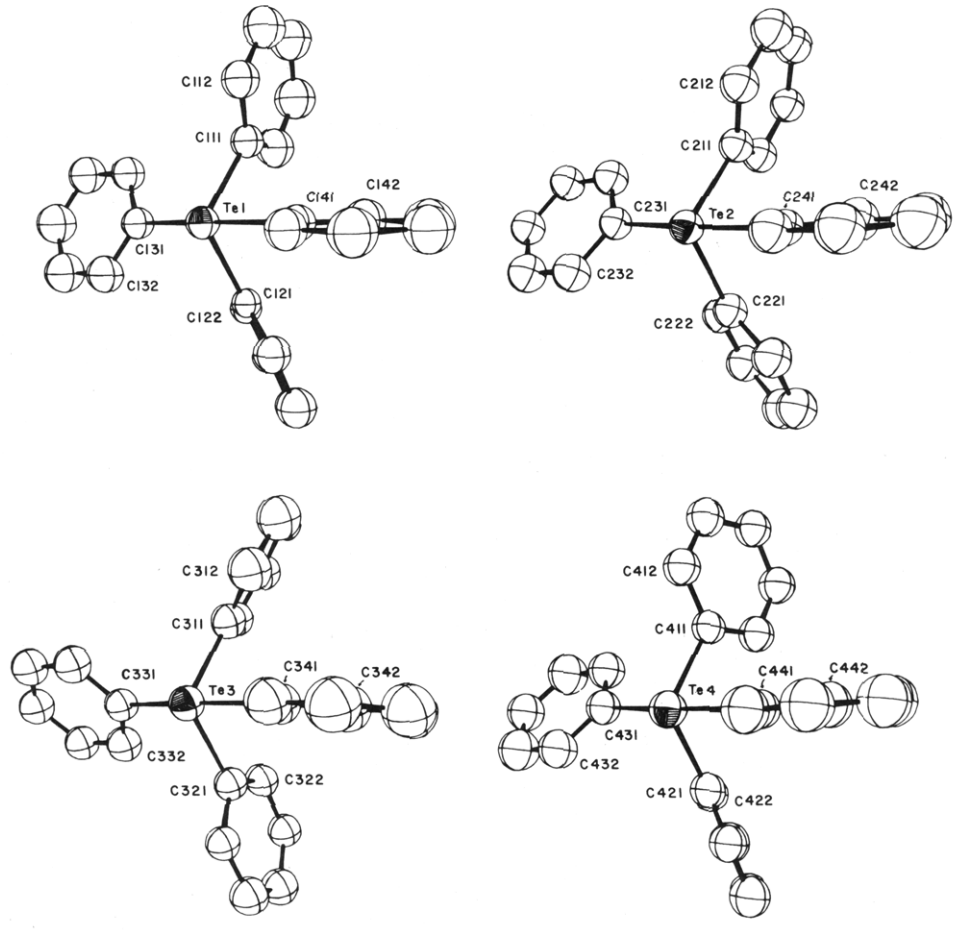

Figure 1. Atom labeling scheme of the four independent molecules of $(C_6H_5)_4Te$.

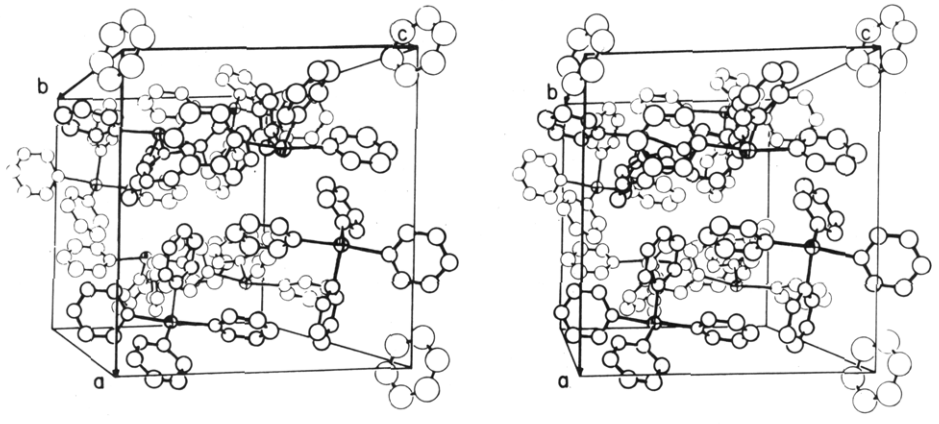

Figure 2. Stereoscopic unit cell drawing of $(C_6H_5)_4Te \cdot {}^1/_8C_6H_6$.

identical with those calculated for the axial distances in other trigonal-bipyramidal molecules such as $(CH_3)_2TeCl_2$[5] and $(C_6H_5)_2TeBr_2$.[16] These long distances are also in keeping with the strong trans influence observed for the phenyl group in several Te(II) complexes[32,33] and in the seven-coordinate Te(IV) compound tris(diethyldithiocarbamato)phenyltellurium(IV).[34] Various bonding models have been used to explain the axial elongation in the AB_4E molecules.[26,35]

Assuming that the R_4Te [and $(R{=})_2Te$][38] compounds require the ψ-tbp geometry, it is reasonable to suggest that the thermal stability of the R_nTeX_{4-n} (n = 2, 4) compounds depends, in part, on the stability of the long, axial $M^{\delta+}\cdots L^{\delta-}$ bonds.[36] Thus, ligand groups of low electronegativity, e.g., CH_3, would be expected to yield less stable structures than groups of higher electronegativity such as phenyls or halogens. Many R_2TeX_2 compounds are known and their thermal stability is well established.[4] In contrast, few R_4Te compounds are known. The thermal stability of these

(31) For comparison, a significantly short intramolecular Te(IV)–C distance is 2.945 (9) Å, in 2-biphenylyltellurium tribromide.[37]
(32) Foss, O.; Husebye, S. *Acta Chem. Scand.* **1966**, *20*, 132.
(33) Foss, O. *Pure Appl. Chem.* **1970**, *24*, 31.
(34) Esperas, S.; Husebye, S. *Acta Chem. Scand.* **1972**, *26*, 3293.
(35) Cotton, F. A.; Wilkinson, G. "Advanced Inorganic Chemistry", 4th ed.; Interscience: New York, 1980; Chapter 5.
(36) Evidence for the polarization of the axial bond has been noted in $(CH_3)_2TeCl_2$.[11]
(37) Knobler, C.; McCullough, J. D. *Inorg. Chem.* **1977**, *16*, 612.
(38) The tellurium catecholate, $Te(C_6H_4O_2)_2$, has a ψ-tbp structure (Lindqvist, O. *Acta Chem. Scand.* **1967**, *21*, 1473) as does $Te(C_6H_{12}O_2)_2$ (Day, R. O.; Holmes, R. R. *Inorg. Chem.* **1981**, *20*, 3071).

Table I. Positional ($\times 10^4$) and Thermal Parameters for Atoms in $(C_6H_5)_4Te \cdot {}^1/_8(C_6H_6)$

atom	x	y	z	B, Å^2	atom	x	y	z	B, Å^2
Te1	2172 (1)	4014 (0)	2755 (1)	3.416 (2)	C313	5828 (10)	6926 (7)	1175 (12)	6.69 (4)
Te2	1055 (1)	6095 (0)	6663 (1)	3.454 (3)	C314	5496 (9)	6470 (7)	359 (11)	5.70 (3)
Te3	3795 (1)	8442 (0)	1505 (1)	4.278 (2)	C315	4687 (10)	6568 (7)	−183 (11)	5.96 (3)
Te4	3046 (1)	645 (0)	5845 (1)	4.154 (2)	C316	4203 (8)	7137 (6)	105 (10)	4.61 (3)
C111	3052 (8)	4759 (5)	2606 (9)	3.80 (2)	C321	2384 (8)	8250 (6)	1667 (9)	4.04 (2)
C112	2751 (9)	5363 (6)	2960 (10)	5.02 (3)	C322	1965 (8)	7690 (6)	1171 (9)	4.63 (3)
C113	3304 (10)	5880 (7)	2821 (12)	6.81 (4)	C323	1022 (9)	7607 (6)	1303 (10)	4.87 (3)
C114	4117 (10)	5777 (7)	2328 (11)	6.35 (3)	C324	523 (9)	8068 (6)	1931 (10)	5.36 (3)
C115	4427 (10)	5159 (7)	1990 (11)	6.60 (4)	C325	953 (10)	8630 (7)	2443 (11)	6.03 (3)
C116	3900 (9)	4626 (7)	2129 (11)	5.89 (3)	C326	1896 (9)	8730 (6)	2305 (10)	4.83 (3)
C121	2950 (7)	3170 (5)	2645 (8)	3.46 (2)	C331	3436 (8)	8479 (6)	−205 (9)	4.56 (3)
C122	3486 (8)	2950 (5)	1792 (9)	3.94 (3)	C332	2580 (9)	8398 (6)	−709 (11)	5.73 (3)
C123	3981 (8)	2379 (6)	1725 (9)	4.65 (3)	C333	2426 (10)	8552 (7)	−1706 (11)	6.12 (3)
C124	3893 (9)	2031 (6)	2519 (10)	5.06 (3)	C334	3141 (10)	8785 (7)	−2160 (11)	6.40 (3)
C125	3342 (9)	2252 (6)	3363 (10)	5.44 (3)	C335	4010 (10)	8866 (7)	−1675 (11)	6.18 (3)
C126	2888 (8)	2834 (6)	3437 (9)	4.69 (3)	C336	4165 (10)	8723 (7)	−667 (11)	5.95 (3)
C131	2027 (8)	3777 (5)	959 (9)	3.99 (3)	C341	3982 (8)	8212 (6)	3110 (10)	4.95 (3)
C132	1622 (9)	3185 (6)	540 (11)	5.59 (3)	C342	3651 (10)	7680 (7)	3408 (12)	7.25 (4)
C133	1392 (10)	3068 (7)	−576 (12)	6.69 (4)	C343	3773 (11)	7583 (8)	4432 (13)	7.89 (4)
C134	1539 (10)	3501 (7)	−1157 (12)	6.36 (4)	C344	4235 (10)	8030 (8)	5186 (12)	6.99 (4)
C135	1902 (10)	4075 (7)	−729 (12)	6.43 (4)	C345	4545 (10)	8560 (7)	4914 (12)	6.83 (4)
C136	2170 (8)	4222 (6)	357 (10)	4.81 (3)	C346	4438 (9)	8666 (6)	3870 (11)	5.65 (3)
C141	2636 (8)	4227 (5)	4461 (9)	4.13 (3)	C411	2349 (8)	1532 (6)	5874 (9)	4.21 (3)
C142	3564 (9)	4270 (6)	4810 (10)	5.07 (3)	C412	2921 (8)	2050 (6)	6009 (10)	4.98 (3)
C143	3815 (10)	4393 (7)	5907 (12)	6.24 (4)	C413	2451 (10)	2655 (7)	6059 (11)	5.99 (3)
C144	3105 (10)	4447 (7)	6607 (11)	6.09 (3)	C414	1519 (10)	2680 (7)	5992 (11)	6.06 (4)
C145	2189 (10)	4414 (6)	6295 (11)	6.26 (3)	C415	982 (10)	2149 (7)	5864 (11)	6.00 (3)
C146	1953 (8)	4305 (6)	5195 (10)	4.56 (3)	C416	1409 (9)	1547 (6)	5805 (10)	5.26 (3)
C211	2459 (7)	6342 (5)	6588 (8)	3.70 (2)	C422	1400 (8)	0 (6)	6617 (9)	5.64 (3)
C212	2978 (8)	5953 (6)	5886 (9)	4.51 (3)	C423	804 (9)	−514 (6)	6658 (10)	7.42 (3)
C213	3933 (10)	6090 (7)	5815 (11)	6.04 (3)	C424	916 (11)	−1068 (8)	5940 (12)	7.06 (4)
C214	4304 (8)	6634 (6)	6470 (10)	4.90 (3)	C425	1587 (10)	−1153 (7)	5227 (12)	6.76 (4)
C215	3745 (8)	7029 (6)	7174 (10)	4.96 (3)	C426	2184 (10)	−644 (7)	5169 (12)	5.75 (4)
C216	2814 (8)	6877 (6)	7232 (9)	4.59 (3)	C421	2069 (9)	−74 (7)	5877 (11)	4.51 (3)
C221	376 (8)	6968 (5)	7265 (9)	3.81 (2)	C431	3000 (8)	879 (6)	7610 (10)	4.97 (3)
C222	574 (8)	7301 (6)	8270 (9)	4.44 (3)	C432	3529 (10)	458 (7)	8051 (11)	6.45 (3)
C223	116 (9)	7865 (6)	8654 (10)	5.05 (3)	C433	3589 (11)	554 (8)	9199 (13)	7.79 (4)
C224	−530 (9)	8108 (6)	8017 (11)	5.68 (3)	C434	3153 (11)	1072 (8)	9800 (12)	7.08 (4)
C225	−720 (9)	7771 (6)	7011 (10)	5.10 (3)	C435	2681 (11)	1506 (8)	9355 (13)	8.08 (4)
C226	−269 (8)	7205 (6)	6601 (9)	4.42 (3)	C436	2586 (9)	1409 (6)	8227 (11)	5.75 (3)
C231	1355 (8)	6002 (5)	8355 (9)	4.01 (3)	C441	2778 (9)	463 (6)	4068 (10)	4.92 (3)
C232	566 (9)	5859 (6)	8846 (10)	5.48 (3)	C442	1946 (10)	504 (7)	3560 (12)	6.71 (4)
C233	631 (10)	5744 (7)	9878 (11)	6.05 (3)	C443	1865 (11)	391 (7)	2418 (13)	7.82 (4)
C234	1482 (10)	5755 (6)	10364 (11)	5.75 (3)	C444	2685 (12)	271 (8)	1942 (13)	7.50 (4)
C235	2263 (9)	5874 (6)	9885 (11)	5.70 (3)	C445	3500 (11)	216 (7)	2390 (12)	7.27 (4)
C236	2207 (8)	5993 (6)	8853 (10)	4.79 (3)	C446	3589 (10)	313 (7)	3523 (11)	6.14 (3)
C241	907 (8)	6326 (5)	5028 (9)	3.99 (3)	C1	−887 (12)	39 (9)	390 (14)	8.79 (5)
C242	1279 (9)	6848 (6)	4742 (10)	5.22 (3)	C2	−289 (13)	−457 (9)	524 (13)	8.59 (4)
C243	1171 (9)	6924 (7)	3688 (11)	6.34 (3)	C3	587 (13)	−490 (9)	158 (14)	8.94 (5)
C244	705 (10)	6465 (7)	2975 (11)	6.08 (3)					
C245	357 (9)	5932 (7)	3220 (11)	5.66 (3)					
C246	463 (8)	5863 (6)	4286 (9)	4.55 (3)					
C311	4515 (8)	7588 (6)	964 (9)	4.69 (3)					
C312	5331 (10)	7495 (7)	1517 (11)	6.62 (4)					

compounds increases in the series alkyl, phenyl, pentafluorophenyl, and 2,2′-biphenylylene, with the solid tetraalkyl- or dialkyldiaryl telluriums not yet isolated.[4] Tetraphenyltellurium decomposes just above 100 °C while the latter two decompose above 200 °C.[4] Similarly, the R_nTeX_{4-n} (n = 2, 4) compounds show greater thermal stability than the analogous selenium compounds where M is less electropositive, although in this case both steric and electronic factors may be important. To our knowledge, no R_4Se compounds have been prepared. If the solid-state geometry of $(C_6H_5)_4Te$ makes any contribution to the structure of the molecule in solution, the axial elongation might facilitate intramolecular and intermolecular processes. Recent solution studies of some organotellurium compounds show that $(C_6H_5)_4Te$ appears to decompose by an intramolecular process[3] and that several ψ-tbp tetraalkoxytellurium compounds undergo both intramolecular and intermolecular ligand reorganization.[40]

The four independent molecules in $(C_6H_5)_4Te$ are separated by normal van der Waals distances. The intermolecular Te–C (aromatic) distances fall between those observed in dibenzotellurophene[41] and those in trimethyltelluronium tetraphenylborate.[14] The Te–C (aromatic) intermolecular distances less than 4.0 Å are Te3–C445 [x, 1 − y, z] at 3.80 (1) Å, Te2–C145 at 3.93 (1) Å and Te4–C346 [x, y − 1, z] at 3.94 (1) Å. These contacts are in the general direction of one of the two vacant octahedral sites around tellurium and involve conformationally, nearly the same carbon atom (*n*45 meta or 346 ortho) on the three

(39) See, for example: Zingaro, R. A.; Cooper, W. C. "Selenium"; Van Nostrand: New York, 1974. Klayman, D. L.; Gunther, W. H. H. "Organic Selenium Compounds: Their Chemistry and Biology", Wiley-Interscience: New York, 1973.

(40) Denney, D. B.; Denney, D. Z.; Hammond, P. J.; Hsu, Y. F. *J. Am. Chem. Soc.* **1981**, *103*, 2340.

(41) McCullough, J. D. *Inorg. Chem.* **1975**, *14*, 2639.

Table II. Interatomic Distances (Å) and Angles (Deg)[44]

Distances[a]			
Te1-Te2′	4.803 (2)	Te3-C321	2.13 (1)
Te3-Te4′	5.757 (3)	Te3-C331	2.27 (1)
Te1-C111	2.12 (1)	Te3-C341	2.30 (1)
Te1-C121	2.12 (1)	Te4-C411	2.13 (1)
Te1-C131	2.27 (1)	Te4-C421	2.16 (1)
Te1-C141	2.31 (1)	Te4-C431	2.27 (1)
Te2-C211	2.13 (1)	Te4-C441	2.30 (1)
Te2-C221	2.14 (1)	C1-C2	1.41 (3)
Te2-C231	2.30 (1)	C2-C3	1.38 (3)
Te2-C241	2.31 (1)	C3-C1′	1.41 (3)
Te3-C311	2.12 (1)		

Angles			
C111-Te1-C121	109.4 (4)	C311-Te3-C321	110.0 (4)
C131-Te1-C141	167.9 (4)	C341-Te3-C331	167.9 (4)
C111-Te1-C131	87.1 (4)	C311-Te3-C331	88.2 (4)
C121-Te1-C131	87.2 (4)	C321-Te3-C331	87.9 (4)
C111-Te1-C141	85.9 (4)	C311-Te3-C341	85.8 (5)
C121-Te1-C141	85.8 (4)	C321-Te3-C341	84.2 (4)
C211-Te2-C221	104.8 (4)	C411-Te4-C421	110.0 (4)
C231-Te2-C241	170.8 (4)	C441-Te4-C431	168.3 (4)
C211-Te2-C231	88.5 (4)	C411-Te4-C431	86.5 (4)
C221-Te2-C231	87.7 (4)	C421-Te4-C431	86.8 (5)
C211-Te2-C241	84.4 (4)	C411-Te4-C441	85.6 (4)
C221-Te2-C241	88.5 (4)	C421-Te4-C441	87.8 (5)

[a] Primes indicate symmetry-related atoms.

different molecules. The contacts in the indium and gallium phenyls similarly involve either ortho or meta carbons,[13] but in the present case distances are not less than the van der Waals sums which are 3.76 Å after Bondi[42] and 3.90 Å after Pauling,[28c] using 1.70 Å for the half-thickness of an aromatic molecule[28c] in both sums. No evidence is seen for a π donor–acceptor interaction as observed in $(C_6H_5)_3SeNCS$.[43] Thus, tellurium in $(C_6H_5)_4Te$ appears to have a genuine fourfold configuration devoid of secondary bonding as defined by Alcock.[8] As in the case of $(CH_3)_3TeB(C_6H_5)_4$,[14] it is not clear whether the absence of secondary bonding is due to electronic or steric constraints or to a combination of the two. The Te···C contacts in the present case appear to be favored electrostatically and are taken as an indication of packing efficiency in the structure. We note that, within the limits of a error, the volume observed for $(C_6H_5)_4Te$ is exactly four-thirds that of the $(C_6H_5)_3Te^+$ ion as calculated from the unit-cell volume of $(C_6H_5)_3TeCl$.[29] An examination of the dihedral angles between the planes of the phenyl rings[44] of the independent molecules revealed no trends in the orientations of the rings which are assumed to be governed by the packing forces.

A stereoscopic drawing of the unit cell appears in Figure 2. The molecules pack with the C–Te–C axis in the general direction of the crystallographic *c* axis and the equatorial plane in the general direction of the *ab* plane. The closest Te–Te approach is 4.803 (1) Å. The benzene of crystallization appears normal[45] and is located at the cell origin. The presence or absence of solvent is expected to have little or no effect on the molecular geometry of $(C_6H_5)_4Te$. This is in contrast to the effect of solvent on the structures of the R_3TeX compounds.[7]

Registry No. $(C_6H_5)_4Te \cdot {}^1/_8(C_6H_6)$, 79768-49-3.

Supplementary Material Available: A listing of the observed and calculated structure factors and tables of the hydrogen atom positional and thermal parameters and of the least-squares planes of the phenyl rings (51 pages). Ordering information is given on any current masthead page.

(42) Bondi, A. *J. Phys. Chem.* **1964**, *68*, 441.
(43) Ash, P.; Lee, J.-S.; Titus, D. D.; Mertz, K.; Ziolo, R. F. *J. Organomet. Chem.* **1977**, *135*, 91.
(44) The 16 independent phenyl rings appear normal. The mean value and its estimated variance[23] for the 96 C–C distances is 1.40 (0) Å and for the 96 C–C–C angles is 120 (0)°. The least-squares planes of the 16 rings and the average atom deviation for each plane are given as supplementary material. The rings are planar with the largest average atom deviation being 0.029 Å for the C11*n* (*n* = 1–6) plane. The C–C distances range from 1.32 (2) to 1.47 (2) Å and the C–C–C angles from 114 (1) to 127 (2)°.
(45) The average of the three independent C–C distances is 1.40 Å and that of the three angles is 120°.

Organofluorosilicates in Organic Synthesis. 12.[1] Preparation of Organopentafluorosilicates and Their Cleavage Reactions by Halogens and *N*-Bromosuccinimide. Synthetic and Mechanistic Aspects

Kohei Tamao, Jun-ichi Yoshida, Hiraku Yamamoto, Toshio Kakui, Hiroshi Matsumoto, Masatada Takahashi, Atsushi Kurita, Masao Murata, and Makoto Kumada*

Department of Synthetic Chemistry, Faculty of Engineering, Kyoto University, Yoshida, Kyoto 606, Japan

Received July 29, 1981

This report describes synthetic and mechanistic aspects of a new method for the regio- and stereoselective transformation of olefins and acetylenes to the corresponding alkyl and alkenyl halides, respectively, via halogen or NBS cleavage of the carbon–silicon bond in organopentafluorosilicates derived from hydrosilylation products. Potassium organopentafluorosilicates ($K_2[RSiF_5]$) have been prepared from the corresponding organotrichlorosilanes which are readily obtained by the well-established highly regio- and stereoselective hydrosilylation of olefins and acetylenes with trichlorosilane catalyzed by chloroplatinic acid. Treatment of the organotrichlorosilanes with potassium fluoride in water or ethanol at 0 °C affords the silicates as white, air-stable powder. The organosilicates containing other alkali-metal countercations (Na, Rb, and Cs) have also been prepared by the reaction of the corresponding organotrifluorosilanes with NaF, RbF, and CsF, respectively. The silicates have been found to react with Cl_2, Br_2, I_2, IBr, and NBS under mild conditions to give the corresponding organic halides. In both the halogen and NBS cleavage reactions a halogen atom is regioselectively introduced onto the carbon to which the silicon atom has been attached. The present procedure provides a new general method for anti-Markownikoff hydrohalogenation of olefins. The NBS cleavage tolerates some functional groups such as the alkoxycarbonyl, oxo, halo, and alkenyl groups. The reaction of (*E*)-alkenylsilicates with NBS affords (*E*)-alkenyl bromides with high stereoselectivity, while stereoselectivity of the bromine cleavage is relatively low. Stereochemistry at the aliphatic carbon in the cleavage reaction of alkylsilicates has also been investigated. Reactions of *exo*- and *endo*-2-norbornylpentafluorosilicates with Br_2 and NBS proceed stereospecifically with predominant inversion of configuration. Partial stereochemical scrambling has been observed, however, in the reaction of the exo silicate with Br_2 in nonpolar solvents. On the basis of these experimental results, a mechanism involving the initial one-electron transfer has been proposed for the bromine cleavage reaction of alkylsilicates. The reaction of alkylsilicates with IBr giving both alkyl iodide and bromide also supports the proposed mechanism. The NBS cleavage of alkylsilicates and all reactions of alkenyl- and arylsilicates, however, seem to proceed by an electrophilic mechanism.

The last decade has seen considerable progress in applications of organosilicon compounds in organic synthesis: many new reactions have been discovered and many new techniques have been developed.[2] However, all these organosilicon compounds, with a few exceptions, have been restricted to ordinary tetracoordinate silicon derivatives. This paper is concerned with one of the intriguing aspects of organosilicon chemistry—the chemistry of hexacoordinate organosilicon compounds, particularly, the preparation and applications in organic synthesis of potassium organopentafluorosilicates, together with some of the results of mechanistic studies.

It is known that silicon can expand its valence shell by use of vacant d orbitals[3] and that several types of penta- and hexacoordinate silicon compounds are obtained in the presence of electronegative ligands which cause contraction of d orbitals.[4-6] Organopentafluorosilicates, $M_2[RSiF_5]$, have been known for some 20 years.[4] The first compounds of this class were prepared by Tansjoe in 1961, who treated phenyltriaminosilanes with water-free hydrogen fluoride in ether solution.[4a]

$$PhSi(NHR)_3 + 6HF \xrightarrow{\text{ether}} (RNH_3)_2[PhSiF_5] + RNH_3F$$

Since then several research groups have reported the synthesis, reactions, and structural studies based on spectroscopies, of organopentafluorosilicates.[4p,s,x,y,5] Especially, Mueller and collaborators had worked most ex-

(1) For part 11, see ref 7l.

(2) (a) Rubottom, G. M. *J. Organomet. Chem. Libr.* **1979**, *8*, 263; **1980**, *10*, 277. (b) Hudrlik, P. F. In "New Applications of Organometallic Reagents in Organic Synthesis"; Seyferth, D., Ed.; Elsevier: Amsterdam, 1976; p 127. (c) Rasmussen, J. K. *Synthesis* **1977**, 91. (d) Chan, T. H.; Fleming, I. *Ibid.* **1979**, 761. (e) Chan, T. H. *Acc. Chem. Res.* **1977**, *10*, 442. (f) Colvin, E. W. *Chem. Soc. Rev.* **1978**, *7*, 15. (g) Fleming, I. In "Comprehesive Organic Chemistry"; Barton, D. H. R., Ollis, W. D., Eds.; Pergamon Press: Oxford; 1979; Vol. 3, p 539. (h) Birkofer, L.; Stuhl, O. *Top. Curr. Chem.* **1980**, *88*, 33.

(3) For example: (a) Kwart, H.; King, K. "*d*-Orbitals in the Chemistry of Silicon, Phosphorus and Sulfur"; Springer-Verlag: Berlin, 1977. (b) Buerger, H. *Angew. Chem., Int. Ed. Engl.* **1973**, *12*, 474.

(4) Hexacoordinate organofluorosilicates: (a) Tansjoe, L. *Acta Chem. Scand.* **1961**, *15*, 1583. (b) Tansjoe, L. *Ibid.* **1964**, *18*, 456, 465. (c) Mueller, R. *Organomet. Chem. Rev.* **1966**, *1*, 359. (d) Mueller, R.; Dathe, C. *J. Prakt. Chem.* **1963**, *22*, 232. (e) Mueller, R.; Dathe, C. *Chem. Ber.* **1965**, *98*, 235. (f) Mueller, R.; Dathe, C.; Mose, D. *Ibid.* **1965**, *98*, 241. (g) Mueller, R.; Reichel, S. *Ibid.* **1965**, *98*, 3874. (h) Mueller, R.; Dathe, C. *Z. Anorg. Allg. Chem.* **1965**, *341*, 41. (i) Mueller, R.; Dathe, C. *Ibid.* **1965**, *341*, 49. (j) Mueller, R.; Dathe, C. *Ibid.* **1966**, *343*, 150. (k) Mueller, R.; Dathe, C. *Chem. Ber.* **1966**, *99*, 1609. (l) Mueller, R.; Dathe, C.; Frey, H. J. *Ibid.* **1966**, *99*, 1614. (m) Mueller, R.; Reichel, S.; Dathe, C. *Ibid.* **1968**, *101*, 783. (n) Mueller, R.; Koehne, R.; Model, H. J.; Dathe, C. *Z. Anorg. Allg. Chem.* **1969**, *368*, 243. (o) Mueller, R.; Dressler, H.; Dathe, C. *J. Prakt. Chem.* **1970**, *312*, 150. (p) Licht, K.; Peuker, C.; Dathe, C. *Z. Anorg. Allg. Chem.* **1971**, *380*, 293. (q) Ishikawa, N.; Kuroda, K. *Nippon Kagaku Zasshi* **1968**, *89*, 421. (r) Ishikawa, N.; Kuroda, K. *Ibid.* **1968**, *89*, 699. (s) Kuroda, K.; Ishikawa, N. *Ibid.* **1970**, *91*, 77. (t) Kuroda, K.; Ishikawa, N. *Kogyo Kagaku Zasshi* **1971**, *74*, 2132. (u) Moscony, J. J.; MacDiarmid, A. G. *Chem. Commun.* **1965**, *307*. (v) Kurosawa, H.; Fukumoto, T.; Okawara, R. *Inorg. Nucl. Chem. Lett.* **1969**, *5*, 473. (w) Kurosawa, H.; Yasuda, M. *J. Chem. Soc., Chem. Commun.* **1978**, 716. (x) Mart, R. K.; Janzen, A. F. *Can. J. Chem.* **1977**, *55*, 1167. (y) Mart, R. K.; Janzen, A. F. *J. Chem. Soc., Chem. Commun.* **1977**, 671.

(5) Pentacoordinate organofluorosilicates: Klanberg, F.; Muetterties, E. L. *Inorg. Chem.* **1968**, *7*, 155. See also ref 4s and 4u.

0276-7333/82/2301-0355$01.25/0

tensively during the period of 1963–1970 and disclosed much chemistry.[4c-o] Recently, the hexacoordination around the silicon atom in solution has been confirmed by ^{19}F NMR.[4s,y]

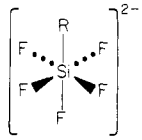

Because organopentafluorosilicates contain a doubly negatively charged, coordinatively saturated, hexacoordinate silicon atom, their reactivities are expected to be quite different from those of neutral, coordinatively unsaturated, tetracoordinate ordinary organosilicon compounds. IR studies also imply the higher reactivitiy of the silicates, where the force constant of the carbon–silicon bond in methylpentafluorosilicate $[CH_3SiF_5]^{2-}$ has been shown to be much smaller than that in tetracoordinate methyltrifluorosilane.[4p] In fact, some noteworthy examples of facile carbon–silicon bond cleavage reactions have been recorded in the literature. (1) A reaction of potassium methylpentafluorosilicate with bromine in water containing fluoride ions affords methyl bromide.[4i] (2) Ammonium methylpentafluorosilicate reacts with $NH_4F{\cdot}HF$ to give the protonolysis product methane.[4i] (3) Oxidation of ammonium or potassium methylpentafluorosilicate by $KMnO_4$ gives carbon dioxide together with a trace amount of methane.[4i] (4) Homo coupling products are obtained from vinyl- and perfluorovinylpentafluorosilicates (Na^+, K^+, or ammonium salts) by the action of $AgNO_3$ or $CuSO_4$.[4o] (5) The organic group is transferred to other metals such as silver,[4e,i] thallium,[4v,w] and antimony[4k] by treatment of the organosilicate with a salt of the corresponding metals.

In spite of these successful fundamental studies on preparation and reactions of organopentafluorosilicates, little attention had been paid to the synthetic applications of the organosilicates as useful and versatile intermediates until 1977 when we initiated systematic studies with this end in view.[7]

We were interested in the synthetically useful electrophilic cleavage reactions of the carbon–silicon, particularly the alkyl carbon–silicon, bond in organosilicon compounds. The addition of silicon hydrides to olefins and acetylenes has become one of the most important methods of forming silicon–carbon bonds.[8] However, the synthetic use of alkylsilanes thus obtained has been rather limited, while alkenylsilanes have recently been recognized as useful intermediates by many synthetic chemists.[2d] The major reason of this situation is that there has been virtually no method for transformation of the alkyl–silicon bonds into functional groups whereas the cleavage of the alkenyl–silicon bonds is quite easy. Tetraalkylsilanes are indeed cleaved by certain activated electrophiles such as H^+, RCO^+, R^+, or halonium ion, but there is no difference in selectivity between the alkyl group under consideration and other alkyl groups on silicon, being of little synthetic value.[9] Substitution of the alkyl groups by electronegative groups diminishes the reactivity of the remaining carbon–silicon bond toward electrophilic cleavage. For example, monoalkylsilicon compounds such as obtainable by hydrosilylation of olefins with trichlorosilane are inert to electrophilic reagents under usual conditions. We anticipated that an organopentafluorosilicate might solve this dilemma, because it contains only one organic group under consideration and an electron-rich alkyl group. Indeed, major part of our expectation has been realized, and several synthetically useful reactions have so far been developed.[7] We report herein the full details of the cleavage reactions of the carbon–silicon bond in organopentafluorosilicates by halogens and NBS providing a new synthetically useful route to organic halides from olefins and acetylenes.

olefin or acetylene $\rightarrow RSiCl_3 \rightarrow K_2[RSiF_5] \rightarrow RX$

Cleavage of the carbon–metal bonds in organometallics by halogens provides one of the unique and useful methods for preparation of organic halides.[10] Especially, the transformation involving hydrometalation of terminal olefins followed by halogenolysis leading to anti-Markownikoff alkyl halides has been successfully achieved by using organoboron,[11] organoaluminum,[12] and organozirconium compounds.[13] Our present development provides a useful alternative to the published procedures. The interest of the present reaction also stems from the expected unique feature of the reaction mechanisms due to the extracoordinate doubly negatively charged silicon atom. Investigation into this virgin field may contribute to the elucidation of the whole view of electrophilic cleavage of carbon–metal bonds.

(6) Other representative extracoordinate organosilicon compounds. $[RSi(-OC_6H_4O)_2]^-$: (a) Frye, C. L. *J. Am. Chem. Soc.* **1964**, *86*, 3170. (b) Boer, F. R.; Flynn, J. N.; Turley, J. W. *Ibid.* **1968**, *90*, 6973. $[RSi(-C_6H_4C(CF_3)_2O)_2]^-$: (c) Perozzi, E. F.; Martin, J. C. *Ibid.* **1979**, *101*, 1591. $[RSi(acac)_2]^+$: (d) Schott, F.; Golz, K. *Z. Anorg. Allg. Chem.* **1973**, *399*, 7. $[RSi(OCH_2CH_2)_3N]$: (e) For example, Vornokov, M. G. *Pure Appl. Chem.* **1966**, *13*, 35. (f) Voronkov, M. G. *Top. Curr. Chem.* **1979**, *84*, 77. $[RXSi(bpy)_2]^{2+}$: (g) Kummer, D.; Geisser, K. E.; Seshadri, T. *Chem. Ber.* **1977**, *110*, 1950. [PcSiRX] (Pc = phthalocyaninato): (h) Esposito, J. N.; Lloyd, J. E.; Kenney, M. E. *Inorg. Chem.* **1966**, *5*, 1979. (i) Pommier, J. C. *Rev. Silicon, Germanium, Tin, Lead Compd.* **1979**, *4*, 91. (j) Tamao, K.; Akita, M.; Kumada, M., unpublished results, 1979.

(7) (a) Tamao, K.; Yoshida, J.; Takahashi, M.; Yamamoto, H.; Kakui, T.; Matsumoto, H.; Kurita, A.; Kumada, M. *J. Am. Chem. Soc.* **1978**, *100*, 290. (b) Tamao, K.; Kakui, T.; Kumada, M. *Ibid.* **1978**, *100*, 2268. (c) Yoshida, J.; Tamao, K.; Kurita, A.; Kumada, M. *Tetrahedron Lett.* **1978**, 1809. (d) Yoshida, J.; Tamao, K.; Takahashi, M.; Kumada, M. *Ibid.* **1978**, 2161. (e) Tamao, K.; Kakui, T.; Kumada, M. *Ibid.* **1979**, 619. (f) Tamao, K.; Matsumoto, H.; Kakui, T.; Kumada, M. *Ibid.* **1979**, 1137. (g) Yoshida, J.; Tamao, K.; Kakui, T.; Kumada, M. *Ibid.* **1979**, 1141. (h) Tamao, K.; Kakui, T.; Kumada, M. *Ibid.* **1980**, *21*, 111. (i) Tamao, K.; Yoshida, J.; Murata, M.; Kumada, M. *J. Am. Chem. Soc.* **1980**, *102*, 3267. (j) Yoshida, J.; Tamao, K.; Kumada, M.; Kawamura, T. *Ibid.* **1980**, *102*, 3269. (k) Tamao, K.; Hayashi, T.; Matsumoto, H.; Yamamoto, H.; Kumada, M. *Tetrahedron Lett.* **1979**, 2155. (l) Tamao, K.; Kakui, T.; Kumada, M. *Ibid.* **1980**, *21*, 4105. (m) Tamao, K.; Yoshida, J.; Kumada, M. *Yuki Gosei Kagaku Kyokaishi* **1980**, *38*, 769.

(8) (a) Eaborn, C.; Bott, R. W. In "Organometallic Compounds of the Group IV Elements"; MacDiarmid, A. G., Ed.; Marcel Dekker: New York; 1968; Vol. 1, p 105. (b) Lukevits, E. Y.; Voronkov, M. G. "Organic Insertion Reactions of Group IV Elements"; Consultant Bureau: New York, 1966. (c) Lukevics, E.; Belyakova, Z. V.; Pomerantseva, M. G.; Voronkov, M. G. *J. Organomet. Chem. Libr.* **1977**, *5*, 1. (d) Speier, J. L. *Adv. Organomet. Chem.* **1979**, *17*, 407. (e) Speier, J. L.; Webster, J. A.; Barnes, G. H. *J. Am. Chem. Soc.* **1957**, *79*, 974. (f) Benkeser, R. A.; Burrous, M. L.; Nelson, L. E.; Swisher, J. V. *Ibid.* **1961**, *83*, 4385. (g) Benkeser, R. A.; Cunico, R. F.; Dunny, S. *J. Org. Chem.* **1967**, *32*, 2634.

(9) (a) Eaborn, C. *J. Chem. Soc.* **1949**, 2755. (b) Sakurai, H.; Tominaga, K.; Watanabe, T.; Kumada, M. *Tetrahedron Lett.* **1966**, 5493. (c) Frainnet, E. *Bull. Soc. Chim. Fr.* **1965**, 1259. (d) Sommer, L. H. *J. Am. Chem. Soc.* **1953**, *75*, 2932. (e) Olah, G.; Ho, T.-L.; Prakash, G. K. S.; Gupta, D. G. B. *Synthesis* **1977**, 677.

(10) Negishi, E. "Organometallics in Organic Synthesis"; Wiley: New York, 1980; Vol. 1.

(11) (a) Brown, H. C.; Rathke, M. W.; Rogic, M. M. *J. Am. Chem. Soc.* **1968**, *90*, 5038. (b) Brown, H. C.; Lane, C. F. *Ibid.* **1970**, *92*, 6660. (c) Lane, C. F.; Brown, H. C. *Ibid.* **1970**, *92*, 7212. (d) Brown, H. C. "Organic Syntheses via Boranes"; Wiley: New York, 1978. (e) Kabalka, G. W.; Gooch III, E. E. *J. Org. Chem.* **1980**, *45*, 3578.

(12) Isagawa, K.; Tatsumi, K.; Otsuji, Y. *Chem. Lett.* **1976**, 1145. (b) Sato, F.; Sato, S.; Sato, M. *J. Organomet. Chem.* **1976**, *122*, C25. (c) Sato, F.; Sato, S.; Sato, M. *Ibid.* **1977**, *131*, C26. (d) Sato, F.; Sato, S.; Kodama, H.; Sato, M. *Ibid.* **1977**, *142*, 71.

(13) (a) Hart, D. W.; Schwartz, J. *J. Am. Chem. Soc.* **1974**, *96*, 8115. (b) Schwartz, J. In "New Applications of Organometallic Reagents in Organic Synthesis"; Seyferth, D., Ed.; Elsevier: Amsterdam, 1976; p 461. (c) Schwartz, J. *Angew. Chem.* **1976**, *88*, 402.

Table I. Preparation of Alkylpentafluorosilicates via Hydrosilylation of Olefins

olefin	hydrosilylation[a] conditns	product	yield, %	silicate formation[b] yield, %
n-$C_6H_{13}CH{=}CH_2$	rt,[c] 3 h	n-$C_8H_{17}SiCl_3$	86	98
n-C_8H_{16}[d]	140 °C, 9 h	n-$C_8H_{17}SiCl_3$[e]	82	98
t-$C_4H_9CH{=}CH_2$	rt,[c] 12 h	t-$C_4H_9CH_2CH_2SiCl_3$	71	64
n-$C_{10}H_{21}CH{=}CH_2$	60-70 °C, 6.5 h	n-$C_{12}H_{25}SiCl_3$	73	78
n-$C_{16}H_{33}CH{=}CH_2$	50-60 °C, 5 h	n-$C_{18}H_{37}SiCl_3$	90	91[f]
$PhCH{=}CH_2$	reflux, 3 h[g]	$PhCH_2CH_2SiCl_3$	92	96
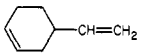	rt,[c] 22 h	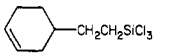	88	73
$Br(CH_2)_9CH{=}CH_2$	50 °C, 11 h	$Br(CH_2)_{11}SiCl_3$	77	72
$CH_3CO(CH_2)_2CH{=}CH_2$	50-60 °C, 4 h	$CH_3CO(CH_2)_4SiCl_3$	85	87
$CH_3O_2C(CH_2)_8CH{=}CH_2$	60 °C, 7 h	$CH_3O_2C(CH_2)_{10}SiCl_3$	91	91
$NCCH{=}CH_2$	100 °C, 5 h[h]	$NC(CH)_2SiCl_3$	54	100
$CH_2{=}CHCH_2OCH_2CH{=}CH_2$	reflux, 2 h[i]	$CH_2{=}CHCH_2O(CH_2)_3SiCl_3$	28	81
	100 °C, 20 h[j]	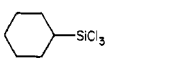	78	76

[a] Hydrosilylation of olefins was carried out with excess (1.2-2.0 parts) trichlorosilane in the presence of chloroplatinic acid unless otherwise stated. [b] Alkyltrichlorosilane was added dropwise to excess (25 parts) aqueous KF at 0 °C. [c] rt = room temperature. An exothermic reaction took place when trichlorosilane was added to a mixture of the olefins and the catalyst. After it ceased, the reaction mixture was stirred at room temperature. [d] A mixture of terminal and internal olefins. [e] Only the terminal adduct was obtained. [f] The alkyltrichlorosilane was treated with KF in ethanol. [g] Hydrosilylation was carried out in THF. [h] Hydrosilylation was carried out in the presence of pyridine catalyst. [i] One equivalent of trichlorosilane was used. [j] The reaction was carried out in a sealed tube.

Results and Discussion

Preparation of Organopentafluorosilicates via Hydrosilylation of Olefins and Acetylenes. Various methods have been reported for the preparation of potassium organopentafluorosilicates from tetracoordinate organofluoro-, organochloro-, and organoalkoxysilanes.[4] Among these precursors organotrichlorosilanes may be the most practical from the synthetic viewpoint since a variety of organotrichlorosilanes can be directly prepared by hydrosilylation of olefins and acetylenes (Scheme I).

We will make a brief mention of the hydrosilylation relevant to our present study at first and then describe the preparation of organopentafluorosilicates. Hereafter, unless otherwise stated, the word "organopentafluorosilicates" refers to the "potassium" salts.

Hydrosilylation of Olefins and Acetylenes. Many types of catalysts such as transition-metal compounds and radical initiators have been developed.[8] Of these catalysts, chloroplatinic acid (Speier's catalyst) is best established, is widely used, and is most convenient.[8d] The hydrosilylation of terminal olefins with trichlorosilane in the presence of H_2PtCl_6 proceeds regioselectively to give exclusively the terminal adducts. Internal olefins are less reactive than terminal ones, and hence selective monohydrosilylation can be achieved on polyenes which contain both terminal and internal double bonds, as exemplified by 4-vinylcyclohexene. Under rather drastic conditions internal olefins are also hydrosilylated with isomerization of the double bond to give terminal adducts. The hydrosilylation with trichlorosilane is compatible with various functional groups such as alkoxycarbonyl, oxo,[14] cyano, halo, ether, and alkenyl groups. Advantages also reside in that the hydrosilylation is usually conducted in the absence of solvent. Experimental results for these transformations are summarized in Table I.

Scheme I

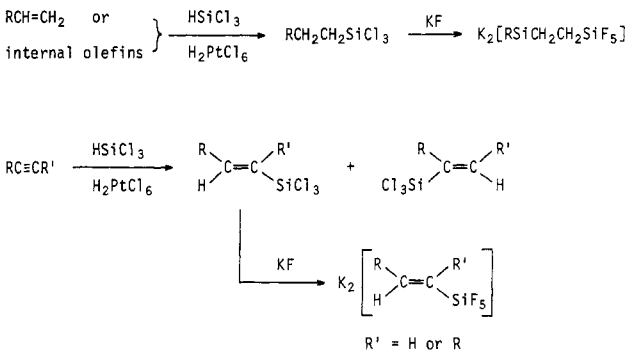

For hydrosilylation of acetylenes, regio- and stereoselectivity problems arise additionally. In the presence of H_2PtCl_6 as a catalyst a monoadduct is usually formed as a sole product. Although the stereochemistry is exclusively cis addition, two regioisomers are usually formed from terminal acetylenes. The terminal adducts are the major products, but a terminal/internal ratio depends upon the reaction conditions as well as the structure of the acetylenes. While *tert*-butylacetylene and phenylacetylene give only the terminal adducts, 1-hexyne, as a representative example of simple acetylenes, at the reflux temperature forms the two regioisomers in the ratio of ca. 82/18.[15]

Recently we have observed that the regioselectivity is remarkably improved up to 95/5 by using a preactivated catalyst which is prepared by refluxing a mixture of chloroplatinic acid as a catalyst precursor and small amounts of two reactants, 1-hexyne and trichlorosilane.[16] Fortunately the terminal adducts (*E*)-alkenyltrichlorosilanes are readily separated from their internal isomers by fractional distillation. Hydrosilylation of internal acetylenes proceeds without isomerization of the triple

(14) The hydrosilylation product of 1-hexen-5-one tends to undergo the thermal intramolecular condensation to form a cyclic enol silyl ether.

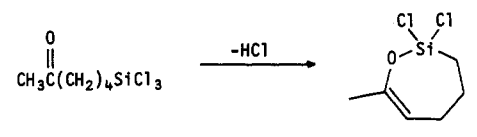

(15) Cf., Miller, R.; McGarvey, G. *J. Org. Chem.* 1978, *43*, 4424.

(16) This procedure is based on the observation made by Dr. K. Nakagawa of our laboratories, who found that the distillation residue of the traditional H_2PtCl_6-catalyzed hydrosilylation was an effective catalyst for the highly regioselective hydrosilylation of terminal acetylenes.

(17) Mueller et al. have noted the formation of $(NH_4)_2[C_3H_7SiF_5]$ in an impure state from allyltrifluorosilane and aqueous NH_4F.[3i]

Table II. Preparation of Alkenylpentafluorosilicates via Hydrosilylation of Acetylenes

acetylene	hydrosilylation[a] conditns	product	terminal, %	yield, %	silicate formation[b] yield, %
n-$C_4H_9C{\equiv}CH$	2 °C or rt,[c] 15 h	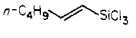	95[d]	75	94
t-$C_4H_9C{\equiv}CH$	rt,[e] 12 h	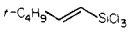	100[f]	72	80
n-$C_6H_{13}C{\equiv}CH$	80 °C, 20 h	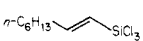	86[d]	92	90
n-$C_{16}H_{33}C{\equiv}CH$	rt,[e] 48 h	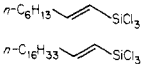	100[f]	83	45[g]
$CH_3O_2C(CH_2)_8C{\equiv}CH$	rt,[e] 20 h	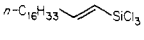	87[d]	93	88
$CH_3OCH_2C{\equiv}CH$	55 °C, 8 h	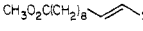	78[d]	85	94
$NC(CH_2)_2OCH_2C{\equiv}CH$	rt,[e] 20 h	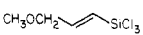	87[d]	93	73
$PhC{\equiv}CH$	rt, 20 h	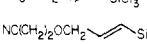	100[f]	88	100[g]
n-$C_4H_9C{\equiv}CC_4H_9$-n	100 °C, 24 h[h]	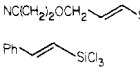		90	93
n-$C_6H_{13}C{\equiv}CC_6H_{13}$-$n$	100 °C, 43 h	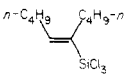		89	55[i]

[a] Hydrosilylation of acetylenes was carried out with excess (1.2–2.0 parts) trichlorosilane in the presence of chloroplatinic acid. [b] The alkenyltrichlorosilane was added dropwise to excess (25 parts) aqueous KF at 0 °C unless otherwise stated. [c] rt = room temperature. A preactivated catalyst was used (see text). [d] Determined by GLC. [e] An exothermic reaction took place when trichlorosilane was added to a mixture of the acetylene and the catalyst. After it ceased, the reaction mixture was stirred at room temperature. [f] GLC analysis and ^1H NMR spectrum of the product showed that only the terminal adduct was formed. [g] The alkenyltrichlorosilane was treated with KF in ethanol. [h] In a sealed tube. [i] The alkenyltrichlorosilane was treated with KF in ethanol-water (1:1).

bond to give the internal (E)-alkenyltrichlorosilanes. Experimental results for these transformations are summarized in Table II.

Preparation of Organopentafluorosilicates. Although Mueller had described briefly the direct preparation of ammonium methylpentafluorosilicate from the corresponding methyltrichlorosilane,[4i] we examined the most convenient and reproducible procedure from the synthetic point of view. Most of potassium organopentafluorosilicates could be prepared by the simple dropwise addition of an organotrichlorosilane (1 mol) to a solution of potassium fluoride (25 mol) in water (1.5 times the weight of KF, almost a saturated solution) at 0 °C with vigorous stirring. The silicate which precipiated as white powder was separated by filtration.

$$\underset{1:25}{RSiCl_3} + KF \xrightarrow[0\ ^\circ C\text{–room temp}]{H_2O} K_2[RSiF_5]$$

For styryltrichlorosilanes and long-chain alkyl- and alkenyltrichlorosilanes such as n-octadecyl-, 1-octadecenyl-, and 7-tetradecenyltrichlorosilanes, this procedure seemed to be less suitable, the silicates being contaminated with substantial amounts of siloxanes (by IR). Switching the reaction medium from water to ethanol afforded satisfactory results for these substrates. Yields of the silicates are given in Tables I and II.

Potassium organopentafluorosilicates thus obtained are all white, air-stable powder. While alkylsilicates can be stored almost indefinitely (longer than 2 years) in a closed polyethylene bottle at room temperature without any noticeable change (IR and reactivity), alkenylsilicates tend to decompose slowly at room temperature and can best be stored in a refrigerator. They exhibit intense IR absorptions in the 400–800-cm^{-1} region which are assigned to Si–F stretching.[4p]

Since they are practially insoluble in water and common organic solvents, purification of organopentafluorosilicates was quite difficult and some of them did not show satisfactory elemental analyses. They were used in further reactions directly as obtained.

Allylic trichlorosilanes gave no organosilicates under similar conditions but only the carbon–silicon bond cleavage product and hexafluorosilicate.[17] The cleavage reaction was accompanied by the allylic transposition, as exemplified by the conversion shown in eq 1.

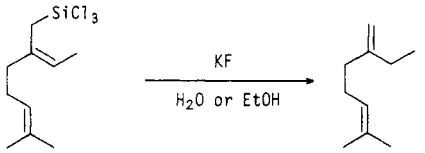

(1)

Several types of organopentafluorosilicates containing other countercations have been known.[2] Since it was expected that their reactivity would depend upon the nature of the countercation, we prepared octylpentafluorosilicates containing other alkali-metal countercations by the reaction of octyltrifluorosilane with NaF, RbF, and CsF in acetonitrile. $Na_2[C_8H_{17}SiF_5]$ was obtained as white powder which was insoluble in water and common organic solvents (75% yield). Its elemental analysis was not satisfactory because of contamination of some impurities, the removal of which was quite difficult due to insolubility of the silicate. $Rb_2[C_8H_{17}SiF_5]$ (87% yield) and $Cs_2[C_8H_{17}SiF_5]$ (85% yield) were also obtained as white powder. Both of them were slightly souble in ethanol. They could be recrystallized from hot ethanol and satisfactory elemental analyses were obtained. These three octyl silicates showed similar characteristic IR absorptions at 400–800 cm^{-1} as their potassium analogues. Octylpentafluorosilicates containing lithium and alkali earth metals such as calcium and barium could not be prepared in a similar fashion.

UV Spectra of Organopentafluorosilicates. In order to get information about the bonding character of hexacoordinate organopentafluorosilicates, we have measured UV spectra of several representative compounds in a solid state (Nujol mull). The results are reproduced in Figure

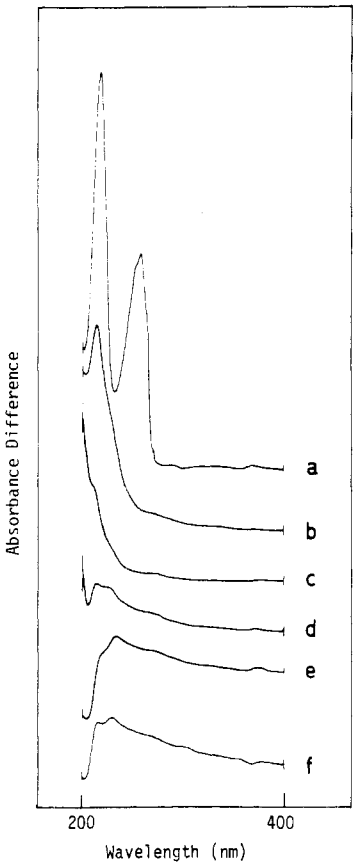

Figure 1. Ultraviolet spectra of (a) $K_2[PhSiF_5]$, (b) $K_2[C_4H_9C{=}CHSiF_5]$, (c) $K_2[cyclo\text{-}C_6H_{11}SiF_5]$, (d) $K_2[n\text{-}C_8H_{17}SiF_5]$, (e) $K_2[MeSiF_5]$, and (f) $K_2[SiF_6]$ in a solid state (Nujol mull).

Table III. UV Spectral Data of $K_2[RSiF_5]$, $RSiF_3$, and $RSiMe_3$

R	λ_{max}, nm (ϵ)		
	$K_2[RSiF_5]$[a]	$RSiF_3$[b]	$RSiMe_3$
Ph-	215[c]	208 (7.4×10^3)[d]	211 (1.03×10^4)[e]
	256	264 (8.3×10^2)	260 (3×10^2)
C_4H_9	211[c]	<200	<200[b]

[a] Solid state (Nujol mull). [b] In cyclohexane. [c] Intensities are not known. [d] Lit. data 210.0 and 263.5 nm: Veszpremi, T.; Reffy, J.; Nagy, J. *Kem. Kozl.* **1976**, *46*, 418; private communication from Professor T. Veszpremi. [e] In ethanol: Nagy, J.; Reffy, J.; Kuszmann-Borbely, A.; Becker, K. P. *J. Organomet. Chem.* **1967**, *7*, 393.

1. While the intensities of absorptions could not be determined, the absorption maxima are reliable. It seems to be interesting to compare the UV data of the phenyl- and hexenylsilicates with those of the corresponding trifulorosilyl and trimethylsilyl counterparts[18] (Table III). For the phenyl series the silicate exhibits an appreciable red shift of the primary band in comparison with the tetracoordinate compounds. A simple comparison of the benzenoid fine-structure band should be avoided owing to the difference of the state. It is also worth noting that hexenylsilicate has an absorption maximum at 211 nm, making a sharp contrast with the trifluorosilyl and trimethylsilyl derivatives which show no absorption maxima above 200 nm. Alkylsilicates and inorganic hexafluorosilicate show similar spectral behavior, but it seems questionable whether the observed rather peculiar absorptions are significant or not. The most significant feature of the UV data is that while there seems to be a tendency that substitution of the methyl groups on silicon by electronegative fluorine atoms ($RSiF_3$ vs. $RSiMe_3$) causes a shift to shorter wavelength,[19] introduction of further fluorine atoms ($RSiF_5^{2-}$) leads conversely to a red shift.

(18) Ramsey, B. G. "Electronic Transitions in Organometalloids"; Academic Press: New York, 1969; Chapter IV, p 65.

Table IV. CNDO/S Calculation Data on $PhSiMe_3$, $PhSiF_3$, and $Na_2[PhSiF_5]$[a]

	$PhSiMe_3$	$PhSiF_3$	$Na_2[PhSiF_5]$
first three IP's (eV)	9.746 (π_3)	10.094 (π_3)	7.707 (π_3)
	9.873 (π_2)	10.248 (π_2)	8.154 (π_2)
	11.469 (Si-C(ar))	12.298 (Si-C)	8.290 (Si-C)
UV absorptions above 200 nm (nm)	209	205	208
	259	255	257
bond order of the Si-C bond	1.039	1.042	0.914

[a] Carried out by Professor T. Veszpremi, private communication. The calculation includes d orbitals.

Recently, Veszpremi carried out the MO calculation (modified CNDO/S)[20] on phenylsilicon compounds including $PhSiMe_3$, $PhSiF_3$, and $Na_2[PhSiF_5]$.[21] Table IV lists the calculated first three ionization potentials, UV absorption maxima (>200 nm), and bond order of the silicon–C(ar) σ bond. Only the results on the calculation with d orbitals are listed, but the calculation without d orbitals shows quite similar results except for the silicate, the results for which will be briefly mentioned below. There are several remarkable features. (1) The ionization potentials decrease in the order $PhSiF_3 > PhSiMe_3 \gg Na_2[PhSiF_5]$. (2) The most striking feature is that in the phenylsilicate the ionization potential of the Si–C σ bond is comparable with those of the phenyl π electrons, while in $PhSiMe_3$ and $PhSiF_3$ the σ-bonding energy level lies much lower than the aromatic π levels. This correlation may be visualized in Figure 2. Interestingly, the calculation without d orbitals for the silicate shows that the ionization potential assignable to the Si–C σ bond (7.006 eV) is lower than π_3 (7.238 eV) and π_2 (7.791 eV). (3) The bond order of the Si–C σ bond in the silicate becomes considerably lower than those in the tetracoordinate silicon compounds. (4) The calculated UV absorption maxima agree with the experimental data shown in Table III.

It seems to be most informative to compare the data on $PhSiF_3$ and the corresponding silicate. Thus, the coordination of extra two fluoride ions to $PhSiF_3$ lowers the

(19) Cf. Petukhov, V. A.; Mironov, V. F.; Kravchenko, A. L. *Izv. Akad. Nauk SSSR, Ser. Khim.* **1966**, 156.

(20) Bene, J. E.; Jaffe, H. H. *J. Chem. Phys.* **1968**, *48*, 1807.

(21) Veszpremi, T., unpublished results (private communication). The calculation assumes the following octahedral geometry for the silicate

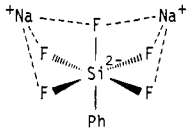

The Si–F bond distance 1.676 Å is based on the published data on the crystal structures of hexafluorosilicates.[22] The Na–F distance of 2.36 Å is estimated to be the summation of the ionic radii of Na^+ and F^-. Since the calculated ionization potentials for $PhSiMe_3$ and $PhSiF_3$ are in good agreement with the experimental data, it is reasonable to suppose that the present calculation gives good estimation also for the phenylsilicate.

(22) Cu^{2+}, Co^{2+}, Ni^{2+}, and Zn^{2+} salts: (a) Ray, S.; Zalkin, A.; Templeton, D. H. *Acta Crystallogr., Sect. B* **1973**, B29, 2741, 2748. Ammonium salt: (b) Hanic, F. *Chem. Zvesti* **1966**, *20*, 738; *Chem. Abstr.* **1967**, *66*, 89253.

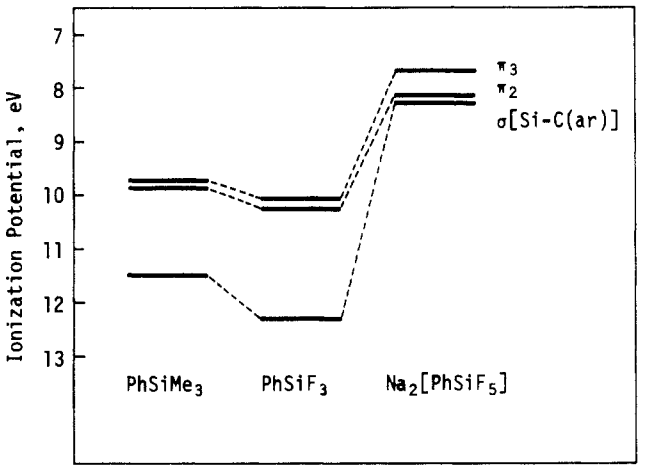

Figure 2. A schematic energy-level diagram for the calculated first three ionization potentials.

Si–C σ bond order and raises extremely the Si–C σ bond energy level up to the levels comparable to the aromatic π-bonding levels. These unique bonding characteristics of organopentafluorosilicates may be responsible for their susceptibility toward various electrophilic or oxidizing agents. It seems interesting to note here that the low ionization potential is comparable with 8.76 eV (by photoelectron spectroscopy)[23] of the silicon–silicon bond which has been well-known to be cleaved by various oxidizing agents including halogen and NBS.[24]

Reaction of Organopentafluorosilicates with Halogens and Interhalogen. Alkylpentafluorosilicates have been found to react exothermically with halogens such as chlorine, bromine, and iodine in carbon tetrachloride to give the corresponding alkyl halides in good yields.

$$K_2[RSiF_5] \xrightarrow{X_2} R\text{-}X \ (X = Cl, Br, I)$$

The results are summarized in Table V. While Mueller observed brominolysis of methylpentafluorosilicate in water containing extra fluoride ions,[4i] our findings revealed that extra fluorides are not requisite for the halogenolysis of organopentafluorosilicates.

The reaction occurred heterogeneously, and the insoluble residue was easily separated by filtration. The IR spectrum of the residue showed only two intense absorptions at 735 and 475 cm^{-1} diagnostic of a hexafluorosilicate, SiF_6^{2-}, salt.[4p]

While the reaction of the primary alkylsilicates proceeded even at 0 °C, the reaction of the secondary alkylsilicates was rather slow and required higher temperatures, indicating that the present halogen-cleavage reaction is subject to the steric hindrance around the carbon. Iodine was less reactive than bromine and chlorine. For example, the reaction of cyclohexylpentafluorosilicate with iodine proceeded appreciably only around 50 °C.

The alkenyl- and arylpentafluorosilicates were also found to react with halogens to give the corresponding organic halides. The halogen atom was regioselectively introduced onto the carbon to which the silicon atom had been attached. Stereoselectivity of the reaction of alkenylsilicates with bromine was not satisfactory. For example, the reaction of (*E*)-1-hexenylpentafluorosilicate with bromine gave both (*E*)- and (*Z*)-1-hexenyl bromides in the ratio of 67/33, while the reaction with iodine gave (*E*)-1-hexenyl iodide almost exclusively.

(23) Bock, H.; Ensslin, W. *Angew. Chem.* **1971**, *83*, 435.
(24) Kumada, M.; Tamao, K. *Adv. Organomet. Chem.* **1968**, *6*, 19.

Table V. Reaction of Organopentafluorosilicates with Halogens[a]

R in $K_2[RSiF_5]$	halogen	product	yield,[b] %
n-C_8H_{17}-	Cl_2	n-$C_8H_{17}Cl$	73
	Br_2	n-$C_8H_{17}Br$	69
	I_2	n-$C_8H_{17}I$	73
t-$C_4H_9CH_2CH_2$-	Br_2	t-$C_4H_9CH_2CH_2Br$	(74)[c]
	Cl_2		(47), (54)[d]
	Br_2		(67), (63)[d]
	I_2		(5),[d] (32)[e]
	Br_2	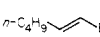 (67% *E*)[f]	(61)
	I_2	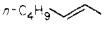 [g]	(48)
Ph-	Br_2	PhBr	(59)

[a] The reactions were carried out on a 5-mmol scale for isolation of the product and on a 1-mmol scale for GLC determination of yields. Halogen in CCl_4 was added dropwise to a mixture of a $K_2[RSiF_5]$ and CCl_4 at 0 °C. After the addition was completed, the mixture was stirred for 2 h at room temperature unless otherwise stated. [b] Isolated yields. Yields determined by GLC analysis are given in parentheses. [c] Stirred at room temperature for 9 h. [d] Carried out at 35 °C for 1 h. [e] Carried out at 50 °C for 1 h. [f] Determined by GLC. [g] (*Z*) isomer was not detected.

Table VI. Reaction of Organopentafluorosilicates with Iodine Monobromide

R in $K_2[RSiF_5]$, mmol	IBr, mmol	temp, °C	time, min	product yield,[b] % R-I	R-Br
n-C_8H_{17}-, 2.0	1.1	0	30	63	6
1.9	0.99[c]	0	10	68	7
 1.0	1.0	20	120	17	27
 , 0.97	0.70	20	120	90	3
Ph-, 1.0	0.37	20	30	83	0

[a] Because iodine monobromide was contaminated by chlorine, a small amount of R-Cl was formed as a byproduct. [b] Yields were based on IBr and determined by GLC analysis. [c] I_2 (0.10 mmol) was added in order to remove free Br_2 in IBr.

Organopentafluorosilicates have been found to react with iodine monobromide (Table VI).

$$K_2[RSiF_5] + IBr \rightarrow RI + RBr$$

The distribution of the products may provide important information about the mechanism of the halogenolysis of organopentafluorosilicates (vide infra). The reaction of the octylsilicate with IBr in carbon tetrachloride gave both octyl iodide and octyl bromide in 63–68 and 6–7% yields, respectively. The cyclohexylsilicate gave cyclohexyl iodide and cyclohexyl bromide in comparable amounts, but the formation of organic bromides was greatly retarded with silicates containing an sp^2 carbon–silicon bond. The reaction of the 1-hexenylsilicate with IBr gave 1-hexenyl iodide almost exclusively, and only iodobenzene was obtained in the reaction of the phenylsilicate.

Reaction of organopentafluorosilicates with NBS. Organopentafluorosilicates were also found to undergo a rapid, usually exothermic reaction with *N*-bromosuccinimide (NBS) to give the corresponding organic bromides in high yields. The bromine atom was regioselectively

introduced onto the carbon to which the silicon atom had been attached. This reaction provides the frst case of the carbon–silicon bond cleavage reaction by NBS.

$$M_2[RSiF_5] + NBS \rightarrow RBr$$

Reactions of octylpentafluorosilicates containing four different alkali-metal countercations were examined. The results are summarized in Table VII. Although the reactions of $K_2[C_8H_{17}SiF_5]$, $Rb_2[C_8H_{17}SiF_5]$, and $Cs_2[C_8H_{17}SiF_5]$ with NBS proceeded smoothly to give octyl bromide in excellent yields, the reaction of $Na_2[C_8H_{17}SiF_5]$ was much slower and the yield was very low. The results, however, do not necessarily reflect the difference in reactivity of the carbon–silicon bond due to the countercation because there is a possibility that impurities in the sodium salt might have retarded the reaction.

The reactivities of the Rb and Cs derivatives were found to be comparable with the reactivity of $K_2[RSiF_5]$, but the use of the latter may be the most practical from the synthetic viewpoint, because they are most readily obtainable and KF is available at relatively low cost in comparison with RbF and CsF.

The stoichiometry of the NBS cleavage reaction may be written as shown in eq 2, based on the deuterium exper-

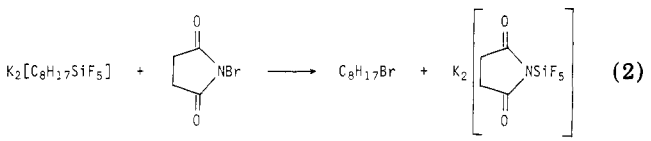

(2)

iments. Thus, the reaction between the octylsilicate and NBS in dry THF under nitrogen gave, together with octyl bromide, yellow insoluble precipitates which showed infrared absorptions at 1690 (C=O) and 800–670 cm^{-1} (fluorosilicates). The precipiates formed succinimide (IR 3150–3050, 1690 cm^{-1}) upon treatment with ethanol and *N*-deuteriosuccinimide (IR 2300, 1690 cm^{-1}) upon treatment with MeOD. The results are consistent with the formation of a succinimidyl–silicon species in the above reaction. Anyway, such a silicon moiety as well as the starting organosilicate is insoluble in the reaction medium, and hence the desired organic product can be readily separated by filtration. This provides one of the advantages of reactions of organopentafluorosilicates.

A wide-spread applicability of the present cleavage reaction is apparent from the data on various alkylsilicates and alkenylsilicates, summarized in Tables VIII and IX, respectively. The nature of the reaction medium did not significantly affect the yield, at least in the reaction of primary alkylsilicates, although aliphatic hydrocarbon and alcoholic solvents seemed to be less favorable. In contrast, methanol was the most suitable for the secondary alkylsilicates. The high yields of primary alkyl halides should particularly be noted, because this procedure provides a new convenient route to anti-Markownikoff hydrohalogenation of olefins under neutral conditions.[25] Rather low yields of alkyl bromides from (3,3-dimethylbutyl)-silicate (t-$C_4H_9CH_2CH_2SiF_5^{2-}$), even at 60 °C for 8 h, and from the secondary alkylsilicates indicate that the reaction with NBS is also subject to the steric hindrance around the reacting carbon. Another significant feature the present reaction is that it is compatible with various functional groups such as alkoxycarbonyl, oxo, halo, and alkenyl groups. Therefore the transformation involving

(25) Halogenolysis of organoboranes requires strongly basic conditions.[11] Procedures using other oganometallic compounds suffer from the rather limited functional group compatibility.

Table VII. Reaction of $M_2[C_8H_{17}SiF_5]$ with NBS[a]

M in $M_2[C_8H_{17}SiF_5]$	yield of $C_8H_{17}Br$,[b] %
Na[c]	31[d]
K	99
Rb	96
Cs	93

[a] $M_2[C_8H_{17}SiF_5]$ (1.0 mmol) was allowed to react with 1.1 mmol of NBS in 5.0 mL of benzene at room temperature for 2 h. [b] The yields were determined by GLC. [c] Purity of the silicate was not satisfactory. See the text for details. [d] The reaction was very slow, and after 160 h $C_8H_{17}Br$ was obtained in 66% yield.

Table VIII. Reaction of Alkylpentafluorosilicates with NBS[a]

R in $K_2[RSiF_5]$	solvent	time, h	product	yield,[b] %
n-C_8H_{17}-	C_6H_6	2	n-$C_8H_{17}Br$	77 (99)
	CCl_4	2		(99)
	THF	2		(98)
	Et_2O	2		(91)
	n-hexane	2		(78)
	MeOH	2		(72)
n-$C_{12}H_{25}$-	C_6H_6	2	n-$C_{12}H_{25}Br$	75
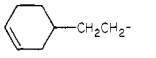	C_6H_6	2	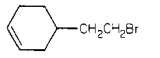	54
t-$C_4H_9CH_2CH_2$-	CCl_4	8[c]	t-$C_4H_4CH_2CH_2Br$	(46)
$PhCH_2CH_2$-	C_6H_6	2	$PhCH_2CH_2Br$	(60)
$MeO_2C(CH_2)_{10}$-	C_6H_6	2	$MeO_2C(CH_2)_{10}Br$	86
$Br(CH_2)_{11}$-	C_6H_6	2	$Br(CH_2)_{11}Br$	92
$CH_3CO(CH_2)_4$-	C_6H_6	28	$CH_3CO(CH_2)_4Br$	(73)
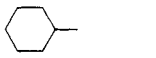	THF	2	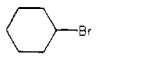	37
	MeOH	9		(79)

[a] The reactions were carried out on a 5-mmol scale for isolation of the product and on a 1-mmol scale for GLC determination of the yields using 1.1 equiv of NBS at room temperature. [b] Isolated yield based on the alkylsilicates. Yields determined by GLC analysis are given in parentheses. [c] Carried out at 60 °C. No reaction was observed at room temperature.

the present reaction can be applied to various types of compounds containing these functional groups.

Stereoselectivity of the reaction of alkenylsilicates with NBS was higher than that with bromine. For example, the reaction of (*E*)-1-hexenylsilicate with NBS gave 1-hexenyl bromide in the ratio of E/Z = 79–91/21–9, depending upon the nature of the reaction medium. In the reaction of the (*E*)-5-decenylsilicate, an example of the internal alkenylsilicate, (*E*)-5-bromo-5-decene was obtained with high stereoselectivity (>99% *E*). The predominant to complete retention of configuration of the double bond in the present transformation seems to be interesting because inversion has been the main stereochemical course of the so far developed preparation of alkenyl bromides from alkenyltrimethylsilanes by bromine cleavage.[15,26]

Synthetic Utility. Although there have been reported several synthetic procedures for the transformation to organic halides by means of hydrometalation of olefins[10-12] or acetylenes[27] such as hydroboration, hydroalumination,

(26) (a) Chan, T. H.; Lau, P. W. K.; Mychajlowskij, W. *Tetrahedron Lett.* **1977**, 3317. (b) Jarvie, A. W. P.; Holt, A.; Thompson, J. *J. Chem. Soc. B* **1969**, 852.

(27) Hydroboration: (a) Brown, H. C.; Hamaoka, T.; Ravindran, N. *J. Am. Chem. Soc.* **1973**, *95*, 5786. (b) Brown, H. C.; Hamaoka, T.; Ravindran, N. *Ibid.* **1973**, *95*, 6456. Hydroalumination: (c) Zweifel, G.; Whitney, C. C. *Ibid.* **1967**, *89*, 2753. (d) Zweifel, G.; Steele, R. B. *Ibid.* **1967**, *89*, 5085. Hydrozirconation: (e) Hart, D. W.; Blackburn, T. F.; Schwartz, J. *Ibid.* **1975**, *97*, 679.

Table IX. Reaction of Alkenyl- and Arylpentafluorosilicates with NBS[a]

R in $K_2[RSiF_5]$	solvent	time, h	product	E/Z[b]	yield,[c] %
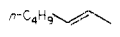	C_6H_6	4	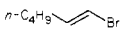	91/9	(75)
	THF	4		79/21	(80)
	MeOH	4		83/17	(73)
	MeOH	24		100/0	(83)
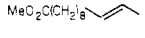	C_6H_6	2	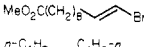	>95/<5[d]	68
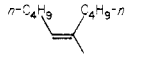	C_6H_6	2	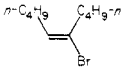	>99/<1	(70)
Ph-	MeOH	10	PhBr		(74)

[a] The reactions were carried out on a 5-mmol scale for isolation of the product and on a 1-mmol scale for determination of the yields using 1.1 equiv of NBS at room temperature. [b] Determined by GLC analysis. [c] Isolated yield based on the organosilicate. Yields determined by GLC analysis are given in parentheses. [d] The Z isomer was not detected by ^1H NMR.

and hydrozirconation, the following features and advantages may prove that the transformation via organopentafluorosilicates is an attractive alternative to these published procedures. (1) Regio and stereoselectivity of

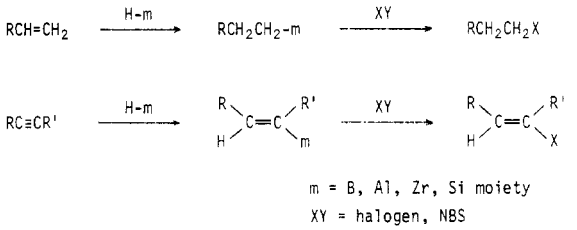

the hydrosilylation have been well established. (2) Various kinds of catalysts exhibiting different selectivities for the hydrosilylation have been discovered.[28] (3) A ready accessibility of less expensive, air-stable trichlorosilane allows a large scale preparation, in comparison with similar conversions using organoboron, -aluminum or -zirconium compounds. (4) In contrast to air-sensitive organoboron or -aluminum analogues, organopentafluorosilicates are air-stable and hence no special precaution in handling is necessary. (5) Reactions with organopentafluorosilicates proceed under mild neutral conditions and give high yields of products with wide functional group compatibility and high regio- and stereoselectivity. (6) Fluorosilicates, either the starting material or the reaction byproduct, mostly hexafluorosilicate, are almost insoluble in common organic solvents. Therefore, the desired organic product can be separated by simple filtration only.

Stereochemistry at Aliphatic Carbon in the Cleavage of the Carbon–Silicon Bond by Bromine and NBS. Not only to elucidate mechanism but also to get the basis for new methods of controlling stereochemistry in organic synthesis using organosilicates, we have examined the stereochemistry at carbon in the reactions of *exo*- and *endo*-2-norbornylpentafluorosilicates with bromine and NBS. Both reactions (eq 3 and 4) were found to

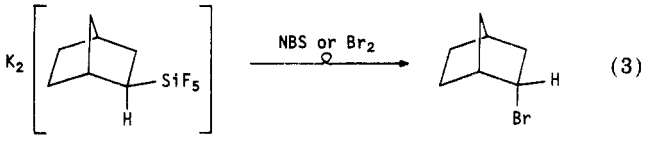

(3)

(4)

(28) For new catalysts for hydrosilylation, see: Yamamoto, K.; Hayashi, T.; Zembayashi, M.; Kumada, M. *J. Organomet. Chem.* **1976**, *118*, 161 and references cited therein.

Scheme II

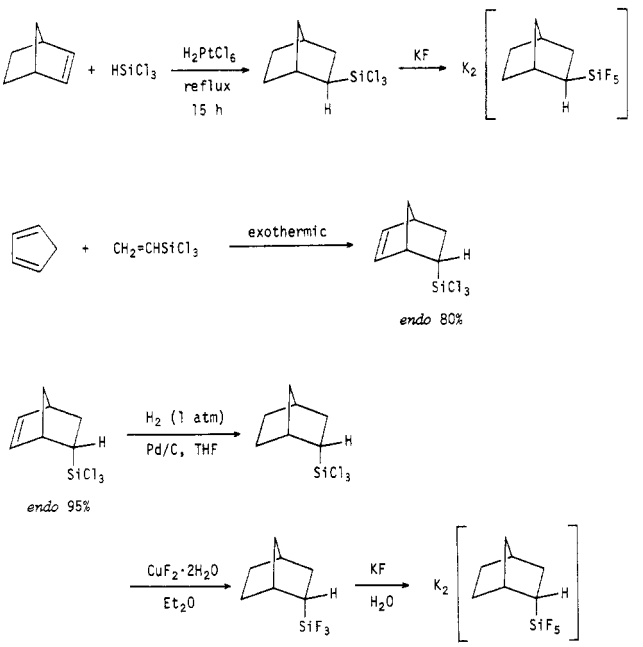

proceed stereospecifically with predominant inversion of configuration. This is the first stereochemical aspect at carbon in electrophilic intermolecular cleavage of aliphatic carbon–silicon bonds.[29]

exo- and *endo*-2-norbornylpentafluorosilicates were prepared as shown in Scheme II. *exo*-2-Norbornyltrichlorosilane was prepared by the stereoselective hydrosilylation of norbornene with trichlorosilane catalyzed by chloroplatinic acid.[30] The silicate formation could be achieved in the usual manner by treatment with aqueous KF. *endo*-2-Norbornyltrichlorosilane (endo 95%) was prepared by the palladium-charcoal-catalyzed hydrogenation (1 atm) of *endo*-norborn-5-en-2-yltrichlorosilane which was obtained by careful fractional distillation of the Diels–Alder adducts[30,31] between vinyltrichlorosilane and

(29) It has been shown that the base-catalyzed intramolecular rearrangement of α-silylbenzyl alcohols to silyl ethers proceeds with inversion at carbon: (a) Biernbaum, M. S.; Mosher, H. S. *J. Am. Chem. Soc.* **1971**, *93*, 6221. (b) Brook, A. G.; Pascoe, J. D. *Ibid.* **1971**, *93*, 6224. Brominolysis of the aryl–silicon bond has been found to proceed with inversion of configuration at silicon: (c) Eaborn, C.; Steward, O. W. *J. Chem. Soc.* **1965**, 521.

(30) (a) Petrov, A. D.; Plate, A. F.; Chernyshev, E. A.; Dolgaya, M. E.; Belikova, N. A.; Krasnova, T. L.; Leites, L. A.; Pryanishnikova, M. A.; Taits, G. S.; Kozyrkin, B. I. *Zh. Obsh. Khim.* **1961**, *31*, 1199. (b) Kuivila, H. G.; Warner, C. R. *J. Org. Chem.* **1964**, *29*, 2845. (c) Green, M.; Spencer, J. L.; Stone, F. G. A.; Tsipis, C. A. *J. Chem. Soc., Dalton Trans.* **1977**, 1159.

(31) (a) Wagner, G. H.; Bailey, D. L.; Pines, A. N.; Dunham, M. L.; McIntire, D. B. *Ind. Eng. Chem.* **1953**, *45*, 367. (b) Cunico, R. F. *J. Org. Chem.* **1971**, *36*, 929.

Table X. Cleavage Reactions of *exo*- and *endo*-Norbornylsilicate with Bromine and NBS To Form 2-Norbornyl Bromide

reagent	solvent	exo/endo ratio[a] (yield of bromide,[b] %) from exo	from endo[c]
Br_2[d]	MeOH	5/95 (57)	96/4 (56)
	THF	5/95 (31)	96/4 (43)
	benzene	42/58 (67)	98/2 (58)
	CCl_4	27/73 (63)	97/3 (57)
NBS[e]	MeOH	2/98 (71)	98/2 (70)
	THF	10/90[f] (33)	96/4[f] (42)
	benzene	7/93 (8)	94/6 (3)
	CCl_4	2/98 (6)	98/2 (3)

[a] Determined by ^1H NMR (≤±5%). [b] Determined by GLC. [c] endo 95%. Ratios are corrected, based on this purity. [d] At 0 °C-room temperature for 4 h. [e] At 50 °C for 4 h. [f] The bromide was contaminated with unknown impurities.

cyclopentadiene. The trichlorosilyl derivative was converted into the trifluorosilyl derivative by treatment with copper(II) fluoride dihydrate in ether and then reacted with aqueous KF to give the *endo*-silicate. During the silicate formation no stereochemical scrambling occurred, as confirmed by comparison of the isomeric purity of 2-norbornyltrimethylsilane[31] obtained by methylation (MeMgBr in ether) of the silicates with that obtained from the trichlorosilyl precursors.

Table X summarizes the stereochemistry of the cleavage of *exo*- and *endo*-2-norbornylpentafluorosilicates with bromine and NBS in methanol, THF, benzene, and carbon tetrachloride. The exo/endo ratios of 2-norbornyl bromide were determined by ^1H NMR analysis (2-methine proton ratio) of a crude product after usual workup.[32] The bromine cleavage in polar solvents proceeded in a highly stereospecific fashion with greater than 95% inversion of configuration at carbon. In nonpolar solvents, a low order of stereoselectivity was observed for the cleavage of the exo isomer, while the cleavage of the endo isomer proceeded with higher than 97% inversion. Predominant inversion (≥93%) has also been observed in the NBS cleavage. The reaction was very sluggish in nonpolar solvents such as benzene and carbon tetrachloride, but stereospecificity was little dependent upon the nature of the solvent.

The present stereospecific cleavage, particularly with NBS in methanol, provides the most efficient and convenient method for the stereoselective preparation of *endo*-2-norbornyl bromide (endo 98%). On the basis of the high stereospecificity, we have recently demonstrated that optically active organic halides can be synthesized from olefins via the chiral phosphine palladium complex catalyzed asymmetric hydrosilylation.[33]

Reaction Mechanism of the Cleavage of Carbon–Silicon Bonds in Organopentafluorosilicates by Halogens and NBS. Since kinetic data are not available owing to the insolubility of organosilicates, the reaction mechanism will be discussed, mainly based on the stereochemical aspects. Much attention has been paid to the stereochemistry of electrophilic cleavage of carbon–metal bonds,[34] and both retention and inversion of configuration

Scheme III

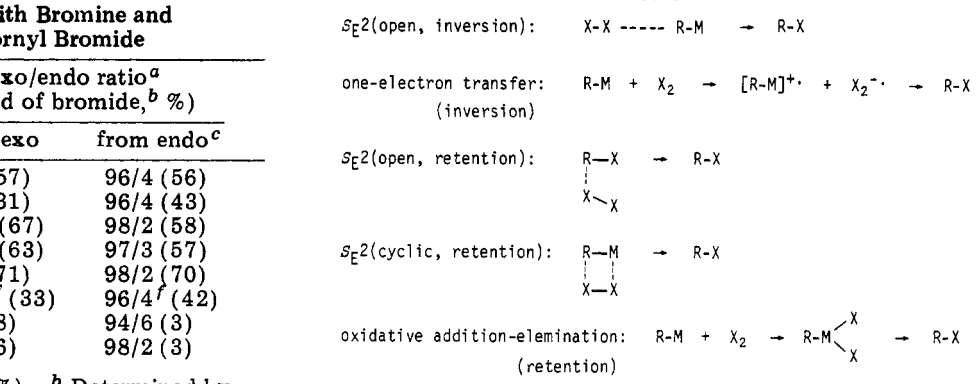

at carbon have been observed.[35,36] Attempts have recently been made to analyze the stereochemistry in terms of initial attack on a HOMO of a metal alkyl.[36j,k,w] Thus, for d^0 and d^{10} systems the HOMO would be a carbon–metal σ-bonding orbital, while for d^1–d^9 systems it would be either a nonbonding orbital of essentially d character or a carbon–metal σ-bonding orbital. Inversion may result from either an S_E2 (inversion) mechanism (attack on carbon) or one-electron transfer (attack on metal) followed by a backside attack by a nucleophile. Retention of configuration may result from either an S_E2 (retention) mechanism (attack on carbon) or an oxidative addition–reductive elimination sequence (attack on metal) (see Scheme III). Evidence for the electron-transfer mechanism has been obtained for halogenolysis of organoiron and -cobalt complexes.[37] For main-group organometallics, data as yet do not seem to be sufficient to rationalize the stereochemical courses. It should be noted that stereochemical observations relevant to our present results have recently been reported by Gielen and his co-workers.[36i] They

(32) We call attention to the ready epimerization of 2-norbornyl bromide on analytical and preparative GLC. In the early stage of this work, we have encountered this trouble, despite the fact that the literature has described the analysis and purification by GLC of this compound.[36a,c]

(33) Hayashi, T.; Tamao, K.; Katsuro, Y.; Nakae, I.; Kumada, M. *Tetrahedron Lett.* **1980**, *21*, 1871.

(34) For example: (a) Matteson, D. S. "Organometallic Reaction Mechanism"; Academic Press: New York, 1974. (b) Kochi, J. K. "Organometallic Mechanism and Catalysis"; Academic Press: New York, 1978; Chapter 18. (c) Johnson, M. D. *Acc. Chem. Res.* **1978**, *11*, 57. (d) Reutov, O. A. *Tetrahedron* **1978**, *34*, 2827.

(35) Jemmis, E. D.; Chendrasekhar, J.; Schleyer, P. V. R. *J. Am. Chem. Soc.* **1979**, *101*, 527.

(36) The halogen-cleavage reaction has been most extensively studied. Inversion of configuration has been shown for *lithium*: (a) Applequist, D. E.; Chmury, G. N. *J. Am. Chem. Soc.* **1967**, *89*, 875. (b) Glaze, W. H.; Selman, C. M.; Ball, A. L.; Bray, L. E. *J. Org. Chem.* **1969**, *34*, 641. *Boron*: (c) Brown, H. C.; Lane, C. F. *J. Chem. Soc. D* **1971**, 521. (d) Brown, H. C.; De Lue, N. R.; Kabalka, G. W.; Hedgecock, H. C., Jr. *J. Am. Chem. Soc.* **1976**, *98*, 1290. (e) Bergbreiter, D. E.; Rainville, D. P. *J. Organomet. Chem.* **1976**, *121*, 19. *Tin*: (f) Jensen, J. R.; Davis, D. D. *J. Am. Chem. Soc.* **1971**, *93*, 4048. (g) Rahm, A.; Pereyre, M. *Ibid.* **1977**, *99*, 1672. (h) McGahey, L. F.; Jensen, F. R. *Ibid.* **1979**, *101*, 4397. (i) Gielen, M.; Fosty, R. *J. Chem. Res., Synop.* **1977**, 214; *J. Chem. Res., Miniprint* **1977**, 2379. *Manganese*: (j) Dong, D.; Hunter, B. K.; Baird, M. C. *J. Chem. Soc., Chem. Commun.* **1978**, 11. (k) Dong, D.; Baird, M. C. *J. Organomet. Chem.* **1979**, *172*, 467. *Iron*: (l) Bock, P. L.; Boschetto, D. J.; Rasmussen, J. R.; Demers, J. P.; Whitesides, G. M. *J. Am. Chem. Soc.* **1974**, *96*, 2814. (m) Flood, T. C.; Miles, D. L. *J. Organomet. Chem.* **1977**, *127*, 33. *Cobalt*: (n) Jensen, F. R.; Madan, V.; Buchanan, D. H. *J. Am. Chem. Soc.* **1971**, *93*, 5283. (o) Anderson, S. N.; Ballard, D. H.; Chrzastowski, J. Z.; Dodd, D.; Johnson, M. D. *J. Chem. Soc., Chem. Commun.* **1972**, 685. (p) Magnuson, H.; Halpern, J.; Levitin, I. Y.; Vol'pin, M. E. *Ibid.* **1978**, 44. (q) Kitchin, J. P.; Widdowson, D. A. *J. Chem. Soc., Perkin Trans. 1* **1979**, 1384. Retention of configuration has been observed for *lithium*: (r) Applequist, D. E.; Peterson, A. H. *J. Am. Chem. Soc.* **1961**, *83*, 862. (s) Walborsky, H. W.; Impastato, F. J.; Young, A. E. *Ibid.* **1964**, *86*, 3283. *Tin*: ref 21 g. (t) Baeckelmans, P.; Gielen, M.; Nasielski, J. *Tetrahedron Lett.* **1967**, 1149. (u) Sisido, K.; Miyanishi, T.; Isida, T.; Kozima, S. *J. Organomet. Chem.* **1970**, *23*, 117. *Manganese*: ref 36j. (v) Johnson, R. W.; Pearson, R. G. *J. Chem. Soc. D* **1970**, 986. *Iron*: (w) Slack, D. A.; Baird, M. C. *J. Am. Chem. Soc.* **1976**, *98*, 5539. *Zirconium*: (x) Labinger, J. A.; Hant, D. W.; Seibert, W. E., III; Schwartz, J. *Ibid.* **1975**, *97*, 3851. *Palladium*: (y) Coulson, D. R. *Ibid.* **1969**, *91*, 200. *Mercury*: (z) Jensen, F. R; Whipple, L. D.; Wedegaertner, D. K.; Landgrebe, J. A. *Ibid.* **1960**, *82*, 2466. (z') Sayre, L. M.; Jensen, F. R. *Ibid.* **1979**, *101*, 1900.

(37) (a) Flood, T. C.; DiSanti, F. J. *J. Chem. Soc., Chem. Commun.* **1975**, 18. (b) Attig, T. G.; Teller, R. G.; Wu, S.-M.; Bau, R.; Wojcicki, A. *J. Am. Chem. Soc.* **1979**, *101*, 619.

have observed that stereochemistry at carbon in brominolysis of a tetraorganostannane dramatically changes from retention to inversion by the addition of a catalytic amount of the fluoride ion which coordinates to the tin atom to prevent the interaction with a nucleophilic part of the reagent.

Inversion stereochemistry observed in the bromine and NBS cleavage reactions of *exo*- and *endo*-2-norbornylpentafluorosilicates may result either from an S_E2 (open, inversion) process involving backside attack on carbon by a bromine or NBS molecule (A) or a one-electron-transfer mechanism leading to backside nucleophilic attack on carbon by a bromide ion (B).

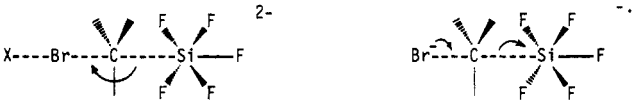

(A) (B)

The MO calculation mentioned above suggests that in alkylsilicates which have no π electrons the Si–C σ bond should be the HOMO having remarkably low ionization potential around 8.3 eV. An electrophilic agent may attack this silicon–carbon bond at first, suggesting the S_E2 (open, inversion) mechanism as a plausible process. We have recently show, however, that the facile reaction of the alkylsilicates with TCNE (tetracyanoethylene) proceeds through an initial one-electron transfer from the alkylsilicates to TCNE.[7j] The electron-transfer process may be favorable also in the present halogenation reactions.

Although no clear distinction between S_E2 and one-electron transfer mechanisms is possible at present, we suggest here the possibility of a one-electron-transfer mechanism for the inversion stereochemistry in bromine cleavage, based on the following arguments (cf. Scheme IV).

(1) The cleavage reaction occurred smoothly irrespective of the nature of the solvent. (2) The stereochemical scrambling observed with *exo*-2-norbornylsilicate in nonpolar solvents suggests the presence of a competing path which proceeds through the formation of an alkyl radical[38] or, if less likely, a carbonium ion.[39] Nucleophilic attack on the exo isomer from the more crowded endo side may be less favorable than that on the endo isomer from the exo side, particularly in nonpolar solvents. Partial diffusion of a norbornyl radical might occur from the "cage" arising from the exo silicate, giving rise to the formation of a mixture of exo and endo bromide. (3) The reaction of the alkylsilicates with IBr gave both the alkyl iodides and bromides. Generally the reaction with interhalogens such as IBr and ICl may provide a useful probe for distinguishing a one-electron-transfer mechanism from electrophilic cleavage.[34b,40] If both halogen atoms of IBr or ICl are transferred to the organic group, a one-electron-transfer mechanism may be operative, while if only the iodine atom is introduced, electrophilic cleavage is considered to be favorable. The present results for the alkylsilicates indicate that both fragments of the IBr might be an active attacking species on the carbon and are consistent with the one-electron-transfer mechanism.

Scheme IV

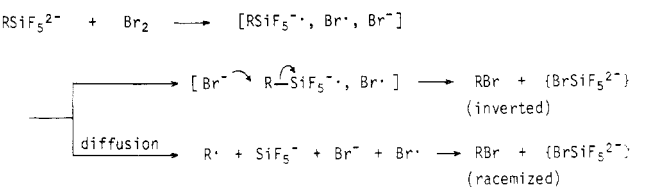

Scheme V

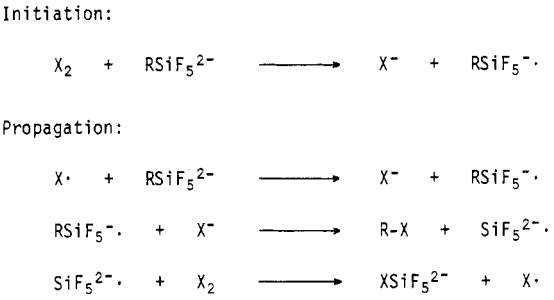

In addition to the nonchain mechanism shown in the above equation, a radical chain mechanism may also be possible, since one-electron transfer from the alkylsilicate to halogen can initiate the following radical chain processes (Scheme V). During the propagation steps the stereochemically inverted alkyl bromide is produced by nucleophilic backside attack of the halide ion on $RSiF_5^{-}\cdot$. Under some conditions $RSiF_5^{-}\cdot$ may decompose to R· and SiF_5^- resulting in racemization (cf. Scheme IV).

The NBS cleavage of the alkylsilicates seems to be mechanistically different from their bromine cleavage. The reaction of primary alkyl-silicates was too fast to observe the solvent effect, but retardation of the reaction of the 2-norbornylsilicates with NBS in nonpolar solvents implies that the transition state might involve a charge-separated species. Thus an S_E2 (inversion) mechanism would be plausible. The fact that the stereochemical scrambling did not occur in nonpolar solvents also supports the electrophilic mechanism.

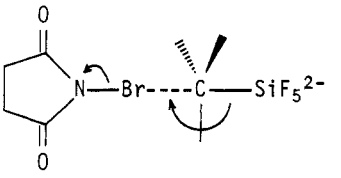

The reactions of aryl- and alkenylpentafluorosilicates with halogens seem to proceed by a different mechanism. Almost exclusive formation of organic iodides in the reactions with IBr inidicates that only potentially positive iodine attacked the carbon and the electrophilic cleavage would be plausible. Predominant formation of the (*E*)-alkenyl halides in the reaction of the (*E*)-alkenylsilicates with halogens and NBS may also support the electrophilic mechanism. It has already been reported that carbon–silicon bonds in the tetracoordinate alkenylsilanes, mostly alkenyltrimethylsilanes, were readily cleaved by bromine with predominant inversion of configuration with respect to the olefinic double bond.[15,16] A mechanism involving trans addition of bromine followed by the base-induced trans elimination of $BrSiMe_3$ has been proposed. Exceptionally, the reaction of styrylsilane with bromine has been observed to proceed with retention of configuration and a mechanism involving the attack of a bromonium ion producing the benzylic carbocation stabilized by the car-

(38) Bartlett, P. D.; Fickes, G. N.; Haupt, F. C.; Helgeson, R. *Acc. Chem. Res.* **1970**, *3*, 177 and reference cited therein.

(39) Interestingly, similar stereochemical phenomena have been observed for the conversion of 2-norbornanol to 2-norbornyl bromide by triphenylphosphine dibromide: Schaefer, J. P.; Weinberg, D. S. *J. Org. Chem.* **1965**, *30*, 2635, 2639.

(40) (a) Stock, L. M.; Spector, A. R. *J. Org. Chem.* **1963**, *28*, 3272. (b) Bhattacharya, S. N.; Raj, P.; Srivastava, R. C. *J. Organomet. Chem.* **1976**, *105*, 45. (c) Dreos, R.; Tauzher, G.; Marsich, N.; Costa, G. *Ibid.* **1976**, *108*, 235. (d) Espenson, J. H.; Samuels, G. J. *Ibid.* **1976**, *113*, 143. (e) Dreos, R.; Tauzher, G.; Marsich, N.; Costa, G. *Ibid.* **1975**, *92*, 227.

bon–silicon σ bond was suggested.[41] The reaction of hexacoordinate alkenylpentafluorosilicates with halogens and NBS is considered to proceed by a mechanism similar to that proposed for the styrylsilane. As shown in eq 5, the carbocation may be stabilized by the electron-rich silicon moiety which is coordinatively saturated and ready for the elimination.

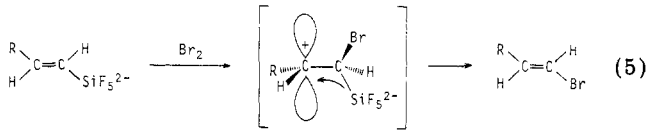

(5)

Formation of the (*Z*)-alkenyl bromide as the minor product in the reaction of the (*E*)-alkenylsilicates with bromine may be ascribed to either the partial radical nature of the reaction or the competing addition–elmination pathway. Further mechanistic studies, currently in progress in our laboratories,[42] on the electrophilic cleavages of alkenylsilicon compounds will hopefully delineate the mechanism in detail.

Summarizing Remarks

We have developed a new methodology for the transformation of olefins and acetylenes to the corresponding alkyl and alkenyl halides, respectively, via a sequence of hydrosilylation, silicate formation, and halogen or NBS cleavage of the silicon–carbon bond. In light of the novel properties of the organosilicates such as air stability and facile reactivity, mildness of reaction conditions, high regio- and stereoselectivity of the cleavage reactions, and high yields of products, the present method may prove to be synthetically useful as an alternative to hitherto developed hydrometalation reactions. The present method is based on the unique reactivity of doubly-negatively charged hexacoordinate organosilicates which may have remarkably low ionization potential assignable to the silicon–carbon σ bond, as suggested by the MO calculation. Further work should be directed to accumulate the experimental data on the bonding character and to establish the structure–reactivity correlation.

Experimental Section

General Remarks. Infrared spectra were recorded on a Hitachi EPI-G3 grating infrared spectrometer. ^{1}H NMR spectra were determined with a JEOL JNM-MH-100 (100-MHz) spectrometer in carbon tetrachloride. Chemical shifts (δ) are recorded in parts per million downfield from Me_4Si. Mass spectra were measured on a JEOL JMS-D300 mass spectrometer connected with a JEOL LGC-20K gas chromatograph, equipped with a 1-m glass column packed with OV-17 (1%) on Chromosorb B, and a JMA-2000 data processing system. Ionization voltage was 24 eV for all compounds. UV spectra of organosilicates in the solid state were recorded on a Shimadzu UV-300 spectrophotometer and other UV spectra on a Hitachi 340 recording spectrophotometer. GLC analyses and preparative purification were performed on a Shimadzu GC-4B gas chromatograph, equipped with a 3-m column packed with 30% Silicone DC550 on Chromosorb B or Celite 545. GC peak integrals were recorded by using a Shimadzu Chromatopac C-E1B integrator. All the elemental analyses were performed at the Microanalysis Center of Department of Pharmacy, Kyoto University, except the analysis of chlorine in organotrichlorosilanes.

Materials. 11-Bromoundecene,[43] 1-hexyne,[44] *tert*-butylacetylene,[45] 5-decyne,[46] 7-tetradecyne,[46] methyl propargyl ether,[47] 2-cyanoethyl propargyl ether,[48] methyl 10-undecynoate,[43] and authentic samples of *exo*-[49] and *endo*-2-norbornyl bromide[36c] were prepared according to the literature procedures. Ethyltrichlorosilane was prepared by the reaction of ethylmagnesium chloride with silicon tetrachloride in ether. Trichlorosilane, methyltrichlorosilane, phenyltrichlorosilane, vinyltrichlorosilane, and a *m*-xylene dispersion of sodium acetylide for the preparation of 1-hexyne[44b] were provided by Shin-etsu Chemical Co., Ltd. An isomeric mixture of octenes was provided by Lion Co., Ltd. Other chemicals including KF, NaF, RbF, CsF, $H_2PtCl_6{\cdot}6H_2O$, $CuF_2{\cdot}2H_2O$, halogens, IBr, NBS, 1-octyne, methyl 10-undenenoate, 4-vinylcyclohexene, 5-hexen-2-one, dially ether, phenylacetylene, 3,3-dimethylbut-1-ene, myrcene, and norbornene were used as obtained commercially. Organic solvents were dried in the usual manner and distilled before use.

Hydrosilylation of Olefins and Acetylenes. Hydrosilylation of olefins and acetylenes catalyzed by chloroplatinic acid was carried out according to the published procedures[8] with minor modifications. Almost all reactions were carried out by the following general procedure. To a mixture of an olefin or an acetylene (1.0 part) and a 0.1 M solution of chloroplatinic acid in 2-propanol (10^{-2}–10^{-3} mol %) was added an excess amount (1.2–2.0 parts) of trichlorosilane. The mixture was allowed to react under the prescribed conditions (Tables I and II). After the reaction was completed (monitored by GLC), the organotrichlorosilane was isolated by distillation.

Hydrosilylation of octene, consisting of terminal and internal olfeins, was carried out under reflux condition, the bath temperature being maintained at 140 °C.[50] Hydrosilylation of cyclohexene (6.0 g, 73 mmol) with trichlorosilane (9.0 mL, 87 mmol) catalyzed by H_2PtCl_6 (2×10^{-3} mol %) was carried out in a sealed glass tube at 100 °C for 20 h. For the selective terminal hydrosilylation of styrene THF was used as a solvent.[51] The amine-catalyzed reaction (Nozakura's method) was employed for the addition of trichlorosilane to acrylonitrile.[52]

Two regioisomers arising from the hydrosilylation of $C_4H_9C{:}CH$, $C_6H_{13}C{:}CH$, $CH_3OCH_2C{:}CH$, and $NC(CH_2)_2OCH_2C{:}CH$ were separated by fractional distillation through a column (ca. 25 cm) packed with glass helices. Since the minor internally silylated products had lower boiling points, the desired (*E*)-alkenyltrichlorosilanes were readily obtained pure by fractional distillation. For example, $CH_3OCH_2(Cl_3Si)C{=}CH_2$ boiled at 70–71 °C (27mmHg), while (*E*)-$CH_3OCH_2CH{=}CHSiCl_3$ at 79.5–80 °C (27mmHg).

For the purpose of improving the regioselectivity of the hydrosilylation of 1-alkynes, a mixture of 1-hexyne (6.5 g, 80 mmol), trichlorosilane (8.0 mL), and a 0.1 M solution of H_2PtCl_6 in 2-propanol (5 drops) was kept at 2 °C in a refrigerator for 15 h. The hydrosilylation was completed and the ratio $C_4H_9(Cl_3Si)C{=}CH_2/C_4H_9CH{=}CHSiCl_3$ was 5/95. With different lots of trichlorosilane the hydrosilylation did not always proceed at such low temperatures and in some cases a vigorous reaction occurred suddenly after a few hours' induction period.[8d] In order to overcome such problems, we have developed a preactivated-catalyst method. For a 0.1-mol scale preparation, the catalyst solution (several drops) was mixed with several millimoles of 1-alkyne and trichlorosilane and the mixture was refluxed for ca. 1 h. To the cooled mixture was added the remaining alkyne and trichlorosilane at room temperature. The mixture was kept at room temperature or in a refrigerator for 15–20 h. The regioisomer ratio was improved to 7/93–5/95 and the total yield was higher than 90%. Alternatively, the distillation residue of the hydrosilylation mixture was also effective for the highly regioselective hydrosilylation, giving essentially the same result as above. Reaction conditions and yields of the organotrichlorosilanes obtained here are sum-

(41) Koenig, K. E.; Weber, W. P. *Tetrahedron Lett.* **1973**, *2533*.
(42) Tamao, K.; Akita, M.; Yoshida, J.; Kumada M. The 27th Symposium on Organometallic Chemistry, Japan, Tokyo, Oct 14–15, 1980; Abstr B104, p 97.
(43) Toubiana, R.; Asselineau, J. *Ann. Chim. (Paris)* **1962**, *7*, 593.
(44) (a) Campbell, K. N.; Campbell, B. K. "Organic Syntheses"; Wiley: New York, 1963; Collect. Vol. 4, p 117. (b) Rutledge, T. F. *J. Org. Chem.* **1959**, *24*, 840.
(45) Kocienski, P. J. *J. Org. Chem.* **1974**, *39*, 3285.
(46) Bried, E. A.; Hennion, G. F. *J. Am. Chem. Soc.* **1937**, *59*, 1310.
(47) Reppe, W. *Justus Liebigs Ann. Chem.* **1955**, *596*, 1 (experimental details are described on p 74).
(48) Shostakovski, M. F.; Egorov, N. V.; Atavin, A. S. *Probl. Poluch. Poluprod. Prom. Org. Sint.* **1967**, 33; *Chem. Abstr.* **1968**, *68*, 49008.
(49) Roberts, J. D.; Trumbull, E. R., Jr.; Bennett, W.; Armstrong, R. *J. Am. Chem. Soc.* **1950**, *72*, 3116.
(50) Saam, J. C.; Speier, J. L. *J. Am. Chem. Soc.* **1958**, *80*, 4104.
(51) Musolf, M. C.; Speier, J. L. *J. Org. Chem.* **1964**, *29*, 2519.
(52) Nozakura, S.; Konotsune, S. *Bull. Chem. Soc. Jpn.* **1956**, *29*, 322.

marized in Tables I and II. Boiling points (°C (mmHg)) and consistent ^{1}H NMR spectral data are given below. n-$C_8H_{17}SiCl_3$: 86–90 (3); δ 0.90 (t, J = 6 Hz, 3 H), 1.1–1.8 (m, 14 H). n-$C_{12}H_{25}SiCl_3$: 124 (3); δ 0.8–1.9 (m, 3 H), 1.1–1.7 (m, 22 H). n-$C_{18}H_{37}SiCl_3$: 182–187 (5); 0.8–1.0 (m, 3 H), 1.0–1.8 (m, 34 H). t-$C_4H_9CH_2CH_2SiCl_3$: 71–73 (22); δ 0.95 (s, 9 H), 1.2–1.6 (m, 4 H). $PhCH_2CH_2SiCl_3$: 85 (6); δ 1.6–1.8 (m, 2 H), 2.7–3.0 (m, 2 H), 6.9–7.3 (m, 5 H). Cyclo-$C_6H_9CH_2CH_2SiCl_3$: 102–103 (8); δ 1.4–1.8 (m, 7 H), 1.9–2.4 (m, 4 H), 5.63 (m, 2 H). $CH_3CO(CH_2)_4SiCl_3$: 99–126 (10); δ 1.2–1.9 (m, 6 H), 2.08 (s, 3 H), 2.44 (t, J = 6 Hz, 2 H). $Br(CH_2)_{11}SiCl_3$: 134–158 (1); δ 1.0–2.1 (m, 20 H), 3.35 (t, J = 7 Hz, 2 H). $CH_3O_2C(CH_2)_{10}SiCl_3$: 151 (1); δ 1.1–1.9 (m, 18 H), 2.36 (t, J = 8 Hz, 2 H), 3.72 (s, 3 H). $NC(CH_2)_2SiCl_3$: 111–114 (35); δ 1.7–2.0 (m, 2 H), 2.5–2.8 (m, 2 H). CH_2=$CHCH_2O(CH_2)_3SiCl_3$: 103–109 (18); δ 1.3–1.7 (m, 2 H), 1.7–2.1 (m, 2 H), 3.43 (t, J = 6 Hz, 2 H), 3.8–4.0 (m, 2 H), 5.0–5.4 (m, 2 H), 5.6–6.1 (m, 1 H). Cyclo-$C_6H_{11}SiCl_3$: 92 (23); δ 1.1–1.6 (m, 6 H), 1.6–2.2 (m, 5 H). (E)-n-C_4H_9CH=$CHSiCl_3$: 84 (30); δ 1.07 (t, J = 6 Hz, 3 H), 1.2–1.7 (m, 4 H), 2.15–2.45 (m, 2 H), 5.79 (d, J = 19 Hz, 1 H), 6.68 (dt, J = 19 (d) and 6 (t) Hz, 1 H). (E)-t-C_4H_9CH=$CHSiCl_3$: 72 (22); δ 1.11 (s, 9 H), 5.67 (d, J = 19 Hz, 1 H), 6.64 (d, J = 19 Hz, 1 H). (E)-n-$C_6H_{13}CH$=$CHSiCl_3$: 130–145 (45); δ 0.90 (t, J = 6 Hz, 3 H), 1.2–1.6 (m, 8 H), 2.15–2.45 (m, 2 H), 5.76 (d, J = 18 Hz, 1 H), 6.66 (dt, J = 18 (d) and 6 (t) Hz, 1 H). (E)-$CH_3O_2C(CH_2)_8CH$=$CHSiCl_3$: 161–163 (5); δ 1.1–1.8 (m, 12 H), 2.15–2.45 (m, 4 H), 3.60 (s, 3 H), 5.76 (d, J = 19 Hz, 1 H), 6.65 (dt, J = 19 (d) and 6 (t) Hz, 1 H). (E)-CH_3OCH_2CH=$CHSiCl_3$: 79.5–80 (27); δ 3.30 (s, 3 H), 3.84–4.05 (m, 2 H), 5.95 (dt, J = 18 (d) and 1 (t) Hz, 1 H), 6.50 (dt, J = 18 (d) and 2 (t) Hz, 1 H). (E)-$NC(CH_2)_2OCH_2CH$=$CHSiCl_3$: 150–155 (12); δ 2.57 (t, J = 6 Hz, 2 H), 3.69 (t, J = 6 Hz, 2 H), 4.12 (q, J = 2 Hz, 2 H), 6.12 (dt, J = 19 (d) and 2 (t) Hz, 1 H), 6.64 (dt, J = 19 (d) and 3.5 (t) Hz, 1 H). (E)-$PhCH$=$CHSiCl_3$: 156–159 (45); δ 6.38 (d, J = 19.5 Hz, 1 H), 7.34 (d, J = 19.5 Hz, 1 H), 7.3–7.6 (m, 5 H). (E)-n-C_4H_9CH=$C(C_4H_9$-$n)SiCl_3$: 130 (25); δ 0.94 (t, J = 6 Hz, 6 H), 1.1–1.7 (m, 8 H), 2.05–2.5 (m, 4 H), 6.40 (t, J = 7 Hz, 1 H). (E)-n-$C_6H_{13}CH$=$C(C_6H_{13}$-$n)SiCl_3$: 122–125 (2); δ 0.90 (t, J = 6 Hz, 6 H), 1.1–1.9 (m, 16 H), 2.05–2.5 (m, 4 H), 6.40 (t, J = 7 Hz, 1 H).

Preparation of Potassium Organopentafluorosilicates. We have adopted the following two procedures for the preparation of potassium organopentafluorosilicates from organotrichlorosilanes depending upon the nature of the organic group.

Method A. Almost all of the organotrichlorosilanes could be transformed into the silicates by this method. An organotrichlorosilane (0.10 mol) was added *dropwise* to a solution of KF (145 g, 2.50 mol) in 220 mL of water at 0 °C with *vigorous stirring*. The reaction was exothermic, and it was essential to maintain the reaction temperature at 0 °C. The organopentafluorosilicate began to precipitate immediately as white solid matters. After the addition was completed, the mixture was stirred at room temperature for 2 h to overnight. The silicate formed was separated by filtration with suction using two sheets of filter paper (No. 131, Toyo Roshi, Co., Ltd.) followed by washing successively with cold water (300 mL), ethanol (or THF) (100 mL), and ether (100 mL) and then dried over P_2O_5 in a vacuum desiccator. In some cases, the silicate so obtained was contaminated by some siloxanes (IR a broad absorption in 1000–1100 cm^{-1} region) and purified by trituration with THF followed by filtration, washing with THF and ether, and drying in vacuo.

Method B. Styryl-, n-octadecyl-, 1-octadecenyl-, and 7-tetradecenylsilicates were most satisfactorily prepared by the following method. An organotrichlorosilane (0.10 mol) was added dropwise to a suspension of KF (145 g, 2.50 mol) in 300 mL of ethanol at 0 °C. After the addition was completed the mixture was stirred at room temperature for 20 h. After the mixture was coded to 0 °C, 500 mL of water was added in order to dissolve the excess KF and the resulting KCl. The silicate was then separated by filtration followed by washing with water, ethanol and ether and was dried under vacuum, as above.

Yield of the organopentafluorosilicates are given in Tables I and II.

Preparation of Octylpentafluorosilicates Containing Na, Rb, and Cs Countercations. Octyltrifluorosilane was prepared as follows. To a suspension of CuF_2·$2H_2O$ (5.15 g, 37.4 mmol) in 15 mL of ether was added dropwise octyltrichlorosilane (5.14 g, 20.8 mmol) at 0 °C. After being stirred at room temperature for 20 h the mixture was diluted with pentane (15 mL) and filtered. The solid matters were washed with pentane. The combined filtrate was dried over Na_2SO_4 and distilled (78–85 °C (120mmHg)) to give 2.61 g of octyltrifluorosilane (63% yield): ^{1}H NMR δ 0.65–1.1 (m, 2 H), 0.88 (t, J = 6 Hz, 3 H), 1.1–1.7 (m, 12 H).

To a suspension of MF (M = Na, Rb, or Cs) (10 mmol) in 5.0 mL of acetonitrile was added octyltrifluorosilane (995 mg, 5.01 mmol) dropwise at room temperature. After the mixture was stirred at room temperature overnight, 10 mL of dry ether was added. The silicate that precipitated as white powder was separated by filtration, washed with ether, and then dried under vacuum. Analytical samples of $Rb_2[C_8H_{17}SiF_5]$ and $Cs_2[C_8H_{17}SiF_5]$ were purified by recrystallization from hot ethanol. $Na_2[C_8H_{17}SiF_5]$ was not purified in a similar manner, and satisfactory elemental analysis was not obtained.

$Na_2[C_8H_{17}SiF_5]$: 75% yield; IR (KBr) 2955 (w), 2915 (m), 2845 (w), 1608 (m, br), 1469 (m), 1380 (w), 1215 (m), 765 (s), 710 (w), 650 (vs), 540 (m), 454 (m) cm^{-1}.

$Rb_2[C_8H_{17}SiF_5]$: 87% yield; IR (KBr) 2955 (w), 2920 (m), 2850 (w), 2800 (w), 1520 (w), 1465 (w), 1376 (w), 1256 (w), 1176 (w), 740 (s), 640 (vs), 532 (m), 445 (m) cm^{-1}. Anal. Calcd for $C_8H_{17}F_5Rb_2Si$: C, 23.60; H, 4.21; F, 23.33. Found: C, 23.55; H, 4.45; F, 23.25.

$Cs_2[C_8H_{17}SiF_5]$: 85% yield; IR (KBr) 2950 (w), 2915 (m), 2845 (w), 2800 (w), 1470 (w), 1380 (w), 740 (s), 643 (vs), 535 (w), 520 (w), 483 (w), 448 (w) cm^{-1}. Anal. Calcd for $C_8H_{17}F_5SiCs_2$: C, 19.14; H, 3.12; F, 18.92. Found: C, 19.33; H, 3.40; F, 19.14.

Potassium Fluoride Treatment of 2-Methyl-6-(trichlorosilylmethyl)-2,6-Octadiene. To a solution of KF (1.7 g) in water (3 mL) was added dropwise the titled chlorosilane[53] (0.363 g, 1.33 mmol) at 0 °C with stirring. Immediately white precipitate deposited. The mixture was filtered, and the solid was washed with ethanol and ether. The white solid was identified as $K_2[SiF_6]$ by IR. The filtrate was extracted with ether. GLC analysis of the ether layer showed that 2-methyl-6-methylene-2-octene, Me_2C=$CHCH_2CH_2C(C_2H_5)$=CH_2, was formed in 55% yield. The product was isolated by flash distillation and preparative GLC: n^{20}_D 1.4471; ^{1}H NMR δ 1.05 (t, J = 5 Hz, 3 H), 1.60 (s, 3 H), 1.68 (s, 3 H), 1.85–2.2 (m, 6 H), 4.65 (s, 2 H), 4.95–5.15 (m, 1 H); mass spectrum, m/e (%) 138 (M^+, 4), 54 (100). Similar results were obtained by the reaction in ethanol.

UV Spectra of Organopentafluorosilicates. The spectra reproduced in Figure 1 were observed on 0.3–0.5 M Nujol mulls of silicates, except the phenylsilicate for which the data were obtained with a 0.05 M Nujol mull. The Nujol mull was spread on a small piece of filter paper and a piece of filter paper applied by Nujol only was used as the reference.

Reaction of Organopentafluorosilicates with Halogens and IBr. General Procedure. To a mixture of an organopentafluorosilicate (5.0 mmol) in 10 mL of a solvent was added a halogen in CCl_4 dropwise at 0 °C until a slight color of the halogen remained. The mixture was stirred at room temperature for 2 h. The reaction of cyclohexylsilicate with halogens, especially with iodine, was rather slow and hence, after the addition of 1 equiv of halogen, the still colored mixture was heated at 35 or 50 °C for 1 h. After the reaction aqueous $Na_2S_2O_3$ was added and the mixture was filtered. The organic layer of the filtrate was separated, washed with water, dried over Na_2SO_4, and concentrated by evaporation. The residue was distilled (bulb-to-bulb distillation) to give the corresponding organic halide. Yields of some organic halides, especially the products arising from the reaction with IBr, were determined by GLC analysis of the reaction mixture. The halides obtained were identified by comparison of their retention time on GLC and spectral data with those of commercially available authentic materials, excepting two alkenyl halides. For characterization of (E)-1-hexenyl bromide, see the section of the NBS clevage (vide infra). Because (E)-1-hexenyl iodide was thermally less stable, it was isolated by column chromatography on silica gel (pentane): n^{20}_D 1.5069 (lit.[27c] 1.5072); IR (liquid film) 3055, 2965, 2930, 2875, 2860, 1609, 1464, 1433, 1378, 1282, 1250, 1218, 1180, 950, 920, 658 cm^{-1}; ^{1}H NMR δ 0.7–1.1 (m, 3 H), 1.1–1.6 (m, 4 H), 1.9–2.1 (m, 2 H), 5.95 (dt, J = 1.5 (t) and 15 (d) Hz, 1 H), 6.45 (dt, J = 7 (t) and 15 (d) Hz,

(53) Ojima, I.; Kumagai, M. *J. Organomet. Chem.* **1978**, *157*, 359.

1 H); mass spectrum, m/e (%) 211 ($M^+ + 1$, 7), 210 (M^+, 100), 83 ($M^+ - I$, 21).

Reaction of Organopentafluorosilicates with NBS. General Procedure. An organopentafluorosilicate (1.0 mmol), NBS (1.1 mmol), and a solvent (5.0 mL) were combined. An exothermic reaction started almost immediately. After the mixture was stirred for 2 h at room temperature, hexane was added. The mixture was filtered, and the insoluble white precipitate was washed with hexane. The combined filtrate was washed with water, dried over Na_2SO_4, and concentrated by evaporation. The product was isolated by distillation, column chromatography, or preparative GLC. The yields of some organic halides were determined by GLC analysis of the reaction mixture.

Preparation of *exo*-2-Norbornylpentafluorosilicate. *exo*-2-Norbornyltrichlorosilane.[30] A mixture of norbornene (45.1 g, 0.479 mol), trichlorosilane (97 mL, 0.958 mol), and 50 μL of 0.1 M solution of chloroplatinic acid in 2-propanol was refluxed at 1100–1300mmHg for 40 h. Distillation of the mixture (97–105 °C (17mmHg)) gave 86.3 g (79% yield) of *exo*-2-norbornyltrichlorosilane. GLC analysis and ^1H NMR of the product showed that the exo isomer was formed exclusively.

***exo*-2-Norbornylpentafluorosilicate.** To a solution of KF (66.8 g, 1.15 mol) in 100 mL of deionized water was added *exo*-2-norbornyltrichlorosilane (10.312 g, 44.9 mmol) dropwise at 0 °C. The mixture was stirred at room temperature overnight. White solid formed was separated by filtration followed by washing with water, acetone, and ether and was dried under vacuum at room temperature (10.714 g, 80% yield); IR (KBr) 2950 (s), 2860 (m), 1450 (w), 1260 (w), 975 (w), 910 (w), 875 (w), 840 (w), 780 (w), 690 (sh), 645 (s), 615 (m), 525 (m), 450 (w) cm^{-1}. Anal. Calcd for $C_7H_{11}F_5K_2Si$: C, 28.36; H, 3.74; F, 32.04. Found: C, 28.55; H, 3.96; F, 31.78.

In order to confirm the stereochemistry, the exo silicate thus obtained was methylated. To the exo-2-norbornylsilicate (889 mg, 3.0 mmol) was added 10 mL of a 2.9 M solution of methylmagnesium bromide in ether at 0 °C. After the mixture was refluxed for 2 h, the usual workup and bulb-to-bulb distillation gave *exo*-2-norbornyltrimethylsilane (372 mg, 74% yield). The exo stereochemistry was confirmed by comparison of its ^1H NMR spectrum with that reported for an authentic sample.[30b]

Preparation of *endo*-2-Norbornylpentafluorosilicate. *endo*-Norborn-5-en-2-yltrichlorosilane.[30,31] To 64.0 g (0.396 mol) of vinyltrichlorosilane was added freshly distilled cyclopentadiene (26.5 g, 0.401 mol) dropwise with stirring. During the addition an exothermic reaction began to take place. The addition was continued with gentle reflux. After the addition the reaction mixture was allowed to stand overnight at room temperature. GLC analysis of the mixture showed that endo and exo adducts were formed in a ratio of 75/25. A careful fractional distillation (105 °C (53mmHg)) of the reaction mixture through a short column (25 cm) packed with glass helices gave *endo*-norborn-5-en-2-yltrichlorosilane (95% endo) (14.4 g, 16% yield).

***endo*-2-Norbornyltrichlorosilane.** A mixture of *endo*-norborn-5-en-2-yltrichlorosilane (95% endo) (24.989 g, 0.110 mol), dry THF (50 mL), and palladium on charcoal (10%, 500 mg) was placed in a 200-mL bottle. The bottle was alternately evacuated and filled with hydrogen, and the mixture was stirred under the hydrogen atmosphere (1 atm). After 7 h additional palladium on charcoal (500 mg) was added. In 15 h 0.12 mol of hydrogen was taken up and the absorption ceased. The reaction mixture was filtered under a stream of nitrogen. The filtrate was concentrated and distilled (98 °C (16mmHg)) to give 19.191 g (76% yield) of *endo*-2-norbornyltrichlorosilane: ^1H NMR δ 1.1–2.1 (m, 9 H), 2.42 (br s, 1 H), 2.62 (br s, 1 H). Anal. Calcd for $C_7H_{11}Cl_3Si$: Cl, 46.32. Found: Cl, 46.19. The stereochemical purity was unable to be determined by GLC or ^1H NMR.

***endo*-2-Norbornyltrifluorosilane.** To a suspension of 18.40 g (134 mmol) of $CuF_2 \cdot 2H_2O$ in 50 mL of ether was added dropwise 18.807 g (82.1 mmol) of *endo*-2-norbornyltrichlorosilane at 0 °C with stirring. The color changes from light blue to brown. After being stirred at room temperature overnight, the mixture was diluted with pentane (50 mL) and filtered and the yellow-green solid matters were washed with pentane several times. The combined filtrate was concentrated and distilled (69–70 °C (117mmHg)) to give 10.627 g (72% yield) of *endo*-2-norbornyltrifluorosilane: ^1H NMR δ 1.0–1.75 (m, 9 H), 1.95–2.25 (m, 2 H).

***endo*-2-Norbornylpentafluorosilicate.** To a solution of KF (50 g, 860 mmol) in 75 mL of deionized water was added *endo*-2-norbornyltrifluorosilane (10.554 g, 58.6 mmol) dropwise at 0 °C. After the addition was completed, the mixture was stirred at room temperature for 3 h. White solid matters thus obtained were separated by filtration, washed with water, ethanol, and ether, and then dried under vacuum (8.811 g, 51% yield): IR (KBr) 2990 (w), 2945 (m), 2910 (w), 2860 (m), 1475 (w), 1450 (w), 1263 (w), 1253 (w), 1195 (w), 1163 (w), 1040 (w), 1000 (w), 980 (w), 915 (w), 870 (w), 835 (w), 775 (w), 695 (s), 645 (w), 620 (s), 552 (m), 543 (m), 465 (w), 455 (w), 445 (w) cm^{-1}. Anal. Calcd for $C_7H_{11}F_5K_2Si$: C, 28.36; H, 3.74; F, 32.04. Found: C, 27.67; H, 3.78; F, 32.09. 3 h. White solid matters thus obtained were separated by filtration, washed with water, ethanol, and ether, and then dried under vacuum (8.811 g, 51% yield): IR (KBr) 2990 (w), 2945 (m), 2910 (w), 2860 (m), 1475 (w), 1450 (w), 1263 (w), 1253 (w), 1195 (w), 1163 (w), 1040 (w), 1000 (w), 980 (w), 915 (w), 870 (w), 835 (w), 775 (w), 695 (s), 645 (w), 620 (s), 552 (m), 543 (m), 465 (w), 455 (w), 445 (w) cm^{-1}. Anal. Calcd for $C_7H_{11}F_5K_2Si$: C, 28.36; H, 3.74; F, 32.04. Found: C, 27.67; H, 3.78; F, 32.09.

In order to confirm the stereochemical purity, the *endo*-2-norbornylsilicate was methylated. Thus a 3.0 M solution of methylmagnesium bromide in ether (7.0 mL) was added to the silicate (593 mg, 2.0 mmol) at 0 °C. The mixture was stirred at room temperature for 5 h. Usual workup followed by distillation gave *endo*-2-norbornyltrimethylsilane in 78% yield. ^1H NMR analysis of the product showed that its stereochemical purity was higher than 95%.[30b]

Reaction of *exo*- and *endo*-2-Norbornylpentafluorosilicates with Br_2. To a mixture of either the *exo*- or *endo*-2-norbornylsilicate (296 mg, 1.0 mmol) and a solvent (5.0 mL) was added dropwise excess bromine (ca. 2 mmol) at 0 °C. After the addition was completed, the mixture was stirred at room temperature for 4 h. Aqueous Na_2SO_3 was added in order to reduce the excess of bromine, and the product was extracted with pentane. The pentane layer was dried over Na_2SO_4 and concentrated by evaporation. The residue, crude 2-norbornyl bromide, was submitted to ^1H NMR analysis. The exo/endo ratio of the product was determined by relative intensities of 2-methine protons. The results are summarized in Table X. An analytical sample of the product was purified by preparative GLC (partial exo–endo isomerization took place) and identified by comparison of its spectral data with those of an authentic material.

Reaction of *exo*- and *endo*-2-Norbornylpentafluorosilicates with NBS. A mixture of either *exo*- or *endo*-2-norbornylpentafluorosilicate (296 mg, 1.0 mmol), NBS (196 mg, 1.1 mmol), and a solvent (5.0 mL) was stirred at 50 °C for 4 h. Pentane (20 mL) was added, and the insoluble matters were removed by filtration. The filtrate was washed with water, dried over Na_2SO_4, and evaporated. The residue, crude 2-norbornyl bromide, was submitted to ^1H NMR analysis. The exo/endo ratio of the product was determined by relative intensities of 2-methine protons. The results are summarized in Table X.

Acknowledgment. We thank the Ministry of Education for the Grant-in-Aid for Scientific Research (Grants 143022, 203518, 265253, 303523), The Yamada Science Foundation, Shin-etsu Chemical Co., Ltd., and the Kurata Foundation (K.T.) for support of this work. We also acknowledge Dr. M. Wada and Dr. H. Kurosawa of Department of Petroleum Chemistry, Osaka University, for valuable suggestions for measuring UV spectra of solid samples, Professor O. Hayaishi and Dr. K. Takai of Department of Medical Chemistry, Kyoto University, for the use of their spectrophotometer which was used for recording UV spectra of organosilicates in solid states, and Professor T. Veszpremi, Technical University of Budapest, Hungary, for helpful discussion on the UV spectral data during his stay in Japan and generous permission of citing the MO calculation data prior to publication.

Registry No. *n*-$C_6H_{13}CH{=}CH_2$, 111-66-0; *t*-$C_4H_9CH{=}CH_2$, 592-41-6; *n*-$C_{10}H_{21}CH{=}CH_2$, 112-41-4; *n*-$C_{16}H_{33}CH{=}CH_2$, 112-88-9; $PhCH{=}CH_2$, 100-42-5; $Br(CH_2)_9CH{=}CH_2$, 7766-50-9; CH_3CO(C-

$H_2)_2CH{=}CH_2$, 109-49-9; $CH_3O_2C(CH_2)_8CH{=}CH_2$, 111-81-9; NCCH=$CH_2$, 107-13-1; $CH_2{=}CH\text{-}CH_2OCH_2CH{=}CH_2$, 557-40-4; *n*-$C_8H_{17}SiCl_3$, 5283-66-9; *t*-$C_4H_9CH_2CH_2SiCl_3$, 928-65-4; *n*-$C_{12}H_{25}SiCl_3$, 4484-72-4; *n*-$C_{18}H_{37}SiCl_3$, 112-04-9; $PhCH_2CH_2SiCl_3$, 940-41-0; Br($CH_2)_{11}SiCl_3$, 79769-48-5; $CH_3CO(CH_2)_4SiCl_3$, 4848-05-9; $CH_3O_2C(CH_2)_{10}SiCl_3$, 4211-29-4; $NC(CH_2)_2SiCl_3$, 1071-22-3; $CH_2{=}CHCH_2O(CH_2)_3SiCl_3$, 79745-60-1; (*E*)-*n*-$C_4H_9CH{=}CHSiCl_3$, 13095-00-6; (*E*)-*n*-$C_6H_{13}CH{=}CHSiCl_3$, 79745-61-2; (*E*)-*n*-$C_{16}H_{33}CH{=}CHSiCl_3$, 79745-62-3; (*E*)-$CH_3O_2C(CH_2)_8CH{=}CHSiCl_3$, 79745-63-4; (*E*)-$CH_3OCH_2CH{=}CHSiCl_3$, 79769-49-6; (*E*)-$NC(CH_2)_2OCH_2CH{=}CHSiCl_3$, 79745-64-5; (*E*)-PhCH=$CHSiCl_3$, 3412-59-7; (*E*)-*n*-$C_4H_9CH{=}C(C_4H_9\text{-}n)SiCl_3$, 79745-65-6; (*E*)-*n*-$C_6H_{13}CH{=}C(C_6H_{13}\text{-}n)SiCl_3$, 79745-66-7; $K_2[(E)\text{-}n\text{-}C_4H_9CH{=}CHSiF_5]$, 68732-24-1; $K_2[(E)\text{-}n\text{-}C_6H_{13}CH{=}CHSiF_5]$, 70995-82-3; $K_2[(E)\text{-}n\text{-}C_{16}H_{33}CH{=}CHSiF_5]$, 71686-43-6; $K_2[(E)\text{-}CH_3O_2C(CH_2)_8CH{=}CHSiF_5]$, 70995-86-7; $K_2[(E)\text{-}CH_3OCH_2CH{=}CHSiF_5]$, 70995-85-6; $K_2[(E)\text{-}NC(CH_2)_2OCH_2CH{=}CHSiF_5]$, 74463-90-4; $K_2[(E)\text{-}PhCH{=}SiF_5]$, 68901-41-7; $K_2[(E)\text{-}n\text{-}C_4H_9CH{=}C(C_4H_9\text{-}n)SiF_5]$, 70995-87-8; $K_2[(E)\text{-}n\text{-}C_6H_{13}CH{=}C(C_6H_{13}\text{-}m)SiF_5]$, 71686-45-8; $K_2[PhSiF_5]$, 5507-59-5; KF, 7789-23-3; $K_2[n\text{-}C_8H_{17}SiF_5]$, 65599-39-5; $K_2[t\text{-}C_4H_9CH_2CH_2SiF_5]$, 79746-13-7; $K_2[n\text{-}C_{12}H_{25}SiF_5]$, 65599-40-8; $K_2[n\text{-}C_{18}H_{37}SiF_5]$, 71686-42-5; $K_2[PhCH_2CH_2SiF_5]$, 79746-14-8; $K_2[Br(CH_2)_{11}SiF_5]$, 79618-87-4; $K_2[CH_3CO(CH_2)_4SiF_5]$, 79618-86-3; $K_2[CH_3O_2C(CH_2)_{10}SiF_5]$, 65599-43-1; $K_2[NC(CH_2)_2SiF_5]$, 79746-15-9; $K_2[CH_2{=}CHCH_2O(CH_2)_3SiF_5)$, 79618-88-5; $C_6H_{11}SiCl_3$, 98-12-4; $K_2[cyclo\text{-}C_6H_{11}SiF_5]$, 65599-42-0; *n*-$C_4H_9C{\equiv}CH$, 693-02-7; *n*-$C_6H_{13}C{\equiv}CH$, 629-05-0; *n*-$C_{16}H_{33}C{\equiv}CH$, 629-89-0; $CH_3O_2C(CH_2)_8C{\equiv}CH$, 2777-66-4; $CH_3OCH_2C{\equiv}CH$, 627-41-8; $NC(CH_2)_2OCH_2C{\equiv}CH$, 1904-22-9; PhC≡CH, 536-74-3; *n*-$C_4H_9C{\equiv}CC_4H_9$, 1942-46-7; *n*-$C_6H_{13}C{\equiv}CC_6H_{13}\text{-}n$, 35216-11-6; NaF, 7681-49-4; RbF, 13446-74-7; CsF, 13400-13-0; $Na_2[PhSiF_5]$, 16924-58-6; Cl_2, 7782-50-5; Br_2, 7726-95-6; I_2, 7553-56-2; *n*-$C_8H_{17}Cl$, 111-85-3; *n*-$C_8H_{17}Br$, 111-83-1; *n*-$C_8H_{17}I$, 629-27-6; *t*-$C_4H_9CH_2CH_2Br$, 1647-23-0; *c*-$C_6H_{11}Cl$, 542-18-7; *c*-$C_6H_{11}Br$, 108-85-0; *c*-$C_6H_{11}I$, 626-62-0; (*E*)-*n*-$C_4H_9CH{=}CHBr$, 13154-13-7; (*Z*)-*n*-$C_4H_9CH{=}CHBr$, 13154-12-6; (*E*)-*n*-$C_4H_9CH{=}CHI$, 16644-98-7; PhBr, 108-86-1; IBr, 7789-33-5; Ph-I, 591-50-4; $Na_2[C_8H_{17}SiF_5]$, 79746-11-5; $Rb_2[C_8H_{17}SiF_5]$, 79746-10-4; $Cs_2[C_8H_{17}SiF_5]$, 79746-12-6; NBS, 128-08-5; *n*-$C_{12}H_{25}Br$, 143-15-7; $PhCH_2CH_2Br$, 103-63-9; $MeO_2C(CH_2)_{10}Br$, 6287-90-7; $Br(CH_2)_{11}Br$, 16696-65-4; $CH_3CO(CH_2)_4Br$, 10226-29-6; (*E*)-PhCH=CHBr, 588-72-7; (*E*)-$MeO_2C(CH_2)_8CH{=}CHBr$, 79745-67-8; (*E*)-*n*-$C_4H_9CH{=}C(C_4H_9\text{-}n)Br$, 72612-74-9; $K_2[SiF_6]$, 16871-90-2; $K_2[CH_3SiF_5]$, 17979-70-3; $K_2[C_2H_5SiF_5]$, 17193-21-4; 4-(2-bromoethyl)cyclohexene, 63540-01-2; 5-decyne, 1942-46-7; (*Z*)-5-bromo-5-decene, 72612-75-0; potassium (2-(cyclohexen-4-yl)ethyl)pentafluorosilicate, 65599-41-9; 4-ethenylcyclohexene, 100-40-3; cyclohexene, 110-83-8; 4-[2-(trichlorosilyl)ethyl]cyclohexene, 18290-60-3; norborene, 498-66-8; trichlorosilane, 10025-78-2; *exo*-2-norbornyltrichlorosilane, 65118-93-6; *exo*-2-norbornyltrimethylsilane, 79745-68-9; *endo*-norborn-5-en-2-yltrichlorosilane, 27544-82-7; vinyltrichlorosilane, 75-95-5; cyclopentadiene, 542-92-7; *endo*-2-norbornyltrichlorosilane, 79812-96-7; *endo*-2-norbornyltrifluorosilane, 79745-69-0; potassium *endo*-2-norbornylpentafluorsilicate, 74410-83-6; *endo*-2-norbornyltrimethylsilane, 79745-70-3; potassium *exo*-2-norbornylpentafluorosilicate, 74380-89-5; *exo*-2-norbornyl bromide, 2534-77-2; *endo*-2-norbornyl bromide, 13237-87-1; 2-methyl-6-methylene-2-octene, 10054-09-8; 2-methyl-6-(trichlorosilylmethyl)-2,6-octadiene, 68898-14-6; *t*-$C_4H_9C{\equiv}CH$, 917-92-0; *t*-$C_4H_9CH{=}CHSiCl_3$, 79745-71-4; $K_2[t\text{-}C_4H_9CH{=}CHSiF_5]$, 70995-83-4; octyltrifluorosilane, 58589-72-3.

Supplementary Material Available: A listing of IR spectral data and/or elemental analyses for the alkali-metal organopentafluorosilicates in Tables I and II and of IR and mass spectral data, refractive indexes, ^1H NMR spectra, and analyses of the organic bromides prepared in this work (6 pages). Ordering information is given on any current masthead page.

Organofluorosilicates in Organic Synthesis. 13.[1] Copper(II) Oxidation of Organopentafluorosilicates

Jun-ichi Yoshida, Kohei Tamao, Toshio Kakui, Atsushi Kurita, Masao Murata, Kozaburo Yamada, and Makoto Kumada*

Department of Synthetic Chemistry, Faculty of Engineering, Kyoto University, Yoshida, Kyoto 606, Japan

Received July 30, 1981

The carbon–silicon bond in organopentafluorosilicates ($K_2[RSiF_5]$, R = alkyl, alkenyl, and phenyl) has been found to be cleaved by copper(II) chloride or bromide to give the corresponding organic halides in high yields. The reaction obeys a stoichiometry of $K_2[RSiF_5]/CuX_2 = 1/2$. A halogen atom is regioselectively introduced to the carbon atom to which the silicon atom has been attached. (*E*)-Alkenyl halides are obtained stereoselectively from (*E*)-alkenylsilicates. Since organopentafluorosilicates can be readily prepared from olefins and acetylenes, the present reaction provides a synthetically useful route to organic halides. A two-step mechanism involving initial formation of an organic radical followed by ligand transfer from CuX_2 has been suggested by (1) spin trapping of the alkyl radical intermediate, (2) formation of an aldehyde in the presence of oxygen, and (3) stereochemical scrambling in the reaction of *exo*- and *endo*-2-norbornylpentafluorosilicates. Alkylsilicates undergo conjugate addition to α,β-enones in the presence of copper(II) acetate under rather forced conditions. In contrast to the inertness of alkylsilicates, alkenylsilicates react with some copper(II) pseudohalides. The reaction of (*E*)-alkenylsilicates with copper(II) thiocyanate gives (*E*)-alkenyl thiocyanates. The reaction with copper(II) selenocyanate prepared from $Cu(OAc)_2$ and KSeCN in situ gives a dialkenyl selenide. Copper(II) acetate induces the oxidative solvolytic cleavage of the carbon–silicon bond in alkenylsilicates. The reaction in the presence of an alcohol or water gives the alkenyl ethers or aldehydes, respectively.

In another paper,[1] we report full details of the cleavage reactions of the carbon–silicon bonds in hexacoordinate organopentafluorosilicates, $M_2[RSiF_5]$, by halogens and *N*-bromosuccinimide which do not affect those in neutral tetracoordinate silanes. This paper deals with the oxidative cleavage of organopentafluorosilicates by copper(II) salts. We have recently reported that copper(II) chloride and bromide cleave the carbon–silicon bond to produce the corresponding organic halides in good yields (eq 1).[2]

$$K_2[RSiF_5] + CuX_2 \rightarrow R\text{–}X \quad (X = Cl, Br, SCN) \quad (1)$$

Copper(II) thiocyanate has also been found to react with alkenylpentafluorosilicates to give alkenyl thiocyanates (eq 1).[3] We have recently found also that copper(II) acetate induces the solvolytic cleavage of alkenylpentafluorosilicates to form, with alcohols, the corresponding alkenyl ethers (eq 2).[4]

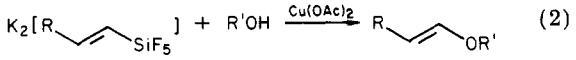

(2)

Although copper(II) cleavage of the silicon–hydrogen[5] and silicon–aryl bonds[6] has been known, the former reaction (eq 1) is the first case of the copper(II) cleavage of silicon–alkyl and –alkenyl bonds involving a ligand transfer from copper to the organic group. The latter reaction (eq 2) is also the first example of copper(II) induced solvolytic cleavage of the carbon–silicon bond.[7] Investigation into the reaction of organopentafluorosilicates with copper(II) salts may not only provide a synthetically useful route to a variety of functionalyzed organic compounds but also contribute to the elucidation of a whole view of copper(II) cleavage of carbon–metal bonds.

Table I. Reaction of Octylpentafluorosilicate with Copper(II) Chloride and Bromide in Ether[a]

molar ratio of $CuX_2/K_2[C_8H_{17}SiF_5]$	yield of $C_8H_{17}X$, %[b]	
	X = Cl	X = Br
1.0	58	62
1.3	65	65
2.0	70[c]	70
4.0[d]	73[e]	69

[a] The reactions were carried out on a 1-mmol scale in 5.0 mL of dry ether at room temperature for 2 h (for $CuCl_2$) or 5 h (for $CuBr_2$). [b] Yields were determined by GLC and based on the octylsilicate. [c] Octyltrifluorosilane was formed in 3% yield. [d] For $CuCl_2$ the ratio was 4.1. [e] Octyltrifluorosilane was formed in 30% yield.

Copper(II) cleavages of carbon–metal bonds have been intensively investigated for a variety of metals including boron,[8] aluminum,[9] lead,[10] zirconium,[11] cobalt,[12] palladium,[11,13,14] mercury,[11,15] and thallium.[16] The reactions, in most cases, are undoubtedly of the redox type and are considered to proceed by a two-step mechanism.[17] First an organic radical is formed by the reaction of organometallic compounds with a copper(II) salt (eq 3), and in

(1) For part 12, see: Tamao, K.; Yoshida, J.; Yamamoto, H.; Kakui, T.; Matsumoto, H.; Takahashi, M.; Kurita, A.; Murata, M.; Kumada, M. *Organometallics*, preceding paper in this issue.
(2) Yoshida, J.; Tamao, K.; Kurita, A.; Kumada, M. *Tetrahedron Lett.* **1978**, 1809.
(3) Tamao, K.; Kakui, T.; Kumada, M. *Tetrahedron Lett.* **1980**, *21*, 111.
(4) Tamao, K.; Kakui, T.; Kumada, M. *Tetrahedron Lett.* **1980**, *21*, 4105.
(5) (a) Cunico, R. F.; Dexheimer, E. M. *Synth. React. Inorg. Met.-Org. Chem.* **1974**, *4*, 23. (b) Anderson, H. H. *J. Am. Chem. Soc.* **1958**, *80*, 5083.
(6) Akhrem, I. S.; Vertanyan, R. S.; Topuzyan, V. O.; Vol'pin, M. E. *Izv. Akad. Nauk SSSR, Ser. Khim.* **1975**, 1387.
(7) The only documented oxidative solvolysis of the carbon–silicon bond is methanolysis of (ferrocenylmethyl)trimethylsilane and its derivatives induced by Fe(III), giving ferrocenylmethyl methyl ether. Kondo, T.; Yamamoto, K.; Omura, T.; Kumada, M. *J. Organomet. Chem.* **1973**, *60*, 287. Kondo, T.; Yamamoto, K.; Kumada, M. *Ibid.* **1973**, *60*, 303.
(8) Lane, C. F. *J. Organomet. Chem.* **1971**, *31*, 421.
(9) Sato, F.; Mori, Y.; Sato, M. *Chem. Lett.* **1978**, 833.
(10) Clinton, N. A.; Kochi, J. K. *J. Organomet. Chem.* **1973**, *56*, 243.
(11) Budnik, R. A.; Kochi, J. K. *J. Organomet. Chem.* **1976**, *116*, C3.
(12) Yamamoto, H.; Yokoyama, T.; Kwan, T. *Chem. Pharm. Bull.* **1975**, *23*, 2186.
(13) Henry, R. M. *J. Org. Chem.* **1974**, *39*, 3871.
(14) Backvall, J. E.; Nordberg, R. E. *J. Am. Chem. Soc.* **1980**, *102*, 393, and references cited therein.
(15) Beletskaya, I. P.; Artamikina, Y. A.; Reutov, O. A. *J. Organomet. Chem.* **1975**, *99*, 343.
(16) Uemura, S.; Toshimitsu, A.; Okano, M.; Ichikawa, K. *Bull. Chem. Soc. Jpn.* **1975**, *48*, 1925.
(17) Kochi, J. K. "Organometallic Mechanism and Catalysis"; Academic Press: New York, 1978; Chapter 2.

0276-7333/82/2301-0369$01.25/0

$$R\text{-}M + Cu^{II}X_2 \rightarrow R\cdot + Cu^{I}X + M\text{-}X \quad (3)$$

the second step the radical is oxidized by another copper(II) salt via the ligand-transfer or the electron-transfer process, depending on the nature of the organic group and the copper(II) salt (eq 4). The present results will be

$$R\cdot + Cu^{II}X_2 \rightarrow R\text{-}X \text{ or } R_{ox} + Cu^{I}X \quad (4)$$

$$R_{ox} = R(-H) \text{ etc.}$$

discussed in the light of these mechanistic aspects, with emphasis on the high susceptibility of organopentafluorosilicates to the carbon–silicon bond cleavage by copper(II) salts.

Throughout this paper, only potassium organopentafluorosilicates, $K_2[RSiF_5]$, have been used, and hence the countercation will be omitted from the individual name of the silicates.

Results and Discussion

I. Reaction of Organopentafluorosilicates with Copper(II) Halides. A. Stoichiometry. When a mixture of octylpentafluorosilicates and anhydrous copper(II) chloride or bromide was stirred in dry ether at room temperature, the color of the reaction mixture gradually faded, possibly indicating the reduction of copper(II) to copper(I), and octyl chloride or bromide respectively, was produced. The yields of organic halides increased with an increase in the amount of copper(II) halide (Table I). In order to elucidate the stoichiometry, we determined the amount of copper(I) produced during the reaction. Thus octylpentafluorosilicate (1 part) was allowed to react with copper(II) chloride (2 parts) in acetonitrile, and the amount of the resulting soluble copper(I) was determined by titration.[18] The amount of copper(I) was found to be essentially equal to twice the amount of octyl chloride (see Experimental Section for details). Therefore the present reaction is reasonably considered to obey a stoichiometry (eq 5) analogous to that previously reported for the cop-

$$K_2[RSiF_5] + 2Cu^{II}X_2 \rightarrow RX + 2Cu^{I}X + K_2[XSiF_5] \quad (5)$$

per(II) oxidation reactions of other organometallic compounds.[17] When 1 equiv of copper(II) halide was used, the yield of the organic halide exceeded 50% (Table I) against the stoichiometry (eq 5). This is probably due to the oxidation of copper(I) to copper(II) by molecular oxygen under the reaction conditions. The regenerated copper(II) might again react with the organosilicate. Indeed the reaction under a nitrogen atmosphere with 1 equiv of copper(II) chloride resulted in reduction of the yield of octyl chloride to 50%.

B. Solvent Effect. Yields of organic halides were greatly dependent upon the nature of the solvent as shown in Table II. In nonpolar solvents such as carbon tetrachloride and benzene the yield of octyl chloride was very low and most of the organosilicate was recovered unchanged. Ether was the most suitable solvent among those examined for the reaction of the octylsilicate with copper(II) chloride. The choice of solvent, however, also depends upon the nature of the organosilicate. Generally the reaction of the alkylsilicates seems to proceed most smoothly in ether or THF, whereas methanol seems to be better for the alkenylsilicates.

C. Synthetic Applications. The present reaction has been applied to various types of organopentafluorosilicates

Table II. Solvent Effect on the Reaction of Octylpentafluorosilicate with Copper(II) Chloride[a]

solvent	yield of octyl chloride, %[b]
CCl_4	3
C_6H_6	4
Et_2O	70
THF	51
CH_3CN	60
CH_3OH	20

[a] Octylpentafluorosilicate (1.0 mmol) was allowed to react with 2.0 mmol of copper(II) chloride in 5.0 mL of a solvent at room temperature for 2 h. [b] The yields are based on the octylsilicate and were determined by GLC.

such as primary alkyl-, secondary alkyl-, alkenyl-, and arylpentafluorosilicates, and the corresponding organic halides have been obtained in high yields. The results are summarized in Table III. As mentioned in the previous paper, alkyl- and alkenylsilicates are readily obtainable via regio- and stereoselective hydrosilylation of olefins and acetylenes,[19] and a halogen atom is selectively introduced onto the carbon atom to which the silicon atom has been attached. Therefore the present method provides a new regio- and stereoselective route to organic halides from olefins and acetylenes (eq 6 and 7), an attractive alternative

$$\text{RCH=CH}_2 \text{ (internal olefins)} \xrightarrow[H_2PtCl_6]{HSiCl_3} RCH_2CH_2SiCl_3 \xrightarrow{KF} K_2[RCH_2CH_2SiF_5] \xrightarrow{CuX_2} RCH_2CH_2X \quad (6)$$

$$RC{\equiv}CR' \xrightarrow[H_2PtCl_6]{HSiCl_3} \underset{H}{\overset{R}{\diagdown}}C{=}C\underset{SiCl_3}{\overset{R'}{\diagup}} \xrightarrow{KF} K_2\left[\underset{H}{\overset{R}{\diagdown}}C{=}C\underset{SiF_5}{\overset{R'}{\diagup}}\right] \xrightarrow{CuX_2} \underset{H}{\overset{R}{\diagdown}}C{=}C\underset{X}{\overset{R'}{\diagup}} \quad (7)$$

(X = Cl, Br; R' = H, R)

to the conventional hydrohalogenation procedures using organoboron, organoaluminum, and organozirconium compounds[20] and also the NBS cleavage of organosilicates mentioned elsewhere.[1] An efficient preparation of the anti-Markovnikov alkyl chloride should be noted, since alkylsilicates are not cleaved by *N*-chlorosuccinimide, as described previously.[1]

The reaction of organopentafluorosilicates with copper(II) halides was compatible with a number of functional

(18) (a) Knop, J. *J. Am. Chem. Soc.* **1924**, *46*, 263. (b) Jenkins, C. L.; Kochi, J. K. *Ibid.* **1972**, *94*, 843. (c) Jenkins, C. L.; Kochi, J. K. *Ibid.* **1972**, *94*, 856.

(19) (a) Eaborn, C.; Bott, R. W. In "Organometallic Compounds of the Group IV Elements"; MacDiarmid, A. G., Ed.; Marcel Dekker: New York, 1968; Vol. 1, p 105. (b) Lukevits, E. Y.; Voronkov, M. G. "Organic Insertion Reactions of Group IV Elements"; Consultants Bureau: New York, 1966. (c) Lukevits, E.; Belyakova, Z. V.; Pomerantseva, M. G.; Voronkov, M. G. *J. Organomet. Chem. Libr.* **1977**, *5*, 1. (d) Speier, J. L. *Adv. Organomet. Chem.* **1979**, *17*, 407.

(20) Hydroboration: (a) Brown, H. C.; Rathke, M. W.; Rogic, M. M. *J. Am. Chem. Soc.* **1968**, *90*, 5038. (b) Brown, H. C.; Lane, C. F. *Ibid.* **1970**, *92*, 6660. (c) Lane, C. F.; Brown, H. C. *Ibid.* **1970**, *92*, 7212. (d) Brown, H. C.; Hamaoka, T.; Ravindran, N. *Ibid.* **1973**, *95*, 5786. (e) Brown, H. C.; Hamaoka, T.; Ravindran, N. *Ibid.* **1973**, *95*, 6456. (f) Brown, H. C. "Organic Syntheses via Boranes"; Wiley: New York, 1978. See also ref 8. Hydroalumination: (g) Isagawa, K.; Tatsumi, K.; Otsuji, Y. *Chem. Lett.* **1976**, 1145. (h) Sato, F.; Sato, S.; Sato, M. *J. Organomet. Chem.* **1976**, *122*, C25. (i) Sato, F.; Sato, S.; Sato, M. *Ibid.* **1977**, *131*, C26. (j) Sato, F.; Sato, S.; Kodama, H.; Sato, M. *Ibid.* **1977**, *142*, 71. (k) Zweifel, G.; Whitney, C. C. *J. Am. Chem. Soc.* **1967**, *89*, 2753. (l) Zweifel, G.; Steele, R. B. *Ibid.* **1967**, *89*, 5085. See also ref 9. Hydrozirconation: (m) Hart, D. W.; Schwartz, J. *Ibid.* **1974**, *96*, 8115. (n) Hart, D. W.; Blackburn, F. F.; Schwartz, J. *Ibid.* **1975**, *97*, 679. (o) Schwartz, J. In "New Applications of Organometallic Reagents in Organic Synthesis"; Seyferth, D., Ed.; Elsevier: Amsterdam, 1976, p 461. (p) Schwartz, J. *Angew. Chem.* **1976**, *88*, 402.

Table III. Reaction of Organopentafluorosilicates with Copper(II) Halides[a]

R in $K_2[RSiF_5]$	X in CuX_2	solvent	time, h	product	yield, %[b]
n-C_8H_{17}	Cl	Et_2O	2	n-$C_8H_{17}Cl$	(70)
	Br	Et_2O	5	n-$C_8H_{17}Br$	(70)
	Br	THF	20	n-$C_8H_{17}Br$	(88)
$CH_3O_2C(CH_2)_{10}$	Cl	Et_2O	1	$CH_3O_2C(CH_2)_{10}Cl$	70
$CH_3CO(CH_2)_4$	Cl	Et_2O	2	$CH_3CO(CH_2)_4Cl$	46 (66)
$Br(CH_2)_{11}$	Cl	Et_2O	2	$Br(CH_2)_{11}Cl$	60
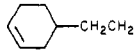	Cl	Et_2O	20	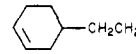	51 (73)
CH_2=$CHCH_2O(CH_2)_3$	Br	THF	4	CH_2=$CHCH_2O(CH_2)_3Br$	45 (52)
CH_2=$CH(CH_2)_4$	Br	THF	5	CH_2=$CH(CH_2)_4Br$	45
	Cl	Et_2O	2		(18)
			54		(58)
	Cl	THF	2	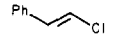	(46)
	Br	MeOH	4	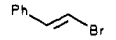	59[c]
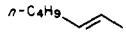	Br	MeOH	4	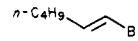	(61)[d]
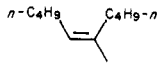	Cl	MeOH	2	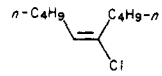	(76)
	Br	MeOH	2	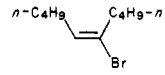	(55)[e]
Ph	Cl	THF	14	PhCl	(75)
	Br	THF	14	PhBr	(79)

[a] The reactions were carried out on a ~1-5-mmol scale with 2 equiv of CuX_2 at room temperature. [b] Isolated yield, based on the organopentafluorosilicate. Yields determined by GLC analysis are given in parentheses. [c] E 100% by GLC. [d] E 99% by GLC. [e] E > 95% by ^1H NMR.

groups, such as bromo, oxo, alkoxy, alkoxycarbonyl, and alkenyl groups, as shown in Table III. Since both the hydrosilylation and silicate preparation are also compatible with these functional groups, the overall transformation can be applied to various olefins and acetylenes containing these functional groups.

It should also be mentioned that the copper(II) cleavage of alkenylsilicates occurs with retention of configuration of the alkenyl group and the stereoselectivity is higher than the halogenation by NBS and halogen. For example, (*E*)-1-hexenyl bromide is formed in >99% isomeric purity with $CuBr_2$ and in 91% with NBS in benzene.[1] It seems interesting to note here that while the stereochemistry of the alkenyl group is predominantly retained, almost complete stereochemical scrambling has been observed in the cleavage of alkylsilicates (vide infra).

D. Mechanistic Studies. On the basis of the stoichiometry the present reaction seems to proceed by the following mechanism. In the first step an alkyl radical is formed by alkyl transfer or electron transfer from the alkylsilicate to copper(II) (eq 8). In the second step a

$$[RSiF_5]^{2-} + Cu^{II}X_2 \rightarrow R\cdot + [XSiF_5]^{2-} + Cu^{I}X \quad (8)$$

$$R\cdot + Cu^{II}X_2 \rightarrow R\text{-}X + Cu^{I}X \quad (9)$$

ligand transfer from another copper(II) halide to the alkyl radical takes place, producing an alkyl halide (eq 9). In order to obtain further information on the reaction mechanism, we performed stereochemical studies and studies on trapping of the alkyl radical intermediate.

Spin Trapping of the Alkyl Radical Intermediate. A successful spin trapping of the alkyl radical intermediate gave a support to the proposed two-step mechanism. Shaking a mixture of octylpentafluorosilicate, copper(II) chloride, 2,3,5,6-tetrakis(trideuteriomethyl)nitrosobenzene, and ether in an ESR sample tube at room temperature gave ESR absorptions. The spectrum (a_N = 13.4 mT, a_H = 10.5 mT, g = 2.0061) was clearly assigned to a *n*-alkyl, in our present case undoubtedly the *n*-octyl, radical adduct of the nitroso compound[21] (eq 10 and Figure 1).

$$[n\text{-}C_8H_{17}SiF_5]^{2-} + Ar\text{-}NO \xrightarrow{CuCl_2} n\text{-}C_8H_{17}\text{-}\overset{O\cdot}{\underset{|}{N}}\text{-}Ar \quad (10)$$

In order to test whether the trapped alkyl radical is the intermediate of the main reaction leading to the alkyl halide or only the intermediate of a side reaction, we examined the effect of a nitroso compound on the yield of an organic halide. If the alkyl radical is the intermediate of the main reaction, the yield of the organic halide must decrease in the presence of the trapping agent. Table IV summarizes a comparison of the yields of organic halides in the reaction of several organopentafluorosilicates with copper(II) halides carried out in the presence or absence of nitrosobenzene or 2,4,6-tri-*tert*-butylphenol. In all cases except cyclohexylsilicate, notrosobenzene caused a great decrease in the yields of the organic halides, indicating that the main reaction proceeded through the organic radical intermediate. A radical-chain mechanism may be ruled out by the fact that an inhibitor such as 2,4,6-tri-*tert*-butylphenol did not affect the yield of the organic halide. In the reaction of cyclohexylsilicate with a copper(II) halide the yield of cyclohexyl halide did not change appreciably in the presence of nitrosobenzene. The reason is not clear at present. It should be noted that also in the case of the alkenylsilicates nitrosobenzene caused a decrease in the

(21) Terabe, S.; Kuruma, K.; Konaka, R. *J. Chem. Soc., Perkin Trans. 2* **1973**, 1252, and references cited therein.

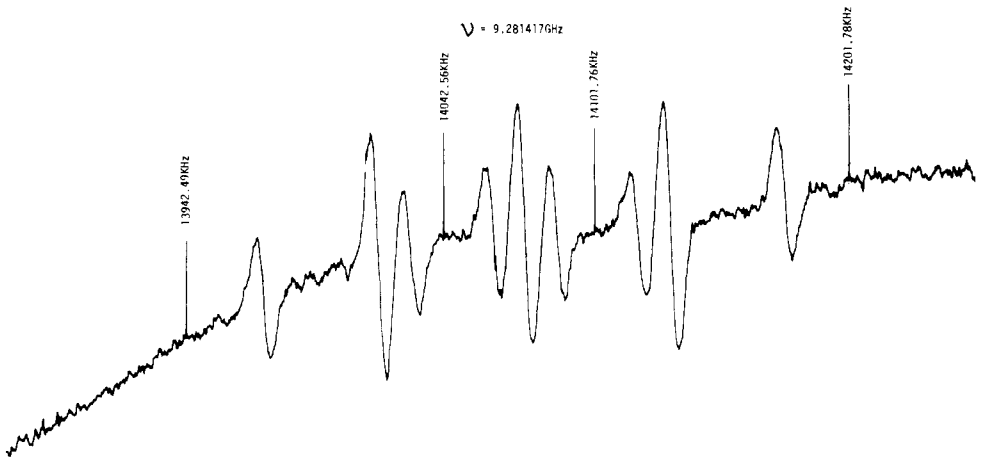

Figure 1. ESR spectrum of the spin adduct of *n*-octyl radical and 2,3,5,6-tetrakis(trideuteriomethyl)nitrosobenzene during the reaction of $K_2[n\text{-}C_8H_{17}SiF_5]$ with $Cu^{II}X_2$ in ether.

Table IV. Reaction of Organopentafluorosilicates with Copper(II) Halides in the Presence of a Radical Trapping Agent[a]

R in $K_2[RSiF_5]$	CuX_2	trapping agent[b]	solvent	time, h	yield of RX, %[c]
$n\text{-}C_8H_{17}$	$CuBr_2$		THF	6	61
		PhNO			22
		TBP[d]			57
		TBP[e]			59
$n\text{-}C_{12}H_{25}$	$CuCl_2$		Et_2O	4	54
		PhNO			19
	$CuCl_2$		Et_2O	50	47
		PhNO			41
	$CuBr_2$		THF	48	42
		PhNO			48
	$CuBr_2$		THF[f]	4	42
		PhNO			30
	$CuBr_2$		THF[f]	4	37
		PhNO			19
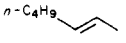	$CuBr_2$		MeOH	4	61[g]
		PhNO			31[g]

[a] Reactions were carried out on a 1-mmol scale in 5.0 mL of a solvent at room temperature unless otherwise stated. [b] One equivalent of a trapping agent was used. [c] Yields are based on the organosilicate and were determined by GLC analysis. [d] 2,4,6-Tri-*tert*-butylphenol (0.01 equiv) was used. [e] 2,4,6-Tri-*tert*-butylphenol (1.0 equiv) was used. [f] The reaction was carried out at 50 °C. [g] (*E*)-1-Hexenyl bromide was formed in 99% stereoselectivity.

yield of the alkenyl halide whereas the halogen transfer reaction occurs with a high stereoselectivity (*E* ≥91%). If the reaction proceeded through the alkenyl radical intermediate, isomerization should occur to produce a mixture of the (*E*)- and (*Z*)-alkenyl halide.[22] The reason cannot readily be explained, but there might be a possibility that while the halogenation reaction is a rapid cage process, possibly keeping an interaction between the alkenyl group and a copper species (vide infra), the addition of nitrosobenzene has influenced the course of the reaction, giving rise to the formation of the spin-trapping product.

Table V. Reaction of Octylpentafluorosilicate with Copper(II) Chloride under an Atmosphere of Molecular Oxygen[a]

conditions	time, h	yield, %[b] $n\text{-}C_8H_{17}Cl$	yield, %[b] $n\text{-}C_7H_{15}CHO$
in Et_2O under N_2	2	67	0
in Et_2O under O_2	2	62	6
in MeOH under N_2	2	21	0
in MeOH under O_2	2	4	14
in MeOH under O_2	50	0	18
in MeOH under O_2[c]	50	0	35

[a] $K_2[n\text{-}C_8H_{17}SiF_5]$ (1.0 mmol) was allowed to react with 2.0 mmol of $CuCl_2$ in 5.0 mL of a solvent under an atmospheric pressure of nitrogen or oxygen unless otherwise stated. [b] Yields are based on the octylsilicate and were determined by GLC analysis. [c] The reaction was carried out with 0.5 mmol of $CuCl_2$.

Molecular Oxygen as a Scavenger for the Alkyl Radical Intermediate. Alkyl radicals have been known to be trapped by molecular oxygen at diffusion-controlled rates to produce alcohols, ketones, aldehydes, and/or peroxides, depending on their structure.[23] In our case, the alkyl radical intermediate was indeed scavenged by molecular oxygen to produce the corresponding aldehyde (eq 11). Table V summarizes the results of the reaction of

$$K_2[n\text{-}C_8H_{17}SiF_5] + CuCl_2 + O_2 \xrightarrow{MeOH} n\text{-}C_7H_{15}CHO \quad (11)$$

octylpentafluorosilicate with copper(II) chloride under an atmospheric pressure of oxygen in ether or methanol. While in ether octanal was formed in only 6% yield together with octyl chloride (62% yield), in methanol the chlorine transfer was greatly retarded and the oxygenation became the major course of the reaction to produce octanal in 35% yield.

(22) The configurational stability of alkenyl radicals is very low. The rate constant of inversion of 1-propenyl radical has been estimated as ca. 10^9 s^{-1} at 25 °C. The mechanism of decomposition of alkenyl–copper complexes has also been studied. Whitesides, G. M.; Casey, C. P.; Krieger, J. K. *J. Am. Chem. Soc.* **1971**, *93*, 1379.

(23) (a) Chen, J. Y.; Fardner, H. C.; Kochi, J. K. *J. Am. Chem. Soc.* **1976**, *98*, 6150. (b) Chen, J. Y.; Kochi, J. K. *Ibid.* **1977**, *99*, 1450.

Table VI. Reaction of *exo*- and *endo*-2-Norbornylpentafluorosilicates with Copper(II) Bromide[a]

solvent	exo/endo ratio[b] and yield (%)[c] of 2-norbornyl bromide: from *exo*-silicate	from *endo*-silicate[d]
MeOH	71/29 (39)	78/22 (20)
THF	73/27 (51)	76/24 (48)
C_6H_6	70/30 (46)	84/16 (38)
CCl_4	80/20 (35)	87/13 (18)

[a] The reactions were carried out on a 2-mmol scale at 50 °C for 4 h. [b] Determined by ^1H NMR (≤±5%). [c] The yields (given in parentheses) are based on the norbornyl silicate and were determined by GLC analysis. [d] The isomeric purity of the silicate was 95% endo. The product ratios are corrected based on this purity.

The result is consistent with the following sequence of reactions involving the trapping of the octyl radical by molecular oxygen (eq 12, 13). The absence of octyl alcohol

$$n\text{-}C_8H_{17}\cdot + O_2 \rightarrow n\text{-}C_8H_{17}OO\cdot \quad (12)$$

$$2n\text{-}C_8H_{17}OO\cdot \rightarrow n\text{-}C_7H_{15}CHO + n\text{-}C_8H_{17}OH + O_2 \quad (13)$$

may be attributed to further oxidation of the alcohol under the reaction conditions.

It should be noted here that the present oxidation is the first example of metal-assisted oxygenation of an alkyl–silicon bond and the overall result corresponds to the conversion of an olefin to a terminal aldehyde. Our efforts to improve the yield of the aldehyde were unfortunately fruitless, possibly owing to the susceptibility of the aldehyde to copper(II) salts.[24]

Stereochemistry at Carbon. The mechanism involving the alkyl radical intermediate also receives support from stereochemical studies. We have examined the stereochemistry of cleavage of the carbon–silicon bond in *exo*- and *endo*-2-norbornylpentafluorosilicates[1] by copper(II) bromide. The cleavage proceeded nonstereospecifically at carbon to form a mixture of *exo*- and *endo*-2-norbornyl bromide in an exo/endo ratio of (70–87)/(30–13) (eq 14). Table VI summarizes the results. The ratio was

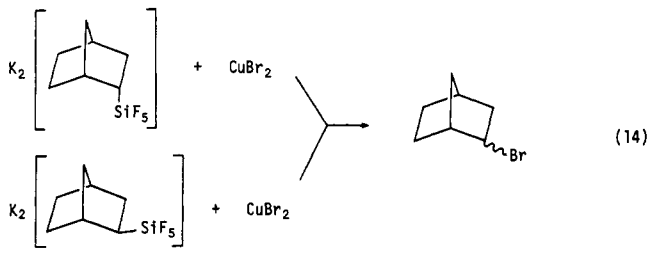

(14)

essentially independent of the stereochemistry of the starting material and of the nature of the solvent. The complete loss of the stereospecificity clearly indicates that a norbornyl radical is involved in the stereochemistry-determining step, consistent with the proposed mechanism. The exo/endo ratios observed here are essentially the same as those shown in the reactions of norbornyl and substituted norbornyl radicals with halogenating agents.[25] Stereochemical scrambling at carbon has also been reported for the copper(II) bromide cleavage of alkyl–zirconium, alkyl–mercury, and alkyl–palladium bonds in the 3,3-dimethylbutyl-*1,2-d*$_2$ and tricyclo[2.2.1.0^{2,6}]heptyl systems.[11]

Reaction of 5-Hexenylpentafluorosilicate with Copper(II) Bromide. The irreversible intramolecular cyclization of the 5-hexenyl radical to the cyclopentylmethyl radical has been used to examine the behavior of radical intermediates in a number of systems,[26] and the rate of the isomerization has been reported to be 1×10^5 s^{-1} at 25 °C.[26] 5-Hexenylpentafluorosilicate was thus allowed to react with copper(II) bromide (Table III). No cyclization product was detected (eq 15). Therefore the

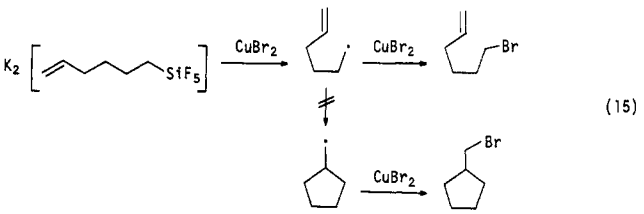

(15)

rate of bromine transfer to the 5-hexenyl radical intermediate is considered to be too fast for the cyclization to compete effectively. The present observation is consistent with the results reported by Kochi and his co-workers for the reaction of 5-hexenyl radical from 6-heptenoyl peroxide with copper(II) bromide.[27]

II. Reaction of Organopentafluorosilicates with Copper(II) Pseudohalides and Acetate. In order to explore the scope of the reaction of organopentafluorosilicates with copper(II) salts, we examined their reactions with some copper(II) pseudohalides and acetate.

A. Reaction of Alkylpentafluorosilicates with Copper(II) Triflate, Copper(II) Acetate, and Copper(II) Thiocyanate. Copper(II) triflate caused merely dissociation of the alkylsilicate. Thus, when octylpentafluorosilicate was allowed to react with copper(II) triflate in ether, octyltrifluorosilane was formed as the only detectable product in 66% yield. With copper(II) acetate or copper(II) thiocyanate in ether under the usual conditions, the octylsilicate was recovered unchanged and no other product was detected. It follows that the alkyl carbon–silicon bond in organopentafluorosilicates is cleaved only by copper(II) halides, but not with copper(II) thiocyanate, acetate, and triflate. The crucial step of the copper(II) cleavage reaction of alkylsilicates may be the initial step in which an alkyl radical species is oxidatively released (cf. eq 8).

B. Conjugate Addition of Alkylpentafluorosilicates to α,β-Unsaturated Ketones Induced by Copper(II) Acetate. Under forced conditions alkylsilicates have also been found to be cleaved by copper(II) acetate, conjugate addition products being formed with α,β-unsaturated ketones. Thus a heterogeneous mixture of octylpentafluorosilicate, methyl vinyl ketone, and copper(II) acetate was heated at 135 °C for 3 h in a sealed tube (eq 16). After

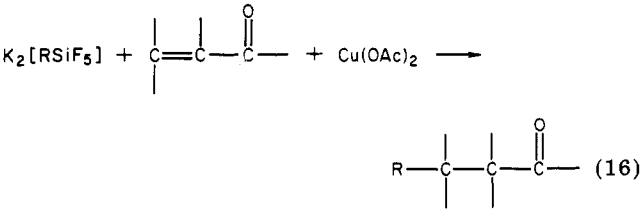

(16)

hydrolytic workup, 2-dodecanone, the conjugate addition

(24) Nigh, W. G. In "Oxidation in Organic Chemistry"; Trahanovsky, W. S., Ed.; Academic Press: New York, 1973; Part B, Chapter 1, p 1.
(25) (a) Bartlett, R.; Fickers, G.; Haupt, F.; Helgeson, R. *Acc. Chem. Res.* **1970**, *3*, 177. (b) Kooyman, E. C.; Vegter, G. C. *Tetrahedron* **1958**, *4*, 382. (c) Cristol, S. J.; Gaston, L. K.; Tiedeman, T. *J. Org. Chem.* **1964**, *29*, 1279. (d) Green, F. D.; Chu, C. C.; Walia, J. *Ibid.* **1964**, *29*, 1285.
(26) Lal, D.; Griller, D.; Husband, S.; Ingold, K. U. *J. Am. Chem. Soc.* **1974**, *96*, 6355, and references cited therein.
(27) Jenkins, C. L.; Kochi, J. K. *J. Org. Chem.* **1971**, *36*, 3103.

Table VII. Conjugate Addition of Alkylpentafluorosilicate to α,β-Unsaturated Ketones in the Presence of Copper Salts[a]

R in $K_2[RSiF_5]$	α,β-enone	copper salt	product	yield, %[b]
n-C_8H_{17}	CH_2=CHCOCH$_3$	$Cu(OAc)_2$	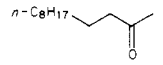	70
		CuCl		28
		CuI		4
		$Cu(OAc)_2$	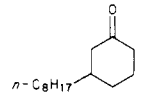	16
$CH_3O_2C(CH_2)_{10}$	CH_2=CHCOCH$_3$	$Cu(OAc)_2$	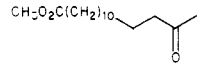	43

[a] A mixture of $K_2[RSiF_5]$ (1.0 mmol), an α,β-unsaturated ketone (20.0 mmol), and a copper salt (1.0 mmol) was heated at 135 °C for 3 h in a sealed tube. [b] Yields are based on $K_2[RSiF_5]$ and were determined by GLC analysis.

product, was obtained in 70% yield. IR analysis of the solid residue showed only characteristic bands of the hexafluorosilicate. Although the reaction occurred with copper(I) chloride and iodide, copper(II) acetate was the most effective among the examined substrates, as shown in Table VII.

Cyclohexenone also reacted with the octylsilicate under similar conditions to give 3-octylcyclohexanone, but the yield was low. The present reaction is compatible with an alkoxycarbonyl group. 10-(Methoxycarbonyl)decanylsilicate reacted with methyl vinyl ketone to produce methyl 2-oxopentadecanoate in 43% yield. The alkenylsilicate did not undergo a similar conjugate addition reaction.

A conjugate addition of organocopper(I) species to α,β-enones has been well-known.[28] Although a mechanism involving an alkylcopper species cannot be ruled out at the present time, we favor the following radical mechanism (eq 17–20) for our present system in the light of the aforementioned discussion concerning the copper(II) induced formation of an alkyl radical from an alkylsilicate. The proposed mechanism is reminiscent of that of the Meerwein arylation reaction.[29]

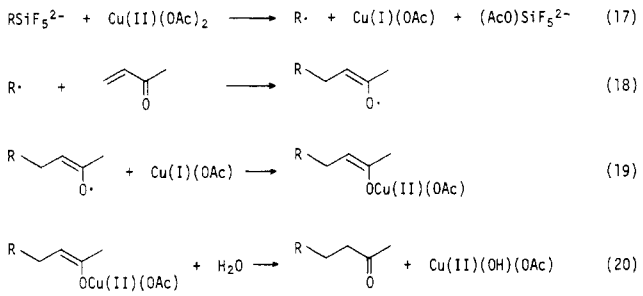

C. Reaction of Alkenylpentafluorosilicates with Copper(II) Thiocyanate. In contrast to the inertness of alkylpentafluorosilicates, alkenylsilicates were found to react with copper(II) thiocyanate to give the corresponding alkenyl thiocyanates.[3] When a mixture of (*E*)-1-octenylpentafluorosilicate, copper(II) thiocyanate, and DMF was stirred at room temperature, the color of the reaction mixture changed from black to yellow-brown, indicative of the reduction of copper(II) to copper(I) (eq 21). After the workup, (*E*)-1-octenyl thiocyanate was obtained in 67% yield. The nature of the solvent influenced the yield of the product, and DMF was the most suitable solvent among those examined, i.e., the yield of octenyl thiocyanate in the reaction of octenylsilicate with 2 equiv of $Cu(NCS)_2$ was 33% in benzene, 40–45% in ethanol, acetonitrile, or ether, 51% in acetone, and 59% in DMF. The use of 3 equiv of $Cu(NCS)_2$ improved the yield to 74% in DMF. Thus, the most satisfactory results were obtained under the conditions where an alkenylsilicate was allowed to react with 3 equiv of $Cu(NCS)_2$ in DMF at room temperature.

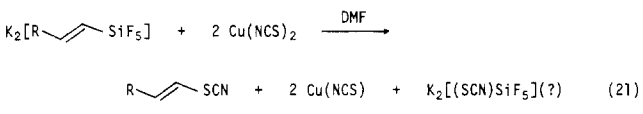

Table VIII. Reaction of Organopentafluorosilicates with Copper(II) Thiocyanate[a]

R in $K_2[RSiF_5]$	product	yield, %[b]
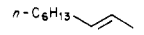	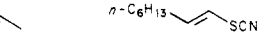	67 (74)
	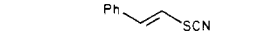	53
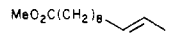	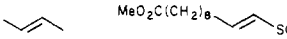	70
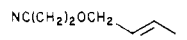	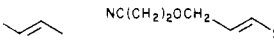	49
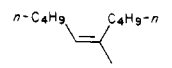	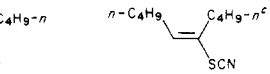	78
Ph	PhSCN	49
n-C_8H_{17}	n-C_8H_{17}SCN	trace

[a] An organopentafluorosilicate (3.0 mmol) was allowed to react with copper(II) thiocyanate (9.0 mmol) in 10 mL of DMF at room temperature for 3 h. [b] Isolated yields based on the organosilicates. The yield in parenthesis was determined by GLC analysis. [c] Contaminated with 7% of the other isomer.

The present reaction was successfully applied to some alkenyl- and phenylsilicates, and the corresponding organic thiocyanates were obtained in high yields, as summarized in Table VIII. The reaction is highly stereoselective at least for terminal (*E*)-alkenylsilicates, isomerically pure (*E*)-alkenyl thiocyanates being selectively produced. The product from 1-butyl-1-hexenylsilicate was also assigned analogously to the *E* isomer, which was contaminated with a small amount (ca. 7%) of the other isomer which was not fully characterized. The phenylsilicate also formed phenyl thiocyanate in 42% yield.

The IR spectra of alkenyl thiocyanates exhibit, in addition to a sharp strong band at 2155 cm^{-1} due to thiocyanate, a weak to medium broad band in the 2100-cm^{-1} region, which is characteristic of isothiocyanate. However, GLC analysis, ^1H NMR and mass spectral data, and a comparison with literature data of the known compound (PhCH=CHSCN)[30] were inconsistent with the presence of any isothiocyanate as an impurity. The infrared behavior remains to be further examined.

(28) Posner, G. H. *Org. React. (N. Y.)* **1972**, *19*, 1.
(29) Rondestvedt, C. S. *Org. React. (N. Y.)* **1960**, *11*, 189; **1976**, *24*, 225.
(30) Guy, R. G.; Pearson, I. *Bull. Chem. Soc. Jpn.* **1976**, *49*, 2310.

The mechanism is not clear, but may be similar to that for the halogen transfer from copper(II) halides to organopentafluorosilicates and other organometallics. The reaction may obey the stoichiometry $RSiF_5^{2-}/Cu(NCS)_2 = 1/2$, but an excess amount (3 equiv) of the latter may be required, owing to its great tendency to decompose into Cu(NCS) and $(SCN)_2$.[18b] The main difference from the halogen transfer reaction is that copper(II) thiocyanate does not react with alkylsilicates.

While there have been many methods for the preparation of alkyl thiocyanates,[31] only a few methods have been developed for the preparation of alkenyl derivatives. The present reaction provides a simple and general method for the preparation of alkenyl thiocyanates which are expected to be versatile in organic synthesis.[31]

D. Reaction of Alkenylpentafluorosilicate with Copper(II) Selenocyanate. (*E*)-1-Hexenylsilicate was allowed to react in DMF with copper(II) selenocyanate prepared from copper(II) acetate (2 equiv) and KSeCN (4 equiv) in situ to form (*E,E*)-di-1-hexenyl selenide in 58% yield (eq 22). Hexenyl selenocyanate was not obtained.

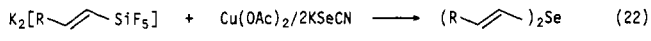

The nature of the solvent influenced the yield of the product, and DMF was the most suitable among the examined solvents, as in the reaction with copper(II) thiocyanate; the yield in benzene, acetonitrile, and ether was 34%, 25%, and 17%, respectively. The use of either an excess amount or 1 equiv of $Cu(SeCN)_2$ was also less satisfactory.

Although the reaction mechanism is not clear, the alkenyl selenocyanate was possibly produced by the reaction of the alkenylsilicate with copper(II) selenocyanate in the first step. Then the alkenyl selenocyanate may be attacked by a further equiv of alkenylsilicate to give the dialkenyl selenide (eq 23 and 24).

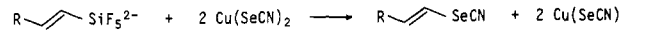

(23)

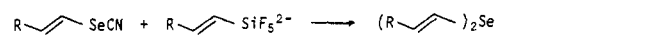

(24)

E. Oxidative Solvolysis of Alkenylpentafluorosilicates Catalyzed by Copper(II) Acetate. Copper(II) acetate was also found to cleave alkenylpentafluorosilicates. For example, the reaction of 1-octenylpentafluorosilicate with copper(II) acetate in DMF gave 1-octenyl acetate[32] in 30% yield. In alcoholic solvents the reaction course has been dramatically changed. Thus, we find that isomerically pure (*E*)-alkenyl ethers are obtained from (*E*)-alkenylpentafluorosilicates by treatment with a catalytic amount of copper(II) acetate in alcohol under an oxygen atmosphere (eq 25). Since the starting silicates are readily

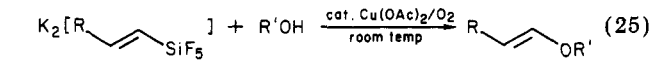

(25)

obtained from acetylenes via hydrosilylation, the overall reaction is regarded as a regio- and stereoselective transformation of acetylenes to (*E*)-alkenyl ethers. Data in Table IX reveal that the reaction requires only a catalytic amount of copper(II) acetate, provided it is conducted under an air or oxygen atmosphere.

Table IX. Reaction of 1-Octenylpentafluorosilicate with Copper(II) Acetate in Ethanol[a]

$Cu(OAc)_2$, mmol	condition	1-octenyl ethyl ether yield, %[b]
2.0	under air[c]	44
1.0	under air[c]	46
0.50	under air[c]	64
0.25	under air[c]	64
0.25	under O_2[d]	66
0.125	under O_2[d]	59

[a] 1-Octenylpentafluorosilicate (1.0 mmol) was allowed to react with $Cu(OAc)_2$ in 5.0 mL of ethanol. [b] Yields are based on the octenylsilicate and determined by GLC analysis. [c] The reactions were carried out in an open flask. [d] The reactions were carried out under an atmospheric pressure of oxygen.

Table X. Alcoholysis of $K_2[RSiF_5]$ Catalyzed by $Cu(OAc)_2$[a]

R in $K_2[RSiF_5]$	alcohol	product	yield, %[b]
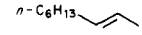	MeOH	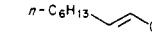	56 (66)
	EtOH	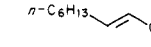	(64)[c]
	i-PrOH	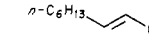	(23)[c]
	t-BuOH	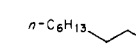	(0)[c]
	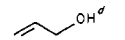	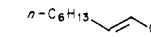	50 (62)[c]
	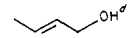	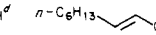	55
	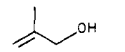	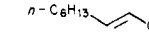	31
	MeOH	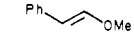	51 (55)
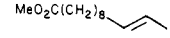	MeOH	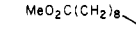	67[e]
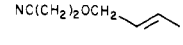	MeOH	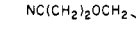	55
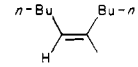	MeOH	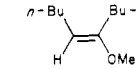	52[f]

[a] Unless otherwise noted, a mixture of $K_2[RSiF_5]$ (3 mmol), dry alcohol (10 mL), and $Cu(OAc)_2$ (0.75 mmol, 25 mol%) was stirred at room temperature for 21 h under air to maintain the blue color of the reaction mixture. [b] Isolated yield based on the silicate (column chromatography, silica gel, pentane or pentane/benzene). GLC yields are given in parentheses. [c] As byproducts, *n*-$C_6H_{13}CH{=}CHOAc$ (2–8%) and/or octanal (2–23%) were formed. [d] In these reactions, 5 mL of alcohol was used. [e] As a byproduct, $MeO_2C(CH_2)_8CH{=}CH_2$ was isolated in 16% yield. [f] Isolated by distillation. As a byproduct, (*Z*)-5-decene was formed in 16% yield. GLC purification caused partial cis/trans isomerization of the product.

Representative results on the synthetic applications are summarized in Table X. There are several significant features. (1) The transformation is highly stereoselective and gives (*E*)-alkenyl ethers in isomeric purities over 99%. (2) The reaction is sensitive to the steric bulkiness of alcohols. The yields of alkenyl ethers decrease in the order MeOH > EtOH > *i*-PrOH ≫ *t*-BuOH (with *t*-BuOH no alkenyl ether was formed). (3) Allylic alcohols gave allyl alkenyl ethers, useful synthetic intermediates which undergo the Claisen rearrangement.[33] (4) Some functional

(31) (a) Guy, R. G. "The Chemistry of Cyanates and Their Thio Derivatives"; Patai, S., Ed.; Wiley: New York, 1977; Part 2, Chapter 18, pp 819–886. (b) Arase, A.; Masuda, Y.; Suzuki, A. *Bull. Chem. Soc. Jpn.* **1974**, *47*, 2511.

(32) Enol esters have been known to be valuable intermediates in organic synthesis. See: Larock, R. C.; Oertle, K.; Beatty, K. M. *J. Am. Chem. Soc.* **1980**, *102*, 1966, and references cited therein.

groups such as ester and cyano groups are compatible with the present reaction. (5) An internal alkenyl ether is also prepared with comparable efficiency.

The present reaction is quite different from other copper(II) cleavage reactions of alkenylsilicates in that while copper(II) chloride, bromide, thiocyanate, and selenocyanate yield the ligand-transfer products, copper(II) acetate induces a solvolytic cleavage of the carbon–silicon bond. Although the mechanism of the present novel solvolytic cleavage has not yet been fully clarified, several points should be mentioned. (1) If the reaction is carried out under an inert-gas atmosphere, copper(II) acetate is reduced to a copper(I) species. The stoichiometry could not be determined, but the formation of a Cu(I) species was confirmed by titration.[18] Under an oxygen atmosphere the resulting Cu(I) is oxidized to regenerate a copper(II) salt, making the reaction to proceed catalytically with respect to copper(II) acetate. (2) Since no alkenyl ether was formed when a mixture of alkenyl acetate, copper(II) acetate, and methanol was stirred under similar conditions, the observed alkenyl ether is considered to be the direct reaction product, not via the ligand-transfer product. (3) Reaction with CH_3OD gave no deuterium-incorporated product. The result may rule out, at the least, the mechanism involving the trans addition of alcohol–anti elimination of a silicon hydride species.

In the light of these observations, coupled with aforementioned mechanistic aspects on the copper(II) oxidation of organosilicates and Kochi's works of the oxidative solvolysis of alkyl radicals by copper(II) salts,[17,18b] the present reaction may be visualized by the mechanism shown in eq 26–29. Thus, the reaction may proceed

$$RSiF_5^{2-} + Cu(OAc)_2 \rightarrow RSiF_5^{-}\cdot + Cu(OAc) + OAc^- \quad (26)$$

$$RSiF_5^{-}\cdot + Cu(OAc)_2 \rightarrow RCu(OAc)_2 + SiF_5^- \quad (27)$$

$$RCu(OAc)_2 + R'OH \rightarrow ROR' + Cu(OAc) + AcOH \quad (28)$$

$$RSiF_5^{2-} + R'OH + 2Cu(OAc)_2 \rightarrow ROR' + 2Cu(OAc) + AcOH + SiF_5(OAc)^{2-} \quad (29)$$

through one-electron transfer from silicate to copper(II) species (eq 26) followed by transfer of the organic group from silicon to copper, forming an organocopper(III) species (eq 27) from which may be formed the observed solvolytic product together with the copper(I) species (eq 28). Since the reaction is highly stereoselective, no free radical can be involved. The present oxidative solvolysis is observed only with alkenylsilicates, but not with alkylsilicates. Therefore, there may be an interaction (complex formation) between the alkenyl group and a copper species throughout the reaction.

While alkenyl ethers have been prepared mainly from the corresponding carbonyl compounds, there have also been a few methods for their preparation from acetylenes.[34] They involve solvomercuration–demercuration of terminal acetylenes producing 2-alkoxy-1-alkenes,[34c] addition of alcohols to certain electron withdrawing group substituted acetylenes,[34b] and acidic solvolysis of α,β-epoxysilanes,[34a,35] the last being probably the most general method so far developed. Our present method provides a useful alternative to these existing procedures.

Table XI. Reaction of Alkenylpentafluorosilicates with Copper(II) Acetate in the Presence of Water[a]

R in $K_2[RSiF_5]$	solvent	H_2O, μL	product	yield, %[b]
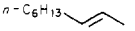	C_6H_6	200	n-$C_6H_{13}CH_2CHO$	trace
	DMF	200		13
	THF	200		42
	i-PrOH	200		46
	CH_3CN	200		50
	CH_3CN	100		52
	CH_3CN	50		45
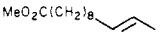	CH_3CN	100	$MeO_2C(CH_2)_8CH_2CHO$	50

[a] Alkenylpentafluorosilicates (1.0 mmol) were allowed to react with copper(II) acetate (0.25 mmol) in the presence of water in 5.0 mL of a solvent under air at room temperature for 2 days. [b] Yields were based on the alkenylsilicate and determined by GLC analysis.

Scheme I

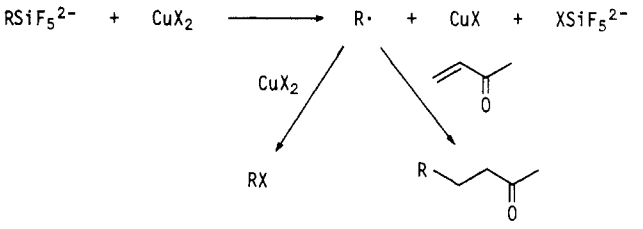

Scheme II

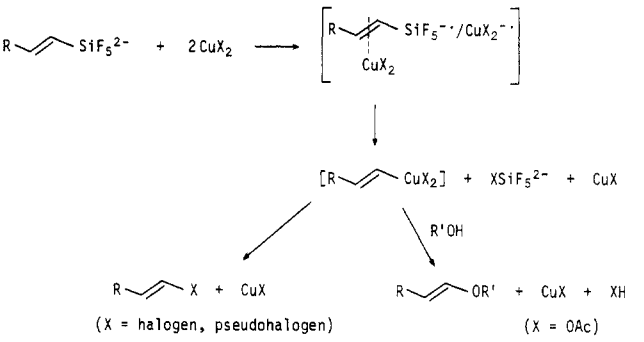

Oxidative hydrolysis of alkenylsilicates has also been observed. Thus, in the presence of a catalytic amount of copper(II) acetate (25 mol %) an alkenylsilicate reacted with water under an air atmosphere in acetonitrile at room temperature in 2 days to give an aldehyde (eq 30). As

$$K_2[RCH{=}CHSiF_5] + H_2O \xrightarrow[CH_3CN]{Cu(OAc)_2} RCH_2CHO \quad (30)$$

shown in Table XI, acetonitrile was the most suitable among the examined solvents. The reaction may apparently proceed through the formation of an enol.

Summarizing Remarks

Several copper(II) induced cleavage reactions of organopentafluorosilicates have been presented. Alkylsilicates give alkyl halides and undergo conjugate addition to α,β-unsaturated ketones. Alkenylsilicates afford alkenyl halides, thiocyanates, selenides, and ethers. We have demonstrated that these reactions are initiated by one-electron transfer from silicate to copper(II) species. In the case of alkylsilicates an alkyl radical is considered to be a crucial species responsible for the observed ligand-transfer products and conjugate addition to α,β-enones (Scheme I).

(33) Rhoads, S. J.; Raulins, N. R. *Org. React (N. Y.)* **1975**, *22*, 1.
(34) (a) Hudrlik, P. F.; Hudrlik, A. M. "The Chemistry of the Carbon–Carbon Triple Bond"; Patai, S., Ed.; Wiley: New York, 1978; Part 1, Chapter 7, pp 199–273. (b) Dickstein, J. I.; Meller, S. I. *Ibid.*; Part 2, Chapter 19, pp 813–955. (c) Hudrlik, P. F.; Hudrlik, A. M. *J. Org. Chem.* **1973**, *38*, 4254.
(35) Hudrlik, P. F.; Hudlik, A. M.; Rona, R. J.; Misra, R. N.; Withers, G. P. *J. Am. Chem. Soc.* **1977**, *99*, 1993.

In the case of alkenylsilicates an alkenyl radical might not be involved, but an alkenyl–copper species may play an important role in the observed reactions, in the light of the reactivity and stereochemical differences between alkyl- and alkenylsilicates. The mechanistic difference may arise from the complex formation between a silicate and copper(II) species, possibly through the carbon–carbon double bond (Scheme II).

Experimental Section

General. Infrared spectra were recorded on a Hitachi EPI-G3 grating infrared spectrometer. ^{1}H NMR spectra were determined with a JEOL JNM-MH-100 (100 MHz) spectrometer in carbon tetrachloride. Chemical shifts (δ) are recorded in ppm downfield from Me_4Si. Mass spectra were measured on a JEOL JMS-D300 mass spectrometer connected with a JEOL LGC-20K gas chromatograph, equipped with a 1-m glass column packed with OV-17 (1%) on Chromosorb B, and a JMA-2000 data processing system. Ionization voltage was 24 eV for all compounds. ESR spectra were observed on a JEOL-PE2X spectrometer modified with a JEOL ES-SCXA gun diode microwave unit. GLC analyses and preparative purification were performed on a Shimadzu GC-4B gas chromtograph, equipped with a 3-m column packed with 30% Silicone DC550 on Chromosorb B or Celite 545. GC peak integrals were recorded with a Shimadzu Chromatopac C-E1B integrator.

Materials. Organopentafluorosilicates except 5-hexenylpentafluorosilicate were prepared as described elsewhere.[1] Copper(II) chloride and bromide of ordinary commercial grade were used without further purification. Anhydrous copper(II) acetate was obtained by refluxing copper(II) acetate hydrate with acetic anhydride.[36] Copper(II) triflate[18b] and thiocyanate[18b] and 5-hexenyl bromide[37] were prepared according to the published procedures. All solvents were dried in the usual manner and distilled before use.

Titration of Copper(I). A mixture of octylpentafluorosilicate (200 mg, 0.636 mmol), copper(II) chloride (180 mg, 1.339 mmol), and acetonitrile (20 mL) was stirred at room temperature under a nitrogen atmosphere for 17 h. GLC analysis of the reaction mixture showed that 0.403 mmol (63% yield) of octyl chloride was formed. After addition of 80 mL of acetonitrile a 20-mL aliquot of the reaction mixture was titrated as follows.[18] The aliquot was poured into a mixture of $FeCl_3 \cdot 6H_2O$ (1.09 g) in 18 mL of 2 N H_2SO_4. This was followed by addition of concentrated H_2SO_4 (2.0 mL), H_3PO_4 (2.0 mL), and water (114 mL). The mixture was titrated with 0.10 N $K_2Cr_2O_7$ with diphenylamine as indicator. The titration showed that 0.825 mmol of copper(I) had been formed in the reaction mixture.

Reaction of Organopentafluorosilicate with Copper(II) Halides. General Procedure. A mixture of organopentafluorosilicate (5.0 mmol), copper(II) halide (10.0 mmol), and solvent (10 mL) was stirred at room temperature for a given period of time. After addition of pentane (20 mL), the mixture was filtered and the insoluble precipitate was washed with pentane. The combined filtrate was washed with water, dried over Na_2SO_4, and evaporated. The product was isolated by distillation. Further purification, if necessary, was carried out by preparative GLC or column chromatography. Spectral and elemental analytical data of some organic halides are given below. The other organic halides were identified by comparison of their ^{1}H NMR and IR spectra and their retention time on GLC with those of authentic materials.

Methyl 11-chloroundecanoate (isolated by bulb-to-bulb distillation): n^{20}_D 1.4487; IR (liquid film) 2920, 2845, 1745, 1469, 1437, 1360, 1250, 1195, 1171, 883, 720 cm^{-1}; ^{1}H NMR 1.1–1.9 (m, 16 H), 2.22 (t, J = 7 Hz, 2 H), 3.45 (t, J = 7 Hz, 2 H), 3.59 (s, 3 H); MS, m/e (%) 87 (34), 74 (100), 55 (55), 41 (59); high-resolution MS, m/e 234.1353 (calcd for $C_{12}H_{23}{}^{35}ClO_2$, 234.1381), 236.1400 (calcd for $C_{12}H_{23}{}^{37}ClO_2$, 236.1351). (The molecular peak was detected only at higher ion multiplicity, around 300.)

1-Chloro-5-hexanone (isolated by bulb-to-bulb distillation): n^{20}_D 1.4405; IR (liquid film) 2995, 2950, 2870, 1712, 1441, 1406, 1360, 1310, 1278, 1165, 950, 797, 725, 645 cm^{-1}; ^{1}H NMR 1.5–1.9 (m, 4 H), 2.09 (s, 3 H), 2.42 (t, J = 7 Hz, 2 H), 3.51 (t, J = 6 Hz, 2 H); MS, m/e (%) 121 (0.7), 119 (2), 99 (M^+ – Cl, 4), 98 (15), 58 (28), 55 (13), 43 (100); high-resolution MS, m/e 134.0531 (calcd for $C_6H_{11}{}^{35}ClO$, 134.0496), 136.0544 (calcd for $C_6H_{11}{}^{37}ClO$, 136.0466). (The molecular peak was detected only at higher ion multiplicity, around 300.)

1-Bromo-11-chloroundecane [isolated by column chromatography on silica gel (pentane)]: n^{20}_D 1.4777; IR (liquid film) 2910, 2845, 1460, 1300, 1285, 1250, 719, 645, 557 cm^{-1}; ^{1}H NMR 1.1–1.6 (m, 14 H), 1.6–2.1 (m, 4 H), 3.35 (t, J = 6 Hz, 2 H), 3.47 (t, J = 6 Hz, 2 H); MS, m/e (%) 270 (M^+ + 2, 0.3), 191 (2), 189 (7), 151 (12), 149 (14), 137 (95), 135 (100). Anal. Calcd for $C_{11}H_{22}BrCl$: C, 49.00; H, 8.22. Found: C, 48.72; H, 8.33.

4-(2-Chloroethyl)cyclohexene (isolated by bulb-to-bulb distillation): n^{20}_D 1.4822; IR (liquid film) 3020, 2910, 2830, 1651, 1449, 1432, 1368, 1332, 1312, 1292, 1280, 1262, 1208, 1140, 1067, 1040, 1030, 895, 862, 850, 773, 740, 715, 649 cm^{-1}; ^{1}H NMR 1.0–2.4 (m, 9 H), 3.53 (t, J = 7 Hz, 2 H), 5.4–5.7 (m, 2 H); MS, m/e (%) 146 (M^+ + 2, 5), 144 (M^+, 18), 81 (100); high-resolution MS, m/e 144.0699 (calcd for $C_8H_{13}{}^{35}Cl$, 144.0703), 146.0660 (calcd for $C_8H_{13}{}^{37}Cl$, 146.0673).

3-(3-Bromopropoxy)prop-1-ene (isolated by bulb-to-bulb distillation): n^{20}_D 1.4651; IR (liquid film) 3075, 3010, 2850, 1648, 1475, 1342, 1285, 1255, 1210, 1140, 1105, 1080, 990, 920 cm^{-1}; ^{1}H NMR 2.09 (tt, J = 6 and 7 Hz, 2 H), 3.48 (t, J = 7 Hz, 2 H), 3.51 (t, J = 6 Hz, 2 H), 3.8–4.1 (m, 2 H), 5.0–5.4 (m, 2 H), 5.6–6.1 (m, 1 H); MS, m/e (%) 180 (M^+ + 2, 2), 178 (M^+, 2), 123 (16), 121 (17), 58 (98), 41 (100); high-resolution MS, m/e 177.9977 (calcd for $C_6H_{11}{}^{79}BrO$, 177.9990), 180.0000 (calcd for $C_6H_{11}{}^{81}BrO$, 179.9970).

(*E*)-5-Chloro-5-decene (isolated by preparative GLC): n^{20}_D 1.4458; IR (liquid film) 3030, 2955, 2925, 2865, 1654, 1470, 1383, 1218, 1144, 1105, 953, 847, 745, 680 cm^{-1}; ^{1}H NMR 0.7–1.1 (m, 6 H), 1.1–1.7 (m, 8 H), 1.9–2.2 (m, 2 H), 2.29 (t, J = 7 Hz, 2 H), 5.49 (t, J = 8 Hz, 1 H); MS, m/e (%) 176 (M^+ + 2, 13), 174 (M^+, 41), 83 (100). Anal. Calcd for $C_{10}H_{19}Cl$: C, 68.75; H, 10.96; Cl, 20.29. Found: C, 68.65; H, 11.10; Cl, 20.13.

Isomeric Purity of Alkenyl Halides. Isomeric purities of 1-hexenyl bromide and 5-bromo-5-decene were determined as described previously.[1] The results are given in Table III. The isomeric purity of 5-chloro-5-decene was not fully determined, but its spectral data showed that only a single isomer had been formed.

Spin Trapping. Shaking an Ar-bubbled mixture of octylpentafluorosilicate, copper(II) chloride, 2,3,5,6-tetrakis(trideuteriomethyl)nitrosobenzene, and dry ether in an ESR sample tube at room temperature gave ESR absorptions (a_N = 13.4 mT, a_H = 10.5 mT, g = 2.0061) due to the spin adduct of a *n*-alkyl radical. They coincide with the ESR spectrum of the spin adduct of ethyl radical with tetramethylnitrosobenzene (a_N = 13.68 mT, a_H = 10.97 mT, g = 2.0061).[21]

Reaction of Octylpentafluorosilicate with Copper(II) Chloride in the Presence of Molecular Oxygen. Oxygen was bubbled into a mixture of copper(II) chloride (269 mg, 2.0 mmol) in 5.0 mL of a solvent. Octylpentafluorosilicate (315 mg, 1.0 mmol) was then added, and the mixture was stirred at room temperature for a given period of time under an atmosphere of oxygen. After the reaction was complete, the mixture was analyzed by GLC. The products, octanal and/or octyl chloride, were isolated by preparative GLC and identified by comparison of their spectral data with those of authentic materials. Results are summarized in Table V.

Reaction of *exo*- and *endo*-2-Norbornylpentafluorosilicates with Copper(II) Bromide. A mixture of *exo*- or *endo*-2-norbornylpentafluorosilicate[1] (592 mg, 2.0 mmol), copper(II) bromide (893 mg, 4.0 mmol), and a solvent (10 mL) was stirred at 50 °C for 4 h. Pentane (30 mL) was added and the insoluble matters were removed by filtration. The filtrate was washed with water, dried over Na_2SO_4, and evaporated. The residue, crude 2-norbornyl bromide, was submitted to ^{1}H NMR analysis. The exo/endo ratio of the product was determined by relative intensities of 2-methine protons (see ref 1). The results are summarized in Table VI.

Preparation of 5-Hexenylpentafluorosilicate. To a solution of silicon tetrachloride (4.0 mL, 35.0 mmol) in 20 mL of dry ether

(36) Fieser, L. F.; Fieser, M. "Reagents for Organic Synthesis"; Wiley: New York, 1967; Vol. 1, p 159.

(37) Lyle, R. E.; DeWitt, E. J.; Pattison, I. C. *J. Org. Chem.* **1956**, *21*, 61.

was added at 0 °C 5-hexenylmagnesium bromide which was prepared from 5-hexenyl bromide (2.44 g, 15.0 mmol) and magnesium (400 mg, 16.5 mmol) in 15 mL of dry ether. After stirring at room temperature for 2 h, white precipitate was removed by filtration. Distillation of the filtrate gave 1.75 g (54% yield) of 5-hexenyltrichlorosilane: ^{1}H NMR 0.9–1.9 (m, 6 H), 1.9–2.3 (m, 2 H), 4.8–5.2 (m, 2 H), 5.5–6.0 (m, 1 H). 5-Hexenyltrichlorosilane (1.245 g, 5.7 mmol) was added dropwise to a solution of KF (7.25 g, 125 mmol) in 11 mL of deionized water at 0 °C. After the addition was completed the mixture was stirred at room temperature for 5 h. 5-Hexenylpentafluorosilicate (1.505 g, 65% yield) was obtained as white powder which was separated by filtration, washed with water, THF, and ether, and dried in vacuo: IR (KBr) 3070 (w), 2915 (m), 1634 (m), 918 (m), 747 (s), 650 (s), 523 (m), 478 (m), 446 (m) cm^{-1}. The product was not analytically pure, but was used in the following cleavage reaction without further purification.

Reaction of 5-Hexenylpentafluorosilicate with Copper(II) Bromide. 5-Hexenylpentafluorosilicate (569 mg, 2.0 mmol) was allowed to react with copper(II) bromide (893 mg, 4.0 mmol) in 10 mL of THF at room temperature for 5 h. Pentane (30 mL) was added and the mixture was filtered. The filtrate was washed with water and dried over Na_2SO_4. After evaporation of the solvent, bulb-to-bulb distillation of the residue gave 146 mg (45% yield) of 5-hexenyl bromide. The product was identified by comparison of its ^{1}H NMR and IR spectra with those of an authentic sample. Cyclopentylmethyl bromide was not detected by GLC.

Reaction of Octylpentafluorosilicate with Copper(II) Pseudohalides and Acetate. A mixture of octylpentafluorosilicate (315 mg, 1.0 mmol), copper(II) triflate, and 5.0 mL of ether was stirred at room temperature for 2 h. GLC analysis of the reaction mixture showed the formation of octyltrifluorosilane in 66% yield. After workup octyltrifluorosilane[1] was isolated by preparative GLC and identified by comparison of its ^{1}H NMR and IR spectra and their retention time on GLC with those of an authentic material.

Reaction of octylpentafluorosilicate with copper(II) thiocyanate and copper(II) acetate was also attempted in a similar fashion, but in neither case was product observed by GLC analysis of the reaction mixture. The insoluble matters which were separated by filtration from the reaction mixture showed an IR absorption only due to the octylsilicate, and no absorption due to hexafluorosilicate was detected, indicating that most of the octylsilicate remained unchanged.

Conjugate Addition of Alkylpentafluorosilicates to α,β-Unsaturated Ketones in the Presence of a Copper Salt. General Procedure. A heterogeneous mixture of an alkylpentafluorosilicate (1.0 mmol), α,β-unsaturated ketone (20.0 mmol), and a copper salt (1.0 mmol) was heated at 135 °C for 3 h in a sealed tube. After the reaction was completed, ether and water were added and the organic layer was analyzed by GLC. After filtration, extraction with ether, and evaporation of the solvent, the product was isolated by preparative GLC. Spectral data and elemental analyses of the conjugate addition products are given below.

2-Dodecanone: n^{20}_D 1.4330; IR (liquid film) 2955, 2925, 2855, 1720, 1465, 1410, 1355, 1165 cm^{-1}; ^{1}H NMR 0.88 (t, J = 6 Hz, 3 H), 1.1–1.7 (m, 16 H), 2.03 (s, 3 H), 2.32 (t, J = 7 Hz, 2 H); MS, m/e (%) 185 (M^+ + 1, 2) 184 (M^+, 11), 169 (4), 126 (9), 85 (10), 71 (32), 59 (36), 58 (100). Anal. Calcd for $C_{12}H_{24}O$: C, 78.20; H, 13.12. Found: C, 78.00; H, 13.11.

Methyl 14-oxopentadecanoate: mp 34–35 °C; IR (KBr) 2920, 2850, 1737, 1710, 1467, 1438, 1375, 1357, 1307, 1252, 1230, 1205, 1175 cm^{-1}; ^{1}H NMR 1.1–1.75 (m, 20 H), 2.02 (s, 3 H), 2.22 (t, J = 7 Hz, 2 H), 2.32 (t, J = 7 Hz, 2 H), 3.61 (s, 3 H); MS, m/e (%) 270 (M^+, 12), 239 (34), 213 (100), 181 (70), 98 (56). Anal. Calcd for $C_{16}H_{30}O_3$: C, 71.07, H, 11.18. Found: C, 71.01; H, 11.19.

3-Octylcyclohexanone: IR (liquid film) 2960, 2925, 2855, 1715, 1450, 1225 cm^{-1}; ^{1}H NMR 0.90 (t, J = 6 Hz, 3 H), 1.28 (br s, 14 H), 1.5–2.4 (m, 5 H); MS, m/e (%) 211 (M^+ + 1, 4), 210 (M^+, 24), 167 (31), 96 (100). Anal. Calcd for $C_{14}H_{26}O$: C, 79.93; H, 12.46. Found: C, 79.96; H, 12.62.

Reaction of Alkenylpentafluorosilicates with Copper(II) Thiocyanate. The following preparation of (*E*)-1-octenyl thiocyanate is representative of the procedure for the reaction of the alkenylsilicates with copper(II) thiocyanate.

(*E*)-1-Octenyl Thiocyanate. A mixture of (*E*)-1-octenylpentafluorosilicate (936 mg, 3.0 mmol), copper(II) thiocyanate (1.620 g, 9.0 mmol), and dry DMF (10 mL) was stirred at room temperature for 3 h. After the addition of ether, the mixture was filtered. The filtrate was washed with water and 10% brine and dried over $MgSO_4$. After evaporation of the solvent, bulb-to-bulb distillation of the residue under reduced pressure gave 338 mg (67% yield) of (*E*)-1-octenyl thiocyanate as a colorless liquid: n^{20}_D 1.4815; IR (liquid film) 3040, 2950, 2920, 2850, 2155, 1468, 1460, 1380, 945 cm^{-1}; ^{1}H NMR 0.88 (t, J = 6 Hz, 3 H), 1.32 (br s, 8 H), 2.18 (q, J = 6 Hz, 2 H), 5.74 (q, J = 16 Hz, 1 H), 6.16 (dt, J = 16 and 6 Hz, 1 H); MS, m/e (%) 169 (M^+, 28), 99 (23), 86 (32), 83 (35), 68 (100). Anal. Calcd for $C_9H_{15}NS$: C, 63.85; H, 8.93. Found: C, 64.14; H, 8.73.

The following organic thiocyanates were prepared in a similar fashion.

2-Phenylethenyl thiocyanate [isolated by column chromatography on silica gel, pentane/benzene (1:1)]: n^{20}_D 1.6226 (lit.[30] n^{24}_D 1.6178); IR (liquid film) 3060, 2155, 2100, 1610, 1570, 1494, 1444, 1230, 1073, 947, 850, 783, 738, 690 cm^{-1}; ^{1}H NMR 6.43 (d, J = 15 Hz, 1 H), 6.94 (d, J = 15 Hz, 1 H), 7.30 (s, 5 H); MS, m/e (%) 161 (M^+, 100), 134 (48), 117 (41), 91 (23), 77 (22). Anal. Calcd for C_9H_7NS: C, 67.05; H, 4.38. Found: C, 67.22; H, 4.56.

3-(2-Cyanoethoxy)propenyl thiocyanate (isolated by bulb-to-bulb distillation): n^{20}_D 1.5106; IR (liquid film) 3050, 2920, 2875, 2250, 2155, 2100, 1627, 1475, 1448, 1408, 1356, 1325, 1285, 1255, 1220, 1113, 1055, 938 cm^{-1}; ^{1}H NMR 2.63 (t, J = 6 Hz, 2 H), 3.22 (t, J = 6 Hz, 2 H), 4.15 (t, J = 2 Hz, 2 H), 6.22 (t, J = 2 Hz, 2 H); MS, m/e (%) 168 (M^+, 1.7), 110 (100), 98 (34), 57 (57), 54 (39). Anal. Calcd for $C_7H_8N_2OS$: C, 49.98; H, 4.79. Found: C, 50.13; H, 4.79.

10-Methoxycarbonyl-1-decenyl thiocyanate (isolated by column chromatography on silica gel, benzene): n^{20}_D 1.4851; IR (liquid film) 3040, 2925, 2850, 2155, 2100, 1738, 1458, 1432, 1358, 1244, 1196, 1170, 945 cm^{-1}; ^{1}H NMR 1.15–1.7 (m, 12 H), 2.1–2.35 (m, 4 H), 3.61 (s, 3 H), 5.82 (d, J = 15 Hz, 1 H), 6.15 (dt, J = 15 and 7 Hz, 1 H); MS, m/e (%) 255 (M^+, 34), 224 (52), 112 (85), 100 (58), 99 (100), 87 (48). Anal. Calcd for $C_{13}H_{21}NO_2S$: C, 61.14; H, 8.29. Found: C, 60.98; H, 8.51.

1-Butyl-1-hexenyl thiocyanate (isolated by bulb-to-bulb distillation): n^{20}_D 1.4368; IR (liquid film) 2960, 2930, 2875, 2860, 2155, 2080, 1615, 1465, 1379, 936, 858 cm^{-1}; ^{1}H NMR 0.8–1.1 (m, 6 H), 1.1–1.7 (m, 8 H), 1.9–2.3 (m, 2 H), 2.40 (t, J = 7 Hz, 1 H), 6.15 (dt, J = 15 and 7 Hz, 1 H); MS, m/e (%) 197 (M^+, 44), 99 (59), 98 (100), 95 (54), 83 (57), 55 (77). Anal. Calcd for $C_{11}H_{19}NS$: C, 66.95; H, 9.70. Found: C, 66.83; H, 9.61.

Phenyl thiocyanate (isolated by bulb-to-bulb distillation): n^{20}_D 1.5685; IR (liquid film) 3060, 2145, 1580, 1475, 1440, 1325, 1085, 1067, 1040, 998, 905, 739, 685 cm^{-1}; ^{1}H NMR 7.3–7.6 (m); MS, m/e (%) 135 (M^+, 100), 112 (14), 111 (25), 84 (11), 79 (26).

Reaction of (*E*)-1-Hexenylpentafluorosilicate with Copper(II) Acetate–KSeCN. A mixture of (*E*)-1-hexenylpentafluorosilicate (289 mg, 1.0 mmol), copper(II) acetate (361 mg, 2.0 mmol), KSeCN (582 mg, 4.0 mmol), and dry DMF (10 mL) was stirred at room temperature for 6 h. GLC analysis of the reaction mixture showed that (*E*,*E*)-bis(1-hexenyl) selenide was produced in 58% yield. After addition of benzene the mixture was filtered. The filtrate was washed with brine and water and dried over Na_2SO_4. After evaporation of the solvent the product was isolated by bulb-to-bulb distillation: n^{25}_D 1.5047; IR (liquid film) 3010, 2955, 2920, 2870, 2850, 1740, 1610, 1462, 1435, 1377, 1225, 945, 923 cm^{-1}; ^{1}H NMR 0.92 (t, J = 6 Hz, 6 H), 1.1–1.6 (m, 8 H), 1.9–2.3 (m, 4 H), 5.91 [dt, J = 15 (d), and 6 Hz (t), 2 H], 6.20 (d, J = 15 Hz, 2 H); MS, m/e (%) 248 (18), 247 (14), 246 (100), 244 (48), 243 (18), 242 (19). Anal. Calcd for $C_{12}H_{22}Se$: C, 58.76; H, 9.04. Found: C, 58.89; H, 9.01.

Reaction of Octenylpentafluorosilicate with Copper(II) Acetate in DMF. A mixture of octenylpentafluorosilicate (312 mg, 1 mmol), copper(II) acetate (364 mg, 2 mmol), and dry DMF (5 mL) was stirred at room temperature for 20 h. GLC analysis of the reaction mixture showed that 1-octenyl acetate was formed in 31% yield. After hydrolysis followed by extraction with pentane, the pentane layer was evaporated. The residue was flash distilled and subjected to preparative GLC to purify the product. (*E*)-1-octenyl acetate: IR (liquid film) 3080, 3025, 2960, 2925, 2855,

1760, 1675, 1655, 1468, 1370, 1223, 1105, 936, 908 cm^{-1}; ^{1}H NMR 0.90 (t, 3 H), 1.30 (br s, 8 H), 1.75–2.0 (m, 2 H), 2.04 (s, 3 H), 5.26 (dt, J = 12 and 7 Hz, 1 H), 6.97 (dt, J = 12 and 1 Hz, 1 H); MS, m/e (%) 170 (M$^+$, 69), 110 (100). Anal. Calcd for $C_{10}H_{18}O_2$: C, 70.55; H, 10.66. Found: C, 70.35; H, 10.76.

Reaction of Alkenylpentafluorosilicates with Copper(II) Acetate in the Presence of an Alcohol. Titration of Copper(I) Species in the Reaction of Octenylpentafluorosilicate with Copper(II) Acetate. A mixture of (*E*)-1-octenylpentafluorosilicate (0.306 g, 0.979 mmol), anhydrous copper(II) acetate (0.365 g, 2.01 mmol), and dry methanol (10 mL) was stirred under nitrogen at room temperature for 2 h. Acetonitrile (20 mL), through which dry nitrogen had been bubbled, was added; this resulted in separation into white precipitates and a green supernatant liquid. An aliquot (20.00 mL) of the liquid layer was titrated as described for the titration of copper(I) chloride, and this showed that 0.992 mmol of a copper(I) species was formed. GLC analysis of the reaction mixture showed that the amount of methyl octenyl ether was 0.356 mmol (36.4% yield). Several repeated experiments, changing the ratio of reactants and/or the reaction time, showed similar results.

General Procedure. A mixture of an alkenylpentafluorosilicate (3.0 mmol), copper(II) acetate (138 mg, 0.75 mmol), and an alcohol (10 mL) was stirred in an open flask at room temperature for 21 h. The color of the reaction mixture gradually changed from green to blue. After addition of ether, the mixture was filtered. The filtrate was washed with brine and dried over $MgSO_4$. After evaporation of the solvent, the product was isolated by distillation, preparative GLC, or column chromatography. Spectral data and elemental analyses of the products are given below.

(*E*)-1-Methoxy-1-octene (isolated by bulb-to-bulb distillation): n^{20}_D 1.4299; IR (liquid film) 3060, 3000, 2955, 2920, 2850, 1663, 1656, 1462, 1375, 1207, 1162, 1130, 933 cm^{-1}; ^{1}H NMR 0.90 (t, 3 H), 1.30 (br s, 8 H), 1.75–2.05 (m, 2 H), 3.44 (s, 3 H), 4.59 (dt, J = 13 and 7 Hz, 1 H), 6.18 (d, J = 13 Hz, 1 H); MS, m/e (%) 142 (M$^+$, 15), 71 (100). Anal. Calcd for $C_9H_{18}O$: C, 76.00; H, 12.76. Found: C, 75.91; H, 13.00.

(*E*)-1-Ethoxy-1-octene (isolated by preparative GLC): n^{20}_D 1.4311; IR (liquid film) 3050, 2955, 2920, 2845, 1662, 1653, 1475, 1463, 1438, 1390, 1377, 1193, 1169, 1130, 933 cm^{-1}; ^{1}H NMR 0.90 (t, 3 H), 1.25 (t, J = 7 Hz, 3 H), 1.30 (br s, 8 H), 1.70–2.10 (m, 2 H), 3.62 (q, J = 7 Hz, 2 H), 4.58 (dt, J = 13 and 7 Hz, 1 H), 6.09 (d, J = 13 Hz, 1 H); MS, m/e (%) 156 (M$^+$, 28), 85 (100). Anal. Calcd for $C_{10}H_{20}O$: C, 76.86; H, 12.90. Found: C, 76.69; H, 13.07.

(*E*)-1-Isopropoxy-1-octene (isolated by preparative GLC): IR (liquid film) 3060, 2995, 2975, 2945, 2875, 1770, 1680, 1660, 1470, 1387, 1376, 1340, 1198, 1168, 1142, 930 cm^{-1}; ^{1}H NMR 0.90 (t, 3 H), 1.15 (d, J = 7 Hz, 6 H), 1.30 (br s, 8 H), 1.70–2.0 (m, 2 H), 3.97 (septet, J = 7 Hz, 1 H), 4.69 dt, J = 13 and 7 Hz), 5.94 (d, J = 13 Hz, 1 H); MS, m/e (%) 170 (M$^+$, 45), 55 (100). Anal. calcd for $C_{11}H_{22}O$: C, 77.58; H, 13.02. Found: C, 77.42; H, 13.27.

(*E*)-1-Allyloxy-1-octene (isolated by bulb-to-bulb distillation): n^{20}_D 1.4462; IR (liquid film) 3055, 2960, 2925, 2855, 1675, 1658, 1460, 1425, 1380, 1195, 1168, 1126, 995, 930 cm^{-1}; ^{1}H NMR 0.90 (t, 3 H), 1.31 (br s, 8 H), 1.70–2.15 (m, 2 H), 4.12 (dt, J = 5 and 1.5 Hz, 2 H), 4.67 (dt, J = 13 and 8 Hz, 1 H), 5.05–5.35 (m, 2 H), 5.7–6.05 (m, 1 H), 6.14 (d, J = 13 Hz, 1 H); MS, m/e (%) 168 (M$^+$, 8), 85 (100). Anal. Calcd for $C_{11}H_{20}O$: C, 78.51; H, 11.98. Found: C, 78.74; H, 12.16.

(*E*)-1-[(*E*)-2-Butenyloxy]-1-octene (isolated by column chromatography on silica gel, pentane): n^{20}_D 1.4492; IR (liquid film) 3080, 3050, 2980, 2950, 2877, 1770, 1683, 1663, 1470, 1385, 1227, 1203, 1172, 1134, 976, 940, 930 cm^{-1}; ^{1}H NMR 0.90 (t, 3 H), 1.27 (br s, 8 H), 1.72 (br d, J = 5 Hz, 3 H), 1.8–2.1 (m, 2 H), 4.01 (br d, J = 5 Hz, 2 H), 4.61 (dt, J = 13 and 7 Hz, 1 H), 5.3–5.85 (m, 2 H), 6.10 (d, J = 13 Hz, 1 H); MS, m/e (%) 182 (M$^+$, 10), 71 (100). Anal. Calcd for $C_{12}H_{22}O$: C, 79.06; H, 12.16. Found: C, 78.95; H, 12.27.

(*E*)-1-(2-Methyl-2-propenyloxy)-1-octene (isolated by column chromatography on silica gel, pentane): n^{20}_D 1.4476; IR (liquid film) 3050, 2950, 2915, 2850, 1675, 1653, 1452, 1376, 1197, 1162, 1135, 932, 920, 902 cm^{-1}; ^{1}H NMR 0.90 (t, 3 H), 1.31 (br s, 8 H), 1.75 (s, 3 H), 1.8–2.15 (m, 2 H), 4.00 (s, 3 H), 4.68 (dt, J = 13 and 7 Hz, 1 H), 4.89 (br d, J = 8 Hz, 2 H), 6.11 (d, J = 13 Hz, 1 H); MS, m/e (%) 182 (M$^+$, 7), 53 (100). Anal. Calcd for $C_{12}H_{22}O$: C, 79.06; H, 12.16. Found: C, 78.88; H, 12.26.

(*E*)-1-Methoxy-2-phenylethene [isolated by column chromatography on silica gel, pentane/benzene (3:1)]: n^{20}_D 1.5642; IR (liquid film) 3070, 3025, 2955, 2930, 2830, 1660, 1645, 1604, 1576, 1490, 1460, 1448, 1433, 1341, 1330, 1313, 1238, 1190, 1153, 1126, 1075, 1032, 1000, 935, 868, 818, 753, 697, 650 cm^{-1}; ^{1}H NMR 3.63 (s, 3 H), 5.69 (d, J = 13 Hz, 1 H), 6.94 (d, J = 13 Hz, 1 H), 7.11 (s, 5 H); MS, m/e (%) 134 (M$^+$, 100), 119 (14), 91 (52).

(*E*)-5-Methoxy-5-decene (bulb-to-bulb distillation gave a mixture of (*Z*)-5-decene (n^{20}_D 1.4327) and (*E*)-5-methoxy-5-decene, the yields of which were 18% and 52%, respectively; isolated by preparative GLC): n^{20}_D 1.4368; IR (liquid film) 3070, 2965, 2930, 2865, 1668, 1466, 1380, 1237, 1209, 1200, 1180, 1115 cm^{-1}; ^{1}H NMR 0.90 (t, J = 7 Hz, 6 H), 1.1–1.6 (m, 8 H), 1.8–2.2 (m, 4 H), 3.40 (s, 3 H), 4.21 (t, J = 7 Hz, 1 H); MS, m/e (%) 170 (M$^+$, 28), 72 (100). Anal. Calcd for $C_{11}H_{22}O$: C, 77.58; H, 13.02. Found: C, 77.48; H, 13.32.

(*E*)-1-Methoxy-10-(methoxycarbonyl)-1-decene (isolated by column chromatography on silica gel, benzene): n^{20}_D 1.4509; IR (liquid film) 3055, 3000, 2925, 2850, 1745, 1675, 1657, 1460, 1436, 1360, 1205, 1175, 1130, 935 cm^{-1}; ^{1}H NMR 1.38 (br s, 10 H), 1.45–1.7 (m, 2 H), 1.7–2.0 (m, 2 H), 2.20 (t, J = 7 Hz, 2 H), 3.42 (s, 3 H), 3.59 (s, 3 H), 4.56 (dt, J = 13 and 7 Hz, 1 H), 6.17 (d, J = 13 Hz, 1 H). Anal. Calcd for $C_{13}H_{24}O_3$: C, 68.38; H, 10.59. Found: C, 68.27; H, 10.81.

(*E*)-1-Methoxy-6-cyano-4-oxahex-1-ene [isolated by column chromatography on silica gel, pentane/ether (1:4)]: n^{20}_D 1.4519; IR (liquid film) 3070, 3010, 2935, 2870, 2255, 1655, 1460, 1450, 1412, 1365, 1327, 1215, 1175, 1113, 1095, 1000, 945, 918 cm^{-1}; ^{1}H NMR 2.48 (t, J = 6 Hz, 2 H), 3.56 (s and t, J = 6 Hz, 5 H), 3.71 (d, J = 7 Hz, 2 H), 4.78 (dt, J = 13 and 7 Hz, 1 H), 6.48 (d, J = 13 Hz, 1 H); MS, m/e (%) 141 (M$^+$, 8), 140 (12), 54 (100). Anal. Calcd for $C_7H_{11}NO_2$: C, 59.56; H, 7.85. Found: C, 59.46; H, 7.80.

Reaction of (*E*)-Octenylpentafluorosilicate with CH_3OD in the Presence of Copper(II) Acetate. A mixture of (*E*)-octenylpentafluorosilicate (312 mg, 1 mmol), copper(II) acetate (46 mg), and CH_3OD (3 mL) was stirred at room temperature for 21 h. Usual workup and distillation gave 64.5 mg of (*E*)-1-methoxyoctene: ^{1}H NMR and MS, m/e (%) 142 (M$^+$, 25.5), 143 (M$^+$ + 1, 2.5); spectral data correspond to the nondeuterated product, $C_6H_{13}CH{=}CHOCH_3$.

Reaction of Alkenylpentafluorosilicates with Copper(II) Acetate in the Presence of Water. The following preparation of octanal is representative of the procedure for the reaction of the alkenylsilicates with copper(II) acetate in the presence of water. A mixture of 1-octenylpentafluorosilicate (1.575 g, 5.0 mmol), copper(II) acetate (114 mg, 0.63 mmol), deionized water (500 μL, 28 mmol), and acetonitrile (15 mL) was stirred in an open flask at room temperature for 2 days. After addition of ether, the mixture was filtered. The filtrate was washed with water and dried over Na_2SO_4. After evaporation of the solvent, bulb-to-bulb distillation of the residue gave 295 mg (46% yield) of octanal. The product was identified by comparison of its spectral data with those of an authentic material.

10-(Methoxycarbonyl)decanal was prepared in a similar fashion: n^{20}_D 1.4450; IR (neat) 2920, 2845, 2715, 1735, 1460, 1433, 1360, 1252, 1190, 1168, 1100 cm^{-1}; ^{1}H NMR 1.32 (br s, 10 H), 1.4–1.75 (m, 4 H), 2.22 (t, J = 7 Hz, 2 H), 2.35 (t, J = 7 Hz, 2 H), 3.62 (s, 3 H), 9.64 (t, J = 1 Hz, 1 H).

Acknowledgment. We thank the Ministry of Education for Grants-in-Aid for Scientific Research (143022, 203518, 265253, 303523), and the Yamada Science Foundation, Shin-etsu Chemical Co., Ltd., and the Kurata Foundation (K.T.) for support of this work. We also acknowledge Dr. Takashi Kawamura, Department of Hydrocarbon Chemistry, Kyoto University, for measuring the ESR spectra concerning the spin trapping.

Registry No. Octylpentafluorosilicate, 65599-39-5; (11-(methoxycarbonyl)decyl)pentafluorosilicate, 65599-43-1; (5-oxyhexyl)-pentafluorosilicate, 79618-86-3; (11-bromoundecyl)pentafluorosilicate, 79618-87-4; (2-(3-cyclohexenyl)ethyl)pentafluorosilicate, 65599-41-9; (3-(2-propenyloxy)propyl)pentafluorosilicate, 79618-88-5; 5-hexenylpentafluorosilicate, 79618-89-6; cyclohexylpentafluoro-

silicate, 65599-42-0; ((*E*)-2-phenylethenyl)pentafluorosilicate, 68901-41-7; (*E*)-1-hexenylpentafluorosilicate, 68732-24-1; 5-(5-decenyl)pentafluorosilicate, 70995-87-8; phenylpentafluorosilicate, 66712-45-6; dodecylpentafluorosilicate, 65599-40-8; (*exo*)-2-norbornylpentafluorosilicate, 74380-89-5; (*endo*)-2-norbornylpentafluorosilicate, 74410-83-6; (*E*)-octenylpentafluorosilicate, 70995-82-3; ((*E*)-10-(methoxycarbonyl)-1-decenyl)pentafluorosilicate, 70995-86-7; ((*E*)-3-(2-cyanoethoxy)propenyl)pentafluorosilicate, 74463-90-4; (*Z*)-5-decen-5-ylpentafluorosilicate, 70995-87-8; octyl bromide, 111-83-1; octyl chloride, 111-85-3; methyl 11-chloroundecanoate, 17696-12-7; 6-chloro-2-hexanone, 10226-30-9; 1-bromo-11-chloroundecane, 30295-21-7; 4-(2-chloroethyl)cyclohexene, 63540-00-1; 3-(3-bromopropoxy)prop-1-ene, 15424-07-4; 6-bromo-1-hexene, 2695-47-8; chlorocyclohexane, 542-18-7; (*E*)-1-chloro-2-phenylethene, 4110-77-4; (*E*)-1-bromo-2-phenylethene, 588-72-7; (*E*)-1-bromo-1-hexene, 13154-13-7; (*E*)-5-chloro-5-decene, 10124-72-8; (*E*)-5-bromo-5-decene, 72612-74-9; chlorobenzene, 108-90-7; bromobenzene, 108-86-1; dodecyl chloride, 112-52-7; cyclohexyl bromide, 108-85-0; *exo*-2-norbornyl bromide, 2534-77-2; *endo*-2-norbornyl bromide, 13237-87-1; 2-dodecanone, 6175-49-1; 3-octylcyclohexanone, 57242-85-0; methyl 14-oxopentadecanoate, 54889-71-3; (*E*)-1-octenyl thiocyanate, 74458-26-7; (*E*)-2-phenylethenyl thiocyanate, 61807-26-9; (*E*)-10-(methoxycarbonyl)-1-decenyl thiocyanate, 74458-28-9; (*E*)-3-(2-cyanoethoxy)propenyl thiocyanate, 74458-27-8; (*E*)-5-thiocyanato-5-decene, 74458-29-0; phenyl thiocyanate, 103-72-0; 1-octenyl ethyl ether, 30989-68-5; (*E*)-1-methoxy-1-octene, 62427-06-9; (*E*)-1-isopropoxy-1-octene, 77149-61-2; (*E*)-1-*tert*-butoxy-1-octene, 79618-58-9; (*E*)-1-(allyloxy)-1-octene, 77149-62-3; (*E*)-1-[(*E*)-2-butenyloxy]-1-octene, 79618-59-0; (*E*)-1-(2-methyl-2-propenyloxy)-1-octene, 77149-64-5; (*E*)-1-methoxy-2-phenylethene, 4110-75-2; (*E*)-1-methoxy-10-(methoxycarbonyl)-1-decene, 77149-65-6; (*E*)-1-methoxy-6-cyano-4-oxahex-1-ene, 77149-66-7; (*E*)-5-methoxy-5-decene, 77149-67-8; octanal, 124-13-0; 10-(methoxycarbonyl)decanal, 1931-65-3; copper(II) chloride, 7447-39-4; copper(II) bromide, 7789-45-9; copper(II) acetate, 142-71-2; copper(I) chloride, 7758-89-6; copper(I) iodide, 7681-65-4; copper(II) thiocyanate, 15192-76-4; 3-buten-2-one, 78-94-4; 2-cyclohexenone, 930-68-7; (*E*)-1-ethoxy-1-octene, 77149-60-1; methanol, 67-56-1; ethanol, 64-17-5; 2-propanol, 67-63-0; 2-methyl-2-propanol, 75-65-0; 2-propen-1-ol, 107-18-6; (*E*)-2-buten-1-ol, 504-61-0; 2-methyl-2-propen-1-ol, 513-42-8.

Poly(phenylene oxide) Catalyst Supports Containing (Cyclopentadiene)metal Complexes

L. Verdet and J. K. Stille*

Colorado State University, Fort Collins, Colorado 80523

Received September 15, 1981

Poly(2,6-dimethyl-1,4-phenylene oxide) containing cyclopentadienyl ligands attached to the benzyl carbons was prepared by the reaction of cyclopentadienylsodium with polymer that had been brominated at the benzyl position. Cross-linking took place during the reaction through the cyclopentadiene group. The reaction of 2-norbornen-7-one with poly(2,6-diphenyl-1,4-phenylene oxide) lithiated at the 3-position gave the norbornen-7-ol derivative which was converted to the polymer-attached 7-chloronorbornene. Cyclopentadiene ligands were generated via a retro Diels–Alder reaction of the anion produced from the 7-chloronorbornene. These polymers were converted to polymer-bound cyclopentadienyldicarbonylcobalt, cyclopentadienyldicarbonylrhodium, and titanocene catalysts. The cobalt and rhodium complexes were effective hydroformylation catalysts while the immobilized titanocene hydrogenated cyclohexene 10–70 times faster than the homogeneous analogue.

Introduction

Because there are many advantages to be gained by binding homogeneous catalysts to solid supports, the chemistry of homogeneous catalysts attached to polymers has been the subject of considerable research activity.[1] Cross-linked polystyrene has been the favorite polymer support, primarily because it is available commercially in various bead sizes with varying degrees of cross-link density.

Polystyrene beads, however, are mechanically, chemically, and thermally unstable.[2,3] For example, macroporous styrene–divinylbenzene resins will slough off polymer, particularly in a solvent that swells the bead. In addition, the reduction of carbon monoxide to hydrocarbons (Fischer–Tropsch), the reduction of carbon monoxide to methanol, and the hydroformylation of olefins in which water is used as the hydrogen source (water gas shift) are reactions that require temperatures higher than those usually necessary in homogeneous catalysis and are above or near the ceiling temperature of polystyrene ($T_c \approx 150$ °C). Further, polystyrene has poor chemical stability and will not endure a number of catalytic processes such as oxidation or photochemical reactions.

Poly(phenylene oxides) are a class of thermally stable engineering plastics.[4] Although the *thermooxidative* stability of the 2,6-dimethyl-substituted polymer is lower than other thermally stable polymers, its thermal stability under a nonoxidizing atmosphere is good;[5] however, the 2,6-diphenyl polymer has excellent thermal and oxidative stability. Consequently, we have explored the attachment of cyclopentadiene ligands to poly(2,6-dimethyl-1,4-phenylene oxide) and poly(2,6-diphenyl-1,4-phenylene oxide), the conversion of these cyclopentadiene sites to η^5-cyclopentadiene complexes with cobalt, rhodium, and titanium, and some of the catalytic reactions of these polymer-supported complexes.

Results and Discussion

Preparation of Poly(phenylene oxide)-Attached Cyclopentadiene Ligands. Cyclopentadiene has been chemically bonded to polystyrene either by the reaction of cyclopentadienyl sodium with chloromethylated polystyrene or by the reaction of cyclopentenone with lithiated

(1) Pittman, C. U. In "Polymer Supported Reactions in Organic Synthesis"; Hodge, P., Sherrington, D. C., Eds.; Wiley: New York, 1980; Chapter 5.
(2) Sherrington, D. C., ref 1, Chapter 1.
(3) International Workshop on Heterophase Attached Homogeneous Catalysis, Grenoble, France, 1977. CNRS and NSF.
(4) Arnold, C. *Macromol. Rev.* **1979**, *14*, 265.
(5) Jachowicz, J.; Kryszewski, M.; Sobol, A. *Polymer* **1979**, *20*, 995.

0276-7333/82/2301-0380$01.25/0

silicate, 65599-42-0; ((*E*)-2-phenylethenyl)pentafluorosilicate, 68901-41-7; (*E*)-1-hexenylpentafluorosilicate, 68732-24-1; 5-(5-decenyl)pentafluorosilicate, 70995-87-8; phenylpentafluorosilicate, 66712-45-6; dodecylpentafluorosilicate, 65599-40-8; (*exo*)-2-norbornylpentafluorosilicate, 74380-89-5; (*endo*)-2-norbornylpentafluorosilicate, 74410-83-6; (*E*)-octenylpentafluorosilicate, 70995-82-3; ((*E*)-10-(methoxycarbonyl)-1-decenyl)pentafluorosilicate, 70995-86-7; ((*E*)-3-(2-cyanoethoxy)propenyl)pentafluorosilicate, 74463-90-4; (*Z*)-5-decen-5-ylpentafluorosilicate, 70995-87-8; octyl bromide, 111-83-1; octyl chloride, 111-85-3; methyl 11-chloroundecanoate, 17696-12-7; 6-chloro-2-hexanone, 10226-30-9; 1-bromo-11-chloroundecane, 30295-21-7; 4-(2-chloroethyl)cyclohexene, 63540-00-1; 3-(3-bromopropoxy)prop-1-ene, 15424-07-4; 6-bromo-1-hexene, 2695-47-8; chlorocyclohexane, 542-18-7; (*E*)-1-chloro-2-phenylethene, 4110-77-4; (*E*)-1-bromo-2-phenylethene, 588-72-7; (*E*)-1-bromo-1-hexene, 13154-13-7; (*E*)-5-chloro-5-decene, 10124-72-8; (*E*)-5-bromo-5-decene, 72612-74-9; chlorobenzene, 108-90-7; bromobenzene, 108-86-1; dodecyl chloride, 112-52-7; cyclohexyl bromide, 108-85-0; *exo*-2-norbornyl bromide, 2534-77-2; *endo*-2-norbornyl bromide, 13237-87-1; 2-dodecanone, 6175-49-1; 3-octylcyclohexanone, 57242-85-0; methyl 14-oxopentadecanoate, 54889-71-3; (*E*)-1-octenyl thiocyanate, 74458-26-7; (*E*)-2-phenylethenyl thiocyanate, 61807-26-9; (*E*)-10-(methoxycarbonyl)-1-decenyl thiocyanate, 74458-28-9; (*E*)-3-(2-cyanoethoxy)propenyl thiocyanate, 74458-27-8; (*E*)-5-thiocyanato-5-decene, 74458-29-0; phenyl thiocyanate, 103-72-0; 1-octenyl ethyl ether, 30989-68-5; (*E*)-1-methoxy-1-octene, 62427-06-9; (*E*)-1-isopropoxy-1-octene, 77149-61-2; (*E*)-1-*tert*-butoxy-1-octene, 79618-58-9; (*E*)-1-(allyloxy)-1-octene, 77149-62-3; (*E*)-1-[(*E*)-2-butenyloxy]-1-octene, 79618-59-0; (*E*)-1-(2-methyl-2-propenyloxy)-1-octene, 77149-64-5; (*E*)-1-methoxy-2-phenylethene, 4110-75-2; (*E*)-1-methoxy-10-(methoxycarbonyl)-1-decene, 77149-65-6; (*E*)-1-methoxy-6-cyano-4-oxahex-1-ene, 77149-66-7; (*E*)-5-methoxy-5-decene, 77149-67-8; octanal, 124-13-0; 10-(methoxycarbonyl)decanal, 1931-65-3; copper(II) chloride, 7447-39-4; copper(II) bromide, 7789-45-9; copper(II) acetate, 142-71-2; copper(I) chloride, 7758-89-6; copper(I) iodide, 7681-65-4; copper(II) thiocyanate, 15192-76-4; 3-buten-2-one, 78-94-4; 2-cyclohexenone, 930-68-7; (*E*)-1-ethoxy-1-octene, 77149-60-1; methanol, 67-56-1; ethanol, 64-17-5; 2-propanol, 67-63-0; 2-methyl-2-propanol, 75-65-0; 2-propen-1-ol, 107-18-6; (*E*)-2-buten-1-ol, 504-61-0; 2-methyl-2-propen-1-ol, 513-42-8.

Poly(phenylene oxide) Catalyst Supports Containing (Cyclopentadiene)metal Complexes

L. Verdet and J. K. Stille*

Colorado State University, Fort Collins, Colorado 80523

Received September 15, 1981

Poly(2,6-dimethyl-1,4-phenylene oxide) containing cyclopentadienyl ligands attached to the benzyl carbons was prepared by the reaction of cyclopentadienylsodium with polymer that had been brominated at the benzyl position. Cross-linking took place during the reaction through the cyclopentadiene group. The reaction of 2-norbornen-7-one with poly(2,6-diphenyl-1,4-phenylene oxide) lithiated at the 3-position gave the norbornen-7-ol derivative which was converted to the polymer-attached 7-chloronorbornene. Cyclopentadiene ligands were generated via a retro Diels–Alder reaction of the anion produced from the 7-chloronorbornene. These polymers were converted to polymer-bound cyclopentadienyldicarbonylcobalt, cyclopentadienyldicarbonylrhodium, and titanocene catalysts. The cobalt and rhodium complexes were effective hydroformylation catalysts while the immobilized titanocene hydrogenated cyclohexene 10–70 times faster than the homogeneous analogue.

Introduction

Because there are many advantages to be gained by binding homogeneous catalysts to solid supports, the chemistry of homogeneous catalysts attached to polymers has been the subject of considerable research activity.[1] Cross-linked polystyrene has been the favorite polymer support, primarily because it is available commercially in various bead sizes with varying degrees of cross-link density.

Polystyrene beads, however, are mechanically, chemically, and thermally unstable.[2,3] For example, macroporous styrene–divinylbenzene resins will slough off polymer, particularly in a solvent that swells the bead. In addition, the reduction of carbon monoxide to hydrocarbons (Fischer–Tropsch), the reduction of carbon monoxide to methanol, and the hydroformylation of olefins in which water is used as the hydrogen source (water gas shift) are reactions that require temperatures higher than those usually necessary in homogeneous catalysis and are above or near the ceiling temperature of polystyrene ($T_c \approx 150$ °C). Further, polystyrene has poor chemical stability and will not endure a number of catalytic processes such as oxidation or photochemical reactions.

Poly(phenylene oxides) are a class of thermally stable engineering plastics.[4] Although the *thermooxidative* stability of the 2,6-dimethyl-substituted polymer is lower than other thermally stable polymers, its thermal stability under a nonoxidizing atmosphere is good;[5] however, the 2,6-diphenyl polymer has excellent thermal and oxidative stability. Consequently, we have explored the attachment of cyclopentadiene ligands to poly(2,6-dimethyl-1,4-phenylene oxide) and poly(2,6-diphenyl-1,4-phenylene oxide), the conversion of these cyclopentadiene sites to η^5-cyclopentadiene complexes with cobalt, rhodium, and titanium, and some of the catalytic reactions of these polymer-supported complexes.

Results and Discussion

Preparation of Poly(phenylene oxide)-Attached Cyclopentadiene Ligands. Cyclopentadiene has been chemically bonded to polystyrene either by the reaction of cyclopentadienyl sodium with chloromethylated polystyrene or by the reaction of cyclopentenone with lithiated

(1) Pittman, C. U. In "Polymer Supported Reactions in Organic Synthesis"; Hodge, P., Sherrington, D. C., Eds.; Wiley: New York, 1980; Chapter 5.
(2) Sherrington, D. C., ref 1, Chapter 1.
(3) International Workshop on Heterophase Attached Homogeneous Catalysis, Grenoble, France, 1977. CNRS and NSF.
(4) Arnold, C. *Macromol. Rev.* **1979**, *14*, 265.
(5) Jachowicz, J.; Kryszewski, M.; Sobol, A. *Polymer* **1979**, *20*, 995.

0276-7333/82/2301-0380$01.25/0

polystyrene followed by dehydration.[1] Poly(phenylene oxides) can be lithiated directly, and while lithiation of poly(2,6-diphenyl-1,4-phenylene oxide) takes place at the 3-position of the phenylene oxide unit,[6] lithiation of poly(2,6-dimethyl-1,4-phenylene oxide) is not as selective, taking place both at the 3-position and at the methyl group.[7] Although the reaction of sodium cyclopentadienide with halomethylated aromatics is a relatively clean reaction, the reaction of cyclopentenone with aryllithium is not.[8]

Bromination of the poly(phenylene oxides) is more selective and can be directed either to the phenylene oxide ring or to the benzyl positions.[9] Consequently, this reaction was chosen as an entry to substituted poly(phenylene oxides). This pathway also has the advantage that the degree of functionalization at the bromination stage could be determined readily. Free radical bromination of poly(2,6-dimethyl-1,4-phenylene oxide) (1) with *N*-

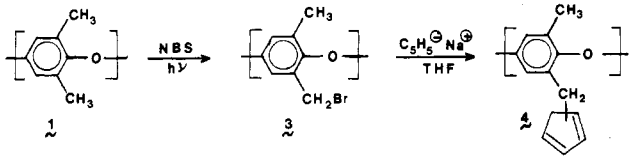

bromosuccinimide gave only the bromomethyl derivative (3) as confirmed by ^{1}H NMR. Products containing 0.17 and 0.35 bromine unit per repeat unit were obtained from 0.25 and 0.5 mol of *N*-bromosuccinimide per mole of recurring unit, respectively. The reaction of a solution of 3 with cyclopentadiene gave polymer 4 containing the

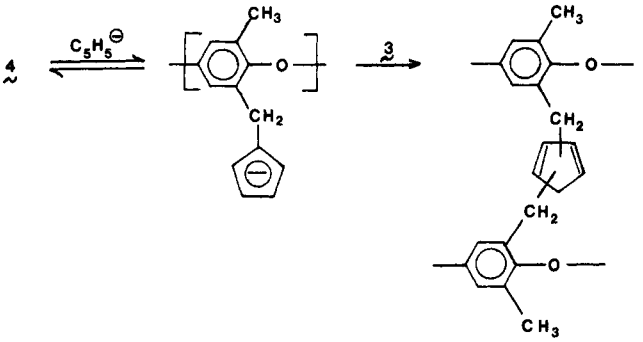

pendant cyclopentadiene groups. This reaction produced an insoluble polymer resulting from cross-linking that occurred either by a 4 + 2 dimerization reaction between cyclopentadiene units on two different chains or by alkylation of a second chain by an attached cyclopentadienyl anion. Analysis of the resulting polymer showed that 75% of the bromine had been displaced, even in the presence of excess cyclopentadienylsodium. Thus, in the case of polymer 3 containing 0.17 bromine unit per recurring unit, 0.04 bromine unit remained after the reaction, indicating 0.13 cyclopentadiene unit per polymer repeat unit. An incomplete reaction of cyclopentadienylsodium also has been observed with chloromethylated polystyrene.[10]

The presence of the pendant cyclopentadiene groups was difficult to verify by NMR or IR spectra of the insoluble polymer. The reaction of polymer 4 with maleic anhydride, however, produced a polymer containing the Diels–Alder adduct as shown by the strong carbonyl anhydride bands

Scheme I. Syntheses of Cyclopentadiene Derivatized Poly(2,6-diphenyl-1,4-phenylene oxide)

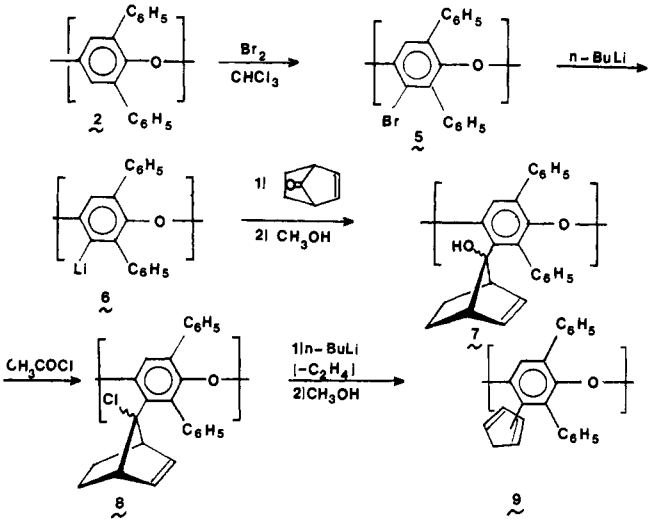

(1850 and 1775 cm^{-1}) in the infrared.

The electrophilic aromatic bromination of the 2,6-diphenyl-substituted polymer (2) was carried out in chloroform solution[9] to yield polymer 5 containing 0.18 bromine unit per repeat unit (Scheme I). Although bromination of the phenylene ether ring would be expected, it was not possible to distinguish the position(s) of bromination by NMR. Direct metalation of 2 with butyllithium yields polymer that had undergone reaction at the 3-position, although the maximum degree of lithiation was low even in the presence of a large excess of butyllithium.[6] Brominated polymer undergoes a more facile metalation with butyllithium, and the degree of lithiation can be more readily controlled.[9] Thus, the reaction of 5 with butyllithium gave the metalated polymer 6 which was allowed to react with 2-norbornen-7-one to yield polymer 7 containing the 7-attached 2-norbornen-7-ol unit.

The presence of norbornenol in the polymer was confirmed by the OH stretching in the infrared and by the characteristic vinyl and bridgehead proton absorptions in the ^{1}H NMR spectrum.[11] Less than 0.1% bromine remained in polymer 7. Chlorination of 7 with acetyl chloride gave polymer 8 containing 0.21 chlorine unit per repeat unit in which the OH stretching in the infrared was absent. Thus, the sequence of transformations, 5 through 8, appears to be quantitative.

Conversion of 8 to polymer 9 containing the cyclopentadiene pendants was achieved by reaction with butyllithium[8] to generate the benzyl anion which undergoes a retro Diels–Alder reaction with the evolution of ethylene.[12] Polymer 9 bearing the aryl cyclopentadiene ligands is soluble in a variety of solvents, indicating no cross-linking occurred during functionalization. Cyclopentadiene groups directly attached to the aromatic polymer backbone and sterically protected by the adjacent phenyl and phenoxide units apparently are prevented from undergoing an interchain Diels–Alder reaction.

Catalyst Preparation. Conversion of polymers 4 and 9 containing pendant cyclopentadiene ligands to supported catalysts corresponding to homogeneous complexes of cobalt, rhodium, and titanium was effected by methods used for the synthesis of the homogeneous analogues. In each case, only half the equivalent amount of transition metal

(6) Chalk, A. J.; Hoogeboom, T. J. *J. Polym. Sci., Polym. Chem. Ed.* **1971**, *9*, 3067.
(7) Chalk, A. J.; Hay, A. S. *J. Polym. Sci., Polym. Chem. Ed.* **1969**, *7*, 691.
(8) Sekiya, A.; Stille, J. K. *J. Am. Chem. Soc.* **1981**, *103*, 5096.
(9) White, D. M.; Orlando, C. M. *ACS Symp. Ser.* **1975**, *No. 6*, 178.
(10) Bonds, W. D.; Brubaker, C. H.; Chandrasekaran, E. S.; Gibbons, C.; Grubbs, R. H.; Kroll, L. C. *J. Am. Chem. Soc.* **1975**, *97*, 2128.
(11) Clark, F. R. S.; Warkentin, J. *Can. J. Chem.* **1971**, *49*, 2223.
(12) Bowman, E. S.; Hughes, G. B.; Grutzner, J. B. *J. Am. Chem. Soc.* **1976**, *98*, 8273.

Table I. Hydroformylation of 1-Octene with 10[a]

catalysts	loading mequiv of Co/g of support	Co/Cp ratio[b]	molar ratio octene/Co	T, °C	t, h	selectivity linear/branch
10a	0.54	0.45	329	135	12	2.4
10a	1.09	0.62	252	135	24	1.5
recycled 10a				135	24	1.5
10a	1.09	0.62	448	170	1	1.6
10a	1.09	0.62	469	135	12	1.7
10b	0.30	0.37	898	135	12	1.3

[a] Conditions: 1500 psi of H_2/CO (1:1); 2 mL of 1-octene in 10 mL of benzene. 100% conversion was achieved in every run. [b] For catalyst **10a**, the amount of available cyclopentadiene (Cp) units was based on the loss of bromide in the conversion of **3** to **4**. For **10b**, the cyclopentadiene (Cp) content was based on the chlorine analysis of **8**.

per cyclopentadiene was allowed to react in order to ensure that all of the metal reacted and to allow for uncertainties in cyclopentadiene content. Both **4** and **9** reacted with dicobalt octacarbonyl to give gray catalysts (**10**), the infrared spectra of which exhibited two characteristic carbonyl bands at 2010 and 1950 cm^{-1}, close to the carbonyl frequencies observed for cyclopentadienyldicarbonylcobalt[13] (Scheme II). Polymer **4**, containing the higher concentration of cyclopentadiene groups per repeat unit, also exhibited low-intensity carbonyl stretching frequencies at 1900 and 1875 cm^{-1}, characteristic of bridging carbonyls and a cobalt dimer.

The reaction of the cyclopentadiene-containing polymers with methyllithium was used to generate the cyclopentadiene anion. The anion-bearing supports reacted with the chlorodicarbonylrhodium dimer to yield catalysts which exhibited two metal carbonyl bands. In the case of polymer **11a**, containing benzyl-attached cyclopentadienyl groups, the carbonyl stretching frequencies were 2030 and 1970 cm^{-1}, and in polymer **11b**, in which the cyclopentadienyl ligand is attached directly to the aromatic ring, frequencies of 2050 and 1955 cm^{-1} were observed. The reported[14] bands for (η^5-cyclopentadienyl)dicarbonylrhodium are 2051 and 1987 cm^{-1}.

Finally, polymers **4** and **9** were converted to the corresponding anions and allowed to react with cyclopentadienyltitanium trichloride. Polymer **12** was red-brown, a darker color being obtained with a higher degree of cyclopentadiene substitution. This polymer was converted to titanocene by reaction with butyllithium; reaction of the reduced complex with carbon monoxide gave polymer attached dicyclopentadienyltitanium dicarbonyl complexes[13] which exhibited two metal carbonyl bands in the infrared spectrum at 1955 and 1875 cm^{-1}.

Catalytic Reactions. Catalyst **10** showed no activity in a Fischer–Tropsch reaction. Although **10a** containing the benzyl-bound cyclopentadienyl group was not expected to be a catalyst,[15] **10b** containing a phenyl-bound cyclopentadienyl ligand also did not effect the reduction of carbon monoxide in a 3:1 H_2–CO mixture at 150 or 200 °C.[15] However, these polymer-bound complexes (**10**) did catalyze the hydroformylation of 1-octene to a mixture of linear and branched aldehydes at 135 °C and 1500 psi (Table I). This same type of catalyst bound to crosslinked polystyrene has been shown to catalyze the hydroformylation of 1-olefins.[16]

Insoluble catalyst **10a** could be readily recovered by filtration at the end of the hydroformylation reaction and reused without apparent decrease in the catalytic activity.

Scheme II. Catalysts from Cyclopentadiene Attached Poly(phenylene oxides)

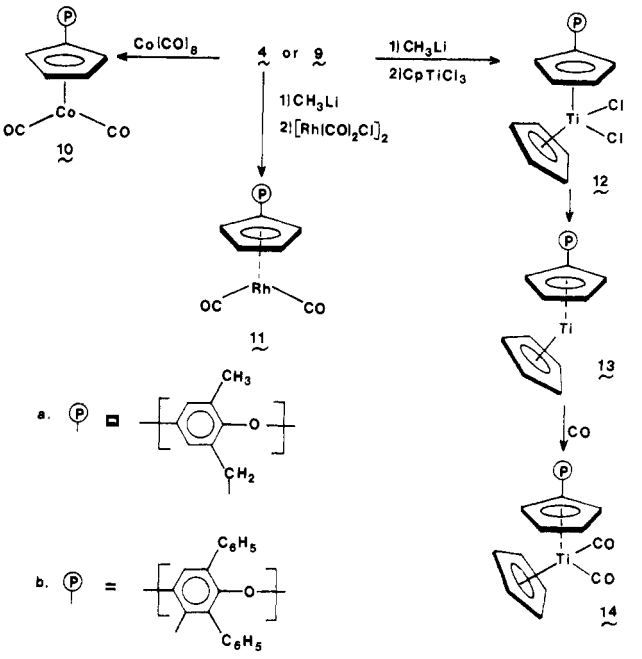

Some broadening and a slight decrease in intensity of the carbonyl bands of the recovered catalyst were observed. In addition, at long reaction times the presence of a weak absorption at 1710 cm^{-1} was observed. Nevertheless, no carbonyl absorption assignable to hydridocobalt tetracarbonyl was observed as was detected in the final reaction mixture after a hydroformylation with the homogeneous analogue.[18] Hydroformylation using soluble **10b** was carried out by using homogeneous conditions; recovery of this catalyst could be achieved by precipitation into a nonsolvent, e.g., ether, followed by filtration.

Catalyst **11** also was effective for the hydroformylation of 1-octene. Under the same reaction conditions as reported for hydroformylation with the similar polystyrene attached cyclopentadienyldicarbonylrhodium,[16,17] complete conversion to the isomeric aldehydes was achieved (Table II).

No attempt was made to optimize the reaction conditions or increase the selectivity to linear aldehyde, which has been shown to be dependent on temperature and pressure.[18] While there was no change in the infrared carbonyl band of catalyst **11a**, the carbonyl absorption for polymer **11b** disappeared after several runs, consistent with the loss of catalyst activity observed with recycled **10b**. At

(13) Piper, T. S.; Cotton, F. A.; Wilkinson, G. *J. Inorg. Nucl. Chem.* **1955**, *1*, 165.
(14) Fischer, E. O.; Bittler, K. *Z. Naturforschg.* **1961**, *16b*, 225.
(15) Perkins, P.; Vollhardt, K. P. C. *J. Am. Chem. Soc.* **1979**, *101*, 3985.
(16) Chang, B. H.; Grubbs, R. H.; Brubaker, C. H., Jr. *J. Organomet. Chem.* **1979**, *172*, 81.
(17) Grubitosa, G.; Brintzinger, H. H. *Colloq. Int. C.N.R.S.* **1977**, *No. 281*, 173.
(18) Pruett, R. L. *Adv. Organomet. Chem.* **1979**, *17*, 1.

Table II. Hydroformylation of 1-Octene with 11[a]

catalyst	loading: mequiv of Rh/g of support	loading: Rh/Cp ratio[b]	solvent	molar ratio substrate/Rh	selectivity linear/branch
11a	0.55	0.57	C_6H_6	258	0.6
recycled 11a			C_6H_6		1.3
11b	0.46	0.59	n-C_6H_{14}	771	1.2
recycled 11b			n-C_6H_{14}		1.5[c]

[a] Conditions: 1000 psi of H_2/CO (1:1); 50 °C; 24 h. [b] For catalyst 11a, the amount of available cyclopentadiene (Cp) units was based on the loss of bromide in the conversion of 3 to 4. For 11b, the cyclopentadiene (Cp) content was based on the chlorine analysis of 8. [c] Only a 68% conversion of 1-octene to aldehyde was achieved.

Table III. Hydrogenation of Cyclohexene with Polymer Attached Titanocene Catalyst 13

catalyst	loading: mequiv of Ti/g of polymer	loading: Ti/Cp[b] ratio	hydrogenation rate: relative rate, n-hexane, 25 °C (mequiv of Ti)	hydrogenation rate: mPH_2/min/mequiv of Ti, n-octane, 0 °C (mequiv of Ti)
13a	0.57	0.40	70 (0.057)	71 (0.042)
	0.86	0.30	52 (0.086)	39 (0.042)
13b	0.11	0.13	53 (0.022)	39 (0.016)
Cp_2Ti	0.10	0.5	3.7 (0.22)	<1

[a] Catalyst/solvent (10 mL)/n-BuLi (1 mL, 2.5 min in hexane)/cyclohexane (1 mL). [b] For 13a, the amount of available cyclopentadiene (Cp) units was based on the loss of bromide in the conversion of 3 to 4. For 13b, the cyclopentadiene (Cp) content was based on the chlorine analysis of 8.

long reaction times (90 h) and at a higher temperature (100 °C) both catalysts **10a** and **10b** reduced nonanal to n-nonanol giving a 1:9 mixture of aldehyde to alcohol.

Reduction of poly(phenylene oxide)-bound titanocene dichloride (**12**) with butyllithium gave the polymer-supported titanocene catalyst (**13**) containing isolated catalytic sites. Hydrogenation of cyclohexene was effected under conditions described[10,19] for polystyrene-bound titanocene (Table III). Although the reported hydrogenation rates differ depending on the polymer support, the degree of crosslinking, and the physical state of the heterogenized catalyst, the rate of hydrogenation is 10–70 times faster with the poly(phenylene oxide)-supported catalyst than with the homogeneous titanocene. The fact that the rate of hydrogenation increased when better site isolation was provided (**13a**, lower mmol of Ti/g of polymer) supports the necessity for preventing catalyst site interaction. Even uncross-linked polymer **13b** maintained as much as a 40-fold activity over homogeneous titanocene. The enhanced activity in this case may be due to the steric protection of the titanocene sites.

Experimental Section

All manipulations involving air-sensitive compounds were performed under argon in Schlenk-type vessels. Transfers and filtrations were carried out in an argon-filled glovebox. Recovery of the soluble polymer-bound catalyst was facilitated by precipitation of the polymers into ether and suction filtration through a fritted filter; insoluble polymer-bound catalysts were recovered simply by suction filtration of the reaction mixture.

Infrared spectra were recorded on a Beckman IR 4240 spectrophotometer; KBr pellets of the samples were prepared in a drybox. GLC was carried out on columns consisting of SE30 or Carbowax 2017 on Chromosorb W.

Elemental analyses were performed by Micro Tech Laboratories, Inc., Skokie, IL, and Galbraith Laboratories, Inc., Knoxville, TN. All solvents were purified and dried by usual procedures. Poly(phenylene oxides) were obtained from General Electric Co., Schnectady, NY. Dicobalt octacarbonyl, chlorodicarbonylrhodium, bis(cyclopentadienyltitanium dichloride), cyclopentadienyltitanium trichloride, and organolithium reagents were obtained commercially.

Bromination of Poly(2,6-dimethyl-1,4-phenylene oxide) (1). To a refluxing solution of 50 g (0.42 mol of repeating unit) of polymer 1 in 500 mL of carbon tetrachloride (the complete dissolution of polymer needed 4 h in stirred, refluxing carbon tetrachloride) was added 18 g (0.10 mole) of freshly recrystallized N-bromosuccinimide over a 10-min period while the solution was irradiated with a 100-W flood lamp at a distance of 10 cm. After 1 h, the mixture was filtered to remove the succinimide. The filtrate was added dropwise to methanol. After filtering, the precipitated polymer was ground vigorously in a blender and washed thoroughly with methanol. The recovered brominated polymer (**3**), dried under reduced pressure, contained 10.43% of bromine, indicating 17% of the repeating units had been brominated. With twice as much N-bromosuccinimide (36 g, 0.20 mol) and the same conditions, the resulting polymer contained 18.84% of bromine (~0.35 Br/unit): ^{1}H NMR ($CDCl_3$) δ 2.05 (CH_3), 4.3 ($-CH_2Br$), 6.45, and 6.65 (aromatic).

Bromination of Poly(2,6-diphenyl-1,4-phenylene oxide) (2). A solution of 25 g (0.10 mol of repeating unit) of polymer **2** in 150 mL of chloroform was added to a solution of 4 g (0.02 mol) of bromine in 10 mL of chloroform. The mixture was heated to a gentle reflux and after 30 min allowed to cool to room temperature. Stirring was continued overnight. The polymer was precipitated into methanol, ground vigorously in a blender, and washed thoroughly with methanol. After being dried under reduced pressure, **5** contained 5.44% Br (~0.18 Br/unit): ^{1}H NMR ($CDCl_3$) δ 5.9, 6.15, and 6.3 (aromatic protons).

Reaction of Sodium Cyclopentadienide with Brominated Poly(2,6-dimethyl-1,4-phenylene oxide) (3). Under an argon atmosphere, 100 mL of dry THF was distilled directly into a flask containing 5 g of brominated polymer **3** (10.43% Br/g). Into this solution, cooled by an ice bath, was syringed 5 mL of a 2.5 M THF solution of freshly prepared cyclopentadienyl sodium.[20] The solution immediately became dark red and very thick. After 3 h of stirring, the red solution was allowed to warm to room temperature. The mixture was poured into 200 mL of deaerated methanol. The precipitated brown polymer (**4**) was filtered, washed with methanol, and dried under reduced pressure for 3 days. The resulting polymer contained 2.70% Br/g (0.04 Br/unit).

Attachment of Cyclopentadiene to Poly(2,6-diphenyl-1,4-phenylene oxide). Reaction of Norbornen-7-one with Lithiated Polymer 6. Into a flask containing 4 g of brominated polymer **5** (5.4% Br/g) was distilled 100 mL of dry THF under

(19) (a) Grubbs, R. H.; Gibbons, C.; Kroll, L. C.; Bonds, W. D.; Brubaker, C. H. *J. Am. Chem. Soc.* **1973**, *95*, 2373. (b) Chandrasekaran, E. S.; Grubbs, R. H.; Brubaker, C. H. *J. Organomet. Chem.* **1976**, *120*, 49. (c) Grubbs, R. H.; Lau, C. P.; Cukier, R.; Brubaker, C. H. *J. Am. Chem. Soc.* **1977**, *99*, 4517.

(20) Wilkinson, G. "Organic Syntheses"; Wiley: New York, 1900; Coll. Vol. IV, p 473.

argon. The stirred yellow solution was cooled to −70 °C and 2 mL of a 2.5 M hexane solution of *n*-butyllithium was added via syringe. After 2 h, 0.70 g (6.4 mmol) of norbornen-7-one[21] was distilled into the reaction mixture at −70 °C. After 1 h, the flask was allowed to warm to room temperature. The mixture was stirred overnight and then poured into deaerated methanol. The precipitated polymer (**7**) was then stirred overnight in methanol, filtered, ground, washed for 24 h in methanol, and then dried: Ir (KBr) 3560 cm^{-1} (–OH stretch); ^1H NMR ($CDCl_3$) δ 5.2, 5.1 (vinyl), 2.8 (bridgehead), 2.2 (H, alcohol), 1.4, 1.2, 0.5 (CH_2). Anal.: <0.1% Br.

Preparation of Polymer-Attached 7-Chloronorbornene (8). Under argon, 60 mL of dried THF was distilled directly into the reaction flask containing 3 g of polymer **7**. To this solution was added 0.80 mL (11 mmol) of acetyl chloride. After being stirred for 48 h, the yellow solution was poured into anhydrous diethyl ether to precipitate a white polymer. After filtration, the polymer was ground, washed with pentane, and dried under reduced pressure. Anal.: 2.78% Cl (0.21 Cl/repeat unit).

Preparation of Polymer-Attached Cyclopentadiene (9). Dry THF, 60 mL, was distilled directly in the reaction flask containing 2 g of polymer **8** containing the attached 7-chloronorbornene units. A solution of 2 mL of 0.25 M *n*-butyllithium in *n*-hexane was added, and the mixture was cooled to −70 °C. The color of the solution turned from yellow to dark red. After 1 h the mixture was allowed to warm to room temperature and then poured into deaerated methanol. The white polymer which precipitated was filtered, washed with methanol, and dried under reduced pressure. Anal.: 0.11% Cl.

Polymer-Supported Cyclopentadienylcobalt Carbonyl Catalysts (10). In a typical experiment, 0.4 g (0.4 mmol of cyclopentadiene for **4**; 0.3 mmol of cyclopentadiene for **9**) of polymer containing attached cyclopentadiene units was allowed to swell (or dissolve in the case of **9**) in methylene chloride (60 mL). Under argon, a solution of 0.40 g (1.2 mmol) of dicobalt octacarbonyl in 10 mL of methylene chloride was added. The black mixture, protected from the light, was stirred at room temperature for 72 h and then poured into a dried deaerated hexane/diethyl ether mixture. The gray precipitate was filtered, washed with ether, and dried under reduced pressure: IR (KBr) 2010, 1950 cm^{-1} (C≡O).

Polymer-Supported Cyclopentadienylrhodium Dicarbonyl (11). In a typical experiment 0.2 g (0.2 mmol of cyclopentadiene for **4**; 0.15 mmol of cyclopentadiene for **9**) of polymer containing attached cyclopentadiene units was suspended in anhydrous diethyl ether cooled to −70 °C, and 0.4 mL of a 1.2 M methyllithium solution in ether was added. The mixture was allowed to warm to room temperature and was stirred for 72 h under argon. The polymer was recovered by filtration and washed under argon with ether. After being dried, the polymer was suspended in 20 mL of hexane that was directly distilled into the reaction flask. A yellow solution of 0.031 g (0.080 mmol) of $[(Rh(CO)_2Cl]_2$ in 10 mL of hexane was added to the polymer suspension at −70 °C. The yellow suspension became orange and then was allowed to warm to 0 °C during which the suspension became dark red and then gray. The suspension was kept for 24 h at 0 °C and then filtered. The gray solid recovered was washed with hexane until the washings were colorless. The polymer was dried under reduced pressure: IR (KBr) 2030, 1970 cm^{-1} (C≡O) (**11a**) and 2050, 1995 cm^{-1} (**11b**).

Preparation of Polymer-Attached Titanocene Dichloride (12). In a typical experiment 1 g (1.0 mmol of cyclopentadiene for **4** and 0.15 mmol of cyclopentadiene for **9**) was suspended in 80 mL of diethyl ether that had been directly distilled into the reaction flask. After the suspension was cooled to −70 °C, 2 mL of a 1.2 M methyllithium solution in ether was added and after 1 h the mixture was allowed to warm to room temperature. Stirring was continued for 5 days. The polymer was filtered, washed, and dried. To 0.8 g of the polymer-supported cyclopentadienide anion, swollen (or dissolved in the case of **9**) in 60 mL of benzene, was added 0.3 g (1.4 mmol) of cyclopentadienyltitanium trichloride dissolved in benzene. After 5 days the polymer was washed with ether (or precipitated into ether, polymer **9**) and dried. A red brown product was obtained.

Preparation of Attached Dicyclopentadienyltitanium Dicarbonyl (14). To a suspension of 0.2 g (0.2 mmol titanium) of polymer attached dichlorotitanocene **12** suspended in 40 mL of hexane and cooled to −70 °C was added 0.75 mL of 2.5 M *n*-butyllithium in hexane. The mixture was allowed to warm to room temperature and after 3 h was transferred to a 100-mL Parr reactor. The reactor was purged with carbon monoxide and then left for 12 h at room temperature with a carbon monoxide pressure of 1100 psi. After release of the pressure, the brown polymer was filtered, washed with 200 mL of hexane, and dried under reduced pressure: Ir (KBr) 1955, 1872 cm^{-1} (C≡O).

Hydroformylation Reactions with Rhodium and Cobalt Catalysts 10 and 11 (Tables I and II). To a 100-mL reactor containing the rhodium catalyst **11** or the cobalt catalyst **10** suspended in 10 mL of benzene or hexane was added 2.0 mL (13 mmol) of 1-octene. The mixture was stirred for 15 min under a hydrogen pressure of 500 psi and, after release of the pressure, for another 15 min under a carbon monoxide pressure of 500 psi. After release of the gas, the reactor was repressurized to 100 psi with a mixture of H_2/CO (1:1) and heated to 50 °C for 24 h. The reactor was cooled to −70 °C, and the pressure was released slowly. At room temperature, the reactor was flushed with argon and the brown-gray suspension was filtered. The recovered polymer-bound catalyst was washed and dried overnight before being reused. The branched and linear aldehydes were characterized by GC analysis of the filtrate. The linear to branched aldehyde ratio was directly determined from the ^1H NMR spectrum of the filtrate when the solvent was hexane and by GC analysis when the solvent was benzene.

Hydrogenation of Aldehyde with Rhodium Catalyst 11. A 100-mL reactor was charged with polymer-bound catalyst **11**, 10 mL of benzene or hexane, and 2 mL (12 mmol) of freshly distilled 1-nonanal. The bomb was flushed with hydrogen, then pressurized to 1000 psi of hydrogen, and finally heated at 100 °C for 86 h. After release of the pressure, the reactor was cooled to −78 °C, the reaction mixture was filtered, the catalyst was washed and dried, and the filtrate was examined by GC and ^1H NMR.

Hydrogenation with Titanium Catalyst 13 (Table III). In a typical experiment, 0.2 g of polymer-bound catalyst **12** was suspended in 10 mL of hexane (or octane) under argon. The flask was flushed with hydrogen and left under 1 atm of hydrogen. The flask was cooled to 0 °C, and 1 mL of a 2.5 M *n*-butyllithium solution in hexane was added. The mixture was allowed to warm to room temperature (or kept at 0 °C), and when the level of hydrogen in a gas delivery apparatus connected to the reaction flask had stabilized, 1 mL of cyclohexene, which was freshly distilled under argon, was added. The rate of hydrogen uptake was determined by monitoring the level in the gas delivery apparatus.

Acknowledgment. This research was supported by a Grant DMR-80 16503 from the National Science Foundation. We wish to thank Dr. A. S. Hay, General Electric, for supplying us with the polymer samples and Dr. A. Sekiya for assisting with the initial bromination experiments.

Registry No. 1 homopolymer, 25134-01-4; 1 repeating unit, 24938-67-8; 2 homopolymer, 26353-84-4; 2 repeating unit, 24938-68-9; sodium cyclopentadienide, 4984-82-1; norbornen-7-one, 694-71-3; dicobalt octacarbonyl, 10210-68-1; cyclopentadienyltitanium trichloride, 1270-98-0; 1-nonanal, 124-19-6; 1-octene, 111-66-0; cyclohexene, 110-83-8; Cp_2Ti, 1271-29-0; $[(Rh(CO)_2Cl]_2$, 14523-22-9.

(21) Gassman, P. G.; Pape, P. G. *J. Org. Chem.* **1964**, *29*, 160.

New Platinacyclobutanes from *exo*-Tricyclo[3.2.1.$0^{2,4}$]oct-6-ene and *exo,exo*-Tetracyclo[3.3.1.$0^{2,4}$.$0^{6,8}$]nonane

Mark D. Waddington and Paul W. Jennings*

Department of Chemistry, Montana State University, Bozeman, Montana 59717

Received July 24, 1981

Two new platinacyclobutane complexes have been prepared from tricyclooctene 1 and tetracyclononane 2. They are, in fact, the compounds in solution when one dissolves the rather insoluble, initially formed platinum complexes in THF or Me_2SO. They were characterized by ^1H, ^{13}C, and ^{195}Pt NMR spectroscopy as platinacyclobutanes which have the exo configuration relative to the bicyclic structure. Moreover, they are unique in that there are no previously characterized platinacyclobutanes which have cis disubstitution.

Metallocyclobutane complexes have received considerable attention over the last few years because they are thought to be intermediates in a number of organic transformations.[1-3] Platinacyclobutanes have been particularly interesting because they often have slow reaction rates and stable intermediates. Moreover, the phenyl-substituted platinacyclobutanes have been shown to exhibit a very intriguing stereospecific intramolecular rearrangement.[4,5]

In 1969, Volger[6] reported on the reactions of *exo*-tricyclo[3.2.1.$0^{2,4}$]oct-6-ene, **1**, and *exo,exo*-tetracyclo[3.3.1.$0^{2,4}$.$0^{6,8}$]nonane, **2**, with various transition-metal complexes. He found that **1** was quantitatively converted to **3** by using $Rh_2(CO)_4Cl_2$ via an uncharacterized yellow intermediate. Katz[7] subsequently reported that the rhodium complex $(Ph_3P)_3RhCl$ not only converted **1** to **3** but also to **4** and **5**. From the results of an elegant deuterium-labeling experiment, he suggested that an endo rhodium π-allyl complex was responsible for the formation of **4** and **5**. According to Volger,[6] the tetracyclohydrocarbon **2** also reacted with $Rh_2(CO)_4Cl_2$, forming a yellow complex, but failed to rearrange to analogues of **3** and **4**.

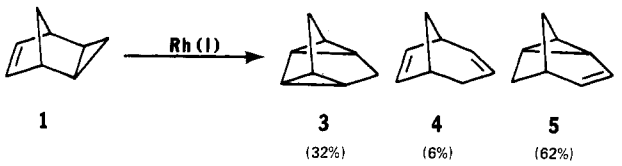

1 **3** (32%) **4** (6%) **5** (62%)

Volger further showed that Zeise's dimer, $[(C_2H_4)PtCl_2]_2$, reacted with **1** and **2** to form insoluble pale yellow derivatives which he postulated to have structures **7** and **8**,

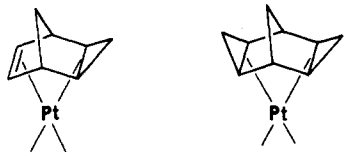

7 **8**

respectively. These platinum complexes were proposed to require bis-endo coordination to the edge of the cyclopropane.

In 1980, Johnson[8] reported further on the reactions of complex **8**. He found it to be insoluble in THF and CH_3CN. When it reacted with pyridine, starting hydrocarbon **2** was regenerated, rather than forming the typical bis(pyridine), six-coordinate platinacyclobutane. In Me_2SO, a facile and quantitative rearrangement occurred to yield **6**, which is analogous to the π-allyl rearrangement advanced by Katz. Like Volger, Johnson concluded that **8** was indeed a bis-endo edge-bound platinum complex.

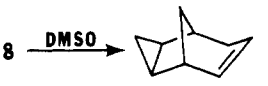

6

Results

In this article, we present evidence which shows that complexes **7** and **8** are, or are easily converted to, platinacyclobutanes **9** and **10**, respectively. In these experiments, hydrocarbon **1** or **2** was added dropwise to Zeise's dimer in ether. The characteristically orange solid, Zeise's dimer, was quickly consumed and replaced by a pale yellow suspension which was filtered, washed with ether, and dried in a vacuum desiccator containing anhydrous calcium sulfate. The platinum complex of **1** was darker yellow than that from **2**. In order to characterize these two initially formed solids, they were solubilized in THF.

9 **10**

NMR Spectral Interpretation. Although these complexes were not very soluble in THF as previously reported, they were sufficiently soluble to determine ^{13}C NMR spectra by using a high-field 250-MHz spectrometer. The NMR data for the proposed complexes **9** and **10** are shown in Table I.

When these data were first observed, the most striking characteristic was the unexpected number of unique ^{13}C resonances. If structures **7** and **8** were correct, one would have observed five and four unique resonance lines, respectively. The data obtained and listed in Table I were totally inconsistent with **7** and **8**. The fact that only one ^{195}Pt NMR resonance was observed for complex **8** ensured the homogeneity of the sample. In discussing the ^{13}C NMR

(1) Ivin, K. J.; Rooney, J. J.; Stewart, C. D.; Green, M. L. H.; Mahtab, R. *J. Chem. Soc., Chem. Commun.* **1978**, 604.
(2) Grubbs, R. H. *Proc. Inorg. Chem.* **1978**, *24*, 1.
(3) Bishop, K. C., III. *Chem. Rev.* **1976**, *76*, 461.
(4) Al-Essa, R. J.; Puddephatt, R. J.; Thompson, P. J.; Tipper, C. F. H. *J. Am. Chem. Soc.* **1980**, *102*, 7546.
(5) Casey, C. P.; Scheck, D. M.; Shusterman, A. J. *J. Am. Chem. Soc.* **1979**, *101*, 4233.
(6) Volger, H. C.; Hogeveen, H.; Gaasbeek, M. M. P. *J. Am. Chem. Soc.* **1969**, *91*, 218, 2137.
(7) Katz, T. J.; Cerefice, S. A. *J. Am. Chem. Soc.* **1969**, *91*, 2405; **1971**, *93*, 1049.
(8) Johnson, T. H.; Cheng, S. S. *Synth. Commun.* **1980**, *10*, 381.

0276-7333/82/2301-0385$01.25/0

Table I. ^{13}C NMR Data for 9 and 10 in Tetrahydrofuran

	9			10		
carbon	δ	$J_{Pt,C}$, Hz	$J_{C,H}$, Hz	δ	$J_{Pt,C}$, Hz	$J_{C,H}$, Hz
1	−3.1 t[a]	435	148	−11.3 t	421	149
2	54.0 d	88	144	57.5 d	102	146
3	13.4 d	457	159	14.8 d	451	157
4	47.3 d	12	151	40.5 d	13	148
5	134.4 d	56	169	12.2 d	61	169
6	137.8 d		169	14.3 d		170
7	47.3 d	33	151	42.2 d	33	148
8	45.2 t		134	22.8 t		133
9				2.0 t		160

[a] Multiplicity of resonance peak with gated decoupling.

assignments in detail, structure **10** will be exemplified. Structures **2**, **11**, **12**, and **13**, which have well-characterized NMR spectra, will be used as analogues.[9]

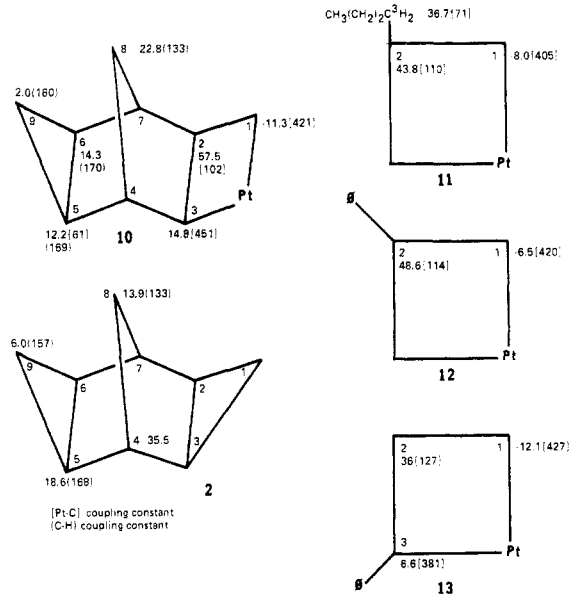

Carbon 1 has three unique characteristics. First, it is coupled to ^{195}Pt by 421 Hz which is consistent with a σ bond to platinum. Second, it exhibits triplet multiplicity in the gated decoupled spectrum, confirming that it is a CH_2 moiety. Third, it is upfield of Me_4Si, which is in accord with the analogous carbons of structures **11**, **12**, and **13**.

The large platinum coupling constant of 451 Hz and the doublet character of the gated decoupled spectrum established the resonance for C-3. The reduced ^{195}Pt coupling to C-2 and its chemical shift are consistent with the analogous carbons of structures **11**, **12**, and **13**.

There are two additional carbons that exhibit triplet multiplicity in the gated decoupled spectrum. The high-field resonance at 2.0 ppm with a $^1J_{C-H}$ value of 160 is assigned to the cyclopropyl carbon 9, basically because of the analogous $^1J_{C-H}$ coupling in structure **2**. The 4.0 ppm shift to higher field for C-9 in structure **10** vs. that carbon in structure **2** is not understood. The other triplet resonance at 22.8 ppm with a $^1J_{C-H}$ of 133 Hz was consequently assigned to C-8.

Carbons 4 and 7 have not been adequately investigated to permit accurate assignment. However, we tentatively suggest that C-4 is at 40.5 ppm with a $^2J_{Pt,C}$ value of 13 Hz and C-7 is at 42.2 ppm with a $^3J_{Pt,C}$ value of 33 Hz.

(9) NMR resonance positions for compounds **2**, **11**, **12**, and **13** were established in our own laboratory after synthesizing the compounds by literature methods.

Carbons 5 and 6 are obviously part of an intact cyclopropane moiety because of their C–H coupling constants which are analogous to those in structure **2**. Carbon 5 is also unique in that the $^3J_{Pt,C}$ value is 61 Hz. This is analogous to C-3 of structure **11**. To explain the relatively large coupling constant to C-5, we propose to employ a Karplus-type relationship. For C-5, the dihedral angle is near 180°. If this idea is extended to C-7, a value of 33 Hz is reasonable for an estimated angle of 100° in either of the two possibilities. Finally, the $^3J_{Pt,C}$ value for C-8 is near 0, suggesting an angle of 80–90° which is also reasonable if the platinacyclobutane moiety is puckered at an angle of 150–160°. A similar distortion in platinacyclobutanes has been observed previously.[10] The Karplus-type relationship has also been used previously to explain coupling constants in organotin[11] and organoselenium[12] complexes.

Arguments similar to those used above can be employed to justify structure **9**. The exo stereochemistry for both platinacyclobutane moieties is assumed from the stereochemistry of the starting hydrocarbons **1** and **2**.

Chemical Characterization. If the initially formed platinum complexes were dissolved in Me_2SO-d_6 at room temperature, they slowly formed compounds **5** and **6**. During this dissolution and subsequent rearrangement, we were able to detect complexes **9** and **10** by ^1H NMR spectroscopy. Their half-lives at 25 °C were 3.0 h and 28 min, respectively.

If, to a $CDCl_3$ suspension of the initially formed platinum complexes of **1** or **2** in an NMR tube, 2.5 equiv of pyridine were added, the complexes dissolved to form **9** and **10**, respectively. There was no NMR spectral evidence for the formation of **1** or **2** as previously reported.[8] Addition of 3.5 equiv of Ph_3P to this pyridine derivative in $CDCl_3$ did regenerate compounds **1** and **2**. When 3.5 equiv of Ph_3P were added to either of the $CDCl_3$ suspensions, **1** and **2** were quantitatively regenerated.

Discussion

In this reaction sequence, Zeise's dimer in ether reacts rapidly with hydrocarbon **1** or **2** to form initial platinum complexes (IPC) which have not been fully characterized. They have been proposed to be endo-platinum complexes which are bound to the edge of the cyclopropane moiety.[6,8] However, in the present work we show that dissolution of these IPC complexes in THF, $CHCl_3$ containing pyridine, or Me_2SO yields the *exo*-platinacyclobutanes **9** and **10**, respectively.

(10) Rajaram, J.; Ibers, J. A. *J. Am. Chem. Soc.* **1978**, *100*, 829.
(11) Doddrell, Y. K.; Burfitt, I.; Kitching, W.; Bullpit, M.; Lee, C. H.; Mynott, R. J.; Considine, J. L.; Kuivila, H. G.; Sarma, R. H. *J. Am. Chem. Soc.* **1974**, *96*, 1640.
(12) Harris, R. K.; Mann, B. E. "NMR and the Periodic Table"; Academic Press: New York, 1978; p 409.

Evidence for proposing structures **9** and **10** is garnered from ^{13}C and ^{195}Pt NMR spectroscopy. The chemical shift values observed are consistent with the proposed structures when compared to model systems **2**, **11**, **12**, and **13**. A great deal of structural assignment weight was put on the $J_{Pt,C}$ values which are not only indicative of platinum–carbon σ bonds but also are analogous to known platinacyclobutanes.

The only piece of information for which there are little data is the exo configuration of the platinacyclobutane. However, the facts that the original cyclopropane moieties in **1** and **2** were exo and that they were regenerated from complexes **9** and **10** on treatment with Ph_3P strongly suggest that the exo platinacycle is correct. There is a 1–2 ppm downfield shift for one proton on C-8 in going from **1** to **9** or **2** to **10**, but there is inadequate precedent to use these data for structural assignments.

These complexes (**9** and **10**) are the first examples to be characterized as cis-1,2-disubstituted platinacyclobutanes. All previous examples of stable 1,2-disubstituted platinacyclobutanes were derived from trans-disubstituted cyclopropanes. However, there are three reports in which cis-substituted cyclopropanes were reacted with platinum. McQuillin[13] reported in 1972 that *cis*-1-methyl-2-*n*-butylcyclopropane reacted with Zeise's dimer to form a mixture of 2- and 3-octene. Further, he found that bicyclo[4.1.0]heptane reacted to give a platinum complex which, upon treatment with KCN, gave methylenecyclohexane, 1-methylcyclohexene, and cycloheptene. In neither of these two cases was a platinacyclobutane characterized or proposed.

In 1979, Johnson[14] reported that *cis*-1,2-dimethylcyclopropane reacted with Zeise's dimer to give 1-pentene (23%), *cis*-2-pentene (20%), 2-methyl-1-butene (15%), 3-methyl-1-butene (6%), and 2-methyl-2-butene (36%). Although a platinacyclobutane was not observed, it was proposed as a possible intermediate.

Finally, in 1980, Puddephatt[4] reported that *cis*-1,2-diphenylcyclopropane reacted sluggishly with Zeise's dimer to yield possibly a diphenylallyl derivative of platinum. Further characterization was not carried out, but a platinacyclobutane was proposed as an intermediate.

Thus, it appears that hydrocarbons **1** and **2** either form platinum complexes which are different from the cis-disubstituted cyclopropanes previously investigated or the decomposition reaction of the platinacyclobutanes from **1** or **2** is retarded. In fact, McQuillin[13] favored a π-allylplatinum complex over the platinacyclobutane to explain the differences in reactivity and products between cis and trans complexes. It is therefore reasonable to suggest that the exo platinum complexes **9** and **10** are unusually stable because they are unable to achieve coplanarity with the β hydrogen to form olefinic products via β elimination. Further investigation is continuing on these aspects.

Experimental Section

General. NMR spectra were recorded on a Bruker WM 250 spectrometer. K_2PtCl_4 was obtained from Aldrich and used without further purification. THF-d_8 was purchased from Stohler and Me_2SO-d_6 from Wilmad. Analytical analyses were carried out by Galbraith Laboratories.

Preparation of Zeise's Dimer $[(C_2H_4)PtCl_2]_2$. This compound was prepared from K_2PtCl_4 exactly as described by Littlecott.[15]

Preparation of *exo*-Tricyclo[3.2.1.$0^{2,4}$]oct-6-ene (1) and *exo,exo*-Tetracyclo[3.3.1.$0^{2,4}$.$0^{6,8}$]nonane (2). These compounds were prepared by the methods described by Kottwitz.[16] The NMR spectral data for these hydrocarbons agreed with the published values.[6]

Reaction of 1 and 2 with Zeise's Dimer. To a vial containing 110 mg (0.185 mmol) of $[(C_2H_4)PtCl_2]_2$ in 10 mL of dry ether was added dropwise 80 μL($\sim$0.8 mmol) of **1** or **2**. The orange dimer was quickly consumed, as the yellowish cream-suspended product formed. After the mixture was stirred with a magnetic stirrer for 10 min, the suspension was filtered and the solid product was crushed, resuspended in 10 mL of ether, and again filtered by suction. After this was dried in a vacuum desiccator containing anhydrous $CaSO_4$, a yield of 80–90% was obtained. Larger quantities (to 1.5 g) were prepared in a similar manner.

The products **7** and **8** gradually darkened in color with increasing temperature: **7**, mp 130–140 °C dec; **8**, mp 145–155 °C dec. Anal. Calcd for $C_8H_{10}PtCl_2$ (**7**): C, 25.82; H, 2.71. Found: C, 25.60; H, 2.70. Anal. Calcd for $C_9H_{12}PtCl_2$ (**8**): C, 27.99; H, 3.13. Found: C, 27.98; H, 3.23.

Dissolution of 7 and 8 in THF. To 1.5–2 mL of THF was added 100 mg of **7** or **8**, resulting in a yellow solution for ^{13}C NMR analysis. During the time required for the ^{13}C determinations (at 35 °C), the solutions of **7** and **8** gradually darkened, with the production of small amounts of **1** and **2** as the only detectable decomposition products. Solutions of 2–4 mg of **7** or **8** in 100 μL of THF-d_8 were used for ^1H NMR analysis.

Dissolution of 7 and 8 in $CdCl_3$ and Pyridine, and Subsequent Reaction with Ph_3P. The addition of 6 μL (0.075 mol) of pyridine to a suspension of 5 mg ($\sim$0.014 mmol) of **7** or **8** in 0.5 mL of $CDCl_3$ resulted in a yellow solution for ^1H NMR analysis. Larger quantities were used to prepare solutions suitable for ^{13}C NMR analysis. The addition of 0.5 mL of a 0.095 M solution of Ph_3P in $CDCl_3$ (containing 0.048 mmol of Ph_3P) to the above 0.5-mL solutions of **9** or **10** resulted in the quantitative production of **1** and **2**, respectively, as determined by ^1H NMR spectroscopy.

Reaction of 7 and 8 with Ph_3P in $CdCl_3$. To $\sim$0.5 mL of a 0.095 M solution of Ph_3P in $CDCl_3$ (containing 0.048 mmol of Ph_3P) was added 5 mg ($\sim$0.014 mmol) of **7** or **8**, resulting in dissolution of the platinum compound and quantitative production of **1** and **2**, respectively as determined by ^1H NMR spectroscopy.

Dissolution of 7 and 8 in Me_2SO-d_6. To 0.6 (or 1.5) of mL Me_2SO-d_6 was added 23 (or 100) mg of **7** or **8**, yielding yellow solutions of **9** or **10**, respectively, as determined by ^1H NMR spectroscopy. The slow decomposition to form **5** or **6**, respectively, along with small amounts of **1** and **2**, respectively, was followed by ^1H NMR spectroscopy.[17] The products were identified by ^1H and ^{13}C NMR spectroscopy:[18,19] ^{13}C NMR for **5** (ppm) 13.4 (d, 2C), 15.4 (d), 27.5 (t, 2 C), 31.4 (d), 127.2 (d), 128.8 (d); ^{13}C NMR for **6** (ppm) 6.1 (t), 17.7 (d), 25.6 (d), 26.9 (t), 33.5 (d), 33.7 (d), 34.7 (t), 125.2 (d), 136.3 (d).

Acknowledgment. We are grateful to Montana State University and to NSF (Grant CHE-7826160) for their support of this research. We also wish to thank J. A. S. Pribanic and J. Campbell for their technical advise.

Registry No. **1**, 3635-94-7; **2**, 24506-61-4; **5**, 3725-23-3; **6**, 42836-55-5; **9**, 79647-66-8; **10**, 79647-67-9; $[(C_2H_4)PtCl_2]_2$, 12073-36-8.

(13) McQuillin, F. J.; Powell, K. G. *J. Chem. Soc., Dalton Trans.* **1972**, 2123.
(14) Johnson, T. H.; Hefty, E. C. *J. Org. Chem.* **1979**, *44*, 4896.
(15) Littlecott, G. W.; McQuillin, F. J.; Powell, K. G. *Inorg. Synth.* **1976**, *16*, 113.
(16) Kottwitz, J.; Vorbruggen, H. *Synthesis* **1975**, 636.
(17) NMR analysis suggests the presence of other minor decomposition products from **9**, but no **4** was detected.
(18) ^1H NMR of **5**: Sauers, R. R.; Shurpik, A. J. *J. Org. Chem.* **1968**, *33*, 799.
(19) ^{13}C NMR of **6** agrees with data of Johnson.[8]

1,3-Diene Complexes of Zirconium and Hafnium Prepared by the Reaction of Enediylmagnesium with MCl_2Cp_2. A Remarkable Difference between the Zirconium and Hafnium Analogues As Revealed by ^1H NMR and Electronic Spectra

H. Yasuda, Y. Kajihara, K. Mashima, K. Nagasuna, K. Lee, and A. Nakamura*

Department of Macromolecular Science, Faculty of Science, Osaka University, Toyonaka, Osaka 560, Japan

Received August 25, 1981

1,3-Butadiene, isoprene, and 2,3-dimethyl-1,3-butadiene complexes of Zr and Hf were prepared by the 1:1 reaction of $ZrCl_2Cp_2$ or $HfCl_2Cp_2$ with the corresponding enediylmagnesium $[MgCH_2CR{=}CRCH_2]_n$, where R is H or CH_3. The variable ^1H NMR spectra of the zirconium–diene complexes showed a limiting *s-cis*-η^4-1,3-diene structure below −40 °C, although they are fluxional at higher temperatures. The ^1H NMR parameters for these Zr complexes at −70 °C were determined by computer simulation. The corresponding Hf complexes showed a strong preference for the metallacyclopentene structure in the temperature range of −90 to +80 °C. A clear difference between the Zr and Hf complexes was also observed in the electronic spectra. In contrast, the Cp_2Zr(1,4-diphenyl-1,3-butadiene) complex favored the *s-trans*-η^4-diene structure at −80 to +50 °C, although the Hf analogue preferred the *s-cis*-η^4-diene structure. All these complexes released the coordinated 1,3-dienes quantitatively on reaction with oxygen. 3,4-Dideuterated butene (or 1,4) or its methyl or phenyl derivatives were formed on treatment of these complexes with D_2O.

Introduction

The 1,3-diene complexes of group 4A metals reported so far show enhanced chemical reactivity. Zirconium(0)- and zirconium(II)-diene complexes with bidentate phosphine ligands are among the well-characterized examples of the 4A metal–diene complexes.[1,2] We have previously communicated (1) a novel method for preparation of a series of Cp_2M(diene) complexes (where M = Zr of Hf) utilizing enediylmagnesium,[3] (2) solution structure,[3] and (3) some regioselective reactions of these complexes with nitriles, carbonyl compounds,[4] alkenes, dienes, and alkynes.[5] Independent of our work, Erker and Krüger recently have reported the synthesis and structure of a series of Cp_2Zr(diene) complexes which were obtained by photochemical reactions between $Cp_2Zr(C_6H_5)_2$ and conjugated dienes.[6]

In this paper, we wish to report the details of our method, the unique reactivity of the resulting diene complexes, and the remarkable difference in fluxional behavior between the Zr and Hf complexes as observed in the variable-temperature ^1H NMR spectra. Since some of the complexes involve a new type of mononuclear *s-trans*-diene structure, the NMR data are compared with those of zirconium, hafnium, and related metal complexes having the *s-cis*-diene structure.

Preparation and Characterization of Cp_2M(1,3-diene) Complexes

A zirconium complex of isoprene was prepared by the 1:1 reaction of $ZrCl_2Cp_2$ with $[Mg(C_5H_8)]_n$ in THF at 20 °C for 2–3 h. After evaporation of the reaction mixture to dryness, the Cp_2Zr(isoprene) complex was extracted into hot benzene–hexane (1:2) and was isolated in the form of extremely air-sensitive dark red crystals by recrystallization from hexane in ca. 70% yield. When the original reaction mixture was cooled to −40 °C, orange crystals of an adduct formulated as $[Cp_2Zr(isoprene)][MgCl_2{\cdot}2THF]$ precipitated in high yield (65–75%). The adduct of Cp_2Zr(isoprene) with magnesium salts is thermally unstable, and hence heating the crystals in refluxing hexane resulted in the precipitation of the magnesium salt. From the hexane-soluble fraction, red crystals of Cp_2Zr(isoprene) were obtained in good yield when the solution was concentrated and cooled to −20 °C. The Zr complexes obtained by this method did not contain any magnesium salt as checked by chemical analysis. The process for the formation of the diene complexes is summarized in eq. 1.

In the case of the hafnium products, the complexes are readily separated from salts by extraction with hexane at 20–30 °C. The interaction of 4–6 with magnesium salts seems to be weaker than that of the Zr derivatives 1–3.

$$MCl_2Cp_2 + [MgCHR^1CR^2{=}CR^3CHR^1]_n \xrightarrow{THF} [Cp_2M(CHR^1{=}CR^2CR^3{=}CHR^1)][MgCl_2{\cdot}2THF] \xrightarrow{\Delta} Cp_2M(CHR^1CR^2{=}CR^3CHR^1) + MgCl_2{\cdot}2THF \quad (1)$$

M = Zr	M = Hf
1, $R^1 = R^2 = R^3 = H$	4, $R^1 = R^2 = R^3 = H$
2, $R^1 = R^2 = H$, $R^3 = CH_3$	5, $R^1 = R^2 = H$, $R^3 = CH_3$
3, $R^1 = H$, $R^2 = R^3 = CH_3$	6, $R^1 = H$, $R^2 = R^3 = CH_3$
7, $R^2 = R^3 = H$, $R^1 = C_6H_5$	8, $R^2 = R^3 = H$, $R^1 = C_6H_5$

A series of butadiene, isoprene, 2,3-dimethylbutadiene, and 1,4-diphenyl-1,3-butadiene complexes of Zr and Hf thus was prepared by the reaction with the corresponding enediylmagnesium $[MgCHR^1CR^2{=}CR^3CHR^1]_n$ where R^1, R^2, and R^3 are H, CH_3, and/or C_6H_5.[7,8] The compositions of the complexes were established by chemical analysis, molecular weight determination, and the ^1H NMR spectra (Table I). All the Zr and Hf complexes exist in monomeric form as proved by the cryoscopic method or by mass spectroscopy.

(1) S. Datta, S. S. Wreford, R. P. Beatty, and T. J. McNeese, *J. Am. Chem. Soc.*, **101**, 1053 (1979).
(2) R. P. Beatty, S. Datta, and S. S. Wreford, *Inorg. Chem.*, 18, 3139 (1979).
(3) (a) H. Yasuda, Y. Kajihara, K. Mashima, K. Lee, and A. Nakamura, *Chem. Lett.*, 519 (1981). (b) For a preliminary report: H. Yasuda, Y. Kajihara, and A. Nakamura, "Proceedings of the Ninth International Conference on Organometallic Chemistry", Dijon, 1979, Abstr. C47.
(4) H. Yasuda, Y. Kajihara, K. Mashima, K. Nagasuna, and A. Nakamura, *Chem. Lett.*, 671 (1981).
(5) H. Yasuda, Y. Kajihara, K. Nagasuna, K. Mashima, and A. Nakamura, *Chem. Lett.*, 719 (1981).
(6) G. Erker, J. Wicher, K. Engel, F. Rosenfeldt, W. Dietrich, and C. Krüger, *J. Am. Chem. Soc.*, **102**, 6346 (1980).
(7) K. Fujita, Y. Ohnuma, H. Yasuda, and H. Tani, *J. Organomet. Chem.*, **113**, 201 (1976).
(8) H. Yasuda, Y. Nakano, K. Natsukawa, and H. Tani, *Macromolecules*, 11, 586 (1978).

0276-7333/82/2301-0388$01.25/0

Table I. Characterization of Cp_2M(diene)

complex	mp, °C	metal content,[a] %		Cp/diene ratio,[b] mol/mol		mol wt [c]	
		calcd	found	calcd	found	calcd	found
1	73	33.1	33	2.00	1.98	275	291
2	64	31.5	32	2.00	2.00	290	301
3	101 dec	30.0	30	2.00	2.01	304	325
4	78	49.2	48	2.00	2.00	363	374
5	68	47.4	48	2.00	2.02	377	388
6	115 dec	45.7	45	2.00	1.99	391	401
7	231 dec	21.3	21	2.00	2.00	426.4 (^{90}Zr), 39.3[d]	426
						427.4 (^{91}Zr), 20.0	427
						428.4 (^{92}Zr), 17.8	428
						430.4 (^{94}Zr), 13.1	430
8	233 dec	34.7	33	2.00	2.00	513.4 (^{177}Hf), 16.8	513
						514.4 (^{178}Hf), 26.4	514
						515.4 (^{179}Hf), 17.5	515
						516.4 (^{180}Hf), 31.3	516

[a] Determined by the metal oxide method and calculated by using atomic weight defined by IUPAC rule. [b] Determined from ^{1}H NMR signal intensity ratio. [c] Molecular weight for **1–6** were determined cryoscopically in benzene and that for **7** and **8** by MS. [d] Intensity ratio (%) of the parent peaks for individual isotopes.

Table II. Hydrolysis and Air Oxidation Product of Cp_2M(diene) Complexes (M = Zr, Hf)

complex	hydrolysis products (distribution, %)	combined yield,[a] mol %	oxidation product	yield,[a] mol %
1	1-butene (98) 2-butene (2)	99	1,3-butadiene	94
2	3-methyl-1-butene (94) 2-methyl-2-butene (4)	99	isoprene	99
3	2,3-dimethyl-1-butene (96) 2,3-dimethyl-2-butene (4)	100	2,3-dimethyl-1,3-butadiene	97
4	1-butene (91) 2-butene (9)	98	1,3-butadiene	95
5	3-methyl-1-butene (94) 2-methyl-1-butene (1) 2-methyl-2-butene (5)	98	isoprene	96
6	2,3-dimethyl-1-butene (92) 2,3-dimethyl-2-butene (8)	100	2,3-dimethyl-1,3-butadiene	95
7	1,4-diphenyl-1-butene (24) 1,4-diphenyl-2-butene (76)	100	(*E*,*E*)-1,4-diphenylbutadiene	93
8	1,4-diphenyl-1-butene (18) 1,4-diphenyl-2-butene (82)	98	(*E*,*E*)-1,4-diphenylbutadiene	99

[a] Yields were determined by gas chromatographic analysis and are given in mol % to the diene complexes.

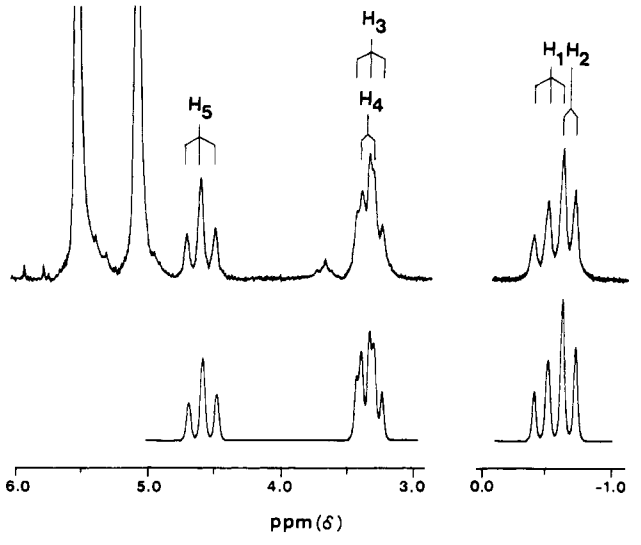

Figure 1. ^{1}H NMR (100-MHz) spectrum of Cp_2Zr(*s-cis*-η^4-isoprene) (**2**) at −70 °C in toluene-d_8 (above) and the simulated spectrum (below).

The diene complexes **1–8** immediately released the coordinated diene quantitatively when the benzene solution was exposed to dry air or oxygen (Table II). The complexes are sensitive also to water and readily hydrolyzed with aqueous HCl. The distribution of hydrolysis products is given in Table II. Addition of deuterium oxide decomposes the Zr and Hf complexes **1–6** to give dideuterated olefins where two deuterons occupy the 3,4-positions regioselectively; e.g., 3,4-dideuterio-1-butene, 3,4-dideuterio-3-methyl-1-butene, or 3,4-dideuterio-2,3-dimethyl-1-butene was produced, respectively. No difference was observed in the hydrolysis between Zr and Hf complexes. Production of 1,4-dideuterated isomer was only 1–9% and of 1,2-dideuterated compounds, which are possible for **2** and **5**, was negligible. Exceptional are the 1,4-diphenyl-1,3-butadiene complexes **7** and **8**, which produced a 1,4-dideuterated olefin exclusively (80%), with minor amounts of a 1,2-dideuterated one. Intermediacy of metallacyclopropane, which may be in equilibrium with a metallacyclo-3-pentene (eq 2) or deuterioxy (η^3-allyl)-

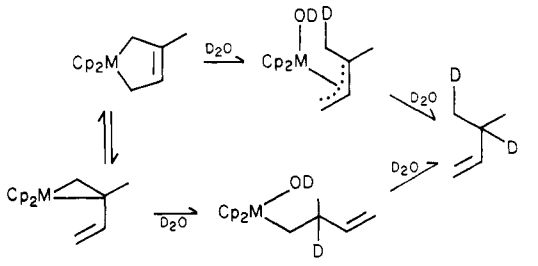

(2)

metal species, is invoked to account for the selective deuteration of **1–6**. Equation 2 illustrates possible routes for the selective deuteration of **2** to afford 3,4-di-

deuterio-3-methyl-1-butene.

Thermolysis of metallacyclopentanes of Ti,[9] Zr,[10] Pt,[11] Ta,[12] and Ni[13] is known to proceed by (a) β-hydrogen elimination, (b) reductive elimination, or (c) C–C bond cleavage, depending critically on the transition metals and ligands present in the complex. Such types of elimination or C–C bond cleavage were not observed in the thermolysis of **1–6** at 130 °C for 8 h in toluene or decane. The sole products obtained in thermolysis were coupling products between the Cp ligand and the diene. For example, complex **2** gradually decomposed at this temperature to give a mixture of $C_{10}H_{14}$ isomers (which corresponds to the 1:1 cyclopentadiene–isoprene adduct) as confirmed by MS ($M^+ = 134$) and by gas chromatography (three components in 15–25% yield).

Nuclear Magnetic Resonance of $Cp_2M(1,3\text{-diene})$ Complexes with *s-cis*-η^4-Diene Structure. The ^1H NMR (100-MHz) spectra of **1–3** were temperature dependent and revealed the fluxional character of the zirconium–diene bonding at room temperature. When the temperature was lowered, the signals broadened at 0–10 °C and split into two groups assignable to syn and anti protons at the diene termini below −40 °C to reach the limiting η^4-1,3-diene structure. For example, $Cp_2Zr(2,3\text{-dimethyl-1,3-butadiene})$ (**3**) in toluene-d_8 at 30 °C showed three broad singlets at 1.19, 1.80, and 5.31 ppm in a 2:3:5 ratio assignable to CH_2, CH_3, and Cp groups, respectively. At −40 °C, the terminal CH_2 signal split into two doublets of equal intensity at 3.16 (syn) and −0.72 ppm (anti).

Chemical shift values of the complexes **1–3** (at −70 °C in toluene-d_8) and a set of ^1H NMR parameters determined by iterative computer simulation are given in Table III. Parameters for related (*s-cis*-diene)metal complexes also are given for comparison. On the basis of the proton coupling constants, $J_{15(26)}$, $J_{35(46)}$, and J_{56}, the butadiene complex **1** most likely has a *s-cis*-η^4-1,3-diene structure rather than a metallacyclopentene structure.

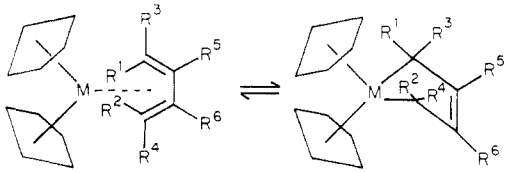

(3)

If **1** favored the metallacyclo-3-pentene structure, the value of $J_{15(26)}$ and $J_{35(46)}$ must be smaller and J_{12} should be larger. We note that magnitude of $J_{15(35)}$ and J_{12} for 1,1-dimethylsilacyclo-3-pentene, 1,1-dimethylgermacyclo-3-pentene,[14] oxo- or thiacyclo-3-pentene[15] and cyclopentene[16] are known to be 1.6–4.6 and 1.7–7.0 Hz, respectively.

Computer analysis of the spectrum of the isoprene complex **2** offered parameters comparable to **1**, although the NMR pattern is rather complicated due to the overlap of the proton signals at C_1 and C_4 (Figure 1). Chemical shift and coupling constant values for **3** also resemble those for **1**. The ^1H NMR data on **1–3** compare closely with those of tricarbonyliron and -ruthenium complexes of *s-*

Table III. ^1H NMR Parameters for *s-cis*-η^4-Diene Complexes at −70 °C and for Related Complexes[a]

complexes	chemical shift, ppm				coupling constant, Hz							
	ν_1 (ν_2)	ν_3 (ν_4)	ν_5 (ν_6)	ν_{Cp}	J_{12}	$J_{13(24)}$	$J_{14(23)}$	$J_{15(26)}$	$J_{16(25)}$	J_{34}	$J_{35(46)}$	$J_{36(45)}$	J_{56}
1 (cis isomer)	−0.69	3.45	4.78	4.84	0.5	−10.0	0.2	10.5	−0.8	0.2	9.5	−1.5	8.0
				5.37									
2	−0.57 (R_1)	3.32 (R_3)	4.52 (R_5)	4.96	0.8	−9.6	0.3	11.0	−0.2	0.4	10.2	−1.5	
	−0.73 (R_2)	3.29 (R_4)	1.88	5.45				(J_{15})			(J_{35})	(J_{45})	
			($R_6 = CH_3$)										
3				5.03									
	−0.72	3.16		5.44	1.0	−10.0	0.2			0.5			
				4.84									
8 (cis isomer)	0.90		5.57	5.38	0.5			11.1	−1.8				10.7
$Fe(CO)_3(C_4H_6)^b$	−0.03	1.46	4.89		−0.31	−2.42	−0.09	9.33	−1.11	0.05	6.93	1.14	4.70
$Ru(CO)_3(C_4H_6)^b$	0.12	1.44	4.88		−0.30	−2.77	−0.13	8.65	−1.10	0.02	6.94	1.10	4.60
$Os_3(CO)_{10}(C_4H_6)^c$	0.49	2.32	5.27		?	2.89	?	8.53	−0.79	?	7.17	1.02	4.66

[a] Spectra were observed at 100 MHz in toluene-d_8 and were analyzed by the computer simulation. Chemical shifts were calibrated by using the internal benzene peak, assumed to be 7.20 ppm. The numbering system follows that shown in eq 3. [b] Data by Philipsborn.[17,18] [c] Data by Shapley.[26]

(9) J. X. McDermott, M. E. Wilson, and G. M. Whitesides, *J. Am. Chem. Soc.*, **98**, 6529 (1976).
(10) G. Erker and K. Krop, *J. Am. Chem. Soc.*, **101**, 3659 (1979).
(11) J. X. McDermott, J. F. White, and G. M. Whitesides, *J. Am. Chem. Soc.*, **98**, 6521 (1976).
(12) S. J. McLain, C. D. Wood, and R. R. Schrock, *J. Am. Chem. Soc.*, **101**, 4558 (1979).
(13) R. H. Grubbs, A. Miyashita, M. Liu, and P. Burk, *J. Am. Chem. Soc.*, **100**, 2418 (1979).
(14) M. L. Filleux-Blanchard, N.-D. An, and G. Manuel, *J. Organomet. Chem.*, **137**, 11 (1977).
(15) R. Lazach and B. Braillon, *J. Magn. Reson.* **12**, 244 (1973).
(16) B. Lemarié, R. Lozach, and B. Braillon, *J. Chem. Phys.*, **72**, 1253 (1975).

Table IV. ^{1}H NMR (100 MHz) Spectral Data for *s-cis*-Diene Complexes at 38 °C[a]

complexes	chemical shift, ppm				coupling constant, Hz		
	ν_1 (ν_3)	ν_2 (ν_4)	ν_5 (ν_6)	ν_{Cp}	$J_{15(26)}$	$J_{35(46)}$	J_{56}
1[b]	1.43 (b s)	1.43 (b s)	4.74 (dt)	5.25	9.9	9.9	10.7
2	1.27 (d)	1.23 (s)	4.58 (t)	5.28	10.1 (J_{15})	10.1 (J_{35})	
3	1.19 (s)	1.19 (s)		5.31			
4[c]	1.14 (m)	1.14 (m)	5.04 (m)	5.23	10.1	10.1	11.1
5	1.00 (d)	1.05 (s)	4.90 (t)	5.27	9.9 (J_{15})	9.9 (J_{35})	
6	0.93 (s)	0.93 (s)		5.36			

[a] Toluene-d_8 was used as a solvent. [b] Measured at 60 °C. [c] Simulated spectrum was given in ref 3. Numbering system follows that for metallacyclopentene given in eq 3.

Table V. ^{1}H NMR Parameters for *s-trans*-η^4-Diene Complexes at 38 °C[a]

complexes	chemical shift, ppm				coupling constant, Hz							
	ν_1 (ν_2)	ν_3 (ν_4)	ν_5 (ν_6)	ν_{Cp}	J_{12}	$J_{13(24)}$	$J_{14(23)}$	$J_{15(26)}$	$J_{16(25)}$	J_{34}	$J_{35(46)}$	$J_{36(45)}$
1 (trans isomer)	3.22	1.22	2.90	4.92	0.5	−4.0	0.02	7.1	−0.5	0.5	16.4	−1.1
7		3.23	3.91	4.89						0.2	15.8	−0.8
8 (trans isomer)		3.11	3.87	4.88						0.2	15.5	−0.8
$Os_3(CO)_{10}(C_4H_6)$[b]	1.43	2.26	3.40		?	2.47	?	7.38	−0.65	?	11.13	−0.48
C_4H_6[c]	4.97	5.08	6.25		1.3	1.7	0.6	10.1	−0.8	0.7	16.9	−0.8

[a] Spectral data were collected at 100 MHz in toluene-d_8 and analyzed by simulation. [b] Data by Shapley.[26] [c] Data by Segre.[25] The numbering system follows that given in eq 7.

cis-butadiene.[17-19] On the basis of these facts, the solution structure of **1–3** was concluded to be the conventional *s-cis*-η^4-diene structure below −40 °C, in line with the crystal structure of Cp_2Zr(2,3-dimethyl-1,3-butadiene).[6]

The chemical shift difference between the syn and anti protons for **1**, **2**, and **3** at −70 °C was found to be exceedingly large (3.88–4.14 ppm) compared with those (1.3–2.3 ppm) for $[Zr(C_4H_6)_2(dmep)](dmep)$,[1] $Fe(CO)_3(C_4H_6)$,[17] $RhCp(C_4H_6)$, $RhCp(C_5H_8)$,[20] or similar complexes. The resonance of the anti protons appears at remarkably high magnetic field, indicating their presence in a magnetically highly shielded environment. The diamagnetic shielding zone due to the Cp–Zr bond seems responsible for this observation. The chemical shift of the syn protons was significantly lowered compared with that of $M(CO)_3(C_4H_6)$ (M = Fe, Ru, Os) but is similar to that of tricarbonyl(cyclic diene)iron complexes.[21] The chemical shift values of the terminal protons at diene termini observed at 38 °C fit well to the averaged value of chemical shifts of syn and anti protons observed at −70 °C. A single Cp proton resonance at 38 °C also showed the averaged chemical shift value of the two Cp resonances detected at −70 °C (Table V).

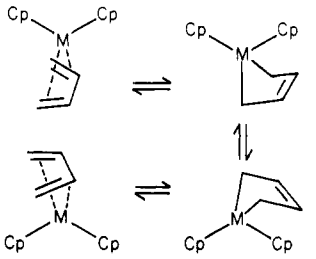

(4)

Therefore, the fluxional mode of the 1,3-diene coordinated to Zr may be explained in terms of the equilibrium between (*s-cis*-η^4-diene)metal and metallacyclo-3-pentene species (a flip mechanism) rather than the rotation of the diene group around the coordination axis. Equation 4 illustrates the fluxional mode of the butadiene complex as an example. The rate of fluxionalization seems to be in an order **1** < **2** ≃ **3** because the coalescence temperature observed for the butadiene complex (ca. 0 °C) is higher than those (ca. −40 °C) observed for the isoprene and 2,3-dimethyl-1,3-butadiene complexes. The ^{1}H NMR data gave no evidence in support of a fluxionalization process via (η^3-allyl)metal species shown in eq 5.

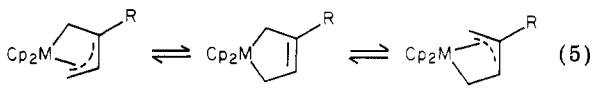

(5)

Since the metallacyclopentene is a 16-electron species with an electron-rich alkenyl group, complexation with electron donors or electron acceptors seems plausible. If an electron donor occupies the vacant d orbital of the metal, the equilibrium (eq 6) may shift to the right to give

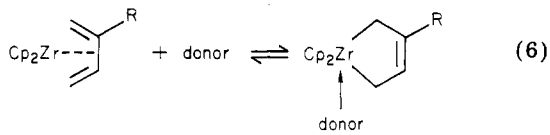

(6)

a stable metallacyclo-3-pentene which has two Zr–C σ bonds, as in $Cp_2Zr(CH_3)_2$ or dicyclopentadienylzirconacyclopentane. To examine this possibility, an excess of an electron donor such as $P(Bu)_3$, $P(C_6H_5)_3$, pyridine, or triethylamine was added to **2**. However, no remarkable change was observed on the variable-temperature NMR spectra. An electron acceptor such as trimethylaluminium or triethylaluminium also showed no interaction with **2** although **2** forms an adduct with $MgCl_2$·2THF as noted above. Thus, the addition of usual electron donors or acceptors had no effect on the presumed equilibration (eq 6, cf. eq 4).

The ^{1}H NMR patterns of the Hf complexes **4–6** were very simple and did not (Table IV) change on lowering the temperature from +60 °C to −85 °C. However, when the temperature was lowered to −110 °C, the spectra of **4** and **6** were converted to the pattern of *s-cis*-η^4-diene coordination as has been found for **1** and **3** at −40 °C, respectively. Broad signals of the anti and syn protons of **4** appeared at −0.65 and 3.36 ppm and Cp proton signals at 4.78 and 5.21 ppm. Corresponding signals of **6** appeared

(17) K. Bachmann and W. von Philipsborn, *Org. Magn. Reson.* **8**, 648 (1976).
(18) S. Ruh and W. von Philipsborn, *J. Organomet. Chem.*, **127**, C59 (1977).
(19) E. A. Koerner von Gustorf, F.-W. Grevels, and I. Fischler, "The Organic Chemistry of Iron", Academic Press, New York, 1978, p 113.
(20) S. M. Nelson, M. Sloan and M. G. B. Drew, *J. Chem. Soc., Dalton Trans.* 2195 (1973).
(21) S. D. Ittel, F. A. Van-Catledge, and J. P. Jesson, *J. Am. Chem. Soc.*, **101**, 3874 (1979).

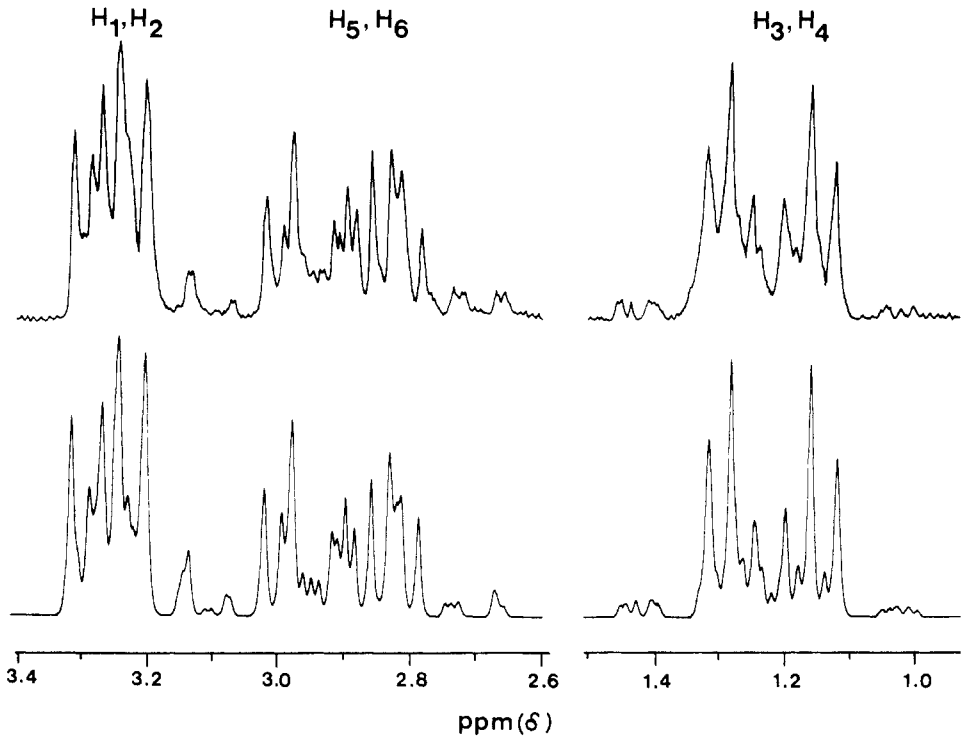

Figure 2. ^{1}H NMR (100-MHz) spectrum of $Cp_2Zr(s\text{-}trans\text{-}\eta^4\text{-butadiene})$ at 38 °C in toluene-d_8 (above) and the simulated spectrum (below).

at −0.65 (anti), 3.05 (syn), 4.98, and 5.30 (Cp) ppm, respectively, at this temperature. Thus, the rate of fluxionalization of the hafnium–diene complexes is very rapid at temperatures above −85 °C.

When the chemical shift values of the Hf complexes 4–6 were compared with those of the Zr complexes 1–3 at 38 °C, the resonance of the terminal protons appears at a higher field by 0.26–0.29 ppm. This difference may be attributed to the stronger M–C σ-bonding character of Hf than Zr, in accord with the general trend that the metal–hydrogen or metal–carbon σ bond is stronger for the third-row transition-metal complexes than the corresponding bond in the second-row isostructural ones. For example, calculation of the Cotton–Kraihanzel force constants for the CO vibration of $M(CO)_2Cp_2$ (M = Ti, Zr, Hf)[22] showed that the force constants (mdyn/Å) decrease from Ti, 15.18, and Zr, 15.06, to Hf, 14.96. The interaction force constants increase in the order Ti, 0.61, Zr, 0.70, Hf, 0.71, to indicate enhanced bonding with CO for the Hf derivative. In the related pentamethylcyclopentadienyl compounds, $M(CO)_2(Me_5C_5)_2$,[22] the same trend was observed. Thus, the remarkably different NMR temperature dependency observed between Zr and Hf complexes is reasonably explained as follows: The hafnium complexes prefer the σ-M–C bonding (when compared with the isostructural Zr complexes), while the Zr complexes prefer the π-M–C bonding.

The detection of subtle differences in the electronic properties between Zr and Hf is worth noting because these two elements are known to have similar electronegativities, ionic potentials, and ionic radii due to the lanthanide contraction. The difference is amplified in the dynamic structure of organometallic complexes with multicenter ligands. Similar spectral differences have been observed between tetrakis(η-allyl)zirconium and tetrakis(η-allyl)-hafnium.[23] The former showed the limiting AM_2X_2 pattern at temperatures below −40 °C, while the latter has an AX_4 pattern even at −60 °C, suggesting ease in rotation at the CH_2 group. The X-ray structures of $(C_5H_5)_4M$ also showed a critical difference; i.e., $(C_5H_5)_4Hf$ was formulated with two η^1- and two η^5-cyclopentadienyl units, while $(C_5H_5)_4Zr$ has one η^1- and three η^5-bonded Cp ligands.[24] Lack of X-ray analyses of organozirconium and -hafnium complexes does not allow meaningful comparisons of the metal–carbon bond distances at present.

Despite the presence of a clear spectral difference between Zr and Hf complexes, these complexes showed no difference in the hydrolysis and air oxidation as noted above. This is presumably due to the ease in conversion of the η^4-diene species to the metallacyclic form by the attack (coordination) of H_2O or O_2 that results in the production of the same compounds from the Zr and Hf analogues.

Nuclear Magnetic Resonance of Cp_2M(1,3-diene) with *s-trans*-η^4-Diene Structure. Cp_2Zr(butadiene), which was recrystallized from hot hexane, showed the *s-cis*-η^4-diene structure as mentioned above. However, when the Cp_2Zr(butadiene) was prepared and extracted into hexane below 30 °C, it comprises two species: *s-cis*-η^4-butadiene (75%) and *s*-trans-η^4-butadiene (25%). The ^{1}H NMR parameters for the latter were obtained by computer simulation (Figure 2) and are given in Table V. The large values of $J_{35(46)}$ and J_{56} clearly show that this species has the *s-trans*-η^4-diene structure. The magnitude of both J_{35} and J_{56} is larger than those for butadiene[25] and a trinuclear osmium–*s-trans*-butadiene complex.[26]

(22) D. J. Sikora, M. D. Rausch, R. D. Rogers, and J. L. Atwood, *J. Am. Chem. Soc.*, **103**, 1265 (1981). Calculation of force constants were made referring to F. A. Cotton and C. S. Kraihanzel, *J. Am. Chem. Soc.*, **84**, 4432 (1962).

(23) J. K. Becconsall, B. E. Job, and S. J. O'Brien, *J. Chem. Soc. A*, 423 (1961).

(24) (a) V. I. Kulishov, E. M. Braina, N. G. Bokiy, and Yu. T. Struchkov, *J. Organomet. Chem.*, **36**, 333 (1972); (b) R. D. Rogers, R. V. Bynum, and J. L. Atwood, *J. Am. Chem. Soc.*, **103**, 692 (1981).

(25) A. L. Segre, L. Zetta, and A. Di. Corato, *J. Mol. Spectrosc.* **32**, 296 (1969).

(26) M. Tachikawa, J. R. Shapley, R. C. Haltiwanger, and C. G. Pierpont, *J. Am. Chem. Soc.*, **98**, 4652 (1976).

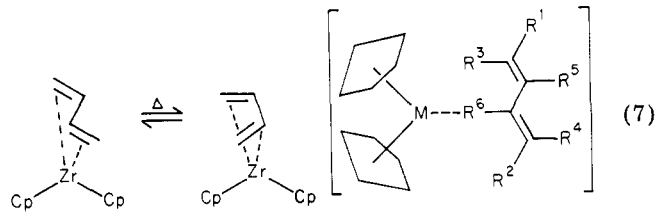

(7)

M = Zr, Hf

Athough the coordination of a *s-trans*-diene to metals was already reported for dinuclear manganese[27] and trinuclear osmium complexes,[26] the coordination of a *s-trans*-diene to mononuclear complexes now has confirmed by ^{1}H NMR studies for the first time. An X-ray analysis of Cp_2Zr(*s-trans*-butadiene) has recently been reported. However, there is some uncertainty with respect to the *s-trans* conformation because of the large positional ambiguity of the central two carbon atoms of the diene.[6]

The *s-trans*-butadiene complex is thermally unstable and readily can be converted to the *s-cis*-butadiene complex by heating in toluene at 80 °C for 30 min. The complexes **2–6** which were prepared at low temperature (25 °C) showed no contamination with the isomer of the *s-trans*-η^4-diene structure as revealed by ^{1}H NMR. The ratio of the *s-cis*- to *s-trans*-diene complex prepared by the present method at 25 °C is summarized in Table VI.

When 1,4-diphenyl-1,3-butadiene was used as a ligand, the *s-trans*-diene coordination to Zr becomes predominant. The NMR parameters of Cp_2Zr(1,4-diphenyl-1,3-butadiene) (**7**) which was prepared from (1,4-diphenyl-2-butene-1,4-diyl)magnesium fit well to those for $Os_3(CO)_{10}$(*s-trans*-C_4H_6) in their chemical shifts while J_{56} is larger.

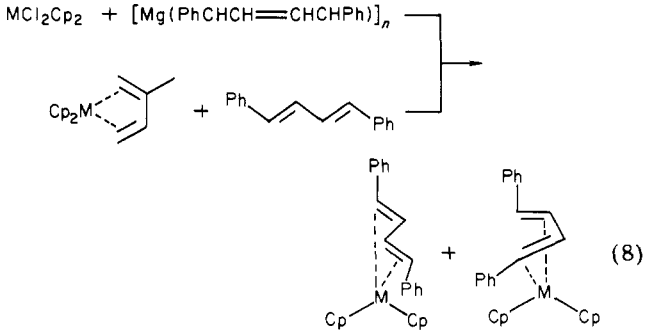

(8)

We have found a novel method for preparation of **7** by a ligand-exchange reaction. The reaction of the isoprene complex with an equimolar amount of (*E,E*)-1,4-diphenylbutadiene gave **7** quantitatively (>90%) when the mixture was heated to 60 °C in benzene (eq 8). Release of isoprene was confirmed by GC. This is the first example for the synthesis of zirconium(IV)–diene complexes by a ligand exchange reaction. The ratio of *s-trans*- to *s-cis*-diene species (97/3) observed for **7** was the same irrespective of the two different synthetic routes described above. Although Cp_2Zr(*s-trans*-butadiene) can readily be converted into Cp_2Zr(*s-cis*-butadiene) by heating at 80 °C in toluene, no such transformation was observed for **7** even when it was heated at 120 °C for 16 h. Complex **1** represents the thermally stable mononuclear *s-trans*-diene complexes.

Surprising was the observation that Cp_2Hf(1,4-diphenyl-1,3-butadiene) (**8**) favors the *s-cis*-η^4-diene structure (76%) over the *s-trans*-η^4-diene structure (24%) even when the complex was prepared by the ligand-exchange reaction under mild reaction conditions (60 °C in benzene). Complex **8** prepared by reaction of [Mg(PhCHCH=CHCHPh)]$_n$ with Cp_2HfCl_2 also favored the *s-cis*-diene configuration. The ratio of *s-cis* to *s-trans* was 75/25, in good agreement with the ratio obtained by the ligand-exchange reaction.

Table VI. Molar Ratio of *s-cis*- to *s-trans*-Diene Species for Cp_2M(diene) Prepared from Enediylmagnesium at 25 °C[a]

complex	M	diene	*s-cis*- to *s-trans*-diene, mol/mol	
1	Zr	butadiene	75	25
2		isoprene	100	0
3		2,3-dimethylbutadiene	100	0
4		1,4-diphenylbutadiene	3	97
5	Hf	butadiene[b]	100	0
6		isoprene[b]	100	0
7		2,3-dimethylbutadiene[b]	100	0
8		1,4-diphenylbutadiene	75	25

[a] Determined by ^{1}H NMR at −70 °C in toluene-d_8. [b] Species of hafnacyclo-3-pentene structure is counted as *s-cis*-diene species.

Table VII. IR and Electronic Spectral Data for Cp_2M(*s-cis*-diene) Complexes in THF[a]

complex	λ_{max}, nm	ϵ mol^{-1}/L cm^{-1}	$\nu_{C=C}$ of diene, cm^{-1}	$\nu_{C=C}$ of Cp, cm^{-1}
1	432	1080	1479 (m) 1515 (w)	1442
2	438	1110	1477 (m) 1516 (w)	1443
3	448	1140	1477 (m) 1516 (w)	1444
4	350	970	1487 (m) 1515 (w)	1442
5	370	990	1480 (m) 1516 (w)	1442
6	394	1040	1476 (m) 1516 (w)	1443
7	385 495	3180 1500		1443
8[b]	438	1130		1443

[a] Spectral data were collected at 25 °C, and the absorption of THF were compensated with a variable cell. [b] A mixture (25/75) of *s-cis*- and *s-trans*-diene species.

Computer simulation of the ^{1}H NMR spectrum of the *s-cis*-diene species of **8** (cf. Figure 3) revealed J values similar to those for **1** and **2** of the *s-cis*-diene structure, indicating similar bonding. However, the fluxionalization rate for **8** of *s-cis*-diene structure was extremely slow when compared to **1–6** and no significant spectral change was observed in the temperature range −40 to +60 °C. Interconversion of the *s-cis*- to the *s-trans*-diene structure has not been achieved by irradiation of UV in benzene. It is not clear at present why **7** prefers the *s-trans*-diene and **8** prefers the *s-cis*-diene coordination.

The IR and the Electronic Spectrum of Cp_2M(diene) in THF. The IR data on the complexes **1–6** were collected (Table VII) in order to obtain more information on the fluxional structure since IR data on metal complexes of mono- and polyolefins have revealed that the vibrational frequencies associated with C=C bond are correlated to the σ- or π-type of M–C bonding.[28] The C=C frequencies of η^4-butadiene coordinated to metals such as Co, Mn, V, and Fe generally appears at 1380–1480 cm^{-1} [29] and of metallacyclo-3-pentenes at 1550–1600 cm^{-1},

(27) H. D. Sasse and M. L. Ziegler, *Z. Anorg. Allg. Chem.*, **392**, 167 (1972).

(28) M. Herberhold, "Metal π-Complexes", Vol. II, Elsevier, Amsterdam, 1972.

(29) E. O. Fischer and H. Werner, "Metall-π-Komplexe mit Di- und Oligoolefinishen Liganden", Verlag Chemie, 1963.

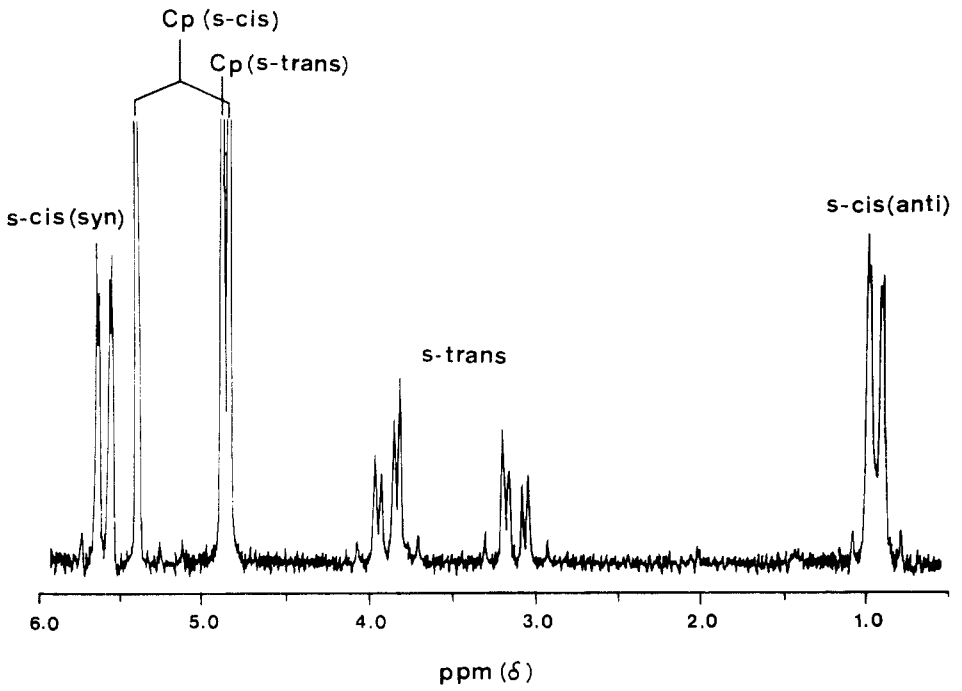

Figure 3. ^{1}H NMR (100-MHz) spectrum of Cp_2Hf(1,4-diphenyl-1,3-butadiene) (8) in toluene-d_8 at 38 °C.

as observed for silacyclo-3-pentene (1600 cm^{-1})[30] or (2-butene-1,4-diyl)magnesium (1550 cm^{-1}).[7]

Although *s-cis*-η^4-diene coordination is unambiguous for 1–6 at low temperatures (−80 ± 30 °C) from the ^{1}H NMR data, it is not clear how much η^4 diene species exists at ambient temperature when they are fluxional in solution. The observed C=C frequencies of 1–6 in THF at 30 °C (1515 and 1481 ± 5 cm^{-1}) are close to the values reported for η^4-diene structures rather than the metallacyclopentene structures. Therefore, on this basis, one can conclude that both the zirconium complexes 1–3 and hafnium complexes 4–6 prefer the η^4-diene structure even when they become fluxional at higher temperatures (0–60 °C). No clear difference in bonding character between zirconium and hafnium complexes has been revealed from the IR data.

The electronic spectra of 1–6, however, showed a remarkable difference between them. The absorption maxima of the zirconium complexes appeared at longer wavelength than those of the corresponding hafnium complexes (Table VII). This result suggests that electronic delocalization over the diene group in the Zr complexes is higher than that in the corresponding Hf derivatives. This means that the zirconium complexes have less σ-bonding character compared to the Hf analogues, in line with the conclusion obtained from the NMR studies. Substitution of phenyl groups at the η^4-diene (complexes 7 and 8) results in longer wavelength shift of the maximum. Meaningful comparison between 7 and 8 cannot be made because the former has the *s-trans*-diene species while the latter involves the *s-cis*-diene species.

Experimental Section

All operations were conducted with Schlenk techniques under argon atmosphere. All the reagents and solvents were distilled after being dried over appropriate drying agents: calcium hydride for olefins and dienes; Na/K alloy for THF and toluene. $ZrCl_2Cp_2$ and $HfCl_2Cp_2$ were prepared by the known method and purified by recrystallization or sublimation. The purity of these complexes was confirmed to be >97% by elemental analysis, mass and ^{1}H NMR spectroscopies, and measurement of melting point: 249 °C for $ZrCl_2Cp_2$ (lit.,[31] 247–249 °C); 305 °C dec for $HfCl_2Cp_2$ (lit.[32] 300 °C). The gas chromatographic analysis of the reaction products was made with a Hitachi Model 163 gas chromatograph equipped with a capillary column, HB-2000 or CW (45 m), and the separation of the products with a Varian-Aerograph Model 700 gas chromatograph using a column packed with Celite-silicone DC-550. NMR spectra were recorded on a Varian XL-100 instrument with a VFT-100-620L Fourier transform accessory and analyzed with a Varian spin simulation program. Mass spectra were recorded on a JEOL OISG-2 spectrometer. IR spectra were obtained on a Hitachi EPI-2 spectrometer and the electronic spectra on a JASCO Model UVIDEC-5A spectrometer. Elemental analyses of the diene complexes were carried out only for 1,4-diphenylbutadiene complexes with a Yanagimoto Model MT-2 CHN analyzer since other complexes were decomposed immediately in the air. Melting points were measured with a sealed glass capillary and were uncorrected.

Activation of Magnesium. The activation of magnesium was carried out in essentially the same way as described previously.[4] To 6.1 g (0.25 mol) of magnesium turnings (suitable for Grignard reaction) in 80 mL of dried THF was added at ambient temperature 0.3 g (2.5 mmol) of iodine and 2.5 mL (0.025 mol) of dry isoprene or 2,3-dimethyl-1,3-butadiene. The mixture was shaken for 30 h at 70 °C in a temperature-controlled water bath, the resulting yellow-green solution was removed by using a syringe, and the residual magnesium was washed with 20 mL of THF. The resulting lusterless magnesium turnings (5.4 g) were used as the activated magnesium for reaction with 1,3-dienes. When the magnesium is inactive, the above-mentioned procedure should be repeated again or the above-mentioned yellow green solution (0.3 mL) should be added to the magnesium. The use of commercial turnings without activation or the use of insufficiently dried THF resulted in no reaction between magnesium and the dienes even at 60 °C. Increase of the reaction temperature exceeding 15 °C or further addition of iodine for activation of magnesium turnings should be avoided because it causes contamination by the magnesium–1,3-diene (1/2) addition compound.

Preparation of (2,3-Dimethyl-2-butene-1,4-diyl)magnesium. Magnesium–butadiene (1/1) adduct ((2-butene-1,4-diyl)-magnesium–bis(tetrahydrofuran)) and magnesium–isoprene (1/1) adduct ((2-methyl-2-butene-1,4-diyl)magnesium–bis(tetrahydrofuran)) were prepared as previously reported.[3,4] Magnesium-2,3-dimethyl-1,3-butadiene (1/1) adduct, [$MgCH_2C$-

(30) (a) T. H. Chao and J. Laane, *Spectrochem. Acta, Part A.*, **A28**, 2443 (1972); (b) J. Laane, *J. Chem. Phys.*, **50**, 776 (1969).

(31) A. F. Reid and P. C. Wailes, *Aust. J. Chem.*, **19**, 309 (1966).

(32) P. M. Druce, B. M. Kingston, M. F. Lappert, T. R. Spalding, and R. C. Privastava, *J. Chem. Soc. A*, **1969**, 2106.

$(CH_3)=C(CH_3)CH_2 \cdot 2THF]_n$, was prepared in exactly the same way. Freshly distilled 2,3-dimethyl-1,3-butadiene (5.6 mL, 50 mmol) was added to an excess of activated magnesium (12 g, 0.5 mol) in THF (100 mL) and a mixture was shaken for 5 days at 10 °C at a water bath incubator. The resulting yellow solution was evaporated to dryness, and the residue was washed with anhydrous benzene to give the 1/1 adduct as pale yellow powder in 77% yield; mp 71 °C dec. The adduct is flammable in the air and immediately decomposes upon hydrolysis in toluene to give 2,3-dimethyl-1-butene (38%) and 2,3-dimethyl-2-butene (62%) besides 2 mol of THF originally coordinated to the magnesium atom: M content, 9.5% by 8-quinolinol method; 9.7% calcd for $C_{14}H_{28}O_2Mg$. ^1H NMR (THF-d_8): 1.03 (s, 4 H, CH_2) 1.81 ppm (s, 6 H, CH_3). The CH_3 proton signal was measured by WEFT (water eliminated Fourier transform) method because it overlapped partially the signal of coordinated THF.

Preparation of (1,4-Diphenyl-2-butene-1,4-diyl)magnesium. A mixture of (*E,E*)-1,4-diphenyl-1,3-butadiene (5 g, 25 mmol) and activated magnesium turnings (6.1 g, 250 mmol) in THF (120 mL) was shaken for 5 days at 15 °C in a shaking apparatus. The resulting deep red solution was separated from magnesium turnings with a syringe, concentrated to 50 mL and cooled to −20 °C to induce the precipitation of (1,4-diphenyl-2-butene-1,4-diyl)magnesium–tris(tetrahydrofuran) as an orange powder in 80% yield. One recrystallization from THF was sufficient for purification (0.6 g of sample per 10 mL of THF). The structure determination was based on the GC analysis of the hydrolysis products, 1,4-diphenyl-2-butene (55%) and 1,4-diphenyl-1-butene (45%), and on the analysis of the metal content (5.4% by 8-quinolinol method; 5.44%, calcd for $C_{28}H_{38}O_3Mg$). The X-ray structure will be reported elsewhere.

Preparation of Cp_2Zr(butadiene) Complex 1. To a stirred slurry of $ZrCl_2Cp_2$ (2.9 g, 10 mmol) in THF (25 mL) in a 100-mL Schlenk tube was added a suspension of (2-butene-1,4-diyl)-magnesium, $[Mg(butadiene) \cdot 2THF]_n$ (2.2 g, 10 mmol), in THF (150 mL) at −40 °C. The mixture was stirred for 1 h at 30 °C and then heated to 60 °C for 10 min. The solution turned from pale yellow to deep red. After evaporation of the solution to dryness, a mixture of hexane (50 mL) and benzene (15 mL) was added and the mixture was heated at reflux for 10 min under an argon atmosphere. The precipitated $MgCl_2 \cdot 2THF$ was separated by centrifugation using a two-necked glass tube fitted with rubber stoppers. Removal of benzene–hexane by trap-to-trap distillation gave Cp_2Zr(butadiene) as deep red crystals in 70% yield. The sample was purified by recrystallization from hexane at −20 °C. Characterization of the complex was based on the ratio of metal to hydrolysis product (analyzed by GC) in addition to the ratio of Cp to the diene group determined by ^1H NMR as shown in Tables I and II.

Preparation of Cp_2Zr(isoprene) Complex 2. A solution of (2-methyl-2-butene-1,4-diyl)magnesium, $[Mg(C_5H_8) \cdot 2THF)]_n$ (2.4 g, 10 mmol), dissolved in THF (80 mL) was added at once at −40 °C to a stirred slurry of $ZrCl_2Cp_2$ (2.9 g, 10 mmol) in THF (25 mL). The mixture was allowed to warm to ambient temperature, stirred for 2h, heated to 60 °C for 5 min, and evaporated to dryness. Hexane (50 mL) was added to the residue, and the mixture was refluxed for 10 min and separated from the salts with a syringe. The products were further extracted from the salts with two portions of 1/2 benzene–hexane (40 mL). Evaporation of the combined solutions gave deep red crystals of Cp_2Zr-(isoprene) in 70% yield. The pure complex was obtained by recrystallization from hexane at −20 °C. When the above-mentioned THF solution was kept at −20 °C for 20 h, prismatic orange crystals were precipitated in 70% yield. The metal content of the crystals agreed with the value calculated for $[Cp_2Zr(C_5H_8)][MgCl_2 \cdot 2THF]$: Zr, 16.5% by oxidation method (calcd 17.2%) and Mg, 5.1% by 8-quinolinol method (calcd 4.5%). When hexane (40 mL) was added at 30 °C to the concentrated THF solution (30 mL) and the mixture was kept at −20 °C for 1 day, orange crystals whose metal content agreed with that of $[Cp_2Zr(C_5H_8)][MgCl_2 \cdot 2THF]_{2.2}$ were precipitated: Zr, 11.1% (calcd 11.17%) and Mg, 6.5% (calcd 6.55%); yield 55%. When the isolated adduct $[Cp_2Zr(C_5H_8)][MgCl_2 \cdot 2THF]$ (5.3 g, 10 mmol) was heated for 10 min in refluxing hexane (80 mL), it decomposed to release Cp_2Zr(isoprene) into the hexane. The hexane solution was concentrated to 6 mL and cooled to −20 °C to give crystals of pure $Cp_2Zr(C_5H_8)$ which contained no magnesium salts as checked by chemical analysis. The yield of **2** was 65%. No appreciable difference was observed between $[Cp_2Zr(C_5H_8)]$-$[MgCl_2 \cdot 2THF]$ and **2** in the ^1H NMR and electronic spectra in THF.

Preparation of Cp_2Zr(2,3-dimethylbutadiene) (3). A solution of (2,3-dimethyl-2-butene-1,4-diyl)magnesium, $[Mg(C_6H_{10}) \cdot 2THF]_n$ (2.5 g, 10 mmol), in THF (80 mL) was added to finely divided $ZrCl_2Cp_2$ (2.9 g, 10 mmol) stirred in THF (30 mL) at −20 °C. The mixture was stirred for 2 h at 30 °C and heated to 60 °C for 5 min. The resulting orange solution was evaporated to dryness, and the residue was extracted with two portions of hot hexane (50 mL). Evaporation of the solution gave **3** as orange crystals in 75% yield. Further purification was effected by recrystallization from hexane at 0 °C.

Preparation of Cp_2Hf(butadiene) (4). A suspension of (2-butene-1,4-diyl)magnesium (2.2 g, 10 mmol) in THF was syringed onto finely divided $HfCl_2Cp_2$ (3.8 g, 10 mmol) stirred in THF at 0 °C, and the mixture was stirred for 2 h at 25–30 °C. The resulting orange-colored homogeneous solution was evaporated to dryness, and the residue was extracted with a mixture of benzene (10 mL) and hexane (40 mL). Separation of the solution from salts by centrifugation followed by trap-to-trap distillation gave Cp_2Hf(butadiene) as orange crystals in 80% yield. Recrystallization was carried out in hexane at −20 °C.

Preparation of Cp_2Hf(isoprene) (5). A solution of (2-methyl-2-butene-1,4-diyl)magnesium (2.4 g, 10 mmol) in THF (80 mL) was syringed onto a stirred suspension of $HfCl_2Cp_2$ (3.8 g, 10 mmol) at 0 °C. The mixture was stirred for 1 h at 30 °C and then refluxed for 5 min. The solution was evaporated to dryness and the desired complex was extracted into hexane (60 mL) at 30 °C. The solution was concentrated to 3 mL and kept at −20 °C to induce the precipitation of orange crystals of Cp_2Hf-(isoprene). Typical isolated yield was 82%.

Preparation of Cp_2Hf(2,3-dimethylbutadiene) (6). A solution of (2,3-dimethyl-2-butene-1,4-diyl)magnesium (2.5 g, 10 mmol) in THF (80 mL) was syringed onto a stirred suspension of $HfCl_2Cp_2$ (3.8 g, 10 mmol) at 0 °C. The mixture was stirred for 2 h at 30 °C and then heated to 60 °C for 5 min. After evaporation of the solution to dryness, the desired complex was extracted with hexane (60 mL). Concentration of the solution to 10 mL and cooling to −20 °C gave orange crystals of Cp_2Hf-(2,3-dimethyl-1,3-butadiene) in 85% yield. Recrystallization was done in hexane at 20 °C.

Preparation of 7 and 8 by Reaction with Enediylmagnesium. To a suspension of powdered $ZrCl_2Cp_2$ (2.9 g, 10 mmol) in THF (30 mL) was added at 0 °C a solution of 1,4-diphenyl-2-butene-diyl)magnesium–tris(tetrahydrofuran) (4.5 g, 10 mmol) in THF (100 mL). The mixture was stirred at ambient temperature for 3 h, heated to 60 °C for 10 min, and then evaporated to dryness. Benzene (60 mL) was added to the residue, and the solution was separated from the salts by centrifugation. Concentration of the solution to 10 mL gave deep red crystals of Cp_2Zr(1,4-diphenyl-1,3-butadiene) (**7**) in 75% yield. A pure sample was obtained by recrystallization from benzene. Anal. Calcd for $C_{26}H_{24}Zr$: C, 73.03; H, 5.62. Found: C, 72.95; H, 5.81. Preparation of Cp_2Hf(1,4-diphenyl-1,3-butadiene) (**8**) was carried out in exactly the same manner as described for **7**; yield 80% based on $HfCl_2Cp_2$. Anal. Calcd for $C_{26}H_{24}Hf$: C, 60.64; H, 4.70. Found: C, 60.42; H, 4.72.

Preparation of 7 and 8 by Ligand Exchange Reaction. To a stirred benzene solution (5 mL) of (*E,E*)-1,4-diphenyl-1,3-butadiene (0.7 g, 3.6 mmol) was added a benzene solution (10 mL) of complex **2** (1.1 g, 3.5 mmol) at ambient temperature. The mixture was stirred for 10 h at 40 °C and concentrated to 4 mL by trap-to-trap distillation. Addition of excess hexane (20 mL) resulted in the precipitation of complex **7**. The hexane-soluble part was taken out by a syringe, and the residue was recrystallized from benzene to give deep red needles of **7** in 75% yield based on the complex **2**. Anal. Calcd for $C_{26}H_{24}Zr$: C, 73.03; H, 5.62. Found: C, 72.83; H, 5.90. Preparation of **8** by reaction of **5** (1.3 g, 3.5 mmol) with (*E,E*)-1,4-diphenyl-1,3-butadiene (0.7 g, 3.6 mmol) was carried out under the same reaction conditions as those for **7** except for the reaction temperature (60 °C); yield 82% based on **2**. Anal. Calcd for $C_{26}H_{24}Hf$: C, 60.64; H, 4.66. Found: C, 60.39; H, 4.84.

Hydrolysis and Oxidation of Cp_2M(diene) Complexes. All the complexes were hydrolyzed with 2 N HCl or 2 N DCl in benzene at 5–10 °C. The resulting 1-butene, 2-butene, 2-methyl-1-butene, 3-methyl-1-butene, 2,3-dimethyl-1-butene, or the dideuterated compounds were isolated with a preparative gas chromatograph and were identified by comparison of their MS and ^1H NMR spectra with those of authentic samples previously identified.[4,5] 1,4-Diphenyl-1-butene and 1,4-diphenyl-2-butene obtained by hydrolysis of **7** and **8** were identified with reference to the data reported by Bumgardner.[33] The yield of each olefin (Table II) was determined by gas chromatographic analysis within an error of 3%. The purity of the dideuterated olefins was determined to be 96–99% by mass spectroscopy with the use of the corresponding undeuterated olefins as standards. Oxidation was carried out in a closed system; i.e., an excess of dry oxygen (300 mL, dried over P_2O_5) was introduced into the reaction tube containing a toluene solution of a diene complex (3 mmol in 30 mL of toluene) (Schlenk technique). The solution turned colorless after being stirred, for 1–10 min at 25 °C. The formation of 0.93–0.97 molar equiv of the respective conjugated diene was confirmed by GC. Addition of dried air gave the identical result.

(33) C. L. Bumgardner and H. Iwerks, *J. Am. Chem. Soc.*, **88**, 5518 (1966).

Registry No. **1**, 75374-50-4; **2**, 75361-73-8; **3**, 75361-74-9; **4**, 80185-89-3; **5**, 80161-02-0; **6**, 80161-03-1; **7**, 75361-76-1; **8**, 80161-04-2.

Communications

An Intramolecular Silene Ene Reaction

Robert T. Conlin,* Mel P. Bessellieu, Paul Ronald Jones,* and Richard A. Pierce

Department of Chemistry, North Texas State University Denton, Texas 76203

Received September 22, 1981

Summary: The flash vacuum pyrolysis of 2,2-dimethyl-3-neopentyl-2-silabicyclo[2.2.1]hept-5-ene (**1**) gives nearly quantitative yields of cyclopentadiene. In addition to the 1,3-disilacyclobutane dimers of 1,1-dimethyl-2-neopentylsilene (**4**), two novel silene-derived products, isobutene and dimethylvinylsilane, are produced. Evidence that the latter products are formed in an intramolecular ene-type reaction of the silene, **4**, is presented.

To a large extent, the resurgence of interest in the intramolecular ene reactions derives from the facility with which heteroatom π bonds undergo pericyclic processes.[1] With the widespread recognition of the extraordinary reactivity of π bonds between silicon and carbon,[2] it is somewhat surprising that there are no demonstrated examples of ene reactions initiated by a silicon–carbon π bond. In this communication we report a new and mild thermal method for generating silenes in the gas phase as well as an example of an intramolecular ene reaction of a silene.

Flash vacuum pyrolysis[3] of a mixture of the endo and exo isomers of 2,2-dimethyl-3-neopentyl-2-silabicyclo-[2.2.1]hept-5-ene (**1**)[4] at 550 °C leads cleanly to cyclopentadiene in nearly quantitative yield. Four other products are isolated: the cis and trans isomers of 1,1,3,3-tetramethyl-2,4-dineopentyl-1,3-disilacyclobutane (**2**),[5] isobutene, and dimethylvinylsilane (**3**).[6] These products were all characterized by comparison of their spectral and chromatographic properties with those of authentic samples.

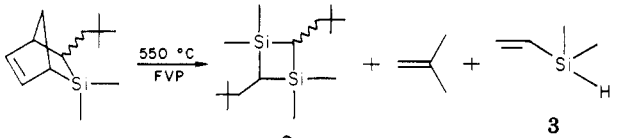

1 2 3

The formation of cyclopentadiene and the 1,3-disilacyclobutanes (**2**) is consistent with a [2 + 4] cycloreversion of **1**, giving cyclopentadiene and 1,1-dimethyl-2-neopentylsilene (**4**) which undergoes the usual head-to-tail dimerization[2] to form **2**. Analogous, possibly concerted, retro Diels–Alder eliminations are known for both the parent hydrocarbon bicyclo[2.2.1]heptene[8] and the related 7,7-dimethyl-7-silabicyclo[2.2.2]octa-2,5-diene.[9] It is noteworthy that the ratio of *cis*- and *trans*-disilacyclobutanes formed in the gas phase at 550 °C, 1.15, is the *same ratio* observed when the silene, **4**, is generated at low temperature in hydrocarbon solvents by the reaction of *tert*-butyllithium with chlorodimethylvinylsilane.[5] The absence of a temperature effect on this cis/trans ratio is consistent with earlier reports that there is no appreciable energy barrier to silene dimerization[10] and that **4** is produced in the low-temperature reaction.[4,5]

Especially intriguing is the mechanism of formation of isobutene and **3**, which are isolated in nearly equal amounts from the reaction mixture.[11] We have established that the disilacyclobutanes, **2**, do not give rise to these

(1) (a) Oppolzer, W.; Snieckus, V. *Angew. Chem., Int. Ed. Engl.* **1979**, *17*, 476. (b) Hoffmann, H. M. R. *Ibid.* **1969**, *8*, 566.

(2) Gusel'nikov, L. E.; Nametkin, N. S. *Chem. Rev.* **1979**, *79*, 529.

(3) Pyrolyses were carried out at 10^{-4}–10^{-5} torr, employing a seasoned hot zone consisting of 10-mm i.d. × 30 cm quartz tube. Residence time in the hot zone was on the order of milliseconds.

(4) Jones, P. R.; Lim, T. F. O.; Pierce, R. A. *J. Am. Chem. Soc.* **1980**, *102*, 4970.

(5) Jones, P. R.; Lim, T. F. O. *J. Am. Chem. Soc.* **1977**, *99*, 2013, **1977**, *99*, 8447.

(6) Recently, Auner and Grobe[7] have reported that 2,2-dimethyl-2-silabicyclo[2.2.1]hept-5-ene, formed as a transient by the addition of 1,1-dimethylsilene to cyclopentadiene, isomerizes through a series of unprecedented steps and eventually leads to benzene as the only isolated product. We have not been able to reproduce their results.

(7) Auner, N.; Grobe, J. *J. Organomet. Chem.* **1980**, *190*, 129.

(8) Herndon, W. C.; Cooper, W. B.; Chambers, M. J. *J. Phys. Chem.* **1964**, *68*, 2016.

(9) Barton, T. J.; Kline, E. *J. Organomet. Chem.* **1972**, *42*, C21.

(10) (a) Gusel'nikov, L. E.; Konobeevski, V. M.; Vdovin, V. M.; Nametkin, N. S. *Dokl. Akad. Nauk SSSR* **1977**, *235*, 1086. (b) Basu, S.; Davidson, I. M. T.; Laupert, R.; Potzinger, P. *Ber. Bunsenges. Phys. Chem.* **1979**, *83*, 1282.

(11) In all of our experiments the yield of isobutene appears to be higher than that of **3**. This might be due to the difficulty in determining an accurate response factor for the highly volatile isobutene. It is also possible that side reactions provide another source of isobutene or that some of **3** is consumed by subsequent reactions. We have no evidence which resolves this discrepancy at this time.

0276-7333/82/2301-0396$01.25/0

Hydrolysis and Oxidation of Cp_2M(diene) Complexes. All the complexes were hydrolyzed with 2 N HCl or 2 N DCl in benzene at 5–10 °C. The resulting 1-butene, 2-butene, 2-methyl-1-butene, 3-methyl-1-butene, 2,3-dimethyl-1-butene, or the dideuterated compounds were isolated with a preparative gas chromatograph and were identified by comparison of their MS and ^1H NMR spectra with those of authentic samples previously identified.[4,5] 1,4-Diphenyl-1-butene and 1,4-diphenyl-2-butene obtained by hydrolysis of **7** and **8** were identified with reference to the data reported by Bumgardner.[33] The yield of each olefin (Table II) was determined by gas chromatographic analysis within an error of 3%. The purity of the dideuterated olefins was determined to be 96–99% by mass spectroscopy with the use of the corresponding undeuterated olefins as standards. Oxidation was carried out in a closed system; i.e., an excess of dry oxygen (300 mL, dried over P_2O_5) was introduced into the reaction tube containing a toluene solution of a diene complex (3 mmol in 30 mL of toluene) (Schlenk technique). The solution turned colorless after being stirred, for 1–10 min at 25 °C. The formation of 0.93–0.97 molar equiv of the respective conjugated diene was confirmed by GC. Addition of dried air gave the identical result.

(33) C. L. Bumgardner and H. Iwerks, *J. Am. Chem. Soc.*, **88**, 5518 (1966).

Registry No. **1**, 75374-50-4; **2**, 75361-73-8; **3**, 75361-74-9; **4**, 80185-89-3; **5**, 80161-02-0; **6**, 80161-03-1; **7**, 75361-76-1; **8**, 80161-04-2.

Communications

An Intramolecular Silene Ene Reaction

Robert T. Conlin,* Mel P. Bessellieu, Paul Ronald Jones,* and Richard A. Pierce

Department of Chemistry, North Texas State University Denton, Texas 76203

Received September 22, 1981

Summary: The flash vacuum pyrolysis of 2,2-dimethyl-3-neopentyl-2-silabicyclo[2.2.1]hept-5-ene (**1**) gives nearly quantitative yields of cyclopentadiene. In addition to the 1,3-disilacyclobutane dimers of 1,1-dimethyl-2-neopentylsilene (**4**), two novel silene-derived products, isobutene and dimethylvinylsilane, are produced. Evidence that the latter products are formed in an intramolecular ene-type reaction of the silene, **4**, is presented.

To a large extent, the resurgence of interest in the intramolecular ene reactions derives from the facility with which heteroatom π bonds undergo pericyclic processes.[1] With the widespread recognition of the extraordinary reactivity of π bonds between silicon and carbon,[2] it is somewhat surprising that there are no demonstrated examples of ene reactions initiated by a silicon–carbon π bond. In this communication we report a new and mild thermal method for generating silenes in the gas phase as well as an example of an intramolecular ene reaction of a silene.

Flash vacuum pyrolysis[3] of a mixture of the endo and exo isomers of 2,2-dimethyl-3-neopentyl-2-silabicyclo-[2.2.1]hept-5-ene (**1**)[4] at 550 °C leads cleanly to cyclopentadiene in nearly quantitative yield. Four other products are isolated: the cis and trans isomers of 1,1,3,3-tetramethyl-2,4-dineopentyl-1,3-disilacyclobutane (**2**),[5] isobutene, and dimethylvinylsilane (**3**).[6] These products were all characterized by comparison of their spectral and chromatographic properties with those of authentic samples.

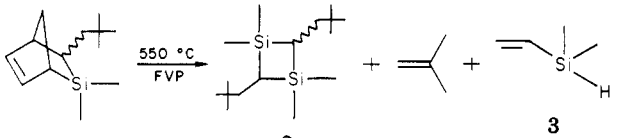

1 2 3

The formation of cyclopentadiene and the 1,3-disilacyclobutanes (**2**) is consistent with a [2 + 4] cycloreversion of **1**, giving cyclopentadiene and 1,1-dimethyl-2-neopentylsilene (**4**) which undergoes the usual head-to-tail dimerization[2] to form **2**. Analogous, possibly concerted, retro Diels–Alder eliminations are known for both the parent hydrocarbon bicyclo[2.2.1]heptene[8] and the related 7,7-dimethyl-7-silabicyclo[2.2.2]octa-2,5-diene.[9] It is noteworthy that the ratio of *cis*- and *trans*-disilacyclobutanes formed in the gas phase at 550 °C, 1.15, is the *same ratio* observed when the silene, **4**, is generated at low temperature in hydrocarbon solvents by the reaction of *tert*-butyllithium with chlorodimethylvinylsilane.[5] The absence of a temperature effect on this cis/trans ratio is consistent with earlier reports that there is no appreciable energy barrier to silene dimerization[10] and that **4** is produced in the low-temperature reaction.[4,5]

Especially intriguing is the mechanism of formation of isobutene and **3**, which are isolated in nearly equal amounts from the reaction mixture.[11] We have established that the disilacyclobutanes, **2**, do not give rise to these

(1) (a) Oppolzer, W.; Snieckus, V. *Angew. Chem., Int. Ed. Engl.* **1979**, *17*, 476. (b) Hoffmann, H. M. R. *Ibid.* **1969**, *8*, 566.

(2) Gusel'nikov, L. E.; Nametkin, N. S. *Chem. Rev.* **1979**, *79*, 529.

(3) Pyrolyses were carried out at 10^{-4}–10^{-5} torr, employing a seasoned hot zone consisting of 10-mm i.d. × 30 cm quartz tube. Residence time in the hot zone was on the order of milliseconds.

(4) Jones, P. R.; Lim, T. F. O.; Pierce, R. A. *J. Am. Chem. Soc.* **1980**, *102*, 4970.

(5) Jones, P. R.; Lim, T. F. O. *J. Am. Chem. Soc.* **1977**, *99*, 2013, **1977**, *99*, 8447.

(6) Recently, Auner and Grobe[7] have reported that 2,2-dimethyl-2-silabicyclo[2.2.1]hept-5-ene, formed as a transient by the addition of 1,1-dimethylsilene to cyclopentadiene, isomerizes through a series of unprecedented steps and eventually leads to benzene as the only isolated product. We have not been able to reproduce their results.

(7) Auner, N.; Grobe, J. *J. Organomet. Chem.* **1980**, *190*, 129.

(8) Herndon, W. C.; Cooper, W. B.; Chambers, M. J. *J. Phys. Chem.* **1964**, *68*, 2016.

(9) Barton, T. J.; Kline, E. *J. Organomet. Chem.* **1972**, *42*, C21.

(10) (a) Gusel'nikov, L. E.; Konobeevski, V. M.; Vdovin, V. M.; Nametkin, N. S. *Dokl. Akad. Nauk SSSR* **1977**, *235*, 1086. (b) Basu, S.; Davidson, I. M. T.; Laupert, R.; Potzinger, P. *Ber. Bunsenges. Phys. Chem.* **1979**, *83*, 1282.

(11) In all of our experiments the yield of isobutene appears to be higher than that of **3**. This might be due to the difficulty in determining an accurate response factor for the highly volatile isobutene. It is also possible that side reactions provide another source of isobutene or that some of **3** is consumed by subsequent reactions. We have no evidence which resolves this discrepancy at this time.

0276-7333/82/2301-0396$01.25/0

Table I. Results from the Flash Vacuum Pyrolysis of 1 [a] at 550 °C

expt	flow, μL of 1/min	% decompn	% of dimers	2 (cis/trans)	% of isobutene	% of 3	ene/dimer ratio [b]
1	0.7	90	8	1.15	50	40	5.00
2	3.2	76	22	1.15	39	23	1.05
3	30.0	83	48	1.14	19	12	0.25
4 [c]	7.0	36	36	1.15	36	25	0.69

[a] Percent yields determined by VPC using di-*n*-butyl ether as an internal standard. [b] Based on yield of 3/yield of 2. [c] Pyrolysis carried out in the presence of a 6-fold excess of methylene chloride.

products at 550 °C. Based on the evidence presented below, we propose that these products arise from a unimolecular ene reaction of 4.

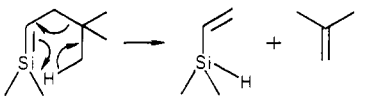

4 3

If dimerization is second order in silene while the ene reaction is first order in silene, one would predict the dimerization to be favored over the ene reaction with increasing silene concentration. The results in Table I support this hypothesis. With increasing flow rates and therefore increasing silene concentration, the ratio of disilacyclobutanes to dimethylvinylsilane increases 20-fold. At low flow, 3 is obtained in 5 times greater yield than the dimers 2; at high flow, the situation is reversed, with dimers being produced in yields 4 times greater than the ene product. Thus, dimethylvinylsilane production is clearly of lower kinetic order than the case for silene dimerization and is most probably first order.

In addition to the ene pathway for the formation of 3, a radical mechanism, involving a rate-determining homolysis of the carbon–carbon bond β to silicon in the silane, 4, followed by hydrogen abstraction could account for the

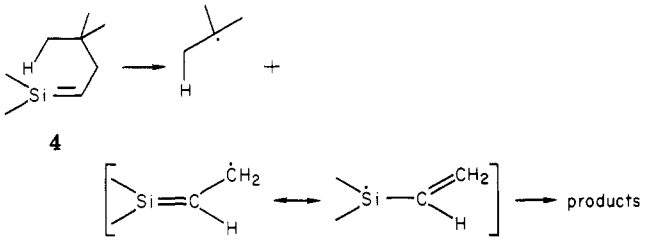

4

ene products. In order to assess the importance of such a pathway, we carried out the pyrolysis of 1 in the presence of a large excess of methylene chloride. If silyl radicals are produced in the pyrolysis, rapid chlorine abstraction should surpress the hydrogen abstraction[12] and chlorodimethylvinylsilane should appear as the main silicon-containing product of the ene pathway.

We have tested this method for detecting silyl radicals by carrying out the copyrolysis of methylene chloride with allyltrimethylsilane, a known source of silyl radicals.[13] The trimethylsilyl radicals are scavenged in nearly quantitative yield to give trimethylchlorosilane. None of the secondary products usually associated with silyl radicals are produced in the presence of methylene chloride.[14]

When the flash vacuum pyrolysis of 1 is carried out in the presence of an excess of methylene chloride, the product distribution is not affected (experiment 4). Because of the increased pressure differential across the reaction zone, the residence time of 1 is decreased, resulting in a correspondingly lower percent decomposition. The relative amounts of isobutene and 3 remain nearly constant (cf. experiment 2), and the ene/dimer ratio is consistent with the flow rate. No chlorodimethylvinylsilane is detected in the reaction mixture. Silyl radicals are thus eliminated as precursors to the isobutene and 3, products of the silene 4. In light of these results, the most reasonable alternative is an intramolecular ene reaction of 1,1-dimethyl-2-neopentylsilene.

In a large number of bimolecular reactions between silenes and organic systems such as propene,[15] isoprene,[16] and acetone,[17] acyclic products containing the exchanged fragments of both reaction partners are found. For the most part, these reactions have been described in terms of the sequence: cycloaddition and ring opening to biradicals, followed by hydrogen atom migration. However, it is conceivable that these reactions proceed by an *intermolecular* concerted pericyclic process. Experiments to explore this possibility are currently in progress in our laboratories.

Acknowledgment is made to the Robert A. Welch Foundation, the Research Corp., and the North Texas State University Faculty Research Fund for their support of this work.

Registry No. *endo*-1, 74107-88-3; *exo*-1, 74107-87-2; *cis*-2, 62518-77-8; *trans*-2, 62518-76-7; 3, 18243-27-1; 4, 79991-59-6; isobutene, 115-11-7; cyclopentadiene, 542-92-7.

(12) (a) Sakurai, H. In "Free Radicals"; Kochi, J. K., Ed.; Wiley-Interscience: New York, 1973; Vol. 2, pp 741–808. (b) Cadman, P.; Tilsley, G. M.; Trotman Dickenson, A. F. *J. Chem. Soc., Faraday Trans. 1* **1973**, *69*, 914.

(13) Davidson, I. M. T.; Wood, I. T. *J. Organomet. Chem.* **1980**, *202*, C65.

(14) Namavari, M.; Conlin, R. T., unpublished results.

(15) Nametkin, N. S.; Gusel'nikov, L. E.; Ushakova, R. L.; Vdovin, V. M. *Izv. Akad. Nauk SSSR, Ser. Khim.* **1971**, 1740.

(16) Barton, T. J.; Hoekman, S. K. *J. Am. Chem. Soc.* **1980**, *102*, 1584.

(17) (a) Golino, C. M.; Bush, R. D.; Roark, D. N.; Sommer, L. H. *J. Organomet. Chem.* **1974**, *66*, 129. (b) Gusel'nikov, L. E.; Nametkin, N. S.; Vdovin, V. M. *Acc. Chem. Res.* **1975**, *8*, 18.

Condensation of Propiolic Esters with Olefins Catalyzed by the $C_5H_5Fe(CO)_2$ Cation

Myron Rosenblum* and Daniel Scheck

Department of Chemistry, Brandeis University
Waltham, Massachusetts 02254

Received September 22, 1981

Summary: Methyl propiolate or tetrolate condense with a number of olefins in a reaction catalyzed by either η^5-$C_5H_5Fe(CO)_2$(isobutylene)BF_4 or η^5-$C_5H_5Fe(CO)_2$(THF)-BF_4 to give 1,3-dienes, cyclobutenes, and 5,6-dihydro-2-pyrones.

The $C_5H_5Fe(CO)_2$ cation (Fp^+) is known to activate olefins in $Fp(\eta^2\text{-olefin})^+ x^-$ complexes toward addition by

0276-7333/82/2301-0397$01.25/0

Table I. Results from the Flash Vacuum Pyrolysis of 1 [a] at 550 °C

expt	flow, μL of 1/min	% decompn	% of dimers	2 (cis/trans)	% of isobutene	% of 3	ene/dimer ratio [b]
1	0.7	90	8	1.15	50	40	5.00
2	3.2	76	22	1.15	39	23	1.05
3	30.0	83	48	1.14	19	12	0.25
4 [c]	7.0	36	36	1.15	36	25	0.69

[a] Percent yields determined by VPC using di-*n*-butyl ether as an internal standard. [b] Based on yield of 3/yield of 2. [c] Pyrolysis carried out in the presence of a 6-fold excess of methylene chloride.

products at 550 °C. Based on the evidence presented below, we propose that these products arise from a unimolecular ene reaction of 4.

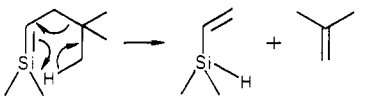

4 3

If dimerization is second order in silene while the ene reaction is first order in silene, one would predict the dimerization to be favored over the ene reaction with increasing silene concentration. The results in Table I support this hypothesis. With increasing flow rates and therefore increasing silene concentration, the ratio of disilacyclobutanes to dimethylvinylsilane increases 20-fold. At low flow, 3 is obtained in 5 times greater yield than the dimers 2; at high flow, the situation is reversed, with dimers being produced in yields 4 times greater than the ene product. Thus, dimethylvinylsilane production is clearly of lower kinetic order than the case for silene dimerization and is most probably first order.

In addition to the ene pathway for the formation of 3, a radical mechanism, involving a rate-determining homolysis of the carbon–carbon bond β to silicon in the silane, 4, followed by hydrogen abstraction could account for the

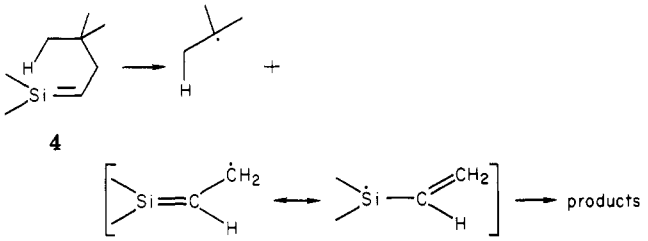

4

ene products. In order to assess the importance of such a pathway, we carried out the pyrolysis of 1 in the presence of a large excess of methylene chloride. If silyl radicals are produced in the pyrolysis, rapid chlorine abstraction should surpress the hydrogen abstraction[12] and chlorodimethylvinylsilane should appear as the main silicon-containing product of the ene pathway.

We have tested this method for detecting silyl radicals by carrying out the copyrolysis of methylene chloride with allyltrimethylsilane, a known source of silyl radicals.[13] The trimethylsilyl radicals are scavenged in nearly quantitative yield to give trimethylchlorosilane. None of the secondary products usually associated with silyl radicals are produced in the presence of methylene chloride.[14]

When the flash vacuum pyrolysis of 1 is carried out in the presence of an excess of methylene chloride, the product distribution is not affected (experiment 4). Because of the increased pressure differential across the reaction zone, the residence time of 1 is decreased, resulting in a correspondingly lower percent decomposition. The relative amounts of isobutene and 3 remain nearly constant (cf. experiment 2), and the ene/dimer ratio is consistent with the flow rate. No chlorodimethylvinylsilane is detected in the reaction mixture. Silyl radicals are thus eliminated as precursors to the isobutene and 3, products of the silene 4. In light of these results, the most reasonable alternative is an intramolecular ene reaction of 1,1-dimethyl-2-neopentylsilene.

In a large number of bimolecular reactions between silenes and organic systems such as propene,[15] isoprene,[16] and acetone,[17] acyclic products containing the exchanged fragments of both reaction partners are found. For the most part, these reactions have been described in terms of the sequence: cycloaddition and ring opening to biradicals, followed by hydrogen atom migration. However, it is conceivable that these reactions proceed by an *intermolecular* concerted pericyclic process. Experiments to explore this possibility are currently in progress in our laboratories.

Acknowledgment is made to the Robert A. Welch Foundation, the Research Corp., and the North Texas State University Faculty Research Fund for their support of this work.

Registry No. *endo*-1, 74107-88-3; *exo*-1, 74107-87-2; *cis*-2, 62518-77-8; *trans*-2, 62518-76-7; 3, 18243-27-1; 4, 79991-59-6; isobutene, 115-11-7; cyclopentadiene, 542-92-7.

(12) (a) Sakurai, H. In "Free Radicals"; Kochi, J. K., Ed.; Wiley-Interscience: New York, 1973; Vol. 2, pp 741–808. (b) Cadman, P.; Tilsley, G. M.; Trotman Dickenson, A. F. *J. Chem. Soc., Faraday Trans. 1* **1973**, *69*, 914.

(13) Davidson, I. M. T.; Wood, I. T. *J. Organomet. Chem.* **1980**, *202*, C65.

(14) Namavari, M.; Conlin, R. T., unpublished results.

(15) Nametkin, N. S.; Gusel'nikov, L. E.; Ushakova, R. L.; Vdovin, V. M. *Izv. Akad. Nauk SSSR, Ser. Khim.* **1971**, 1740.

(16) Barton, T. J.; Hoekman, S. K. *J. Am. Chem. Soc.* **1980**, *102*, 1584.

(17) (a) Golino, C. M.; Bush, R. D.; Roark, D. N.; Sommer, L. H. *J. Organomet. Chem.* **1974**, *66*, 129. (b) Gusel'nikov, L. E.; Nametkin, N. S.; Vdovin, V. M. *Acc. Chem. Res.* **1975**, *8*, 18.

Condensation of Propiolic Esters with Olefins Catalyzed by the $C_5H_5Fe(CO)_2$ Cation

Myron Rosenblum* and Daniel Scheck

Department of Chemistry, Brandeis University
Waltham, Massachusetts 02254

Received September 22, 1981

Summary: Methyl propiolate or tetrolate condense with a number of olefins in a reaction catalyzed by either η^5-$C_5H_5Fe(CO)_2$(isobutylene)BF_4 or η^5-$C_5H_5Fe(CO)_2$(THF)-BF_4 to give 1,3-dienes, cyclobutenes, and 5,6-dihydro-2-pyrones.

The $C_5H_5Fe(CO)_2$ cation (Fp^+) is known to activate olefins in $Fp(\eta^2\text{-olefin})^+ x^-$ complexes toward addition by

0276-7333/82/2301-0397$01.25/0

Table I. Reactions of Alkenes and Acetylenic Esters with Fp^+

alkene	ester	$FpL^+BF_4^-$ (mol %)	products (yield)
	2	4 (10)[a]	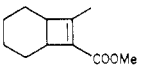 (46)
	2	3 (10)[a]	5 (53)
	2	4 (50)[a]	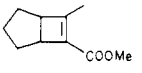 (32)
			6
	2	4 (20)[a]	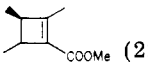 (22) 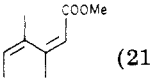 (21)
			7 8
	2	4 (20)[a]	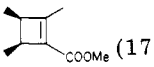 (17) 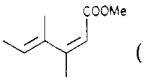 (16)
			9 10
	1	3 (100)[b]	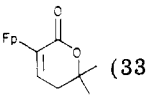 (33)
			11
	2	3 (100)[b]	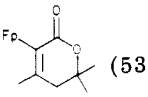 (53)
			12
	1	3 (100)[b]	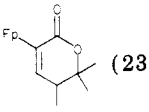 (23) 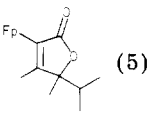 (5)
			13 14
	2	2 (100)[b]	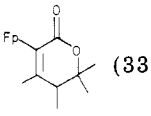 (33) 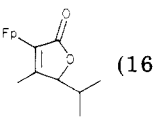 (16)
			15 16
	2	3 (100)[b]	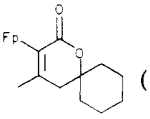 (66)
			17

[a] Reaction time, 24 h. [b] Reaction time, 5 h.

carbon[1] and heteroatomic nucleophiles,[2] and we have earlier applied this chemistry in metal-assisted Michael reactions,[3] enolate vinylations[4] and β-lactam synthesis.[5] Similar activation of acetylenic ligands is less extensively explored, but these too have been shown to be effective substrates for nucleophilic attack in Fp(η²-acetylene) cations.[6] We now find that Fp^+ may function as a unique *catalyst* for cycloaddition and ene[7] type reactions involving

Scheme I

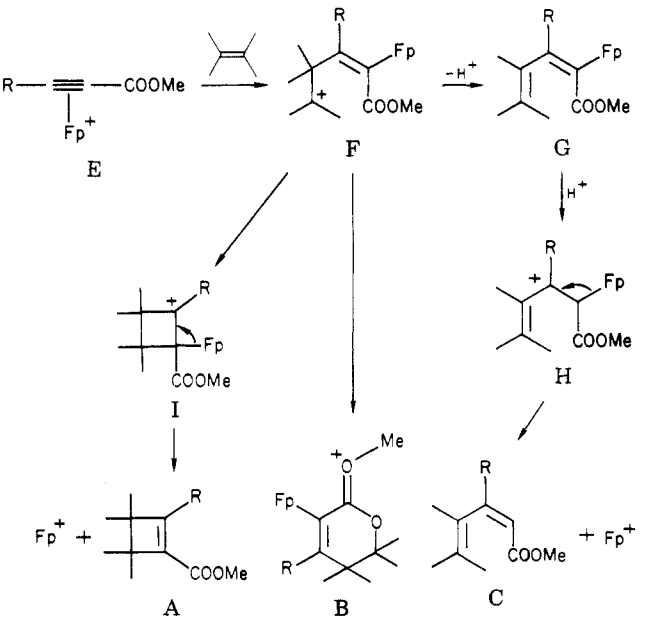

the cocondensation of acetylenic esters and olefins. The overall transformation is given by eq 1, and experimental

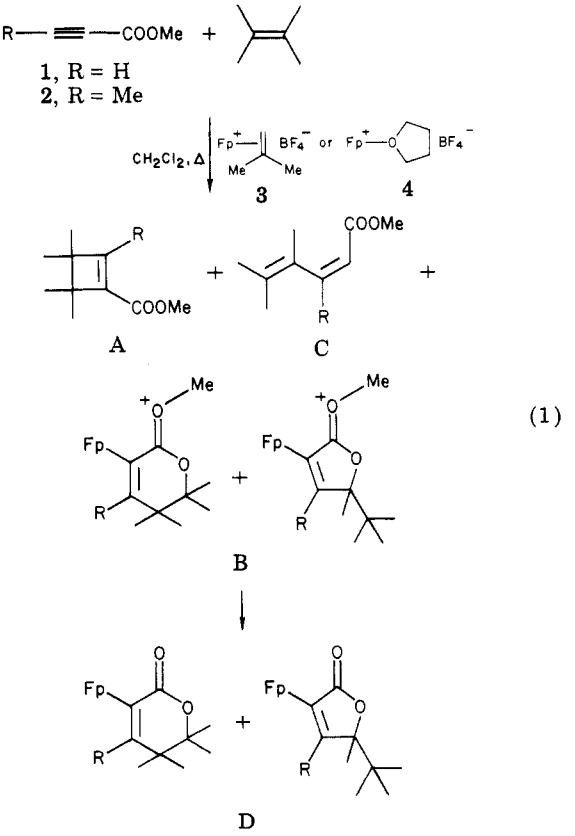

(1)

results, obtained with methyl propiolate **1** or methyl tetrolate **2** and a number of alkenes, using Fp(isobutylene)[8] or Fp(tetrahydrofuran) tetrafluoroborate[9] salts as a source

(1) Rosan, A.; Rosenblum, M.; Tancrede, J. *J. Am. Chem. Soc.* **1973**, *95*, 3062. Lennon, P.; Rosan, A. M.; Rosenblum, M. *Ibid.* **1977**, *99*, 8426. Foxman, B.; Marten, D. F.; Rosan, A.; Raghu, S.; Rosenblum, M. *Ibid.* **1977**, *99*, 2160.

(2) Lennon, P.; Madhavarao, M.; Rosan, A.; Rosenblum, M. *J. Organomet. Chem.* **1976**, *108*, 93.

(3) Rosan, A.; Rosenblum, M. *J. Org. Chem.* **1975**, *40*, 3621.

(4) Chang, T. C. T.; Rosenblum, M.; Samuels, S. B. *J. Am. Chem. Soc.* **1980**, *102*, 5930.

(5) Wong, P. K.; Madhavarao, M.; Marten, D. F.; Rosenblum, M. *J. Am. Chem. Soc.* **1977**, *99*, 2823.

(6) Bates, D. J.; Rosenblum, M.; Samuels, S. B. *J. Organomet. Chem.* **1981**, *209*, C55.

(7) Snider, B. B. *Acc. Chem. Res.* **1980**, *13*, 426.

(8) (a) Giering, W. P.; Rosenblum, M. *J. Organomet. Chem.* **1970**, *25*, C71. (b) Giering, W. P.; Rosenblum, M. *J. Chem. Soc., Chem. Commun.* **1971**, 441. (c) Cutler, A.; Ehntholt, D.; Giering, W. P.; Lennon, P.; Raghu, S.; Rosan, A.; Rosenblum, M.; Tancrede, J.; Wells, D. *J. Am. Chem. Soc.* **1976**, *98*, 3495.

(9) Reger, D. L.; Coleman, C. *J. Organomet. Chem.* **1977**, *131*, 153. A more convenient and less expensive method for making this compound than the method used in the above references (FpX + $AgBF_4$ in THF) consists in simply heating complex **3** in THF–CH_2Cl_2 solution for 3.5 h and filtering off the product **4** (79% yield).

of the Fp cation, are summarized in Table I.

In general a mixture of acetylenic ester, complex **3** or **4**, and the olefin, dissolved in methylene chloride, was heated at reflux for several hours (see Table I). The solution was cooled and concentrated under reduced pressure, and ether was added to precipitate the salt B. This was collected and washed thoroughly with ether. Treatment of these with sodium iodide in acetone solution at 25 °C for 1–2 h gave the lactone products, which were purified by column chromatography on neutral, activity IV alumina, eluting with 10% ether–hexane followed by 70% ether–hexane. The ether-soluble products were concentrated in vacuo and Kugelrohr distilled. Separation of mixtures of products and determination of yields was achieved by gas chromatography.[10,11]

Several features of the reaction are noteworthy with respect to its mechanism and synthetic scope. The formation of cyclobutene A and diene C products is catalytic with respect to complexes **3** or **4**, but it can be shown in a separate experiment that the lactone salts B do not promote the conversion of acetylene and olefin to A and C. Both the dienes **8** and **10** and cyclobutenes **7** and **9** are formed stereospecifically from *cis*- and *trans*-2-butene,[12] consistent with, but not requiring, a concerted mechanism for their formation.[13] Futhermore, the structures of the product olefins **8** and **10** are such as to exclude their formation from cyclobutenes **7** and **9** by a thermal or metal-catalyzed electrocyclic reaction. Finally, the course of the reaction is strongly dependent on the structure of the olefin reactant; 1,2-disubstituted cyclic and acyclic alkenes yield cyclobutenes and 1,3-dienes in addition to some lactone salts, while 1,1-disubstituted or trisubstituted alkenes gave only the latter products. Monosubstituted olefins yield principally their Fp complexes.

The mechanism shown in Scheme I plausibly accounts for these experimental results.

Initial transfer of Fp^+ from **3** or **4** to the acetylenic ester gives the highly reactive complex E. We have already provided evidence for the formation of such a species in exchange reactions with **3**[6] and for its reaction with nucleophiles competitive[6,14] with rearrangement to a cationic vinylidene complex.[15] The cation F, formed by the reaction of the acetylene complex with an olefin, may be expected to undergo several competing reactions. Proton transfer (F → G → H → C) results in the formation of diene and regeneration of Fp^+ catalyst. Although this sequence bears some resemblance to the Lewis acid promoted ene reactions of propiolic esters with olefins,[7,16] an important distinction lies in the formation of 1,4-dienes in these latter reactions, apparently due to proton loss through a six-membered dipolar transition state or intermediate.[16] Significantly, such a transition state is not available to F.[17] The stereochemistry assigned to F follows from anticipated trans addition[1] of olefin to the acetylene complex E and allows for the observed formation of both δ- and γ-lactone salts B, by either direct closure of F or by carbonium ion rearrangement prior to closure. These latter complexes, unlike intermediate G, should be resistant to proton-initiated demetalation owing to their charge, and hence the formation of B irreversibly consumes the catalyst Fp^+. Alternatively, cyclization of F may proceed through the cyclobutyl cation I and thence by elimination of Fp^+ to product A, in a second catalytic cycle. Throughout, the Fp group plays an important role in promoting the cyclization of F to B and I and in the demetalation of G through the stabilization of cationic charge β to it in these substances.[18]

Facile demetalation of **12** is also achieved by treatment with I_2 (CH_2Cl_2, 3 h, 25 °C) or with 48% HBr (Et_2O, 3 h, 25 °C) to give lactones **18a**,[19]**b** (73% and 61% yields, respectively). Similarly, treatment of **17** with Br_2 (CH_2Cl_2, 1 h, 25 °C) gave the spirolactone **19** (55% yield).

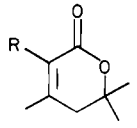

18a, R = I
b, R = H

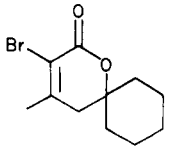

19

Cationic oligomerization and polymerization of alkenes and alkynes by transition-metal salts is well recognized,[20] and an example of such reactions by a discrete organometallic complex dication has recently been given.[21] We had earlier reported the catalytic dimerization of phenylacetylene to give 2-phenylnaphthalene in the presence of **3**.[14] The reactions reported here represent the first examples of carbon–carbon bond formation catalyzed by Fp^+, involving a mixed acetylene–olefin system. Further experiments designed to examine the generality of the reaction and its synthetic applications are in progress.

Acknowledgment. This research was supported by a grant from the National Science Foundation (No. CHE-7816863) which is gratefully acknowledged.

Registry No. **1**, 922-67-8; **2**, 23326-27-4; **3**, 41707-16-8; **4**, 63313-71-3; **5**, 79953-73-4; **6**, 79970-17-5; **7**, 73588-18-8; **8**, 79953-74-5; **9**, 79953-75-6; **10**, 79953-76-7; **11**, 69627-24-3; **12**, 79972-23-9; **13**, 79972-24-0; **14**, 79972-25-1; **15**, 79972-26-2; **16**, 79972-27-3; **17**, 79972-28-4; **18a**, 79953-77-8; **19**, 79953-78-9; cyclohexene, 110-83-8; cyclopentene, 142-29-0; *trans*-2-butene, 624-64-6; *cis*-2-butene, 590-18-1; isobutylene, 115-11-7; 2-methyl-2-butene, 513-35-9; methylenecyclohexane, 1192-37-6; **18b**, 6970-56-5.

(10) Final purification and analysis was carried out by GLC on a 6 ft × 1/4 in. DEGS on chromosorb W column at 85 °C.

(11) All new products have been fully characterized by IR and ^1H NMR spectra and by elemental or ^{13}C NMR spectral analysis.

(12) Assignments of **7** and **9** were made by decoupling the ring protons from the methyl proton resonances: $J_{H\text{-}3,H\text{-}4}(7) = 1.5$ Hz, $J_{H\text{-}3,H\text{-}4}(9) = 4.6$ Hz. The stereochemistry of the C(2),C(3) double bond in **8** and **10** is consistent with the chemical shifts observed: for C(3) methyl groups, **8**, **10** ($CDCl_3$) δ 1.90; for *cis*-crotonic ester, δ 2.14; for *trans*-crotonic ester, δ 1.88. The stereochemistry of the C(4),C(5) double bond in **8** and **10** is in accord with methyl group carbon resonances in their ^{13}C spectra: **8** ($CDCl_3$) δ 23.9, 21.8, 14.1; **10** ($CDCl_3$) δ 25.5, 15.1, 13.4.

(13) Bartlett, Q. *Rev., Chem. Soc.* **1970**, *4*, 473. Hoffmann, R. W.; Bressel, U.; Gehlhaus, J.; Häuser, H. *Chem. Ber.* **1971**, *104*, 873. Gompper, R. *Angew. Chem., Int. Ed Engl.* **1969**, *8*, 312.

(14) Samuels, S. B.; Berryhill, S. R.; Rosenblum, M. *J. Organomet. Chem.* **1979**, *166*, C9.

(15) Davidson, A.; Solar, P. *J. Organomet. Chem.* **1978**, *155*, C8.

(16) Snider, B. B.; Roush, D. M.; Rodini, D. J.; Gonzalez, D.; Spindell, D. *J. Org. Chem.* **1980**, *45*, 2773.

(17) The stereospecific formation of dienes **8** and **10** precludes the possibility that nonconjugated diene is first formed and subsequently isomerized to a conjugated diene.

(18) These interactions are evident in the unusual chemical stability of lactones B, which are only partially hydrolyzed after being stirred in contact with aqueous bicarbonate solutions for several hours. The neutral lactones, derived from B by iodide treatment, also show the effects of Fp group interactions with electron-defficient centers in their unusually low lactone carbonyl frequencies: for **13** and **15**, 1670 cm^{-1}; for **14** and **16**, 1710 cm^{-1}.

(19) Korte, F.; Scharf, D. *Chem. Ber.* **1962**, *95*, 443.

(20) Khan, M. M. T.; Martell, A. E. "Homogeneous Catalysis by Metal Complexes"; Academic Press: New York, 1974; Vol. II, Chapter 6.

(21) Sen, A.; Lai, T.-W. *J. Am. Chem. Soc.* **1981**, *103*, 4627.

Heterobimetallic Cooperativity in the Reduction of Methyl Isocyanide by $(C_5H_5)_2W(SH)_2$

Thomas B. Rauchfuss* and Charles J. Ruffing

School of Chemical Sciences, University of Illinois Urbana, Illinois 61801

Received August 25, 1981

Summary: The metallodithiol $(C_5H_5)_2W(SH)_2$ reacts with $[Pd(CH_3NC)_2(Ph_2PCH_2CH_2PPh_2)](PF_6)_2$ to form the *N*-methyldithiocarbamate $[(C_5H_5)_2WS_2CN(H)CH_3]PF_6$ (**3**) via a novel hydrogen-transfer reaction. An independent synthesis of **3** and $(C_5H_5)_2W$ derivatives of other sulfur ligands is also reported.

Metallothiols are a class of compounds characterized by the presence of the M–SH functional group. As such, soluble mononuclear metallothiols can be considered to be the simplest analogues of surface and cluster polymetallothiols which are of likely relevance to certain biological and industrial catalysts.[1] $Cp_2W(SH)_2$, **1** (Cp = $^5\eta$-C_5H_5), is a metallo*dithiol* which was first reported by Green[2] but is otherwise a neglected chemical entity. Since it shows enhanced nucleophilicity relative to other similar compounds, e.g., $Cp_2Ti(SH)_2$,[3,4] it was selected for the study described herein.

With the objective of assessing the ability of metallothiols for hydrogen atom transfer to small molecules, we examined the reactivity of **1** toward methyl isocyanide. Although **1** does not react directly with methyl isocyanide, we have found an interesting reaction with its transition-metal derivative $[Pd(CH_3NC)_2(dppe)](PF_6)_2$,[5] **2** (dppe = 1,2-bis(diphenylphosphino)ethane). Thus, reaction of equimolar quantities of **1** and **2** in acetonitrile under an atmosphere of N_2 at 25 °C resulted in a rapid color change from deep red to yellow. After 2 h the reaction mixture was evaporated to dryness and the residue was extracted with dichloromethane leaving the *N*-methyldithiocarbamate complex **3** as an orange solid which was recrystallized from acetonitrile (90%) (eq 1). Analytical[7]

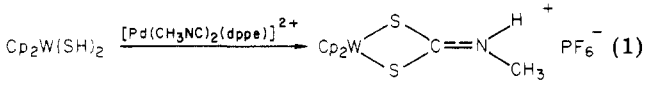

(1)

3

and spectroscopic data for **3** were consistent with our formulation, the most important observations being the IR absorptions (Nujol mull) at 3380 cm^{-1} (ν_{N-H}) and 1549 cm^{-1} ($\nu_{C=N}$), the D_2O-collapsible *N*-methyl doublet at 2.8 ppm in the ^1H NMR (CD_3CN solution), and a molecular ion (m/e = 420) in the field desorption mass spectrum. Final confirmation of the identity of **3** follows from the preparation of a spectroscopically identical compound from

Scheme I

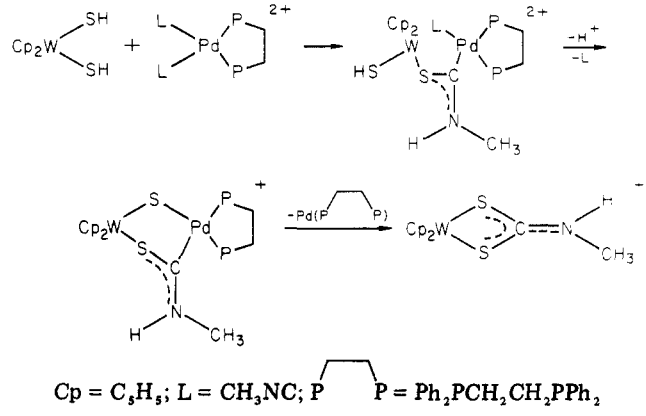

Cp = C_5H_5; L = CH_3NC; P P = $Ph_2PCH_2CH_2PPh_2$

Cp_2WCl_2[8] and methylammonium *N*-methyldithiocarbamate[9] (eq 2). This synthetic method appears to be

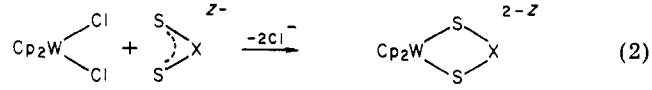

(2)

3, X = C–N(H)CH_3, Z = 1
4a, X = C–N$(CH_3)_2$, Z = 1
b, X = C–N$(C_2H_5)_2$, Z = 1
c, X = C–N(H)(C_6H_5), Z = 1
5, X = MoS_2, Z = 2

a general one, and we have utilized it to prepare other, related derivatives such as **4a–c**[10] and the tetrathiomolybdate **5**.[11] These complexes were characterized by elemental analyses, IR, and when soluble, ^1H NMR.

A reasonable mechanism for the formation of **3** can be proposed on the basis of the precedents in monometallic chemistry. Addition of the WS–H unit to a coordinated isocyanide would form the heterobimetallic carbene[13] (Scheme I), via a reaction analogous to that previously observed between organic thiols and $[Pd(CH_3NC)_4](PF_6)_2$.[6] Deprotonation of the remaining metallothiol group followed by displacement of the unreacted isocyanide ligands affords a cyclic intermediate which, upon reductive elimination of palladium(0) as Pd(dppe),[14] gives the dithiocarbamate **3**.

The reactivity of coordinated isocyanide toward RSH, where R = H[15,16] and alkyl,[6] has been reported previously.

(1) Rakowski, DuBois, M.; VanDerveer, M. C.; DuBois, D. L.; Haltiwanger, R. C.; Miller, W. K. *J. Am. Chem. Soc.* **1980**, *102*, 7456 and references therein.

(2) Green, M. L. H.; Lindsell, W. E. *J. Chem. Soc. A* **1967**, 1455.

(3) Köpf, H.; Schmidt, M. *Angew. Chem., Int. Ed. Engl.* **1965**, *4*, 953. McCall, J. M.; Shaver, A. *J. Organomet. Chem.* **1980**, *193*, C37.

(4) Ruffing, C. J.; Rauchfuss, T. B., unpublished results.

(5) $[Pd(CH_3NC)_2(dppe)](PF_6)_2$ was synthesized from equimolar quantities of $[Pd(CH_3NC)_4](PF_6)_2$[6] and dppe in acetonitrile and was recrystallized from CH_2Cl_2/Et_2O. Anal. Calcd for $C_{30}H_{30}F_{12}N_2P_4Pd$: C, 40.89; H, 3.41; P, 14.54. Found: C, 40.68; H, 3.38; P, 14.22. IR (Nujol mull): 2260 cm^{-1} (ν_{CN}). ^1H NMR (CD_3CN): 7.5 (m, 10 H), 3.25 (s, 3 H), 3.20 (m, 2 H).

(6) Miller, J. S.; Balch, A. L. *Inorg. Chem.* **1972**, *11*, 2069.

(7) Anal. Calcd for $C_{12}H_{14}F_6WS_2NP$: C, 25.49; H, 2.47; N, 2.47. Found: C, 25.66; H, 2.52; N, 2.53. Melting point: 260 °C dec.

(8) Cooper, R. L.; Green, M. L. H. *J. Chem. Soc. A* **1967**, 1155.

(9) Methylammonium *N*-methyldithiocarbamate was synthesized in a manner analogous to that for $NH_4S_2CNH_2$. Fackler, J. P.; Coucouvanis, D. *Inorg. Chem.* **1967**, *6*, 2047.

(10) In a typical preparation, a suspension of 0.15 mmol each of Cp_2WCl_2 and 1,1-dithio ligand in 10 mL of absolute ethanol was heated under reflux for 2 h. Addition of an ethanolic solution of 0.6 mmol of NH_4PF_6 precipitated an orange solid. The suspension was then evaporated to dryness and washed with CH_2Cl_2. Addition of Et_2O to the CH_2Cl_2 extract afforded orange microcrystalline solids in 60–80% yield. Compounds **4a–c** gave satisfactory elemental analyses and were spectroscropically analogous to **3**.

(11) Compound **5** was synthesized by refluxing 0.15 mmol each of Cp_2WCl_2 and NH_4MoS_4 in 10 mL of absolute ethanol. After 2 h the product was filtered from the reaction mixture and air-dried. The IR spectrum (Nujol mull) of compound **5** shows absorptions characteristic of terminal (502, 488 cm^{-1}) and bridging (446 cm^{-1}) Mo–S vibrations of chelating MoS_4^{2-}.[12] Anal. Calcd for $C_{10}H_{10}WS_4Mo$: C, 22.30; H, 1.85; S, 23.79. Found: C, 22.21; H, 1.92; S, 23.90.

(12) Coucouvanis, D.; Simhon, E. D.; Baenziger, N. C. *J. Am. Chem. Soc.* **1980**, *102*, 6646.

(13) The intermediacy of carbenes has been invoked in the heterobimetallic reduction of carbon monoxide: Marsella, J. A.; Folting, K.; Huffman, J. C.; Caulton, K. G. *J. Am. Chem. Soc.* **1981**, *103*, 5596.

(14) The palladium product(s) of this reaction have been isolated but identified only to the extent that it contains the fragment Pd^{II}dppe(MeNC)PF_6. Anal. Found: C, 46.35; H, 3.69; N, 1.89; Cl, 3.15. IR (Nujol mull): 2220 (ν_{NC}), 1050 (dppe Pd), 850 cm^{-1} (ν_{PF}). FDMS: ions observed at m/e = 398 ($dppe^+$), 504 ($Pd(dppe)^+$), 545 (Pd(dppe)$(MeNC)^+$), and 569.

(15) Treichel, P. M.; Knebel, W. J. *Inorg. Chem.* **1972**, *11*, 1285.

0276-7333/82/2301-0400$01.25/0

The present work demonstrates that metallothiols can function similarly and in so doing reduce unsaturated organic substrates. This hydrogen transfer behavior is of likely relevance to the chemistry which occurs on metal sulfide catalysts under hydrogenation conditions.[17]

Acknowledgment. This research was supported by the National Science Foundation. The University of Illinois field desorption mass spectrometry facility is supported by the National Cancer Institute.

Registry No. 1, 12245-02-2; 2, 79681-97-3; 3, 79681-99-5; 4a, 79682-00-1; 4b, 79682-01-2; 4c, 79682-02-3; 5, 78356-91-9; Cp_2WCl_2, 12184-26-8.

(16) Grundy, K. R.; Roper, W. R. *J. Organomet. Chem.* **1976**, *113*, C45.
(17) Landa, S.; Weisser, O. "Sulphide Catalysts; Their Properties and Applications"; Pergamon Press: New York, 1973.

Cyclopentadienylnickel Cyclooctadiene: A Stable Organometallic π Radical Containing a Nonconjugated Polyolefin

Gregg Lane and William E. Geiger*

Department of Chemistry, University of Vermont Burlington, Vermont 05405

Received October 7, 1981

Summary: Reduction of cyclopentadienylnickel cyclooctadiene cation, $CpNiCod^+$, in which the polyolefin ring is bonded as a nonconjugated diene to the metal, has been accomplished electrochemically in weakly polar nonaqueous media. An E° value of −0.46 V was found for the redox process in CH_2Cl_2/0.1 M Bu_4NPF_6. The reduction is chemically and electrochemically reversible and gives the neutral free radical, 19-electron CpNiCod, which is stable without decomposition for over 1 h at −10 °C in dichloromethane. Eventual decomposition occurs through disproportionation to nickelocene and bis(cyclooctadiene)nickel. The stability of the 1,5-diene Cod in the radical is in marked contrast to the behavior of the isoelectronic cobalt complex $CpCoCod^-$, in which isomerization of Cod to the 1,3-diene isomer has been observed. Differences in preferred isomeric form of the Cod ligand are discussed in terms of the probable electronic structures of the radicals.

We wish to report electrochemical data showing that the neutral organometallic π complex radical (η^5-cyclopentadienyl)nickel cyclooctadiene, CpNiCod, can be generated via facile one-electron reduction of the cationic precursor, $CpNiCod^+$. Furthermore, our data show that in the 19-electron radical the Cod ligand retains its 1,5-diene mode of coordination, whereas in the isoelectronic cobalt anion, $(CpCoCod)^-$, isomerization of the polyolefin from a η^4-1,5-diene to a η^4-1,3-diene had been observed (Scheme I)[1]

Reduction of $[CpNiCod]^+PF_6^{-2}$ in either dichloromethane or THF solutions containing 0.1 M Bu_4NPF_6 occurred in a diffusion-controlled one-electron step to yield

Scheme I

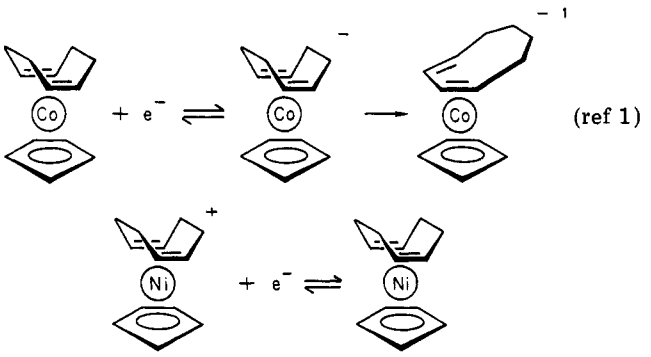

Scheme II

$CpNiCod^+ + e^- \rightleftharpoons CpNiCod$

$CpNiCod \longrightarrow {}^1/_2Cp_2Ni + {}^1/_2Cod_2Ni$

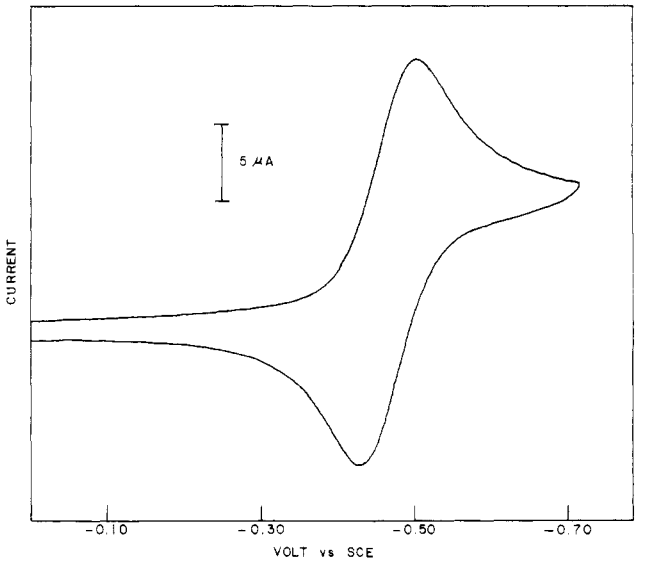

Figure 1. Cyclic voltammogram of 1.0×10^{-3} M $CpNiCod^+PF_6^-$ in CH_2Cl_2 at a platinum bead electrode in CH_2Cl_2/0.1 M Bu_4NPF_6 (scan rate = 100 mV/s).

the neutral radical. Direct current polarography gave an $E_{1/2}$ of −0.49 V[3] in CH_2Cl_2. The slope of the plot[4] of applied potential vs. log $[i/(i_d - i)]$ was −53 mV in CH_2Cl_2, consistent with the reduction being a reversible one-electron process. This was confirmed through cyclic voltammetry (CV) measurements[5] at either a platinum microelectrode or a hanging mercury drop electrode (E° = −0.46 V in CH_2Cl_2). At scan rates as low as 100 mV/S, the ratio of the anodic to cathodic currents was unity, implying a very stable one-electron reduction product (Figure 1). Peak potential separations were also consistent the process being electrochemically reversible.[6]

(1) Moraczewski, J.; Geiger, W. E. *J. Am. Chem. Soc.* **1981**, *103*, 4779.
(2) Salzer, A.; Count, T. L.; Werner, H. *J. Organomet. Chem.* **1973**, *54*, 325.

(3) Potentials are reported vs. the aqueous saturated calomel electrode.
(4) i is the current at any point on the rising portion of the polarographic wave, and i_d is the diffusion limited current measured on the plateau of the wave. A slope of −59 mV/n, where n is the number of electrons transferred, is calculated for reversible electron-transfer processes.
(5) Procedures for the electrochemical experiments were as described in ref 1. Spectrograde dichloromethane was distilled from calcium hydride before use. Anhydrous tetrahydrofuran (Aldrich) was distilled from lithium aluminum hydride. Since the nickel cation is an air-stable compound, all of the voltammetric measurements except those associated with bulk electrolytic reductions were carried out by using inert atmosphere purging techniques. Bulk coulometry and handling of solutions of electrolysis products were accomplished inside a Vacuum Atmosphere drybox.

0276-7333/82/2301-0401$01.25/0

The present work demonstrates that metallothiols can function similarly and in so doing reduce unsaturated organic substrates. This hydrogen transfer behavior is of likely relevance to the chemistry which occurs on metal sulfide catalysts under hydrogenation conditions.[17]

Acknowledgment. This research was supported by the National Science Foundation. The University of Illinois field desorption mass spectrometry facility is supported by the National Cancer Institute.

Registry No. 1, 12245-02-2; 2, 79681-97-3; 3, 79681-99-5; 4a, 79682-00-1; 4b, 79682-01-2; 4c, 79682-02-3; 5, 78356-91-9; Cp_2WCl_2, 12184-26-8.

(16) Grundy, K. R.; Roper, W. R. *J. Organomet. Chem.* **1976**, *113*, C45.
(17) Landa, S.; Weisser, O. "Sulphide Catalysts; Their Properties and Applications"; Pergamon Press: New York, 1973.

Cyclopentadienylnickel Cyclooctadiene: A Stable Organometallic π Radical Containing a Nonconjugated Polyolefin

Gregg Lane and William E. Geiger*

Department of Chemistry, University of Vermont Burlington, Vermont 05405

Received October 7, 1981

Summary: Reduction of cyclopentadienylnickel cyclooctadiene cation, $CpNiCod^+$, in which the polyolefin ring is bonded as a nonconjugated diene to the metal, has been accomplished electrochemically in weakly polar nonaqueous media. An E° value of −0.46 V was found for the redox process in CH_2Cl_2/0.1 M Bu_4NPF_6. The reduction is chemically and electrochemically reversible and gives the neutral free radical, 19-electron CpNiCod, which is stable without decomposition for over 1 h at −10 °C in dichloromethane. Eventual decomposition occurs through disproportionation to nickelocene and bis(cyclooctadiene)nickel. The stability of the 1,5-diene Cod in the radical is in marked contrast to the behavior of the isoelectronic cobalt complex $CpCoCod^-$, in which isomerization of Cod to the 1,3-diene isomer has been observed. Differences in preferred isomeric form of the Cod ligand are discussed in terms of the probable electronic structures of the radicals.

We wish to report electrochemical data showing that the neutral organometallic π complex radical (η^5-cyclopentadienyl)nickel cyclooctadiene, CpNiCod, can be generated via facile one-electron reduction of the cationic precursor, $CpNiCod^+$. Furthermore, our data show that in the 19-electron radical the Cod ligand retains its 1,5-diene mode of coordination, whereas in the isoelectronic cobalt anion, $(CpCoCod)^-$, isomerization of the polyolefin from a η^4-1,5-diene to a η^4-1,3-diene had been observed (Scheme I)[1]

Reduction of $[CpNiCod]^+PF_6^{-2}$ in either dichloromethane or THF solutions containing 0.1 M Bu_4NPF_6 occurred in a diffusion-controlled one-electron step to yield

Scheme I

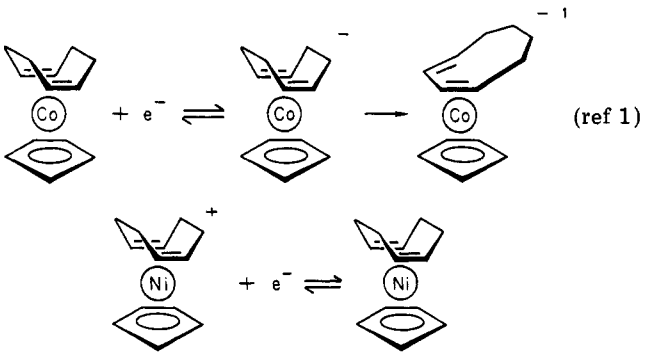

Scheme II

$CpNiCod^+ + e^- \rightleftharpoons CpNiCod$

$CpNiCod \longrightarrow {}^1/_2Cp_2Ni + {}^1/_2Cod_2Ni$

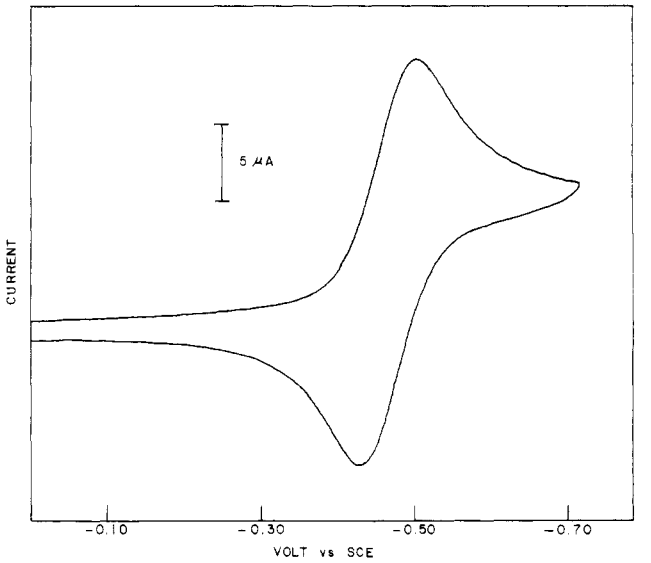

Figure 1. Cyclic voltammogram of 1.0×10^{-3} M $CpNiCod^+PF_6^-$ in CH_2Cl_2 at a platinum bead electrode in CH_2Cl_2/0.1 M Bu_4NPF_6 (scan rate = 100 mV/s).

the neutral radical. Direct current polarography gave an $E_{1/2}$ of −0.49 V[3] in CH_2Cl_2. The slope of the plot[4] of applied potential vs. log $[i/(i_d - i)]$ was −53 mV in CH_2Cl_2, consistent with the reduction being a reversible one-electron process. This was confirmed through cyclic voltammetry (CV) measurements[5] at either a platinum microelectrode or a hanging mercury drop electrode (E° = −0.46 V in CH_2Cl_2). At scan rates as low as 100 mV/S, the ratio of the anodic to cathodic currents was unity, implying a very stable one-electron reduction product (Figure 1). Peak potential separations were also consistent the process being electrochemically reversible.[6]

(1) Moraczewski, J.; Geiger, W. E. *J. Am. Chem. Soc.* **1981**, *103*, 4779.
(2) Salzer, A.; Count, T. L.; Werner, H. *J. Organomet. Chem.* **1973**, *54*, 325.

(3) Potentials are reported vs. the aqueous saturated calomel electrode.
(4) i is the current at any point on the rising portion of the polarographic wave, and i_d is the diffusion limited current measured on the plateau of the wave. A slope of −59 mV/n, where n is the number of electrons transferred, is calculated for reversible electron-transfer processes.
(5) Procedures for the electrochemical experiments were as described in ref 1. Spectrograde dichloromethane was distilled from calcium hydride before use. Anhydrous tetrahydrofuran (Aldrich) was distilled from lithium aluminum hydride. Since the nickel cation is an air-stable compound, all of the voltammetric measurements except those associated with bulk electrolytic reductions were carried out by using inert atmosphere purging techniques. Bulk coulometry and handling of solutions of electrolysis products were accomplished inside a Vacuum Atmosphere drybox.

0276-7333/82/2301-0401$01.25/0

Room temperature controlled potential electrolysis measurements at a platinum basket resulted in a change from green to yellow and consumption of one-electron (n = 0.95 e^-). Voltammograms taken immediately after electrolysis showed mainly the reversible couple for $CpNiCod^{0/+}$ at −0.46 V, but a small reverisible wave was also present at −0.02 V, together with another minor wave (irreversible) at +1.04 V. As time went on, the wave due to CpNiCod diminished and the others grew in. By matching these waves with potentials measured independently for the pure compounds, we have identified the wave at −0.02 V as arising from the oxidation of nickelocene and the wave at +1.04 V as being due to bis(cyclooctadiene)nickel. Therefore, there is good evidence that the ultimate fate of the 19-electron radical is disproportionation into compounds containing metals with 20 valence electrons (Cp_2Ni) and 18 valence electrons (Cod_2Ni) (Scheme II). The reaction appears to be quantitative.

Electrolysis at subambient temperatures slowed down the disproportionation reaction and allowed production of stable solutions of the radical. Thus, electrolysis at −10 °C in CH_2Cl_2 gave only the wave for the neutral radical. By voltammetry at the rotating platinum electrode it was shown that the original reduction wave at −0.46 V had been quantitatively replaced by an oxidation wave at the identical potential. Solutions at this temperature were stable for at least 1 h after electrolysis before any wave for Cp_2Ni was noticed.

The stability of this radical is noteworthy. It is a very rare example of a neutral π-complex radical containing a nonconjugated polyolefin ligand. Previous examples of stable metal π radicals have been generally restricted to "sandwich"-type compounds like Cp_2Co,[7] $CpFe(C_6R_6)$,[8] $(C_6R_6)_2V$,[9] $CpV(C_7H_7)$,[10] $CpCr(C_6H_6)$,[11] and $CpTi(\eta^8$-cyclooctatetraene).[12] The present example suggests that metal–olefin compounds without extensively delocalized orbitals may in certain cases be isolable in free radical form.

Electronic Structure of the Radical. CpNiCod is also of interest because it is isoelectronic with $CpCoCod^-$, in which the cyclooctadiene ligand prefers the 1,3-diene mode of coordination.[1] Electron spin resonance measurements and molecular orbital calculations agree that the half-occupied orbital in the cobalt anion is predominantly metal in character.[13] Because ^{61}Ni is present in low natural abundance (1.2%), no hyperfine splitting is observed from ESR spectra of solutions of CpNiCod, but frozen solution spectra in dichloromethane (163 K) are indicative that, qualitatively, reduction of the cation has again involved a metal-based orbital. An axially symmetric **g** tensor was observed, with $g_{\parallel} = 2.182$ and $g_{\perp} = 2.025$. The fact that the unique g value is at low-field is consistent with findings for other d^9 metal π complexes[13,14] and inconsistent with a ligand-based orbital (because of large g value anisotropy) or a d^7 metal configuration. The latter is ruled out because in that case, the unique g value is expected to be the high-field component.[8] Thus, the ESR is consistent with CpNiCod being a formal Ni(I), with appreciable spin density on the metal.

Bonding Mode of the Cod Ligand. In spite of the isoelectronic nature of $CpCoCod^-$ and CpNiCod, the cyclooctadiene ligand prefers the nonconjugated (1,5-diene) mode of coordination in the nickel complex. The electrochemical data clearly supports this conclusion, since changes in the ligand coordination mode would give an electrolysis product with a different $E°$ potential. In the analogous CpCo(diene) complexes, the differences in reduction potentials varied from ca. 200 mV (diene = cyclooctatetraene) to almost 1 V (diene = Cod) when alterations from 1,5 to 1,3 bonding occurred.[1]

The question arises as to why the ligand isomerizes from the nonconjugated to the conjugated form in the cobalt anion but remains as the 1,5 diene in the nickel complex. The obvious difference between the two isoelectronic compounds is the negative charge on the cobalt species, suggesting that delocalization of the excess charge into the Cod ring in $CpCoCod^-$ may be an important factor in dictating the isomerization of the polyolefin ligand to the conjugated isomer.

Acknowledgment. We gratefully acknowledge support of this work by the National Science Foundation (Grant CHE80-04242).

Registry No. $CpNiCod^+ PF_6^-$, 42088-01-7; CpNiCod, 80010-11-3.

(6) ΔE_p values of ca. 70 mV were found for 5×10^{-4} M $CpNiCod^+$ in CH_2Cl_2/0.1 M Bu_4NPF_6, virtually identical with those of ferrocene under identical experimental conditions. The increase from the theoretical value of 60 mV is undoubtedly due to uncompensated iR loss common to these weakly polar nonaqueous electrolytes.

(7) Wilkinson, G. *J. Am. Chem. Soc.* **1954**, *76*, 209.
(8) Hamon, J.-R.; Astruc, D.; Michaud, P. *J. Am. Chem. Soc.* **1981**, *103*, 758.
(9) Henrici-Olive, G.; Olive, S. *Z. Phys. Chem. (Wiesbaden)* **1967**, *56*, 223 and references therein.
(10) Engelbretson, G.; Rundle, R. E. *J. Am. Chem. Soc.* **1963**, *85*, 481.
(11) Evans, S.; Green, J. C.; Jackson, S. E. *J. Chem. Soc., Faraday Trans. 2* **1972**, *68*, 249 and references therein.
(12) Van Oven, H. O.; de Leifde Meijer, H. J. *J. Organomet. Chem.* **1969**, *19*, 373.
(13) Albright, T. A.; Geiger, W. E.; Moraczewski, J.; Tulyathan, B. *J. Am. Chem. Soc.* **1981**, *103*, 4787.
(14) Van Willigen, H.; Geiger, W. E.; Rausch, M. D. *Inorg. Chem.* **1977**, *16*, 581.

(15) Notes Added in Proof: Dr. Ulrich Koelle and co-workers have recently prepared the title compound (*J. Organomet. Chem.*, in press). We thank Dr. Koelle for informing us of this prior to publication of his data. A series of related $CpNiL_2$ compounds (L = phosphines or other Lewis bases) has also been reported recently by Barefield and co-workers (*J. Am. Chem. Soc.*, **1981**, *103*, 6219).

Umpolung with Rhodium Iminoacyls. The Use of Metal Oxidation State To Control the Nucleophilicity or Electrophilicity of Acyl Carbons

J. William Suggs* and Sherman D. Cox
Bell Laboratories
Murry Hill, New Jersey 07974

Received September 28, 1981

Summary: Rhodium(III) iminoacyl hydrides are reduced with dimethylcadmium to give rhodium(I) iminoacyl compounds. These show acyl anion-like reactivity. The same functional group can exhibit acyl anion or acyl cation reactivity depending upon the oxidation state of the attached transition metal.

Hydroacylation, the addition of an aldehyde's C–H bond across an olefin to give a ketone, can be achieved with stable acylrhodium(III) hydrides, or their derivatives, (iminoacyl)rhodium(III) hydrides, and unhindered olefins.[1] However, this methodology cannot be used to append several classes of carbon groups to aldehydes. Methyl groups cannot be appended, since this requires insertion of methylene between the aldehyde C–H bond. Similarly,

*To whom correspondence should be addressed at the Department of Chemistry, Brown University, Providence, Rhode Island 02912.

(1) Suggs, J. W. *J. Am. Chem. Soc.* **1979**, *101*, 489.

0276-7333/82/2301-0402$01.25/0

Room temperature controlled potential electrolysis measurements at a platinum basket resulted in a change from green to yellow and consumption of one-electron (n = 0.95 e^-). Voltammograms taken immediately after electrolysis showed mainly the reversible couple for $CpNiCod^{0/+}$ at −0.46 V, but a small reverisible wave was also present at −0.02 V, together with another minor wave (irreversible) at +1.04 V. As time went on, the wave due to CpNiCod diminished and the others grew in. By matching these waves with potentials measured independently for the pure compounds, we have identified the wave at −0.02 V as arising from the oxidation of nickelocene and the wave at +1.04 V as being due to bis(cyclooctadiene)nickel. Therefore, there is good evidence that the ultimate fate of the 19-electron radical is disproportionation into compounds containing metals with 20 valence electrons (Cp_2Ni) and 18 valence electrons (Cod_2Ni) (Scheme II). The reaction appears to be quantitative.

Electrolysis at subambient temperatures slowed down the disproportionation reaction and allowed production of stable solutions of the radical. Thus, electrolysis at −10 °C in CH_2Cl_2 gave only the wave for the neutral radical. By voltammetry at the rotating platinum electrode it was shown that the original reduction wave at −0.46 V had been quantitatively replaced by an oxidation wave at the identical potential. Solutions at this temperature were stable for at least 1 h after electrolysis before any wave for Cp_2Ni was noticed.

The stability of this radical is noteworthy. It is a very rare example of a neutral π-complex radical containing a nonconjugated polyolefin ligand. Previous examples of stable metal π radicals have been generally restricted to "sandwich"-type compounds like Cp_2Co,[7] $CpFe(C_6R_6)$,[8] $(C_6R_6)_2V$,[9] $CpV(C_7H_7)$,[10] $CpCr(C_6H_6)$,[11] and $CpTi(\eta^8$-cyclooctatetraene).[12] The present example suggests that metal–olefin compounds without extensively delocalized orbitals may in certain cases be isolable in free radical form.

Electronic Structure of the Radical. CpNiCod is also of interest because it is isoelectronic with $CpCoCod^-$, in which the cyclooctadiene ligand prefers the 1,3-diene mode of coordination.[1] Electron spin resonance measurements and molecular orbital calculations agree that the half-occupied orbital in the cobalt anion is predominantly metal in character.[13] Because ^{61}Ni is present in low natural abundance (1.2%), no hyperfine splitting is observed from ESR spectra of solutions of CpNiCod, but frozen solution spectra in dichloromethane (163 K) are indicative that, qualitatively, reduction of the cation has again involved a metal-based orbital. An axially symmetric **g** tensor was observed, with $g_{\parallel} = 2.182$ and $g_{\perp} = 2.025$. The fact that the unique g value is at low-field is consistent with findings for other d^9 metal π complexes[13,14] and inconsistent with a ligand-based orbital (because of large g value anisotropy) or a d^7 metal configuration. The latter is ruled out because in that case, the unique g value is expected to be the high-field component.[8] Thus, the ESR is consistent with CpNiCod being a formal Ni(I), with appreciable spin density on the metal.

Bonding Mode of the Cod Ligand. In spite of the isoelectronic nature of $CpCoCod^-$ and CpNiCod, the cyclooctadiene ligand prefers the nonconjugated (1,5-diene) mode of coordination in the nickel complex. The electrochemical data clearly supports this conclusion, since changes in the ligand coordination mode would give an electrolysis product with a different $E°$ potential. In the analogous CpCo(diene) complexes, the differences in reduction potentials varied from ca. 200 mV (diene = cyclooctatetraene) to almost 1 V (diene = Cod) when alterations from 1,5 to 1,3 bonding occurred.[1]

The question arises as to why the ligand isomerizes from the nonconjugated to the conjugated form in the cobalt anion but remains as the 1,5 diene in the nickel complex. The obvious difference between the two isoelectronic compounds is the negative charge on the cobalt species, suggesting that delocalization of the excess charge into the Cod ring in $CpCoCod^-$ may be an important factor in dictating the isomerization of the polyolefin ligand to the conjugated isomer.

Acknowledgment. We gratefully acknowledge support of this work by the National Science Foundation (Grant CHE80-04242).

Registry No. $CpNiCod^+ PF_6^-$, 42088-01-7; CpNiCod, 80010-11-3.

(6) ΔE_p values of ca. 70 mV were found for 5×10^{-4} M $CpNiCod^+$ in CH_2Cl_2/0.1 M Bu_4NPF_6, virtually identical with those of ferrocene under identical experimental conditions. The increase from the theoretical value of 60 mV is undoubtedly due to uncompensated iR loss common to these weakly polar nonaqueous electrolytes.

(7) Wilkinson, G. *J. Am. Chem. Soc.* **1954**, *76*, 209.
(8) Hamon, J.-R.; Astruc, D.; Michaud, P. *J. Am. Chem. Soc.* **1981**, *103*, 758.
(9) Henrici-Olive, G.; Olive, S. *Z. Phys. Chem. (Wiesbaden)* **1967**, *56*, 223 and references therein.
(10) Engelbretson, G.; Rundle, R. E. *J. Am. Chem. Soc.* **1963**, *85*, 481.
(11) Evans, S.; Green, J. C.; Jackson, S. E. *J. Chem. Soc., Faraday Trans. 2* **1972**, *68*, 249 and references therein.
(12) Van Oven, H. O.; de Leifde Meijer, H. J. *J. Organomet. Chem.* **1969**, *19*, 373.
(13) Albright, T. A.; Geiger, W. E.; Moraczewski, J.; Tulyathan, B. *J. Am. Chem. Soc.* **1981**, *103*, 4787.
(14) Van Willigen, H.; Geiger, W. E.; Rausch, M. D. *Inorg. Chem.* **1977**, *16*, 581.

(15) Notes Added in Proof: Dr. Ulrich Koelle and co-workers have recently prepared the title compound (*J. Organomet. Chem.*, in press). We thank Dr. Koelle for informing us of this prior to publication of his data. A series of related $CpNiL_2$ compounds (L = phosphines or other Lewis bases) has also been reported recently by Barefield and co-workers (*J. Am. Chem. Soc.*, **1981**, *103*, 6219).

Umpolung with Rhodium Iminoacyls. The Use of Metal Oxidation State To Control the Nucleophilicity or Electrophilicity of Acyl Carbons

J. William Suggs* and Sherman D. Cox
Bell Laboratories
Murry Hill, New Jersey 07974

Received September 28, 1981

Summary: Rhodium(III) iminoacyl hydrides are reduced with dimethylcadmium to give rhodium(I) iminoacyl compounds. These show acyl anion-like reactivity. The same functional group can exhibit acyl anion or acyl cation reactivity depending upon the oxidation state of the attached transition metal.

Hydroacylation, the addition of an aldehyde's C–H bond across an olefin to give a ketone, can be achieved with stable acylrhodium(III) hydrides, or their derivatives, (iminoacyl)rhodium(III) hydrides, and unhindered olefins.[1] However, this methodology cannot be used to append several classes of carbon groups to aldehydes. Methyl groups cannot be appended, since this requires insertion of methylene between the aldehyde C–H bond. Similarly,

*To whom correspondence should be addressed at the Department of Chemistry, Brown University, Providence, Rhode Island 02912.

(1) Suggs, J. W. *J. Am. Chem. Soc.* **1979**, *101*, 489.

0276-7333/82/2301-0402$01.25/0

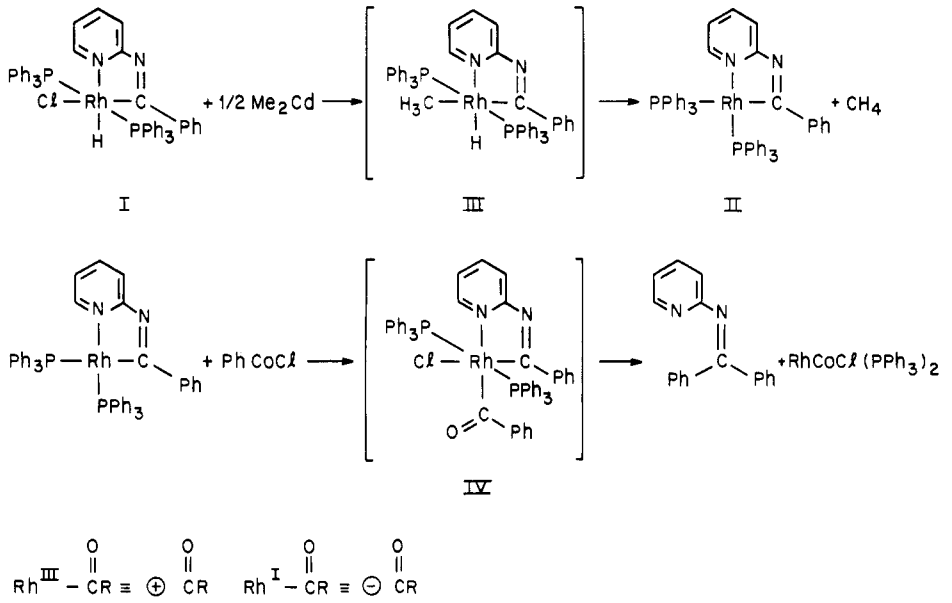

Figure 1. Formation and reaction of the rhodium(I) iminoacyl.

phenyl groups cannot be added, since this corresponds to addition of benzyne. We have developed a way to overcome this limitation which, although stoichiometric in rhodium, does permit efficient recovery of the metal. This new method also illustrates the use of a metal's oxidation state to switch reactivity of a bound acyl derivative between nucleophilicity and electrophilicity.

When a solution of the (iminoacyl)rhodium(III) hydride I is dissolved in a 1:1 mixture of CH_2Cl_2 and THF at −20 °C (0.05 M solution) under argon and a solution of $(CH_3)_2Cd$ in THF (0.5 equiv) added dropwise over 10 min, the initial yellow color is replaced over 15 min by a deep red color, characteristic of Rh(I). Methane is evolved as detected by mass spectrometry, corresponding to 0.75 equiv/mol of rhodium, and the hydride resonance at δ −11.1 disappears. Apparently, chloride–methyl exchange occurs, followed by reductive elimination of methane (expected to be fast) to give the (iminoacyl)rhodium(I) compound II.[2] Although we have not been able to isolate II in crystalline form, ^{31}P NMR spectroscopy (as well as the chemical reactions described below) provides strong evidence for its formation.[3] The ^{31}P resonance of I at δ −32.5 (J_{Rh-P} = 117 Hz) is cleanly replaced with two doublets of doublets at δ −42.2 and −38.8 (downfield from 85% H_3PO_4), with J_{P-P} = 32.6 Hz and J_{Rh-P} = 144 Hz for both phosphines.[4]

The iminoacyl group of II could be alkylated by addition of CH_3I or $C_6H_5CH_2Br$ and heating the solution at reflux for 30 min. Bubbling CO through the warm solution and addition of ether precipitates the rhodium as $RhCOCl(PPh_3)_2$, with greater than 90% recovery of the metal. The ketimine, which remains in solution, can be hydrolyzed over wet silica gel, and thin-layer chromatography gives acetophenone and desoxybenzoin, respectively, in 70–80% yield. No ketone formation occurs if the dimethylcadmium reduction step is omitted.

Of the two products (diketone or monoketone), which could arise from II and benzoyl chloride, only one is formed. Although oxidative addition apparently forms the bisacyl IV, the two acyl carbons do not couple to give (after hydrolysis) any 1,2 diketone. Instead decarbonylation intervenes, followed by reductive elimination to give benzophenone (72% yield after hydrolysis and chromatography).[5] In this case, the rhodium can be recovered as $RhCOCl(PPh_3)_2$ without adding additional CO. Reaction of II with secondary bromides or branched acid chlorides gives no branched ketones. Instead, the intermediate *sec*-alkylrhodium(III) iminoacyl compounds undergo β elimination rather than coupling. This is consistent with the observation that I catalyzes olefin isomerization in internal olefins but gives no branched ketone products.

Several other rhodium-based procedures for ketone synthesis are presently in the literature.[8] Each may be useful for preparing small amounts of valuable ketones under mild conditions. The most useful feature of this work is, however, the illustration of how changes in a metal's oxidation state can be used to switch the reactivity of its ligands between two states. In the sense complex I, with the iminoacyl group bound to rhodium in the metal's higher oxidation state, reacts with olefins to give ketones, the masked acyl has the reactivity of an acyl cation.[9] With the iminoacyl bound to rhodium in a lower oxidation state, the reactivity pattern is that of an acyl anion.[10] Thus the same functional group can exhibit opposite reactivities, controlled by the charge density of the metal to which it is bound.

Registry No. I, 80399-45-7; II, 80409-35-4; $(CH_3)_2Cd$, 506-82-1; CH_3I, 71-88-4; $C_6H_5CH_2Br$, 100-39-0; $RhCOCl(PPh_3)_2$, 13938-94-8.

(2) Dimethylcadmium was chosen since it is a mild alkylating agent and will not attack the carbon–nitrogen double bond in I. Even under the above conditions, however, small amounts of methyl ketones are formed by the reaction of II with dimethylcadmium.

(3) Purification of II was apparently hampered by the presence of $CdCl_2$.

(4) Pregosin, P. S.; Kunz, R. W. *NMR: Basic Princ. Prog.* **1979**, *16*.

(5) In the hydroacylation procedure of Schwartz and Cannon,[6] an intermediate acylmetal alkyl couples to give a ketone rather than first decarbonylating. Our result may reflect the reluctance of acyl groups to couple[7] as well as perhaps a barrier to reductive elimination due to one of the carbons being constrained by chelation.

(6) Schwartz, J.; Cannon, J. B. *J. Am. Chem. Soc.* **1974**, *96*, 4721.

(7) Casey, C. P.; Bunnell, C. A. *J. Am. Chem. Soc.* **1976**, *98*, 436.

(8) (a) Larock, R. C.; Oertle, K.; Potter, G. F. *J. Am. Chem. Soc.* **1980**, *102*, 190. (b) Hegedus, L. S.; Kendall, P. M.; Lo, S. M.; Sheats, J. R. *Ibid.* **1975**, *97*, 5448. (c) Reference 6.

(9) The mechanism of insertion involves addition of a rhodium hydride to a double bond, followed by carbon–carbon coupling. Since two anionic groups are on the metal, it must be in at least the +2 state.

(10) Acylcarbonylferrates provide an interesting example of a species which reacts with both electrophiles (alkyl halides)[11] and nucleophiles (olefins)[12] without a change in metal oxidation state.

(11) Collman, J. P. *Acc. Chem. Res.* **1975**, *8*, 342.

(12) McMurry, J. E.; Andrus, A. *Tetrahedron Lett.* **1980**, *21*, 4687.

Chelate and Open Structures in Complexes of Bis(stannyl)methanes with Dimethyl Sulfoxide

Jeffrey R. Hyde, Thomas J. Karol, John P. Hutchinson, Henry G. Kuivila,* and Jon Zubieta*

Department of Chemistry
State University of New York at Albany
Albany, New York 12222

Received August 28, 1981

Summary: Structures are given for the complexes bis(dichloromethylstannyl)methane–bis(dimethyl sulfoxide), (chlorodimethylstannyl)(dichloromethylstannyl)methane–dimethyl sulfoxide, and bis(trichlorostannyl)methane–tetrakis(dimethyl sulfoxide).

Organic derivatives of tin(IV) bearing at least one electronegative group have long been known to form complexes with a wide variety of ligands.[1-3] Among the halomethyltins the number of ligands depends upon the number of halogen atoms on the tin atom. For example, trimethylchlorostannane forms a complex with one molecule of dimethyl sulfoxide (Me_2SO),[4] while dimethyldichlorostannane[5] and methyltrichlorostannane[6] form complexes with two molecules of Me_2SO. No studies appear to have been made with compounds containing more than one Lewis acid tin center in the molecule. In such species the possibility for chelation by the acceptor molecule, by analogy with the abundant examples of chelation by donor molecules, exists. We are examining systems in which this phenomenon might be observed and report here on the first examples of chelation by organotin acceptors, bis(chloromethylstannyl)methanes, with Me_2SO.

Bis(dichloromethylstannyl)methane, **1**, (chlorodimethylstannyl)(dichloromethylstannyl)methane, **2**, and bis(trichlorostannyl)methane, **3**, each reacted with excess dimethyl sulfoxide (Me_2SO) to form crystalline solids which were characterized by NMR spectroscopy and elemental analysis.[7] Their compositions were as follows: $1(Me_2SO)_2$, $2(Me_2SO)$, and $3(Me_2SO)_4$. Thus the ratios Sn/Me_2SO are 1, 0.5, and 2, respectively, reflecting substantial differences in coordinative behavior.

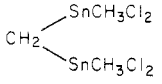

1

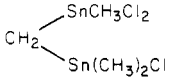

2

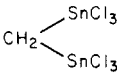

3

The structures of the complexes were shown by X-ray diffraction to be **4**, **5**, and **6**. As illustrated in the structures, they consist of discrete molecules. In **4** each tin atom is found in a pseudooctahedral environment (supplementary material), face sharing through the bridging methylene carbon and the oxygens of the Me_2SO groups with the adjacent Sn polyhedron. A crystallographic mirror plane passes through Sn1, Sn2, the bridging methylene carbon

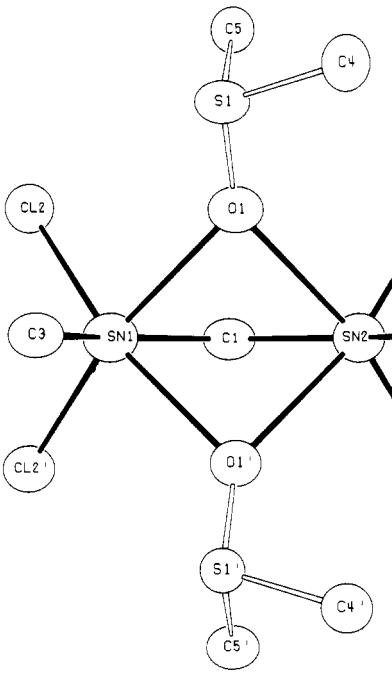

4

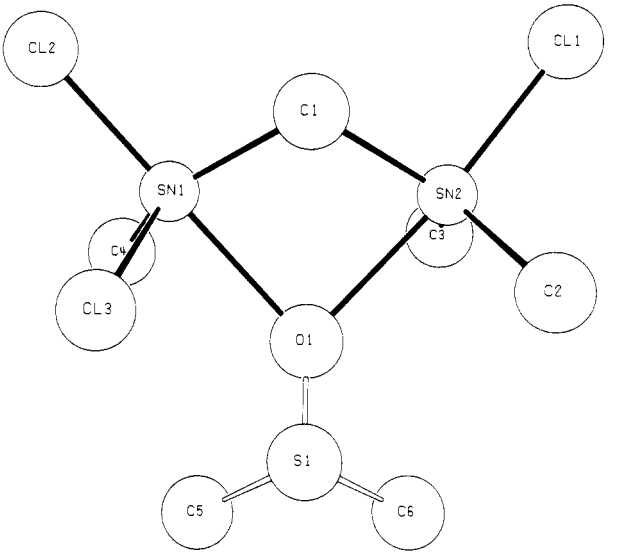

5

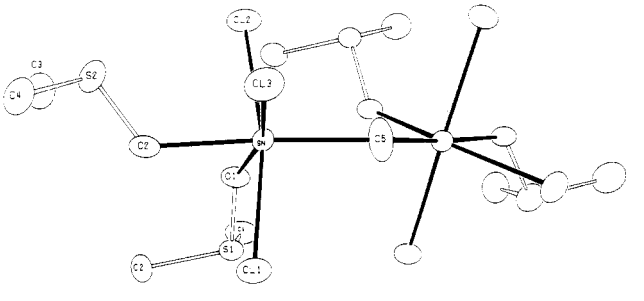

6

(1) H. C. Clark and R. J. Puddephatt in "Organometallic Compounds of Group IV Elements", Vol. 2, Part II, A. G. McDiarmid, Ed., Marcel Dekker, New York, 1972.

(2) J. A. Zubieta and J. J. Zuckerman in "progress in Inorganic Chemistry", Vol. 24, S. J. Lippard, Ed., Wiley, New York.

(3) V. S. Petrosyan, N. S. Yashina, and O. A. Reutov, *Adv. Organomet. Chem.* **14** (1976).

(4) Y. Kawasaki, M. Hori, and K. Uenaka, *Bull. Chem. Soc. Jpn.*, **40**, 2463 (1967).

(5) H. D. Langer, and A. H. Blut, *J. Organomet. Chem.*, **5**, 288 (1966).

(6) V. S. Petrosyan, N. S. Yashina, and O. A. Reutov, *J. Organomet. Chem.*, *52*, 315 (1973).

(7) Experimental details on the preparation and properties of the complexes and their precursors will be described in another manuscript. In general the complexes were prepared by addition of excess Me_2SO to a solution of chlorostannane in carbon tetrachloride. Melting points were as follows: **4**, 150–153 °C; **5**, 107–108 °C; **6**, 169–172 °C.

0276-7333/82/2301-0404$01.25/0

C1, and the terminal methyl carbons C2 and C3.

The geometry about the tin atoms in structure **5**, on the other hand, is distorted trigonal bipyramidal, with edge sharing between tin polyhedra provided by the bridging methylene carbon and Me_2SO oxygen atoms. The bridging methylene group occupies an equatorial position in both the Sn1 and Sn2 polyhedra while O1 is found in an apical position in both cases. The tin environments are nonequivalent: Sn1 bound to a methyl carbon, C4, and C13 in the equatorial plane, in addition to the bridging C1, while the trigonal plane about Sn2 is defined by C1 and two methyl carbons C2 and C3. As anticipated, the Sn1–C13 distance of 2.372 (4) Å is significantly shorter than the Sn1–C12 and Sn2–C11 distances, 2.434 (4) Å average, reflecting the equatorial and axial occupancies, respectively.

The crystallographically identical tin atoms in **6** enjoy pseudooctahedral geometry, with a single bridging group, the methylene carbon C5, connecting the vertex-sharing polyhedra. A noteworthy feature of the structure is the short terminal Sn–O(Me_2SO) bond length of 2.118 (6) Å (average) in contrast to bridging Sn–O(Me_2SO) distances of 2.588 (6) and 2.572 (8) Å in **4** and **5**, respectively.

In comparing the structures, the tin–tin distances increase from 3.426 (1) Å in the triply-bridged structure **4** to 3.529 (1) Å in the doubly bridged **5** to 3.760 (1) Å in the singly bridged case **6**, a trend reflected in the Sn–methylene carbon–Sn valence angle which opens from 108.5 (4)° in **4** to an exceptionally large value of 130.8 (6)° in **6**.

These results show that the composition and structure of the most readily formed complexes are strongly dependent on the number of chlorines on the tin atoms. Presumably the high Lewis acidity of the trichlorostannyl groups of **3** leads to pseudooctahedral coordination in **6**. But this occurs at the expense of expanding the Sn–C–Sn bond angle to the remarkably large value of 130.8°. In **4** a more distorted octahedral configuration is achieved by two bridging oxygens of Me_2SO molecules. But **5** finds both tins pentacoordinate. Further studies should reveal structure/composition patterns and may lead to some understanding of the driving forces involved.

Crystal Data. $Sn_2(CH_2)(CH_3)_2Cl_4(Me_2SO)_2$, **4**, crystallizes in the orthorhombic space group *Pbnm* with a = 9.821 (2) Å, b = 12.411 (2) Å, c = 15.540 (3) Å, V = 1894.2 Å^3, D_{calcd} = 2.03 g cm^{-3}, Z = 4, and μ = 34.2 cm^{-1} (Mo Kα, λ = 0.710 73 Å).[8] A total of 1498 independent reflections were measured on a Nicolet R3/m diffractometer and 1109 reflections with $F_o \geq 6\sigma(F_o)$ were used in the subsequent solution and least-squares refinement, which have produced current discrepancy factors of 0.048 and 0.047 for R and R_w, respectively.

$Sn_2(CH_2)(CH_3)_3Cl_3(Me_2SO)$, **5**, crystallizes in the triclinic space group $P\bar{1}$ with a = 7.551 (2) Å, b = 7.945 (2) Å, c = 13.354 (3) Å, α = 80.63 (2)°, β = 89.13 (3)°, γ = 72.96 (2)°, and V = 755.3 Å^3 to give D_{calcd} = 2.11 g cm^{-3} for Z = 2 (μ = 39.6 cm^{-1}, Mo Kα). A total of 1932 reflections were collected as above of which 1609 with $F_o \geq 6\sigma(F_o)$ were used in the structure solution and refinement. The current discrepancy factors are R = 0.045 and R_w = 0.055.

$Sn_2(CH_2)Cl_6(Me_2SO)_4$, **6**, crystallizes in the monoclinic space group $C2/c$ with a = 20.998 (5) Å, b = 7.925 (3) Å, c = 16.535 (4) Å, β = 98.79 (3)°, and V = 2719.3 Å^3 with D_{calcd} = 1.90 g cm^{-3} for Z = 4 (μ = 27.5 cm^{-1}, Mo Kα). The structure solution and least-squares refinement are based on 1277 reflections with $F_o \geq 6\sigma(F_o)$, collected on the Nicolet R3/m diffractometer. The current residuals are 0.034 and 0.038 for R and R_w, respectively.

All data was collected on a Nicolet R3/m automated four-circle diffractometer, in the range $0° \geq 2\theta \geq 50°$, and processed on a Nova 3 computer, using local versions of the SHELXTL crystallographic computing package. Lorentz and polarization corrections and absorption corrections were carried out in the usual fashion. Details of the usual procedures may be found in ref 9 and 10.

Acknowledgment. Support of this work has been provided by the National Science Foundation (Grant CHE 750075402) and by the National Institutes of Health (partially by Grant GM22566 and funding for the diffraction from Grant GM27459). Acknowledgement is also made to the donors of the Petroleum Research Fund, administered by the American Chemical Society, for partial support of this work.

Registry No. **1**, 79992-66-8; **2**, 79992-67-9; **3**, 79992-68-0; **4**, 79992-48-6; **5**, 79992-49-7; **6**, 79992-50-0.

Supplementary Material Available: Tables of bond distances, angles, final fractional coordinates, thermal parameters, and observed and calculated structure factors are available (28 pages). Ordering information is given on any current masthead page.

(8) The alternative space group $Pbn2_1$ was discarded on the basis of the Hamilton significance test.

(9) G. M. Shedrick, "Nicolet SHELXTL Operations Manual", Nicolet XRD Corp., Cupertino, CA, 1979.

(10) M. W. Bishop, J. Chatt, J. R. Dilworth, P. Dahlstrom, J. Hyde, and J. Zubieta, *J. Organomet. Chem.*, **213**, 109 (1981).

A New Organometallic Photoreaction: Interconversion of Metal–Alkylidene Geometric Isomers

Fred B. McCormick, William A. Kiel, and J. A. Gladysz*[1]

Department of Chemistry, University of California Los Angeles, California 90024

Received October 21, 1981

Summary: Benzylidene complex $[(\eta\text{-}C_5H_5)Re(NO)(PPh_3)(=CHC_6H_5)]^+PF_6^-$ (**1**), which exists as a >99:1 mixture of anticlinal (**1t**, "thermodynamic") and synclinal (**1k**, "kinetic") Re=C bond geometric isomers at room temperature, is isomerized when irradiated between −20 and −78 °C in CD_2Cl_2, CD_3CN, or $(CD_3)_2CO$ to a (55 ± 3):(45 ± 3) **1t/1k** photostationary state. Propylidene $[(\eta\text{-}C_5H_5)Re(NO)(PPh_3)(=CHCH_2CH_3)]^+PF_6^-$ (**2**), which exists as a (95±1):(5±1) mixture of anticlinal (**2t**) and synclinal (**2k**) isomers at room temperature, is similarly isomerized to a (59 ± 2):(41 ± 2) photostationary state. Absorption spectra of **1t** and **2t** and unsuccessful attempts to photosensitize **1t** → **1k** (azulene, rose bengal, eosin Y) are reported. Thermal isomerization rates for **1k** → **1t**, measured between 4 °C ($t_{1/2}$ = 443 min) and 29.5 °C ($t_{1/2}$ = 17 min), yield $\Delta H^\ddagger$ = 20.9 ± 0.4 kcal/mol and $\Delta S^\ddagger$ = −3.8 ± 0.2 eu. The benzylidene complex $[(\eta\text{-}C_5H_5)Fe(CO)(PPh_3)(=CHC_6H_5)]^+CF_3CO_2^-$ (**3**) decomposes upon low-temperature irradiation.

We recently reported the synthesis of a series of rhenium–alkylidene complexes $[(\eta\text{-}C_5H_5)Re(NO)(PPh_3)(=$

(1) Fellow of the Alfred P. Sloan Foundation (1980–1982) and Camille and Henry Dreyfus Teacher-Scholar Grant Recipient (1980–1985); after 6/30/82, address correspondence to this author at the Department of Chemistry, University of Utah, Salt Lake City, UT 84112.

0276-7333/82/2301-0405$01.25/0

C1, and the terminal methyl carbons C2 and C3.

The geometry about the tin atoms in structure **5**, on the other hand, is distorted trigonal bipyramidal, with edge sharing between tin polyhedra provided by the bridging methylene carbon and Me_2SO oxygen atoms. The bridging methylene group occupies an equatorial position in both the Sn1 and Sn2 polyhedra while O1 is found in an apical position in both cases. The tin environments are nonequivalent: Sn1 bound to a methyl carbon, C4, and C13 in the equatorial plane, in addition to the bridging C1, while the trigonal plane about Sn2 is defined by C1 and two methyl carbons C2 and C3. As anticipated, the Sn1–C13 distance of 2.372 (4) Å is significantly shorter than the Sn1–C12 and Sn2–C11 distances, 2.434 (4) Å average, reflecting the equatorial and axial occupancies, respectively.

The crystallographically identical tin atoms in **6** enjoy pseudooctahedral geometry, with a single bridging group, the methylene carbon C5, connecting the vertex-sharing polyhedra. A noteworthy feature of the structure is the short terminal Sn–O(Me_2SO) bond length of 2.118 (6) Å (average) in contrast to bridging Sn–O(Me_2SO) distances of 2.588 (6) and 2.572 (8) Å in **4** and **5**, respectively.

In comparing the structures, the tin–tin distances increase from 3.426 (1) Å in the triply-bridged structure **4** to 3.529 (1) Å in the doubly bridged **5** to 3.760 (1) Å in the singly bridged case **6**, a trend reflected in the Sn–methylene carbon–Sn valence angle which opens from 108.5 (4)° in **4** to an exceptionally large value of 130.8 (6)° in **6**.

These results show that the composition and structure of the most readily formed complexes are strongly dependent on the number of chlorines on the tin atoms. Presumably the high Lewis acidity of the trichlorostannyl groups of **3** leads to pseudooctahedral coordination in **6**. But this occurs at the expense of expanding the Sn–C–Sn bond angle to the remarkably large value of 130.8°. In **4** a more distorted octahedral configuration is achieved by two bridging oxygens of Me_2SO molecules. But **5** finds both tins pentacoordinate. Further studies should reveal structure/composition patterns and may lead to some understanding of the driving forces involved.

Crystal Data. $Sn_2(CH_2)(CH_3)_2Cl_4(Me_2SO)_2$, **4**, crystallizes in the orthorhombic space group *Pbnm* with a = 9.821 (2) Å, b = 12.411 (2) Å, c = 15.540 (3) Å, V = 1894.2 Å^3, D_{calcd} = 2.03 g cm^{-3}, Z = 4, and μ = 34.2 cm^{-1} (Mo Kα, λ = 0.710 73 Å).[8] A total of 1498 independent reflections were measured on a Nicolet R3/m diffractometer and 1109 reflections with $F_o \geq 6\sigma(F_o)$ were used in the subsequent solution and least-squares refinement, which have produced current discrepancy factors of 0.048 and 0.047 for R and R_w, respectively.

$Sn_2(CH_2)(CH_3)_3Cl_3(Me_2SO)$, **5**, crystallizes in the triclinic space group $P\bar{1}$ with a = 7.551 (2) Å, b = 7.945 (2) Å, c = 13.354 (3) Å, α = 80.63 (2)°, β = 89.13 (3)°, γ = 72.96 (2)°, and V = 755.3 Å^3 to give D_{calcd} = 2.11 g cm^{-3} for Z = 2 (μ = 39.6 cm^{-1}, Mo Kα). A total of 1932 reflections were collected as above of which 1609 with $F_o \geq 6\sigma(F_o)$ were used in the structure solution and refinement. The current discrepancy factors are R = 0.045 and R_w = 0.055.

$Sn_2(CH_2)Cl_6(Me_2SO)_4$, **6**, crystallizes in the monoclinic space group $C2/c$ with a = 20.998 (5) Å, b = 7.925 (3) Å, c = 16.535 (4) Å, β = 98.79 (3)°, and V = 2719.3 Å^3 with D_{calcd} = 1.90 g cm^{-3} for Z = 4 (μ = 27.5 cm^{-1}, Mo Kα). The structure solution and least-squares refinement are based on 1277 reflections with $F_o \geq 6\sigma(F_o)$, collected on the Nicolet R3/m diffractometer. The current residuals are 0.034 and 0.038 for R and R_w, respectively.

All data was collected on a Nicolet R3/m automated four-circle diffractometer, in the range $0° \geq 2\theta \geq 50°$, and processed on a Nova 3 computer, using local versions of the SHELXTL crystallographic computing package. Lorentz and polarization corrections and absorption corrections were carried out in the usual fashion. Details of the usual procedures may be found in ref 9 and 10.

Acknowledgment. Support of this work has been provided by the National Science Foundation (Grant CHE 750075402) and by the National Institutes of Health (partially by Grant GM22566 and funding for the diffraction from Grant GM27459). Acknowledgement is also made to the donors of the Petroleum Research Fund, administered by the American Chemical Society, for partial support of this work.

Registry No. **1**, 79992-66-8; **2**, 79992-67-9; **3**, 79992-68-0; **4**, 79992-48-6; **5**, 79992-49-7; **6**, 79992-50-0.

Supplementary Material Available: Tables of bond distances, angles, final fractional coordinates, thermal parameters, and observed and calculated structure factors are available (28 pages). Ordering information is given on any current masthead page.

(8) The alternative space group $Pbn2_1$ was discarded on the basis of the Hamilton significance test.

(9) G. M. Shedrick, "Nicolet SHELXTL Operations Manual", Nicolet XRD Corp., Cupertino, CA, 1979.

(10) M. W. Bishop, J. Chatt, J. R. Dilworth, P. Dahlstrom, J. Hyde, and J. Zubieta, *J. Organomet. Chem.*, **213**, 109 (1981).

A New Organometallic Photoreaction: Interconversion of Metal–Alkylidene Geometric Isomers

Fred B. McCormick, William A. Kiel, and J. A. Gladysz*[1]

Department of Chemistry, University of California Los Angeles, California 90024

Received October 21, 1981

Summary: Benzylidene complex $[(\eta\text{-}C_5H_5)Re(NO)(PPh_3)(=CHC_6H_5)]^+PF_6^-$ (**1**), which exists as a >99:1 mixture of anticlinal (**1t**, "thermodynamic") and synclinal (**1k**, "kinetic") Re=C bond geometric isomers at room temperature, is isomerized when irradiated between −20 and −78 °C in CD_2Cl_2, CD_3CN, or $(CD_3)_2CO$ to a (55 ± 3):(45 ± 3) **1t/1k** photostationary state. Propylidene $[(\eta\text{-}C_5H_5)Re(NO)(PPh_3)(=CHCH_2CH_3)]^+PF_6^-$ (**2**), which exists as a (95±1):(5±1) mixture of anticlinal (**2t**) and synclinal (**2k**) isomers at room temperature, is similarly isomerized to a (59 ± 2):(41 ± 2) photostationary state. Absorption spectra of **1t** and **2t** and unsuccessful attempts to photosensitize **1t** → **1k** (azulene, rose bengal, eosin Y) are reported. Thermal isomerization rates for **1k** → **1t**, measured between 4 °C ($t_{1/2}$ = 443 min) and 29.5 °C ($t_{1/2}$ = 17 min), yield $\Delta H^\ddagger$ = 20.9 ± 0.4 kcal/mol and $\Delta S^\ddagger$ = −3.8 ± 0.2 eu. The benzylidene complex $[(\eta\text{-}C_5H_5)Fe(CO)(PPh_3)(=CHC_6H_5)]^+CF_3CO_2^-$ (**3**) decomposes upon low-temperature irradiation.

We recently reported the synthesis of a series of rhenium–alkylidene complexes $[(\eta\text{-}C_5H_5)Re(NO)(PPh_3)(=$

(1) Fellow of the Alfred P. Sloan Foundation (1980–1982) and Camille and Henry Dreyfus Teacher-Scholar Grant Recipient (1980–1985); after 6/30/82, address correspondence to this author at the Department of Chemistry, University of Utah, Salt Lake City, UT 84112.

0276-7333/82/2301-0405$01.25/0

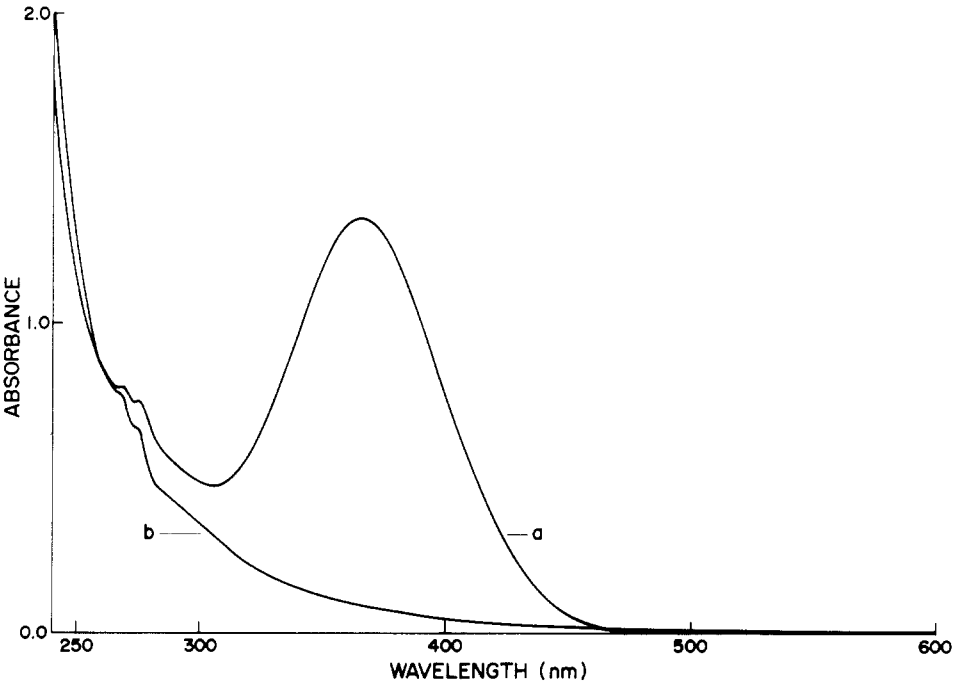

Figure 1. Absorption spectra of **1t** (trace a) and **2** (trace b) in CH_3CN.

CHR)]$^+PF_6^-$, which are capable of existing in two isomeric forms:[2] a "kinetic" isomer (**k**), which is stereospecifically generated at −78 °C by the reaction of $(\eta\text{-}C_5H_5)Re(NO)(PPh_3)(CH_2R)$ alkyls (R = C_6H_5 or primary alkyl) with $Ph_3C^+PF_6^-$, and a "thermodynamic" isomer (**t**) obtained in 94–100% equilibrium yields upon warming the kinetic isomer to 10–25 °C. X-ray crystallographic[3] and theoretical[4] studies indicate these isomers to have the general structures I(**k**) and II(**t**), respectively (Newman

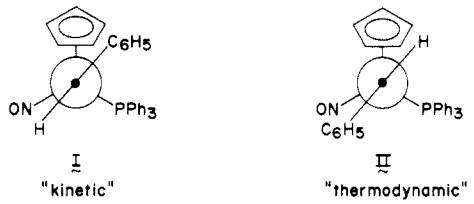

projections down the alkylidene–rhenium bond). Since geometric isomerism arising from metal–carbon multiple bonding is without precedent, we have undertaken additional studies of this phenomenon. In this communication, we report that these isomers can be photochemically interconverted. Photostationary states result, as has previously been observed upon olefin irradiation.[5]

Direct irradiation of CD_2Cl_2, CD_3CN, or $(CD_3)_2CO$ solutions[6] of isolated "thermodynamic" benzylidene [$(\eta\text{-}C_5H_5)Re(NO)(PPh_3)(=CHC_6H_5)]^+PF_6^-$ (**1t**) between −20 °C and −78 °C afforded, after 3 h, clean (55 ± 3):(45 ± 3) mixtures of **1t** and **1k** (eq 1) as determined by NMR in-

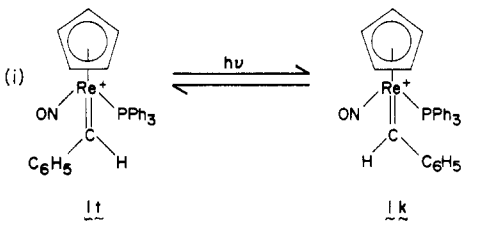

tegration of the C_5H_5 proton resonances. Continued irradiation (up to 9 h) did not alter the **1t**/**1k** ratio. These solutions were allowed to relax back to thermal equilibrium in the dark (**1t**/**1k** > 99:1); a sample to which *p*-di-*tert*-butylbenzene standard had been added indicated >95% of the original **1t** to be present. Additional irradiation cycles could be conducted without noticeable sample deterioration.

Similar experiments were conducted in $(CD_3)_2CO$ with propylidene [$(\eta\text{-}C_5H_5)Re(NO)(PPh_3)(=CHCH_2CH_3)]^+PF_6^-$ (**2**),[6] which exists (depending somewhat upon solvent) as a 96–94:4–6 mixture of **2t**/**2k** at room temperature. Photostationary states (**2t**/**2k**) of (59 ± 2):(41 ± 2) were obtained. Considerable sample darkening accompanied the irradiation of **2**; however, after allowing relaxation back to thermal equilibrium, ^1H NMR integration against *p*-di-*tert*-butylbenzene standard indicated >80% of the original **2** to be present.

Absorption spectra of **1t** and **2** were measured.[7] Benzylidene **1t** (yellow crystals) displayed a λ_{max} (ϵ 13 000) at 365 nm in CH_3CN (Figure 1). Propylidene **2** (cream-colored) showed only a featureless tail into the visible. The absorption spectrum of pure **1k** could not be obtained; low-temperature spectra of $(\eta\text{-}C_5H_5)Re(NO)(PPh_3)(CH_2C_6H_5)/Ph_3C^+PF_6^-$ reaction mixtures were complicated by starting material and byproduct (e.g., Ph_3CH) absorbances. However, a series of spectra (Figure 2) were recorded as a CH_2Cl_2 **1k**/**1t** photostationary state solution was warmed from −78 °C to room temperature. An isos-

(2) Kiel, W. A.; Lin, G.-Y.; Gladysz, J. A. *J. Am. Chem. Soc.* **1980**, *102*, 3299.
(3) Kiel, W. A. UCLA, unpublished results.
(4) Eisenstein, O.; Hoffmann, R. Cornell University, unpublished results.
(5) (a) Saltiel, J.; D'Agostino, J.; Megarity, E. D.; Metts, L.; Neuberger, K. R.; Wrighton, M.; Zafiriou, O. C. In "Organic Photochemistry"; Chapman, O. L., Ed.; Marcel Dekker: New York, 1973; Vol. 3, pp 1–113. (b) Saltiel, J.; Charlton, J. L. In "Rearrangements in Ground and Excited States"; de Mayo, P., Ed.; Academic Press: New York, 1973; Vol. 3, p 25.
(6) All irradiations were conducted through Pyrex with a Hanovia 450-W lamp. Samples were contained in septum-capped 5-mm NMR tubes; those which were rigorously degassed gave results identical with those which were undegassed.
(7) (a) Spectra were obtained on a Cary 219 spectrophotometer. (b) Benzylidene **1t** does not luminesce (single crystal, 10 K). We thank Professor J. I. Zink for conducting this experiment and informing us of the results.

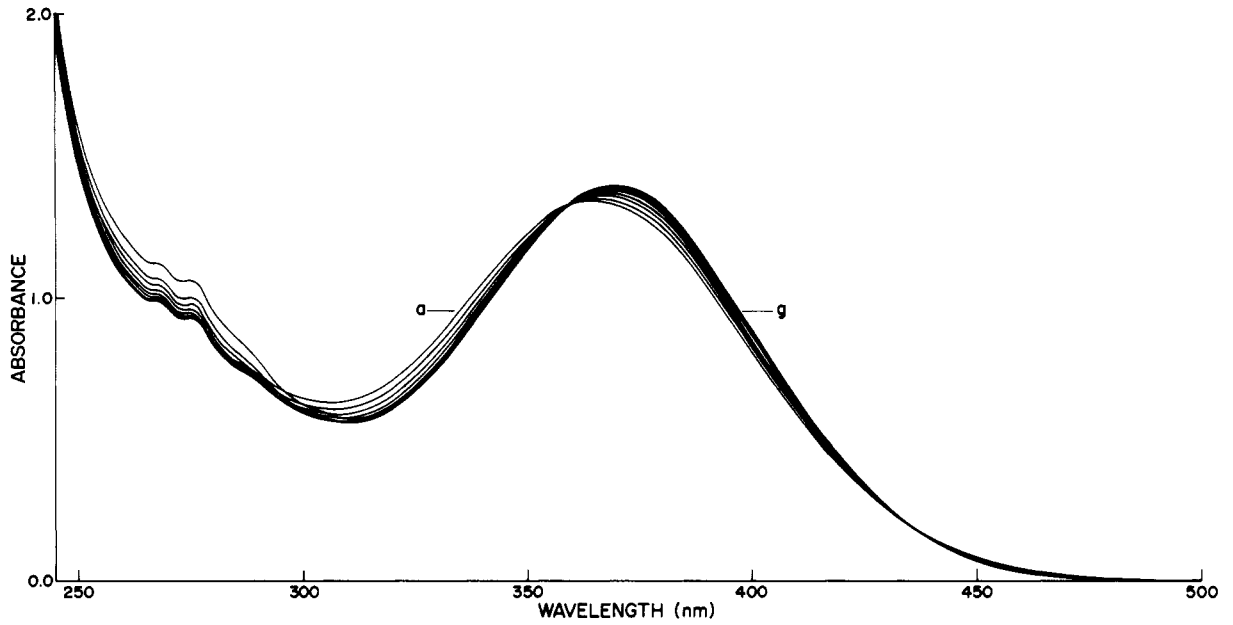

Figure 2. Absorption spectra recorded as a (55 ± 3):(45 ± 3) **1t**/**1k** mixture in CH_2Cl_2 (prepared by photolysis at −78 °C) was warmed to room temperature: initial spectrum, trace a; final spectrum, trace g.

Table I. Rate Constants for the Re=C Bond Rotation **1k** → **1t** in CD_2Cl_2[a]

entry	temp, ±0.1 °C	$10^5 k_{obsd}$, s^{-1}
1	29.5	69.2 ± 0.6
2	24.0	37.6 ± 0.6
3	19.0	20.5 ± 0.2
4	19.0	19.2 ± 0.2
5[b]	19.0	20.9 ± 0.3
6	14.0	11.5 ± 0.2
7	10.0	4.81 ± 0.10
8	10.0	6.93 ± 0.10
9	4.0	2.61 ± 0.03

[a] $[\mathbf{1k}]_0$ = 0.038 − 0.042 M; generated in situ from $(\eta\text{-}C_5H_5)Re(NO)(PPh_3)(CH_2C_6H_5)$ and $Ph_3C^+PF_6^-$ at the temperature of measurement unless noted. Entries 1-5 were followed through $>2t_{1/2}$, others were followed through at least one $t_{1/2}$. [b] **1k** photochemically generated at −78 °C.

bestic point is evident as **1k** isomerizes to **1t**, and it can be concluded that λ_{max} for **1k** is at shorter wavelength than that for **1t**.[8]

Since photoisomerization of **1t** offered the only means of generating **1k** without significant quantities of byproducts, the first-order rate constant for equlibration back to **1t** (in CD_2Cl_2) was measured by ^1H NMR at 19 °C (entry 5, Table I). The k_{obsd} determined was in good agreement with the k_{obsd} obtained (19 °C) from **1k** prepared in situ from $(\eta\text{-}C_5H_5)Re(NO)(PPh_3)(CH_2C_6H_5)$ and $Ph_3C^+PF_6^-$ (entries 3 and 4, Table I). Hence, data obtained by the latter route can reliably be used to calculate activation parameters for rotation about rhenium–alkylidene bonds. Rate constants for **1k** → **1t** were measured from 4 °C ($t_{1/2}$ = 443 min) to 29.5 °C ($t_{1/2}$ = 17 min), as summarized in Table I; these yielded $\Delta H^\ddagger$ = 20.9 ± 0.4 kcal/mol and $\Delta S^\ddagger$ = −3.8 ± 0.2 eu.

The possibility that geometric isomerization of L_nM=C(X)Y complexes might be a general photoreaction was considered. However, isomerization would be degenerate for substrates in which the =CXY plane is bisected by a L_nM fragment mirror plane such as octahedral group 6B carbonyls $(CO)_5M$=C(X)Y (for which some photochemical studies have been reported).[9] A second consideration is that there must be a sufficient activation energy barrier to prevent rapid thermal isomerization of the less stable geometric isomer to the more stable one. However, these barriers are generally much lower than that measured for **1k** → **1t**. For instance, $\Delta G^\ddagger$ for methylidene rotation in $[(\eta\text{-}C_5H_5)Fe[P(C_6H_5)_2CH_2CH_2P(C_6H_5)_2](=CH_2)]^+CF_3SO_3^-$ is only 10.4 ± 0.1 kcal/mol over the temperature range of −65 to −14 °C;[10] furthermore, this $\Delta G^\ddagger$ is likely higher than normal because of the strong donor ligands (and absence of good π-accepting ligands) on the iron. Nonetheless, we attempted a similar photolysis with the Brookhart benzylidene complex $[(\eta\text{-}C_5H_5)Fe(CO)(PPh_3)(=CHC_6H_5)]^+CF_3CO_2^-$ (**3**).[11] Irradiation of **3** generated from $(\eta\text{-}C_5H_5)Fe(CO)(PPh_3)[CH(OCH_3)C_6H_5]$ and 3.5 equiv of CF_3CO_2H in degassed CD_2Cl_2 at −78 °C resulted (over the course of 30 min) in complete disappearance of the benzylidene ^1H NMR resonance (δ 17.30). The color of the sample turned from deep red to green-brown, and no new low-field ^1H NMR resonances appeared. Thus **3** is not stable to conditions which photoisomerize **1t** and **2**.

In summary, this study has shown that alkylidene complexes can exhibit a heretofore totally unexpected mode of photoreactivity. The closest analogy of which we are aware is the photoequilibration of endo/exo iron and ruthenium π-allyl isomers.[12] Two speculative extensions of our observations merit note. First, photoinitiation of transition metal mediated catalysis is well documented.[13] However, since metal alkylidenes are propagating inter-

(8) Studies are in progress to determine the nature of the photoreactive state for the conversion **1t** → **1k**. The following attempts at triplet sensitization ($(CD_3)_2CO$ solutions, −78 °C) have been unsuccessful: azulene, 1.2 equiv, 574-nm Corning 2-73 filter; rose bengal, 1.0 equiv, 514-nm Corning 3-69 filter; eosin Y, 1.0 equiv, 514-nm Corning 3-69 filter.

(9) (a) Fischer, E. O.; Fischer, H. *Chem. Ber.* **1974**, *107*, 657. (b) Dahlgren, R. M.; Zink, J. I. *Inorg. Chem.*, **1977**, *16*, 3154; (c) Lappert, M. F.; Pye, P. L.; McLaughlin, G. M. *J. Chem. Soc., Dalton Trans.* **1977**, 1272.
(10) Brookhart, M.; Tucker, J. R.; Flood, T. C.; Jensen, J. *J. Am. Chem. Soc.* **1980**, *102*, 1203.
(11) Brookhart, M.; Nelson, G. O. *J. Am. Chem. Soc.* **1977**, *99*, 6099.
(12) (a) Fish, R. W.; Giering, W. P.; Marten, D.; Rosenblum, M. *J. Organomet. Chem.* **1976**, *105*, 101. (b) Gibson, D. H.; Hsu, W.-L.; Steinmetz, A. L.; Johnson, B. V. *Ibid.* **1981**, *208*, 89.
(13) (a) Wrighton, M. S.; Ginley, D. S.; Schroeder, M. A.; Morse, D. L. *Pure Appl. Chem.* **1975**, *41*, 671. (b) Geoffroy, G. L.; Wrighton, M. S. "Organometallic Photochemistry"; Academic Press: New York, 1979.

mediates in olefin metathesis[14] (and possibly in some olefin polymerizations),[15] a new type of photochemical effect upon metal-catalyzed reactions may be possible: both olefin metathesis and polymerization can exhibit high stereoselectivity, which conceivably could be altered if the alkylidene intermediates were photoisomerized to new geometric isomers. Second, it is possible that the excited states of 1 and 2 might, like their ground-state counterparts, exist in two isomeric forms. These and related photochemical and photophysical questions are presently under investigation.

Acknowledgment. We are grateful to the Department of Energy and the donors of the Petroleum Research Fund, administered by the American Chemical Society, for support of this research. We thank Professors J. I. Zink and M. A. El-Sayed for helpful discussions and the Regents of the University of California for a fellowship (W.A.K.).

Registry No. 1k, 74540-78-6; **1t**, 74561-64-1; **2k**, 74540-85-5; **2t**, 74561-68-5; **3**, 80387-86-6.

(14) Calderon, N.; Lawrence, J. P.; Ofstead, E. A. *Adv. Organomet. Chem.* **1979**, *17*, 449 and reviews cited therein.
(15) Ivin, K. J.; Rooney, J. J.; Stewart, C. D.; Green, M. L. H.; Mahtab, R. *J. Chem. Soc., Chem. Commun.* **1978**, 604.

Coordinatively Unsaturated Clusters of Rhodium Incorporating Chelating Bidentate Ligands. Synthesis of $[\{(CH_3O)_2PCH_2CH_2P(OCH_3)_2\}RhH]_4$ and $[\{(\mathit{i}\text{-}C_3H_7O)_2PCH_2CH_2P(O\text{-}\mathit{i}\text{-}C_3H_7)_2\}RhH]_2$

Michael D. Fryzuk

Department of Chemistry, University of British Columbia Vancouver, British Columbia, Canada V6T 1Y6

Received September 23, 1981

Summary: The reaction of (1,2-bis(dimethoxyphosphino)ethane)(2-methylallyl)rhodium(I), $[\eta^3\text{-}(2\text{-}MeC_3H_4)Rh(dmope)]$, **1**, and (1,2-bis(diisopropoxyphosphino)ethane)(2-methylallyl)rhodium(I), $[\eta^3\text{-}(2\text{-}MeC_3H_4)Rh(dipope)]$, **3**, with hydrogen produces, respectively, $[(dmope)RhH]_4$, **2**, and $[(dipope)RhH]_2$, **4**. The hydride resonance of **2** is an overlapping quintet of nonets, while for **4**, a broad, overlapping triplet of quintets is observed. The solution structures of these new rhodium hydride clusters are discussed in terms of the rhodium– and phosphorus–hydride coupling constants which suggest that **2** may have a tetrahedral array of rhodium atoms with face-bridging hydrides.

Our interest in the effect of chelating ligands[1] on the reactivity of metal complexes has recently turned to didentate phosphine and phosphinite derivatives of rhodium(I).[2,3] Specifically we have undertaken a study of the use of (2-methylallyl)rhodium(I) complexes incorporating chelating ligands as catalyst precursors[4] for the hydrogenation of unsaturated substrates. Herein we report the synthesis and characterization of two new catalytically active hydridorhodium derivatives that belong to the class of coordinatively unsaturated clusters of the general formula $[P_2RhH]_x$[5].

(1) Fryzuk, M. D.; MacNeil, P. A. *J. Am. Chem. Soc.* **1981**, *103*, 3592.
(2) Fryzuk, M. D., submitted for publication in *Inorg. Chem.*
(3) Fryzuk, M. D. *Inorg. Chim. Acta* **1981**, *54*, L265–266.
(4) The use of allylrhodium(I) complexes of monodentate phosphines and phosphites as hydrogenation catalyst precursors is known.[5]
(5) Sivak, A. J.; Muetterties, E. L. *J. Am. Chem. Soc.* **1979**, *101*, 4878.

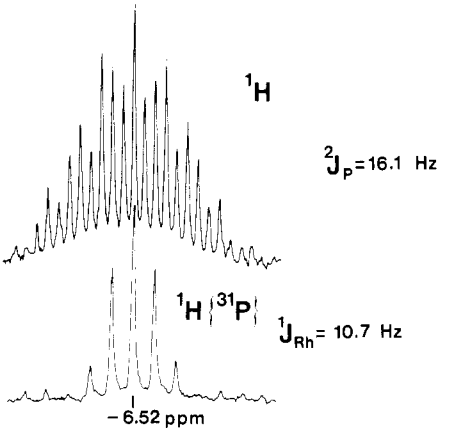

Figure 1. Hydride resonance of $[\{(CH_3O)_2PCH_2CH_2P(OCH_3)_2\}RhH]_4$, **2**; a binomial quintet (lower spectrum) is obtained when phosphorus decoupled.

When bright yellow toluene solutions of the (2-methylallyl)rhodium(I) complex of 1,2-bis(dimethoxyphosphino)ethane, $[\eta^3\text{-}(2\text{-}Me\text{-}C_3H_4)Rh(dmope)]$[2], **1**, are exposed to medium pressures of hydrogen, a slow color change to deep, black-red is observed; from these solutions, dark maroon crystals of the formula $[(dmope)RhH]$[6] can be isolated in 60–70% yield. On the basis of ^1H NMR studies and a solution molecular weight determination[7] we formulate this complex as the tetramer $[(dmope)RhH]_4$, **2**. At room temperature the hydride resonance appears

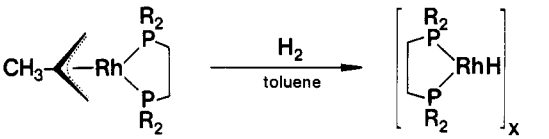

2: R = OCH_3, x = 4
4: R = O-i-C_3H_7, x = 2

as a beautifully symmetric 23-line multiplet which simplifies to a binomial *quintet* when phosphorus is decoupled (Figure 1). This quintet is due to the coupling of *four* magnetically equivalent rhodium nuclei (^{103}Rh, 100% abundance, spin $^1/_2$) with the four equivalent hydrides. Thus the fully coupled spectrum is in fact an overlapping quintet of *nonets* due to the additional coupling of *eight* magnetically equivalent phosphorus nuclei. One must invoke a fluxional process which might involve rapid hydride migration about the cluster on the NMR time scale to explain the apparent symmetry in solution. Indeed, as the temperature is lowered, the 23-line multiplet broadens until finally, at −90 °C, a very broad triplet is observed which collapses to a broad singlet with phosphorus decoupling; in addition, the methoxy protons appear as a doublet at ambient temperatures, but a −90 °C, three doublets (phosphorus coupled) in the ratio 2:1:1 are observed. We are at present unable to account for this temperature-dependent behavior but note that freezing out the conformational flipping of the chelate ring may be

(6) **2**: mp 183 °C dec; ^1H NMR (C_6D_6) $P(OCH_3)$, 3.83 ppm (d, 48, J_P = 11.7 Hz); PCH_2, 1.51 ppm (br d, 16, J_P = 21.0 Hz); RhH, −6.52 ppm (q of nonets, 4, J_{Rh} = 10.7 Hz, J_P = 16.1 Hz). Anal. Calcd for $C_6H_{17}O_4P_2Rh$: C, 22.66; H, 5.39. Found: C, 22.25; H, 5.27.
(7) The molecular weights of both **2** and **4** were determined via isothermal distillation using the Signer method.[8] Accurately made up solutions (C_6D_6) of the cluster and a standard were prepared and maintained at 24.9 °C for 7–10 days in an inverted U-tube assembly under vacuum. Molecular weight found for **2**: 1280 ± 50 (theoretical 1272). Molecular weight found for **4**: 830 ± 30 (theoretical 861). Analysis by ^1H NMR immediately after the determination showed no measurable decomposition.
(8) (a) Signer, R. *Justus Liebigs Ann. Chem.* **1930**, *478*, 246. (b) Clark, E. P. *Ind. Eng. Chem., Anal. Ed.* **1941**, *13*, 820.

0276-7333/82/2301-0408$01.25/0

mediates in olefin metathesis[14] (and possibly in some olefin polymerizations),[15] a new type of photochemical effect upon metal-catalyzed reactions may be possible: both olefin metathesis and polymerization can exhibit high stereoselectivity, which conceivably could be altered if the alkylidene intermediates were photoisomerized to new geometric isomers. Second, it is possible that the excited states of 1 and 2 might, like their ground-state counterparts, exist in two isomeric forms. These and related photochemical and photophysical questions are presently under investigation.

Acknowledgment. We are grateful to the Department of Energy and the donors of the Petroleum Research Fund, administered by the American Chemical Society, for support of this research. We thank Professors J. I. Zink and M. A. El-Sayed for helpful discussions and the Regents of the University of California for a fellowship (W.A.K.).

Registry No. 1k, 74540-78-6; **1t**, 74561-64-1; **2k**, 74540-85-5; **2t**, 74561-68-5; **3**, 80387-86-6.

(14) Calderon, N.; Lawrence, J. P.; Ofstead, E. A. *Adv. Organomet. Chem.* **1979**, *17*, 449 and reviews cited therein.
(15) Ivin, K. J.; Rooney, J. J.; Stewart, C. D.; Green, M. L. H.; Mahtab, R. *J. Chem. Soc., Chem. Commun.* **1978**, 604.

Coordinatively Unsaturated Clusters of Rhodium Incorporating Chelating Bidentate Ligands. Synthesis of $[\{(CH_3O)_2PCH_2CH_2P(OCH_3)_2\}RhH]_4$ and $[\{(\mathit{i}\text{-}C_3H_7O)_2PCH_2CH_2P(O\text{-}\mathit{i}\text{-}C_3H_7)_2\}RhH]_2$

Michael D. Fryzuk

Department of Chemistry, University of British Columbia Vancouver, British Columbia, Canada V6T 1Y6

Received September 23, 1981

Summary: The reaction of (1,2-bis(dimethoxyphosphino)ethane)(2-methylallyl)rhodium(I), $[\eta^3\text{-}(2\text{-}MeC_3H_4)Rh(dmope)]$, **1**, and (1,2-bis(diisopropoxyphosphino)ethane)(2-methylallyl)rhodium(I), $[\eta^3\text{-}(2\text{-}MeC_3H_4)Rh(dipope)]$, **3**, with hydrogen produces, respectively, $[(dmope)RhH]_4$, **2**, and $[(dipope)RhH]_2$, **4**. The hydride resonance of **2** is an overlapping quintet of nonets, while for **4**, a broad, overlapping triplet of quintets is observed. The solution structures of these new rhodium hydride clusters are discussed in terms of the rhodium– and phosphorus–hydride coupling constants which suggest that **2** may have a tetrahedral array of rhodium atoms with face-bridging hydrides.

Our interest in the effect of chelating ligands[1] on the reactivity of metal complexes has recently turned to didentate phosphine and phosphinite derivatives of rhodium(I).[2,3] Specifically we have undertaken a study of the use of (2-methylallyl)rhodium(I) complexes incorporating chelating ligands as catalyst precursors[4] for the hydrogenation of unsaturated substrates. Herein we report the synthesis and characterization of two new catalytically active hydridorhodium derivatives that belong to the class of coordinatively unsaturated clusters of the general formula $[P_2RhH]_x$[5].

(1) Fryzuk, M. D.; MacNeil, P. A. *J. Am. Chem. Soc.* **1981**, *103*, 3592.
(2) Fryzuk, M. D., submitted for publication in *Inorg. Chem.*
(3) Fryzuk, M. D. *Inorg. Chim. Acta* **1981**, *54*, L265–266.
(4) The use of allylrhodium(I) complexes of monodentate phosphines and phosphites as hydrogenation catalyst precursors is known.[5]
(5) Sivak, A. J.; Muetterties, E. L. *J. Am. Chem. Soc.* **1979**, *101*, 4878.

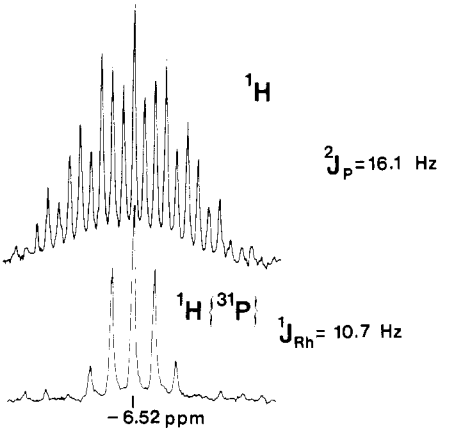

Figure 1. Hydride resonance of $[\{(CH_3O)_2PCH_2CH_2P(OCH_3)_2\}RhH]_4$, **2**; a binomial quintet (lower spectrum) is obtained when phosphorus decoupled.

When bright yellow toluene solutions of the (2-methylallyl)rhodium(I) complex of 1,2-bis(dimethoxyphosphino)ethane, $[\eta^3\text{-}(2\text{-}Me\text{-}C_3H_4)Rh(dmope)]$[2], **1**, are exposed to medium pressures of hydrogen, a slow color change to deep, black-red is observed; from these solutions, dark maroon crystals of the formula $[(dmope)RhH]$[6] can be isolated in 60–70% yield. On the basis of ^1H NMR studies and a solution molecular weight determination[7] we formulate this complex as the tetramer $[(dmope)RhH]_4$, **2**. At room temperature the hydride resonance appears

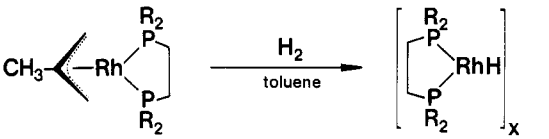

2: R = OCH_3, x = 4
4: R = O-i-C_3H_7, x = 2

as a beautifully symmetric 23-line multiplet which simplifies to a binomial *quintet* when phosphorus is decoupled (Figure 1). This quintet is due to the coupling of *four* magnetically equivalent rhodium nuclei (^{103}Rh, 100% abundance, spin $^1/_2$) with the four equivalent hydrides. Thus the fully coupled spectrum is in fact an overlapping quintet of *nonets* due to the additional coupling of *eight* magnetically equivalent phosphorus nuclei. One must invoke a fluxional process which might involve rapid hydride migration about the cluster on the NMR time scale to explain the apparent symmetry in solution. Indeed, as the temperature is lowered, the 23-line multiplet broadens until finally, at −90 °C, a very broad triplet is observed which collapses to a broad singlet with phosphorus decoupling; in addition, the methoxy protons appear as a doublet at ambient temperatures, but a −90 °C, three doublets (phosphorus coupled) in the ratio 2:1:1 are observed. We are at present unable to account for this temperature-dependent behavior but note that freezing out the conformational flipping of the chelate ring may be

(6) **2**: mp 183 °C dec; ^1H NMR (C_6D_6) $P(OCH_3)$, 3.83 ppm (d, 48, J_P = 11.7 Hz); PCH_2, 1.51 ppm (br d, 16, J_P = 21.0 Hz); RhH, −6.52 ppm (q of nonets, 4, J_{Rh} = 10.7 Hz, J_P = 16.1 Hz). Anal. Calcd for $C_6H_{17}O_4P_2Rh$: C, 22.66; H, 5.39. Found: C, 22.25; H, 5.27.
(7) The molecular weights of both **2** and **4** were determined via isothermal distillation using the Signer method.[8] Accurately made up solutions (C_6D_6) of the cluster and a standard were prepared and maintained at 24.9 °C for 7–10 days in an inverted U-tube assembly under vacuum. Molecular weight found for **2**: 1280 ± 50 (theoretical 1272). Molecular weight found for **4**: 830 ± 30 (theoretical 861). Analysis by ^1H NMR immediately after the determination showed no measurable decomposition.
(8) (a) Signer, R. *Justus Liebigs Ann. Chem.* **1930**, *478*, 246. (b) Clark, E. P. *Ind. Eng. Chem., Anal. Ed.* **1941**, *13*, 820.

0276-7333/82/2301-0408$01.25/0

Table I. A Comparison of the Rhodium Hydride Coupling Constants for the $[P_2RhH]_x$ Family of Clusters

entry	cluster	δ(Rh*H*)	$^1J_{Rh-H}$, Hz	$^2J_{P-H}$, Hz	ref
4	[(dipope)RhH]$_2$	−4.30	34.0	33–35	this work
5	[{(i-$C_3H_7O)_3P$}$_2$RhH]$_2$	−7.11	34.2	36.6	5
6	[{$(CH_3O)_3P$}$_2$RhH]$_3$	−9.56	16.5	25.0	5
2	[(dmope)RhH]$_4$	−6.52	10.7	16.1	this work

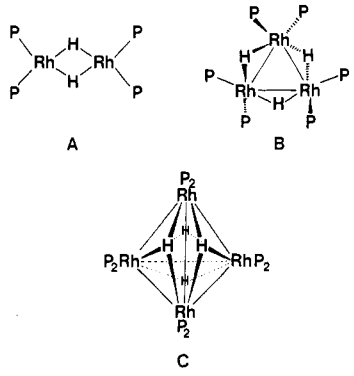

Figure 2. Structures of the $[P_2RhH]_x$ family of clusters: structures A and B have been verified crystallographically whereas structure C is tentative.

adding to the complexity in the low temperature regime.

We have also investigated the reactions of hydrogen with the (2-methylallyl)rhodium(I) complex of 1,2-bis(diisopropoxyphosphino)ethane, [η^3-(2-Me-C_3H_4)Rh(dipope)], **3**; in this case the dimeric[7] derivative [(dipope)RhH]$_2$,[9] **4**, is obtained as bright red crystals. The hydride resonance of **4** appears as a broad, unsymmetrical *septet* which upon phosphorus decoupling simplifies to a binomial *triplet*, indicating coupling with *two* magnetically equivalent rhodium nuclei ($^1J_{Rh}$ = 34.0 Hz). Because of the broadness of the phosphorus-coupled hydride pattern of **4**, we have been unable to extract an accurate phosphorus coupling constant; however, on the basis of previous work[5] with the closely related rhodium hydride dimer utilizing monodentate triisopropyl phosphite ligands, [{(i-$C_3H_7O)_3P$}$_2$RhH]$_2$, **5**, the observed seven-line pattern can be considered as an overlapping triplet of *quintets* which would require a phosphorus coupling constant between 33 and 35 Hz, indicating *four* magnetically equivalent phosphorus nuclei. Interestingly both the rhodium– and phosphorus–hydride coupling constants of **4** are nearly identical with those of **5** (Table I), suggesting that these binuclear complexes are isostructural: all four phosphorus atoms and two rhodium atoms coplanar as in Figure 2, structure A.[10]

The factors that determine the nuclearity of the $[P_2RhH]_x$ clusters are clearly steric in origin. In our case, the choice of the bidentate ligand $(CH_3O)_2PCH_2CH_2P(OCH_3)_2$ allows for the formation of the *tetranuclear* cluster **2**, the largest member of this family of clusters; this contrasts the use of $P(OCH_3)_3$, a monodentate ligand, which generates[5] the *trinuclear* cluster [{$(CH_3O)_3P$}$_2$RhH]$_3$, **6** (structure B, Figure 2). With relatively small substituents such as methoxy groups of the phosphorus donors, the bidentate $(CH_3O)_2PCH_2CH_2P(OCH_3)_2$ ligand exerts a smaller steric influence than two monodentate $P(OCH_3)_3$ ligands; with larger substituents such as isopropoxy, the steric influence of the bidentate ligand must be similar to two monodentate ligands since in both cases binuclear clusters are isolated.

All the members of the $[P_2RhH]_x$ family of clusters are formally electron deficient and therefore coordinatively unsaturated. For example, the tetranuclear complex **2** is a 56-electron cluster,[11] electronically identical with the 56-electron cluster $H_4Re_4(CO)_{12}$, the structure of which is known[12] to be a tetrahedral array of rhenium atoms with face-bridging hydrides. That **2** is similar in structure to $H_4Re_4(CO)_{12}$ can only be speculation in the absence of crystallographic data; however, a comparison of the hydride coupling constants (Table I) of these clusters does provide support for **2** having structure C (Figure 2). Thus one observes a decrease in $^1J_{Rh-H}$ on going from doubly edge bridging hydrides as in **4** and **5** (structure A) to singly edge bridging for **6** (structure B). That a further decrease of $^1J_{Rh-H}$ is observed in **2** may be evidence for face-bridging hydrides and therefore structure C. We are attempting to grow suitable crystals of **2** for crystallographic studies to verify this hypothesis.

Each rhodium center in **2** and **4** is formally in the +1 oxidation state and therefore susceptible to oxidative addition. Indeed, both **2** and **4** readily exchange their hydrides with deuterium at atmospheric pressure in minutes to form the corresponding deuterides. A consequence of this facile oxidative addition of H_2 or D_2 and their inherent coordinative unsaturation is that both **2** and **4** are extremely efficient hydrogenation catalysts for simple olefins. Whether or not the integrity of the cluster is maintained[5] throughout the hydrogenation cycle is under active investigation and will be the subject of future publications.

Acknowledgment. Financial support from the Natural Sciences and Engineering Research Council of Canada, Research Corp., and the President's Emergency Research Fund (UBC) are gratefully acknowledged. We also thank Mr. Peter Borda for the chemical analyses and Dr. S. O. Chan and his staff for help with the NMR experiments. The generous loan of hydrated rhodium trichloride from Johnson-Matthey is also acknowledged.

Registry No. 1, 80105-91-5; 2, 80105-92-6; 3, 80105-93-7; 4, 80126-87-0.

(9) 4: mp 153 °C dec; ^{1}H NMR (C_7D_8) P(OC*H*(CH_3)$_2$), 5.35 ppm (m, 8, J = 6.4 Hz); P(OCH(CH_3)$_2$, 1.35 and 1.45 ppm (d, 48); PCH_2, 1.49 ppm (br m, 8); Rh*H*, −4.3 ppm (br sep, 2, J_{Rh} = 34.05 Hz, J_P = 33–35 Hz); ^{31}P{^{1}H} NMR (C_6D_6, ppm relative to $P(OMe)_3$ at +141.0 ppm) 196.4 (AA′A″A‴XX′, $|^1J_{Rh} + {}^3J_{Rh}|$ = 212.4 Hz). Anal. Calcd for $C_{14}H_{33}O_4P_2Rh$: C, 39.08; H, 7.73. Found: C, 39.01; H, 7.62.

(10) Teller, R. G.; Williams, J. M.; Koetzle, T. F.; Burch, R. R.; Gavin, R. M.; Muetterties, E. L. *Inorg. Chem.* **1981**, *20*, 1806.

(11) A saturated tetranuclear cluster formally contains 60 electrons; see: Johnson, B. F. G.; Benfield, R. E. *Top. Stereochem.* **1981**, *12*, 253.

(12) Wilson, R. D.; Bau, R. *J. Am. Chem. Soc.* **1976**, *98*, 4687.

Synthesis and ^{31}P NMR Characterization of $[W_2(CO)_{10}PPh_2]^-$, $[W_2(CO)_9(PPh_2H)PPh_2]^-$, $[W_2(CO)_8(PPh_2)_2]^{2-}$, and $W_2(CO)_8(PPh_2)_2$

Richard L. Keiter* and Matthew J. Madigan

Chemistry Department, Eastern Illinois University Charleston, Illinois 61920

Received September 14, 1981

Summary: Tetrahydrofuran solutions of $(OC)_5WPPh_2H$ are converted to $[W_2(CO)_{10}PPh_2]^-$, $[W_2(CO)_9(PPh_2)(PPh_2H)]^-$,

Table I. A Comparison of the Rhodium Hydride Coupling Constants for the $[P_2RhH]_x$ Family of Clusters

entry	cluster	δ(Rh*H*)	$^1J_{Rh-H}$, Hz	$^2J_{P-H}$, Hz	ref
4	[(dipope)RhH]$_2$	−4.30	34.0	33–35	this work
5	[{(i-$C_3H_7O)_3P$}$_2$RhH]$_2$	−7.11	34.2	36.6	5
6	[{$(CH_3O)_3P$}$_2$RhH]$_3$	−9.56	16.5	25.0	5
2	[(dmope)RhH]$_4$	−6.52	10.7	16.1	this work

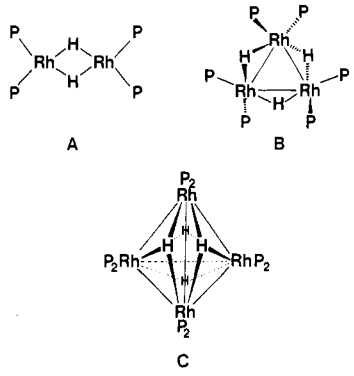

Figure 2. Structures of the $[P_2RhH]_x$ family of clusters: structures A and B have been verified crystallographically whereas structure C is tentative.

adding to the complexity in the low temperature regime.

We have also investigated the reactions of hydrogen with the (2-methylallyl)rhodium(I) complex of 1,2-bis(diisopropoxyphosphino)ethane, [η^3-(2-Me-C_3H_4)Rh(dipope)], **3**; in this case the dimeric[7] derivative [(dipope)RhH]$_2$,[9] **4**, is obtained as bright red crystals. The hydride resonance of **4** appears as a broad, unsymmetrical *septet* which upon phosphorus decoupling simplifies to a binomial *triplet*, indicating coupling with *two* magnetically equivalent rhodium nuclei ($^1J_{Rh}$ = 34.0 Hz). Because of the broadness of the phosphorus-coupled hydride pattern of **4**, we have been unable to extract an accurate phosphorus coupling constant; however, on the basis of previous work[5] with the closely related rhodium hydride dimer utilizing monodentate triisopropyl phosphite ligands, [{(i-$C_3H_7O)_3P$}$_2$RhH]$_2$, **5**, the observed seven-line pattern can be considered as an overlapping triplet of *quintets* which would require a phosphorus coupling constant between 33 and 35 Hz, indicating *four* magnetically equivalent phosphorus nuclei. Interestingly both the rhodium– and phosphorus–hydride coupling constants of **4** are nearly identical with those of **5** (Table I), suggesting that these binuclear complexes are isostructural: all four phosphorus atoms and two rhodium atoms coplanar as in Figure 2, structure A.[10]

The factors that determine the nuclearity of the $[P_2RhH]_x$ clusters are clearly steric in origin. In our case, the choice of the bidentate ligand $(CH_3O)_2PCH_2CH_2P(OCH_3)_2$ allows for the formation of the *tetranuclear* cluster **2**, the largest member of this family of clusters; this contrasts the use of $P(OCH_3)_3$, a monodentate ligand, which generates[5] the *trinuclear* cluster [{$(CH_3O)_3P$}$_2$RhH]$_3$, **6** (structure B, Figure 2). With relatively small substituents such as methoxy groups of the phosphorus donors, the bidentate $(CH_3O)_2PCH_2CH_2P(OCH_3)_2$ ligand exerts a smaller steric influence than two monodentate $P(OCH_3)_3$ ligands; with larger substituents such as isopropoxy, the steric influence of the bidentate ligand must be similar to two monodentate ligands since in both cases binuclear clusters are isolated.

All the members of the $[P_2RhH]_x$ family of clusters are formally electron deficient and therefore coordinatively unsaturated. For example, the tetranuclear complex **2** is a 56-electron cluster,[11] electronically identical with the 56-electron cluster $H_4Re_4(CO)_{12}$, the structure of which is known[12] to be a tetrahedral array of rhenium atoms with face-bridging hydrides. That **2** is similar in structure to $H_4Re_4(CO)_{12}$ can only be speculation in the absence of crystallographic data; however, a comparison of the hydride coupling constants (Table I) of these clusters does provide support for **2** having structure C (Figure 2). Thus one observes a decrease in $^1J_{Rh-H}$ on going from doubly edge bridging hydrides as in **4** and **5** (structure A) to singly edge bridging for **6** (structure B). That a further decrease of $^1J_{Rh-H}$ is observed in **2** may be evidence for face-bridging hydrides and therefore structure C. We are attempting to grow suitable crystals of **2** for crystallographic studies to verify this hypothesis.

Each rhodium center in **2** and **4** is formally in the +1 oxidation state and therefore susceptible to oxidative addition. Indeed, both **2** and **4** readily exchange their hydrides with deuterium at atmospheric pressure in minutes to form the corresponding deuterides. A consequence of this facile oxidative addition of H_2 or D_2 and their inherent coordinative unsaturation is that both **2** and **4** are extremely efficient hydrogenation catalysts for simple olefins. Whether or not the integrity of the cluster is maintained[5] throughout the hydrogenation cycle is under active investigation and will be the subject of future publications.

Acknowledgment. Financial support from the Natural Sciences and Engineering Research Council of Canada, Research Corp., and the President's Emergency Research Fund (UBC) are gratefully acknowledged. We also thank Mr. Peter Borda for the chemical analyses and Dr. S. O. Chan and his staff for help with the NMR experiments. The generous loan of hydrated rhodium trichloride from Johnson-Matthey is also acknowledged.

Registry No. 1, 80105-91-5; 2, 80105-92-6; 3, 80105-93-7; 4, 80126-87-0.

(9) 4: mp 153 °C dec; ^{1}H NMR (C_7D_8) P(OC*H*(CH_3)$_2$), 5.35 ppm (m, 8, J = 6.4 Hz); P(OCH(CH_3)$_2$, 1.35 and 1.45 ppm (d, 48); PCH_2, 1.49 ppm (br m, 8); Rh*H*, −4.3 ppm (br sep, 2, J_{Rh} = 34.05 Hz, J_P = 33–35 Hz); ^{31}P{^{1}H} NMR (C_6D_6, ppm relative to $P(OMe)_3$ at +141.0 ppm) 196.4 (AA′A″A‴XX′, $|^1J_{Rh} + {}^3J_{Rh}|$ = 212.4 Hz). Anal. Calcd for $C_{14}H_{33}O_4P_2Rh$: C, 39.08; H, 7.73. Found: C, 39.01; H, 7.62.

(10) Teller, R. G.; Williams, J. M.; Koetzle, T. F.; Burch, R. R.; Gavin, R. M.; Muetterties, E. L. *Inorg. Chem.* **1981**, *20*, 1806.

(11) A saturated tetranuclear cluster formally contains 60 electrons; see: Johnson, B. F. G.; Benfield, R. E. *Top. Stereochem.* **1981**, *12*, 253.

(12) Wilson, R. D.; Bau, R. *J. Am. Chem. Soc.* **1976**, *98*, 4687.

Synthesis and ^{31}P NMR Characterization of $[W_2(CO)_{10}PPh_2]^-$, $[W_2(CO)_9(PPh_2H)PPh_2]^-$, $[W_2(CO)_8(PPh_2)_2]^{2-}$, and $W_2(CO)_8(PPh_2)_2$

Richard L. Keiter* and Matthew J. Madigan

Chemistry Department, Eastern Illinois University Charleston, Illinois 61920

Received September 14, 1981

Summary: Tetrahydrofuran solutions of $(OC)_5WPPh_2H$ are converted to $[W_2(CO)_{10}PPh_2]^-$, $[W_2(CO)_9(PPh_2)(PPh_2H)]^-$,

Table I. ^{31}P NMR [a] of Phosphido-Bridged Tungsten Carbonyls (CD_3CN)

complex	δ_{PPh_2}	δ_{PPh_2H}	J_{PP}, Hz	J_{WPPh_2}, Hz	J_{WPPh_2H}, Hz
I	−63.5			168.7	
II	−61.6	7.4	19.5	163.2 [b]	228.0
III	−99.2			156.0	
IV	180.0			162.0	

[a] Spectra were recorded at 40.5 MHz on a Varian XL-100 100 NMR spectrometer equipped with Fourier transform and a pulsed deuterium lock. [b] See ref 7.

and $[W_2(CO)_8(PPh_2)_2]^{2-}$ upon treatment with potassium *tert*-butoxide. The dianion reacts with O_2 to form $W_2(CO)_8(PPh_2)_2$. These complexes have been isolated and characterized with ^{31}P NMR and IR spectroscopy.

The metal–metal bonded doubly bridged complexes $M_2(CO)_8(PR_2)_2$ (M = Cr, Mo, W) have been extensively studied.[1] Although most frequently synthesized from the thermal reaction of R_2PPR_2 and $M(CO)_6$,[2] they also have been prepared from the UV irradiation of $(OC)_5MPPh_2H$ or $(OC)_5MPPh_2Li$ in THF.[3] For the latter reaction, intermediates such as $[(OC)_4M(PR_2)_2M(CO_4)]^-$ or $[(OC)_4M(PPh_2)_2M(CO)_4]^{2-}$ may be proposed but neither has been verified. The change in oxidation state of tungsten from 0 to +1 requires an oxidizing agent, and it has been speculated that the reaction solvent serves that function.[3]

In this work we have investigated the reaction of $(OC)_5WPPh_2H$ with potassium *tert*-butoxide and have isolated and characterized $[PPN][W_2(CO)_{10}PPh_2]$ (I), $[PPN][W_2(CO)_9(PPh_2H)PPh_2]$ (II), $K_2[W_2(CO)_8(PPh_2)_2]$ (III), and $W_2(CO)_8(PPh_2)_2$ (IV).

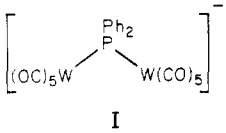

I

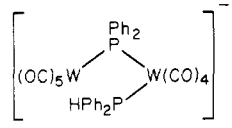

II

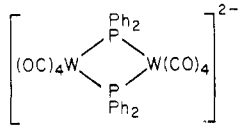

III

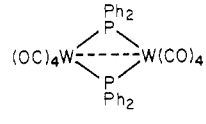

IV

Products I, II, and III were generated when equimolar quantities (2.0 mmol) of $(OC)_5WPPh_2H$, KO-*t*-Bu, and [PPN]Cl were dissolved in CD_3CN and allowed to react for 3 days at ambient temperature. They were identified in the crude reaction mixture, contained in a sealed NMR tube, by ^{31}P NMR spectroscopy (Table I).[4] Procedures were developed for isolating these products, and their structures were further substantiated by IR spectroscopy (Table II).

Compound I was obtained by refluxing equimolar quantities (1.0 mmol) of $(OC)_5WPPh_2H$, KO-*t*-Bu, and [PPN]Cl with excess $W(CO)_6$ (1.8 mmol) in THF (50 mL) for 1.0 h. Recrystallization from CH_2Cl_2/Et_2O gave the pure yellow solid (55%). It is stable in air both in the solid state and in solution (CH_2Cl_2, $CHCl_3$, CH_3CN, THF, Et_2O). Its ^{31}P NMR spectrum consists of a signal at 20.1 ppm for PPN^+ and a signal at −63.5 ppm, flanked by ^{183}W satellites (J_{WP} = 168.7 Hz). The observed intensities (1:6:1) for the anion are consistent with two tungsten atoms coupled to phosphorus. This pattern provides a useful means of distinguishing such compounds from those which have a single tungsten atom coupled to phosphorus. Although many other anionic monobridged group 6 complexes, $[M_2(CO)_{10}X]^-$ (X = Cl^-, Br^-, I^-, CN^-, NCS^-, SR^-, H^-), have been synthesized,[5] the only example in which X is PR_2^- is $[Mo_2(CO)_{10}PH_2]^-$.[6] The infrared spectrum of the carbonyl region of I shows a spectral complexity which also has been observed for other $[M_2(CO)_{10}X]^-$ systems.[5]

When equimolar quantities of $(OC)_5WPPh_2H$, KO-*t*-Bu, and [PPN]Cl were heated under reflux in THF for 3 h, KCl precipitated from solution, and upon evaporation of the filtrate, II was precipitated. Recrystallization of II from CH_2Cl_2/Et_2O gave pure yellow solid (39%). The ^{31}P spectrum of II consisted of a doublet at −61.6 ppm (J_{PP} = 19.5 Hz, J_{WP} = 163.2 Hz), attributed to bridging PPh_2[7] and a doublet at 7.4 ppm (J_{PP} = 19.5 Hz, J_{WP} = 228.0 Hz) which was assigned to coordinated PPh_2H. The magnitude of J_{PP} is consistent with a cis arrangement of phosphorus atoms.[8] A proton-coupled ^{31}P spectrum revealed the expected phosphorus–hydrogen coupling ($^1J_{PH}$ = 325.2 Hz, $^3J_{PH}$ = 6.4 Hz). The IR spectrum can be seen as a superimposition of absorptions for $W(CO)_4$ and $W(CO)_5$ moieties and provides further confirmation of the structure. II slowly decomposes in solution to give I and III.

Table II. Infrared Data [a] of Bridged Complexes

complex	metal carbonyl stretching freq cm^{-1}
I [b]	2064 (w), 2051 (m), 1963 (sh), 1934 (vs), 1901 (s), 1877 (s)
II [b]	2056 (m), 2004 (m), 1960 (w), 1924 (vs), 1874 (s), 1832 (m)
III [c]	1923 (m), 1880 (s), 1840 (m), 1793 (m)
IV [b]	2034 (s), 1957 (vs)

[a] Spectra were recorded with a Perkin-Elmer 337 infrared spectrometer and expanded with an E-H Sargent recorder. [b] CH_2Cl_2. [c] CH_3CN.

Scheme I

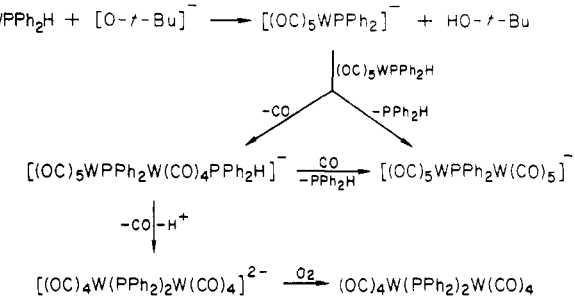

(1) Madach, T.; Vahrenkamp H. *Chem. Ber.* **1981**, *114*, 513. Vahrenkamp, H. *Ibid.* **1978**, *111*, 3472. Shaik, S.; Hoffmann, R.; Fisel, C. R.; Summerville, R. H. *J. Am. Chem. Soc.* **1980**, *102*, 4555.

(2) Hayter, R. G. *Inorg. Chem.* **1964**, *3*, 711. Chatt, J.; Thorton, D. A. *J. Chem. Soc.* **1964**, 1005, Chatt, J.; Thompson, D. T. *Ibid.* **1964**, 2713. Linck, M. H.; Nassimbeni *Inorg. Nucl. Chem. Lett.* **1973**, *9*, 1105.

(3) Treichel, P. M.; Dean, W. K.; Douglas, W. M. *J. Organomet. Chem.* **1972**, *145*, 42.

(4) Several signals observed in the ^{31}P NMR spectrum of the crude reaction mixture have not been assigned to specific structures. These are found at 59.6 ppm (J_{WP} = 247.0 Hz) and −50.9 ppm (J_{WP} unresolved).

(5) Ruff, J. K. *Inorg. Chem.* **1968**, *7*, 1818, 1821; **1969**, *8*, 86, 180; **1972**, *11*, 2265. Cooper, M. K.; Duckworth, P. A.; Henrick, K.; McPartlin, M. *J. Organomet. Chem.* **1981**, *212*, C10. Darensbourg, M. Y.; Deaton, J. C. *Inorg. Chem.* **1981**, *20*, 1644.

(6) Becker, G.; Ebsworth, E. A. V. *Angew. Chem., Int. Ed. Engl.* **1971**, *10*, 186.

(7) We were not able to resolve the two tungsten–phosphorus coupling constants expected for bridging PPh_2 and so we must consider our value to be an average of the two.

(8) Keiter, R. L.; Sun, Y. Y.; Brodack, J. W.; Cary, L. W. *J. Am. Chem. Soc.* **1979**, *101*, 2638.

Refluxing a THF solution of $(OC)_5WPPh_2H$ (1.0 mmol) and KO-*t*-Bu (1.0 mmol) for 6 h resulted in the precipitation of III (10%). The ^{31}P NMR spectrum of III shows signals at -99.2 ppm (J_{WP} = 156.0 Hz). The infrared spectrum of III, consisting of three medium and one strong absorption, matches in appearance that reported for $[Cr_2(CO)_8(PMe_2)]_2^{2-}$, an anion previously obtained electrochemically.[9] The yellow anion, III, reacts rapidly with air to give red IV but is stable in oxygen-free dry THF or CH_3CN. The infrared spectrum of IV is in agreement with literature reports.[2] ^{31}P resonance occurs at 180.0 ppm (J_{WP} = 162 Hz).

A reasonable reaction sequence for the production of I, II, III, and IV is presented in Scheme I.

Of particular interest is the dramatic change in the ^{31}P chemical shift which accompanies formation of a metal–metal bond. Thus our work adds further support to the notion that ^{31}P chemical shifts diagnose the presence or absence of metal–metal bonds in phosphido bridged complexes.[10]

Acknowledgment is made to the donors of the Petroleum Research Fund, administered by the American Chemical Society, for support of this research. We thank David Vander Velde and Dennis Warrenfeltz of the University of Illinois for obtaining ^{31}P spectra.

Registry No. I, 80049-78-1; II, 80049-80-5; III, 80049-81-6; IV, 80049-82-7; $(OC)_5WPPh_2H$, 18399-62-7.

(9) Dessey, R. E.; Weiczorek, L. *J. Am. Chem. Soc.* **1969**, *91*, 4963. Dessey, R. E.; Rheingold, A. L.; Howard, G. D. *Ibid.* **1972**, *94*, 746.
(10) Carty, A. J.; Mott, G. N.; Taylor, N. J.; Yule, J. E. *J. Am. Chem. Soc.* **1978**, *100*, 3051. Garrou, P. E. *Chem. Rev.* **1981**, *81*, 229. Brandon, J. B.; Dixon, K. R. *Can. J. Chem.* **1981**, *59*, 1188.

Role of Heteroatoms in the Formation of Higher Nuclearity Transition-Metal Carbonyl Cluster Compounds. The Condensation of Small Clusters

Richard D. Adams,* Zain Dawoodi, and Donald F. Foust
Department of Chemistry, Yale University
New Haven, Connecticut 06511

Received November 9, 1981

Summary: The molecules $HOs_3(\mu_3\text{-}S)(\mu\text{-}HCNR)(CO)_9$, R = C_6H_5, Ia, and *p*-C_6H_4F, Ib, lose carbon monoxide when heated and condense to form the higher nuclearity carbonyl clusters $H_2Os_6(\mu_4\text{-}S)(\mu_3\text{-}S)(\mu\text{-}HC{=}NR)_2(CO)_{17}$, R = C_6H_5, IIa, and *p*-C_6H_4F, IIb, and $H_2Os_6(\mu_4\text{-}S)(\mu_3\text{-}S)(\mu\text{-}HC{=}NR)_2(CO)_{16}$, R = C_6H_5, III. The compounds have been characterized by IR and ^1H NMR spectroscopies, and IIb and III have also been characterized by X-ray crystallographic methods. For IIb: space group $P\bar{1}$ at 28 °C; a = 9.865 (7) Å, b = 14.735 (6) Å, c = 15.926 (10) Å, α = 69.08 (5)°, β = 79.63 (6)°, γ = 86.40 (6)°, Z = 2, ρ_{calcd} = 3.01 g/cm^3. The structure was solved by a combination of Patterson and difference Fourier techniques. Refinement on 3584 reflections ($F^2 \geq 3.0\sigma(F^2)$) produced the final residuals R_1 = 0.032 and R_2 = 0.030. For III: space group $P2_1/n$ at 28 °C; a = 10.506 (4) Å, b = 23.145 (12) Å, c = 16.933 (5) Å, β = 97.60 (3)°, Z = 4, ρ_{calcd} = 3.03 g/cm^3. This structure was solved by a combination of direct methods and difference Fourier techniques. Refinement on 2347 reflections ($F^2 \geq 3.0\sigma(F^2)$) produced the final residuals R_1 = 0.052 and R_2 = 0.043. IIb contains two groups of "open" clusters of three metal atoms linked by a tetracoordinate bridging sulfur atom. The metal–metal bonding in each of the "open" cluster groups is analogous to that in the molecules I. In III the metal atoms are arranged in groups of four and two with the two groups linked by a tetracoordinate bridging sulfur atom. It is believed that III is formed by the decarbonylation of IIa. A reorganization of the metal–metal bonding then occurs in which an $Os(CO)_3$ unit is shifted from one group of three to the other.

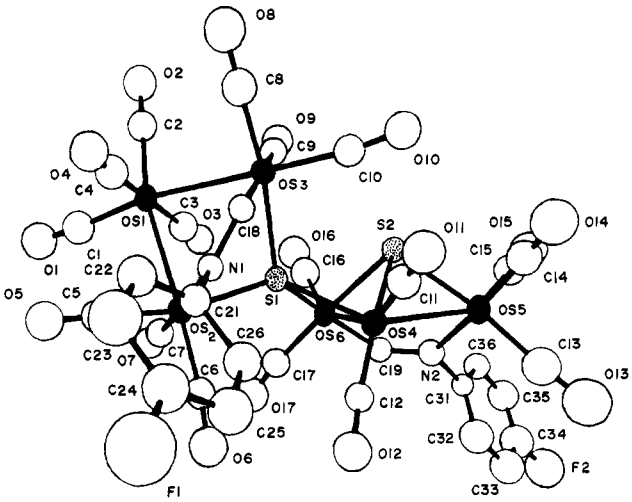

Figure 1. An ORTEP drawing of $H_2Os_6(\mu_4\text{-}S)(\mu_3\text{-}S)(\mu\text{-}HC{=}N\text{-}p\text{-}C_6H_4F)_2(CO)_{17}$, IIb, showing 50% electron density probability ellipsoids.

The decarbonylation of metal carbonyl compounds is the most successful and widely used method for the preparation of high nuclearity transition-metal carbonyl cluster compounds.[1] In this process, metal–metal bonds replace the metal–carbon bonds of the eliminated ligands. It is well-known that heteronuclear bridging ligands will enhance the stability of polynuclear metal complexes.[2] Recently it has been proposed that these heteronuclear bridging ligands can play an important role in the systematic synthesis of higher nuclearity cluster compounds.[3]

We wish to report that we have now observed an example of the aggregation of two transition-metal clusters which unequivocally shows the importance and role of the heteronuclear bridging ligand in preliminary cluster condensation and the eventual reorganization of the metal–metal bonds within the clusters.

We have recently reported the synthesis of the cluster compounds $HOs_3(\mu_3\text{-}S)(\mu\text{-}HC{=}NR)(CO)_9$, R = C_6H_5, Ia, and *p*-C_6H_4F, Ib.[4] When heated to reflux in octane solvent

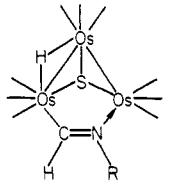

I

(1) (a) Chini, P.; Longoni, G.; Albano, V. G. *Adv. Organomet. Chem.* **1976**, *14*, 285. (b) Eady, C. R.; Johnson, B. F. G.; Lewis, J. *J. Chem. Soc., Dalton Trans.* **1975**, 2606. (c) Lewis, J.; Johnson, B. F. G. *Gazz. Chim. Ital.* **1979**, *109*, 271. (d) Lewis, J.; Johnson, B. F. G. *Pure Appl. Chem.* **1975**, *44*, 43.
(2) (a) Vahrenkamp, H. *Angew. Chem., Int. Ed. Engl.* **1975**, *14*, 322. (b) Marko, L. *Gazz. Chim. Ital.* **1979**, *109*, 247.
(3) Vahrenkamp, H.; Wucherer, E. J. *Angew. Chem., Int. Ed. Engl.* **1981**, *20*, 680.

0276-7333/82/2301-0411$01.25/0

Refluxing a THF solution of $(OC)_5WPPh_2H$ (1.0 mmol) and KO-*t*-Bu (1.0 mmol) for 6 h resulted in the precipitation of III (10%). The ^{31}P NMR spectrum of III shows signals at -99.2 ppm (J_{WP} = 156.0 Hz). The infrared spectrum of III, consisting of three medium and one strong absorption, matches in appearance that reported for $[Cr_2(CO)_8(PMe_2)]_2^{2-}$, an anion previously obtained electrochemically.[9] The yellow anion, III, reacts rapidly with air to give red IV but is stable in oxygen-free dry THF or CH_3CN. The infrared spectrum of IV is in agreement with literature reports.[2] ^{31}P resonance occurs at 180.0 ppm (J_{WP} = 162 Hz).

A reasonable reaction sequence for the production of I, II, III, and IV is presented in Scheme I.

Of particular interest is the dramatic change in the ^{31}P chemical shift which accompanies formation of a metal–metal bond. Thus our work adds further support to the notion that ^{31}P chemical shifts diagnose the presence or absence of metal–metal bonds in phosphido bridged complexes.[10]

Acknowledgment is made to the donors of the Petroleum Research Fund, administered by the American Chemical Society, for support of this research. We thank David Vander Velde and Dennis Warrenfeltz of the University of Illinois for obtaining ^{31}P spectra.

Registry No. I, 80049-78-1; II, 80049-80-5; III, 80049-81-6; IV, 80049-82-7; $(OC)_5WPPh_2H$, 18399-62-7.

(9) Dessey, R. E.; Weiczorek, L. *J. Am. Chem. Soc.* **1969**, *91*, 4963. Dessey, R. E.; Rheingold, A. L.; Howard, G. D. *Ibid.* **1972**, *94*, 746.
(10) Carty, A. J.; Mott, G. N.; Taylor, N. J.; Yule, J. E. *J. Am. Chem. Soc.* **1978**, *100*, 3051. Garrou, P. E. *Chem. Rev.* **1981**, *81*, 229. Brandon, J. B.; Dixon, K. R. *Can. J. Chem.* **1981**, *59*, 1188.

Role of Heteroatoms in the Formation of Higher Nuclearity Transition-Metal Carbonyl Cluster Compounds. The Condensation of Small Clusters

Richard D. Adams,* Zain Dawoodi, and Donald F. Foust
Department of Chemistry, Yale University
New Haven, Connecticut 06511

Received November 9, 1981

Summary: The molecules $HOs_3(\mu_3\text{-}S)(\mu\text{-}HCNR)(CO)_9$, R = C_6H_5, Ia, and *p*-C_6H_4F, Ib, lose carbon monoxide when heated and condense to form the higher nuclearity carbonyl clusters $H_2Os_6(\mu_4\text{-}S)(\mu_3\text{-}S)(\mu\text{-}HC{=}NR)_2(CO)_{17}$, R = C_6H_5, IIa, and *p*-C_6H_4F, IIb, and $H_2Os_6(\mu_4\text{-}S)(\mu_3\text{-}S)(\mu\text{-}HC{=}NR)_2(CO)_{16}$, R = C_6H_5, III. The compounds have been characterized by IR and ^1H NMR spectroscopies, and IIb and III have also been characterized by X-ray crystallographic methods. For IIb: space group $P\bar{1}$ at 28 °C; a = 9.865 (7) Å, b = 14.735 (6) Å, c = 15.926 (10) Å, α = 69.08 (5)°, β = 79.63 (6)°, γ = 86.40 (6)°, Z = 2, ρ_{calcd} = 3.01 g/cm^3. The structure was solved by a combination of Patterson and difference Fourier techniques. Refinement on 3584 reflections ($F^2 \geq 3.0\sigma(F^2)$) produced the final residuals R_1 = 0.032 and R_2 = 0.030. For III: space group $P2_1/n$ at 28 °C; a = 10.506 (4) Å, b = 23.145 (12) Å, c = 16.933 (5) Å, β = 97.60 (3)°, Z = 4, ρ_{calcd} = 3.03 g/cm^3. This structure was solved by a combination of direct methods and difference Fourier techniques. Refinement on 2347 reflections ($F^2 \geq 3.0\sigma(F^2)$) produced the final residuals R_1 = 0.052 and R_2 = 0.043. IIb contains two groups of "open" clusters of three metal atoms linked by a tetracoordinate bridging sulfur atom. The metal–metal bonding in each of the "open" cluster groups is analogous to that in the molecules I. In III the metal atoms are arranged in groups of four and two with the two groups linked by a tetracoordinate bridging sulfur atom. It is believed that III is formed by the decarbonylation of IIa. A reorganization of the metal–metal bonding then occurs in which an $Os(CO)_3$ unit is shifted from one group of three to the other.

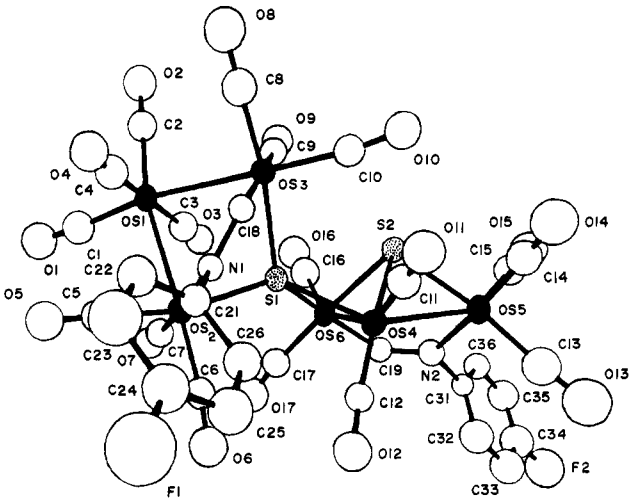

Figure 1. An ORTEP drawing of $H_2Os_6(\mu_4\text{-}S)(\mu_3\text{-}S)(\mu\text{-}HC{=}N\text{-}p\text{-}C_6H_4F)_2(CO)_{17}$, IIb, showing 50% electron density probability ellipsoids.

The decarbonylation of metal carbonyl compounds is the most successful and widely used method for the preparation of high nuclearity transition-metal carbonyl cluster compounds.[1] In this process, metal–metal bonds replace the metal–carbon bonds of the eliminated ligands. It is well-known that heteronuclear bridging ligands will enhance the stability of polynuclear metal complexes.[2] Recently it has been proposed that these heteronuclear bridging ligands can play an important role in the systematic synthesis of higher nuclearity cluster compounds.[3]

We wish to report that we have now observed an example of the aggregation of two transition-metal clusters which unequivocally shows the importance and role of the heteronuclear bridging ligand in preliminary cluster condensation and the eventual reorganization of the metal–metal bonds within the clusters.

We have recently reported the synthesis of the cluster compounds $HOs_3(\mu_3\text{-}S)(\mu\text{-}HC{=}NR)(CO)_9$, R = C_6H_5, Ia, and *p*-C_6H_4F, Ib.[4] When heated to reflux in octane solvent

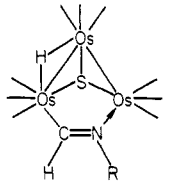

I

(1) (a) Chini, P.; Longoni, G.; Albano, V. G. *Adv. Organomet. Chem.* **1976**, *14*, 285. (b) Eady, C. R.; Johnson, B. F. G.; Lewis, J. *J. Chem. Soc., Dalton Trans.* **1975**, 2606. (c) Lewis, J.; Johnson, B. F. G. *Gazz. Chim. Ital.* **1979**, *109*, 271. (d) Lewis, J.; Johnson, B. F. G. *Pure Appl. Chem.* **1975**, *44*, 43.
(2) (a) Vahrenkamp, H. *Angew. Chem., Int. Ed. Engl.* **1975**, *14*, 322. (b) Marko, L. *Gazz. Chim. Ital.* **1979**, *109*, 247.
(3) Vahrenkamp, H.; Wucherer, E. J. *Angew. Chem., Int. Ed. Engl.* **1981**, *20*, 680.

0276-7333/82/2301-0411$01.25/0

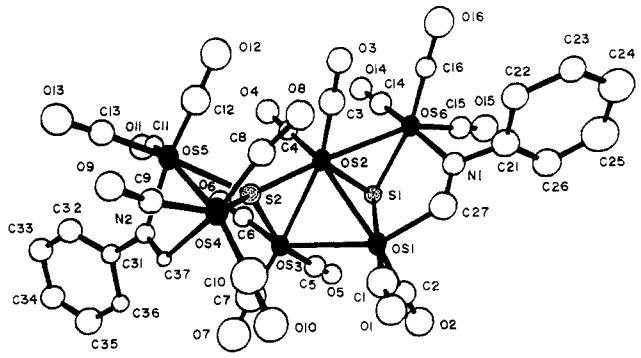

Figure 2. An ORTEP drawing of $H_2Os_6(\mu_4\text{-}S)(\mu_3\text{-}S)(\mu\text{-}HC{=}NC_6H_5)_2(CO)_{16}$, III, showing 50% electron density probability ellipsoids.

for 3 h, these molecules are converted into a number of new higher nuclearity clusters, two of which have now been isolated and characterized by IR and ^1H NMR spectroscopic and X-ray crystallographic methods.[5,6] The first of these has the formula $H_2Os_6(\mu_4\text{-}S)(\mu_3\text{-}S)(\mu\text{-}HC{=}NR)_2(CO)_{17}$, R = C_6H_5, IIa, and $p\text{-}C_6H_4F$, IIb.[7] They can be assumed to be formed by the condensation of two moles of I accompanied by the loss of 1 mol of CO. The molecular structure of IIb is shown in Figure 1.[8,9] The molecule consists of two "open" cluster groupings of three osmium atoms which are linked by a tetrahedrally coordinated bridging sulfur atom, S(1). The cluster group Os(4)–Os(5)–Os(6) is very similar to I with the exception that two of the equatorially coordinated carbonyl ligands have been replaced by donor bonds from the bridging sulfur atom, S(1). Cluster Os(1)–Os(2)–Os(3) differs from I in that the sulfur atom is bonded only to two of the metal atoms, Os(1) and Os(2), while Os(3) has four carbonyl ligands. As in I, each cluster grouping in IIb contains an η^2-formimidoyl ligand bridging the open edge of the cluster.

The formation of II was probably initiated via a dissociative loss of CO from I. The empty coordination site was then filled by donation of the lone pair of electrons of the triply bridging sulfur atom from a second molecule of I. In this close proximity, an intercluster carbonyl shift might easily follow the cleavage of an osmium–sulfur bond in the added cluster and this would complete the formation of II.

Scheme I

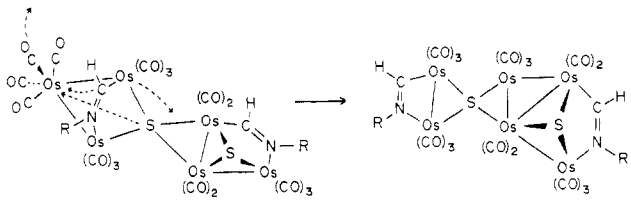

The second type of molecule isolated from the pyrolysis of I has the formula $H_2Os_6(\mu_4\text{-}S)(\mu_3\text{-}S)(\mu\text{-}HC{=}NR)_2(CO)_{16}$, R = C_6H_5, III.[10] The molecular structure of III is shown in Figure 2.[6,11,12] III contains six osmium atoms which are arranged in groups of four and two. Within the group of four osmium atoms, three, namely, Os(1), Os(2), and Os(6), can be compared with Os(4), Os(5), and Os(6) in the "open" cluster in IIb. These three metal atoms contain a triply bridging sulfur atom and an η^2-formimidoyl ligand bridging the nonbonded pair of metal atoms, Os(1) and Os(6). The fourth metal atom, Os(3), in the form of an $Os(CO)_3$ unit bridges the Os(1)–Os(2) edge of this grouping of three. A tetrahedrally coordinated sulfur atom, S(2), bridges the Os(2)–Os(3) bond and links the two atom group Os(4)–Os(5) to the first four. The Os(4)–Os(5) group consists of two $Os(CO)_3$ units joined by a metal–metal bond and contains a bridging η^2-formimidoyl ligand.

We feel it is significant that III contains one carbonyl ligand less than II and thus believe that the molecules II are precursors to III. The transformation of II into III can be imagined in the following way (see Scheme I). If the $Os(CO)_4$ unit in II loses one carbonyl ligand, the formimidoyl ligand can then move either its carbon or nitrogen atom to that metal atom. According to the labeling scheme in IIb, the remaining $Os(CO)_3$ unit, either that of Os(2) or Os(3), can then insert into the Os(6)–S(1) bond. This involves cleavage of either the Os(1)–Os(2) or the Os(1)–Os(3) metal–metal bond and formation of metal–metal bonds to both Os(4) and Os(6). A metal–sulfur bond between Os(1) and S(1) is also formed.

The principal steps represented by II and III in the condensation of the clusters of I are (1) metal–sulfur coordination which leads to the initial link between the clusters and (2) reorganization of the metal–metal bonds which occurs in the formation of III. The first step is facilitated by the ability of the sulfur ligand to serve as a polycoordinate multielectron donor.[13]

(4) Adams, R. D.; Dawoodi, Z. *J. Am. Chem. Soc.* **1981**, *103*, 6510.

(5) In a typical preparation 180 mg of Ia was refluxed 3 h in octane solvent under a nitrogen atmosphere. The products were isolated by TLC on silica gel plates using a hexane/10% CH_2Cl_2 solvent mixture. At least six compounds were isolated in yields ranging from 5 to 15%. Accurate yields are difficult to obtain because of the small amounts of material involved. Of the six product bands which followed residual starting material on the plate, IIa and IIIa were the fifth and second bands, respectively. All the products are air-stable. ^1H NMR spectra were recorded at 270 MHz on a Bruker HX-270 spectrometer.

(6) X-ray crystallographic data were collected on an Enraf-Nonius CAD-4 automatic diffractometer using molybdenum radiation. Structure solution and refinement calculations were done on a Digital PDP 11/45 computer by using the Enraf-Nonius SDP program library, Version 16.

(7) For IIa: IR ν (CO) (in hexane) 2111 (m), 2096 (m), 2085 (sh), 2066 s), 2053 (sh), 2044 (vs), 2029 (vs), 2008 (s), 1990 (s), 1979 (s), 1960 (m); ^1H NMR (in $CDCl_3$), δ 12.38 (s, 1 H), 11.25 (s, 1 H), 7.30 (m, 10 H), −13.82 (s, 1 H), −17.44 s, 1 H). For IIb: IR ν(CO) (in hexane), 2110 (m), 2095 (m), 2080 (w), 2067 (vs), 2050 (sh), 2043 (s), 2025 (s), 2005 (m), 1980 (m), 1975 (m), 1955 (w); ^1H NMR (in $CDCl_3$), δ 12.40 (s, 1 H), 11.27 (s, 1 H), 7.20 (m, 8 H), −13.87 (s, 1 H), −17.46 (s, 1 H).

(8) For IIb: space group $P\bar{1}$ at 28 °C; a = 9.865 (7) Å, b = 14.735 (6) Å, c = 15.926 (10) Å, α = 69.08 (5)°, β = 79.63 (6)°, γ = 86.40 (6)°, Z = 2, ρ_{calcd} = 3.01 g/cm^3. The structure was solved by a combination of Patterson and difference Fourier techniques. Least-squares refinement on 3584 reflections ($F^2 \geq 3.0\sigma(F^2)$) produced the final residuals R_1 = 0.032 and R_2 = 0.030.

(9) Selected bond distances (Å) and angles (deg) for IIb: Os(1)–Os(2) = 2.914 (1), Os(1)–Os(3) = 2.918 (1), Os(4)–Os(5) = 2.951 (1), Os(4)–Os(6) = 2.803 (1), Os(3)–C(18) = 2.10 (1), Os(2)–N(1) = 2.12 (1), Os(6)–C(19) = 2.02 (2), Os(5)–N(2) = 2.16 (1); Os(2)–S(1) = 2.447 (4), Os(3)–S(1) = 2.481 (3), Os(4)–S(1) = 2.441 (4), Os(6)–S(1) = 2.509 (4); Os(2)–Os(1)–Os(3) = 75.28 (2), Os(5)–Os(4)–Os(6) = 80.93 (2), Os(2)–S(1)–Os(3) = 92.54 (13), Os(4)–S(1)–Os(6) = 68.96 (10), Os(2)–S(1)–Os(4) = 124.05 (13), Os(2)–S(1)–Os(6) = 129.54 (15), 68.96 (10), Os(2)–S(1)–Os(4) = 124.05 (13), Os(2)–S(1)–Os(6) = 129.54 (15), Os(3)–S(1)–Os(4) = 113.61(14), Os(3)–S(1)–Os(6) = 129.38 (14), Os(4)–S(1)–Os(6) = 68.96 (10).

(10) For III: Ir ν(CO) (in hexane) 2100 (m), 2077 (vs), 2054 (vs), 2039 (s), 2024 (s), 2007 (vs), 1979 (s), 1953 (m), 1932 (w); ^1H NMR (in $CDCl_3$) δ 10.89 (s, 1 H), 10.38 (s, 1 H), 7.30 (m, 10 H), −17.57 (s, 1 H), −17.72 (s, 1 H).

(11) For III: space group $P2_1/n$ at 28 °C; a = 10.506 (4) Å, b = 23.145 (12) Å, c = 16.933 (5) Å, β = 97.60 (3)°, Z = 4, ρ_{calcd} = 3.03 g/cm^3. The structure was solved by a combination of direct methods (MULTAN) and difference Fourier syntheses. Least-squares refinement on 2347 reflections ($F^2 \geq 3.0\sigma(F^2)$) produced the final residuals R_1 = 0.052 and R_2 = 0.043.

(12) Selected bond distances (Å) and angles (deg) for III: Os(1)–Os(2) = 2.865 (2), Os(1)–Os(3) = 3.070 (2), Os(2)–Os(3) = 2.839 (2), Os(2)–Os(6) = 2.917 (2), Os(4)–Os(5) = 2.769 (2), Os(2)–S(2) = 2.372 (8), Os(3)–S(2) = 2.417 (7), Os(4)–S(2) = 2.425 (7), Os(5)–S(2) = 2.403 (8), Os(1)–C(27) = 2.07 (4), Os(6)–N(1) = 2.16 (3), Os(4)–C(37) = 2.11 (3), Os(5)–N(2) = 2.11 (2); Os(2)–S(2)–Os(3) = 72.7, Os(2)–S(2)–Os(4) = 132.2 (3), Os(3)–S(2)–O(4) = 130.5 (4), Os(3)–S(2)–Os(5) = 131.9 (3), Os(4)–S(2)–Os(5) = 70.0 (2), Os(1)–Os(2)–Os(6) = 81.04 (5), Os(1)–Os(2)–Os(3) = 65.13 (5), Os(1)–Os(3)–Os(2) = 57.85 (5), Os(2)–Os(1)–Os(3) = 57.02 (5), Os(3)–Os(2)–Os(6) = 128.76 (6).

Further loss of carbon monoxide from III should lead to the formation of clusters with still more metal–metal bonds. These studies are now in progress.

Acknowledgment. This work was supported by the Office of Basic Energy Sciences of the U.S. Department of Energy under Contract No. DE-AC02-78ER04900 and the Alfred P. Sloan Foundation through a fellowship to R. D. A. NMR studies were supported by Grant No. CHE-7916210 to the Northeast Regional NSF-NMR Facility from the National Science Foundation. We wish to thank Engelhard Industries for a loan of osmium tetroxide.

Registry No. Ia, 80399-46-8; Ib, 79790-55-9; IIa, 80409-94-5; IIb, 80409-95-6; III, 80409-96-7.

Supplementary Material Available: Tables of final fractional atomic coordinates, bond distances and angles, and structure factors (35 pages). Ordering information is given on any current masthead page.

(13) Coleman, J. M.; Wojcicki, A.; Pollick, P. J.; Dahl, L. F. *Inorg. Chem.* **1967**, *6*, 1236.

Direct Observation of a Cationic Intermediate in the Acid-Catalyzed Decomposition of (2-Hydroxy-, (2-Ethoxy-, and (2-Phenoxyethyl)cobaloximes

Kenneth L. Brown* and Sheela Ramamurthy

Department of Chemistry
The University of Texas at Arlington
Arlington, Texas 76019

Received October 21, 1981

Summary: The kinetics of the acid-catalyzed decomposition of the title compounds to form ethylene and cobaloxime(III) have been studied by UV and visible spectroscopy as well as manometrically in both weakly and strongly acidic H_2SO_4/H_2O mixtures. Compelling kinetic evidence has been obtained for formation of a cationic intermediate (upon loss of the β-leaving group) which accumulates in strongly acidic media where the activity of water is low. The ^1H NMR spectrum of the intermediate and its temperature dependence are consistent with its assignment as a cobaloxime(III)–ethylene π complex with two preferred conformations, although a σ-bonded ethylcobaloxime carbonium ion cannot be ruled out.

Cobalt(III) olefinic π complexes and/or electronically equivalent σ-bonded alkylcobalt carbonium ions have been suggested as intermediates in the alcoholysis of (2-acetoxyalkyl)cobaloximes,[1-4] in the acid-catalyzed rearrangements of (2-hydroxy-*n*-propyl)- and (2-hydroxyisopropyl)cobaloximes[5,6] and decomposition of (2-hydroxyethyl)cobaloxime[6] as well as in the synthesis of organocobalt complexes from vinyl ethers and cobalt(III) complexes in nucleophilic solvents.[4,7-9] To date, all evidence presented for the existence of such intermediates has been indirect. We would now like to report firm kinetic evidence for the existence of an intermediate in the acid-catalyzed decomposition of (2-hydroxyethyl)cobaloxime to cobaloxime(III) and ethylene[10] and direct observation of this intermediate by ^1H NMR spectroscopy.

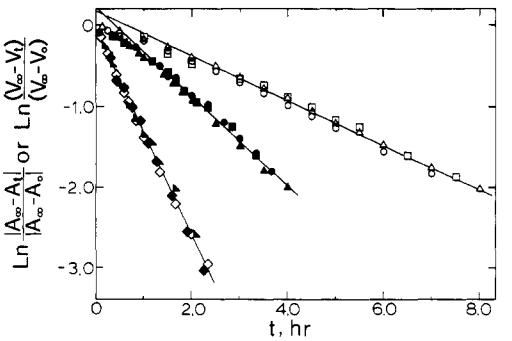

Figure 1. Normalized, semilogarithmic plots of the UV (255 nm), visible (445 nm), and manometric kinetics of the decomposition of **1a**, **1b**, and **1c** at $H_o = 1.70 \pm 0.01$, 25.0 ± 0.1 °C: **1c**, UV (○), visible (△), manometric (□), $k_{obsd} = (7.65 \pm 0.18) \times 10^{-5}$ s^{-1}; **1b**, UV (●), visible (▲), manometric (■), $k_{obsd} = (1.53 \pm 0.04) \times 10^{-4}$ s^{-1}; **1a**, UV (♦), visible (◇), manometric (◣), $k_{obsd} = (3.53 \pm 0.05) \times 10^{-4}$ s^{-1}.

Scheme I

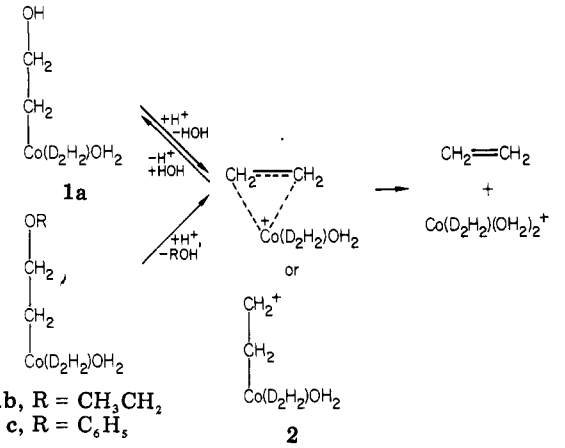

The decomposition of (2-hydroxyethyl)aquocobaloxime (**1a**)[11] in weakly acidic H_2SO_4/H_2O mixtures ($H_o = 1.70 \pm 0.01$)[14-16] (Figure 1) was found to be a strictly first-order process when monitored by UV or visible spectroscopy, as well as manometrically. In contrast, the decomposition of (2-ethoxyethyl)-(**1b**) and (2-phenoxyethyl)aquocobaloxime (**1c**) in the same media shows a distinct lag followed by a first-order decay using the same three techniques. The observed first-order rate constants decrease markedly

(1) Golding, B. T.; Holland, H. L.; Horn, U.; Sakrikar, S. *Angew. Chem., Int. Ed. Engl.* **1970**, *9*, 959–960.
(2) Golding, B. T.; Sakrikar, S. *J. Chem. Soc., Chem. Commun.* **1972**, 1183–1184.
(3) Silverman, R. B.; Dolphin, D.; Babior, B. M. *J. Am. Chem. Soc.* **1972**, *94*, 4028–4030.
(4) Silverman, R. B.; Dolphin, D. *J. Am. Chem. Soc.* **1976**, *98*, 4626–4633.
(5) Brown, K. L.; Ingraham, L. L. *J. Am. Chem. Soc.* **1974**, *96*, 7681–7686.
(6) Espenson, J. H.; Wang, D. M. *Inorg. Chem.* **1979**, *18*, 2853–2859.
(7) Silverman, R. B.; Dolphin, D. *J. Am. Chem. Soc.* **1973**, *95*, 1686–1688.
(8) Silverman, R. B.; Dolphin, D. *J. Am. Chem. Soc.* **1974**, *96*, 7094–7096.
(9) Silverman, R. B.; Dolphin, D.; Carty, T. J.; Krodel, E. K.; Abeles, R. H. *J. Am. Chem. Soc.* **1974**, *96*, 7096–7097.
(10) Schrauzer, G. N.; Windgassen, R. J. *J. Am. Chem. Soc.* **1967**, *89*, 143–147.
(11) The title complexes were synthesized by published procedures[10,12,13] and characterized by ^1H NMR spectroscopy and elemental analysis.
(12) Brown, K. L.; Awtrey, A. W. *Inorg. Chem.* **1978**, *17*, 111–119.
(13) Brown, K. L. *J. Am. Chem. Soc.* **1979**, *101*, 6600–6606.
(14) Hammett, L. P.; Deyrup, A. J. *J. Am. Chem. Soc.* **1932**, *54*, 2721–2739.
(15) Bascombe, K. N.; Bell, R. P. *J. Chem. Soc.* **1959**, 1096–1104.
(16) Ryabova, R. S.; Medvetskaya, I. M.; Vinnik, M. T. *Zh. Fiz. Khim.* **1966**, *40*, 339–345.

0276-7333/82/2301-0413$01.25/0

Further loss of carbon monoxide from III should lead to the formation of clusters with still more metal–metal bonds. These studies are now in progress.

Acknowledgment. This work was supported by the Office of Basic Energy Sciences of the U.S. Department of Energy under Contract No. DE-AC02-78ER04900 and the Alfred P. Sloan Foundation through a fellowship to R. D. A. NMR studies were supported by Grant No. CHE-7916210 to the Northeast Regional NSF-NMR Facility from the National Science Foundation. We wish to thank Engelhard Industries for a loan of osmium tetroxide.

Registry No. Ia, 80399-46-8; Ib, 79790-55-9; IIa, 80409-94-5; IIb, 80409-95-6; III, 80409-96-7.

Supplementary Material Available: Tables of final fractional atomic coordinates, bond distances and angles, and structure factors (35 pages). Ordering information is given on any current masthead page.

(13) Coleman, J. M.; Wojcicki, A.; Pollick, P. J.; Dahl, L. F. *Inorg. Chem.* **1967**, *6*, 1236.

Direct Observation of a Cationic Intermediate in the Acid-Catalyzed Decomposition of (2-Hydroxy-, (2-Ethoxy-, and (2-Phenoxyethyl)cobaloximes

Kenneth L. Brown* and Sheela Ramamurthy

Department of Chemistry
The University of Texas at Arlington
Arlington, Texas 76019

Received October 21, 1981

Summary: The kinetics of the acid-catalyzed decomposition of the title compounds to form ethylene and cobaloxime(III) have been studied by UV and visible spectroscopy as well as manometrically in both weakly and strongly acidic H_2SO_4/H_2O mixtures. Compelling kinetic evidence has been obtained for formation of a cationic intermediate (upon loss of the β-leaving group) which accumulates in strongly acidic media where the activity of water is low. The ^1H NMR spectrum of the intermediate and its temperature dependence are consistent with its assignment as a cobaloxime(III)–ethylene π complex with two preferred conformations, although a σ-bonded ethylcobaloxime carbonium ion cannot be ruled out.

Cobalt(III) olefinic π complexes and/or electronically equivalent σ-bonded alkylcobalt carbonium ions have been suggested as intermediates in the alcoholysis of (2-acetoxyalkyl)cobaloximes,[1-4] in the acid-catalyzed rearrangements of (2-hydroxy-*n*-propyl)- and (2-hydroxyisopropyl)cobaloximes[5,6] and decomposition of (2-hydroxyethyl)cobaloxime[6] as well as in the synthesis of organocobalt complexes from vinyl ethers and cobalt(III) complexes in nucleophilic solvents.[4,7-9] To date, all evidence presented for the existence of such intermediates has been indirect. We would now like to report firm kinetic evidence for the existence of an intermediate in the acid-catalyzed decomposition of (2-hydroxyethyl)cobaloxime to cobaloxime(III) and ethylene[10] and direct observation of this intermediate by ^1H NMR spectroscopy.

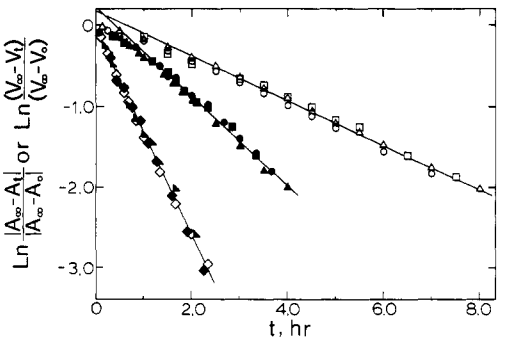

Figure 1. Normalized, semilogarithmic plots of the UV (255 nm), visible (445 nm), and manometric kinetics of the decomposition of **1a**, **1b**, and **1c** at $H_o = 1.70 \pm 0.01$, 25.0 ± 0.1 °C: **1c**, UV (○), visible (△), manometric (□), $k_{obsd} = (7.65 \pm 0.18) \times 10^{-5}$ s^{-1}; **1b**, UV (●), visible (▲), manometric (■), $k_{obsd} = (1.53 \pm 0.04) \times 10^{-4}$ s^{-1}; **1a**, UV (♦), visible (◇), manometric (◣), $k_{obsd} = (3.53 \pm 0.05) \times 10^{-4}$ s^{-1}.

Scheme I

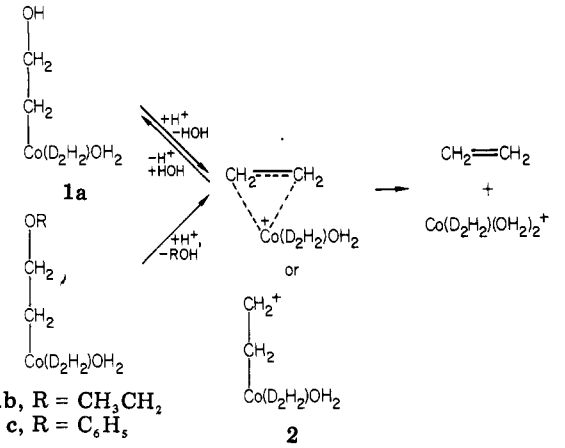

The decomposition of (2-hydroxyethyl)aquocobaloxime (**1a**)[11] in weakly acidic H_2SO_4/H_2O mixtures ($H_o = 1.70 \pm 0.01$)[14-16] (Figure 1) was found to be a strictly first-order process when monitored by UV or visible spectroscopy, as well as manometrically. In contrast, the decomposition of (2-ethoxyethyl)-(**1b**) and (2-phenoxyethyl)aquocobaloxime (**1c**) in the same media shows a distinct lag followed by a first-order decay using the same three techniques. The observed first-order rate constants decrease markedly

(1) Golding, B. T.; Holland, H. L.; Horn, U.; Sakrikar, S. *Angew. Chem., Int. Ed. Engl.* **1970**, *9*, 959–960.
(2) Golding, B. T.; Sakrikar, S. *J. Chem. Soc., Chem. Commun.* **1972**, 1183–1184.
(3) Silverman, R. B.; Dolphin, D.; Babior, B. M. *J. Am. Chem. Soc.* **1972**, *94*, 4028–4030.
(4) Silverman, R. B.; Dolphin, D. *J. Am. Chem. Soc.* **1976**, *98*, 4626–4633.
(5) Brown, K. L.; Ingraham, L. L. *J. Am. Chem. Soc.* **1974**, *96*, 7681–7686.
(6) Espenson, J. H.; Wang, D. M. *Inorg. Chem.* **1979**, *18*, 2853–2859.
(7) Silverman, R. B.; Dolphin, D. *J. Am. Chem. Soc.* **1973**, *95*, 1686–1688.
(8) Silverman, R. B.; Dolphin, D. *J. Am. Chem. Soc.* **1974**, *96*, 7094–7096.
(9) Silverman, R. B.; Dolphin, D.; Carty, T. J.; Krodel, E. K.; Abeles, R. H. *J. Am. Chem. Soc.* **1974**, *96*, 7096–7097.
(10) Schrauzer, G. N.; Windgassen, R. J. *J. Am. Chem. Soc.* **1967**, *89*, 143–147.
(11) The title complexes were synthesized by published procedures[10,12,13] and characterized by ^1H NMR spectroscopy and elemental analysis.
(12) Brown, K. L.; Awtrey, A. W. *Inorg. Chem.* **1978**, *17*, 111–119.
(13) Brown, K. L. *J. Am. Chem. Soc.* **1979**, *101*, 6600–6606.
(14) Hammett, L. P.; Deyrup, A. J. *J. Am. Chem. Soc.* **1932**, *54*, 2721–2739.
(15) Bascombe, K. N.; Bell, R. P. *J. Chem. Soc.* **1959**, 1096–1104.
(16) Ryabova, R. S.; Medvetskaya, I. M.; Vinnik, M. T. *Zh. Fiz. Khim.* **1966**, *40*, 339–345.

0276-7333/82/2301-0413$01.25/0

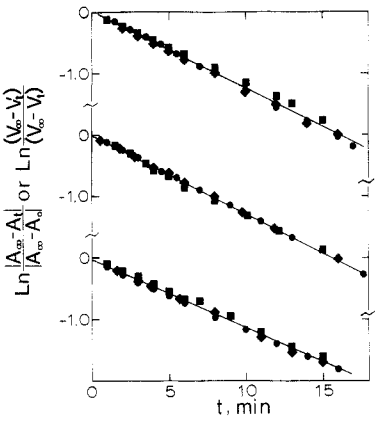

Figure 2. Normalized, semilogarithmic plots of the kinetics of decomposition of **1a** (●), **1b** (♦), and **1c** (■), at H_0 ca. −5.0, 25.0 ± 0.1 °C. Upper plot: UV (255 nm), $H_0 = -5.02 \pm 0.02$, $k_{obsd} = (2.08 \pm 0.03) \times 10^{-3}$ s^{-1}. Center plot: visible (445 nm), $H_0 = -4.99 \pm 0.02$, $k_{obsd} = (2.12 \pm 0.03) \times 10^{-3}$ s^{-1}. Lower plot: manometric, $H_0 = -5.06 \pm 0.03$, $k_{obsd} = (1.85 \pm 0.03) \times 10^{-3}$ s^{-1}.

Scheme II

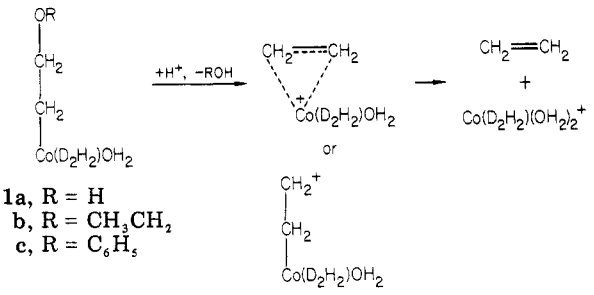

1a, R = H
b, R = CH_3CH_2
c, R = C_6H_5

2

in the order **1a** > **1b** > **1c** (Figure 1). These results suggest a mechanism such as that shown in Scheme I in which the decomposition of the three complexes is linked via a common cationic intermediate (**2**). Further evidence for such a scheme comes from the following observations. (i) The kinetics of decomposition of **1b** and **1c** in such media are unaffected by the presence of added alcohol leaving group over the concentration range ca. 3.7×10^{-5} to 3.7×10^{-2} M. (ii) Both the duration and severity of the lag as well as the observed first-order rate constant for decomposition of **1b** and **1c** are substantially altered by initiation of the reaction with various mixtures of **1b** or **1c** with **1a**. (iii) Complex **1a** may be obtained, after neutralization, from the partial decomposition of **1b** or **1c** at $H_0 = 1.50$.[17]

This situation is substantially altered in much more strongly acidic H_2SO_4/H_2O mixtures (Figure 2). At H_0 ca. −5.0 (ca. 9.95 M H_2SO_4) spectrophotometric observations of the decomposition of all three complexes show a rapid "burst" of absorbance change (too fast to quantitate under these conditions) followed by a much slower first-order decay which is identical for all three compounds. Significantly, manometric measurements of the rate of ethylene evolution are also identical for all three compounds under these conditions and are in excellent agreement with the spectrophotometric results (Figure 2). These observations require a common intermediate in the decomposition of all three complexes and suggest that in such strongly acidic media the activity of water is sufficiently reduced[18,19] to prevent the hydration of the intermediate to form **1a** and that Scheme II now applies.[20]

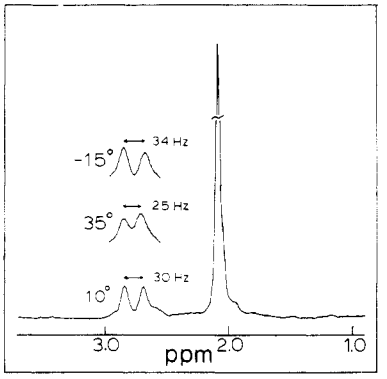

Figure 3. ^{1}H NMR spectrum of the intermediate formed from **1a** in ca. 13.0 M D_2SO_4/D_2O at 10 °C (insets 35 and −15 °C) using a JEOL JNM-FX200 FT NMR spectrometer operating at 199.5 MHz. The chemical shifts indicated are relative to external Me_4Si.

Because of the relatively slow rate of decomposition of the intermediate in such strongly acidic media, it is possible to observe it directly by Fourier transform ^{1}H NMR spectroscopy. Figure 3 shows the ^{1}H NMR spectrum observed at 199.5 MHz and 10 °C as soon as possible after makeup of a sample of **1a** in ca. 13.0 M D_2SO_4/D_2O (D_0 ca. −6.6).[21,22] The spectrum is characterized by a 12.0 proton singlet resonance at 2.06 ppm (relative to external Me_4Si) representing the cobaloxime equatorial methyls and two rather broad singlets of approximately equal intensity at 2.66 and 2.81 ppm integrating to a total of four protons. Similar spectra may be observed at D_0 ca. −6, as well as in samples of **1b** and **1c** in similar media.[23] When the intermediate is observed at 60 MHz, the organic ligand gives a broad singlet ($w_{1/2}$ ca. 15 Hz) centered at 2.74 ppm. Figure 3 also shows the temperature dependence of the two organic ligand resonances (at 199.5 MHz). The separation between the two resonances can be seen to decrease from 34 Hz at −15 °C to 25 Hz at 35 °C while the relative intensity of the two resonances changes such that the upfield member increases at the expense of the downfield member as the temperature is increased. These observations are consistent with the formulation of the intermediate as a cobaloxime(III)–ethylene π complex in which rotation about the π bond axis is relatively slow (on the NMR time scale) and two different preferred conformations exist, presumably one in which the ethylene hydrogens point toward the equatorial oxime oxygens and one in which the ethylene hydrogens point toward the equatorial methyls, leading to a chemical shift difference of about 0.15 ppm for the ethylene hydrogens in the two conformations. However, as the temperature-dependent change in intensity of the two organic ligand resonances is quite small, it is not possible to rule out a σ-bonded ethylcobaloxime carbonium ion undergoing relatively slow topomerization (on the NMR time scale) as the intermediate.

Acknowledgment. This research was supported by the Robert A. Welch Foundation, Houston, Texas, Grant

(17) E.g., decomposition of 4.46 mmol of **1b** for 50 min at 25.0 °C in 500 mL of 0.0217 M H_2SO_4 ($H_0 = 1.50$) provided, after neutralization, reaction with pyridine, concentration, and workup by silica gel chromatography, 0.84 mmol of unreacted starting material (18.8%) and 0.25 mmol (5.7%) of (2-hydroxyethyl)(pyridine)cobaloxime.

(18) Wyatt, P. A. H. *Discuss. Faraday Soc.* **1957**, *24*, 162–170.
(19) Yates, K.; Wai, H. *J. Am. Chem. Soc.* **1964**, *86*, 5408–5413.
(20) Expected equatorial ligand protonations have been observed and will be discussed fully in a forthcoming publication. For simplicity these have been omitted from Schemes I and II but their occurrence in no way affects the conclusions drawn herein.
(21) Hogfeldt, E.; Bigeleisen, J. *J. Am. Chem. Soc.* **1960**, *82*, 15–20.
(22) Sierra, J.; Ojeda, M.; Wyatt, P. A. H. *J. Chem. Soc. B* **1970**, 1570–1573.
(23) Spectra of the intermediate obtained from **1b** or **1c** show additional resonances due to the alcohol leaving groups.

Y-749. We are grateful to the Chemistry Department of The University of Texas at Dallas for the use of the JEOL JNM-FX200 FT-NMR spectrometer and particularly to Dr. Dean Sherry for his assistance with the FT NMR measurements.

Registry No. 1a, 15218-80-1; 1b, 80422-34-0; 1c, 64707-51-3; 2, 80422-35-1.

Catalytic Polymerization of Acetylenes and Olefins by Tetrakis(acetonitrile)palladium(II) Bis(tetrafluoroborate)

Ayusman Sen* and Ta-Wang Lai

Chandlee Laboratory, Department of Chemistry
Pennsylvania State University
University Park, Pennsylvania 16802

Received October 23, 1981

Summary: The cationic Pd(II) compound $[Pd(CH_3CN)_4](BF_4)_2$ was found to catalyze the polymerization of H—C≡C—R (R = Ph, COOMe), styrene, α-methylstyrene, 1,3-cyclohexadiene, norbornylene, and norbornadiene under very mild conditions. The polyacetylenes are highly colored and have relatively high molecular weights. The poly(phenylacetylene) has a trans configuration around the C=C bond. The polymerization of 1,3-cyclohexadiene leads predominantly to the 1,2 polymer with only minimal cross-linking. The norbornane framework is retained during the polymerization of norbornylene. The poly(norbornadiene) is a highly cross-linked material.

We wish to report that the cationic Pd(II) compound $[Pd(CH_3CN)_4](BF_4)_2$, 1,[1] is a versatile catalyst for the polymerization of a wide range of acetylenes and olefins under relatively mild conditions. Except for a few halides of transition metals in high oxidation states, e.g., $TiCl_4$ and $FeCl_3$, transition-metal compounds in general have not been found to catalyze the cationic polymerization of olefins.[2] This is particularly true for the "softer" transition metals belonging to the second and third period of group 8. However, we have recently presented evidence for the generation of carbonium ions by the interaction of olefins with 1.[3] Therefore, it should be expected that 1 would act as a good initiator for cationic polymerization reactions. Indeed, we find this to be true, and our results are summarized in Table I. These reactions all involved the addition of 100 equiv of the monomer to a 1×10^{-2} M solution of 1 and were carried out under air- and moisture-free conditions by using standard vacuum line techniques. Consistent with a cationic polymerization mechanism, we found that compared to phenylacetylene, the polymerization of the electron-deficient methyl propiolate took place only at a significantly higher temperature and led to a polymer with lower molecular weight. Similarly, no polymerization was observed for the electron-deficient olefins, acrylonitrile and methyl acrylate.

The polyacetylenes are soluble in organic solvents and are highly colored, consistent with the presence of extensive conjugation. The poly(phenylacetylene) shows a maxima at 237 nm (ϵ 1.8×10^6 M^{-1} cm^{-1}, mol wt 9000) with a shoulder at 339 nm (ϵ 6.4×10^5 M^{-1} cm^{-1}) in THF. The corresponding maxima and shoulder for poly(methyl propiolate) are at 232 nm (ϵ 1.85×10^5 M^{-1} cm^{-1}, mol wt 3000) and 291 cm (ϵ 9×10^4 M^{-1} cm^{-1}), respectively. The poly(phenylacetylene) that we have obtained has one of the highest molecular weights recorded thus far.[4] Its infrared spectrum (KBr pellet) exhibits an absorption at 1595 cm^{-1}, indicating the presence of polyconjugated C=C bonds. Two strong bands appear at 755 and 695 cm^{-1}, and these correspond to the C–H out-of-plane deformations of monosubstituted benzene rings. The region between 2000 and 1700 cm^{-1} also exhibits the characteristic absorption of monosubstituted benzenes. In addition, a band at 910 cm^{-1} indicates a trans configuration around C=C bond.[5] When $CHCl_3$, instead of CH_3CN, was used as the solvent, a slightly different polymer exhibiting infrared bands at both 910 and 870 cm^{-1} was obtained. The latter band can be ascribed to a cis configuration around the C=C bonds.[5] Thus the stereostructure of the poly(phenylacetylene) obtained appears to be solvent dependent—in acetonitrile predominantly trans polymer

Table I. Catalytic Polymerization of Olefins and Acetylenes by $[Pd(CH_3CN)_4](BF_4)_2$[a]

monomer	solvent	temp, °C	time	yield,[b] %	$\bar{M}_n$[c]
H—C≡C—Ph	CH_3CN	25	5 min	30	9000
H—C≡C—CO_2Me	CH_3CN	70	12 h	>90	3000
CH_2=CHPh	CH_3CN	25	5 min	>90	70000
CH_2=C(Me)Ph	CH_3NO_2	0	5 min	75	8000
	CH_3CN	25	30 min	40	2000
	CH_3NO_2	25	5 min	>90	*d*
	CH_3NO_2	25	60 min	>90	*d*

[a] A monomer to catalyst ratio of 100:1 was used in all cases. [b] Yields reported are those of isolated pure materials. [c] Molecular weights of polymers were determined by gel permeation chromatography using solutions of polymers in tetrahydrofuran. A 500-Å microstyragel column was used. The weights reported are those of standard polystyrene samples having GPC traces similar to those observed. [d] The polymer was insoluble in THF.

Table II. Expected ^1H NMR Data for Poly(1,3-cyclohexadiene)

	1,2-polycyclohexadiene	1,4-polycyclohexadiene
	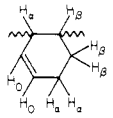	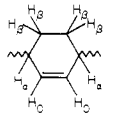
$H_o/(H_\alpha + H_\beta)$	1/3	1/3
H_α/H_β	1/1	1/2

(1) Schramm, R. F.; Wayland, B. B. *J. Chem. Soc., Chem. Commun.* **1968**, 898.
(2) Kennedy, J. P. "Cationic Polymerization of Olefins: A Critical Inventory"; Wiley-Interscience: New York, 1975.
(3) Sen, A.; Lai, T.-W. *J. Am. Chem. Soc.* **1981**, *103*, 4627.
(4) For other synthetic routes to high molecular weight poly(phenylacetylene), see: (a) Katz, T. J.; Lee, S. J. *J. Am. Chem. Soc.* **1980**, *102*, 422. (b) Navarro, F. R.; Farona, M. F. *J. Polym. Sci. Polym. Chem. Ed.* **1976**, *14*, 2335. (c) Masuda, T.; Sasaki, N.; Higashimura, T. *Macromolecules* **1975**, *8*, 717.
(5) For discussions on the infrared spectra of poly(phenylacetylene) samples, see: (a) Reference 3c. (b) Tsonis, C.; Farona, M. F. *J. Polym. Sci., Polym. Chem. Ed.* **1979**, *17*, 1779. (c) Simionescu, C. I.; Percec, V.; Dumitreecu, S. *Ibid.* **1977**, *15*, 2497. (d) Kern, R. J. *J. Polym. Sci., Polym. Chem. Ed.* **1969**, *7*, 621. (e) Furlani, A.; Collamati, I.; Sartori, G. *J. Organomet. Chem.* **1969**, *17*, 463.

0276-7333/82/2301-0415$01.25/0

Y-749. We are grateful to the Chemistry Department of The University of Texas at Dallas for the use of the JEOL JNM-FX200 FT-NMR spectrometer and particularly to Dr. Dean Sherry for his assistance with the FT NMR measurements.

Registry No. 1a, 15218-80-1; 1b, 80422-34-0; 1c, 64707-51-3; 2, 80422-35-1.

Catalytic Polymerization of Acetylenes and Olefins by Tetrakis(acetonitrile)palladium(II) Bis(tetrafluoroborate)

Ayusman Sen* and Ta-Wang Lai

Chandlee Laboratory, Department of Chemistry
Pennsylvania State University
University Park, Pennsylvania 16802

Received October 23, 1981

Summary: The cationic Pd(II) compound $[Pd(CH_3CN)_4](BF_4)_2$ was found to catalyze the polymerization of H—C≡C—R (R = Ph, COOMe), styrene, α-methylstyrene, 1,3-cyclohexadiene, norbornylene, and norbornadiene under very mild conditions. The polyacetylenes are highly colored and have relatively high molecular weights. The poly(phenylacetylene) has a trans configuration around the C=C bond. The polymerization of 1,3-cyclohexadiene leads predominantly to the 1,2 polymer with only minimal cross-linking. The norbornane framework is retained during the polymerization of norbornylene. The poly(norbornadiene) is a highly cross-linked material.

We wish to report that the cationic Pd(II) compound $[Pd(CH_3CN)_4](BF_4)_2$, 1,[1] is a versatile catalyst for the polymerization of a wide range of acetylenes and olefins under relatively mild conditions. Except for a few halides of transition metals in high oxidation states, e.g., $TiCl_4$ and $FeCl_3$, transition-metal compounds in general have not been found to catalyze the cationic polymerization of olefins.[2] This is particularly true for the "softer" transition metals belonging to the second and third period of group 8. However, we have recently presented evidence for the generation of carbonium ions by the interaction of olefins with 1.[3] Therefore, it should be expected that 1 would act as a good initiator for cationic polymerization reactions. Indeed, we find this to be true, and our results are summarized in Table I. These reactions all involved the addition of 100 equiv of the monomer to a 1×10^{-2} M solution of 1 and were carried out under air- and moisture-free conditions by using standard vacuum line techniques. Consistent with a cationic polymerization mechanism, we found that compared to phenylacetylene, the polymerization of the electron-deficient methyl propiolate took place only at a significantly higher temperature and led to a polymer with lower molecular weight. Similarly, no polymerization was observed for the electron-deficient olefins, acrylonitrile and methyl acrylate.

The polyacetylenes are soluble in organic solvents and are highly colored, consistent with the presence of extensive conjugation. The poly(phenylacetylene) shows a maxima at 237 nm (ϵ 1.8×10^6 M^{-1} cm^{-1}, mol wt 9000) with a shoulder at 339 nm (ϵ 6.4×10^5 M^{-1} cm^{-1}) in THF. The corresponding maxima and shoulder for poly(methyl propiolate) are at 232 nm (ϵ 1.85×10^5 M^{-1} cm^{-1}, mol wt 3000) and 291 cm (ϵ 9×10^4 M^{-1} cm^{-1}), respectively. The poly(phenylacetylene) that we have obtained has one of the highest molecular weights recorded thus far.[4] Its infrared spectrum (KBr pellet) exhibits an absorption at 1595 cm^{-1}, indicating the presence of polyconjugated C=C bonds. Two strong bands appear at 755 and 695 cm^{-1}, and these correspond to the C–H out-of-plane deformations of monosubstituted benzene rings. The region between 2000 and 1700 cm^{-1} also exhibits the characteristic absorption of monosubstituted benzenes. In addition, a band at 910 cm^{-1} indicates a trans configuration around C=C bond.[5] When $CHCl_3$, instead of CH_3CN, was used as the solvent, a slightly different polymer exhibiting infrared bands at both 910 and 870 cm^{-1} was obtained. The latter band can be ascribed to a cis configuration around the C=C bonds.[5] Thus the stereostructure of the poly(phenylacetylene) obtained appears to be solvent dependent—in acetonitrile predominantly trans polymer

Table I. Catalytic Polymerization of Olefins and Acetylenes by $[Pd(CH_3CN)_4](BF_4)_2$[a]

monomer	solvent	temp, °C	time	yield,[b] %	$\bar{M}_n$[c]
H—C≡C—Ph	CH_3CN	25	5 min	30	9000
H—C≡C—CO_2Me	CH_3CN	70	12 h	>90	3000
CH_2=CHPh	CH_3CN	25	5 min	>90	70000
CH_2=C(Me)Ph	CH_3NO_2	0	5 min	75	8000
	CH_3CN	25	30 min	40	2000
	CH_3NO_2	25	5 min	>90	*d*
	CH_3NO_2	25	60 min	>90	*d*

[a] A monomer to catalyst ratio of 100:1 was used in all cases. [b] Yields reported are those of isolated pure materials. [c] Molecular weights of polymers were determined by gel permeation chromatography using solutions of polymers in tetrahydrofuran. A 500-Å microstyragel column was used. The weights reported are those of standard polystyrene samples having GPC traces similar to those observed. [d] The polymer was insoluble in THF.

Table II. Expected ^1H NMR Data for Poly(1,3-cyclohexadiene)

	1,2-polycyclohexadiene	1,4-polycyclohexadiene
	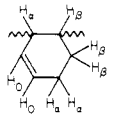	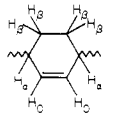
$H_o/(H_\alpha + H_\beta)$	1/3	1/3
H_α/H_β	1/1	1/2

(1) Schramm, R. F.; Wayland, B. B. *J. Chem. Soc., Chem. Commun.* **1968**, 898.
(2) Kennedy, J. P. "Cationic Polymerization of Olefins: A Critical Inventory"; Wiley-Interscience: New York, 1975.
(3) Sen, A.; Lai, T.-W. *J. Am. Chem. Soc.* **1981**, *103*, 4627.
(4) For other synthetic routes to high molecular weight poly(phenylacetylene), see: (a) Katz, T. J.; Lee, S. J. *J. Am. Chem. Soc.* **1980**, *102*, 422. (b) Navarro, F. R.; Farona, M. F. *J. Polym. Sci. Polym. Chem. Ed.* **1976**, *14*, 2335. (c) Masuda, T.; Sasaki, N.; Higashimura, T. *Macromolecules* **1975**, *8*, 717.
(5) For discussions on the infrared spectra of poly(phenylacetylene) samples, see: (a) Reference 3c. (b) Tsonis, C.; Farona, M. F. *J. Polym. Sci., Polym. Chem. Ed.* **1979**, *17*, 1779. (c) Simionescu, C. I.; Percec, V.; Dumitreecu, S. *Ibid.* **1977**, *15*, 2497. (d) Kern, R. J. *J. Polym. Sci., Polym. Chem. Ed.* **1969**, *7*, 621. (e) Furlani, A.; Collamati, I.; Sartori, G. *J. Organomet. Chem.* **1969**, *17*, 463.

0276-7333/82/2301-0415$01.25/0

being obtained, while a cis–trans mixture resulted in chloroform. The ^1H NMR spectrum of poly(phenylacetylene) exhibits only a broad featureless absorption between 7.5 and 6.5 ppm.

The ^1H NMR spectrum of poly(1,3-cyclohexadiene) exhibits three broad resonances at 5.8 ppm (H_0), 2.0 ppm (H_α), and 1.6 ppm (H_β), the first two representing respectively the vinylic and allylic protons present in the polymer. Two possible types of polymers (1,2 and 1,4) may arise through the cationic polymerization of 1,3-cyclohexadiene,[6] and these are shown in Table II. The ratio, H_α/H_β, in the polymer that we have obtained is approximately 1, thus indicating it is predominantly 1,2-poly(1,3-cyclohexadiene). The ratio, $H_0/(H_\alpha + H_\beta)$, is a measure of the degree of branching or cross-linking that is present in the polymer ($H_0/(H_\alpha + H_\beta) = 0.33$ for unbranched polymer and 0 for completely cross-linked polymer). In the present case, $H_0/(H_\alpha + H_\beta) = 0.28$, thus indicating the presence of a very modest degree of cross-linking.

The polymerization of norbornylene has been reported to yield either of the following two polymeric structural units I[7] and II.[8] Structure I, having vinyl cyclopentane

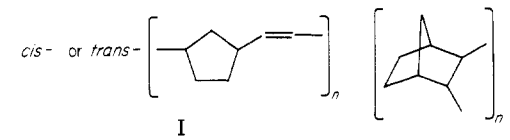

I II

as the repeating unit, is characterized by vinylic resonance at ~5.3 ppm in the ^1H NMR spectrum and C=C stretch at 1680 cm^{-1} and vinylic C-H bending mode at 960 cm^{-1} in the infrared spectrum respectively.[7] On the other hand, the above olefinic features are absent in poly(norbornylene) having II as the structural unit. Instead, the latter type of polymer exhibits an intense absorption at 1300 cm^{-1} in the infrared spectrum, characteristic of the bridging methylene group. The poly(norbornylene) that we have obtained appears to have structure II. It shows none of the spectral features ascribable to the presence of olefinic functionality, while its infrared spectrum (KBr pellet) shows an intense absorption at 1298 cm^{-1} due to the presence of the bridging methylene group.

It has been reported that the cationic polymerization of norbornadiene leads to a polymer with the structural unit III.[9] This repeating unit, nortricyclene, is characterized

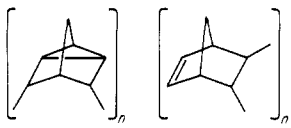

III IV

by a strong infrared absorption band at 810–800 cm^{-1}.[10] On the other hand, the polymerization of norbornadiene by π-allyl compounds of Pd(II) results in a polymer with the repeating unit IV.[11] The NMR and IR data presented

Scheme I

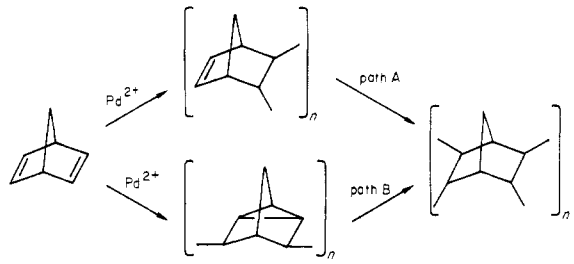

appear to support this conclusion.[11] The absence of an infrared absorption at 810–800 cm^{-1} would seem to exclude the presence of the nortricyclene repeating unit. On the other hand, an absorption at 1620 cm^{-1} together with a resonance at 6.2 ppm in the ^1H NMR spectrum indicate the presence of C=C bond. The infrared spectrum of the poly(norbornadiene) that we have obtained show bands at *both* 800 cm^{-1}, which is characteristic of nortricyclene derivatives, and at 1620 cm^{-1}, which indicates the presence of C=C bonds in the polymer. Support for the presence of C=C bonds in our poly(norbornadiene) was also obtained by reacting norbornadiene with 1 in CH_3CN. A soluble polymer with resonance at 6.2 ppm in the ^1H NMR spectrum was obtained. Thus it appears that our poly(norbornadiene) incorporates both repeating units III and IV.

We find our poly(norbornadiene) to be virtually insoluble in all common organic solvents, and this insolubility is probably a consequence of the presence of extensive cross-linking. The cross-linking may arise out of the reaction of the remaining C=C bonds (path A, Scheme I) or through ring-opening polymerization of notricyclene (path B, Scheme I). While our observation of the polymerization of norbornylene by 1 (vide supra) constitutes support for path A, some evidence for path B is provided by the fact that 1 was found to catalyze the instantaneous conversion of quadricyclane to norbornadiene; the latter, if left in the reaction mixture, is then slowly polymerized (eq 1).

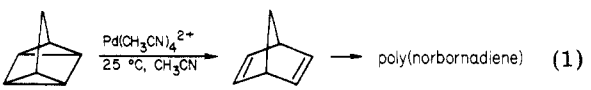

(1)

In conclusion, it is obvious that the cationic Pd(II) compound $[Pd(CH_3CN)_4](BF_4)_2$ containing weakly coordinating CH_3CN ligands, is capable of polymerizing a wide variety of acetylenes and olefins. There are also several reports in the literature concerning the catalytic oligomerization and cooligomerization of olefins by Pd(II) compounds which attest to the increased activity of the cationic Pd(II) species as compared to their corresponding neutral precursors.[12] Moreover, the recent report[13] of polymerization of 1,3-butadiene and 1,3-cyclohexadiene by the related cationic Rh compound $[Rh(NO)(CH_3CN)_4](BF_4)_2$ appears to indicate a common reactivity pattern for cationic transition-metal compounds containing weakly coordinating ligands. Indeed, we have observed similar catalytic chemistry for the cationic compounds $[M(NO)_2(CH_3CN)_4](BF_4)_2$ (M = Mo, W).[14] On the other

(6) (a) Imanishi, Y.; Matsuzaki, K.; Yamane, T.; Kohjiya, S.; Okamura, S. *J. Macromol. Sci., Chem.* **1969**, *A3*, 249. (b) Reference 2, p 192.
(7) (a) Michellotti, F. W.; Keaveney, W. P. *J. Polym. Sci., A* **1965**, *3*, 895. (b) Truett, W. L.; Johnson, D. R.; Robinson, I. M.; Montague, B. A. *J. Am. Chem. Soc.* **1960**, *82*, 2337.
(8) (a) Kennedy, J. P.; Makowski, H. S. *J. Macromol. Sci., Chem.* **1967**, *A1*, 345. (b) Tanielian, C.; Kiennemann, A.; Osparpucu, T. *Can. J. Chem.* **1979**, *57*, 2022.
(9) (a) Kennedy, J. P.; Hinlicky, J. A. *Polymer* **1965**, *6*, 133. (b) Reference 2, p 223.
(10) Roberts, J. D.; Trumbull, E. R.; Bennett, W.; Armstrong, R. *J. Am. Chem. Soc.* **1950**, *72*, 3116.
(11) Hojabi, F. *J. Appl. Chem. Biotechnol.* **1973**, *23*, 601.
(12) (a) Oehme, G.; Pracejus, H. *Tetrahedron Lett.* **1979**, 343. (b) Kaneda, K.; Terasawa, M.; Imanaka, T.; Teranishi, S. *Ibid.* **1977**, 2957. (c) Hattori, S.; Munakata, H.; Tatsuoka, K.; Shimuzu, T. U.S. Patent, 3 803 254, 1974.
(13) Connelly, N. G.; Draggett, P. T.; Green, M. *J. Organomet. Chem.* **1977**, *140*, C10.
(14) Sen, A.; Thomas, R. R. *Organometallics*, submitted for publication.

hand, the Ni(II) and Co(II) compounds $[M(CH_3CN)_6](BF_4)_2$ (M = Ni, 2; M = Co, 3)[15] were inactive as polymerization catalysts under conditions employed for the reactions involving the Pd(II) compound, 1, even though from a consideration of charge/radius ratios, one might expect Co^{2+} and Ni^{2+} to be more electrophilic than Pd^{2+}.[16] One reason for this remarkable difference in reactivity may be that the CH_3CN ligands in 2 and 3 are held more strongly[17] than those in 1. For example, we find that while the coordinated CH_3CN molecules in 1 exchange "instantaneously" with the solvent when 1 is dissolved in CD_3CN at 25 °C, no exchange was observed in case of 2 even on heating the corresponding solution of 2 to 60 °C for 8 h. Thus, it would appear that the replacement of CH_3CN by olefins or acetylenes in the coordination sphere of the metal is a prerequisite for the polymerization of these substrates.

Finally, from a practical standpoint, an important advantage of using 1 as a catalyst for cationic polymerizations as compared to traditional initiators such as $HBF_4 \cdot Me_2O$ is that the latter does not initiate the polymerization of acetylenes such as phenylacetylene and methyl propiolate under the mild conditions that are employed when 1 is used as the initiator.

Acknowledgment. Financial support of this research by grants from the Department of Energy, Office of Basic Energy Sciences, and by the donors of the Petroleum Research Fund, administered by the American Chemical Society, is gratefully acknowledged.

Registry No. $(H-C\equiv C-Ph)_n$, 25038-69-1; $(H-C\equiv C-CO_2Me)_n$, 27342-21-8; $(CH_2=CHPh)_n$, 9003-53-6; $(CH_2=C(Me)Ph)_n$, 25988-53-8; (1,3-cyclohexadiene)$_n$, 27986-50-1; (norbornene)$_n$, 25038-76-0; (norbornadiene)$_n$, 27859-77-4; $[Pd(CH_3CN)_4](BF_4)_2$, 21797-13-7.

(15) Hathaway, B. J.; Underhill, A. E. *J. Chem. Soc.* **1960**, 3705.
(16) Such a comparison is complicated by the fact that 1 is diamagnetic, while 2 and 3 are paramagnetic compounds.
(17) For rates of exchange of CH_3CN for 2 and 3, see: (a) Yano, Y.; Fairhurst, M. T.; Swaddle, T. W. *Inorg. Chem.* **1980**, *19*, 3267. (b) Meyer, F. K.; Newman, K. E.; Merbach, A. E. *Ibid.* **1979**, *18*, 2142. (c) Newman, K. E.; Meyer, F. K.; Merbach, A. E. *J. Am. Chem. Soc.* **1979**, *101*, 1470.

Book Reviews

Reactivity of Metal-Metal Bonds. Edited by M. H. Chisholm. ACS Symposium Series No. 155. American Chemical Society, Washington, D.C. 1981. vii + 327 pages. $39.00.

This 300+ page collection of 15 lectures presented on August 25–26, 1980, at the 180th National ACS Meeting in Las Vegas continues in the tradition of the many excellent ACS Symposium Series in the past. The premise of the symposium on "Reactivity of Metal–Metal Bonds" was that the chemistry of compounds containing metal–metal bonds is shifting from elucidating structures, bonding, and electronic properties to studies concerning reactivity patterns.

About half of the 15 chapters in this book deal with a wide variety of bimetallic systems. Articles by Cotton, Chisholm, McCarley, and Walton discuss group 6 or 7 metal–metal complexes containing triple or quadruple bonds. The first is an historical perspective; the other three present recent results from the authors' labs concerning fundamental reactions of Mo≡Mo complexes, formation of group 6 tetranuclear halo and ternary oxide complexes, and cleavage of metal–metal multiple bonds, respectively. Balch and Puddephatt discuss the preparation and reaction of 1,2-bis[(diphenylphosphino)methane]-bridged Rh, Pd, and Pt complexes containing μ-alkylidene, μ-hydrido, or μ-alkyl ligands, while Curtis presents some recent chemistry of $Cp_2Mo_2(CO)_4$ having to do with addition of reagents across the triple bond. Dyke et al. summarize some fascinating recent chemistry of dimetallacyclic complexes prepared by adding simple molecules (e.g., acetylenes) to metal–metal bonded dimeric complexes. A related paper by Ashworth et al. describes some simple preparative routes to complexes containing two (or three) metals, many of them based on the principle of "oxidizing" Pt(0) by adding a M=C or M≡C bond to it.

Metal cluster chemistry is represented here in two chapters, one by Vidal on polynuclear rhodium carbonyl complexes and a second by Geoffroy on $H_2FeRu_3(CO)_{13}$.

The remaining four chapters are relatively thorough, general accounts of the photochemistry of metal–metal bonds (Wrighton), the kinetics of reactions involving metal carbonyl dimers and trimers (Pöe), the thermochemistry of metal–metal bonds (Connor), and the coordination chemistry of metal surfaces (Muetterties).

Like previous books in this series, this one is assembled from camera-ready manuscripts. While technical quality is sacrificed to some extent for speed of publication, the authors have for the most part made the book more readable by using the same typeface and format. An index is included.

Richard R. Schrock, *Massachusetts Institute of Technology*

Catalytic Activation of Carbon Monoxide. Edited by P. C. Ford. ACS Symposium Series No. 152, American Chemical Society, Washington, D.C. 1981. ix + 358 pages. $36.50.

This volume is a collection of 21 papers presented at a symposium at the American Chemical Society Meeting in Las Vegas in 1980 and is part of the ACS Symposium Series. The field of CO activation is continually gaining importance as the search goes on for replacements for petroleum feedstocks, and this volume presents a good overview of research in this field in the past few years. The majority of the papers deal in some way with homogeneous catalysis of CO activation, either by describing the synthesis and reaction chemistry of compounds which are models for proposed reaction intermediates or by describing actual catalyst systems. There are six papers by various research groups describing different systems for the homogeneous catalysis of the water gas shift reaction. In total, these papers cover nearly all of the most recent work in this field. Of particular note here is a very detailed paper by Slegeir, Sapienza, and Easterling on "Mechanistic Aspects of the Homogeneous Water Gas Shift Reaction". The paper by Dombek on the "Hydrogenation of Carbon Monoxide to Methanol and Ethylene Glycol by Homogeneous Ruthenium Catalysts" and that by Feder, Rathke, Chen, and Curtiss on "Experimental and Theoretical Studies of Mechanisms in the Homogeneous Catalytic Activation of Carbon Monoxide" are good examples of research on the direct production of C_1 and C_2 oxygenated chemicals by CO hydrogenation. The paper by Knifton on "Syngas Homologation of Aliphatic Carboxylic Acids" provides an interesting example of the incorporation of CO into other molecules.

There are seven papers which discuss the synthesis and reaction chemistry of organometallic compounds believed to be models for reactive intermediates in CO hydrogenation. A particularly intriguing paper in this area is the contribution by Gladysz, Kiel, Lim, Wary, and Tam, which discusses the reaction chemistry of